

*11-12-58*  
*3-11-59*

# NASA

## MEMORANDUM

NASA REACTOR FACILITY HAZARDS SUMMARY

VOLUME I

By Lewis Research Center Staff

Lewis Research Center  
Cleveland, Ohio

NATIONAL AERONAUTICS AND  
SPACE ADMINISTRATION

WASHINGTON

January 1959

10

11

12

NASA REACTOR FACILITY HAZARDS SUMMARY

VOLUME I

by Lewis Research Center Staff  
Cleveland, Ohio

October 15, 1956

Edited by  
T. M. Hallman and B. Lubarsky





## TABLE OF CONTENTS

## Volume I

	Page
SUMMARY . . . . .	1
1. <u>INTRODUCTION</u> . . . . .	3
2. <u>THE REACTOR FACILITY</u> . . . . .	7
2.1 GENERAL DESCRIPTION OF FACILITY . . . . .	7
2.2 REACTOR PHYSICS . . . . .	26
2.3 DESCRIPTION OF CONTROL SYSTEM . . . . .	34
2.4 REACTOR AND CONTROL KINETICS . . . . .	52
2.5 REFERENCES . . . . .	56
3. <u>SITE</u> . . . . .	57
3.1 ACCESS TO SITE . . . . .	57
3.2 EXISTING USES OF SURROUNDING AREA . . . . .	57
3.3 POPULATION DISTRIBUTION SUMMARY . . . . .	59
3.4 METEOROLOGY SUMMARY . . . . .	60
3.5 GEOLOGY SUMMARY . . . . .	61
3.6 REFERENCE . . . . .	62
4. <u>EXPERIMENTS</u> . . . . .	63
4.1 DESIGN OF TYPICAL EXPERIMENTS . . . . .	64
4.2 REACTIVITY EFFECTS OF EXPERIMENTS . . . . .	72
4.3 REFERENCE . . . . .	76
5. <u>HANDLING OF FUEL AND RADIOACTIVE MATERIALS</u> . . . . .	77
5.1 FUEL HANDLING AND DISPOSAL . . . . .	77
5.2 DISPOSAL OF RADIOACTIVE WASTE IN NORMAL OPERATION . . . . .	80
5.3 REFERENCES . . . . .	87
6. <u>HAZARDS</u> . . . . .	89
6.1 HAZARDS CREATED BY FAILURE OR MALFUNCTION OF COMPONENTS OF THE REACTOR FACILITY . . . . .	89
6.2 HAZARDS FROM FAILURE OR MALFUNCTION OF EXPERIMENTS . . . . .	100
6.3 HAZARDS RESULTING FROM ACTS OF GOD, WAR, SABOTAGE, NEGLIGENCE, AND EXPLOSIONS EXTERNAL TO THE FACILITY . . . . .	111
6.4 MAXIMUM CREDIBLE ACCIDENT AND ITS CONSEQUENCES . . . . .	117
6.5 REFERENCES . . . . .	125
7. <u>ADMINISTRATIVE ORGANIZATION</u> . . . . .	127
7.1 ORGANIZATIONAL STRUCTURE . . . . .	127
7.2 STAFF TRAINING . . . . .	131
7.3 PROCEDURES FOR HANDLING EXPERIMENTS OR CHANGES IN RE- ACTOR DESIGN AND OPERATION . . . . .	133
7.4 ADDITIONAL REGULATIONS FOR PROMOTING SAFETY . . . . .	135
7.5 HEALTH PHYSICS AND SAFETY . . . . .	135
7.6 SECURITY . . . . .	137
7.7 REFERENCES . . . . .	139

	Page
APPENDIX A. - REACTOR HEAT TRANSFER . . . . .	141
APPENDIX B. - REACTOR PHYSICS CALCULATIONS . . . . .	143
APPENDIX C. - METEOROLOGICAL ASPECTS OF A PROPOSED NUCLEAR FACILITY . . . . .	159
APPENDIX D. - MEMORANDUM ON THE GEOLOGY AND HYDROLOGY OF A PROPOSED REACTOR SITE NEAR SANDUSKY, OHIO . . . .	167
APPENDIX E. - PRIMARY WATER ACTIVITY . . . . .	177
APPENDIX F. - ANALYSES OF THE BORAX-TYPE EXCURSION IN THE NACA REACTOR . . . . .	183
APPENDIX G. - POSSIBLE CHEMICAL REACTIONS . . . . .	195
APPENDIX H. - FORCES ON THE REACTOR CONTAINMENT STRUCTURE . . .	201
APPENDIX I. - STRUCTURAL ANALYSIS . . . . .	205
APPENDIX J. - RADIOLOGICAL HAZARDS FROM THE RELEASE OF FISSION PRODUCTS . . . . .	221
APPENDIX K. - EMERGENCY PROCEDURES IN EVENT OF SERIOUS FISSION PRODUCT RELEASE . . . . .	235

NATIONAL AERONAUTICS AND SPACE ADMINISTRATION

Memorandum 12-8-58E

NASA REACTOR FACILITY HAZARDS SUMMARY

by Lewis Research Center Staff

SUMMARY

The Lewis Research Center of the National Aeronautics and Space Administration proposes to build a nuclear research reactor which will be located in the Plum Brook Ordnance Works near Sandusky, Ohio. The purpose of this report is to inform the Advisory Committee on Reactor Safeguards of the U. S. Atomic Energy Commission in regard to the design of the reactor facility, the characteristics of the site, and the hazards of operation at this location.

The purpose of this research reactor is to make pumped loop studies of aircraft reactor fuel elements and other reactor components, radiation effects studies on aircraft reactor materials and equipment, shielding studies, and nuclear and solid state physics experiments.

The reactor is light water cooled and moderated of the MTR-type with a primary beryllium reflector and a secondary water reflector. The core initially will be a 3 by 9 array of MTR-type fuel elements and is designed for operation up to a power of 60 megawatts.

The reactor facility is described in general terms. This is followed by a discussion of the nuclear characteristics and performance of the reactor. Then details of the reactor control system are discussed. A summary of the site characteristics is then presented followed by a discussion of the larger type of experiments which may eventually be operated in this facility. The considerations for normal operation are concluded with a proposed method of handling fuel elements and radioactive wastes.

The potential hazards involved with failures or malfunctions of this facility are considered in some detail. These are examined first from the standpoint of preventing them or minimizing their effects and second from the standpoint of what effect they might have on the reactor facility staff and the surrounding population. The most essential feature of the design for location at the proposed site is containment of the maximum credible accident.

E-102

CZ-1



## SECTION 1. - INTRODUCTION

The NACA has found it essential in the development of a propulsion system that the programs on the various components of a given system be closely coordinated. It has been severely limited in the nuclear propulsion systems field by the lack of a facility for investigating the reactor. Since 1951, studies have been made of the kind of a facility needed. In 1955 the NACA obtained funds from Congress to build this facility.

The development of an aircraft reactor that will give the performance required for high speed aircraft is hampered by two important factors.

1. Currently known reactor materials are inadequate at the high operating temperatures needed to give the high thrust per unit of powerplant weight required for supersonic aircraft.

2. The high shield weights associated with current reactor designs make for excessively heavy aircraft.

The continuous competition among nations for higher aircraft speeds provides a continuing demand for better materials and better configurations for the reactor and the shield. Refinement in materials and design are justified for the aircraft application beyond the needs of any other known application of nuclear energy. Hence, continuing research for better reactor and shield materials and configurations is essential. The need to save shield weight has led to configurations in which aircraft equipment, fluids, and structure are exposed to radiation damage, and an extensive research program on this subject is required.

The primary objective of the proposed facility is to provide the means for making the various types of investigations needed to assist the development of the aircraft reactor. These include:

- a. Pumped loop studies of the performance and behavior of fuel elements and other reactor components at coolant flow, heat flow, neutron flux, and temperature conditions of interest for aircraft reactors.

- b. Effects of radiation on reactor materials and the interaction between reactor materials.

- c. Effect of radiation on aircraft structure, fluids, and equipment.

- d. Shield studies.

- e. Nuclear physics and solid state physics experiments pertinent to the development of the aircraft reactor.

E-102

CZ-1 back

For realistic evaluation, materials and configurations must be investigated under conditions closely simulating the conditions desired in the aircraft reactor. Under these conditions failures of experimental components can be expected on a routine basis. The rate of progress of the aircraft development will depend on the speed with which experiments can be made. Hence, the facility must be designed to expedite the removal of highly radioactive test objects, and with provisions to minimize hazard or delay in operation from failure of a test object. To insure safety, containment of all radioactive solids, liquids, and gases developed during normal operation and in accidents must be provided.

The pumped loop experiments are of particular importance to the aircraft program and special attention was given in the facility design to reduce the cost, complication, and handling problems associated with these experiments.

Pumped loops can be very costly, and can require much time for development and construction, if their elements must fit into a restricted space, such as a reactor test hole. The shielding plugs for the loops are likewise expensive and introduce complication. An attempt is made in the present design to eliminate the need for shielding plugs and to provide sufficient space near the test area to permit the use of more conventional types of pumps, motors, etc. for loop components.

These objectives are attained in the proposed facility by the following design features: The reactor is provided with only sufficient solid shield for the reactor shutdown period. The remainder of the shielding for the test period is provided by a pool of water that surrounds the solid shield. The water covers and provides shielding also for the pumped loop equipment which resides in the water tank. Because the solid shield is thin, the pumping and other loop equipment can be close coupled to the test unit and the shielding plug is eliminated. During removal of the experiment, a continuous water shielded channel is provided to the storage and hot cell areas so that irradiated experiments can be handled without coffins.

Pumped loop experiments often require that an appreciable length of the loop reside in a region of uniform flux. This is achieved by locating the test holes for pumped loops parallel to the long faces of the reactor and close to these faces.

In a further effort to simplify the handling of experiments, provision is made for easy access from the reactor top to test holes in the fuel element and reflector lattice. This is implemented by location of the control rod actuating mechanism at the bottom of the reactor. Experiments in these test holes can be removed to the storage and hot cell areas through a chute which communicates with the pool system.

For shielding experiments a large test hole is provided which can be filled with graphite to form a thermal neutron column. This hole can also be used for irradiation studies of large pieces of aircraft equipment. A number of small beam holes are provided which permit neutron beams to emerge into a physics test area.

E-102

In an effort to achieve good coordination of the reactor research with programs on the other propulsion systems components, a location for the facility was sought which combined adequate isolation with reasonable distance from Cleveland. By being located close to the Lewis laboratory, the proposed facility would also have the benefit of consultation service of a large staff of specialists in metallurgy, heat transfer, thermodynamics, stress analysis, fluid mechanics, physics, and chemistry, and convenient use of the extensive shop and computing facilities, and purchase and administrative services.

The Plum Brook Ordnance Works which was chosen for the reactor site is a 6500 acre plot fenced in and guarded. The reactor facility is located 3000 feet from the closest border of the site, three miles from Sandusky, a city of 30,000 people, and 50 miles from the Lewis laboratory. Special effort is made in the facility design to provide for containment of radioactive gases, liquids, and solids generated either in normal operation or in accidents. In particular, complete containment of Borax-type explosions was provided.





## SECTION 2. - THE REACTOR FACILITY

The reactor facility is described in section 2.1. The nuclear and engineering characteristics are then described in section 2.2 and finally the control system and the kinetic behavior of the reactor with its control system are described in sections 2.3 and 2.4.

A more detailed discussion of the site, the experiments, the hazards involved with the reactor facility and its experiments, and the administrative organization is contained in the following sections.

### 2.1 GENERAL DESCRIPTION OF FACILITY

This section of the report presents a general description of the proposed NACA Research Reactor Facility. The material presented is intended primarily for orientation purposes. More detailed discussion of the safety and hazard problems associated with some of the important components is contained in subsequent sections of the report.

#### 2.1.1 Location of Facility

Figure 2.1 is a map illustrating the location of the proposed site for the facility relative to Cleveland and Sandusky, Ohio. The facility will be located approximately 50 miles west of Cleveland and 3 miles south-southeast of Sandusky, a city of approximately 30,000 population. The NACA site lies in the north section of the Plum Brook Ordnance Works as illustrated in figure 2.2. It includes an area of approximately 500 acres, and the facility will be located in the south-central section of this area. Figure 2.3 is an enlarged map of the NACA site, and illustrates the location of the reactor and supporting facilities. Figure 2.4 is a plan view showing the relative locations of the various structures included in the facility. Figure 2.5 is a perspective drawing of the facility, and figure 2.6 is an artist's conception of the main building which houses the reactor.

The function of each of the structures shown in figure 2.4 (referred to by the letters on the figure) is as follows:

- A. Main building which houses the reactor.
- B. East wing of the reactor building. It houses pumps, heat exchangers, degasser, and ion-exchanger for the main primary water system.
- C. South wing of the reactor building. It contains the hot laboratory for handling of radioactive equipment, materials, and experiments.

D. West wing of the reactor building. It contains office and laboratory space.

E. A building which houses the ventilating fans for the facility. The exhaust stack is adjacent to the southeast corner of this building.

F. Four hot retention basins for storage of radioactive water from the facility.

G. This building houses electrical control equipment for the primary pump house, B.

H. Overhead storage tank for processed water.

J. Overhead storage tank for deionized water.

K. Cooling tower.

L. A service building which contains softening, filtering, and de-ionizing equipment for raw water. It also houses air compressors, and the diesel-generators for emergency electrical power. The secondary water pumps are located adjacent to the north wall of this building.

M. A substation for incoming electrical power.

N. A concrete retention basin for storage of uncontaminated water.

P. An earthen reservoir for emergency storage of water.

Q. A utility building for general storage purposes.

## 2.1.2 Reactor

The reactor core is essentially a modified version of that of the Materials Testing Reactor now in operation at the National Reactor Testing Station, Arco, Idaho. The active lattice is made up of individual fuel elements of the MTR type. A detailed drawing of a tentative design of one fuel element is shown in figure 2.7. The element consists of assemblies of flat, aluminum clad, plates of an aluminum-enriched uranium alloy and suitable supporting structure. There are 18 plates per element. Sixteen plates are 0.06 inch thick, and the two end plates are at present 0.065 inch thick. Their length is  $24\frac{5}{8}$  inches. The spacing between plates is 0.115 inch. The assembled fuel element, including top and bottom supporting structure, measures 2.995 by 3.145 by  $42\frac{7}{8}$  inches. The fuel elements are cooled by demineralized light water which also serves as a reactor moderator. The reactor core has a primary reflector of beryllium, and a secondary reflector of light water.

E-102

The reactor core is illustrated in figures 2.8(a) and (b). In the initial core loading the fuel elements are arranged in a 3- by 9-element array in a 4 by 11 grid as shown in figure 2.8(a). Positions in the 4 by 11 lattice are identified as follows: There are four columns LA, LB, LC, and LD. In each column are eleven rows. Thus, lattice positions are identified by LA-1, LB-6, etc. Fuel elements, indicated by the letter F, occupy positions LB-2 to LB-10, LD-2 to LD-10, and LC-3, LC-5, LC-7, and LC-9. The grid spaces marked C represent control rod positions, and 10 such positions are indicated. The remaining grid spaces, indicated by the letter R, are occupied by beryllium primary reflector pieces. The 4 by 11 grid is enclosed by a box which extends the full height of the core. The sides are of one inch thick beryllium, and the ends are of aluminum.

CZ-2

On the south side of the 4 by 11 lattice (fig. 2.8(a)) is a 4 by 8 grid of beryllium blocks which surround one of the horizontal test holes (described later) to improve the flux distribution in it. The positions of these blocks are identified by columns RA, RB, RC, and RD, and rows 1 to 8. This grid is enclosed on three sides by aluminum, and on the side adjacent to the 4 by 11 lattice, by beryllium.

Cooling of the reactor is accomplished in two passes. Water flows upward in the secondary region around the 4 by 11 lattice and downward through the fuel elements and primary reflector pieces in the lattice. Water flow in the 4 by 8 reflector grid is upward through cooling holes in the beryllium blocks.

### 2.1.3 Control Rods

There are five control rod positions in the active lattice and five in the beryllium reflector as is indicated by the letter C in figure 2.8(a). Shim-safety rods occupy all five positions in the core, and the three central positions in the reflector. Positions LA-2 and LA-10 in the reflector are occupied by regulating rods, only one of which will be used at a time. All control rods enter the reactor from below. The upper ends of the shim-safety rods contain cadmium. Below the cadmium are fueled sections for the rods in the active lattice and beryllium sections for the rods in the reflector. As poison is removed from the core or reflector, fuel or beryllium is inserted.

The control system is discussed in detail in section 2.3.

### 2.1.4 Reactor Pressure Tank

The reactor is mounted in a vertical, cylindrical, stainless steel clad pressure tank as illustrated in figures 2.9(a), (b), and (c). Figure 2.10 is a cutaway perspective of the reactor and pressure tank. The tank is 9 feet in diameter, and has an over-all height of about 32 feet.

The top of the tank is at approximately grade level. The center of the reactor core is 21 feet below grade. The lower end of the tank is hemispherical in shape, and the upper end is elliptical. The upper end is flanged so that it can be removed. A hatch is also provided to facilitate changing fuel elements and inserting or withdrawing experiments.

Tentatively, three concentric stainless steel clad rings located within the tank, and extending above and below the reactor core, will serve as thermal shields.

The reactor is supported from the lower end of the tank wall by a stainless steel structure which also serves to separate the inlet and outlet cooling water. This structure also supports the entire control rod assembly, and absorbs shock loads resulting from deceleration of the control rods in their respective shock absorbers when the reactor is scrammed. The support is circular at its base and changes to a rectangular shape, the size of the reactor grid, at its upper end.

A drilled plate, extending radially from the lower reactor grid to the inner thermal shield ring, serves to meter and control distribution of water flow outside the lattice.

The cooling, and moderating, water enters the tank at the side, just below the lower level of the reactor. It flows upward through the reflector, and the thermal shield rings, and downward in the aluminum-beryllium box enclosing the 4 by 11 reactor lattice. After passing downward through the reactor supporting structure the water is discharged near the bottom of the tank.

Six horizontally positioned instrumentation tubes enter the pressure tank just below the reactor core (fig. 2.9(a)) and are positioned around the periphery of the tank. Four additional tubes, inclined downward toward the core, are located just above the active lattice. The inner diameters of the lower and upper tubes are  $11\frac{1}{2}$  and  $9\frac{1}{2}$  inches respectively. Four additional tubes, to be used for fission chambers and other instrumentation, enter the tank from near the bottom. They have an inner diameter of four inches, and are inclined slightly from the vertical, terminating just below the reactor core (fig. 2.9(a)).

Fuel elements are removed from the reactor pressure vessel through a discharge chute located just above the reactor core (fig. 2.9(b)).

### 2.1.5 Test Holes

The locations of the various test holes, with respect to the reactor core, are shown in figures 2.8, 2.9, and 2.10.

2.1.5.1 Horizontal through holes. - Two horizontal test holes (designated HT-1 and HT-2) lie parallel to the long horizontal axis of the core. HT-1 is on the south side of the core, and HT-2 is on the north. The walls of these holes are aluminum tubes, or thimbles, both ends of which penetrate the pressure tank wall. For the initial installation both thimbles have an inner diameter of 9 inches and a wall thickness of  $\frac{1}{2}$  inch. The centerlines of HT-1 and HT-2 are 1 inch and  $4\frac{5}{16}$  inches, respectively below the core center. Test hole HT-1 is separated from the active lattice by the 1 inch beryllium wall of the box surrounding the core. HT-2 is further separated by the beryllium reflector pieces.

The 9 inch I.D. aluminum thimbles penetrate the tank wall through  $13\frac{1}{2}$  inch I.D. pipes, or liners, welded to the pressure tank on their inner ends, and provided with flanges on the outer ends. The method of connecting the thimbles and liners outside the pressure tank is shown in figure 2.11(a). A bellows type expansion joint is provided on each thimble to allow for thermal expansion.

As will be described later, it is proposed that experiments will be enclosed in containment tubes for insertion into the test holes. A remotely operable sealing mechanism is therefore provided to seal the clearance space, between the test hole wall and the tube containing the experiment, from water in the shielding pool surrounding the reactor. Connections are provided so that water, at high velocity, can be bypassed from the primary water system, through the annular clearance space, to remove the heat lost from the experiment in the thimble.

The spaces between the 9 inch aluminum thimbles and the 13.5 inch liners are filled by removable steel sleeves. For the initial installation the thimbles are horizontally eccentric with the liners. This arrangement permits test holes up to 12 inches in diameter to be used, if desired, at a later date. With 12 inch test holes the steel sleeves would be eliminated and the test hole thimble and liner would be concentric. The test holes would again lie close to the reactor core. Provision is made for cooling the steel sleeves by bypassing water from the primary system around their inner and outer peripheries.

2.1.5.2 Horizontal beam holes. - There are three horizontal 6 inch I.D. test holes which terminate at the north face of the reactor. These holes, designated HB-1, HB-2, and HB-3 are located above HT-2. Their centerlines lie in a horizontal plane  $6\frac{11}{16}$  inches above the center of the reactor. The thimbles penetrate the pressure tank walls through  $9\frac{1}{2}$  inch I.D. lines in a manner similar to that for the horizontal through holes. Details of a typical beam hole are shown in figure 2.11(b). It is possible to increase these holes to 8 inches I.D., if desired, by removing the

steel sleeves between the aluminum thimbles and the liners. As for the through holes, remotely operable seals will be provided. Provision is again made for cooling inside the aluminum thimbles, and around the steel sleeves, by bypassing water from the primary system.

2.1.5.3 Thermal column. - Provision is made for a thermal column (designated TC) on the same side of the core as HT-1. A 41-inch diameter pipe penetrates the tank wall. The thermal column is inside this pipe and terminates one inch from the beryllium blocks surrounding HT-1. Besides being used as a thermal column this opening can be adapted to shield studies or to irradiation studies of relatively large bodies, such as pieces of electronic equipment. A drawing of the thermal column is shown in figure 2.11(c).

2.1.5.4 Vertical test holes. - Two 8 inch I.D. vertical test holes, designated V-1 and V-2 are provided, one at each end of the core. The walls of these holes are aluminum tubes which penetrate the top cover of the reactor tank and terminate near the bottom of the core. They are closed at the lower end.

A series of 28 holes, each 3 inches in diameter, are also provided in the beryllium blocks (RA through RD) above HT-1.

It is also possible to remove the control rod from position LC-6 in the reactor core, so that this space can be made available as a test hole.

2.1.5.5 Rabbit tubes. - Two pneumatic rabbit tubes, designated RP-1 and RP-2 in figure 2.8, are provided. The carrier tubes are 3/4 inch I.D. and pass the core horizontally and parallel to HT-2. One is located below HT-2 and the other just above the horizontal beam holes. These are through tubes and penetrate the pressure tank wall on both ends.

There are also four hydraulic rabbit tubes designated RH-1, RH-2, RH-3, and RH-4. These have a carrier tube inside diameter of 3/4 inch and terminate in the beryllium blocks surrounding HT-1. They are located in positions RA-1, RD-1, RA-8, and RD-5.

## 2.1.6 Biological Shield

The reactor pressure tank is surrounded by barytes concrete to provide part of the biological shield (fig. 2.9). The concrete below the pressure tank will be cooled by water flowing in pipes embedded in the concrete. The remainder of the shield is provided by water contained in a circular pool surrounding the pressure tank as shown in figure 2.12(a). This pool is approximately 70 feet in diameter, and its vertical center-line is offset 5 feet from that of the pressure tank. The walls of the pool are made of reinforced concrete and are three feet thick. The pool

E-102

is divided into four quadrants (designated A, B, C, and D in fig. 2.12) by water tight partitions (quadrant walls). The concrete surrounding the pressure tank has a minimum thickness of two feet in quadrants A, C, and D. In quadrant B, which contains the thermal column, the concrete is thickened to 9 feet (minimum) to provide adequate shielding without water in the quadrant. The water in quadrants A, C, and D is 25 feet deep. In quadrant B it is 27 feet deep. This additional depth increases the distance from the centerline of the thermal column to the pool floor and provides a better geometry for shield testing (fig. 2.13(b)).

A concrete platform, cantilevered in quadrants A, C, and D, surrounds the pressure tank near the top, at approximately grade level, to provide work space for changing fuel elements, and for handling the various types of experiments that can be done from above the reactor.

The shielding pool is enclosed in a 100 foot diameter cylindrical steel containment tank (discussed later). Surrounding the pool, and inside the containment tank, is an annular space 13 feet wide and 25 feet deep. Part of the annulus is occupied by a canal (discussed later), and the remainder is provided with concrete floors at grade level, and at pool floor level, 25 feet below grade.

Three movable bridges are provided to permit access, from the annular space around the pool, to the concrete platform above the reactor tank.

Quadrant D is covered by a removable steel grating.

#### 2.1.7 Shrapnel Shield

Resting on the massive concrete shield above the reactor pressure tank is a heavy steel cover (figs. 2.9(a) and 2.9(b)). This serves both as a gamma shield, and as a shrapnel shield for protection against damage to the containment tank (discussed later) in the event of an explosion such as might result from a violent power excursion. This shield weighs about 60 tons. In the event of a power excursion violent enough to rupture the reactor pressure tank, the energy associated with the upward directed momentum due to the explosion and resultant flying debris would be absorbed by lifting of the shrapnel shield. This will be discussed in more detail in section 6.4.

#### 2.1.8 Containment Tank

The shielding pool and annular space surrounding it, including work space and canal, are housed by a cylindrical steel tank with an elliptical roof as shown in figures 2.12 and 2.13. In the event of an accident, with

release of radioactivity from the reactor or experiments, this tank is designed to prevent its escape to the atmosphere. This tank has an inner diameter of 100 feet and its wall height above grade is approximately 30 feet. The tank wall extends downward to the pool floor level, 25 feet below grade, and then continues on as the containment tank bottom, passing underneath the entire structure including the subpile room. There is no excavation under the pool floor level except for the subpile room located directly under the reactor tank (see fig. 2.13), and a passageway leading to this room from an elevator and stairway shaft located in the annular space outside quadrant A of the shield pool. The subpile room contains the control rod drive equipment.

The contained volume includes that within the 100 foot diameter tank above grade and extending downward to the pool floor level. It also includes the subpile room, passageway, and elevator and stairway shaft.

The containment tank can be entered, at grade level, by means of three openings. One is a 10- by 10-foot truck opening with a pressure tight door located in the wall adjacent to quadrant D. This opening will be sealed shut when the reactor is in operation. The other two openings are air locks for use of personnel. These are located in the wall adjacent to quadrants A and C, and can be used with the reactor in operation.

There is one additional opening in the containment tank wall. This is located under water in the wall nearest quadrant B. It permits equipment and experiments to be moved under water from the circular portion of the canal within the containment tank to that part which is outside the tank. This opening is sealed by a watertight door, so designed that an increase in pressure within the containment tank will augment the seal. This door also permits the portion of the canal inside the tank to be drained independently of that outside.

Two stairways within the annulus permits access from grade level to the lower level 25 feet below grade. The elevator to the subpile room also permits access to this floor.

A 20 ton crane serves the entire floor area of the containment tank at grade level. A hatch is provided to permit the crane to serve the lower level of the annular work space around the pool.

#### 2.1.9 Canal

The canal is provided for underwater transportation of radioactive materials, equipment, experiments, and fuel elements from the reactor to storage, or to the hot laboratory. As shown in figure 2.12(a), the portion of the canal inside the containment tank extends completely around the outer wall of quadrant B, and partially around quadrants A and C.



It is 13 feet wide and 25 feet deep. Walkways are provided on both sides. Direct access from the shielding pool to the canal is provided from quadrants A and C. Access is by means of underwater doors, designed to be water tight.

E-102

During operation of the reactor it is proposed that the portion of the canal within the containment tank will be drained. Its volume, together with that of the rest of the annular space surrounding the pool, will act as an expansion volume, and will aid in absorbing the energy released in the event of a power excursion severe enough to rupture the reactor pressure tank. The annular portion of the canal, within the containment tank, connects with the outside portion through the underwater opening in the containment tank wall that has been previously mentioned. This opening is on the south side of the containment tank, adjacent to pool quadrant B. The external portion of the canal extends south, and passes through the reactor building surrounding the containment tank, into the hot laboratory. Within the main reactor building, and extending east, is another extension of the canal. This extension provides storage space for fuel elements, and at its closed end space is available for reactivity measurements. Two watertight movable gates are provided in this section of the canal to permit local draining.

A traveling bridge, and a 5-ton monorail hoist, are provided for this section of the canal.

#### 2.1.10 Main Reactor Building

Surrounding the containment tank is a flat roofed, mill type, building measuring approximately 150 by 160 feet (see figs. 2.12 and 2.13). Its height is  $29\frac{1}{2}$  feet. It provides setup and work space around the containment tank at grade level. It also houses shop and personnel facilities, and control panels for experiments. The reactor control room, and offices, are located on a mezzanine extending along the north and west walls (fig. 2.12(a)).

The north half of this building has a basement with its floor 15 feet below grade. The southwest corner has a basement with its floor level 25 feet below grade. These basement areas are connected by a stairway. The lower basement also connects, by a passage paralleling the north-south canal extension, with a vertical shaft which opens into the hot laboratory. Two hot cells will be located in the southwest corner of the 25-foot basement.

#### 2.1.11 Method of Handling Loop Type Experiments

In general, it is proposed to design experiments that are compact enough to be enclosed in water tight boxes with the test section itself

mounted in a closed tube extending from the box. The entire assembly will be taken into the containment tank at grade level, lowered into the shielding pool, and inserted into the proper test hole. The pool water will provide shielding for the experiment. Integral experiments of this type, utilizing either of the horizontal through holes, will occupy either pool quadrant A or C. Inasmuch as both of these quadrants connect with the canal, radioactive experiments from the reactor can be moved under water from the pool, through the canal, to the hot laboratory for dismantling.

For experiments requiring equipment that is too large to be placed in the pool, or that cannot be placed under water, the annular basement area around the pool can be used.

Typical loop type experiments are discussed in more detail in section 4.

#### 2.1.12 Water System

A schematic diagram of the water system for the facility is shown in figure 2.14. Temperatures, pressures, and flow rates at various points in the system are given in table 2.1. Figure 2.15 is a more detailed diagram of the water system showing all valves and connections to the various services. Table 2.2 lists locations, mode of operation, and control point location for all valves in the system. Figure 2.16 is a schematic drawing of the water system shown on a plan view of the facility.

TABLE 2.1 - WATER SYSTEM OPERATING CONDITIONS

Primary water system	
Power output, Mw	60
Total water flow, GPM	17,300
Reactor tank inlet press., psia	160
Reactor tank inlet temp., °F	159
Reactor tank outlet press., psia	120
Reactor tank outlet temp., °F	187
Reactor core press. drop, psi	30
Heat exchanger inlet press., psia	99
Heat exchanger press. drop, psi	10
Pump inlet press., psia	89
Pump power, each, HP	550
Pump outlet press., psia	159
Fuel plate temp., °F (max.)	315
Saturation temp. at outlet press., °F	341
Saturation temp. at critical spot, °F	350

TABLE 2.1 - Concluded. WATER SYSTEM OPERATING CONDITIONS

Secondary water system	
Cooling water flow, GPM	9850
Pump power, HP	200
Cooling water temp. from tower, °F	85
Cooling water press., psia	63
Cooling water temp. to tower, °F	130
Heat exchanger press. drop, psi	20
Water evaporation, GPM	460

2.1.12.1 Primary cooling system. - The main primary cooling system is shown in figure 2.14. Deionized water enters the pressure tank from the side at a point just below the reactor core. It flows upward outside the 4 by 11 lattice, reverses its direction above the reactor, and flows downward through the lattice. The water leaves the pressure tank at the bottom and goes to the main heat exchangers. From the heat exchangers it flows through the primary water pumps and is returned to the reactor tank. A venturi meter, and a strainer, are located in the main water line between the pump discharge and the reactor tank. There are two main heat exchangers operating in parallel (with provision for a third to be added later), and three primary pumps, also in parallel. Only two pumps are in operation at one time, with the third serving as a standby. Each primary pump has a capacity of 8650 gpm with a pressure rise of 70 psi. The water pressure in the primary system is normally set by the head of water in a 5000 gallon tank located 150 feet above grade and feeding into the system at the primary pump inlet. The pressure at this point is approximately 89 psia. At the same level as the 5000 gallon tank, is a 50,000 gallon tank, also filled with deionized water. Normally, only the smaller tank is open to the primary system. However, a line from the bottom of the larger tank connects with the primary system so that its capacity can be made available to the primary system by opening a valve. The use of the small tank for normal operation results in a more sensitive indication of variations in required makeup water for the primary system.

A mixed resin bed ion-exchanger is connected between the primary pump inlet and discharge. Approximately 100 gpm are bypassed continually through the ion-exchanger. The flow is regulated by a valve and metered by a venturi. A heat exchanger is provided to cool the water entering the ion-exchanger to a temperature the resin can withstand.

The method that will be used for degassing the primary water has not yet been decided upon. One possible method of degassing is indicated in figure 2.14. The degasser is located between the reactor tank outlet and the main heat exchanger inlet. Part of the primary water is bypassed through the degasser in which the pressure is reduced by a throttle valve. Degassed water is pumped back into the primary system, and off-gases and water vapor are pumped to the exhaust stack. Two pumps are indicated, only one of which would be in operation at a time.

The main primary pumps, ion-exchanger, degasser, and main heat exchangers are located in the east wing of the main reactor building (marked "B" in fig. 2.4). A tentative layout of the wing is shown in figure 2.17. The heat exchangers and degasser are in one room of the wing, while each of the pumps and the ion-exchanger are located in separate rooms. The concrete walls of the pump and ion-exchanger rooms are thick enough to provide sufficient shielding so that any one of them can be serviced while the others are in operation.

A shutdown cooling system is also provided which has sufficient capacity to cool the reactor a few seconds after shutdown. Cooling immediately after shutdown is taken care of by coast down of the main pumps. This system is shown schematically in figure 2.14, and its arrangement in quadrant D of the shielding pool, where it is located, is shown in figure 2.18.

Referring to figure 2.14, water from the shutdown system enters the pressure tank at a point just below the reactor core, passes upward outside the lattice, down through the lattice and then to a heat exchanger. From the heat exchanger the water is pumped back to the reactor tank. The flow rate is metered by a venturi.

Two pumps, of 1100 gpm capacity each, are provided for the shutdown primary water system. Only one will be in operation at a time. The drive motors for these pumps are powered by either of two diesel-generator sets. One diesel-generator with its pump is continually in operation, even when the main water system is in operation. The pump motors for this system can also be driven from the regular electrical supply.

The main and shutdown heat exchangers are of the shell and tube type with primary water flowing through the tubes. The primary heat exchangers, pumps, ion-exchangers, degasser and piping are made of 300 series stainless steel, either solid or clad. Some valves may be of cast iron.

2.1.12.2 Secondary water system. - The secondary water system removes heat generated in the reactor from the primary water in the main and shutdown heat exchangers and dissipates it in the cooling tower. Water from the cooling tower basin is pumped through the heat exchangers and returned to the tower.

There are three secondary pumps for the main cooling system, each having a capacity of 4925 gpm and a pressure rise of 48 psi. Only two pumps are normally in operation, with the third serving as a standby.

There are also two secondary pumps, each having a capacity of 800 gpm, for the shutdown cooling system. Only one of these is normally in operation. For the shutdown system, one primary and one secondary pump are driven by a diesel-generator set. As stated previously, there are two such diesels, one continuously in operation.

TABLE 2.2 - WATER SYSTEM VALVES AND CONTROL LOCATION

[See figs. 2.14, 2.15, and 2.16.]

[illegible]



Two additional pumps are provided in the secondary water system to supply water for general service use.

2.1.12.3 Water supply system. - Raw water from Lake Erie is normally drawn from a 5,500,000 gallon reservoir which is now in existence at the site. In an emergency, water can also be obtained from a fire protection system, or from city water mains, both of which are available. Also, a 100,000 gallon tank located 100 feet above grade and floating on the processed water line, will be provided for further emergency protection.

For normal operation water is pumped from the reservoir through a clarifier. A portion of the clarified water is used to supply the secondary cooling system, and the balance is passed through gravity type sand filters. Filtered water is supplied to the processed water system, and to the deionizers which further purify the water for the primary system. Dual deionizers, pumps, and filters of 100 gpm capacity each are provided to condition the primary water. Both of these deionizers can operate concurrently with staggered regeneration periods to provide a continuous supply of deionized water to the primary system.

The shielding pool and canal are supplied with processed water. Although not shown in figure 2.14, approximately 500 gpm of the canal and shield water will be continuously circulated through a filter with 100 gpm also passing through a mixed bed deionizer to maintain purity and clarity in the pool and canal. The clarifier, filters, and deionizers which prepare raw water for the primary system, are located in the service building labeled "L" in figure 2.4. The secondary pumps are located just outside the north wall of this building. A tentative layout of this building is shown in figure 2.19.

2.1.12.4 Water disposal. - Retention basins are provided (fig. 2.14) for holdup of water from the facility. A 1,000,000 gallon "cold" basin is available for water of little or no activity such as might normally come from the canal or shielding pool in the event that they need to be drained. There are also four "hot" basins, of 125,000 gallons capacity each, for water that is more radioactive, such as that from the reactor pressure tank, hot laboratory, or primary pump house. An earthen reservoir is provided for emergency storage of water from the facility. This reservoir is labeled P in figure 2.4.

Water in the "cold" retention basin can be either drained into Plum Brook, or pumped back into the raw water system. Provision is also made for filtering and deionizing water from the "cold" retention basin so that it can be reused in the canal or shielding pool.

Water from the reactor tank, leakage from pump seals, and drainage from the hot laboratory flows into sump tanks located under the reactor building. From the sump tanks this water can be pumped to any one of the

four "hot" retention basins. Provision is made for pumping water from any "hot" basin through an ion-exchanger and back to another. By recirculation of water one or more times through an ion-exchanger, together with proper dilution, its activity can be reduced to the point where it can be reused or drained into Plum Brook.

#### 2.1.13 Hot Laboratory

The layout of the laboratory for handling radioactive experiments, equipment, etc., coming from the reactor is shown in figure 2.20. This laboratory is housed in the south wing of the reactor building. Nearest the reactor building are the facilities for handling, storage, and dismantling, of large pieces of equipment, or experiments, that are highly radioactive. This part of the hot laboratory is of heavy concrete construction. It contains part of the north-south extension of the canal, a vault for dry storage of radioactive materials, a hot handling room, a room for dismantling and cutting up of large experiments and one of the hot cells. The canal extension serves to convey experiments from the shielding pool and as a storage area. A removable water tight gate is provided at the entrance to the hot laboratory to permit local drainage.

The dry storage vault is available for equipment or materials which cannot be stored under water. The floor level of the vault is 15 feet below grade, and it has a cover of removable concrete slabs located approximately 14 feet above grade. A shielding window is provided in the north wall of the vault.

The hot handling room has a vertical shaft connecting with the passageway from the basement area of the main building. This provides a means of conveying equipment from the reactor building basement to the hot laboratory. A shielding door at the south end of the hot handling room permits access to the rest of the hot laboratory.

A shielded room for dismantling radioactive experiments and equipment, and a hot cell (no. 1) are adjacent to the west side of the hot handling room. Movable shielding plugs, mounted on rails, permit access from the hot handling room to the dismantling room and hot cell. The ceilings of these rooms are removable concrete slabs.

A General Mills manipulator serves both the dismantling room and the hot cell. A vertically movable wall permits movement of the manipulator between the dismantling room and the hot cell. Shielding windows are located in the west walls of these rooms and manipulator controls are operated from outside these walls.

A 15-ton remotely-controlled crane and a 5-ton auxiliary hoist service the dry storage vault, canal, hot handling room, dismantling room and hot cell.



Adjacent to the south wall of the concrete portion of the hot laboratory is a mill type building housing a semicontaminated work area, decontamination room, and rooms for storage and repair of equipment or materials that are only mildly radioactive. The canal extension terminates in this area. Also, included in this area are seven additional hot cells of heavy concrete construction. Entrance to these cells is from the semicontaminated work area through movable shielding plugs. Shielding windows are provided in the west walls. A General Mills Manipulator, and a crane mounted on the same rails, serve all seven cells. Vertically movable walls between cells permit movement of the manipulator or crane between cells. The ceilings of all cells are made of removable concrete slabs.

A truck entrance is located in the east wall of the laboratory, and an overhead monorail type hoist serves the truck entrance and the end of the canal extension. A crane serves this area of the laboratory.

At the south end of the hot laboratory wing is a personnel decontamination area including showers, toilet facilities, and locker rooms. Entrance to and from the laboratory areas, where contaminated materials are handled, is through the decontamination area.

A clean shop area, housed in a mill type structure, extends along the west wall of the hot laboratory wing. This shop is for work on uncontaminated equipment. Access to and from the personnel decontamination area is through this clean shop area.

#### 2.1.14 Ventilating System

Figure 2.21 is a schematic diagram of the ventilation system for the facility.

2.1.14.1 Containment tank. - Air is drawn into the containment tank through a filter at the rate of 200 cfm. Air leaving the containment tank is pumped by a reciprocating type compressor into one of three tanks. The capacity of each tank represents 2.5 minutes supply of ventilating air. When one tank is filled the compressor discharge is automatically switched to another tank. The air in the tank last filled is monitored for radioactivity. If found to be uncontaminated, the air is discharged to the exhaust stack. If the air is found to be radioactive, it is not released. The two additional tanks give five minutes time in which to stop the flow of air without releasing it to the exhaust stack.

Dehumidifying and air conditioning systems and air circulating fans will be provided in the containment tank.

2.1.14.2 Main building. - Ventilating air for the main building surrounding the containment tank, and for the hot laboratory, is drawn in

through filters in the roof of the building. One fan of 10,000 cfm capacity pumps air from the building above grade level. Another 10,000 cfm fan draws air from the basement area and, after monitoring, discharges it to the exhaust stack. The balance of the air required to ventilate the main building is drawn into the hot laboratory as described below.

2.1.14.3 Hot laboratory. - Ventilating air for the hot laboratory is drawn partly from the main reactor building and partly from the clean shop area along the west side of the hot laboratory. It passes through the personnel decontamination area into the contaminated work area and hot handling room. From these areas the air is drawn out of the dismantling room and the hot cells, and after being filtered and monitored, is discharged to the exhaust stack.

Three ventilating fans of 10,000 cfm capacity each are provided for the hot laboratory. One fan serves the dismantling room and hot cell number 1. Normally one of the other fans serves hot cells (nos. 2 to 8). If, however, one or more of the shielding plugs in the hot cells is removed, more air is required to maintain the desired air velocity in the cells, and the third fan goes into operation. All three fans are interconnected so that any one can perform any other function.

Figure 2.21 also shows a typical hot cell ventilation system. In addition to the exhaust vent, a vacuum hose is provided for use in clean-up of the cells. Individual filters are provided, within the cell, for the exhaust vent and the vacuum hose. Servicing of the filters can be done remotely by use of the manipulators.

#### 2.1.15 Electrical System

Diagrams showing components of the electrical power system are contained in figures 2.22(a) and (b). Primary electrical power will be furnished by the Ohio Edison Company by means of two 34,500 volt lines. These lines will be connected to two existing 34,500 volt lines energized from separate substations at Sandusky. Each 34,500 volt line will be connected to a 34,500/4160 volt step-down transformer located at a substation on the site (M, fig. 2.4). Each 34,500 volt line and transformer will have sufficient capacity to carry the entire electrical load of the facility.

The portion of the 4160 volt distribution system located at the site substation will consist of two separated buses and associated circuit breakers. A tie bus and breaker will be provided to connect the two 4160 volt buses together. Pending approval of the Ohio Edison Company, it is proposed to operate normally with the 4160 volt systems tied together.

From the substation 4160 volt feeder cables will be extended to motor starting and circuit-breaker switchgear located throughout the site.

480-Volt electrical power, supplied by 4160/480 volt step-down transformers, will be distributed to motors and 480-volt circuit breaker panelboards from motor control centers in various buildings at the site.

Operational voltages for motors and equipment will be as follows:

Motors, 200 hp and over	4160 volt - 3 phase
Motors, 3/4 hp to 200 hp	480 volt - 3 phase
Lighting and small power	120/208 volt - single phase

Power for operation of pumps for the shut-down cooling system will be provided by diesel-driven generators at 480 volts. Duplicate diesel generator sets will be provided; each unit being capable of starting and operating the required shut-down pumps.

Duplicate 480-volt feeders will be installed to feed the switchgear containing the starting equipment for the primary and secondary pumps of the shut-down cooling system. In addition to the two 480-volt services from the diesel-generators, a feeder from each of two normal 480-volt supplies will be tied to each set of pump motor switchgear.

Reactor control and instrument power will be supplied by means of two conversion units and a bank of batteries (not shown in fig. 2.22). The first conversion unit will convert A.C. power to D.C. power. The D.C. power will then be used to energize the D.C. motor of a second conversion unit, which motor drives an A.C. generator. The output of this generator will supply A.C. control and instrument needs. The battery system will be connected to the D.C. bus between the first and second conversion units. In normal operation the batteries will float on the line. In case of failure of the normal A.C. power, required to energize the first conversion unit, the batteries will supply power to the second conversion unit to maintain the A.C. control and instrument requirements. Duplicate conversion and battery equipment will be installed for reactor control, instrumentation, and all other systems requiring a guaranteed power supply.

All telephone, operational and emergency intercommunication, fire protection (alarms, etc.) and evacuation (alarms, etc.) systems will be supplied with power from batteries.

The emergency lighting system will be maintained at a level sufficient for periods of loss of normal lighting, and evacuation needs. Power for the emergency lighting system will be supplied by a diesel-generator emergency power system through step-down transformers. Transfer switches will be provided so that lighting power will normally come from the regular power supply.

Electrical power for experiments will normally be drawn from the regular laboratory supply. For emergency power a diesel generator will be provided.

E-102

CZ-4

## 2.2 REACTOR PHYSICS

An important class of experiments to be performed in the NACA reactor is the operation of representative subcritical sections of prototype aircraft reactor cores. Fuel elements, coolant, moderator, and supporting structure composing these representative sections are to be exposed to the neutron fluxes in and around the critical research reactor. The heat generation rate, temperature distribution and fuel burn-up expected in the prototype are to be simulated. Appropriate conditions in the experiment may be maintained by operation of the reactor at various powers up to the maximum design power of 30 megawatts.

One of the cores experimentally studied in detail at MTR was a 9 by 3 array of fuel elements containing 168 gms of enriched uranium and shim-rod fuel elements containing 130 gms of enriched uranium. Inasmuch as the indicated excess reactivity of this loading corresponds to the requirements of the NACA operating cycle, this initial loading for the NACA reactor was selected for analytical study of normal operational behavior and possible hazards. Reactor design conditions, operating cycle, excess reactivity requirements, neutron flux and specific power distributions for this reference core are presented in this section.

### 2.2.1 Reactor Design Conditions

A brief listing of nominal reactor design conditions and of reactor nuclear properties for the loading under consideration, is presented in table 2.3. A discussion of reactor heat transfer is presented in appendix A. A discussion of reactor physics is presented in appendix B.

It is proposed to operate the reactor at approximately constant average power per unit volume as dictated by the desired conditions in a major experiment up to an average over the core volume of 600 watts per cubic centimeter of core. The gross power generated is a function of shim rod position, so that the maximum design power can only be realized toward the end of the operating period when the rods are effectively withdrawn.

TABLE 2.3 - NACA RESEARCH REACTOR DESIGN CONDITIONS

Reactor power	60 megawatts
Coolant flow	Two pass - 15,000 gal/min; 30 ft/sec in core
Core inlet coolant, top	160° F, 150 psia
Core outlet coolant, bottom	187° F, 120 psia
Maximum fuel plate surface temperature	315° F
Saturation temperature at location of maximum fuel surface temperature	350° F
Average core heat flux	490,000 Btu/hr-ft <sup>2</sup>
Maximum heat flux	880,000 Btu/hr-ft <sup>2</sup>
Uranium loading (9×3 slab)	4.4 kilograms (22 - 168 gm fuel elements 5 - 130 gm shim rod elements)
K <sub>eff</sub> (cold, clean)	1.185
Average power density	600 watts/cc
Maximum power density	1100 watts/cc
Average core thermal flux	4×10 <sup>14</sup> neutrons/cm <sup>2</sup> sec
Average core integrated fast flux	17×10 <sup>14</sup> neutrons/cm <sup>2</sup> sec
Average core uncollided flux	2×10 <sup>14</sup> neutrons/cm <sup>2</sup> sec
Percent fissions by thermal neutrons	88
Mean prompt neutron lifetime	90×10 <sup>-6</sup> sec
Temperature coefficient of reactivity	-18×10 <sup>-5</sup> ΔK/K °C; -10×10 <sup>-5</sup> ΔK/K °F
Void coefficient of reactivity	-0.18 ΔK/K/ΔV/V <sub>H<sub>2</sub>O</sub>

## 2.2.2 Reactor Operating Cycle

A continuous operating time of 10 days has been selected as being representative of irradiation times required to simulate aircraft reactor core component fuel burnup. It is expected, however, that the reactor will be operated to meet requirements of major experiments. A 10-day operating cycle may be achieved with a core loading of fresh fuel elements and shim-rod fuel elements which provide sufficient excess reactivity for experiments, reactor operation, and transient xenon override. For reasons of operating economy and minimizing fuel inventory, reactor core loadings for subsequent operating cycles would consist of fresh fuel elements of greater uranium content replacing some of the partially spent elements of the previous loadings. Addition of these fresh fuel elements and relocation of partially spent elements would provide core loadings of the required excess reactivity for a new set of experiments.

As described in reference 2.1, it has been the experience of MTR that larger average fuel burn-ups may be achieved by moving partially spent elements from the corner regions to the center of the slab. New fuel elements with uranium content of about 200 grams inserted in the corner regions maintain acceptable heat generation rates as well as reduce the peak-to-average specific power ratio over the core volume. Prior to startup of each new loading, criticality experiments, control rod calibrations, and instrument calibrations will be performed until reactivity effects of refueling are sufficiently well understood to forego repeated calibrations.

Of course, the startup of the first cold, clean loading must also be carefully executed. A startup procedure manual will be written.

An alternate method of controlling the required excess reactivity is through the use of a burnable poison such as boron uniformly dispersed in the uranium-aluminum alloy of the fuel elements. There are several possible advantages to the use of such fuel elements. These are discussed in appendix B where the results of preliminary burnup studies of burnable poisons applied to the research reactor are presented. Additional studies, using burnable poisons, will be made. The technology of fuel element fabrication containing burnable poisons as evolved at Oak Ridge National Laboratory is being followed. Pending the outcome of these studies, burnable poisons may ultimately be used. Burnable poisons, however, will not be employed in fuel elements for initial loadings of the NACA research reactor. Therefore, for purposes of analyzing the normal operational behavior of the proposed NACA research reactor, and for evaluation of possible hazards, the initial core loading of fresh fuel elements and fresh shim-rod elements has been studied in detail and is presented herein.

### 2.2.3 Excess Reactivity Requirements

The estimated allocation of excess reactivity for an initial loading of 168 gm fuel elements and 130 gm shim-rod elements is listed in table 2.4. The value of  $K_{eff}$  for this cold, clean loading was calculated to be 1.185. A  $\Delta K$  of 0.123 is required to operate the core for a period of 10 days leaving an excess reactivity of 0.062 available for experiments and transient xenon override at the end of core life. Correspondingly larger  $\Delta K$  is available during the operating cycle for overriding transient xenon. Table 2.4 indicates that for a  $\Delta K$  in experiments of 0.05, the transient xenon override potential during the cycle decreases from a  $\Delta K$  of 0.124 at startup to a  $\Delta K$  of 0.012 at 10 days. The reactivity requirements of restart after scram during the operating cycle are covered in the reactor kinetics discussion in section 2.4. The reactivity requirements of representative experiments located in the horizontal through hole and in the center test hole are covered in section 4.2. The results were obtained by solving two-group diffusion equations on a two-dimensional reactor simulator.

TABLE 2.4 - EXCESS REACTIVITY REQUIREMENTS FOR NACA RESEARCH REACTOR  
(9 by 3 Array; 4.4 Kgm  $U^{235}$ ; 600 watt/cc core;  $K_{eff} = 1.185$  cold, clean)

Reactivity $\Delta K$	Operating time (Days)					
	0	2	4	6	8	10
Temperature effects	0.011	0.011	0.011	0.011	0.011	0.011
Xenon buildup	0	.046	.045	.044	.043	.042
Samarium buildup	0	.003	.006	.007	.008	.008
LCSFPP *	0	.003	.006	.008	.010	.012
Fuel burn-out	<u>0</u>	<u>.010</u>	<u>.020</u>	<u>.030</u>	<u>.040</u>	<u>.050</u>
Total allocated	0.011	0.073	0.088	0.100	0.112	0.123
Available for experiments and transient xenon override	0.174	0.112	0.097	0.085	0.073	0.062
Transient xenon override if $\Delta K$ of experiments is 0.05	0.124	0.062	0.047	0.035	0.023	0.012

\*Low cross section fission product poisons.

The data of table 2.4 indicate how the potential excess reactivity of the core loading would be employed during an operating cycle, assuming operation of the entire reactor core at a uniform specific power of 600 watts/cc. The fuel burn-up picture deviates from this assumption because of two things:

1. A nonuniform specific power distribution, and hence, a nonuniform fuel burn-up is actually present. Since the larger burn-ups occur in regions of relatively high statistical weight, the calculated reactivity effects of fuel burn-up may be underestimated for this reason.

2. The critical assembly during the early part of core life is effectively smaller by the insertion depth of the shim rods. Gradual withdrawal of shim rods introduces an additional nonuniformity to the fuel burn-out. In addition, the actual average burn-up of fuel is less than that considered in arriving at the data of table 2.4 because of the changing effective volume of the core. The calculation for operation at a constant average specific power of 600 watts/cc for the entire core volume has overestimated the reactivity effects due to burn-out.

calculate reactivity effects of experiments in this through hole on the basis of two-dimensional considerations, the upper half of a vertical section of the reactor was selected. The two-dimensional simulator geometry is shown in figure 2.24 in which the core, beryllium-water primary reflector, water secondary reflector, and aluminum-water top reflector regions are indicated. The 9-inch diameter experimental space is shown in position as a square area. (Calculated results for experiments in this space are presented in section 4.2.) The dotted areas shown indicate the fineness of the grid used in solving the diffusion equations on the space simulator; 3-inch square areas were used in the outer regions; 1.5-inch square areas were used in the regions around the experimental space; and 0.75-inch square areas were used in the experimental regions. In all, 252 space points are used.

In order to calculate reactivity effects of shim-rods and experiments in the center test hole, one-quarter of a horizontal section of the reactor was selected. The two-dimensional simulator geometry is shown in figure 2.25 in which the core, primary and secondary reflectors, shim-rod positions, and center test hole locations are shown. The fineness of the grid is indicated; in all, 166 space points are used.

The thermal flux and integrated fast flux distributions for the upper half of the vertical section of the unperturbed reference core, that is with primary reflector in the horizontal through hole HT-1 space, are shown in figures 2.26(a) and (b). The fluxes are shown relative to a spatial average thermal neutron flux of unity. The characteristic peaking of thermal flux in the reflector and fall-off toward the corners of the slab may be noted. There is an asymmetry due to the thicker primary reflector on one face of the core.

The thermal and fast flux distributions in the one-quarter horizontal section are shown in figures 2.27(a) and (b) for the unperturbed reference core. In this case the shim-rods are fully withdrawn and replaced by fuel-elements, and a fuel-element occupies the center test hole space. The fluxes are shown relative to a spatial average thermal neutron flux of unity. The relative closeness of the flux contours at the core-reflector interface indicate the sharp flux gradients present here.

With an average specific power of 600 watts/cc of core, the average core thermal flux is  $4 \times 10^{14}$  neutrons/cm<sup>2</sup> second. The maximum thermal flux occurs in a small part of the thick primary reflector and has an unperturbed value of  $10^{15}$  neutrons/cm<sup>2</sup> second. The maximum fast flux occurs in the central fuel element of the lattice at the reactor midplane and has an unperturbed value of  $2.2 \times 10^{15}$  neutrons/cm<sup>2</sup> second.

The two-dimensional two-group neutron flux distributions for the case with all five core shim rods fully inserted are shown in figure 2.28(a) and (b). The shim rods, being water filled cadmium boxes, effectively appear as water diffusing media for the fast flux and as a



black boundary for the thermal flux. The thermal flux is taken as zero at the extrapolated thermal diffusion distance within the walls of the shim rod.

### 2.2.5 Specific Power Distributions

From the flux distributions shown, the specific power variation in the reference slab core may be calculated. Because epithermal fissions, lumped into the fast group, are considered in the two-group formulation employed, the thermal flux distribution does not exactly correspond to the specific power distribution. There is a contribution to the specific power due to epithermal fissions of about 15 percent at the center of the core diminishing to about 10 percent at the core-reflector interfaces. The variations of the specific power along the axes of the unperturbed reference core are presented in figure 2.29. The specific power is shown relative to the average in the core and permits the location of the hot spot at the interface of the core and the thick primary reflector which is shown. The peak-to-average specific power has a value of 1.83; the minimum-to-average specific power has a value of 0.46.

E-102

C-70

## 2.3 DESCRIPTION OF CONTROL SYSTEM

The reactor control and safety-system design and associated instrumentation incorporate many of the desirable features of the system at the Materials Testing Reactor. The margins of safety used are, in general, comparable to the practice at the Materials Testing Reactor in that the design incorporates the following basic features:

1. Maximum use of fail-safe circuitry and of amplifier and instrument circuit-monitoring.
2. Duplication of safety channels of instrumentation.
3. Use of permissive interlocks that exercise certain required supervisory control on operator action.
4. Use of various modes of reversible power cutbacks as corrective measures together with an alarm system to warn operator of any abnormal conditions arising in the reactor system which may lead to a hazardous condition.
5. The fast scram initiated electronically by the safety system upon instrumental detection of a seriously abnormal situation which poses an immediate threat to personnel safety or reactor integrity.

The shim-safety-rod drive and release mechanism design herein described will be subjected to extensive developmental testing. Hence, the design is not to be construed as the final one but rather as the starting point in the development of a design in every way satisfactory from the standpoint of performance and reliability. Table 2.5 gives the basic requirements used in arriving at the given design as the starting point for further development.

TABLE 2.5 - GROUND RULES FOR CONTROL ROD DESIGN

1. Rod motion approximately thirty inches
2. Six inch span between center of rod activators
3. Replaceable poison and fuel element as short as possible
4. Complete disassembly of actuating mechanism with minimum loss of reactor water
5. No twist to be imposed on the control rod
6. Double water seal packing - fresh water pumped between glands

7. Electrical latch to be out of water
8. Prefer scram above packing gland
9. Cannot rely on pressure difference across lattice to help scram rods
10. Ability to release for scram when driving rods in either direction
11. Positive insertion after scram

### 2.3.1 Control-Rod Types and Locations

For the narrow slab fuel-loading (9 fuel-elements long by 3 wide) shown in figure 2.8, the excess reactivity for the cold-clean condition, assuming none taken up or contributed by experiments, has been estimated as 18.5 percent. Eight shim-safety rods are provided to counter this excess reactivity and keep the reactor subcritical by a wide margin ( $K_{eff} \leq 0.85$  with all rods fully inserted, i.e., in maximum absorptive position) at all times. The shim-safety rods serve the dual purpose of providing coarse adjustments of reactivity and nuclear-safety control. The rods are constructed so that dropping a rod introduces cadmium into the active lattice. Five of the rods are in the middle of the fuel slab (positions LC-2, LC-4, LC-6, LC-8, and LC-10 in fig. 2.8) and introduce fuel into the slab as they are raised. The remaining three shim-safety rods are in the beryllium section of the active lattice (positions LA-4, LA-6, and LA-8 in fig. 2.8) and introduce beryllium into the lattice as they are raised. When the rods rest in the lower shock absorber, the rod cadmium sections fill up the lattice.

As explained in section 2.1, the shim-safety rod in position LC-6 of the fuel slab may be removed and the space used instead for experimental purposes. In this case, only 4 shim-safety rods are available in the fuel slab so that, if necessary, the fuel loading will be slightly modified from that indicated in figure 2.8 to give the required margin of shutdown reactivity. It will be the policy of operations to use loadings giving minimum excess-reactivity required for the specific operation.

Space has been provided in two of the beryllium pieces at the edge of the fuel slab (positions LA-2 and LA-10) for two regulating rods. The two regulating rods, which provide the means for continuous fine control of the reactivity, are coupled to the automatic servo-control system described later. Only one rod can be in servo-control at a time while the other rod is used as standby to be manually switched into operation at the discretion of the operator.

### 2.3.2 Shim-Safety Rods

A drawing of the shim-safety rod used in the fuel slab is presented in figure 2.30. The rod consists of six principal sections: (1) the hollow cadmium section, (2) the fuel section, (3) the water-outlet section, (4) the transition section, (5) the guide section, and (6) the drive-release section. The positions of the upper and lower assembly grids relative to the shim-safety rods for rods fully inserted and fully withdrawn are indicated in figure 2.31. For the fully inserted position, the rod rests in its shock absorber (dashpot) located in the reactor tank below the grid assembly as shown in figure 2.31 (described in detail later). In actual operation, the shim-safety rods are never driven to the fully withdrawn position indicated in figure 2.31. Instead, a mechanical stop will be set on the rod drive so that the rod effectiveness is never less than about 20 percent of maximum, as determined by calibration of the rods. The fuel section contains 14 fuel-plates instead of the 18 plates contained in a fuel-element assembly. Water flows downward from above the upper assembly grid through the hollow cadmium section, past the fuel-plates, and out through the water-exit slots to the plenum chamber beneath the lower assembly grid. The rod transition section forms the transition from a rectangular cross-section to the cylindrical cross-section of the rod guide and drive-release sections. The action of engagement and release of the shim-safety rod by the drive-rod occurs at the drive-release section; this action is described in detail later.

### 2.3.3 Shim-Safety Rod Supports and Bearings

Guide bearings are provided for each shim-safety rod at three positions; at the upper assembly grid, at the lower assembly grid, and at the lower bearing grid located 46.625 inches below the lower assembly grid (see fig. 2.31). The position of these guide bearings with respect to the shim-safety rod is shown in figure 2.31. As indicated in figure 2.32, the topmost bearing is an individual unit for each rod and is bolted to the top surface of the upper assembly grid. This bearing consists of 8 spring-loaded rollers each of which bear with a force of about 10 pounds against the flat sides of the shim-safety rod. This floating-bearing guide permits up to 0.040 inch misalignment of the shim-rod from its center position without the shim-rod coming in contact with the grid or adjacent fuel elements. Figure 2.32 shows the rollers, springs, and spring-loading adjustments. Figure 2.33 is a view of the upper assembly grid showing cross-sections of fuel-elements and a shim-safety rod in place and a top view of the shim rod with its bearing guide in place.

The middle bearing guide is identical to the topmost bearing and is bolted to the bottom surface of the lower assembly grid. Hung underneath from the same support as the lower assembly grid (see fig. 2.8) is a bearing grid which holds the lower guide bearings for the shim-safety rods.

As shown in figure 2.34, this bearing consists of 4 concave rollers which bear against the cylindrical surface of the drive-release section of the shim-safety rod. This guide bearing is also of the floating type with each roller loaded to exert a side force of about 100 pounds on the shim-safety rod to keep it centered; the total movement of each roller is limited to about  $1/8$  inch. This bearing is hence a relatively stiff guide compared to the upper 2 guides.

This arrangement and design of guide bearings is to permit free operation of the shim rods in their guides, making due allowance for misalignment and possible distortions of the assembly grids and lower bearing grid. The possibility of rod sticking due to distortion of the structure following a nuclear incident is thus reduced.

The bottom shock-absorbers (dashpots) for the shim-safety rods are located on a plate mounted 50.50 inches below the lower bearing grid (see fig. 2.31). The plate mounting is by means of hanger supports extending downward from the main support for the entire grid assembly. A cross-section of the dashpot is shown at the right side of figure 2.35; the upper drawing shows the shim-safety rod just out of its dashpot and the lower drawing shows the shim-safety rod resting in its dashpot. The dashpot is formed by the annular space between two concentric cylinders (actually tapered) into which the bottom end of the shim-safety rod fits. Since the dashpot is located within the reactor tank, it is always filled with water which acts as the damping fluid to absorb the energy of a rod-drop.

For initial installation, the assembly grids with the shim-safety rods (and regulating rods) and dummy fuel elements, the lower bearing grid, and the shock-absorber mount are assembled and accurately aligned outside the reactor tank. This entire assembly is then placed in position within the reactor tank and aligned to allow free movement of the  $1\frac{1}{4}$ -inch O.D. drive-rods through the  $2\frac{1}{2}$ -inch I.D. holes in the reactor-tank bottom wall and shield and into the drive-release section of each shim-safety rod (see fig. 2.31).

#### 2.3.4 Drive-Rod and Scram Latch Mechanism

The shim-rod drive mechanism is located in the subpile room directly beneath the reactor tank and bottom shield as indicated in figure 2.31. The drive-rod penetrates up into the reactor tank and runs up inside the shim-safety rod to the drive-release section. As indicated in figure 2.35, the release-rod runs up within the hollow drive rod from the subpile room. The scram-release action is shown in detail in figure 2.35. The release of the shim-safety rod from the drive rod, and resultant "scram" action,

is actuated by a 1/4-inch downward movement of the release-rod relative to the drive rod. Three release-buttons at the end of stiff cantilever springs extend upward from the top end of the drive rod. In the locked position shown in the top drawing of figure 2.35, the release-rod is up relative to the drive-rod and the buttons are held out against the tapered surface of the engage shoulder of the shim-safety rod. Line contact is obtained between the release buttons and the engage shoulder and between the release buttons and the plunger of the release rod. The surfaces are inlaid with a hard, wear-resistant material. The bearing pressure at the engage shoulder is due to the weight of the shim-safety rod and the water-flow pressure forces on the shim-safety rod. In the design shown in figure 2.35, no forces on the shim-safety rod are transmitted to the release-rod (other than friction forces due to side pressure on the plunger). As shown in the bottom drawing of figure 2.35, a 1/4-inch downward travel of the release-rod relative to the drive-rod releases the shim-safety rod which then drops into its dashpot under the combined forces of gravity and water-flow pressure. As shown in the middle drawing of figure 2.35, an additional 1/4-inch downward travel of the release-rod (total travel = 1/2 in.) results in a positive gripping of the buttons inward. This feature insures positive disengagement of the drive-rod from the shim-safety rod, as well as eliminating any possible interference between the buttons and the rod shoulder during removal of the shim-safety rod from the top of the reactor tank. In the event a shim-rod binds and will not move down as the drive-rod is lowered, a shoulder on the drive-rod will engage a shoulder in the shim-rod and positively pull it down. These shoulders are slotted like a spline to permit removal of the shim-rod by simply rotating the drive-rod until the shoulders of one piece line up with the slots of the other. A protection tube (which also provides support of dashpot) around each individual shim-safety rod reduces any possible buffeting of the rods by the turbulent high-speed water flow.

As indicated in figure 2.35, the topmost guide for the drive rod is fastened to the bottom of the dashpot support mount. This aluminum guide positions the drive-rod to run up through the inner cylinder of the annular dashpot and into the shim-safety rod to the drive-release section. Downward, as shown in figure 2.31, the drive-rod runs through a hole in the reactor-tank bottom and shield into the subpile room. This hole is lined by a stainless-steel pipe which is cast in the concrete and welded to the reactor-tank. To the flange at the bottom end of the stainless-steel tube liner is bolted a gate valve which, during normal operation, is open to allow the drive-rod to run through the valve body. The valve permits removal of the drive- and release-rod assemblies into the subpile room with only a small loss of reactor-tank water. Mounted on the bottom flange of the gate-valve is a bellows expansion-joint and, in turn, the drive-rod seal assembly. The expansion joint compensates for any slight misalignment of the pipe permanently embedded in the concrete; it gives some flexibility for aligning the drive-rod through the seal-assembly up to the drive-release section of the shim-rod.

E-102

A drawing of the drive-rod seal assembly is presented in figure 2.36. The seal-assembly is designed to keep to a minimum any water-leakage where the drive-rod passes from the pressurized tank-water space above the seal to the subpile room. Two sets of teflon chevron packings are used. The top set of packings is held against the walls of the drive-rod and seal-housing by an adapter. The bottom set is held against the drive-rod and adapter by means of a packing nut screwed into the adapter. The adapter is designed to permit introduction of fresh water to the region between the two sets of seals. The purge water is at a pressure slightly greater than the reactor-tank water-pressure and thus greatly reduces the possibility of leakage of activated tank-water into the subpile room. An O-ring seal between the adapter body and seal-housing is used to reduce the leakage of the buffer purge water. The arrangement of two separate sets of packings permit use of different tightening pressures for the two sets of packings.

As previously described, the "scram" action results from downward movement of the release-rod relative to the drive-rod. Figure 2.37 shows the bottom latch mechanism actuating the "scram" by reduction of current to a solenoid. This mechanism is in the subpile room (fig. 2.31) for convenience of installation, inspection, maintenance, and adjustment. Several important functions are achieved by the design, namely, (1) only a small holding force of the solenoid plunger is required in the latching and unlatching action; (2) the mechanism is locked for proper drive and "scram" function during normal operation but can be conveniently dismantled for pulling the drive and release-rods into the subpile room; (3) after the "scram," the drive-rod must be driven beyond the bottom stop to relatch; (4) after the relatching action, a small upward movement of the drive-rod is required before the shim-safety rods are picked up; (5) rotation of the drive-rod during its motion is prevented, and (6) angular position of the release-rod with respect to the drive-rod is fixed. As shown at the left side of the drawing of figure 2.37, a collar is slipped over the tapered end of the drive-rod shaft and is held tightly in place by a tightening nut and a key which prevents rotation of the collar relative to the drive-rod shaft. A cross-head is held in place over the collar by a snap ring. The collar has a keyed-out section which mates with the cross-head to prevent rotation of the cross-head relative to the drive-rod shaft. Two slots in the cross-head run in a fixed frame guide so as to prevent rotation of the drive-rod assembly as it moves up and down. A bellows connects the drive-rod assembly to the release-rod assembly as shown in figure 2.37. Pressurized water from the reactor tank fills the bellows and tends to force the drive-rod and release-rod apart (tends to move release-rod down with respect to the drive-rod). Keyed to the release-rod assembly just below the bellows is a relatching arm whose function is described later. The drive-rod is made integral with the drive-rod lower assembly by means of the drive-rod extension bolted to the drive-rod collar and welded to the drive-rod lower assembly. The drive-rod lower assembly contains the scram latch and solenoid-actuator

and, in addition, incorporates a set of guide-bearings for the release-rod. The scram latch is a break-leg mechanism as indicated in figure 2.37. The bottom pivot of the lower leg is about a horizontal axis fixed on the drive-rod lower assembly. The top end of the upper leg slides up and down with the release-rod, its position relative to the release-rod being fixed (except for some play allowed for in its motion, such play being restrained by a spring). This action is accomplished by a pin passing through the top end of the upper leg through a hole in the release-rod. At the common pivot junction of the upper and lower legs of the break-leg mechanism is pivoted a latch bar, the lower end of which can be engaged by a trigger arm as shown in the figure. The action of the bottom latch is illustrated in figure 2.37. The solid lines show the latch engaged, i.e., the latch bar is held by the trigger arm so that the break-leg mechanism is holding up the release-rod relative to the drive-rod. The dashed lines show the latch disengaged.

The sequence of actions of the bottom-latch mechanism resulting in its disengagement upon deenergizing the solenoid and the actions involved for reengagement of the latch are described herein. Downward forces on the release-rod due to the release-rod weight, water pressure in the bellows, and, in addition, a compression spring at the bottom end of the release-rod tend to move the release-rod down relative to the drive-rod. The total downward force tending to unlatch the release-rod is resisted by the friction forces due to the side pressure on the release-rod plunger and by a counter-balancing force on the break-leg junction exerted, through the trigger arm and latch bar, by the solenoid plunger when the solenoid is energized. When the current to the solenoid is reduced or stopped and hence the counter-balancing force reduced, the moment on the trigger arm about its pivot is unbalanced resulting in disengagement of the latch bar out of the notch in the trigger arm. The break-leg is then "broken" and the release-rod moves downward under the action of the combined forces due to release-rod weight, bellows, and spring. As previously described, downward movement of 1/4 inch of the release-rod relative to the drive-rod releases the shim-safety rod from the drive rod and results in the "scram" action. When unlatched, the movement of the release-rod down is stopped (and limited to 1/2-inch total distance) by impact of the end of the release-rod against the face of the steel nut screwed into the end of the drive-rod lower assembly. The face of the steel nut and the end of the release-rod are heat-treated to form hardened surfaces. To relatch after a scram, the drive-rod must be driven down to its bottom stop where the relatching arm contacts the relatch stop on the fixed frame guide. Further downward motion of the drive-rod is then required to pull up the release-rod relative to the drive-rod against the action of the downward forces; the release-rod is then in proper position for relatching by solenoid-action.

The relatching arm runs in a slot fastened to the drive-rod extension so that the release-rod cannot rotate relative to the drive-rod.



The total force downward on the latch is about 400 pounds with the release-rod weight contributing 10 pounds, the bellows 230 pounds, and the spring 160 pounds. Due to the mechanical multiplication, this downward force results in a force of about 12 pounds exerted downward on the solenoid plunger and which must be overcome by solenoid action. The spring alone or the bellows alone exert enough force to trip the latch so that if either the spring or the bellows broke, the unlatching action would still occur although the dead time in the unlatching process would be increased.

A slight downward force by means of a torsion spring is also applied on the trigger arm above the solenoid plunger so that in the unlatched position with the solenoid plunger down, the latch is swung away from the release-rod. Note the O-ring seals in figure 2.37 to prevent leakage of water from the reactor tank through the bellow assembly.

In the scram-latch mechanism design shown in figure 2.37, careful consideration has been taken to ensure ease of assembly, disassembly, and inspection of the individual parts. Means for careful adjustment and maintaining constancy of adjustment of the forces actuating the latch are incorporated into the design. The speed of response of the mechanical unlatching action for the design herein described has been calculated as 18 msec (not including solenoid dead-time); part of the developmental work on the mechanism will be aimed at reducing this dead-time.

### 2.3.5 Drive-Rod Actuator

The shim-rod withdrawal speed will be limited to 3 inches per minute. The considerations involved in arriving at this limiting speed are discussed in section 6.1. However, the shim-rods will have two possible limiting speeds for insertion, namely, a slow-speed insertion of 3 inches per minute, and a high-speed insertion of 9 inches per minute. To incorporate the feature of a high-speed insertion without the possibility of it becoming, by any means whatsoever, a high-speed withdrawal, two separate motors are used for each shim-rod drive. One motor gives the low-speed withdrawal and insertion whereas the second motor gives the fast insertion only. The two motors drive, through individual self-locking worm-gears, a common differential epicyclic gear train, the output of which drives the drive-rod by means of a lead screw (see fig. 2.38). The locked worm-gears preclude the possibility of one motor driving the other. The low-speed motor is a reversible 2-phase A.C. motor. The motor will have speed and direction-of-rotation control through the control of the phase and voltage of the one winding in reference to the other. In order to assure a synchronous limited maximum speed, the motors will be selected to have the required torque near the full-speed point; thus any reduction in load torque could give only a very small increase in speed. The high-speed insertion motor is a single-phase, repulsion-induction A.C. motor so wound and connected that only a single direction of rotation is possible. The motor will have a single-shaft output so that it cannot possibly

be assembled to deliver power in the reverse rotational direction. In addition, the high-speed insertion motor is coupled to the self-locking worm-gear by means of a one-way clutch. Standard operational procedure prior to a normal reactor-startup will require that the fast-insertion be checked by the operator at the reactor-console. These precautions ensure no possibility of the fast-insertion becoming a fast withdrawal as a result of failure of the driving mechanism, short-circuit or error in the electrical wiring, wrong assembly of the drive-rod actuator, or reactor-operator error.

Interlocks will be incorporated in the control circuitry of the two motors so that only one of the two motors can drive the shim-safety rod at any given time. Actually, no hazardous condition is involved because the high-speed insertion motor will pull the rod into the reactor regardless of the speed and rotation-direction of the low-speed motor.

#### 2.3.6 Shim-Safety Rod Position Measurements and Travel Limits

Information on the instantaneous positions of the shim-rods is transmitted by selsyn units to the operator. Limit switches are used to limit the travel of the drive-rods (by interruption of current to the drive-motors) and to transmit to the operator such information as the seating of the shim-safety rods in their shock absorbers or the engagement of the bottom latch in the quick-release mechanism.

#### 2.3.7 Developmental Tests of Shim-Safety Rod System

A full-scale mockup of the shim-safety rod drive system and quick-release mechanism is being constructed and will receive thorough testing under the simulated water-flow and purity conditions anticipated in actual operation. The mockup will be subjected to several thousand hours of repetitive testing running through many different cycles of shim-safety rod withdrawal, insertion, and scram-release. Variations will be made in the design described herein in order to arrive at a "best" design from the standpoint of ruggedness, performance, and absolute reliability. The performance and endurance testing will involve determination of the reliability and speed of response of the quick-release mechanism, the degree of misalignment and distortion of the assembly grids relative to each other and to the lower bearing grid which will not (1) interfere with the scram-action, and (2) prevent the pulling-down of the shim-safety rod by the drive-rod, and the leak-tightness of the drive-rod seal assembly under repetitive cycling motion of the drive-rod. Final testing will be performed with water-crudding conditions much more severe than expected in actual operation.

### 2.3.8 Regulating - Rods

No details of rod construction and drive-mechanism are presented herein. Basically, the design objectives for the regulating-rod action are the same as at the Materials Testing Reactor. The regulating-rod drive is actuated from the subpile room. The maximum reactivity controllable by the regulating rod will be limited to not over 0.6 percent. The regulating-rod motion will be velocity-limited. The accidents due to the regulating-rod are discussed in section 6.1.6.

### 2.3.9 Emergency Power Cutbacks

As in the Materials Testing Reactor control and safety system, various modes of corrective action other than the ultimate scram are used, the severity of the action depending on the degree of hazard involved in the abnormal condition requiring the safety action. Hence, many potentially dangerous situations may be corrected before the scram action is involved. The types of emergency reactor-power cutbacks in the order increasing severity of the accident involved are: (1) slow and fast setbacks, (2) slow and fast reverses, and (3) slow and fast scrams. Figure 2.39 gives some indication of the rates of power-reduction resulting from these safety actions. The reverse at 0.04 percent  $\Delta K/K$  per second corresponds to the slow-reverse for shim-rod effectiveness equal to 40 percent of its maximum value; the power-reduction rate corresponding to maximum effectiveness (0.1 percent  $\Delta K/K$  per sec) can be estimated by interpolation between the curves for 0.04 and 0.15 percent. The reverse at 0.1 percent  $\Delta K/K$  per second also corresponds to the fast-reverse for shim-rod effectiveness equal to 1/3 of its maximum value. The scram to -30 percent  $\Delta K/K$  corresponds to the full scram for shim-rod effectiveness equal to about 1/3 maximum effectiveness. It is obvious that the fast-reverse is vastly inferior to the full scram insofar as rate of power reduction is concerned.

### 2.3.10 General Considerations of Safety System

Basically, the control and safety system is comparable to the MTR system. The important safety features of the MTR have been adopted with relatively little change. However, in some phases of the design, it was desirable to take advantage of the improvements in instrumentation and control equipment made since the design of the MTR system and of the experience accumulated at MTR. It is basically in this respect that the design differs from that at MTR.

No specific components are described inasmuch as an investigation is still in progress to obtain more complete information on the performance and reliability that can be expected from presently-available components.

Hence, only the general principles and design objectives are presented. It is to be expected that some of the design objectives may be modified as more complete information on available components is obtained. However, with the more important basic features of the MTR incorporated, as a minimum, in the present design, such design changes as may be required should have little effect on the over-all safety and control of the reactor. Prior to its adoption, the critical components of the control and safety system will be assembled and tested (using simulated ion-chamber signals) to evaluate its over-all performance and reliability.

### 2.3.11 Regulating-Rod Servo-System

The power-level control system provides for automatic control of the neutron flux level as sensed by a suitable ion chamber located close to the reactor core so as to give nearly maximum signal at full power. This system will cover the top three decades of the reactor power spectrum. The reactor will then be on "servo" during the last decades of the period range and for the full power range. As indicated in figure 2.40, the output of the ion chamber feeds into a logarithmic amplifier whose output is proportional to the logarithm of its input. The output of this circuit is compared with the output of a similar circuit and if the difference between the two outputs exceeds a preset minimum, a warning of this condition is indicated to the operator at the reactor control console. By means of a switch the operator can select either of the two logarithmic-amplifier outputs for the servo signal. The signal from the selected log N amplifier is compared, in a servo error-circuit, with a reference (setpoint) signal to give an error signal which, in turn, is fed to the regulating-rod servo-control system. The output of the error circuit is approximately proportional to the logarithm of the ratio of the measured and setpoint flux; the servo-loop gain is thus independent of power level.

### 2.3.12 Setpoint Action

As indicated in figure 2.40 the setpoint signal for the error-circuit is obtained by means of a speed-limited motor-driven setpoint on a linear-resistance slide wire. The setpoint can be driven, through appropriate interlocks, by either the slow-reversible motor or the fast-reversible motor. The manual setting is accomplished by the operator setting the demand-power on the power controller which results in the driving of the setpoint. This results in a power change to the new setting on a 20-second period when the fast-reversible motor is used and on a 90-second period with the slow-reversible motor. The slow and fast setbacks are the result of the automatic lowering, by the control-safety system, of the servo setpoint. The slow setback reduces reactor power on a constant 90-second period; the fast setback causes power-reduction on a 20-second period. These controlled decreases in power occur only within the servo-range limits of full-power to  $10^{-3}$  full power. When the trouble causing

the setbacks has cleared, the power can be increased to the original or desired value by operator action.

Setback error circuits, similar to the one forming the error-signal for the servo-control system, will be provided to place limits upon the motion of the motor-driven setpoint and to cause full-corrective and/or fail-safe power reductions dependent upon certain error-minimum requirements. The error-circuits will perform the following functions:

(a) If the indicated reactor flux exceeds the setpoint by:

1.2 Warning

1.3 Shim-rod out motion will be stopped and locked out (no manual override possible until causative condition cleared).

1.4 Slow-reverse will be initiated.

1.5 Slow scram will be initiated.

(b) If the setpoint exceeds the indicated reactor flux by:

1.2 Warning

1.3 Motor-driven setpoint increase will be stopped and be locked out.

1.4 Shim-rod-out motion will be stopped and locked out.

1.5 Fast setback initiated.

Of the preceding circuits, two will be provided with backups on a separate independent system (by setpoints on the recorder indicated in fig. 2.40). These are:

(a) When measured power exceeds setpoint by more than 1.5, full scram will be initiated.

(b) When setpoint exceeds measured power by more than 1.5, setpoint will be stopped and locked out and all shim-rod-out motion will be stopped and locked out.

Recovery from these conditions, except for full scram can be made through the proper corrective action.

By such close supervision of the error-signal at all levels in the servo-control range, the corrective-action of the control system is initiated at flux levels close to the level where the "accident" or abnormal condition occurs. This system supplements the usual fixed-level and period trips.

When the reactor is started from a power below the lower limit of the motor-driven setpoint system, the motor-driven setpoint must be at its lower limit thus providing a over-power scram at  $1.5 \times 10^{-3}$  of full power. When a power "sag" occurs that is within the range of the motor-driven setpoint, recovery to higher power can be made only by first driving the motor setpoint down to the "sag" power.

### 2.3.13 Regulating- and Shim-Rod Actions

The regulating rod and servo system will be of the high speed type required for proper control of experimental reactors of this type and power capabilities. The system will be of the continuous signal type (as opposed to the on-off type) using an amplidyne driven D.C. motor or similar power system. A tachometer feedback will be used and local and remote position indication will be provided. The usual switches will be provided for travel limits, shim control, and interlocks. Two complete regulating rod assemblies will be provided with one required for operation. Arrangements for transfer of control from one rod to the other during reactor operation will be provided. The regulating rod in control will call for both insertion and withdrawal of the shim rods. The insertion (lowering power) will not require manual supervision but the withdrawal will be subject to both interlock and manual agreement. The regulating rod will be maintained in its area of highest control effectiveness, i.e., near mid-travel during normal operation. The rod not in servo-control will always be withdrawn from the core prior to starting.

A wide range of speed control is available for movement of the shim-safety rods. Manual control of any single shim-safety rod will be possible and both intermittent and very slow shim-rod withdrawal rates will be provided. The usual limit switches will be provided for limiting rod motion and for interlocking. A safe reactor-off position has been provided by the drive-rod relatching system. In the shutdown (or "off") position, the reactor is in the "scram" condition with the drive rods in the full-down position; hence, any motion of the drive rods is incapable of moving the control rods should some accident occur. In order to be able to move the shim-safety rods out of the reactor, the operator must first go through a specific mechanical procedure for rod relatching. To effect the rod relatching, it will be necessary (with manual override required) to drive the rods below the bottom limit, reset the solenoid catch, and reverse the drive to the bottom limit position.

The reverse is a motor-driven insertion of all shim-safety rods, the action being initiated either automatically by the safety system or manually by the operator. When initiated by the safety system, the reverse continues until the condition causing the reverse has cleared and the operator has removed the reverse command of the safety system. In the slow-reverse, the shim-rods are driven at the maximum speed of the low-speed shim-drive motors; the command is transmitted to the motors through

the closing of contacts indicating some abnormal condition. In the fast-reverse, the shim-rods are driven at the maximum speed of the high-speed insertion motors.

The scrams are achieved by reducing or shutting off the current to the shim-rod holding solenoids. Exactly as in the MTR safety system (fig. 2.41), the output of the amplifiers supplying power to the holding solenoids is controlled by a sigma-bus potential which in turn is determined by power-level and period signals originating from ion-chambers. When any one of the duplicate signals of power-level or period is abnormal, the sigma-bus potential changes resulting in a reduction of power to the holding-solenoids thus resulting in the fast scram. This action is electronic so that the fast scram is a quick-response action.

In the slow scram, the current to the holding solenoids is shut off by the action of normally-energized relays whose contacts are in the power supply circuit of the magnet amplifiers. Failure of any relay causes scram.

Every scram action is immediately followed by the fast-reverse.

#### 2.3.14 Activity - Measuring Instrumentation

The reactor activity measuring instrumentation will consist of parallel circular plate and compensated ion chambers, fission chambers, boron thermopiles, and miscellaneous air and water activity measuring instruments. The parallel circular plate and compensated ion chambers and the fission chambers cover, in combination, the entire range of flux levels from that produced by a neutron source to that corresponding to 1.5 full power. The flux range of the fission chambers is increased by making provisions for their movement during reactor startup. The fission-chambers are especially useful in the source-level range and, by moving them to several established fixed positions during startup, can cover the entire flux range of the reactor. The information obtained from the fission chambers is indicated in figure 2.42 which shows the galvanometer system. The parallel circular plate and compensated ion chambers will be of commercial manufacture following the Oak Ridge designs, or fully equal equipment of proven design and operation. The fission chambers and boron thermopiles will also follow Oak Ridge designs with whatever modifications are required to fit this reactor design. The other air and water activity measuring devices will be of standard types now in use or under development. Those activities in the air and the water systems directly associated with the operation of the reactor will be part of the warning and reactor power setback circuits.

### 2.3.15 Other Instrumentation

Instrumentation with indication, time records, warning circuits and reactor shut-down capabilities will be provided as required for measurement of flow, pressure, temperature, power (heat release) electrical power, etc. In general, these systems will use commercially available equipment with only such modifications as may be necessary to perform the required task.

Water flow measurements will be made in the primary water system both in the main flow and the head-tank makeup line. Flow measurements will also be made in the shut-down cooling system. Air flow into and out of the containment vessel will also be measured. Standard flow measuring methods will be used (i.e., flow nozzles, pitot tubes, venturies, etc.). An indication of secondary (heat-exchanger) water flow will be provided. Many pressure measurements will also be made. These will include the critical operating pressures in both the primary and secondary water systems. The head tank pressure (which is also an indication of tank water level) will also be measured. This pressure will be compared with actual tank level as indicated by float gages and any deviation will call for reactor shut-down.

The commercial (purchased) power system as well as the diesel generator and the guaranteed (battery) power systems will be surveyed for indications of off-normal conditions. Loss of power in these systems shall call for automatic corrective action and failing that will shut down the reactor. Under some instances, emergency water flow systems would be brought into play.

Very many temperatures will be measured. Only the more important ones are covered here. In the primary water system, the reactor inlet and outlet temperatures will be measured and the temperature difference computed. Also the water temperatures entering and leaving the heat exchangers and entering the primary deionizer will be measured. The secondary system temperatures will also be monitored. Other temperatures affecting the operation of the reactor will be measured on a scanning monitor. Such temperatures, as shield water, solid shield, pump motor winding and bearing, containment tank air, etc., would be typical of these. The product of the water flow and the water  $\Delta T$  for both the primary and shut-down systems would be computed to give an indication of the power output (heat release) of the reactor.

### 2.3.16 Power Cut-Back Table

Table 2.6 is indicative of the emergency measures that will be incorporated into the reactor safety system. In table 2.6 is presented a compilation of the automatic corrective action invoked by the control and safety system for various abnormal or hazardous conditions which may arise



in the operation of the reactor and reactor supporting systems. The table is arranged according to the source of the trouble. The severity of the power cutback depends on the degree of abnormality involved. As the abnormal condition worsens, the emergency action becomes more drastic, finally culminating in the scram.

E-102

CZ-7



TABLE D.8. - Continued. POWER CUTHACKS

FS - Fast scram; SS - Slow scram; FR - Fast reverse; SR - Slow reverse; FRS - Fast set back;  
SSS - Slow set back; War - Warning.

System	Unit	Trouble	FS	SS	FR	SR	FRS	SSS	War
1. Emergency water system (continued)	B. Emergency system temperature	1. Inlet temperature 1.1 R							X
		2. Inlet temperature 1.2 S							X
		3. Inlet temperature 1.3 R							X
		4. Inlet temperature 1.4 R							X
		5. Leaving temperature 1.1 R							X
		6. Leaving temperature 1.2 R							X
		7. Leaving temperature 1.3 R							X
		8. Leaving temperature 1.4 R							X
		9. AT 1.1 R							X
		10. AT 1.2 R							X
1. Reactor tank conditions		1. Tank not full of water							X
		2. Tank pressure 1.2 R							X
		3. Tank pressure 1.3 R							X
		4. Tank pressure 1.4 R							X
		5. Tank pressure 1.5 R							X
		6. Tank temperature 1.1 R							X
		7. Tank temperature 1.2 R							X
		8. Tank temperature 1.3 R							X
		9. Tank temperature 1.4 R							X
		10. Tank temperature 1.5 R							X
1. Primary detector		1. Flow too low							X
		2. Flow too high							X
		3. AT too high							X
		4. AT too low							X
		5. Inlet temperature too high							X
		6. Inlet temperature too low							X
		7. Leaving temperature too high							X
		8. Leaving temperature too low							X
		9. AT 1.1 R							X
		10. AT 1.2 R							X
1. Secondary water system	A. Loss of one of two pumps in parallel	1. Loss of electrical power to motor							X
		2. Loss of AT across pump							X
		3. Loss of rpm							X
		4. Over current, under voltage							X
		5. High winding or bearing temperature							X
		6. Loss of other pump - both off							X
		7. Loss of electrical power to motor							X
		8. Loss of AT across pump							X
		9. Loss of rpm							X
		10. Over current, under voltage							X
1. Secondary water system (continued)	B. Loss of pump	1. Loss of electrical power to motor							X
		2. Loss of AT across pump							X
		3. Loss of rpm							X
		4. Over current, under voltage							X
		5. High winding or bearing temperature							X
		6. Loss of other pump - both off							X
		7. Loss of electrical power to motor							X
		8. Loss of AT across pump							X
		9. Loss of rpm							X
		10. Over current, under voltage							X
1. Secondary water system (continued)	C. Inlet flow is high	1. Flow too high							X
		2. Flow too low							X
		3. AT too high							X
		4. AT too low							X
		5. Inlet temperature too high							X
		6. Inlet temperature too low							X
		7. Leaving temperature too high							X
		8. Leaving temperature too low							X
		9. AT 1.1 R							X
		10. AT 1.2 R							X
1. Secondary water system (continued)	D. Leaving flow is high	1. Flow too high							X
		2. Flow too low							X
		3. AT too high							X
		4. AT too low							X
		5. Inlet temperature too high							X
		6. Inlet temperature too low							X
		7. Leaving temperature too high							X
		8. Leaving temperature too low							X
		9. AT 1.1 R							X
		10. AT 1.2 R							X
1. Secondary water system (continued)	E. Inlet flow is low	1. Flow too high							X
		2. Flow too low							X
		3. AT too high							X
		4. AT too low							X
		5. Inlet temperature too high							X
		6. Inlet temperature too low							X
		7. Leaving temperature too high							X
		8. Leaving temperature too low							X
		9. AT 1.1 R							X
		10. AT 1.2 R							X
1. Secondary water system (continued)	F. Leaving flow is low	1. Flow too high							X
		2. Flow too low							X
		3. AT too high							X
		4. AT too low							X
		5. Inlet temperature too high							X
		6. Inlet temperature too low							X
		7. Leaving temperature too high							X
		8. Leaving temperature too low							X
		9. AT 1.1 R							X
		10. AT 1.2 R							X
1. Secondary water system (continued)	G. Inlet flow is high	1. Flow too high							X
		2. Flow too low							X
		3. AT too high							X
		4. AT too low							X
		5. Inlet temperature too high							X
		6. Inlet temperature too low							X
		7. Leaving temperature too high							X
		8. Leaving temperature too low							X
		9. AT 1.1 R							X
		10. AT 1.2 R							X
1. Secondary water system (continued)	H. Leaving flow is high	1. Flow too high							X
		2. Flow too low							X
		3. AT too high							X
		4. AT too low							X
		5. Inlet temperature too high							X
		6. Inlet temperature too low							X
		7. Leaving temperature too high							X
		8. Leaving temperature too low							X
		9. AT 1.1 R							X
		10. AT 1.2 R							X
1. Secondary water system (continued)	I. Inlet flow is low	1. Flow too high							X
		2. Flow too low							X
		3. AT too high							X
		4. AT too low							X
		5. Inlet temperature too high							X
		6. Inlet temperature too low							X
		7. Leaving temperature too high							X
		8. Leaving temperature too low							X
		9. AT 1.1 R							X
		10. AT 1.2 R							X
1. Secondary water system (continued)	J. Leaving flow is low	1. Flow too high							X
		2. Flow too low							X
		3. AT too high							X
		4. AT too low							X
		5. Inlet temperature too high							X
		6. Inlet temperature too low							X
		7. Leaving temperature too high							X
		8. Leaving temperature too low							X
		9. AT 1.1 R							X
		10. AT 1.2 R							X

## 2.4 REACTOR AND CONTROL KINETICS

Detailed studies of the material in this section are presented in reference 2.4.

### 2.4.1 Startup

A detailed description of the startup procedures is in preparation. This will include check-out and monitoring procedures before startup, source level considerations, allowable rod motions, and instrumentation for the various types of startup conditions. The role of the servo and the nature of the coupling between the shim-safety and regulating rods will be discussed as well as the degree of automatic and manual control to be used.

### 2.4.2 Restart Times

The Xe buildup after a shutdown has serious consequences in the operation of the reactor as continuity in operation is desired. The buildup will be linear in time and proportional to the operating flux before the scram. The minimum time in which to stop the Xe rise is taken up by (1) a waiting period to ascertain and correct the difficulty and to insert the rod drive and lower the servo set point, (2) the time to withdraw the rods to near critical, and (3) the time to increase flux level high enough to stop the Xe rise.

In a typical startup at constant rod speed, the allowable period (T) is reached subcritically about T seconds before criticality would be reached if rods continued at constant speed. At this time the rods must be slowed down to maintain the allowable period. As the flux level must rise almost to its original value before scram in order to stop the Xe rise, maximum rod speed cannot be used to full advantage.

Figure 2.43 shows the potential ability to restart the reactor after a scram in terms of the maximum allowable down time, from full scram to starting rod withdrawal, at each day of operation over the 10-day cycle, for various excess reactivities allocated for Xe override. The decrease in excess reactivity available was assumed at 0.625 percent  $\Delta K$ /day. A maximum rod withdrawal velocity of 3 in./min and a minimum reactor period of 20 seconds were used. A typical 10-day cycle characteristic at rated conditions for flux level and Xe concentration was assumed; the rate of Xe rise after shutdown being proportional to the product of these two quantities. The shim-rod positions given in figure 2.23 were used.

Figure 2.43 shows that each one percent  $\Delta K$  allocated for Xe override is worth about  $1\frac{1}{2}$  days extra operation, or 3 to 3.5 min extra down time. If 2 percent  $\Delta K$  were allocated for Xe override, there would be

a 2 min allowable down time at the end of 8 days, and a 19 min allowable down time at the end of 2 days.

The long term Xe and Sm effects are given in reference 2.4. Of special interest is the behavior of Sm at high thermal flux. After shutdown from a flux level of  $4 \times 10^{14}$ , the Sm rise will compensate for the Xe decay at about 105 hours after scram; ultimately reaching a quasi-equilibrium value of -5.88 percent  $\Delta K/K$ .

#### 2.4.3 Maximum Xenon Burn-Out After Restart

The rate of Xe burn-out is proportional to the product of the Xe concentration and the thermal flux. After a restart, with Xe buildup, the possible Xe burn-out relative to formation from I decay, even at normal flux levels, is a factor in setting control rod speeds. If the rods cannot keep up with this burn-out, a nuclear excursion will start and the only protection to the reactor are the scrams. This incident would not give large power overshoots if the reactor scrams.

The maximum rates of Xe burn-out, after a restart with Xe buildup, are tabulated below, for restarting at the maximum thermal flux level of  $4 \times 10^{14}$ .

#### MAXIMUM Xe BURN-OUT RATES AFTER RESTARTS

Reactivity effect of Xe at restart	Restart on Xe rise		Restart on Xe decay
	Thermal flux level before scram		
	$4 \times 10^{14}$	$\sim 10^{14}$	
-8 percent $\Delta K$	0.3 percent $\Delta K/\text{min}$	0.6 percent $\Delta K/\text{min}$	0.6 percent $\Delta K/\text{min}$
-20	1.2	1.4	1.5

#### MINIMUM CONTROLLED $\Delta K$ REVERSE RATES

Rod velocity	Minimum rod effectiveness	Controlled $\Delta K$ reverse rate
3 in./min	0.4 percent $\Delta K/\text{in.}$	1.2 percent $\Delta K/\text{min}$
9	0.4	3.6

The extreme possibility of restarting with -20 percent  $\Delta K$  due to Xe in the core was used. The worst case is restarting around peak Xe

or on Xe decay where 1.5 percent  $\Delta K/\text{min}$  may be inserted by Xe burn-out at rated flux level. This reactivity insertion rate must be controlled by the reverse speeds of the shim-safety rods. The minimum controlled reactivity reverse rates are also shown above for rod speeds of 3 in./min and 9 in./min, at the minimum rod effectiveness of 0.4 percent  $\Delta K/\text{in.}$  (20 percent of maximum effectiveness, as estimated from fig. 2.23). The 9 in./min insertion rate is adequate to insure control of Xe burn-out at all times.

#### 2.4.4 Cut-Backs

The effect of various cut-backs on flux level was shown on figure 2.39, for scrams, reverses, and set-back. These results were obtained on a differential analyzer including the effects of five delayed neutron groups. For scrams, the prompt drop is obtained in 0.25 to 0.5 second. For a total of -30.0 percent  $\Delta K/K$ , a cut-back to 2 percent is obtained in 1.16 seconds. If only a total of -10 percent  $\Delta K/K$  is inserted, it takes 11 seconds to reduce flux level to 2 percent.

Cut-backs by reverses are very sensitive to reverse speeds. For a reverse of 0.7 percent  $\Delta K/K/\text{second}$ , a one decade drop is obtained in 5 seconds at which time -3.5 percent  $\Delta K/K$  has been inserted. Immediate recovery from this level is always possible if there were about 0.7 percent  $\Delta K/K$  excess before the reverse. The slower reverse, at 0.04 percent  $\Delta K/K/\text{second}$ , is only slightly more effective than a 20 second period set-back.

#### 2.4.5 Kinetic Parameters

The prompt neutron lifetime, temperature coefficient, and void coefficient were discussed in section 2.2 and appendix B. The effective delayed neutron fraction was calculated from an analysis consistent with the group diffusion equations. The minimum value of this parameter was found to be 0.0085, as compared to the actual yield of 0.0075. The increased effect of the delayed neutrons is caused by their lower average age, about 35  $\text{cm}^2$ , as compared to the average age of the prompt neutrons, 64  $\text{cm}^2$ .

#### 2.4.6 Stability

In normal operation, the inherent stability characteristics of the reactor determine the ease or difficulty of operation in manual control and the dependence on and requirements of the servo in automatic control. Xenon effects are always unstabilizing. The delayed neutrons and negative temperature coefficient are stabilizing influences. Assuming

linearization around the operating condition of interest, the combined equations for reactor kinetics using one average delay group, temperature effects, and Xe effects were analyzed for inherent stability.

The stability criterion was found to be  $\alpha\Delta T > P_0$ , where  $\alpha$  is the negative temperature coefficient,  $\Delta T$  is the difference between the average coolant temperature in the reactor and the average coolant temperature at the inlet to the reactor, and  $P_0$  is the total reactivity effect of Xe; all conditions at the operating point of interest. For this reactor,  $\alpha\Delta T \leq 0.15$  percent  $\Delta K/K$  and  $P_0 \geq 4$  percent  $\Delta K/K$ , and the reactor is inherently unstable. This Xe power instability is manifested as a slow, positive exponential drift in flux level, increasing or decreasing. The time constant of this unstable mode is shown in the following table, for an operating flux of  $4 \times 10^{14}$ , effective delayed neutron fraction of 0.0085, and average mean life of the delayed neutrons of 12.47 seconds.

TIME CONSTANT OF Xe POWER INSTABILITY

$\alpha\Delta T$	Xenon concentration	
	4 Percent $\Delta K/K$ , during normal operation	20 Percent $\Delta K/K$ , during restart with maximum xenon
0 percent $\Delta K/K$	43.5 sec	16.0 sec
0.043	49.8	
*.15	67.0	20.4
.3	96.6	

\*Approximate condition at rated power.

The negative temperature coefficient only increases the time constant of the Xe power instability from 43 seconds to about 60 seconds. The unstable period could be as low as 20 seconds after a restart with maximum Xe buildup. On a restart, this period is also that which would develop, at first, if the control rods do not keep up with Xe burn-out.

#### 2.4.7 Controlled Reactor

A controlled system was analyzed under the same assumptions regarding kinetics as in the preceding section. For pure integral control action, the gains and regulating rod speed requirements to stabilize the Xe power instability are easily met; the speed chosen being about 200 times that required for stability under all conditions.

The requirements on the regulating rod for constant period setbacks are tabulated below:

Setback period	Maximum speed of regulating rod required	Maximum insertion of regulating rod required	Time to reach maximum insertion of regulating rod
20.0 sec	-0.04 percent $\frac{\Delta K/K}{\text{sec}}$	-0.24 percent $\Delta K/K$	15.6 sec
90.0	-.01	-.08	28.5

Using one average delayed neutron group indicates that to maintain a constant period setback, there is a maximum insertion of the regulating rod after which the rod will withdraw and approach its original position. The table shows that the regulating rod speed (given below) is adequate for setbacks but that the range required for a 20 second period setback may be critical. If the regulating rod trips the bottom limit switch, the reverse action called for would be adequate to maintain the 20 second period setback or put the regulating rod back into range.

The regulating rod can control step-wise insertions of reactivity within its range capabilities. For step-wise disturbances in reactivity less than prompt critical, the peak flux would be the irreducible (almost) prompt rise. The required rod velocity is proportional to the reactivity inserted and inversely proportional to the required settling time for the transient. The maximum rod speed chosen, full travel in about one second or 0.6 percent  $\Delta K/K/\text{second}$ , could control a step reactivity disturbance of 0.15 percent for a requirement that the flux level return back to its original value in about one second. In addition, the regulating rod, which must be fully withdrawn before startup, can override all possible shim-safety rod withdrawals and can stop or delay a startup accident.

## 2.5 REFERENCES

- 2.1. Huffman, J. R.: The Materials Testing Reactor: Operational Behavior. Preprint 299, Am. Inst. of Chem. Eng., Nuclear Engineering Science Congress. Dec. 12-16, 1955.
- 2.2. Research Reactors TID 5275. Light-Water-Moderated: Type III. Heterogeneous - Enriched Fuel. Figure 3-52, p. 237.
- 2.3. Spooner, R. B.: Using a Reactor Simulator for Design Analysis. Nucleonics, vol. 12, no. 4, April 1954, pp. 36-39.
- 2.4. Boksenbom, A. S.: Some Preliminary Analyses of Reactor Kinetics and Control. Supplement I to NACA Reactor Facility Hazards Summary. To be published.



### SECTION 3. - SITE

#### 3.1 ACCESS TO SITE

The proposed site, in the Plum Brook Ordnance Works, lies three miles south southeast of the city limits of Sandusky, and approximately four miles from the center of population. The site is surrounded by excellent major highways (see fig. 2.1). Immediately to the west of the site and serving the site area with a spur, is the Baltimore and Ohio Railroad, entering Sandusky from the south.

Travel and truck movements to and from Sandusky and the reactor site on any side appear feasible during an emergency.

#### 3.2 EXISTING USES OF SURROUNDING AREA

##### 3.2.1 Plum Brook Ordnance Works

The Plum Brook Ordnance Works was constructed in 1941 and 1942 for the U.S. Army and was used for TNT and pentolite manufacturing and for ammunition storage. The area is presently inactive except for the ammunition storage area which is being used by the Erie Ordnance Depot, Port Clinton, Ohio.

The relation of the reactor facility to the Plum Brook Ordnance Works is shown in figure 3.1. The reactor facility is located in what formerly was the pentolite manufacturing area. This area will be decontaminated to a condition 5X (fit for civilian use). The areas designated "A," "B," and "C" were formerly TNT manufacturing areas and are now inactive. Area "A" has been decontaminated by Ravenna Arsenal, Inc., 16,000 pounds of TNT being removed in the process.<sup>1</sup>

The magazine storage area is also shown on figure 3.1. This area contains 99 igloos which are of reinforced concrete construction and earth covered. They are limited in storage capacity to 250,000 pounds of TNT (or equivalent) each.<sup>2</sup> The ground shock accelerations and displacements and the air blast which would be produced at the reactor facility due to an accidental explosion of one of the igloos are discussed in section 6.3.7.

##### 3.2.2 Area External to the Plum Brook Ordnance Works

As is shown on the aerial mosaic (fig. 3.2), to the west, south, and east of the Plum Brook Ordnance Works the land is used primarily for

---

<sup>1</sup>Personal communication from Mr. H. M. Krengle, General Manager, Ravenna Arsenal, Inc., Apco, Ohio.

<sup>2</sup>Personal communication from Mr. Joseph Fernan, Erie Ordnance Depot.

farming. North of the reactor site is a suburban residential and manufacturing area of Sandusky.

The following list of manufacturers was compiled from "Directory of Ohio Manufacturers, 1954," as published by the State of Ohio, Department of Industrial Relations. Of the companies listed for the immediate area 29 employ 50 or more people and are listed in the table. Fifty-six companies employ less than 50 each and have a total employment of 731 (7 percent of total) for an average of 13 employees each.

TABLE 3.1. - MANUFACTURERS IN SANDUSKY AREA

Company	Industry	Number of employees	Distance from site, miles	Direction
Waldock Packing Company	Meat Packing	91	3.15	NNW
Lake Erie Canning Company	Canning	83	3.33	NNW
General Motors Corporation, New Departure Division	Ball and Roller Bearings	2671	3.44	NW
Ford Motor Company <sup>a</sup>	Auto Parts	2000	3.50	NW
Esmond Dairy Company	Dairy	72	3.72	NNW
American Crayon Company	Art Supplies	279	3.93	NNW
Flexible Conveyor Company	Conveyors	52	4.00	NW
Brown Industries, Inc.	Foundry	108	4.00	NW
Sandusky Baking Company	Baking	56	4.15	NNW
Diamond Fertilizer Company	Fertilizer	71	4.23	NNW
Universal Clay Products Company	Electrical Insulator	116	4.36	NNW
Farrell Cheek Steel Company	Foundry	429	4.36	NNW
Apex Electrical Mfg. Company	Appliances	697	4.40	N
Lyman Boat Works, Inc.	Boat Building	161	4.44	NNW
Armour Fertilizer Works	Fertilizer	105	4.45	NNW
Barr Rubber Products Company	Rubber	310	4.45	NNW
Industrial Nut Corporation	Bolts and Nuts	135	4.59	NW
Stephens Printing Corp.	Printing	72	4.83	NW
Sandusky Newspapers, Inc.	Printing	69	4.86	NNW
Sandusky Foundry & Machine Co.	Foundry	171	4.94	NNW
G & C Foundry Company	Foundry	63	4.97	NW
Union Chain and Mfg. Company	Power Transmission	272	5.00	NNW
A. H. Vogel and Company, Inc.	Candy	93	5.05	NNW
Sandusky Metal Products, Inc.	Metal Furniture	72	5.05	NNW
Hinde & Dauch Paper Company	Paper	681	5.10	NNW
Scott Paper Company	Paper	119	5.10	NNW
Aluminum & Magnesium, Inc.	Smelting	272	5.30	NW
Celotex Corporation Paper	Paper	56	5.50	SE
Medusa Portland Cement Company	Cement	207	8.60	NW
Total Estimated Workers:		9583		

<sup>a</sup>Plant currently under construction. Employees estimated.

The New Departure Division of the General Motors Corporation Bearing Plant employing more than 2500 persons is being followed by a Ford Motor Company small parts plant now under construction which it is estimated will have over 2000 employees. This trend is expected to continue particularly after completion of the St. Lawrence Seaway which will result in increased shipping on the Great Lakes and greater commercial and manufacturing activities in and around the lake port cities.

### 3.3 POPULATION DISTRIBUTION SUMMARY

The population distribution for different directions and distances from the reactor site is indicated in table 3.2. These values are estimated from the 1950 Census Bureau Tabulation.

TABLE 3.2. - POPULATION DISTRIBUTION

Radius, Mi	NE Quad	SE Quad	SW Quad	NW Quad	Totals
0 - 1	<sup>a</sup> 100	---	---	50	150
1 - 2	300	100	100	200	700
2 - 3	800	80	250	<sup>c</sup> 2,300	<sup>c</sup> 3,430
3 - 4	<sup>b</sup> 510	310	280	<sup>b</sup> 6,150	<sup>b</sup> 7,250
4 - 5	<sup>b</sup> 320	450	300	<sup>b</sup> 21,870	<sup>b</sup> 22,940
5 - 6	540	680	330	<sup>b</sup> 2,430	<sup>b</sup> 3,980
	2570	1620	1260	33,000	38,450

<sup>a</sup>Distance to nearest residence is 3200 feet.

<sup>b</sup>Includes a part of Sandusky.

<sup>c</sup>Includes State of Ohio Soldiers and Sailors Home.

Five to six mile areas to the northwest, the direction of greatest population, are largely in Sandusky Bay; to the northeast, downstream of the prevailing winds, they are largely in Lake Erie.

The city of Sandusky as presently constituted has a very limited area available for new commercial or housing construction. A recent attempt to enlarge the city limits to the south in Perkins Township was defeated by vote. Since waterfront areas are already built up, new manufacturing plants are being located south of the city. The largest of such expansion has been to the southwest - General Motors, New Departure Bearing Division Plant, and the Ford Motor Company small parts plant under construction. As new industries are established, additional commercial and housing construction will be required to serve the people drawn to the area. It appears that such construction being, in effect, an enlargement of Sandusky would be uniformly distributed in an arc to the south of the city and lying north of the Plum Brook Ordnance Works.

No attempt to estimate the future growth of the area is made but the census figures for the city of Sandusky (going back to 1900) are listed below:

1900	19,664
1910	19,989
1920	22,897
1930	24,622
1940	24,874
1950	29,375

The total county population for 1940: 43,201 and for 1950: 52,565, which indicates that for this ten year period the rate of increase in population in the county as a whole was slightly greater than for the city of Sandusky.

### 3.4 METEOROLOGY SUMMARY

The U.S. Weather Bureau, Scientific Services Division, has prepared a report on the meteorology for the proposed site. This report is included as appendix C.

Figure 3.3 summarizes the frequency of surface winds from various directions for each season of the year and figure 3.4(a) shows the annual average for all observations. Due to the location of the recording stations in an urban area and the high percentage of low velocity readings the corresponding mean wind velocities have been omitted. It will be noted that southwesterly winds are predominant with 55 percent of the winds occurring from the directions south through west. Downwind of the site southwesterly winds pass over relatively sparsely populated areas and reach Lake Erie within  $4\frac{1}{2}$  to 5 miles. Winds from the southeast which would present the greatest hazard to Sandusky have the smallest frequency occurring 5 percent of the time for all season. During summer nights this increases to 7 percent and for winter nights to 6 percent.

As pointed out in the meteorological report, there is no major shift in surface wind patterns during precipitating weather. Since the frequency of wind, by directions, is virtually identical with the annual frequencies, no special consideration has been given the direction of travel of "washed out" material or accelerated "fall out." Figure 3.4 shows annual wind frequencies for (a) all observations and (b) annual wind frequencies during precipitation.

Atmospheric stability has been examined using measurements made at Toledo, Ohio. Since inversion and wind direction data are from different stations no plot of frequency of occurrence with wind direction is presented. However, this data is believed to give a fair qualitative picture

of conditions at the proposed site. It is apparent that daytime inversions while not too infrequent are almost entirely eliminated by daytime heating during the summer seasons and probably occur less than 10 percent of the time from the south and southwest for other seasons. Night-time inversions are more frequent with the greatest frequency from the south through west similar to the wind direction frequency.

Upper air wind roses recorded at Cleveland, Ohio (ref. 3.1), are shown in figures 3.5(a) and (b) for different altitudes and seasons. It is seen that during fall and winter the prevailing wind directions change from the southwest to the west with increasing altitudes. During spring and summer the change is from the southwest to the northwest with increasing altitude. The average upper air wind velocities are greatest during the winter season.

More than 75 percent of the recorded surface wind speeds are between 4 and 12 mph with an average speed of 9.7 mph. The strongest winds occur in the winter and spring. Peak wind speeds exceeding 50 mph have been recorded for all months except May with the highest recorded speed of 77 mph occurring in June.

The area is subject to summer thunderstorms and a rare storm may cause winds in excess of 50 mph, 1 to 3 inches of rain in an hour and hailstones 1/2 inch or larger in diameter. Similarly tornadoes are a probability in the area. The Weather Bureau report notes that over a 35 year period 111 tornadoes occurred in Ohio with the largest percentage in the northern and western portions of the state.

### 3.5 GEOLOGY SUMMARY

The U.S. Geological Survey, Water Resources Division, has prepared a memorandum on the geology and hydrology for the site. This report is included as appendix D.

The site area is situated in the Lake Erie drainage basin on a very flat plain at an elevation of about 630 feet, 65 feet above Lake Erie.

The surface drainage from an area of approximately 23 acres immediately surrounding the facility will be impounded by dikes and released to Plum Brook through a monitored discharge.

Test borings taken at the site indicate that limestone bedrock lies twenty-five (25) feet below the surficial deposit of lacustrine clay and glacial till. At 61 feet below the surface the bedrock becomes sandstone. The lower level of the excavation will be 52 feet below grade.

## 3.6 REFERENCE

- 3.1 Airway Meteorological Atlas for the United States. U.S. Department of Commerce, Weather Bureau, Washington, D. C., 1941.

#### SECTION 4. - EXPERIMENTS

The large variety of in-pile experiments necessary to the development of a nuclear reactor for flight application calls for a large variety of test holes in and around the research reactor core. For materials development and radiation effects work, relatively small experiments in high fast neutron-flux fields are desirable. Small pumped loop experiments in which ionizing effects on corrosion compatibility of materials and coolant are simulated also require high fast neutron fluxes and relatively small test space. Experiments such as these are best conducted within the active lattice of the critical assembly. On the other hand, experiments on complete fuel elements or representative sections of a prototype reactor require simulated heat generation rate and radiation effects. For such experiments high thermal neutron fluxes and relatively large test volumes are required which are generally available outside of the active lattice.

As described in section 2.1, the 9-inch diameter horizontal through hole (HT-1) is the prime irradiation facility outside of the active lattice. The proximity of the water quadrants permits the insertion of complete self-contained experiments into this through hole with auxiliary equipment installed in the quadrant under water. Such experiments do not necessarily use the through-hole feature but are likely to have a two-pass primary coolant system so that only one quadrant need be used. The smaller in-pile experiments may be inserted in the center test space vacated by a shim-rod fuel element in the LC-6 position of the active lattice. These consist of 3-inch square special experimental assemblies.

There are in all some 43 test holes around the core into which experiments may be inserted. The designation, number, and size of these are listed in table 4.1.

TABLE 4.1 - EXPERIMENTAL TEST HOLES

Type	Designation	Number	Size, in.
Horizontal through hole	HT	2	9 ID
Horizontal beam hole	HB	3	6 ID
Vertical center hole	LC-6	1	3 sq.
Vertical hole	V	2	8 ID
Thermal column	TC	1	41 OD
Reflector hole	R	28	3 ID
Hydraulic rabbit	RH	4	.75 ID
Pneumatic rabbit	RP	2	.75 ID

#### 4.1 DESIGN OF TYPICAL EXPERIMENTS

The testing of fuel elements to failure requires that the failure of the element presents no hazards to the safety of operation of the facility and that all radioactivity be contained within the experimental equipment. When the test loop becomes contaminated, it must be readily removed from the test hole and handled by remote operating techniques.

These requirements are fulfilled by using a closed coolant loop with the test fuel element located in the horizontal through hole and the auxiliary pumping and heat removal equipment sealed in a large container located in one of the water filled quadrants. With a closed circulating coolant loop of satisfactory design, the activity may be contained within the loop. The coolant flow may be maintained during removal of the experiment from the facility to prevent further damage to the test. The entire loop experiment may then be moved to the reactor canal and allowed to cool as long as required without interfering with the installation of a new experiment in the same test hole.

Three representative experiments have been conceptually designed and are herein described. Two of the experiments, an air-cooled and a liquid-cooled fuel element pumped loop test have been designed for the HT-1 hole. A third capsule experiment for determining radiation effects on corrosion has been designed for insertion into a reflector test hole or in the vertical center hole. The first two experiments were chosen as being typical of the larger gas and liquid-cooled fuel element tests that would be conducted in the HT-1 hole and were selected to point up the problems and attendant hazards.

The reactivity effects and heat generation distributions for the air-cooled experiment in the horizontal through hole and for a fueled and unfueled experiment in the vertical center test hole have been evaluated.

To augment the present reactivity calculations, an experimental program with the Bulk Shielding Reactor at Oak Ridge National Laboratory was jointly planned and executed by BSR and NACA personnel. In these experiments the NACA core loading was mocked up to within the limits of excess reactivity and materials available to BSR. A 7x3 slab loading of 140 gram fuel elements reflected by rows of canned beryllium oxide followed by water provided 2.5 percent excess reactivity. This loading permitted the measurement of reactivity effects of compositional changes in the location of the center fuel element corresponding to the center test hole location in the NACA core. The worth of fuel plates, water passages, and void spaces at various positions along the reactor height were experimentally determined. A complete description of these reactivity measurements and the results obtained is presented in supplement III (ref. 4.1) to this report.



It is recognized that the safe and efficient operation of an aircraft reactor component research facility requires that the reactivity effects of all experiments be known accurately. The theoretical evaluation of reactivity effects of experiments is analytically difficult and limited. It is, therefore, essential that the worth of experiments are determined in temporary position in the reactor proper at zero power, or that another facility, such as a Reactivity Measurement Facility, be made available at the reactor site. The characteristics of such a facility are being explored.

In this section, the experiments, auxiliary loop equipment, and loop operation will first be discussed. This will be followed by a presentation of the reactivity effects of these experiments, the reactor neutron flux distributions, and the specific power distributions in the experiments for normal operation.

#### 4.1.1 Air-Cooled Fuel Element Experiment

The air-cooled fuel element considered is presumed to be a representative subassembly of an air-cooled reactor. The fuel element may be composed of metallic fuel plates surrounded by a suitable solid moderator. The element may be about 3 to 4 inches in diameter and 2 to 3 feet long and is cooled by air which is recirculated in a closed loop.

The arrangement of the experiment in the horizontal through hole is shown in figure 4.1. This particular experiment is smaller than the diameter of the HT-1 hole and hence an eccentric beryllium collar is inserted to position the experiment in the hole. The fuel element and moderator is surrounded by three concentric stainless steel tubes. The air for cooling the element enters the annulus formed by the inner and middle tubes at the quadrant end of the thimble and flows past the test section where it reverses direction and flows back through the fuel element. A honeycomb and screen combination straightens the flow before entering the fuel element. Part of the air bypasses the fuel element to cool the moderator. The middle and outer tubes are sealed at both ends to form a double closure to prevent any fission fragments or gases from escaping outward into the water cooled clearance space between the experiment and the permanent aluminum thimble. By the same token, these stainless steel tubes prevent the water from entering the cooling air annulus and cooling passages of the experiment. In the event of a melt down of the fuel element, the steel tubes prevent the molten metal from making contact with water.

The volume enclosed by these tubes is filled with a monitoring gas and a porous media such as carbon or beryllium oxide powder. The thermal conductivity of these materials is sufficient to conduct the heat generated by gamma absorption to the cooling water flowing between the outer stainless tube and the aluminum thimble. These porous media also permit

the after-heat generated in the fuel element to be conducted away more readily when the experiment is removed to the canal. If a better insulating material were used, the cooling air would have to be kept circulating for longer periods until the after-heat had decayed to a lower value.

In order to size the auxiliary equipment and to design the experiment so that the temperature of the outer stainless steel wall is well below the boiling point of water in the annular water passage, a nominal sub-assembly operating power of 1 Mw was selected with operating temperatures consistent with material limitations.

In order to determine the temperature profiles across the experiment and the amount of heat to be removed by the cooling water, it was assumed that the materials in the experiment exclusive of the test element were subjected to a uniform combined neutron and gamma internal heat generation rate of 12 watts per gram. For these conditions the amount of heat transferred to the water is 0.15 Mw.

4.1.1.1 Description of auxiliary equipment. - The equipment for circulating the cooling air and removing the heat from the air is sealed in a tank 6 feet in diameter and 10 feet long located in the quadrant as shown in figures 4.1(b) and (c).

The pumping system includes two centrifugal compressors operating in parallel, pumping twice the required flow rate. One-half of the flow is bypassed through a throttling valve and cooler, which removes the heat produced in compressing the air. The air required to cool the fuel element passes through a pressure regulating valve and flowmeter to the test. The heated air leaves the test, passes through two water-cooled, shell-and tube-type heat exchangers connected in series, and then flows through a monitored filter. The air then returns to the compressors. Some of the air bypasses the coolers and is used to regulate the compressor inlet temperature.

The size and required utilities for the loop components are listed in table 4.2. A block diagram of the safety and control instrumentation is shown in figure 4.2(d).

4.1.1.2 Operation of air-cooled experiment. - The experiment is assembled and the equipment operated prior to installation in the quadrant. The experiment is then lowered into the quadrant and fastened to the rails which align the experiment with the thimble. The instrumentation and control leads and the utility lines are connected, and the equipment further checked. The experiment is moved forward into the thimble and sealed with a lock ring, shown in figure 2.11(a), that can be operated remotely. The cooling water is connected and the flow rate checked. The circulating air system and the gas volume inside the experiment containment tank are precharged with air via the main supply system to the operating pressure level at the compressor inlet. With cooling water for the experiment set

at the design flow rates, the quadrant is flooded with water. The air compressors are started and the system is checked at design conditions of flow rate and pressure. The experiment is then ready for the start-up of the reactor.

TABLE 4.2 - EQUIPMENT SIZES AND UTILITY REQUIREMENTS

Pumping unit:	
Number required	2
Over-all length	5 ft
Maximum diameter	2 ft
Compressor tip diameter	17 in.
Compressor ratio	1.2
Compressor speed	7200 rpm
Drive motor type	Induction
Power required at 480 volts	45 kw
Motor speed	3600 rpm
Cooling water flow rate	10 gpm
Main cooler:	
Number required	2
Diameter	1 ft
Length	8 ft
Cooling water flow rate	80 gpm
Bypass cooler:	
Number required	1
Diameter	1 ft
Length	6 ft
Cooling water flow rate	30 gpm
Filter:	
Number required	1
Diameter	1 ft
Length	2 ft
Equipment container:	
Diameter	6 ft
Length	10 ft
Piping size	4 in.
Over-all length of experiment	19 ft

The various tie-ins of the experiment with the reactor and the alternatives available to the operators for normal operation and in case accidents occur or equipment malfunctions during the experiment will be described in an operating manual for the experiment to be prepared upon completion of the design of the experiment.

Upon completion of the test, the reactor is shut down, the thimble quadrant seal is removed and the experiment is backed out of the thimble. The experiment is then moved to the rear of the quadrant with the compressors and coolers still in operation. The after-heat will have decayed sufficiently, 180 hours after the reactor has been shut down, that the air compressors can be stopped. The after-heat is then transferred to the stagnant water by conduction.

After a suitable cooling-off period, the experiment is moved to the hot lab where an approved procedure is followed for dismembering the experiment and removing the test fuel element for inspection and analysis. Methods of disposing of used experimental fuel elements is discussed in Section 5.2.4 and methods of decontaminating the loop equipment before it is used for another test is discussed in Section 6.2.3.

#### 4.1.2 Liquid-Cooled Fuel Element Experiment

A representative liquid-cooled fuel element irradiation experiment is shown in figure 4.2(a). The fuel elements consist of metallic pins which may be as long as 2 feet. The liquid coolant indicated is metallic sodium which is recirculated in a closed loop. The fuel pin assembly is located inside an annulus of beryllium moderator. The fuel pins and moderator are enclosed by three concentric stainless steel tubes. The successive annuli making up the test are: 3/16-inch sodium passage, 1/16-inch stainless steel container, 1/8-inch monitoring gas and porous medium of carbon or beryllium oxide powder, and 1/8-inch stainless steel container. Sodium flows through the annulus and then over the fuel pins.

To establish temperature distributions in the experiment and to size auxiliary equipment, a nominal subassembly operating power of one Mw was selected. Operating temperatures were selected to be consistent with material limitations.

Again a combined neutron and gamma internal heat generation rate of 12 watts/gram of materials in the experiment exclusive of the test was assumed.

Primary water at 160 pounds per square inch pressure is used to cool the experimental insert. The outer surface temperature was held at 250° F. This clearance space coolant makes a once through pass over the test entering at one end of the HT-1 hole and discharging at the other end. Other coolants which do not react with sodium are being studied. Approximately 0.15 Mw are removed with a water flow rate of 19 gpm and a corresponding temperature rise from 80° to 145° F. The water velocity in the 1/8-inch clearance annulus is 3.5 feet per second.

4.1.2.1 Description of auxiliary equipment. - A schematic of the sodium loop are shown in figures 4.2(b) and (c). The system is charged

from the sump tank which contains 10 gallons of filtered sodium. Liquid sodium is circulated through the system at the rate of 40 gallons per minute by two canned rotor pumps connected in parallel. Each pump is capable of maintaining full flow rate in the loop so that failure of one pump may be tolerated. Since the canned rotor pumps are driven by induction motors, flow rates must be controlled by throttling. Valves are located before and after each pump so that either can be isolated from the loop.

After flowing through the test, sodium passes to a pair of sodium-to-air heat exchangers connected in parallel. The heat exchangers are of the shell-and-tube design with sodium as the shell fluid and each is capable of transferring 1.3 Mw of heat. A total of 350 tubes, 1/4-inch outside diameter by 1/16 wall, is required for each heat exchanger. Spaced in a triangular array on 3/8-inch center-to-center distance, the heat exchanger dimensions are 7 inches outside diameter by 21 inches long. Valves located before and after each exchanger control the fluid flow and can isolate either heat exchanger from the system in event of a tube failure.

Sodium enters the heat exchangers and is cooled by counter-flow air. Piping connecting the components is 1.75 inches outside diameter. The entire system is welded, with expansion loops located before each pump and between the test and heat exchangers. All piping and components containing sodium are wrapped with beaded nichrome wire to preheat the system. The test tank is connected to the thimble by a lock ring shown in figure 2.11(a).

Each sodium pump has a capacity of 100 gpm, which is approximately twice the design sodium flow rate. Each heat exchanger has a capacity of 1.3 Mw at design temperatures and flow rates. These oversize units are to be installed to allow for normal shutdown in the event of a failure of one component. Total air, water, and electric power required are listed below:

Air	7 pps at 100 psi
Water	2 pps at 160 psi
Electricity	30 kw at 220 volts - 3 phase

A block diagram of the safety and control instrumentation is shown in figure 4.2(d).

4.1.2.2 Operation of sodium-cooled experiment. - The test loop must be thoroughly inspected during assembly. A Freon leak detecting unit is used to insure that the system had been properly welded. All piping and component exposed to sodium is then cleaned. The loop is purged with argon and filled with an initial charge of sodium. Liquid sodium is circulated to remove all oxides and foreign matter within the loop. The sodium is drained from the loop and disposed of.

The loop is again purged and filled with clean sodium and circulation is started. All instrumentation and controls are checked. A sample of sodium is extracted from the system and analyzed for its oxygen content.

After all checks on leaks, sodium purity, and operations of instrumentation and controls have been made, the heated loop with sodium in circulation is inserted into the HT-1 hole. The sodium flow is adjusted for a flow rate of 40 gallons per minute. Coolant flows in the experiment clearance space are set and the quadrant filled with water. The reactor is started and as the power level is increased, the air flow to the heat exchangers is proportionately increased to remove the heat generated in the core of the test. Final adjustments are made when the one megawatt power level has been reached.

After completion of the test, the reactor is shut down and the sodium flow is maintained for an additional 1.5 hours, at which time the power level has dropped to 10 kilowatts. The experiment is then removed from the hole and allowed to cool in the quadrant. To prevent the fuel pins from melting down, sodium must cover the fuel pins. Before the pumps are shut off, the valves before and after the test are closed. Heat is transferred to the water in the quadrant by boiling until the after-heat generated has reached the 8 kilowatt level; then all the heat is transferred by natural convection.

The sodium-cooled experiment can be removed from the water 50 hours after the reactor has been shut down, and cooled by natural convection in air. The power level will then be approximately 2.5 kilowatts and the temperature of the outer stainless steel and core will be 1050° and 1150° F, respectively. After the experiment has cooled sufficiently, the valves are opened and the sodium is drained into the sump, and the experiment is removed to the hot lab.

#### 4.1.3 Reflector Test Hole, Capsule Experiment

A representative capsule experiment has been designed to determine the effect of a corrosion inhibitor in the presence of a radiation field. An experiment containing 4 capsules was selected. Weight loss of corrosion specimens from in-pile tests is compared to tests conducted out of pile.

4.1.3.1 Description of equipment. - A cross sectional view of the experiment is shown in figure 4.3. Each capsule is  $\frac{3}{8}$ -inch diameter by  $\frac{1}{16}$ -inch wall by 6 inches long, and contains 3.2 grams of the test media plus a corrosion specimen. Two of the capsules have an addition of a corrosion inhibitor. The remaining two capsules are control capsules.

The capsules are heated over their filled length by four furnaces. Each furnace consists of a  $\frac{7}{16}$ -inch diameter, by  $\frac{1}{32}$ -inch wall,  $2\frac{1}{4}$  inches long Inconel tube wound with two Calrod type heating coils. The first coil is wound from the bottom of the furnace tube to within  $\frac{3}{4}$  inch from the top, while the second coil is wound about the remaining  $\frac{3}{4}$  of an inch and acts as a guard heater.

The four furnaces are fixed to a  $2\frac{3}{8}$ -inch diameter Inconel plate, and are equally spaced about a circle of  $1\frac{1}{4}$ -inch diameter. The plate is then welded into the bottom of a  $2\frac{3}{8}$ -inch diameter Inconel can, 9 inches long to form a sealed unit. A 3-inch diameter hole bored in a beryllium reflector piece, allowing a  $\frac{5}{16}$ -inch cooling annulus, receives the unit for the test.

Cooling is provided by a capsule cooling line which enters through the top of the can and an annulus cooling line which is vented to the space between the plate and the bottom of the test hole. The capsule cooling air exits through a line welded to the center of the plate, which vents to the space above the can.

Electrical connections for the heaters are brought through the plate by means of machine screws which are insulated from the plate.

Temperature measurements are taken by ten chromel-alumel thermocouples. Each capsule has one thermocouple imbedded in its base and another fixed to the wall to correspond to the test media interface. Two additional thermocouples are attached to the outside of the Inconel can.

A  $\frac{3}{4}$ -inch aluminum tube carries all lines from the test hole out of the reactor tank. At this point the exit air goes to the stack and the remaining air, electrical, and thermocouple lines go to the control point.

Instrumentation consists of a strip chart recorder to read temperatures, a bank of eight variable autotransformers connected in parallel to give eight variable lines and one common line, and valves and pressure gages for control of the cooling air.

4.1.3.2 Operation of the capsule experiment. - The test is completely assembled and checked in the shop, moved to the reactor, rechecked and lowered into the reflector. Connections are made at the control point and the test given a final check. Once the reactor comes to steady state, the heater power and the cooling air are adjusted to give the required temperatures.

If the duration of the test is less than that of reactor power cycle, the furnaces are shut off and the capsule temperatures are held below 600° F by the cooling air until reactor shutdown. At the end of the reactor power cycle, the test is removed to a hot lap where the specimens are extracted for weighing.

#### 4.2 REACTIVITY EFFECTS OF EXPERIMENTS

The air-cooled and liquid-cooled experiments, as modified for two-group diffusion-theory calculations on the two-dimensional reactor simulator are described. The reactivity effects of the air-cooled experiments as normally inserted in the horizontal through-hole are presented. The reactivity effects of a liquid-cooled experiment, with and without fuel, inserted in the center test hole are also presented. Illustrative neutron flux and specific power distributions are given for some of the experiments.

The excess reactivity required by these experiments must be considered in the light of the  $\Delta K$  available. The particular loading for the reference core has tentatively allocated a  $\Delta K$  of 0.05 for experiments. It will be shown that some of the experiments which have been discussed use up the greater part of this allocation. In this case, only one of these experiments would be the major experiment in a particular core loading.

##### 4.2.1 Air-Cooled Through-Hole Experiment

For purposes of calculation on the two-dimensional simulator, the experimental space comprising HT-1 facility was modified to a square geometry 9-inches on a side with 3/4-inch thick zones of different composition as shown in figure 4.4. The HT-1 facility is taken as being separated from the face of the core by  $1\frac{1}{2}$  inches of a beryllium-water region simulating the water-cooled beryllium box surrounding the core. Annular zone 1 contains the aluminum thimble walls and clearance space cooling water. Zone 2 simulates the eccentric water-cooled beryllium insert used to locate the experiment. Annular zone 3 contains the stainless steel experiment container walls, the first pass for the experiment cooling air, and a porous material. This porous material is assumed to have the nuclear properties of beryllium oxide of 20 percent theoretical density. Annular zone 4 contains a portion of the test fuel-element moderator. Finally,



the central fertile zone 5, which is 3 inches on a side, contains the air-cooled fuel elements. Fully enriched uranium fuel is present in zone 5 in the concentration of  $0.00030 \times 10^{24}$  atoms per cc of experiment.

In each zone the contents were homogenized and the two-group diffusion solutions obtained on the two-dimensional simulator. The two-group diffusion parameters used for each zone are given in table B.2 of appendix B.

The over-all geometry of a vertical section of the reactor is shown in figure 2.24. Two positions of the air-cooled fuel element test were taken: the first in which the stainless steel container (zone 3) and contents were directly against the wall of the HT-1 thimble, as shown in figure 4.4; the second in which zone 3 and contents were further separated from the face of the core by the eccentric beryllium insert. The particular air-cooled test studied was assumed to be at appropriately high average temperature. Because of the relatively small size of the experimental region, it was not considered likely that the thermal neutrons would be in equilibrium with this high temperature. The average temperature of neutrons were taken therefore, to be the same as the neutrons in the reactor core.

The values of  $K_{\text{eff}}$  for the unperturbed case and for the two positions of the air-cooled experiment in the horizontal through-hole are shown below. (The calculations have assumed the experiments to be effectively the same length as the 27-in. length of the core):

Configuration	$K_{\text{eff}}$
Unperturbed reference core	1.185
Air-cooled test in HT-1 closest to core	1.158
Air-cooled test in HT-1 farthest from core	1.163

The fast and thermal neutron flux distributions obtained for the air-cooled fuel element test closest to the core are shown in figures 4.5(a) and (b). The thermal fluxes in the core on the side of the experiments are depressed. The fluxes at the opposite core-reflector interface are relatively unperturbed. In the vicinity of the experiment, the significant fission rate of the fertile region boosts the fast fluxes in the reflector around the through-hole. There is a subsequent slowing down and conversion to thermal flux in the surrounding primary reflector. The relatively high absorptivity of the experiment shows up as a sink for the thermal neutrons.

These flux distributions may be compared to the unperturbed flux distributions which have been shown in figures 2.26(a) and (b). The

unperturbed fluxes at the position of the experiment indicate significantly higher thermal fluxes and significantly lower fast fluxes than exist in the core. Therefore, it would appear that an experiment inserted here would not be exposed to a desirable spectrum of fluxes. This may be true for an experiment which did not contain fuel. However, for the fertile experiments studied, which contain fuel concentrations representative of their prototype reactor, the flux distributions of figures 4.5(a) and (b) indicate a significant increase in fast flux and a strong depression in the thermal neutron flux in the experimental regions. It is interesting to note that the excellent moderating properties of the beryllium-water reflector surrounding the experimental through-hole feed thermal neutrons into the experiment from all sides. This reduces the asymmetry of thermal flux across the experiment. The fast flux has about a 15 percent fall-off across the experiment.

The variation in specific power for the air-cooled fuel element experiment in HT-1 closest to the core is shown in figure 4.6(a). The specific power is shown relative to an average specific power in the reactor core of unity and has an average value of 0.49 over the test fuel element. The minimum specific power occurs somewhat removed from the geometric center of the experiment. The maximum-to-average specific power in this experiment is 1.35.

The variation in specific power for the air-cooled fuel element experiment in HT-1 farthest from the core is shown in figure 4.6(b). Average specific power in the test fuel element relative to unity in the reactor core is 0.38. The maximum-to-average specific power in this experiment is 1.45.

#### 4.2.2 Liquid-Cooled Center Test Hole Experiment

The reactivity effects of a liquid cooled experiment for insertion in the center test hole position of the core have been calculated. The experiment may or may not contain fuel.

The composition and geometry used is shown in figure 4.7. Two  $\frac{3}{8}$ -inch zones and a central experiment  $1\frac{1}{2}$  inches in diameter were selected. The first outer zone contains an aluminum thimble and cooling water in the space between the experiment and adjacent core fuel assemblies. The second zone contains stainless steel, thermal insulation and a cooling or monitoring gas passage. The central zone contains a medium consisting of 0.90 liquid and 0.10 metal by volume. Two cases have been considered:

1. Fully enriched uranium fuel is present in the concentration of  $0.00020 \times 10^{24}$  atoms per cc of experiment.

2. The experiment does not contain fuel, but contains absorber of the composition cited above. This composition was taken to represent a passive in-pile irradiation.

The over-all geometry of a horizontal section of the reactor is shown in figure 2.25. The two-group diffusion parameters used are given in tables B.1 and B.2 of appendix B. Although these nuclear parameters are based on the experiment at an appropriately high average temperature, thermal neutrons were assumed to be in equilibrium with the average core temperature.

The values of  $K_{\text{eff}}$  for the unperturbed case and for the two compositions of the center test hole experiment core are given below:

Configuration	$K_{\text{eff}}$
Unperturbed reference core	1.185
Experiment with fuel	1.165
Experiment with absorber	1.150

The greater depression of both fast and thermal fluxes in the region around the center test hole for the experiment with absorber results in a lower  $K_{\text{eff}}$  of 1.150. This highly absorptive experiment would use a large part of the excess reactivity allocated to experiments.

The effect of the fueled center test hole experiment on the reactor neutron fluxes is illustrated by cross plots taken from the two-dimensional flux distributions obtained. The fluxes at the midplane of the core along the core length and core width for the unperturbed reference core and for the fueled experiment in the center hole are shown in figures 4.8(a) and (b). The fluxes are relative to an average thermal neutron flux of unity over the core volume. The fluxes are significantly lowered in the core in the immediate vicinity of the experiment; the fluxes are relatively unperturbed outside of the core.

The variation in specific power in the fueled experiment was perfectly symmetrical and, for the fuel concentration employed, resulted in an experiment average specific power of 1.0 relative to a core average specific power of unity. The ratio of maximum-to-average specific power across the  $1\frac{1}{2}$ -inch diameter experiment was 1.07.

## 4.3 REFERENCE

- 4.1. Bogart, D., and Hallman, T.: Reactivity Measurements with the Bulk Shielding Reactor. Supplement III. NACA Reactor Facility Hazards Summary. To be published.

## SECTION 5. - HANDLING OF FUEL AND RADIOACTIVE MATERIALS

The disposal and handling problems to be discussed here are those to be expected in normal operation of the reactor facility. This normal operation includes those minor accidental situations that must be expected from time to time owing to personnel errors or equipment failure.<sup>1</sup> All of these problems are both administrative and technical in nature.

The disposal of radioactive materials must be predicated on the philosophy that no undue hazard will be presented to the present or succeeding generations of people in the area. To this end the NACA intends to abide by the legal maximum contamination limits and exposures as set forth in the Federal Register (ref. 5.1). NBS Handbook 52 (ref. 5.2) will be used as an additional guide as well as any other publications of the National Committee on Radiation Protection which may become available and are pertinent. Accountability, safety, and security provisions of the AEC license will also be honored. Deviations from any of these provisions and limits will be made only with the prior approval of the AEC wherever it is humanly possible to do so. Obviously, this is not possible for accidents which are not anticipated and for which inadequate protective measures are provided.

Disposal problems can be approached from several points of view such as: administrative procedures, particular operations, the legal limitations, the contamination sources, the kinds and constitution of the radioactive material (gaseous, liquid, and solid), the contamination level, the disposal methods available, and accountability requirements. These are all interrelated, and there is no simple and unique method of presentation. Since many aspects of the facility operations have not been fully explored, it seems best to treat the various kinds of operations in a general way and indicate how some of the problems can be handled.

### 5.1 FUEL HANDLING AND DISPOSAL

The NACA fuel elements are substantially identical to those now used by the MTR (see fig. 2.7). As such, they can be handled, stored, and disposed of by procedures similar to those already tested and approved for MTR assemblies.

#### 5.1.1 Handling of New Fuel Elements

New fuel elements will be stored in movable racks holding 12 units each with 6 on either side. Each element and each rack carries an identifying number. Cadmium sheets are arranged on 3 sides of each fuel element

---

<sup>1</sup>Cleanup and disposal problems involving serious failures in the reactor facility and experiments are discussed in sections 6.1.9 and 6.2.3.2.

socket so that there is no possibility of a critical assembly with any number of filled racks even when surrounded by water. Each rack will have a simple locking device to hold all elements securely during transportation. The same type of rack will be used for underwater transportation of depleted or partially depleted fuel elements in the reactor shielding quadrants and the canals.

Racks containing new fuel elements will be stored in a locked vault requiring the simultaneous use of two separate keys for entry. These keys will be available only to the shift leaders of the Health Physics and the Facility Operation Sections, respectively. The vault will be located on the main floor of the reactor building. All fuel element receipts and releases, together with dates and identities thereof, storage rack number, radiation levels, order numbers, etc. will be entered in a bound log book (kept within the vault) by the Health Physicist responsible at the time of transfer. The vault lock design will permit key removal only when the door is closed and locked. When not in use, the two keys will be kept in separate door type safes provided with 3-tumbler combination locks, the combinations of both of which will not be known to any one individual.

This arrangement may provide a higher level of security and safety than is ordinarily required at isolated AEC reactor sites. Since the NACA reactor does not have such a large exclusion area, this added complication seems advisable as a precaution against deliberate mishandling by demented personnel. Such people do develop in every organization occasionally. These precautions are not interded as a substitute for good administrative controls, but they can assist these controls with very little added complication.

The new fuel elements are taken from the storage racks and individually placed in the reactor lattice grid positions by means of long-handled tools.

#### 5.1.2 Fuel Unloading Procedure

At the completion of a reactor operation cycle, the reactor is shut down and the main coolant pumps are shut off. The shutdown cooling system continues to operate with a flow rate of 1100 gpm in order to remove the after-heat. The 5000 gallon head tank is then isolated from the coolant system to permit reduction of pressure in the reactor tank. Any gases liberated by the water in this reactor tank at the lower pressure will be vented to the stack through a valve in the tank cover. The tank is then flushed out by opening the "high" drain and then admitting deionized water from either the 50,000 gallon head tank or one of the purge tanks mentioned in section 5.2.1.1.

The high drain is designed to prevent uncovering the core during the flushing operation, thereby ensuring the continued removal of after-heat by the shutdown cooling system. The reactor tank can be completely drained by the "low" drain.

After flushing, the 50,000 gallon head tank or purge tank is isolated and the water level allowed to drop to the level of the high drain. The shrapnel shield is then removed and the hatch to the reactor tank opened, allowing access to the fuel elements. The 1100 gpm shutdown cooling system continues to run during the entire unloading operation.

The fuel elements are individually removed by use of long-handled tools and are passed through the fuel element discharge chute shown in figure 2.9(b) to the receiving tube. The receiving tube is then rotated to a vertical position and the fuel element is removed and placed in an underwater transfer rack. Partially depleted fuel elements can be re-placed in the reactor lattice by reversing these steps.

### 5.1.3 Spent Fuel Element Handling

The underwater transfer racks containing spent fuel elements are moved under water from quadrant C to the canal extension in the reactor building. The fuel elements are then placed in stationary underwater storage racks.

The underwater storage racks are also cadmium lined and are designed so as to allow adequate free convection cooling of the fuel elements. These racks will be locked except when inserting or removing elements. The lock on each unit will require the use of a special key near the end of a metal pole for its operation, the same pole being used to handle the fuel elements under water once the rack is unlocked. The suggested key will consist of a simple combination of lugs attached to the pole such that a duplicate cannot be made readily and unnoticed. Each rack will have its own key pole. These poles will be stored in a locked holder adjacent to the canal when not being used for handling fuel elements. Two people with separate keys will be required to unlock this pole holder just as has been described for the fuel vault. A record will be kept of all element transfers, uses, and history.

The spent fuel elements will be allowed to cool in the underwater storage racks in the canal. A second rack will be used in the canal where spent fuel elements can be arranged for gamma irradiation experiments.

The fuel elements will be kept until they can be transported safely in MPR type coffins to a reprocessing plant. Before transfer of spent elements to a coffin, water samples from the vicinity of the storage rack will be monitored as a check on possible fission product leakage.

The off-site transportation of spent fuel elements will be in accordance with any applicable AEC requirements as outlined in the Handbook of Federal Regulations applying to Transportation of Radioactive Materials (ref. 5.3). Each shipment will be recorded and all fuel elements identified in the log book kept in the vault for unused fuel elements. This record will be maintained by the Health Physicist responsible for fuel element security and safety on the particular shift.

## 5.2 DISPOSAL OF RADIOACTIVE WASTE IN NORMAL OPERATION

### 5.2.1 Primary Water Contaminants

Aside from the very short lived  $N^{16}$  activity which determines the shielding requirements around piping, pumps, etc., the activity of the primary water is determined by its impurities, both solid and dissolved. Traces of these impurities are found in the supply water, other impurities result from corrosion within the primary system, and still others are due to recoils from the surfaces of core materials. No definitive information as to the attainable lower limits of these activities seems to exist for practical operating conditions. In most instances the reported activities pertain to systems in which the feed water was not deionized as well as present day practice will permit, nor was dissolved air removed before startup.

Using what are considered to be conservative values for supply and by-pass demineralizer effectiveness, corrosion rates, and recoil contribution, the equilibrium ionic concentrations in the reactor cooling water were calculated. These results, together with the individual activities due to these impurities for a 1000 hour run, are presented in appendix E. The big uncertainty lies in the assumed corrosion rates for the primary system components, plus the fact that there may be some active colloidal material which can pass both the strainer and the mixed-bed. If the corrosion rates chosen are conservative and a minimum of colloidal material is present, then the actual long lived activities should be less than those indicated. In this event, moderate dilution of the primary system water, after a reasonable holdup time, should render this waste suitable for off-site discharge.

MTR experience has demonstrated, however, that fission product leaks must be expected. Once this occurs, the primary system is likely to be so grossly contaminated that this simple disposal procedure may not suffice. Available data on demineralizer effectiveness in removing the last traces of activity are not very encouraging in this respect. For this reason, provisions are made for re-using the bulk of the primary system water over and over again so as to minimize the actual volume of primary water which must be discharged.



5.2.1.1 Activity retention. - All primary system leakage and excess purge water will be discharged to one of the retention tanks shown in figure 2.14. The bulk of the flush water will be discharged to one of a pair of purge tanks not specifically shown in this figure and which may replace one of the retention tanks. Ordinarily one of these tanks will be empty and the other filled with purge water from the previous cycle. At the end of a new cycle the full tank will supply the purge water and the second tank will receive the corresponding primary system discharge. These purge tanks can be vented to the facility stack.

This arrangement minimizes the amount of feed water which has to be demineralized, and also retains the bulk of any fission products which may be in the primary water. Moreover, it reduces the amount of long-lived corrosion or fission products which would otherwise appear in the laboratory waste water system.

When fission leaks occur, the primary system will first be cleaned up to a practical level by the by-pass demineralizer and degassifier units before the purge operation is attempted. In this way the bulk of the fission products will be removed in these units which are suitably shielded and otherwise arranged for eventual disposal of the activities involved. Any residual activities which this procedure contemplates will not be objectionable in the primary system in subsequent operating cycles. As a matter of fact, the primary system will always be contaminated by some fission products once a leak has occurred because some of these materials adhere most tenaciously to metal surfaces (see ref. 5.4).

The installed plumbing will also permit discharge of primary water to the hot retention tanks shown in figure 2.14, should this become advisable. This water can be further demineralized by the mixed-bed units shown in this drawing as explained in section 2.1.

5.2.1.2 By-pass degassifier. - All makeup water for the primary system will be deionized to specific resistances of between  $10^6$  and  $10^7$  ohms per cm by the mixed-bed units shown in figure 2.14 at the right of the 150-foot head tank. This water will be deaerated in the by-pass unit shown on the right side of figure 2.14 before or during the early part of each cycle. The flow capacity of this degassifier is about 200 gpm. The unit is designed for reducing the air concentration to 10 percent or less of the saturation value at one atmosphere. This reduction is believed to be greater than necessary for normal operation. Removal of the oxygen should lessen corrosion problems during most of the operating cycle. Removal of nitrogen should reduce nitrate formation and thus reduce the load on the by-pass demineralizer discussed in the next section.

The degassifier is also intended to remove hydrogen and oxygen during reactor operation should this prove necessary. It can also be used to remove fission gases resulting from a fuel element leak or from possible

diffusion through the cladding (ref. 5.5, p. 239). All such gases can be released to the facility stack at an acceptable rate. In the absence of these situations, the degassifier unit will not be used during the actual operating cycle.

In the event a serious fission leak does occur, careful handling of the gas activities evolved in the degassifier will be required. The demineralizer will serve to remove some of the iodine and bromine, but not all. Some will appear in the degassifier along with the radiokrypton and radioxenon. Because of the small volumes of these gases, their removal by the degassifier might be a slow process. In this case, their direct discharge to the facility stack may be feasible. Otherwise, they will have to be scrubbed out with cooled activated charcoal (ref. 5.6) after removal of water vapor in a CO<sub>2</sub> cold trap. The gases caught in the charcoal trap can later be further concentrated in a smaller volume charcoal trap and held for decay and then slow release to the stack.

5.2.1.3 By-pass demineralizer. - This by-pass circuit is shown in figure 2.14 to the right of the reactor tank. It includes a cleanable filter, a heat exchanger, a combination of resin beds, and a discharge filter, all connected across the primary pumps. Only one resin bed is shown for illustrative purposes. The filter will remove solid suspended matter, thereby reducing the chance of serious blockage of the resin beds. The heat exchanger serves to reduce the water temperature below that at which resin damage occurs. Space for three resin beds is provided: One anion (which may not be installed), one cation, and one mixed-bed having a flow capacity of about 100 gpm. The first two are intended for pH control as in the E.T.R. system (ref. 5.7) with the mixed-bed serving the principal role of contamination and activity control. The single resin units need not handle the full flow except possibly the cation unit. At high water activities, a cation unit does reduce anion resin damage in the mixed-bed (ref. 5.8, p. 309), but this situation is not expected to develop unless a serious fission leak occurs.

Some of the primary system corrosion products will not be water soluble. Such materials either adhere to the system walls or eventually enter the demineralizer by-pass circuit. The strainer should serve to remove most of this material. Provisions for cleaning this strainer in a safe manner during an operating cycle will be incorporated. The refuse can be caught on spent resin as a filter and the combination disposed of as described in the next section.

5.2.1.4 Resin disposal. - The regeneration of all resins used for decontamination purposes is not contemplated. These resins will be flushed into suitably shielded disposable containers and, after a practical decay period, will be shipped out for off-site burial. Resins can be burned to achieve further volume reduction, but in the absence of cost data, this method is not being given serious consideration. It is true that considerable combustible waste is expected from other facility operations

(section 5.2.4). If the volume of such wastes becomes prohibitive, then burning in a properly designed incinerator will be considered at a later date.

Water used in handling spent resin and strainer refuse will pass to one of the purge tanks for reuse in a subsequent cycle.

5.2.1.5 Sampling provisions. - In order to keep tab on primary system activities and fission leaks, several sampling stations must be provided:

1. Reference 5.9 presents a method of using radiiodine picked up by an anion resin as a means of detecting the presence of fission products in the water. This type of monitor can supplement evidence of leaks derived from the degassifier monitor and may well serve to give an earlier warning of fission product leakage. Four sampling circuits across the main heat exchangers will be provided, starting just before the degasser by-pass and ending at the pump inlet. Two of these will serve for  $H_2$ ,  $O_2$ ,  $H_2O_2$ , conductivity, pH, and water analysis. The other two will serve for leak detection.

2. Two circuits across the by-pass demineralizer for determination of activities entering this unit.

3. Two connections at the demineralizer exit for effluent activities, pH, conductivity, and water analysis. Purging water will be discharged to the retention tank system.

4. Two circuits across the repressurizing pumps on the exit side of the degassifier for gas content sampling.

#### 5.2.2 Contamination of Shielding Quadrant and Canal Water

No important direct generation of activities in the shielding quadrant water is expected because of the concrete shield (see fig. 2.9) interposed between the reactor core and this water. Quadrants and canals will be charged with clarified water and demineralized thereafter at a rate of 100 gpm.

All concrete surfaces will be painted with Amercoat to minimize leaching and make decontamination somewhat easier.

As explained in section 5.1.2 the primary tank will be purged with fresh water before exchanging fuel elements. The same is true of the water in thimble passages before insertion or removal of experiments and equipment. With these precautions, the activity of quadrant and canal water should remain reasonably low. The chief source of contamination may well be corrosion products adhering to thimble walls and experiment

surfaces which are dislodged during transfer operations. Also some leakage of thimble water may occur. Contamination attributable to ruptured experiments (section 6.2.3) is likely to be far more serious than the normal conditions considered here. Water from the canals and quadrants can be discharged to hot retention tanks and decontaminated if necessary by passage through the mixed-bed demineralizer shown in figure 2.14.

### 5.2.3 Ventilation of Containment Shell

The ventilation system for the containment shell is outlined in section 2.1 and shown in figure 2.21. No appreciable contamination of the atmosphere in this shell is expected during normal operating conditions. Otherwise the shell interior would not be habitable as assumed. A serious accident, particularly one involving a fueled experiment, could result in excessive contamination as discussed in section 6.2.3 and appendix J.

Adequate monitoring equipment will be installed, both within the shell at selected locations and in the exhaust system, for promptly shutting down the ventilation system should the air become contaminated for any reason. The procedure to be followed thereafter will depend upon circumstances. If necessary the contaminated air can be filtered and discharged at an acceptable rate to the stack.

As presently conceived all air filled passages passing near the core will be sealed and vented to the stack, possibly after suitable hold-up in tanks provided for this purpose. As long as these connections remain intact, the containment shell atmosphere should not experience any contamination from this source. However, in view of the fact that the air in such passages constitutes the only gases subject to high flux, the most likely source of containment shell contamination during normal operation must be associated with their presence. Obviously this is no longer true if an experiment rupture should occur (section 6.2.3).

### 5.2.4 Handling and Disposal of Experiment Wastes

These wastes include all scrap metal, debris from machining operations, air-borne dusts and gases, and all chemicals derived from experiments. Fission products may or may not be involved, depending upon the nature of the experiment. In the absence of fission products the total activity will generally be of a lower level but will otherwise present very nearly the same disposal problems. There are two exceptions. Fueled experiments will generally release fission gases. They also require the recovery of virtually all of the unburned fuel which in turn necessitates recovery of most of the fission products as well.

E-102

Upon removal of experiments from the reactor, the irradiated material will be placed in the wet or dry hot storage areas (see fig. 2.20) and left there for some appropriate time. Large experiments will then be dismembered in the hot cutting and dismantling room and the portion of research interest transferred to the hot cells. The rest will go either to dry storage or to the decontamination shops. Smaller items will be transferred directly to an appropriate hot cell from storage.

A detailed presentation of hot cell operations and methods requires consideration of the kind of investigations contemplated. This type of discussion must await further consideration of the experimental program plus additional experience in conducting operations of this type (see section 7.2). The major operations will presumably be: (1) cutting operations to obtain specimens for metallographic or other study, (2) disassembly and assembly of equipment too radioactive for direct manual operations, (3) recovery of valuable materials or one kind or another, and (4) flushing out or decontaminating experimental apparatus or materials.

Best contamination control is obtained by proper segregation of constituent materials as to type and probable activity level, by keeping all wastes in as concentrated a form as possible, and by minimizing the required cutting operations through good experiment design. Except for small samples, most structural components of experiments will have no further value. The same is true for the bulk of coolant fluids. All such materials can be placed in dry storage and later packaged in some appropriate manner for off-site disposal.

Concentrated liquid wastes will generally be so acid or caustic as to require neutralization before packaging for disposal. Such wastes, as well as those of high activity, will be discharged to a special system terminating in a small tank. Here the solid matter can settle out and the liquid be periodically neutralized. Supernatant water from this tank will be evaporated at a low rate directly from disposable containers. These containers will be directly heated in a ventilated enclosure under conditions which promote evaporation without splashing, bubbling, etc. The off gases will be cooled to condense the water vapor and the air filtered before discharge to the facility stack. Condensed water will be discharged to the retention tank system.

Lower level wastes will generally be in the form of chips and dust from machining operations, or as water solutions and suspensions. The smaller dust particles can be picked up by a vacuum system with a nozzle very near the work point. This dust must then be caught in suitable filters and the filtered air vented to the facility stack. Larger chips and pieces can be caught in suitable trays or receptacles which permit remote handling and packaging. Low level water wastes must be filtered, pumped to one of the retention basins, and then discharged, with or without demineralization, as the nature of the waste dictates. Discharge from these basins will be monitored and diluted as necessary to acceptable activity levels.

In the case of apparatus contaminated with, or containing fission products, an intermediate barrier within the hot cell may be required as a means of keeping all wastes as concentrated as possible. (The same is true of work on some very hazardous chemical materials such as beryllium.) This barrier is usually a transparent plastic container which surrounds the sectioning equipment (ref. 5.10). Its sole purpose is to confine all fission products to as small a volume and area as possible. Similar covers can be attached to items containing fission products to prevent the spread of contamination during transportation. Arrangements can be made to flush all gas-borne activity out of such barrier cells through recovery devices such as filters and chilled activated charcoal traps to remove inert fission gases (ref. 5.11, p. 371). Another possibility is to store the flushing gas under pressure in tanks where it can be monitored and released gradually to the stack. The extent to which these added precautions are necessary depends in part upon the post irradiation decay time which can be tolerated by those responsible for the research program.

These barrier cells can be supplied with an inert gas for cases involving combustible and especially pyrophoric materials. Relatively minor fires can promote the spread of excessive amounts of activity.

In addition to experiment wastes as such, hot cell operation will ordinarily result in secondary wastes of all sorts. These include absorbent and masking paper, plastics (sheet and film), stripable paints, worn out tools, cleaning reagents, filter elements, and a host of other materials of this character. Combustible materials having a low order of contamination might be burned locally, but all other trash will require packaging for off-site disposal. Any secondary wastes exhibiting high activity will have to be handled as are the direct experiment wastes.

#### 5.2.5 Evaporation of Intermediate Level Water Wastes

As outlined in the preceding section, there are some high level concentrated wastes which can be further concentrated most expeditiously by evaporation in small scale equipment. This procedure minimizes shielding requirements, which on large equipment are cumbersome and expensive. Also, there are some "warm" solutions which contain short lived activities which by a combination of retention time and careful demineralization can be rendered suitable for offsite disposal. There are other solutions containing high concentrations of inert solubles and dilute long lived activities for which demineralization may be too expensive and ineffective for activity concentration (ref. 5.12, p. 458).

Concentration by vapor compression evaporation seems to offer the cheapest method of handling such intermediate wastes. This method has proven satisfactory at Brookhaven National Laboratory (ref. 5.13, p. 194). Any evaporation method is inherently expensive, both from a capital and

E-102

operating cost standpoint. Available information suggests that vapor compression is the cheapest of these, at least in terms of operating costs. Demineralization, even if adequate, may actually cost more because of the heavy load of inert solutes likely to be present. Some combination of the two methods may be even cheaper, i.e., demineralization with regeneration and evaporation of the regenerant solutions.

### 5.3 REFERENCES

- 5.1. Federal Register, July 16, 1955, p. 5101.
- 5.2. National Bureau of Standards Handbook 52, Maximum Permissible Amounts of Radioisotopes in the Human Body and Maximum Permissible Concentrations in Air and Water, March 20, 1953.
- 5.3. Handbook of Federal Regulations Applying to Transportation of Radioactive Materials - U.S. Atomic Energy Commission, July 1955.
- 5.4. Campbell, D. O.: Decontamination of Stainless Steel, Survey and Proposed Program. CF 53-5-233.
- 5.5. Research Reactors. TID 5275.
- 5.6. Browning, W. E., and Bolta, C. C.: Measurement and Analysis of the Holdup of Gas Mixtures by Charcoal Absorption Traps. ORNL 2116.
- 5.7. Safeguards Report, Engineering Test Reactor GEAP 0554, KE 56-19-R.
- 5.8. Cox, J. A., Costo, W. R., and Tabor, W. H.: Continuous Repurification of the L.I.T.R. Cooling Water. TID 2018.
- 5.9. Heath, R. L.: Fission Product Monitoring in Reactor Coolant Streams. IDO 16213.
- 5.10. Sullivan, L. O.: Problems and Costs Encountered in the Handling of Irradiated Fuels. KAPL 1443.
- 5.11. McHenry, R. E.: Radioactive Gas Processing Equipment. TID 5280.
- 5.12. Nachrod, F. C., and Schubert, Jack: Ion Exchanger Technology. Academic Press, Inc., 1956.
- 5.13. Manowitz, Bernard, Richards, Powell, and Horrigan, Robert: Vapor Compression Evaporation Handles Radioactive Waste Disposal. Chemical Engineering, March 1955.





## SECTION 6. - HAZARDS

In exploring the possibilities of unplanned release or uncontrolled dispersion of radioactive materials, an analysis of the consequences of failure or malfunction of equipment has been made. The analysis has concerned itself with accidents which introduce hazards from the following sources:

1. Hazards from failure or malfunction of component parts of the reactor or of component parts of the reactor cooling, electrical, or control system.
2. Hazards from failure or malfunction of experiments in any of the radiation facilities of the research reactor.
3. Hazards resulting from acts of God, sabotage, or negligence.
4. Maximum credible accident.

Each of the foregoing categories is itemized and discussed in detail in the following respective sub-sections: 6.1, 6.2, 6.3, and 6.4.

### 6.1 HAZARDS CREATED BY FAILURE OR MALFUNCTION OF COMPONENTS

#### OF THE REACTOR FACILITY

##### 6.1.1 Pump Failure

Both the main primary cooling system and the main secondary cooling system have three pumps, each of which has a capacity equal to one-half of the system flow requirement. Thus, in each system two pumps will operate to provide normal flow with the third pump available to replace a malfunctioning unit.

Separate primary and secondary shut-down systems are available to provide cooling after the reactor is shut down for any cause. Two pumps are installed in each shut-down system with each pump having capacity to fulfill its system flow requirement. These four pumps are powered by one of two diesel-generator sets which are backed up by the commercial power supply. The shut-down cooling systems will be in operation continuously during normal operation and shut-down operation.

Pump failures may be caused by failure of the pumps themselves, failure of the pump motors, or loss of electrical power. A decrease in coolant flow caused by the loss of one pump in either the primary or secondary systems will effect a power cut-back. A third standby pump is available to restore the coolant flow to normal. It is unlikely that both main pumps will fail at the same time unless the electrical power fails. However, if two pumps do fail simultaneously, the reactor will scram and the shut-down system will provide cooling.

E-102

CZ-12

Failure of the electrical power supply to the facility will cause failure of the pumps in both the main primary and secondary systems. The electrical power is supplied by two independent power lines which minimizes the possibility of loss of electrical power. Should both power supplies fail the reactor will automatically scram. The coolant flow rate to the reactor will then decrease to the flow rate supplied by the primary shut-down system which is powered by the diesel-generator set. This flow rate is sufficient to cool the reactor two seconds after scram. Coast down of the main pumps will take care of the first few seconds.

#### 6.1.2 Pipe Failure

Inasmuch as complete loss of coolant would expose the core and result in melting of the fuel elements accompanied by release of the accumulated radioactivity all precautions must be taken to safeguard against this occurrence.

The results of a break in the primary water system naturally depends upon the location and severity of the break. A break in the line at any position, however, will be indicated by a loss in water from the 5000 gallon overhead tank riding on the line. A signal from a flowmeter in the pipe from the 5000 gallon tank will warn the operator of loss of water from the primary system. A low water level in the 5000 gallon tank will automatically scram the reactor and open a valve in the line running from the 50,000 gallon overhead tank to the reactor pressure tank. This line enters the reactor pressure tank at a level above the core. The valve in this line will open fully in 15 seconds.

A severe break in the primary water system will be postulated at all points adjacent to a cavity which can receive water. There are two general locations of this type; one in the pump house and one at the sub-pile room.

A pipe break inside the pump house upstream of the pump will allow water to flow from the 50,000 gallon tank through the core and out the break into the pump house. The resistance in the eight inch pipe from the 50,000 gallon tank is designed for a pressure drop of 150 feet of head for a flow rate of 3000 gpm. Therefore the maximum flow from the 50,000 gallon tank and out the break is 3000 gpm which would drain the 50,000 gallon tank in a minimum of 17 minutes. The reactor pressure tank would remain full of water and the shut-down loop would continue to cool the reactor.

A pipe break inside the pump house downstream of the pump will also allow water to flow from the 50,000 gallon tank through the core and out the break into the pump house. In this case the pump head will add to the tank head if the pumps were not shut off. The head which the pumps can add is equal to their maximum suction lift. This additional head would increase the flow a negligible amount and the 50,000 gallon tank would again empty in about 17 minutes. The main pumps are located above

the core a distance which exceeds their maximum practical suction lift and therefore they cannot expose the core. The centerline of the main pumps is 29 feet above the top of the core. With the core still covered the shut-down loop will continue to cool the reactor.

The pipes adjacent to the sub-pile room are encased in five feet of concrete for shielding purposes. While this concrete reduces the possibility of a severe break, the results of such a failure will be discussed.

If the break is in the main inlet or outlet pipes of the reactor tank the water will flow through the core and out the break. Again the friction head in the supply line from the 50,000 gallon tank limits the flow rate to a maximum of 3000 gpm which will last for 17 minutes. There is also a 100,000 gallon overhead processed water tank available which will supply water to the reactor pressure tank for an additional 33 minutes. The cavities available to receive the water from the break are the sub-pile room and the passageway leading to this room. This passageway connects the sub-pile room with the annulus surrounding the 70 foot tank by means of an elevator and stair shaft. The combined capacity of the sub-pile room and passageway is approximately 46,000 gallons. In addition it requires 180,000 gallons to bring the water level in the annulus to one foot above the level of the top of the core. Therefore motorized valves are provided between the annulus and each of the quadrants to allow water to flow into the annulus. These valves are manually controlled. The resulting water level when these valves are open would be about nine feet above the top of the core. The shut-down loop will continue to cool the reactor.

In the case of a break in both inlet and outlet lines or a break in the bottom of the reactor pressure tank, some of the water from the 50,000 gallon tank will also flow through the reflector and out the break. It is desired to have 1000 gpm flow through the reactor lattice. The ratio of the pressure drop through the lattice to the pressure drop through the reflector during normal operation is 3:1. Assuming the flow proportional to the square root of the pressure drop, the ratio of the flow through the reflector to the flow through the lattice for the same pressure drop will be 1.7:1 or a total flow of approximately 2700 gpm will be required. The 3000 gpm from the 50,000 gallon tank satisfies this requirement. The resulting water level when the quadrant valves are open will be 9 feet above the top of the core as before. The shut-down loop will continue to cool the reactor. If the shut-down loop was to fail also, the fuel elements would cool by free convection after the overhead tanks were drained. According to reference 6.1 the maximum heat flux from the fuel plates without vapor binding is 19,650 Btu/hr-sq ft with free convection restricted to the channel itself. It is estimated that the heat flux reaches this value approximately one minute after shut-down.

E-102

CZ-12 back

A severe break in the pipes or reactor tank would therefore not result in any subsequent failure but could spread radioactive water into the sub-pile room and quadrants. Unless accompanied by a fission break the activity would decay rapidly and would offer no difficult clean-up problem. The core would not be exposed unless an explosion or earthquake were to open up additional cavities to receive water. It is estimated that it would take from 10 to 14 seconds to melt the fuel elements after the core has been exposed.

### 6.1.3 Startup Accident

The maximum rod rates were set by reference to the startup accident, where it is assumed that all control rods are being withdrawn at their maximum possible speeds and the reactor is protected only by the level scrams. It is well known that the higher the rod speed the shorter the period at any level and thus the larger the overshoot after a power level scram.

In the transient heat transfer analysis of reference 2.4 it was found that, for the periods involved, there is a static correspondence between the fuel plate surface heat flux and surface temperature, both lagging the heat release rate with a time constant of 46 milliseconds at normal heat transfer conditions. During nucleate boiling this lag decreases considerably. Neglecting this lag is pessimistic if the plate temperature is well below melting as any additional heat stored would attenuate peak surface heat flux and surface temperature.

Thus, a safe and conservative criterion for the startup accident is that the peak heat release rate for the transient correspond, statically, to a heat flux which is below the burnout heat flux. The burnout heat flux for the reactor is not known although from existing burnout data a value of  $2.2 \times 10^6$  Btu/hr-sq ft appears to be a conservative limit. This value would allow an overshoot to 2.5 times rated power. Pressure build-up on nucleate boiling for the periods involved are not harmful, section 6.4.1.

The analysis of the startup accident requires only the period at the scram level from which overshoots in power can be easily calculated. The overshoot after a one g rod drop is shown on figure 6.1 for a lifetime of  $9 \times 10^{-5}$  seconds and a range of control rod effectiveness. The power level rise during the dead time can be calculated by assuming that the period changes very little during the dead time duration.

For the cases where the scram level is much higher than the initial level where the accident begins, a Newson-type analysis, reference 6.2, was used. In this reference and reference 2.4, it is shown that

$$\text{Minimum possible period at scram signal} = \left( \frac{\lambda}{2R \log \frac{\phi_{ss}}{\phi_{in}}} \right)^{1/2}$$

where  $\lambda$  is prompt neutron lifetime,  $R$  is rod rate in  $\Delta K/K$  per second, and  $\phi_{ss}/\phi_{in}$  is the ratio of scram signal level to initial level. This equation is plotted in figure 6.2 for a lifetime,  $\lambda$ , of  $9 \times 10^{-5}$  seconds and a range of  $R$ .

For cases where the scram level is close to the initial level, the reactor kinetic equations with 5 delayed neutron groups were solved on a differential analyzer for a case of constant rod withdrawal rate and a case of a 0.5 percent  $\Delta K/K$  step in reactivity followed by a constant rod withdrawal rate. The results are plotted in figure 6.2 and also on figures 6.4 and 6.5. For a power increase of 100 fold, the Newson-type analysis is far too pessimistic giving a period of about 100 milliseconds when the actual period would be about 400 milliseconds. The minimum value of  $\phi_{ss}/\phi_{in}$  where the two analyses give the same results is about  $10^4$ .

Figure 6.3 gives the power overshoot as a function of dead time for various values of  $\phi_{ss}/\phi_{in}$ , for a maximum rod withdrawal speed of 3 in./min and a maximum control rod effectiveness, the worst case, of 2 percent/in. Various startup accidents are also tabulated below.

#### STARTUP ACCIDENTS

[ Rod velocity, 3 in./min; rod effectiveness, 2 percent  $\Delta K/\text{in.}$  ]

Accident conditions				Period at scram signal level	Ratio of peak level to scram signal level	Peak level
Initial level	Scram signal level	Ratio of scram signal to initial level	Dead time in scram			
$10^{-14} \phi_f$	$10^{-3} \phi_f$	$10^{11}$	80 Millisec	42 Millisec	9.7	$10^{-2} \phi_f$
$10^{-14} \phi_f$	$10^{-1} \phi_f$	$10^{13}$	80	39	12	$1.2 \phi_f$
* $10^{-14} \phi_f$	$1.5 \phi_f$	$1.5 \times 10^{14}$	40	37	4.6	$6.9 \phi_f$
	$1.5 \phi_f$	2.25	80 Millisec	1.8 Sec		
		1000	80	170 Millisec	1.66	$2.5 \phi_f$
*	$1.5 \phi_f$	4000	40	100	1.66	$2.5 \phi_f$

\* Slow scram inoperative, four simultaneous failures.

Note: If period scram operates with dead time  $< 3$  sec then peak level always  $< 2.5 \phi_f$ .

For the accident beginning at a very low source level and scrambling at the lowest protection level of  $10^{-3} \phi_F$ , where  $\phi_F$  is the rated power level, the period at scram would be 42 milliseconds. Using a dead time of 80 milliseconds for this slow scram gives an overshoot of 9.7 times, which is very safe. If we consider the protection level not acting until  $10^{-1}$  rated power, the period at scram would be 39 milliseconds and the overshoot 12 times which is still very safe. If the slow scram protection does not act at all, the minimum period at scram would be 37 milliseconds and, with a dead time in the fast scram of 40 milliseconds, the peak power would be 6.9 times rated. This accident involves four simultaneous failures: uncontrolled rod withdrawal, failure of the slow scram system and its back-up, and failure of the period scram. Also, as discussed in sections 6.4.1, periods of 37 milliseconds are controllable by the self-regulating features of the reactor, which are not included in this analysis. Also, the conservative limit on peak power of 2.5 times rates is the static burn-out limit; allowable transient peaks being much higher.

In the power range, above  $10^{-3}$  rated power, the protection will be very close whereby the scram level should not exceed the operating level by more than 2.25. The minimum period that could develop from a control rod withdrawal would be 1.8 sec. If this protection takes a level rise of as much as 1000 to act, instead of 2.25, the period at scram would be 170 milliseconds and the excursion would be safe. The fast level scram, set at  $1.5 \phi_F$  with a dead time less than 40 milliseconds, is always in effect. If the slow scram protection does not act at all, a level rise of as much as 4000 would give a period of 100 milliseconds, which, for the fast scram would give a safe peak power.

All cases discussed above were for the period scram inoperative. If only the period scram operates with a dead time less than 3 seconds, then the excursions for any startup accident would be safe.

The drive system providing the rod insertion speed of 9 in./min is designed to insure one-directional operation. Even if this speed should somehow become effective as a withdrawal, and uncontrolled withdrawal should occur, the scram system would keep the excursions safe. In addition, the minimum period that can develop from this higher rod speed, about 21 milliseconds, can be controlled by the self-regulation of the reactor as discussed in section 6.4.1.

#### 6.1.4 Maximum Xe Burnout after Restart

The hazard with respect to Xe burnout at normal flux levels was discussed in section 2.4.3. The insertion speed of the rods is more than adequate.

### 6.1.5 Controllable Accidental Insertions of Reactivity

One of the basic criterions on the design of the reactor, experiments, and control systems is that no possible accident can introduce changes in reactivity which cannot be safely handled by the reactor control system. The basic safety feature of the control system is the level fast scram which is set to trip at a level 50 percent or less above the maximum reactor operating level required for the particular reactor cycle. This safety trip is backed up by the one second period fast scram, the intermediate level slow scrams, as well as reverses and set-backs which are triggered at the first indications of malfunction.

Figure 6.1 can be used to find the minimum allowable period at the scram signal power level. In order to relate these restrictions on reactor periods to allowable reactivity insertions, the transient reactor periods must be considered as well as the stable periods. For step or ramp-wise insertions of reactivity, the transient periods are always smaller than the ultimate stable period. To obtain these effects, the reactor kinetic equations, using 5 delayed neutron groups, were solved on a differential analyzer for cases of continued insertion of reactivity at constant rates. The results are shown on figures 6.4 and 6.5.

In general, the period at the scram signal is determined by the level at the start of the accident, the rate of reactivity insertion, and the total reactivity inserted. For any reactivity insertion rate, figure 6.5 shows that the period decreases continuously until the total reactivity is inserted. At this time the period is the minimum for the transient as, past this point, the period would increase toward the stable period corresponding to the total reactivity inserted. If the smallest allowable period during the transient is set according to figure 6.1, which only specifies minimum periods at scram, a definitely safe and pessimistic relation between reactivity insertion rate and total reactivity inserted can be obtained from figure 6.5.

Ramp-wise accidents are assumed: Each such accident is represented by a point on figure 6.6 corresponding to the reactivity and time at the corner of the ramp. Accidents which so map into a point below the curve under consideration can be safely handled by the control system for that curve. The curves apply to the least favorable power levels at the start of the accident, up to the 60 mw power level, and for the least effective control rod position, and for the conservative criterion on any excursion that the peak power be less than 2.5 times rated.

If only the level fast scram system is operative, a step of 0.5 percent  $\Delta K$  or a slow insertion up to 0.9 percent  $\Delta K$  is always controllable. If only the set-point level scram system is operative, a reactivity insertion of 1.2 percent in 0.6 second is always controllable. If only the one second period scram system is operative, with a dead time less than 40 milliseconds, a reactivity insertion of 1.35 percent in 0.23 second is always controllable.

It is emphasized that these limits are for the least favorable power levels at the start of the accident. If, for example, considering only the fast scram operative, a 2 percent  $\Delta K$  per second accident starts at power levels greater than 20 mw, the reactor scrams before the limiting total reactivity of 0.74 percent is inserted. If the same accident starts at power levels less than 20 mw, then a somewhat larger total insertion of reactivity is controllable as the reactor scrams after the minimum period of the transient. If the accident starts at 60 mw, a reactivity insertion rate of 4 to 5 percent  $\Delta K$  per second is controllable.

#### 6.1.6 Hazards Due to Regulating Rod

The regulating rod will be calibrated to insure reactivity worth of less than 0.6 percent  $\Delta K$ . The rod is velocity limited to give full travel in about one second. This would give for full travel at maximum speed a minimum transient period of 400 milliseconds (fig. 6.5) and a stable period of 1.7 second, which is not at all hazardous. The hazard in the regulating rod is shown on figure 6.6 for full travel of 0.6 percent  $\Delta K$  in one second. The regulating rod could be worth as much as 0.87 percent  $\Delta K$  for only the level fast scram system operative or as much as 1.2 percent  $\Delta K$  for only the set-point level scram system operative and still be safe.

#### 6.1.7 Xe Burnout on Nuclear Excursion

The possibility of burning out an appreciable fraction of the Xe in the core in a short time on a nuclear excursion was investigated. Reference 2.4 shows that this burnout is a function of nuclear energy release only. In order for this burnout to add as little as 0.1 percent  $\Delta K$ , it takes a 1250 mw second nuclear excursion at normal Xe concentration, and a 250 mw second nuclear excursion at maximum possible Xe concentration as during a restart. These nuclear energy releases on a fast excursion are not probable, section 6.4.1, and this type of burn-out hazard is not a factor.

#### 6.1.8 Removal of Fuel Element or Breakage of Fuel Element Plate

The reactivity effects of individual fuel plates or of an entire fuel element accidentally falling out of the active lattice have been experimentally obtained by Oak Ridge personnel at the Bulk Shielding Reactor. These data were obtained for a variety of fuel loadings and reflector compositions incidental to the principal purpose of the experiments and so have not been published. The data were made available to the NACA by personnel at the Bulk Shielding Reactor.



The results indicated that removal of fuel plates and replacement by water introduced negative reactivity for all positions of the lattice. Removal of a single fuel plate in a position of high statistical weight is worth less than 0.1 percent reactivity. For example, a single fuel plate from a standard 140 gram fuel element near the center of a 5 by 6 critical fuel element array was removed. This introduced negative reactivity of 0.067 percent. The loading was designated as no. 33 and was water reflected.

Another experiment involved removal of an entire standard 140 gram fuel element from a critical 5 by 5 fuel element array which was surrounded on three faces by canned beryllium oxide primary reflector and on the fourth side by water. The element removed was adjacent to the central fuel element toward the side reflected by water. A negative reactivity of 3.2 percent was introduced by replacing the fuel element by water. This loading was designated no. 6.

A third series of experiments on a 5 by 5 critical loading removed a fuel element at the corner; its two neighbors along one core-reflector interface were also individually removed. It was found that the 140 gram corner fuel element was worth -0.73 percent  $\Delta K$ , whereas a 70 gram corner fuel element was worth -0.45 percent  $\Delta K$ . Replacement of the corner fuel element and removal of its neighbor introduced negative reactivity of 1.25 percent for a 140 gram fuel element and 0.70 percent for a 70 gram fuel element. Removal of the next fuel element along the core-reflector interface resulted in introduction of negative reactivity of 1.9 percent for a 140 gram fuel element and 1.02 percent for a 70 gram fuel element.

Additional information concerning the worth of fuel has been obtained from an NACA-requested experimental program at the Bulk Shielding Reactor. A description of the reactivity experiments and the results obtained are presented in supplement III to this report (ref. 6.3). In these experiments a slab loading of 7 by 3 - 140 gram fuel elements reflected by rows of canned beryllium oxide followed by water was used. The center fuel element was removed plate by plate, and successive changes in reactivity measured. This program also determined the worth of removal of water between fuel plates, and the worth of voids at various positions along the reactor height. Results confirmed the negative fuel plate worth as mentioned above. An interesting finding was that replacement of water by void near the center of the core introduced positive reactivity.

#### 6.1.9 Fuel Element Cladding Failure

Fission product contamination is caused by two basic types of fuel element cladding failure. In one case a small hole develops somewhere in the fuel element cladding because of some initial imperfection or by slow corrosion. The other type, caused by local or general overheating

E-102

CZ-13

of one or more fuel elements, is likely to be more serious, and in the worst conceivable case, can be catastrophic. This last situation is discussed in section 6.4.

The small leak type of failure has been experienced in the MTR (ref. 5.5). Such leaks release some fission gases plus such solid fission products as may corrode and leach out. The resulting contamination presents disposal and cleanup problems but does not constitute a major personnel hazard. The actual weight of radioatoms released is quite small if the faulty fuel element is removed promptly after the leak is detected by the water monitors. Prompt removal may not always be practical, in which case the contamination may build up until the reactor is shut down and the source of the leak removed. Fortunately MTR experience can serve as a guide for failures of this kind.

Leaks caused by overheating can be very serious even though the primary cooling system remains intact. The dosage rate outside those portions of the system adjacent to inhabited work areas will increase approximately 10,000 fold if all the fission products in one fuel element are released uniformly into the primary water. This is a rough estimate, assuming rated burnup in each fuel element.

Fission products that do escape into the primary cooling system will consist of dissolved inert gases, water soluble material, and insolubles which either remain suspended in the water or settle out on various surfaces. The inert gas content of any one fuel element probably does not exceed 50 ml N.T.P. (ref. 6.4). Inert gases will not be removed as such by the deionizer. The separation of these gases as a separate phase is unlikely at normal operating temperatures unless other gases (as from water decomposition) are also present.

The water soluble material can, in principle, be removed by the deionizer unit although some data (ref. 5.8) indicate that the removal of last traces is difficult. The addition of inactive ions of the same element can be used to improve the removal of the last traces of radioions (ref. 6.5). The deionizer resins cannot be expected to remove colloidal material very effectively. Larger sized material in suspension may be removed either by screens preceding the mixed bed or by the resin itself acting as a filter.

The ability of the deionizer resin to remove contaminating material from fuel element leaks depends upon the concentration of such material and the extent to which the bed capacity is depleted before the leak occurs. Fresh mixed-bed resins will absorb the equivalent of 500+ grams of  $\text{CaCO}_3$  per cubic foot of resin. Since the fission products have higher atomic weights than calcium, and since a good fraction of the material released by a major leak probably will not be ionized, the bypass deionizer should have sufficient capacity for the major portion of the soluble

E-102

fission products released in any non-catastrophic accident. Even so, the demineralizer will not reduce the water activities to permissible discharge levels because of the fantastic decontamination factors required. At the same time it should serve to reduce the water borne radiation to levels where mechanical work on the system becomes practical except near the screens and bypass deionizer. These concentrated sources can be removed and disposed of after a reasonable decay period. There is evidence (ref. 6.6) that some fission products are prone to adhere or combine very tenaciously with metal surfaces. Since it will not be practical (because of size and cost) to decontaminate the interior surfaces of the primary system, some degree of surface contamination will have to be accepted after a major fission leak. The degree of contamination allowed to remain will have to be consistent with the performance of necessary mechanical operations.

CZ-13 back

The fact that mixed-bed resins probably are incapable of reducing fission product activities to acceptable discharge levels, gave rise to the primary water re-use system described in 5.2.1.1. After a major fission product leak, the required cleanup operations may well require the disposal of some excess water. This can first be discharged to one of the hot retention tanks and then either diluted and discharged or possibly concentrated by evaporation.

The problem of cleanup after a major accident has not been thoroughly investigated at this time. The following procedure may be used to handle radioactive material for purposes of disposal:

1. Concentration of radioactive ions on the mixed-bed resins by recirculation after shutdown. More rapid removal of activity could be accomplished by forcing the mixed-bed discharge through the system as a slug with a minimum of intermixing with the contaminated water.

2. Concentration of suspended particulate matter by the filter in the demineralizer circuit.

3. Removal of fission gases by continuous circulation through the degassifier described in section 5.2.1.2. As in (1) above, the degassed water should preferably move through the system as a slug.

4. Concentration of contaminants in all excess water, which must be discharged, by evaporation as outlined in 5.2.5.

5. Dilution of water after sufficient contaminants have been removed.

## 6.2 HAZARDS FROM FAILURE OR MALFUNCTION OF EXPERIMENTS

It is strongly emphasized that the experiments discussed have been chosen as being typical of the larger and potentially more dangerous experiments that would be considered for testing in the reactor. Certainly such experiments would not even be considered for testing until a sufficient amount of operating time and experience had been accumulated to insure a thorough knowledge of the characteristics of the reactor facility. During this interim period, experiments would be limited to relatively small experiments of unquestionable integrity. It is felt, however, that eventually it will be essential to perform experiments of the same general type as described in section 4. It is for these reasons that these particular experiments have been chosen for discussion. All experiments will be rejected, however, which by conceivable accident may introduce potential positive excess reactivities which cannot be safely handled by the reactor control system.

The design of experiments on prototype fuel elements cooled by air or liquids has been based on the concept of minimizing the possibilities of fission product escape from the experiment containers. On the other hand, if the experiments are to yield data of value to the Aircraft Nuclear Propulsion program, they must be operated at high temperature and stress levels. The probability of fission product leakage within the experiments is accordingly large. In fact, there are experiments which will intentionally be operated with gaseous fission products escaping from the test element; the detection of particulate matter, however, may call for immediate cessation of the experiment by cut-back of the reactor.

The degree of contamination and dose rates accompanying dispersion of fission products associated with a one megawatt experiment operating for 10 days is very high. These fission products dispersed in the shielding pool and in the air-filled dome of the containment tank would produce dose rates of 550 r/hr just outside of the reactor containment tank (dose rates at other locations are discussed in appendix J). It is essential therefore, that the experiments are structurally designed to contain failed fuel elements under all foreseeable conditions.

To insure that malfunction of experimental equipment or failure of the fuel element do not proceed to completion, scram signals from as many independent detectors as practical will be transmitted to the reactor safety system. It is also essential that accidents causing changes in composition and geometry of the experiment shall not cause positive step changes or ramps in reactivity which can place the reactor on unsafe periods.

A discipline for the design of experiments should therefore incorporate the following:

1. Absolute local containment of experiment.

2. Accidents to experiments shall not introduce changes in reactivity which cannot be handled safely by the reactor control system.

3. Multiple reactor scram signal tie-ins from experiment instrumentation.

The ways in which the foregoing design discipline has been conceptually applied to an air-cooled and a liquid-cooled experiment are discussed in the following section. Hazards associated with failure of experiments and methods of cleaning up are discussed in sections 6.2.2 and 6.2.3, respectively.

### 6.2.1 Operational Accidents to Experiments

6.2.1.1 Air-cooled experiment. - The air-cooled fuel element experiment in normal operation has been described in section 4.1.1 and shown in figure 4.1(c). The integrity of the experiment is maintained by a multiplicity of stainless steel containers maintained at acceptable temperatures and stresses by water coolant in the clearance space. The cooling water is supplied from the 50,000 gallon overhead, primary-cooling-water tank. This flow is independent of the operation of any other equipment of the reactor facility.

The scram signals can originate from:

1. Activity due to accumulation of particulate matter in a filter downstream of the test fuel element exceeding a prescribed level. The level may be set to cause scram for fission gases passing through the filter. If the experiment calls for operation with cracked fuel elements, fission gases in the airstream may be accepted.

2. Overtemperature on fuel-plate surfaces and in strategic locations in the pumped loop which indicate overheating of element due to distortion of air flow or fuel plates.

3. Failure of an air compressor as indicated by a cooling-air flow reduction in the bypass loop and a change in compressor speed.

4. Loss of water coolant flow in experiment clearance space.

5. Loss of cooling water flow in main coolers.

6. Reduction in air pressure at fuel element due to a leak or break in an air line in the equipment container.

An important accident is failure or reduction of air or cooling water supply and subsequent overheating of the fuel element. The experiment has been designed to handle these accidents in the following manner:

If one of the compressors fail, the reactor is cut-back, and the compressor is isolated from the system by valves located before and after the compressor. The bypass throttling valve is closed and all the flow is diverted through the main loop, removing the afterheat of the fuel element. About 180 hours of forced cooling are required to remove afterheat after which the afterheat can safely be transferred by conduction. If the second compressor fails before 180 hours after reactor shutdown, the fuel element will melt. The remaining afterheat is then transferred to the surrounding water, in which the experiment has been stored, by conduction through the wall of the experiment and by boiling and free convection from the experiment outer container surface.

If a break occurs in one of the air lines inside the experimental tank, changes in the flow rate or air pressure cut-back the reactor. The degree of flow deviation depends upon the location of the break. Inasmuch as the pressure in the tank is maintained at the same level as the compressor inlet, a break downstream of the fuel element would result in very little flow deviation. The contents of the containment tank could become contaminated but still present no hazard since the experiment is contained.

A larger flow adjustment occurs if the break is located upstream of the fuel element because part of the flow is diverted through the break into the experiment containment tank. It is possible to design the system so that sufficient air is circulated over the test fuel elements to remove the afterheat.

If the flow of cooling water to one of the main coolers fails, the reactor is cut-back and the afterheat of the experiment is removed in the remaining cooler. If water flow to both coolers stops simultaneously the reactor scrams; the test fuel element melts down due to afterheat. The remaining afterheat in the molten elements is transferred to the clearance space coolant to maintain containment.

Another hazard is that involving excursions of the main reactor. With the fuel element operating near its peak heat-transfer performance, an excursion of the reactor could result in overheating and consequent failure of the fuel element. Integrity of the thimble is maintained by the clearance space cooling water. Excursions in reactor power resulting in pressure increases in the core large enough to break the thimble and the containment tank for the experiment will contaminate the quadrant. The experiment containment tank, however, is designed to withstand pressures consistent with the design value for the reactor pressure tank.

6.2.1.2 Liquid-cooled experiment. - A representative liquid-cooled experiment using sodium to cool metallic fuel elements has been described in section 4.1.2 and shown in figure 4.2(c). Several stainless steel containers maintained at acceptable temperatures and stresses by water

coolant in the clearance space enclose the experiment. From a safety point of view, it is desirable to have as many sensing elements as practical to detect failure. For this reason additional systems, such as a helium gas monitoring system between two stainless steel concentric containers may be used to detect sodium leaks. In addition, a boiling detector, which acoustically measures the growth and collapse of vapor bubbles, may be installed in the sodium loop.

The reactor scram signals can originate from:

1. (a) Temperatures of sodium leaving the test element above a prescribed limit
- (b) Temperatures of beryllium moderator surface near outer fuel elements exceeding prescribed limits

Both of the foregoing temperatures closely follow fuel element plate temperature since temperature lags through sodium and beryllium are relatively small.

2. Helium gas-monitor circulating through porous media to detect sodium leak through inner stainless steel containment shell
3. Bare-wire, continuous-twin conductors in parallel in porous media to detect sodium leak by shorting
4. Boiling detector to indicate overheating in fuel elements
5. Electromagnetic flowmeter to detect reduction of sodium flow rate
6. Failure of sodium pump
7. Loss of water coolant flow in experiment clearance space
8. Loss of coolant flow in sodium-to-air heat exchangers

If one pump fails, the reduction in flow is noted on the magnetic flowmeter in that line. At a predetermined drop in flow rate the valve controlling the flow rate is completely opened and the pump that failed is isolated from the system. The reactor is scrammed and the afterheat is removed by sodium circulated by the remaining pump. Forced cooling is required for a period of 1.5 hours after scram before the afterheat may be removed by conduction to the water in which the experiment is being stored. If the second pump fails during the latter part of the afterheat forced-cooling period, the experiment will cool by convection to the ambient water. However, failure of the second pump early in the afterheat forced cooling period will result in boiling of both sodium and storage water. The detailed transient heat transfer calculations have not been made - but it is expected that the fuel elements may melt.

If the facility air flow to the heat exchangers stops, a pressure sensitive, cut-out switch will cut-back the reactor. The time required to boil sodium if no heat is removed by the heat exchangers is 50 seconds. The fuel elements may melt down, but the afterheat will be removed by the clearance space cooling water.

An additional hazard exists with this sodium-cooled experiment. If a sodium leak should occur in the air-cooled heat exchangers, the hot walls will corrode very rapidly. This means that such leaks must be detected promptly and the reactor scrammed without delay. Otherwise the leak may quickly enlarge and release enough sodium to prevent adequate cooling of the fueled test section. Presumably, enough of the leaking radioactive sodium will be carried out of the experiment by the cooling air to permit early detection. A leak in either of the heat exchangers is picked up by the leak and flame detector. This signal closes the valves, isolates the heat exchanger, and scrams the reactor.

E-102

#### 6.2.2 Reactivity Effects of Accidents to Experiments

In order to evaluate the hazards due to reactivity changes associated with accidents to the experiments, the effects of several compositional and geometric changes to the experiments and consequent interaction with the reactor core, have been studied. A series of reactivity calculations have been made for:

1. An air-cooled experiment in the horizontal through-hole HT-1 in two positions relative to the face of the core
2. A liquid-cooled experiment in the center test hole for two cases of this experiment; with fuel and without fuel but with an absorber equivalent to the fuel concentration

It is again emphasized that the compositions and locations of these experiments were selected as representative of the type of desirable experiments. The sizes were chosen in order to explore reactivity effects, and because of the complexity of the two-dimensional diffusion solutions, a limited number of configurations were considered.

It is recognized that the most elegant criticality calculations are at best a relative guide. In order to augment the present calculations and to establish effects of fuel worth and void worth in the central fuel element of the active lattice, an experimental program was negotiated with the Oak Ridge National Laboratory, and performed at the Bulk Shielding Reactor. The critical loading consisted of a 7 by 3 array of 140-gram aluminum fuel elements surrounded by rows of canned beryllium-oxide primary reflector elements followed by a water secondary reflector. This was



the best simulation of the NACA reactor possible at the BSR. NACA personnel assisted with the experiments and subsequently analyzed the results. Analysis of these experimental results has provided evidence of the reactivity changes associated with removal or addition of fuel plates, flooding of void spaces with water, and void coefficients due to localized voids in regions of high statistical weight. A complete presentation of these experimental results can be found in supplement III (ref. 6.3).

Analysis of these experimental results permit the estimation of some third-dimensional effects, that is, the finiteness in the length of experiments proposed for the center test hole. It is recalled that the reactivity calculations performed on the two-dimensional simulator assume that the experiments in the critical configuration extend the full height of the core in the case of the center test hole, and the full length of the core in the case of the horizontal test hole.

Insofar as diffusion theory calculations are concerned, there is a reasonable measure of confidence in the group analyses herein employed. The analytical techniques used calculated satisfactorily the criticality of the Oak Ridge homogeneous enriched uranium oxy-fluoride-water solution cylindrical reactor critical mass studies. This analysis has been published as reference 6.7.

6.2.2.1 Reactivity effects of accidents to air-cooled experiments in horizontal through hole. - The various two-dimensional configurations considered for the air-cooled experiment are shown in figure 6.7.

Configuration I shows the normal air-cooled experiment in the closest possible approach to the face of the core.

Configuration II postulates a break in the outer container of the experiment with complete flooding by water of the cooling-air passages in zones 3 and 5.

Configuration III shows the normal air-cooled experiment in the farthest possible position from the face of the core.

Configuration IV postulates a break in the outer container of the experiment with complete flooding by water of the cooling-air passages in zones 3 and 5.

The values of  $K_{eff}$  obtained for each of these configurations relative to the reference core are listed below:

E-102

CZ-14

Configuration		$K_{eff}$
Unperturbed reference core		1.185
I	Air-cooled test closest to core	1.158
II	Cooling-air passages in I flooded	1.158
III	Air-cooled test farthest from core	1.163
IV	Cooling-air passages in III flooded	1.164

It may be seen that complete flooding of the cooling-air passages and, as such, all of the effective void space in the HT-1 hole with the air-cooled fuel element experiment in place, introduces no change in reactivity for configuration I and only  $+0.001 \Delta K/K_{eff}$  for configuration III.

The two-group neutron flux distributions across the reactor horizontal midplane with the air-cooled fuel element experiment in HT-1 are shown in figure 6.8. The distributions for both configurations I and II are shown. The effect of complete flooding with water of the cooling-air passages in zones 3 and 5 results in a large change in fluxes in HT-1, but in a small change in fluxes in the core itself. The effect on reactivity is therefore small. The effects of the stainless steel absorbers in zone 3 and of the moderator in zone 4 in perturbing the local fluxes are readily apparent in figure 6.8.

It has been shown in section 4.2.1 that an average relative specific power of from 0.49 to 0.38 can be obtained in the air-cooled fuel element experiment in HT-1 in respective positions closest and farthest from the face of the core. This specific power is relative to an average specific power of unity over the entire core volume. Inasmuch as the air-cooled fuel element experiment described herein was designed for a total power of one megawatt, and the test fuel element contains about 4000 cc, the average specific power required in the experiment is 250 watts per cc. The core average specific power required to produce this specific power in the experiment is less than the core design value of 600 watts per cc for the position closest to the core.

Specific powers in the experiment may be increased somewhat by increasing the uranium concentration in the experiment. On the other hand, the effective fission cross section may be reduced by neutrons coming into equilibrium with the higher temperature in the immediate vicinity of the experimental fuel element. There is also the possibility of locating the experiment in HT-1 at various distances from the face of the core; movement of the air-cooled experiment by one-inch near the center of HT-1 altered the average specific power by 20 percent.

6.2.2.2 Reactivity effects of accident to liquid-cooled experiments in center test hole. - The compositional changes to the liquid-cooled experiments in the center test hole are shown in figure 6.9. Configurations I and II are the experiments with and without fuel respectively in zone 3.

Configuration II without fuel contains a macroscopic absorber equivalent to the fuel. Configurations III and IV postulate a break in both thimble and stainless-steel containers, and a complete flooding of the gas passage in zone 2.

Configuration V was calculated to estimate the worth of accidental removal of the entire 3-inch square center test hole experiment, or of the core shim-rod fuel element, which ordinarily occupies this space.

The values of  $K_{eff}$  obtained for each of these configurations are listed below:

Configuration	$K_{eff}$
Unperturbed reference core	1.185
I Fueled experiment	1.165
II Unfueled experiment	1.150
III Flooded fueled experiment	1.179
IV Flooded unfueled experiment	1.154
V All water in test space	1.157

It may be seen that the increase in reactivity accompanying flooding of the monitoring gas passage introduces a  $\Delta K/K_{eff}$  of +0.012 for the fueled experiment, and +0.004 for the unfueled absorptive experiment. Response of the reactor to accidental reactivity insertions introduced as ramps is covered in section 6.1.5 in which a discussion of safe ramps for various reactor powers is presented. Precisely how steep a ramp increase in reactivity may be introduced by a specific experiment must be determined by a detailed analysis of how failure of the experiment may proceed. The present calculation for an experiment extending the full height of the core indicates a relatively large positive  $\Delta K/K_{eff}$  due to the complete flooding accident. However, the results of the experiments at the Bulk Shielding Reactor, reported in reference 6.3, indicate that filling of air space with water near the center of the core introduces negative reactivity. This would imply that experiments, which are shorter than the full height of the core and which experience accidents in which air passages are flooded, may not introduce as large a positive reactivity as that calculated.

On the other hand, the calculated reactivity effect of flooding an absorptive but unfueled experiment introduces a  $\Delta K/K_{eff}$  of +0.004 which is controllable even if introduced as a step increase at any operating power and so is completely safe. Of course, the experiment considered is very absorptive, using up a  $\Delta K$  of 0.035.

Very careful studies will be made before any fueled experiment will be considered for insertion into the center test hole. However, materials

irradiations experiments appear to be reasonable for the center test space.

Configuration V estimates the effects of removing a standard fuel element from the center of the lattice and replacement by water. The contribution of this fuel element is calculated to have  $\Delta K$  of 0.028. Removal of the fueled experiment would introduce negative reactivity of  $\Delta K/K_{eff}$  of -0.007. On the other hand, removal of the unfueled experiment would introduce positive reactivity of  $\Delta K/K_{eff}$  of +0.006. This reactivity insertion is controllable.

E-102

### 6.2.3 Failure of Experiments and their Cleanup

**6.2.3.1 Failures.** - The design of equipment for fueled experiments must be such as will minimize the possibility of fission product escape from the experiment container. On the other hand, if these experiments are to yield data of value to the ANP program, these units must be operated at temperature and stress levels such that the margin of safety is much less than that incorporated in the reactor proper. Moreover, there will be less experience on which to base these individual designs of experimental units. The probability of fission product leakage within an experiment is accordingly large. The chance of leakage into the clearance coolant space is presumed to be much lower since the fuel element coolant fluid will tend to carry any molten fuel element material away from influence of the reactor core, thereby reducing the heat release in the experiment in the small interim prior to scram of the reactor.

If leakage to the experiment exterior does occur, it follows that very serious damage to the fueled portion of the unit must have occurred. Minor fuel element rupture in the experiment is unlikely to result in any external leakage because of the protective features inherent in the design. The monitoring and scram instrumentation normally provided are intended to limit the fuel element damage to as low a level as possible. The possibility of external leakage is very remote unless the interior damage is both violent and extensive. Under these circumstances, the external contamination is likely to include both the primary system and the pool water. A major cleanup job must be expected for any external experiment leakage. The activity of the air in the containment tank can be very high if the explosion is sufficiently severe (see appendix J).

If, however, the accident is less violent, such that no large gas bubble rises to the pool surface, then some of the fission gases could remain dissolved in the huge volume of pool water. In this event, the handling of the air activity in the reactor containment tank could be much less of a problem than appendix J indicates.

E-102

In the case of the sodium-cooled experiment, the possible hazard and cleanup problems are somewhat different. Should the sodium ever succeed in escaping through the double-walled experiment test section, the rate of escape is likely to be high because of the extensive interior damage which must precede the leak. If this situation does occur, very high thimble pressures can develop as a result of the sodium-water reaction. The experiment assembly is much too heavy to be blown back quickly enough for any practical thimble protection. The inclusion of a rupture vent at one or both ends of the thimble may offer some protection, but this is problematical. Obviously, a thimble burst must be avoided because of possible damage to the reactor core and the control system. The decontamination required after such an accident is substantially the same as that required for the air-cooled experiment except that a larger fraction of the fission gases is likely to reach the pool surface along with the escaping hydrogen. Any type of external rupture of an experiment will require prolonged and tedious decontamination, the details of which will doubtless depend upon the particular circumstances.

Even though all the fission products released by ruptured fuel elements are within an experiment, the cleanup and disposal programs will not be easy. The detailed procedures will depend upon each design. Some general procedures are discussed in the next section. These are essentially an extension of those presented in section 5.2.4. The activity levels are comparable, the principal difference being that the activity is not as well confined. This tends to make all decontamination procedures more exacting and time consuming. The control procedures are substantially the same.

To what extent the two kinds of experiments considered herein are typical, is problematical. Other types of experiments are likely to present other failure and contamination problems.

6.2.3.2 Cleanup of fueled experiments. - As already stated, the rupture of the fuel elements in any kind of fueled experiment designed for high-level operation is likely to be rapid and the contamination severe throughout the coolant passages. The first trace of a leak can doubtless be detected as soon as the added activity is comparable to that normally present in the coolant stream. The details of this detection have not been worked out but will depend upon each type of coolant. The normal gamma activity of the coolant stream is likely to be high throughout the coolant passage, particularly for sodium. For this reason delayed neutrons might offer the best basis for detection (ref. 6.8). Whether any kind of detection will be rapid enough to permit reduction of reactor power before extensive fuel element damage occurs, is not yet known. If not, then the coolant stream will be extensively contaminated with fission products in the form of metal debris, inert gases, oxides, nitrides, and to some extent, bromides and iodides. The size of these particles is problematical and will depend in part upon the rate of temperature rise and the temperature overshoot that occurs.

The replacement cost, plus that of disposing of such bulky apparatus as these experiments entail, will generally be far greater than the cost of decontamination to a re-use level. This means that a decontamination program will have to be devised for all such experiments and provision made in the original design to facilitate these operations.

Once an experiment has had its interior contaminated by a fission leak, there are several steps which will be generally applicable. These will differ in detail between types of experiments and the extent of the contamination, the latter being a factor which may not be easily evaluated. These steps can be enumerated as follows:

1. The usual instrumentation will scram the reactor once a leak has been detected.

2. Cooling fluid flow must be maintained for a short time thereafter to remove decay heat. After this, the experiment can be pulled back into its quadrant at the earliest opportunity. There will be no particular virtue in minimizing the cooling period because the contamination level within the experiment is not likely to increase once the reactor is shut down. Normal instrumentation will indicate whether any activity has penetrated the experiment walls.

3. After removal of the experiment test piece from the thimble, and resealing of the thimble, the reactor is once more operable for other research. The experiment can be left in its quadrant or moved directly to the hot laboratory canal extension (see section 2.1.9 and fig. 2.20) for such time as is required for activity decay.

4. By this time the experiment can be transferred to the Dry Hot Storage, or directly to the Hot Handling Room (see fig. 2.20) if prompt dismantling is desired. Up to this point all steps are essentially alike irrespective of any internal contamination.

5. Once ready for dismantling, the experiment must next be cleared of coolant fluids. If these are contaminated, this operation is the first requiring additional precautions beyond those normally followed. Since the coolant is either liquid or gaseous, some provision for removal of fission gases in a controlled manner will be necessary. The required precautions are substantially like those outlined for the degassifier in section 5.2.1.2. By straining the coolant fluid during removal, the greater part of any unburned fuel contained therein should be recovered. Under most circumstances, the bulk of unburned fuel will remain within the experiment.

6. The next step involves sawing off the experiment test section and transferring it to one of the hot cells for further dismemberment. Here the bulk of the unburned fuel must be recovered by a combination of chemical and mechanical operations. In general, the complete separation of all fuel from container materials will not be attempted.

E-102

7. The other portion of the experiment must be decontaminated to such a level that any remaining activity will neither interfere with the next use nor be a radiation hazard during further disassembly, repair, and reassembly. The initial decontamination will probably be performed in the Hot Handling Room where adequate shielding exists. The techniques employed will depend upon the particular coolant being used. Flushing the system with fresh coolant may be the logical first step, otherwise an appropriate wash solution. If the rig contains sodium or other reactive material, this must be removed completely prior to flushing with water solutions. The use of inhibited acid solutions may be necessary followed by a water rinse. Water solutions will have to be evaporated as for the hot cells as discussed in section 5.2.4.

8. After completion of such preliminary cleaning, the rig will be transferred to the Decontamination Shop (fig. 2.20). Here the contamination level must be such that dismantling operations are possible with close control of exposure times. Workmen will wear such protective clothing, masks, etc. as may be required. Upon completion of dismantling and further decontamination in this area, the experiment components will be transferred to the adjacent Repair Shop. Here the rig will be reassembled in preparation for the next experimental project. The contamination level should be such that a practical minimum of exposure control is required.

9. All waste and scrap will be controlled rigidly and disposed of in a manner dictated by the nature of such waste.

### 6.3 HAZARDS RESULTING FROM ACTS OF GOD, WAR, SABOTAGE, NEGLIGENCE, AND EXPLOSIONS EXTERNAL TO THE FACILITY

#### 6.3.1 Severe Storms

Records of extreme weather conditions in the Sandusky area are given in appendix C and are summarized here. The two most severe types of storms are thunderstorms and tornadoes. Thunderstorms average 32 days per year occurring primarily in the summer, June and July averaging 7 days apiece. Thunderstorm activity is extremely variable but a rare severe storm may cause winds in excess of 50 mph, 1 to 3 inches of rain in an hour and hailstones 1/2 inch or larger in diameter.

Situations favorable for the formation of severe thunderstorms are also conducive to tornado formation. A 35 year study of the tornadoes in the United States shows that 111 tornadoes occurred in Ohio during this period. The largest percentage of these storms occurred in the northern and western portions of the state. One tornado has occurred in Sandusky in 73 years, that occurring in 1924. The highest wind speed ever recorded at Sandusky, 77 mph, occurred during this tornado.

A tornado is not expected to result in a hazard to the reactor itself although considerable damage may be inflicted to the reactor building (outside the containment tank), the auxiliary buildings, and the water towers. The pump room and the hot labs are both of heavy reinforced-concrete construction so it is extremely unlikely that they will be damaged in a tornado.

Lightning damage might possibly disrupt electrical power but two separate power lines supply the facility. If both of these lines are disrupted, the reactor will scram. A diesel generator runs continuously to supply 1000 gpm through the shutdown water system which is adequate for reactor afterheat. A second diesel generator will automatically take over the load in event the first one fails.

E-102

### 6.3.2 Floods

The land surface in the vicinity of the reactor is 65 feet above Lake Erie, sloping gently towards the lake, so flooding of the complete area is unlikely. However, the reactor building is located within a diked area to prevent surface water runoff in the event of a catastrophe. The heaviest rainfall ever recorded in 24 hours is 6 inches and the heaviest snowfall in 24 hours is 14 inches. In the event of a severe rainstorm (such as 6 in. in a 24 hr period) it is possible that the culverts will be inadequate to keep the area drained. This is not expected to be a hazard because all radioactive waste tanks are covered and the integrity of the containment tank is maintained. To prevent floating of the waste tanks in the event of a flood they will be purposely flooded when this danger exists.

The floor above the handling canals is 1.5 feet above grade so a flooding to this depth is necessary before flood water mixes with canal water. In the unlikely event that radioactivity does appear in the flood water, the monitors on the culvert valves will shut off these valves and prevent the radioactive water from leaking to populated areas.

### 6.3.3 Earthquakes

Earthquakes having epicenters in the Sandusky area have never been recorded. According to Dr. Edward J. Walter, Seismology Laboratory, John Carroll University (personal communication) earthquakes have been centered to the south, east, and west of Sandusky and the maximum intensities of these have been 7 to 8 on the Modified Mercalli intensity scale. The occurrence of such earthquakes is roughly about one in every five or ten years. According to Heck (ref. D.2) there are 11 earthquakes reported having epicenters in Ohio to 1947, including 5 important ones. Table 6.1 lists the major earthquakes reported in Ohio. An additional discussion is given in the geology report (appendix D).



TABLE 6.1. - MAJOR EARTHQUAKES HAVING EPICENTERS IN OHIO

Date	Hour	Locality		Area felt, sq mi	Intensity, Rossi-Forel scale
		North latitude	West longitude		
June 18, 1875	0743	40.2	84.0	40,000	6-7
Sept. 19, 1884	1414	40.7	84.1	125,000	6
Sept. 20, 1931	1705	40.2	84.3	40,000	8
March 2, 1937	0948	40.7	84.0	90,000	8
March 9, 1937	0045	40.6	84.0	150,000	8

The earthquake of 1875 caused minor damage at Sidney, Ohio. The earthquake of 1884 was centered at Columbus, Ohio, and effects of it were felt as far as Washington, D. C., and Michigan. Some property damage was caused by an earthquake at Anna and Sidney, Ohio, in 1931. Two earthquakes which occurred one week apart in March 1937 centered around Anna and Sidney and caused property damage in those towns, in Lima and Bellefontaine, Ohio, and in Ft. Wayne and Indianapolis, Indiana. The second shock was felt in the upper stories of buildings in Chicago, Illinois, Milwaukee, Wisconsin, and Toronto, Canada. The center of this region of earthquakes is approximately 110 miles southwest of the reactor site.

The earthquake hazard to the reactor facility is sufficiently low that no seismograph-operated scram circuit is considered to be necessary.

#### 6.3.4 Bombing

The only bombing considerations will be for bombs of a nonnuclear type. To release fission products would require a direct hit in which the bomb would pierce the containment tank and explode at the bottom of one of the quadrants.

The most serious situation would occur if the bomb exploded in a "wet" quadrant and demolished both the reactor tank wall and the shielding pool wall in one quadrant only. In this event the 5000 gallon head tank would supply water immediately and a 50,000 gallon head tank would supply water automatically in 15 seconds. In addition to this a 100,000 gallon head tank is available which is supplied through a manually actuated valve. Further emergency water is available from the reservoir on the NACA site and from the domestic and fire main systems to prevent core meltdown.

If any of the walls between the quadrants ruptured or if the entire reactor vessel ruptures in addition to either of the walls mentioned above, the core would not be drained. If the motorized valves between the quadrants and the annulus (mentioned in section 6.1.2) were opened, the core would not be drained.

A conservative calculation shows that the core would melt in approximately 10 seconds in event of a complete loss of water at the same time the reactor scrams. If melting occurs, a metal-water explosion conceivably could result (see section 6.4). This would disrupt the core and release a considerable amount of fission products.

#### 6.3.5 Sabotage

Sabotage is probably the most difficult hazard to provide for in a design. It would be difficult for a saboteur to gain entry from the outside since he would be required to first break through the area security fence and then gain access to the containment tank. The entrances to the Plum Brook Ordnance Work area and to the NACA area will be guarded at all times.

A more likely occurrence would be sabotage by a demented or subversive employee. The philosophy which has been adopted is to protect vulnerable points in the facility by maintaining an efficient security force and by using protective methods which require the actions of two individuals to gain access to critical areas.

It is foolhardy to state that a reactor cannot be sabotaged through malicious mishandling of the control system and its wiring. The discussion must, therefore, rest upon how difficult it is to produce damage. The only way to destroy the reactor through its control system is to cause the control rods to withdraw from the core and to remain withdrawn until the reactor destroys itself. In order to do this for the reactor herein described, it is necessary to override all the interlocks placed upon rod-out motion by the power set-back circuits (reverse, fast set-back, slow set-back, and rod stop) as well as the regulating-rod and shim-rod interaction limits. Also, it would be necessary to abrogate all the "slow" scram circuit interlocks that would sense reactor run-away through secondary effects, e.g., temperatures, pressures,  $N^{16}$  activity, etc. Lastly, it would be necessary to completely inactivate the "fast" scram circuits in such a manner that the sigma bus did not collapse and so that all units in the period and safety circuits would remain normal and sound no alarm. If there would be dynamic experiments (e.g., pump loops, etc.) in the reactor flux, it would also be necessary to prevent them from causing the reactor to scram.

The above outlined changes, modifications, and rewirings would involve no small effort upon the part of a saboteur and would limit his employment to that of reactor operator, since, during times when the reactor is shut down, the control system is double locked-out in a full scram condition (i.e., driving rods not latched to control rods). The

saboteur would be required to have considerable knowledge of the wiring and would have to violate locked cabinets (not under his key control). The necessary rewiring would have to be done without error because a misstep would cause reactor scram.

The spent or new fuel elements could possibly be arranged in the water of the canal to form a supercritical assembly. Therefore, the new fuel elements will be stored in movable racks which will be kept in a locked vault requiring the simultaneous use of two separate keys for entry as described in section 5.1.1. The underwater storage racks will be individually locked as described in section 5.1.3.

Sabotaging the main power lines will not result in a hazard because the reactor will automatically scram and the diesel generator will supply a 1100 gpm water flow. It would be necessary to cut out both main power lines and the diesel generator in order to introduce a hazardous condition. Even if the fuel plates do melt as a consequence and cause a metal-water reaction with a resultant explosion the integrity of the containment shell will not be violated. For a discussion of the metal-water reaction and resultant explosion see section 6.4.2 and appendix G.

It is realized that it is impossible to design for complete protection against sabotage. Only the more obvious methods of protection have been considered and a practical limit is reached when the ease of operation of the facility has been impaired.

#### 6.3.6 Negligence

The history of accidents in atomic energy activities has shown that negligence is one of the largest contributing factors to accidents. The most difficult task in preventing negligence is that of promoting continued safety consciousness even though no accidents have occurred.

The operation of the nuclear reactor itself is most hazardous during startup and shutdown operations. It will be required that the shift leader of reactor operations and the console operator both be present in the control room during these operations. When the reactor is on servo control the console will normally be manned by the console operator with the shift leader of reactor operations available for relief. An operating manual for reactor operations will be prepared which will include standard operating procedures and operating restrictions imposed by nuclear safety considerations. A check list will be prepared for startup and shutdown operations which must be checked by the console operator and initialed by the shift leader of reactor operations. During operation, the console operator will be required to maintain a log book and to take meter readings periodically.

The operation of experiments will be handled in a manner similar to that of the reactor except that potentially hazardous experiments must

E-102

CZ-15 back

be very carefully tended. An operating manual which must be rigidly adhered to will be prepared. Check lists will be used for startup and shutdown operations. If there are any changes in the experiments which affect the reactor in any way, the shift leader of reactor operations must be notified.

#### 6.3.7 Explosions in the Magazine Area

Located in the Plum Brook Ordnance Works is an ammunition storage area described in section 3.2.1 and shown on figure 3.1. The 99 igloos located there are each of 250,000 pound TNT (or equivalent) capacity and range from 8000 to 16,000 feet from the reactor site. The igloos are spaced 400 feet apart. It is a matter of concern what effect an accidental explosion in one of these igloos might have on the reactor facility.

This matter was discussed with Mr. J. A. Bately, Jr., Safety Branch Chief of the Intelligence, Security, and Safety Office of the Office of the Chief of Ordnance of the Army. He gave an opinion that the earth tremor would be of insufficient intensity to cause any structural damage to the foundation of the reactor building. He also stated that the air blast would be very low but possibly may cause window damage.

Experimental data on large HE explosions (250,000 and 500,000 lb) in igloos are available from tests made at Arco, Idaho in 1945 and 1946 (refs. 6.9 and 6.10). The horizontal accelerations at the ground surface for various distances from the explosion are shown on figure 6.10. These igloos were situated on about 20 feet of sand and gravel over volcanic rock. The horizontal displacement of the earth at a distance of 8500 feet from these blasts was approximately 0.025 inches.

The air blast was measured in the Arco tests (refs. 6.9 and 6.10) and a slight extrapolation of these data indicates that the peak overpressure would be about 0.4 psi. It is concluded in reference 6.10 that the air blast at distances over 6000 feet from this size explosion should cause very little flying glass from window breakage.

These experimental data indicate that the accelerations in the ground at the reactor site from a 250,000 pound TNT explosion in an igloo will be less than 0.002 g's and the air overpressure will be about 0.4 psi. This acceleration is so low that no damage of any type is expected to the reactor. The air overpressure is likely to cause slight window breakage. These conclusions substantiate those of Mr. Bately.

The probability of an explosion in one igloo setting off another igloo is considered to be very low. In the Arco tests (ref. 6.10) an igloo containing 500,000 pounds of TNT (twice rated capacity) was set off

next to another loaded igloo at a clear distance of 185 feet without causing a sympathetic explosion. It is concluded in reference 6.10 that:

"...there is small probability of propagation of explosion from one igloo magazine containing 500,000 net pounds of TNT to another parallel to the first, at a clear distance of 185 feet...observers with long experience in military high explosions, after examining the condition of the target magazine and its contents were unanimous in the opinion that there was little likelihood of a detonation."

#### 6.4 MAXIMUM CREDIBLE ACCIDENT AND ITS CONSEQUENCES

The accident considered here is the excursion resulting from the inability of the control system to compensate for the addition of a large step-increase in reactivity to the reactor.<sup>1</sup> In this excursion, the reactor power and temperatures increase rapidly until some inherent self-limiting process in the reactor stabilizes the situation or until the reactor disassembles itself. The runaway to destruction in a reactor of this type would probably include the melting of the fuel plates, an explosion in the reactor pressure vessel, and the scattering of radioactive materials. It is an event which could create a considerable hazard both for the operating personnel and the general populace.

For the sake of convenience the type of accident described in the above paragraph will be called a Borax-type accident. Analyses (based on limited information and uncertain theories about the nuclear excursions) have been made of various aspects of a Borax-type accident in the NACA reactor. Some of the results of these analyses are presented in the following order:

1. The nuclear excursion including estimates of the energies released and temperatures attained
2. The chemical reactions which may result from the nuclear excursion
3. The concept of an equivalent TNT explosion
4. The forces acting on the containing structure of the reactor
5. The ability of the reactor containing structure to resist these forces

---

<sup>1</sup>The inability of the control system to compensate for this change in reactivity might occur because of some failure of the control system or because the nuclear events in the reactor occur too rapidly for the control system to be effective. The large step-increase in reactivity is assumed, even if it is difficult to conceive of its actual occurrence, because it represents the worst possible condition.

6. Additional analysis of 4 and 5 above carried out by Armour Research Foundation for the NACA.
7. The radiological hazards from the release of the fission products
8. Emergency procedures in the event of serious fission product release

#### 6.4.1 The Nuclear Excursion

The only inherent self-limiting process, other than reactor disassembly, which will appreciably affect a Borax-type excursion is the formation of steam in the reactor core. The effectiveness of steam formation as a self-limiting process was demonstrated in the series of Borax and Spert tests and is reported in references 6.11, 6.12, and 6.13. Various attempts have been made to predict analytically the results of Borax-type excursions, in water moderated reactors with Borax (MTR) type fuel elements, considering the effect of steam formation as a self-limiting process. Four of these attempts are reported in references 6.14, 6.15, 6.16, and 6.17. All four attained some limited degree of success in predicting the results of the Borax experiments. There is considerable question as to the general validity of any of these analyses, but they were used to evaluate the results of Borax-type excursions in the NACA reactor because no better analyses were available. A discussion of the application of these analyses to the NACA reactor is presented in appendix F; some of the results are discussed below.

The variation of maximum fuel plate temperature with stable reactor period as computed by the four different methods is shown in figure F.2. The variation of nuclear energy release with stable reactor period as computed by three different methods (the method of reference 6.17 did not permit the calculation of energy release) is shown in figure F.3. The variation of maximum pressure with stable reactor period as computed by two different methods (the methods of refs. 6.16 and 6.17 did not permit the calculation of pressures) is shown in figure F.4. The table below summarizes some of the results of figures F.2, F.3, and F.4 of appendix F. The  $\Delta K/K$  corresponding to the various stable reactor periods was calculated in the same manner as was used to obtain figure 6.5.

Stable reactor period, msec	$\Delta K/K$	Maximum fuel plate temperature, °F	Nuclear energy release, Mw-sec	Maximum pressure in the reactor core, psia
40	1.1	350-750	5-35	135-200
20	1.3	400-800	10-40	145-300
10	1.8	900-1200	20-60	200-400
5	2.9	1500-2700	30-120	500-950

Two important assumptions in the analyses described above are the value of the void coefficient of reactivity and the effectiveness of the reactor hydrodynamic system as a means of pressure relief. Both of these topics are discussed in appendix F.

It appears that for periods longer than about 10 milliseconds ( $\Delta K/K$  less than about 1.8 percent) the fuel plates would probably not reach the melting temperature. The maximum predicted energy release for periods down to 5 milliseconds ( $\Delta K/K$  up to 2.9 percent) is about 120 megawatt-seconds. The Borax experiment in which the reactor was destroyed released about 135 megawatt-seconds; the period was 2.6 milliseconds. The NACA reactor, in all the various control rod accidents described in section 6.1, would certainly not reach a period as fast as 5 milliseconds because reactor disassembly would occur at somewhat slower periods. Accidents associated with experiments would cause insertions of reactivity (see section 6.2), but these would certainly not be large enough to result in reactor periods as short as 5 milliseconds.

#### 6.4.2 Possible Chemical Reactions

If the fuel plate temperature in an excursion were to become high enough to melt the aluminum or the aluminum-uranium alloy, a reaction might occur between the metals in the fuel plate and the water in the reactor. The possibilities of such a reaction occurring, the extent to which it might occur, and the energy released by the reaction are discussed in appendix G. How much metal in the fuel plates would react with water is very uncertain. However, to give some idea of the magnitude of the energy releases involved, if all the aluminum and uranium in the fuel plates were to react with water, the energy release would be about 1350 megawatt-seconds.

If all the metal in the fuel plates were to react with water, the reaction products would include about 23 pounds of free hydrogen. The nuclear and chemical energy released by the nuclear excursion and concurrent metal-water reaction would undoubtedly rupture the reactor tank and hurl a portion of the contents of the reactor tank into the air-filled dome of the containment tank. The possibility of the hydrogen reacting with the air in the dome of the containment tank and the energy which could be produced by this reaction are discussed in appendix G. Calculation of the final equilibrium conditions indicate that the final hydrogen-air mixture would be well below the flammability limits for hydrogen-air mixtures. The equilibrium concentration of hydrogen would be about 1 percent by volume while the minimum concentration required for flammability is about 4 percent by volume, and the minimum concentration required for detonability is about 18 percent by volume. The possibility does exist, however, that during the transient a portion of the hydrogen might form a flammable or detonable mixture with the air which could be ignited by hot metallic pieces from the reactor debris.

#### 6.4.3 Equivalent TNT Explosion

A Borax-type excursion severe enough to melt the fuel plates and rupture the reactor tank is sufficiently complex that it is difficult or impossible to estimate theoretically the loads that it would apply to the containing structure. Further, there is very little experimental information on which any detailed estimate could be based. The assumption is therefore made that the destructiveness of a Borax-type excursion can be replaced by the destructiveness of a TNT explosion of the same energy content as the Borax-type excursion. It is felt that this is a conservative assumption for two reasons: the energy release in a TNT explosion is much more rapid than in a reactor excursion; an explosives expert estimated that damage to the containment vessels of the Borax reactor caused by the final destructive excursion could have been caused by about 6 to 17 pounds of TNT (ref. 6.11); the energy released was equivalent to about 70 pounds of TNT.

The nuclear energy release predicted by the different methods of analysis for a Borax-type excursion in the NACA reactor is less than 120 megawatt-seconds for periods down to 5 milliseconds (fig. F.3, appendix F). This predicted energy release is less than the energy release of 135 megawatt-seconds (at a period of 2.6 millisecon) which accompanied the destruction of the Borax reactor. Let us assume that the nuclear energy release for the NACA reactor is 135 megawatt-seconds. Let us further assume that 50 percent of all the metal in the fuel plates react with water. This would release an additional 675 megawatt-seconds of energy which is a very large amount of energy compared to the assumed nuclear energy. Any energy liberated by the reaction of the hydrogen released by the metal-water reaction would occur in the air-filled region above the shielding pool and would not appreciably contribute to the forces in the shielding pool. The effect of possible hydrogen-air reactions will therefore be considered separately. Combining the assumed nuclear energy release of 135 megawatt-seconds with the assumed energy release of the metal-water reaction, 675 megawatt-seconds, we arrive at a figure for the total energy of 810 megawatt-seconds. The weight of TNT which would have an energy equivalent to this is approximately 400 pounds. We will, therefore, consider the effects on the reactor containment structure of an explosion of 400 pounds of TNT at the location of the reactor.

If 50 percent of the metal in the fuel plates were to react with water, approximately 11.5 pounds of hydrogen would be formed. An estimate of the effect on the reactor containment structure of the reaction with air of this hydrogen in the air-filled region above the shielding pool will be made.

#### 6.4.4 Forces on the Reactor Containment Structure

Appendix H presents a discussion of the forces on different parts of the reactor containment structure due to a 400 pound TNT explosion at the



reactor location. Pressure-time and impulse-time histories for the reactor pressure tank and the floors and walls of the reactor shielding pool are shown in figures H.1 and H.2 of appendix H.

The forces which might act on the dome of the reactor containment tank, if a hydrogen explosion occurred in the air above the shielding pool, are discussed in appendix H, as is the equilibrium pressure in the containment tank after an excursion.

#### 6.4.5 Structural Analysis

The ability of the containment structure to resist the forces due to the 400 lb TNT explosion, the concurrent hydrogen-air explosion, and the resultant equilibrium pressure is discussed in appendix I. The following are the conclusions of appendix I.

1. The reactor tank and the concrete adjacent to its sides would fail.
2. The radial quadrant walls would be badly damaged, particularly near the reactor tank. The structural steel reinforcement in the outer sections of the quadrant walls would hold and, except for fragments and debris, the outer section of the walls would lift only about 0.15 inches and shift laterally only about 0.35 inches.
3. The steel reinforcing hoops in the shielding pool wall would elongate about 8 percent. The elongation to rupture of these hoops is about 16 percent and therefore, though the wall might crack badly, it would not fail in a gross sense.
4. The lead and concrete plug underneath the reactor tank would be broken loose and would fall to the bottom of the sub-pile room. The resulting stress would not exceed 4300 psi at the floor surface and would not exceed 2150 psi in the concrete just above the containment tank skin. The dynamic crushing stress in concrete is about 5000-6000 psi and therefore the concrete would not crush through to the containment tank skin.
5. About  $8.1 \times 10^6$  ft lbs of energy is required to crush the concrete in the fillet between the sub-pile room and the shielding pool floor through to the containment tank skin. The energy available would be about  $6.0 \times 10^6$  ft lbs. Therefore the concrete would not crush through to the containment tank skin.
6. About  $4.6 \times 10^5$  ft lbs of energy is required to crush the concrete in the shielding pool floor beyond the fillet through to the containment tank skin. The energy available would be about  $3.6 \times 10^5$  ft lbs. Therefore the concrete would not crush through to the containment tank skin.
7. Even if the concrete crushed through to the containment tank skin in items 4, 5, or 6 above, the containment tank would not fail, since it is backed by pressure grouted limestone bedrock in the regions considered in these items.

E-102

CZ-16

8. The shrapnel shield would raise about fifteen feet but, since the top of the containment tank dome is about 50 feet above the shrapnel shield, no damage would be done to the containment tank.

9. The maximum debris velocity likely to be encountered would be about 160 ft/sec. The maximum weight of steel fragment would not be likely to exceed 18 lbs. The velocity required for an 18 lb fragment to pierce the containment tank is about 1000 ft/sec. Therefore the containment tank would not be pierced by debris.

10. The hydrogen-air explosion, even if it occurred with the hydrogen-air mixture in contact with the containment tank, would not rupture the tank. The maximum biaxial elongation would be about 4.8 percent, if the area of contact were twenty feet in diameter. If the area of contact were two feet in diameter, experimental evidence indicates that a 12 gage (0.109 in.) or 14 gage (0.083 in.) sheet would not be ruptured and therefore the 3/4 inch thick containment shell would certainly be safe.

11. The weakest members of the containment tank from point of view of the equilibrium pressure of 2 psi, are the doors. These have been designed for a steady pressure of 5 psi with a safety factor of three. The containment tank would therefore readily contain the equilibrium pressures.

12. The containment tank would survive, its integrity would be maintained, and it would contain all solids, liquids, and gases present inside of it.

#### 6.4.6 Independent Analysis Carried Out by Armour

##### Research Foundation for the NACA

The problem of containing any possible Borax-type excursion is extremely important. Consequently, a contract was let to Armour Research Foundation for an independent analysis of the NACA reactor containment structure. This analysis has been carried out and the final report is added to this report as supplement II (ref. 6.18). The Armour Research Foundation analyses confirms the analyses carried out at the NACA in finding that the containment tank would survive the 400 lb TNT explosion, the subsequent hydrogen-air explosion, and the equilibrium pressure and that it would contain all solids, liquids, and gases inside of it.

#### 6.4.7 Radiological Hazards from the Release of Fission Products

The extreme importance of containing a Borax-type excursion which is sufficient to melt the fuel plates is indicated by a study of the

hazards associated with the release of fission products in either liquid or gaseous form. The hazards resulting from the release of fission products to the ground in liquid form, the hazards resulting from the release of fission products to the air in gaseous form, and the hazards resulting if all fission products are contained in the containment tank are discussed in appendix J. Some of the results of appendix J will be described below:

The hazards due to the release of all the fission products diluted in water was estimated for two cases. The first case, that of water seepage to the ground, would result in activities of about  $0.5 \mu\text{c}/\text{cm}^3$  at the nearest well, and activities of about  $0.08 \mu\text{c}/\text{cm}^3$  as the water enters Lake Erie. The second case assumed the worst possible conditions, including the assumption that the valves in the dikes surrounding the reactor are left open by mistake, the ground is frozen, and a heavy rainfall occurs shortly after the explosion. This case might contaminate as much as  $4 \times 10^{10}$  cubic feet of lake water to the level of  $3 \times 10^{-2} \mu\text{c}/\text{cm}^3$ .

The hazards due to the release of fission products in the form of a gaseous cloud was estimated in appendix J for several different sets of assumptions. The greatest possible doses which an individual could receive are tabulated below for two locations of interest. The worst dosages for all cases except one occur when fission products from a saturated core operating at 60 megawatts are released instantaneously under severe inversion conditions. The greatest possible inhalation dose to the nearest resident occurs when the fission products are released continuously over 24 hours.

	Dosages		
	External, r	Deposition, r/hr	Inhalation, r
Nearest residence, 3200 feet	38	170	12,000
Center of Sandusky, 4.5 miles	7	3.5	690

The hazards due to the release of large amounts of fission products which are all contained in the reactor containment tank were also estimated in appendix J. Dose rates and integrated doses for three locations of interest, and for various times, are tabulated below for the contained release of fission products resulting from 1000 hours of operation at sixty megawatts.

E-102

CZ-16 back.

Time, days after release of fis- sion products	Just outside the containment tank		Nearest point of NACA fence - 920 ft (see fig. J.16)		Nearest point of Ord- nance Works fence - 3000 ft (see fig. J.16)	
	Dose rate, r/hr	Integrated dose from time zero, r	Dose rate, r/hr	Integrated dose from time zero, r	Dose rate, r/hr	Integrated dose from time zero, r
0	39,000	-----	35	---	0.18	-----
1/4	8,600	200,000	6.8	50	.027	0.060
1	3,700	450,000	4.0	140	.011	.160
7	1,700	1,200,000	.91	410	.0013	.630
14	840	1,300,000	.34	470	.00045	.830
25	270	1,500,000	.10	550	.00011	1.080

The following conclusions may be drawn from the above tabulation:

In view of the extremely high initial dose rates just outside the containment tank, it is doubtful that anyone in the reactor building would survive unless they happen to be shielded. Other personnel on the site farther removed from the containment tank would have to be evacuated as rapidly as possible.

The dose rates at the nearest point of the NACA fence are high and certain portions of Plum Brook Ordnance Works would have to be blocked off. The portions closest to the site would have to be blocked off for a period in excess of twenty-five days. Calculations for longer times indicate that the period would not exceed ninety days. There would be ample time available to warn Ordnance Works personnel who happened to be in the vicinity of the site since the integrated dose in the first six hours would be about 50 r. Also, as may be seen from figure J.16, the sections of the Ordnance Works which would have to be blocked off would not seriously hamper the operation of the works.

The dose rate at the nearest point of the Ordnance Works fence, which represents the closest approach that the general public can make to the reactor, is not too high. The integrated dose which would be picked up at this point in the first week (168 hrs) would be about 630 mr which is only about twice the allowable continuous expose dose of 300 mr/week. The integrated dose for the second week is down to about 300 mr.

#### 6.4.8 Emergency Procedures in Event of Accident

Appendix K presents a description of the emergency procedures to be followed in the event of serious release of radioactive fission products.

## 6.5 REFERENCES

- 6.1. ORNL-120: Heat Dissipation from Fuel Assemblies of High Flux Reactor After Shutdown (declassified).
- 6.2. Newson, H. W.: MonP 271 (classified).
- 6.3. Bogart, D., and Hallman, T. M.: Supplement III. NACA Reactor Facility Hazards Summary. Reactivity Measurements with the Bulk Shielding Reactor. To be published.
- 6.4. Hunter, H. F., and Ballow, N. E.: Simultaneous Slow Neutron Fission of  $U^{235}$  Atoms. I - Individual and Total Rates of Decay of the Fission Products. ADC-65.
- 6.5. Ayers, John A.: Treatment of Radioactive Waste by Ion Exchange, Industrial and Eng. Chem., vol. 43, p. 1526 (1951).
- 6.6. Campbell, D. O.: Decontamination of Stainless Steel. Survey and Proposed Program. CF 53-5-233.
- 6.7. Bogart, D., and Soffer, L.: NACA RM E55L23 (classified).
- 6.8. Wade, G. E., and Berberet, J. A.: KAPL 120 High Pressure Recirculating Water Loop. HW-40919.
- 6.9. Igloo Tests, Naval Proving Ground, Arco, Idaho, 1945. Technical Paper no. 3, Army-Navy Explosives Safety Board, Washington, D. C., Revised Nov. 6, 1947.
- 6.10. Igloo and Revetment Tests, Naval Proving Ground, Arco, Idaho, Oct. 1946. Technical Paper no. 5, Army-Navy Explosives Safety Board, Washington, D. C., Jan. 5, 1948.
- 6.11. Dietrich, J. R.: Experimental Investigation of the Self-Limitation of Power During Reactivity Transients in a Subcooled Water-Moderated Reactor. AECD-3668.
- 6.12. Dietrich, J. R.: Experimental Determinations of the Self-Regulation and Safety of Operating Water-Moderated Reactors. International Conference on the Peaceful Uses of Atomic Energy (Geneva), vol. 13, paper 481, pp. 88-101.
- 6.13. Nyer, W. E., Forbes, S. G., Bentzen, F. L., Bright, G. O., Schroeder, F., and Wilson, T. R.: Experimental Investigation of Reactor Transients. IDO 16285.

- 6.14. Edlund, M. C., and Noderer, L. C.: Analysis of Borax Experiments and Application to Safety Analyses of Research Reactors. To be published.
- 6.15. Gartner, L., and Daane, R.: The Self-Regulation by Moderator Boiling in Stainless Steel  $\text{UO}_2\text{-H}_2\text{O}$  Reactors. NDA report 15-H-1.
- 6.16. Golian, S. E., Bergstrahl, T. A., Harris, E. G., and O'Rourke, R. C.: NRL report 4495 RD 480 (classified).
- 6.17. Booth, M. E.: Behaviour of Water-Moderated Reactors During Rapid Transients. M.S. Thesis, M.I.T.
- 6.18. Hoenig, S., Saleme, E., and Porzel, F. G.: Final Report of National Advisory Committee for Aeronautics Reactor Safety Program, Armour Research Foundation.

## SECTION 7. - ADMINISTRATIVE ORGANIZATION

### 7.1 ORGANIZATIONAL STRUCTURE

The diagram in figure 7.1 shows the suggested organization for the facility. The chief scientist at the facility is the Chief of Research Operations. He will be in charge of operation of the facility and of the research activities at the Plum Brook site. He will be assisted in the consideration and scheduling of experiments for the reactor and of changes to the facility and its operation by a Program Committee. The Program Committee will be headed by a Program Coordinator who will call meetings of this committee and organize the business handled by the committee. The Safeguard Committee will advise the Program Committee with regard to the safety and technical soundness of proposals under consideration. The Chief of Research Operations will also have on his staff a Personnel Training Officer who will study the educational needs of the organization, and make arrangements for the required instruction.

The Chief of Administrative Services at Plum Brook will administer the shop facilities, maintenance, purchase, and plant protection at the Plum Brook site. He will also serve to coordinate the administrative and service operation at the Plum Brook site with those at the Lewis laboratory for handling the construction or purchase of large items, and for handling administrative matters such as records, payrolls, budget, etc. The following is an outline of the responsibilities of the Committees and of the organizational segments shown on the diagram in figure 7.1.

#### 7.1.1 Program Committee

##### 7.1.1.1 Function. -

1. Rules on experiments for insertion in reactor with regard to scheduling and adequacy of equipment.
2. Rules on changes to reactor equipment or operation procedures.

##### 7.1.1.2 Membership of program committee. -

Program Coordinator, Chairman  
Chief of Technical Branch  
Chief of Operating Branch  
Chairman of Safeguard Committee  
Head of Project Engineers Section  
Head of Health Physics Section  
Chief of Technical Services Branch  
Chief of Research Operations (ex officio)

## 7.1.2 Safeguard Committee

7.1.2.1 Function. -

1. Make recommendations to Program Committee with regard to adequacy of design of experiment and whether proper tie-in of experiment with reactor safety system is provided.
2. Make recommendations to Program Committee on proposed changes to facility or operational procedures.

7.1.2.2 Membership of safeguard committee. -

Head Reactor Physics Section  
Head Engineering Design Section  
Head Instrument Research Section  
Head Operations Section  
Health Physicist

## 7.1.3 Technical Branch

7.1.3.1 Reactor Physics Section. -

- a. Analyze distribution in reactor of flux, power, temperature, coolant flow with various reactor fuel and control rod assemblies and various experiments.
- b. Operate zero power mock-up or reactor to determine  $\Delta K$  of reactor components and experiments.
- c. Study startup and transient behavior of reactor and prepare operating manual.
- d. Study methods of improving reactor performance and utility.
- e. Determine parameters needed for reactor analyses.
- f. Provide consultation services.

7.1.3.2 Instrument research section. -

- a. Research on improved instruments for the facility and for experiments.
- b. Improve control systems and safety systems.
- c. Provide consultation service.



7.1.3.3 Irradiated materials laboratory section. -

- a. Operate hot cells.
- b. Assist in making chemical and metallurgical analyses of materials irradiated in experiments in reactor.
- c. Analyze reactor components.

7.1.3.4 Engineering design section. -

- a. Design new equipment for reactor facility.
- b. Make engineering analyses of present and advanced facility operation covering such items as stresses, materials, coolant flow rates, coolant pumping requirements, coolant pressures, and temperatures.
- c. Design experimental equipment proposed to be inserted into reactor.

7.1.3.5 Project engineers section. - Provide project engineer for each proposed experiment or change in facility design who will schedule the project through the various stages, arrange for the cooperation of other groups at the facility, and train operational personnel in the handling of experimental equipment. He will supervise all personnel specifically assigned to a project.

7.1.4 Operations Branch

7.1.4.1 Facility operations section. - Operates reactor facility which includes reactor and all of the accessory equipment necessary for proper operation of the reactor such as coolant pumps, motors, generators, etc.

7.1.4.2 Experimental equipment operations section. - Provides test engineers for assignment to major experiments in reactor who have responsibility for proper operation of this equipment while inserted in reactor.

7.1.4.3 Health physics and safety section. -

- a. Provides safety and health regulations.
- b. Enforces these regulations.
- c. Provides radiation monitors.

- d. Makes periodic inspections.
- e. Studies methods of improving safety of the operation and plant.
- f. Supervises cleanup and maintenance of irradiated areas and equipment.
- g. Supervises disposal of radioactive by-products.
- h. Keep records on health physics.
- i. Keep records on radioactive materials on facility site.

#### 7.1.5 Technical Services Branch

##### 7.1.5.1 Plant protection section. -

- a. Guards
- b. Firemen

##### 7.1.5.2 Shops. -

- a. Operate assembly and construction shops.
- b. Arranges for construction of equipment at Lewis laboratory, and independent shops.

##### 7.1.5.3 Mechanical services section. -

- a. Provide mechanics, electricians, pipe fitters, etc., for construction and installing experiments or reactor facility equipment.

##### 7.1.5.4 Plant maintenance section. -

- a. Maintaining facility equipment in good repair.
- b. Maintaining grounds and building.

#### 7.1.6 Administrative Branch

##### 7.1.6.1 Purchase section. -

- a. Arrange for purchase of equipment.
- b. Obtain cooperation of Purchase Section at Lewis laboratory when required.

7.1.6.2 Clerical section. -

- a. Keep personnel records.
- b. Handle payroll records.
- c. Keep files on letters and documents.

7.1.6.3 Stenographic section. -

- a. Provide typing service.
- b. Handle report preparation and tie-in with Lewis laboratory organization on this subject.

7.1.6.4 Fiscal section. -

- a. Prepare budget.
- b. Keep records on funds and expenditures.
- c. Tie-in operation with Lewis laboratory Fiscal Department.

7.1.6.5 Computing section. -

- a. Make computations for staff.

It is estimated that 61 professional and 119 nonprofessional personnel will be required initially to operate the facility. A breakdown of this staff is shown in table 7.1. The number of personnel required will be adjusted or augmented when experience with operation is obtained.

## 7.2 STAFF TRAINING

This reactor facility, unlike AEC reactor facilities, will have to be staffed largely by people who at present have had little practical experience with the everyday problems of reactor operation which arise and demand prompt and correct operational decisions. To compensate for this situation, key staff members will be sent to several AEC sites for the purpose of gaining this type of experience while the NACA reactor is being built. Obviously, the number of trainees and the period of assignment will depend upon mutually acceptable arrangements being made with the AEC. These trainees will then serve as a cadre for training additional operators and supervisors during the initial performance testing of the NACA reactor. It is intended that they shall also prepare the requisite procedure and control manuals to be used for initial operations.

TABLE 7.1. - PROPOSED INITIAL STAFF FOR FACILITY

	Profes- sional	Nonpro- fessional		Profes- sional	Nonpro- fessional
Chief of Research Operations Secretary Program Coordinator Technical Assistant Personnel Training	1 1 1 1	1	Experimental Equipment Operations Section Mechanical Engineers Scientific Aides	5	4
Technical Branch Chief Secretary	1	1	Health Physics and Safety Section Health Physicists Safety Monitors Records Clerk Engineer Scientific Aides Cleaning hot area Cleaning hot equipment	4	5 1 3 4 2
Reactor Physics Section Nuclear Engineers Physicists Mathematicians Physical Chemists Technical Aides	2 2 3 2	2	Chief, Administration and Technical Service Secretary	1	1 1 1
Instrument Research Section Physicists Electrical Engineers Electronic Technicians	2 3	3	Technical Service Branch Chief Shop Section Machinists Sheetmetal Workers Carpenters Coordination with Lewis shops	1	4 4 3 1
Irradiated Materials Lab Analytical Chemists Metallurgists Physical Chemists Physicists Hot Lab Operators	2 2 2 3	3	Mechanical and Electrical Services Section Electrical Engineers Electricians Instrument Calibration and Repair Mechanics Pipe Fitters	2	2 4 2 2
Engineering Design Section Mechanical Engineers Electrical Engineers Chemical Engineer Metallurgical Engineer Draftsmen	4 2 1 1	4	Plant and Ground Maintenance Section Mechanics Laborers Janitors		3 3 3
Project Engineer Section Mechanical Engineers Chemical Engineer Electrical Engineer Scientific Aides	4 1 1	4	Security and Plant Protection Guards Clerk Firemen		6 1 4
Operations Branch Chief Secretary	1	1	Administrative Branch Chief (Most of these functions will be handled by LPPL staff) Purchase Section Clerical Section Stenographic Section Fiscal Section Computing Section		3 3 6 4 10
Facility Operation Section Shift Leaders Console Operator Auxiliary Equipment Operators	5	5		2	2
			Sub-total	61	119
			Total		180

E-102

As a minimum, this experienced cadre should include the Program Coordinator, the Safeguard Committee Chairman, the Technical Branch Chief, the Operations Branch Chief, and the Heads of the Reactor Physics Section, of the Irradiated Materials Laboratories, of the Project Engineers Section, of the Health Physics and Safety Section, and as many shift leaders from the Facility Operations Section as are available. This totals between 9 and 12 people. Their training periods might vary from 2 to 6 months each. It is hoped that they can be given training assignments which permit their working closely with their counterparts at AEC sites.

This matter of staff training and development is one that receives continuing attention in most well-managed laboratories. This is particularly desirable in a reactor facility because of the necessary and continuing emphasis on safety and teamwork. For this reason the Chief of Research Operations will have on his staff a Personnel Training Officer who has prime responsibility for the proper indoctrination and training of all new employees assigned to radiation work, both technical and non-technical.

The present shortage of people with experience and training in nuclear technology is likely to continue if the nuclear power field develops as rapidly as some enthusiasts predict. Under these circumstances the rate of turnover of qualified personnel is likely to be higher than normal. Replacements for all group leaders must then be available on short notice, hence supervisor development will be emphasized and encouraged. There seems to be no alternative since most of these replacements will generally come from within the available staff.

### 7.3 PROCEDURES FOR HANDLING EXPERIMENTS OR CHANGES

#### IN REACTOR DESIGN AND OPERATION

Experiments for the reactor facility will originate at the Plum Brook facility, at the Lewis laboratory, at the AEC, or with contractors of the AEC or Air Force. In addition, proposed changes to the reactor design and operation may originate at the Plum Brook site or elsewhere.

For the purpose of promoting the safety of the facility operation the following is the procedure through which all proposed experiments and facility and operational changes must pass:

1. The proposed experiment, facility change, or operation change is referred to the Program Committee through the office of the Chief of Research Operations and is presented briefly in conceptional form with regard to the purpose and method.

2. If the Program Committee approves the proposal, it sets a preliminary test date and it authorizes the appointment of a project engineer who brings the project to the Engineering Design Section.

3. The project engineer, together with representatives of the group that have proposed the experiment, and the Engineering Design Section develop the final design. The project engineer has the responsibility of coordinating all of the efforts on the Plum Brook site relating to the design, construction, and testing of the proposal, and supervises all Plum Brook personnel assigned to the proposal. He brings into the project, as is required, the services of other personnel on the site. He obtains the guidance of the Safeguard Committee regarding the compatibility of the design with the safety requirements of the facility, such as the tie-in of the experiment with the reactor scram circuits.

4. After satisfying the Safeguard Committee, the project engineer schedules presentation of the completed design to the Program Committee, and organizes this presentation.

5. On approval of the proposal by the Program Committee with the advice of the Safeguard Committee, the project engineer arranges for construction of the experiment.

6. When the completed apparatus is delivered to the site, the project engineer arranges for the services of experimental equipment operators and supervises them in the operation of the experiment outside of the reactor to obtain familiarity with its handling characteristics. The project engineer, the equipment operators, and the proposer of the experiment prepare an operating manual for the experiment which itemizes the test conditions and procedures and the safety procedures.

7. The project engineer then makes application to the Program Committee for an approval document authorizing insertion of the experiment in the reactor, or the proposed changes to the facility or its operation. The operating manual is submitted to the Program and Safeguard Committees for comment. The Program Committee must be shown that the operators have obtained the required operational experience with the experiment outside the reactor; that the proper tie-ins with the reactor scram system are being provided, and that the experiment has been approved by the Safeguard Committee.

8. If approval is granted by the Program Committee, an approval document is issued which contains the scheduling date and must carry the signatures of the Chairmen of the Program and Safeguard Committees, of the personnel initiating the proposal, of the Chief of the Operations Branch, and of the personnel specifically delegated to make the experiment insertion into the reactor, or the changes in facility design or procedure.

9. Items can be removed from the reactor only through presentation of a document which carries the signatures of the Project Engineer proposing the removal, Head of the Facility Operations Section, and of the Operational personnel specifically designated to make the removal.

10. On removal of an experiment from the reactor, the project engineer arranges for transportation of the experiment to the handling and storage areas, and for the required operations in the hot laboratories.

A project flow diagram illustrating these steps is shown in figure 7.2.

#### 7.4 ADDITIONAL REGULATIONS FOR PROMOTING SAFETY

1. The Technical Branch determines the operational procedure for the facility but cannot operate the facility.

2. The Facility Operation Section operates the facility according to the procedure specified by the Technical Branch but cannot change the procedure, except as specified in the operating manual (see paragraph 7, section 7.3).

3. Insertion or removal of experiments, control rods, fuel elements, moderator rods, and also repairs to the facility system can only be made on presentation of a document that as a minimum must contain the signature of the requester, the Head of the Facility Operation Section and of the person designated to make the actual insertion, removal or repair. The document must contain the date on which the act was completed. (The regulations regarding new experiments or changes to the facility or its operating procedure have been previously discussed.)

4. The operation of the facility can only be started via written and signed order of the Head of the Facility Operation Section.

5. Accident reports must be prepared on all accidents by the group in whose field of responsibility the accidents fall as decided by the Safeguard Committee. The report should cover the causes of the accident and the proposed corrective measures.

#### 7.5 HEALTH PHYSICS AND SAFETY

##### 7.5.1 Some General Comments on Safety

Industrial experience has demonstrated repeatedly that personnel safety cannot be relegated to some subordinate group (or individual) and forgotten, no matter how dedicated such persons may be. Personnel safety has to receive the direct support and continuing encouragement of all supervisors to be successful. This interest must stem from the top-most echelons of the organization. In the absence of this interest, the safety functions (and in the present case Health Physics as well) inevitably become segregated from the main effort with consequent loss of co-operation, initiative, and good will. Under these circumstances, safety operations are reduced to police type actions, with typical police attitudes, rather than being an adjunct to good management as they should be.

In the ideal case, all safety personnel should assist in getting assigned jobs done without relaxing safety standards unduly. They should help to overcome or circumvent the hazards inherent in a job rather than interpose endless restrictions or relax the rules beyond good reason. With a little thought and foresight, most jobs can be performed safely without too much extra cost. Delays often occur because of too little prior planning from a safety point of view.

It is one of the prime functions of good management to recognize this need for teamwork and to promote proper safety attitudes throughout the staff. This cannot be done by paying lip service to safety on the one hand, and encouraging or condoning relaxation of reasonable safety standards at the same time. The Chief of Research Operations of the NACA reactor will have to take a keen personal interest in the safety attitudes of his staff.

It is true that the safe way of doing a particular job might not be the quickest or cheapest, but it will lead to fewer heartaches, sickness, and lost time in most instances. As Stokinger and Laskin have pointed out, "No substance is too harmless to be disregarded, and no substance is too toxic to be used, if recognized as such, and adequate safeguards applied" (ref. 7.1). All too frequently, research people are intolerant of any restrictions on their freedom of action. In most of these cases this attitude is grounded in ignorance - either of the possible hazards, or of the proper techniques for coping with these hazards. Those few individuals who persist in this attitude, in spite of training and good supervision, are simply not suitable for work with radioactive materials.

#### 7.5.2 Functions of Health Physics and Safety Section

There are two aspects to the protection of personnel employed at any reactor facility. One involves control of ordinary mechanical and chemical hazards which suitably trained people can and will recognize. The other involves radiological safety, namely, the maintenance of radiation and contamination levels which are consistent with legal requirements (refs. 7.2, 7.3). This function is commonly called "Health Physics." Those with formal physics and biological damage training are called "Health Physicists" or "Radiological Officers." Those responsible for routine survey work are Radiation Monitors.

In view of the relatively small staff at this facility, the responsibility for ordinary safety will also be assigned to this group. The members of this group frequently visit all parts of the facility and of necessity know what experimental work is underway. With proper supervision and training, they should be able to assume both functions to advantage.



In addition to these strictly safety functions, this group has four other responsibilities, all of which have an indirect relationship to safety. One involves accountability for all source materials, and radioisotopes obtained under license from the AEC. The second is concerned with cleaning and general maintenance in areas subject to radiation and contamination. The third involves control of, and disposal of, all radioactive or contaminated materials at the laboratory which are not needed for further work. The fourth is concerned with personnel exposure records.

Accountability for source materials has to be a precise operation. This is easiest for fabricated units such as reactor fuel elements. It is not so easy for source materials used in fabricating fuel elements at the site for test purposes. Here all fabrication scrap, all hot cell scrap, burnup, and losses have to be evaluated, and a complete inventory maintained. In the case of radioisotopes obtained under license, the records must show receipts, locations at all times, and eventual disposal.

Control of low level contamination is a never ending chore wherever work with dispersible radioactive materials takes place. Walls, floors, and furniture must be washed periodically. Filters require replacement, and provision made for disposal of wastes of all sorts. Such jobs require nonskilled labor which needs the constant supervision and attention of someone who can evaluate the radiation hazard levels involved. For this reason such janitorial and maintenance employees responsible for this type of work will be assigned as a subgroup under Health Physics. Most of this work will be of a routine nature although assistance in handling high level wastes may be required. Individuals responsible for spills or other accidents may be required to clean up after their error, particularly if violation of laboratory rules is involved.

Storage and disposal of all contaminated wastes will be under the control of Health Physics since this group has to provide the monitoring service, packaging supervision, and identity information for shipping. Routine monitoring and control of disposal rate for gases and liquids is included in this function. All necessary radiation signs are posted and maintained by this group.

Finally, Health Physics will be responsible for the maintenance of personnel exposure records, processing dosimeters and badges, calibration of all monitoring equipment, area and air monitoring, inspection of radioactive material received from other sites, and any other duties peculiar to their interests and responsibilities. Special clothing will be provided for all those subject to contamination, the issuance and processing of which will be controlled by the Health Physics group.

## 7.6 SECURITY

The physical security of the NACA Reactor site is most important both as a safety measure and for the protection of classified information. Both

E-102

CZ-18

aspects are fully recognized in present NACA practice. The key personnel will be drawn from the existing NACA plant protection staff and will be given further instruction as to the safety provisions peculiar to this site. These men hold weekly training sessions in all aspects of their job.

These security personnel are usually military veterans who have some minor disability preference but who are nevertheless alert and able to assume the necessary responsibilities inherent in their job. All are required to wear Chief Petty Officer uniforms. Those posted at site entrances wear side arms, the proper use of which receives constant attention. The over-all supervision of this group will remain under Lewis laboratory control.

The Plum Brook Ordnance Works is surrounded by a cyclone-type fence with a guard post at the entrance serving the NACA reactor site. This entrance is located near the intersection of Taylor Road and Columbus Avenue (see fig. 2.3). The reactor site is surrounded by a second fence shown in this same figure. The gatehouse at the south end of the westerly north-south road will be manned by an NACA guard on a continuous three shift basis.

A secondary fence within the reactor site is shown in figure 2.4. It encloses auxiliaries which require special safety control, such as waste water storage ponds; service terminals such as power, fuel, and water; and contaminated equipment which permits outdoor storage.

All employees will receive a preliminary badge check at both the Arsenal and NACA entrances. All visitors (salesmen, technical consultants, truck drivers, etc.) will have their credentials checked at these points also. In general, all technical visitors will be accorded prior clearance by the NACA Headquarters, otherwise, by the Management of the Lewis laboratory.

Fire protection will be provided, at least initially, by Ravenna Arsenal, Inc., operators of the Plum Brook Ordnance Works. The activities at the site will be under the immediate control of the particular operating supervisors with the advice of the Health Physicist in charge at the time the emergency arises. Telephonic (and possibly radio) communication facilities will be available. Emergency medical and hospital arrangements will be made with local authorities.

As a supplementary measure, all important check points within the reactor site will be patrolled and inspected by the security staff on a periodic basis. This patrol function will be coordinated with the operational and radiation monitoring functions wherever possible.

## 7.7 REFERENCES

- 7.1. Stokinger, H. E., and Laskin, S.: "Air Pollution and the Particle Size Toxicity Problem - II." Nucleonics, vol. 6, no. 3, March, 1950, pp. 15-31.
- 7.2. Federal Register, July 11, 1955.
- 7.3. Federal Register, January 11, 1956.

E-102

CZ-18 Back



## APPENDIX A

### REACTOR HEAT TRANSFER

The reactor is designed to produce a total power of 60 MW from 27 MTR type fuel assemblies arranged in a 9 by 3 array. Of the total output of 60 MW it is estimated there will be 57 MW generated in the fuel plates. There are 23 standard fuel assemblies with 18 fuel plates in each assembly and 4 shim control rod fuel assemblies with 14 fuel plates in each assembly having a combined heat transfer surface area of 400 ft<sup>2</sup>. This results in an average heat flux of 490,000 Btu/hr-ft<sup>2</sup>. From neutron flux distribution calculations the ratio of the peak to average power is approximately 1.8:1 which results in a maximum heat flux of 880,000 Btu/hr-ft<sup>2</sup>.

The velocity in the fuel assemblies is 30 ft/sec and the local heat transfer coefficients were calculated from the equation

$$\frac{hD}{k} = 0.023 \text{ Re}^{0.8} \text{ Pr}^{0.4}$$

where the water properties were evaluated at the local bulk temperature. The heat transfer coefficient at the hottest point in the reactor was calculated to be 9000 Btu/hr-ft<sup>2</sup>-°F and a fouling factor of 25,000 Btu/hr-ft<sup>2</sup>-°F was assumed.

The reactor heat is to be transferred to a primary cooling water system, then by means of heat exchangers to a secondary cooling water system which dissipates the heat through the use of water cooling towers. It is therefore desirable to operate the reactor and primary cooling water at a high temperature level in order to dispose of the reactor heat as economically as possible. The maximum allowable fuel plate temperature was taken to be 315° F in order to avoid excessive corrosion of the aluminum. The pressure in the reactor tank was chosen to set the saturation temperature a minimum of 35° F above the calculated surface temperature of the fuel plates in order to prevent any boiling in the reactor during normal operation. This results in a pressure of 150 psia at the inlet to the reactor lattice. The maximum inlet water temperature to the reactor is 160° F so as not to exceed the maximum allowable fuel plate surface temperature. The maximum outlet temperature is achieved by using the same water to cool the reflector as is used to cool the fuel plates, i.e., the reflector cooling is in series with the core cooling. This has been compromised by placing some Be reflector pieces in the lattice (in parallel with the core) to gain flexibility in location of the fuel assemblies.

The primary cooling water enters the bottom of the pressure tank at 160 psia and 159° F, flows upward through the bulk of the reflector and

enters the top of the lattice at 150 psia and an average temperature of 160° F. The water then flows downward through the lattice and out of the pressure tank. The upflow is separated from the downflow by one inch thick Be plates cooled internally by 1/4 inch holes drilled vertically through the plates and spaced 1/2 inch between centers. The total primary water flow is determined by the flow through the fuel elements and through the interstices of the lattice and is approximately 15,000 gpm. Essentially all of the reactor heat goes into the primary water giving an average outlet water temperature of 187° F.

Inasmuch as most of the reflector is in series with the core, the reflector can be greatly overcooled during normal operation without imposing a large increase in cooling water flow. The maximum heat load in the Be adjacent to the core at 60 MW is estimated to be  $3 \times 10^6$  Btu/hr-ft<sup>3</sup>. All Be pieces were designed for the thermal stress caused by this heat load.

Shutdown heat fluxes for the fuel elements were based on the sum of the neutron decay power after scram and the beta and gamma decay power. The neutron decay power as a function of time after scram was obtained from figure 2.39 for a negative reactivity insertion of 10 percent. The beta and gamma decay power was calculated from the following equation of reference A.1

$$p = 5.9 \times 10^{-3} P \left[ (\tau - T_0)^{-0.2} - \tau^{-0.2} \right]$$

for the reactor operating for 10 days at 60 megawatts where  $p$  is the decay power in watts,  $P$  is the reactor operating power in watts,  $T_0$  is the operating time at constant power in days, and  $\tau$  is the number of days after start up. The shutdown cooling system flow rate of 1100 gpm through the lattice is sufficient to cool the fuel elements for this case 2 seconds after scram. The main pump coast down will take care of the first few seconds.

The rate of heat generation in the beryllium reflector was assumed to decrease by a factor of 3 at the instant of scram to  $1 \times 10^6$  Btu/hr-ft<sup>3</sup> and was assumed to decay with time according to the equation of reference A.1 given previously. The shutdown cooling system flow rate is sufficient to cool the beryllium reflector two seconds after scram. The pump coast down will take care of the first few seconds.

#### REFERENCE

- A.1. Glasstone, Samuel: Principles of Nuclear Reactor Engineering, D. Van Nostrand Company, Inc., p. 119, 1955.

APPENDIX BREACTOR PHYSICS CALCULATIONS

The diffusion equations and nuclear parameters used in the reactivity calculations are presented. A brief description is given of the methods used and results obtained in the calculations of reactivity, temperature coefficient, void coefficient, and mean prompt neutron lifetime. Preliminary results of excess reactivity control by burnable poisons are presented.

## LIST OF SYMBOLS

A	constant
$B^2$	total geometric buckling of the reactor
$B_z^2$	buckling in direction normal to direction of solution
D	neutron diffusion coefficient
H	height of reactor core
$K_{eff}$	effective multiplication factor
$K_f$	fast group multiplication constant giving number of fission neutrons produced per epithermal neutron absorbed
$K_{th}$	thermal multiplication constant giving number of fission neutrons produced per thermal neutron absorbed
k	Boltzmann constant
$L_f^2$	mean-square slowing down length of fission neutrons to thermal energy
$L_{th}^2$	mean-square diffusion length of thermal neutrons
$l$	mean lifetime of prompt neutrons
N	atoms per cubic centimeter
P	specific power in fissions/cm <sup>3</sup> -sec
$P_{th}$	fraction of fission neutrons escaping capture in slowing down to thermal energy

$\underline{r}$	vector distance
T	temperature of thermal neutrons
t	time
V	ratio of metal volume to water volume
v	neutron velocity
X	metal equivalence factor
y	fission yield in percentage
$\alpha$	ratio of radiative capture to fission cross section of $U^{235}$
$\delta$	reflector savings
$\eta$	number of neutrons emitted per neutron absorbed by a $U^{235}$ nucleus
$\lambda$	reciprocal period of prompt neutrons in $\text{second}^{-1}$ , also decay constant of a radioactive nuclide
$\nu$	number of neutrons emitted per fission of a $U^{235}$ nucleus
$\rho$	density of $H_2O$ in $\text{gm/cm}^3$
$\Sigma_a$	macroscopic neutron absorption cross section
$\Sigma_F$	macroscopic neutron fission cross section
$\sigma_a$	microscopic neutron cross section for absorption
$\phi$	neutron flux

#### Subscripts:

f	refers to fast neutrons
n	index number
th	refers to thermal neutrons

### DIFFUSION CALCULATIONS

Two-group multiregion diffusion calculations have been made based on the following equations (ref. B1):



$$D_f \nabla^2 \phi_f - (\Sigma_{a,f} + D_f B_z^2) \phi_f + K_f (1 - p_{th}) \Sigma_{a,f} \phi_f + K_{th} \Sigma_{a,th} \phi_{th} = \frac{1}{v_f} \frac{\partial \phi_f}{\partial t} \quad (B1)$$

$$D_{th} \nabla^2 \phi_{th} - (\Sigma_{a,th} + D_{th} B_z^2) \phi_{th} + p_{th} \Sigma_{a,f} \phi_f = \frac{1}{v_{th}} \frac{\partial \phi_{th}}{\partial t} \quad (B2)$$

where all of the quantities have been defined in the list of symbols. Equation (B1) includes a term giving the neutron production due to neutron absorptions above the thermal group. This term is  $K_f (1 - p_{th}) \Sigma_{a,f} \phi_f$  where the following definitions are made

$$\Sigma_{a,f} = D_f / L_f^2 \quad (B3)$$

$$K_f = \frac{v \Sigma_{F,f}}{(1 - p_{th}) \Sigma_{a,f}} \quad (B4)$$

Equations (B1) and (B2) apply for the passive regions with  $K_{th} \equiv K_f \equiv 0$ . At the interface between two regions the fluxes and neutron currents are made continuous. At the extrapolated boundary of the secondary reflector the fluxes are made zero.

The operator  $\nabla^2$  is modified such that the terms in the direction normal to the direction of solution are taken proportional to the flux. In equations (B1) and (B2) effective absorbers are introduced to account for the neutron leakage in these directions; these are  $D_f B_z^2$  and  $D_{th} B_z^2$  for the fast and thermal neutron groups, respectively. The quantity  $B_z^2$  is the geometrical buckling of the equivalent bare dimensions of the reactor normal to the direction of solution. The various geometrical bucklings were determined by iteration on the reactor simulator of the solutions for the dimensions of interest. The applicability of the foregoing two-group diffusion equations for light water moderated assemblies has been shown in reference B2.

The composition of each region was assumed to be homogeneous for purposes of solution. Solutions for the time-independent forms of equations (B1) and (B2) have been obtained using one-dimensional and two-dimensional electric analogs. The rectangular parallelepiped formed by the 9x3 array of fuel elements and surrounding reflectors was indicated in figure 2.8. The active lattice is nominally 9 inches wide, 27 inches long, and 24 inches high. The core has a composition by volume of 0.423 aluminum and 0.577 water and an assumed enriched uranium concentration

$^{235}\text{U}$  of  $0.000110 \times 10^{24}$  atoms/cc reactor (see ref. B.3). Top and bottom reflectors are regions containing 0.77 water and 0.23 aluminum by volume and are 9 inches thick. The primary side reflectors are regions containing 0.95 beryllium and 0.05 water by volume. The secondary side reflectors are regions containing water only and are infinite in thickness insofar as reactivity effectiveness is concerned.

The two-group nuclear parameters used for each reactor region and for the experiments are listed in tables B.1 and B.2 on the following page.

The reactivity and neutron flux distributions were obtained by iterative solutions on the two simulators. The final solution indicated that the value of  $K_{\text{eff}}$  was 1.185 for the cold startup loading of fuel elements containing 168 grams of enriched uranium and shim-rod fuel elements containing 130 grams of enriched uranium. The total buckling  $B^2$ , for the equivalent bare pile was estimated from these solutions to have a value of 0.005405; the vertical buckling  $B_z^2$  was estimated as 0.001622. These values were used in subsequent simplified calculations on the one-dimensional space simulator as an estimation of leakage in the direction normal to the direction of solution. The quantity  $B_z^2$  was computed from the expression

$$B_z^2 = \frac{\pi^2}{(H + \delta_1 + \delta_2)^2} \quad (\text{B5})$$

where

$H$  height of the active lattice in cm

$\delta_1$  reflector savings for top of core

$\delta_2$  reflector savings for bottom of core

values of  $\delta_1$  and  $\delta_2$  were obtained from reference B.4.

In order to calculate conveniently the temperature coefficient, void coefficient, and the mean lifetime of the prompt neutrons, a cylindrical reactor of the same height  $H$  and total buckling  $B^2$  as the reference slab reactor was employed. These cylindrical calculations should be reasonable approximations to the slab reactor and the coefficients calculated should apply for the slab. The radius of the cylindrical reactor core was taken as 22 cm; the primary reflector was 10 cm thick and consisted of 0.95 Be - 0.05  $\text{H}_2\text{O}$ , the secondary water reflector was 40 cm thick.

TABLE B.1 - NUCLEAR CONSTANTS FOR THE REACTOR ( $k_T = 0.025$  ev.)

Parameter	Core (ref. B.3)	Primary side reflector	Secondary side reflector	Top and bottom reflector	Experiment thimble
	0.423 Al, .577 H <sub>2</sub> O, U <sup>235</sup>	0.95 Be, .05 H <sub>2</sub> O,	1.00 H <sub>2</sub> O	0.23 Al, .77 H <sub>2</sub> O	0.67 Al, .33 H <sub>2</sub> O
$L_f^2$	64.0	82.0	31.4	44.0	137.0
$D_f$	1.320	.615	1.146	1.234	1.447
$P_{th}$	.844	1.000	.977	.974	.950
$D_{th}$	.269	.764	.160	.208	.445
$\Sigma_{a,th}$	.0813	.00218	.0196	.0177	.0142
$K_{th}$	1.675				
$K_f$	1.566				
$N_{U-235}$	.110x10 <sup>21</sup>				

TABLE B.2 - NUCLEAR CONSTANTS FOR THE EXPERIMENTS ( $k_T = 0.025$  ev.)

Parameter	Air-cooled fuel - element experiment in HT-1			Liquid-cooled fuel - element experiment in core position LC-6	
	0.33 S.S., .50 air .17 insulation	0.33 S.S., .50 H <sub>2</sub> O .17 insulation	Hydrogenous moderator	0.15 S.S., .85 air U <sup>235</sup>	0.15 metal, .85 H <sub>2</sub> O U <sup>235</sup>
$L_f^2$	6200	72.2	31.2	68,400	38.2
$D_f$	7.770	1.215	.933	6.750	1.123
$P_{th}$	0	.672	.966	0	.708
$D_{th}$	2.590	.246	.444	2.500	.175
$\Sigma_{a,th}$	.0697	.0794	.0192	.2143	.1755
$K_{th}$				1.784	1.655
$K_f$				1.644	1.546
$N_{U-235}$			.300x10 <sup>21</sup>	.300x10 <sup>21</sup>	.300x10 <sup>21</sup>
				3790	125.8
				2.529	1.463
				0	.839
				1.196	.345
				.0528	.0597
					102.0
					1.231
					.523
					.535
					.1494
					1.481
					1.417
					.194x10 <sup>21</sup>

Temperature coefficient of reactivity. - The temperature coefficient of the cylindrical reactor was obtained by solving the time-independent forms of equations (B1) and (B2) on the one-dimensional reactor simulator. The primary effect of an increase in reactor temperature is a decrease in the density of the water with corresponding reduction in the concentration of hydrogen and oxygen atoms. There is also the effect of an increase in the  $kT$  temperature of the thermal neutrons. The most important effect of the reduction of water density is the increase in the mean-square slowing down length  $L_f^2$  of fission neutrons to thermal energies. This increase in  $L_f^2$  tends to decrease the  $K_{eff}$  of the reactor and thus has an important bearing on the stability of the reactor. Values of  $L_f^2$  were computed by the following empiricism (ref. B.5) fitted to the experimental data of reference B.6 for aluminum-water mixture for the range of values of interest.

$$L_f^2 = 31.4 \frac{(1 + V)^2}{(\rho + XV)^2} \quad (B6)$$

where

V ratio of aluminum to water volumes

$\rho$  density of water

X aluminum equivalence to water, 0.292

The calculation of the temperature coefficient showed that the effects of variation of microscopic thermal absorption cross sections were negligible compared to density effects. (All of the  $\sigma_a$ 's were taken as  $1/v$  with the exception of  $U^{235}$ .) The only significant cross section effect was the temperature dependence of the effective microscopic transport cross section  $\sigma_{TR}^H$  for hydrogen due to chemical binding. The effects of chemical binding of hydrogen in water have been evaluated by a method due to Radkowsky. Values of  $\sigma_{TR}^H$  used have been presented as a function of temperature in reference B.7.

The effect of the expansion of the aluminum fuel elements was found to be unimportant. The strongest effect was due to the variation of  $L_f^2$  with temperature as a result of the decreased density of the water.

Two sets of calculations were made on the one-dimensional simulator. One set with the temperature of the reflector varying in the same manner as the temperature of the core. The second set with the temperature of

the core varying and with the reflector kept at the average reactor operating temperature of 82.2° C (180° F). These two sets of calculations gave identical results for the temperature coefficient; this is reasonable since the primary reflector is 0.95 beryllium - 0.05 water and the parameters for this reflector changed but little with temperature.

The results of the simulator calculation are shown in figure B1 where  $\Delta K/K$  °C is plotted as a function of temperature. It is seen that the temperature coefficient is negative and increasingly so with temperature. At the average reactor operating temperature of 82.2° C (180° F) the value of  $\Delta K/K$  °C is  $-18.0 \times 10^{-5}$  ( $-10^{-4}$   $\Delta K/K$  °F).

Void coefficient of reactivity. - Another coefficient of importance in evaluating the kinetic behavior of the reactor is the void coefficient. In making the calculations, voids are introduced in the reactor core, the nuclear parameters varied accordingly, and the diffusion equations solved on the one-dimensional simulator. Reactivity effects of voids are obtained relative to the reference reactor with no void in the core. The effect of voids appears as a change in the density of the water in the core with the effective neutron temperature remaining at 82.2° C (180° F). This computation of the void coefficient was made on the reactor simulator using the cylindrical geometry previously described.

The results of the calculations for uniformly distributed voids are presented as figure B2. On this graph  $\frac{\Delta K}{K}$  is plotted as a function of the percentage void introduced into the reactor core. It is seen from this curve that the void coefficient is always negative. The curve is not quite linear with  $\frac{\Delta K}{K}$  an increasing function of void percentage. Over the linear portion of the curve the change in  $K_{\text{eff}}$  per percentage displacement in water  $\frac{\Delta K_{\text{eff}}/K_{\text{eff}}}{\Delta V_{\text{void}}/V_{\text{H}_2\text{O}}} = -0.180$ .

The foregoing calculations were made assuming a uniform distribution of voids in the core, but in general it can be expected that any mechanism introducing voids would do so in some nonhomogeneous manner. Therefore, three calculations with nonuniform voids in the core were made. In the first calculation a linear radial distribution of voids was introduced into the cylindrical core such that more voids were in the volume elements at the center of the core than at the edge. The total amount of void in the entire reactor was then 9 percent. Solution on the simulator indicated that  $\frac{\Delta K}{K}$  was -4.29 percent for this nonhomogeneous distribution of voids as compared to -3.12 percent for a homogeneous distribution of the same amount of voids. In the second calculation, a linear distribution of voids was introduced into the reactor over the first 12 cm radius of the core

(the core radius is 22 cm), again with more voids near  $r = 0$  cm than at  $r = 12$  cm. This distribution of voids amounted to a total of 3.6 percent over the entire reactor core. It was found that  $\Delta K/K$  was -1.89 percent for this nonhomogeneous distribution as compared to -1.15 percent for a homogeneous distribution of voids. In the third calculation 22.7 percent void was introduced into the volume element of the core extending from  $r = 0$  cm to  $r = 4$  cm. This amounted to an introduction of 0.75 percent void throughout the entire reactor core. It was found that this distribution of voids gave a  $\Delta K/K$  of -0.48 percent as compared to -0.25 percent for the homogeneous distribution of the void.

These solutions point up the higher statistical weight of voids introduced at the axis of the cylindrical core than at the interfaces. It must be kept in mind that in these one-dimensional solutions, the radial distributions of voids extend the full height of the core. As such, they may not properly estimate the worth of comparable voids concentrated at the center of the cylindrical core.

The Oak Ridge-NACA program of experiments at the Bulk Shielding Reactor has provided data on the reactivity effects of completely voiding various numbers of water passages in a single fuel element. These experiments are fully described in Supplement III to this report (ref. B.8) and data for successively voiding water passages in the fuel element at the geometric center of a 7x3 slab loading are presented therein. (This fuel element corresponds to that in the LC-6 position shown in fig. 2.8.) Voided water passages in this fuel element of high statistical weight introduce negative reactivity of greater magnitude than that for comparable homogeneously distributed voids. Analysis of the BSR data for the 7x3 slab loading indicate that the fractional void coefficient for a linear portion of the curve is  $-0.64 \Delta K/K / \Delta V_{\text{void}} / V_{\text{H}_2\text{O}}$ . This is to be compared with a calculated value of fractional void coefficient for homogeneously distributed voids of -0.18 in the NACA reactor 9x3 slab loading.

Similarly, voiding of water passages in the fuel element at the hot-spot position at the core-reflector interface (fuel element in the LD-6 position shown in fig. 2.8) produced a fractional void coefficient of  $-0.41 \Delta K/K / \Delta V_{\text{void}} / V_{\text{H}_2\text{O}}$ . These results indicate the strong spatial statistical dependence of void coefficient.

Mean prompt neutron lifetime. - To compute the mean lifetime of the prompt neutrons in the reference reactor, solutions of equations (B1) and (B2) of the following form are assumed:

$$\phi_f(\underline{r}, t) = \sum_{n=0}^{\infty} A_n \phi_{f,n}(\underline{r}) e^{\lambda_n t} \quad (\text{B7})$$

$$\phi_{th}(\underline{r}, t) = \sum_{n=0}^{\infty} A_n \phi_{th,n}(\underline{r}) e^{\lambda_n t} \quad (B8)$$

where the functions  $\phi_{f,n}$  and  $\phi_{th,n}$  satisfy the time-independent equations

$$D_f \nabla^2 \phi_{f,n} - \left( \Sigma_{a,f} + D_f B_z^2 + \frac{\lambda n}{v_f} \right) \phi_{f,n} + K_f (1 - p_{th}) \Sigma_{a,f} \phi_{f,n} + K_{th} \Sigma_{a,th} \phi_{th,n} = 0 \quad (B9)$$

$$D_{th} \nabla^2 \phi_{th,n} - \left( \Sigma_{a,th} + D_{th} B_z^2 + \frac{\lambda n}{v_{th}} \right) \phi_{th,n} + p_{th} \Sigma_{a,f} \phi_{f,n} = 0 \quad (B10)$$

Again for the reflector, equations (B9) and (B10) apply when  $K_{th} \equiv K_f \equiv 0$ .

Since the delayed neutrons have not been considered, the reciprocal asymptotic period  $\lambda$ , is related to the mean lifetime of prompt neutrons  $l$  by (ref. B.9):

$$\lambda = \frac{\Delta K_{eff}/K_{eff}}{l} \quad (B11)$$

The mean lifetime of the prompt neutrons can be found in the following manner. First, equations (B9) and (B10) are solved with  $\lambda = 0$  to obtain a value for  $K_{eff}$ . Second, an absorber equal to  $\lambda/v_f$  for the fast group and  $\lambda/v_{th}$  for the thermal group is introduced into the reactor core and reflectors and equations (B9) and (B10) are solved again. Finally, knowing  $\lambda$  and  $\Delta K_{eff}/K_{eff}$  the lifetime  $l$  may be computed from equation (B11). Solutions were obtained on the one-dimensional space simulator. As expected the value of  $l$  was independent of the value of  $\lambda$  chosen.

The above method was used to calculate the mean lifetime of the prompt neutrons which was found to be  $90 \times 10^{-6}$  second. This calculation was based on the cylindrical reactor discussed previously except that the primary beryllium reflector thickness was increased to 20 cm and this was followed by a 30 cm water reflector. Also  $v_f$  was taken as  $10 v_{th}$  and the core was assumed to be in the hot-clean condition.

A computation of the mean lifetime of the prompt neutrons in the reactor after 10 days of operation was made and the lifetime was not found to be appreciably different from  $90 \times 10^{-6}$  seconds.

Excess reactivity requirements for reactor operating cycle. - The excess reactivity necessary to operate the reactor for a period of 10 days was estimated from the equivalent bare pile two-group criticality equation (ref. B.2):

$$\frac{K_{th}P_{th}}{(1 + L_f^2 B^2)(1 + L_{th}^2 B^2)} + \frac{K_f(1 - P_{th})}{(1 + L_f^2 B^2)} = K_{eff} \quad (B12)$$

The operating characteristics of the reference reactor core have been computed as a function of time using this criticality equation. The nuclear constants used to compute  $K_{eff}$  for the cold-clean reactor at time  $t = 0$  days are listed on table B.1 and the value of  $B^2$  used was such that  $K_{eff} = 1.185$ . This  $K_{eff}$  was then the same as that computed by the two-dimensional reactor simulator.

The reactor was taken to be operating at a constant specific power of 600 watts/cm<sup>3</sup> with approximately 90 percent of the fissions due to thermal neutrons. It was further assumed that the fast production term of equation (B12) remained constant throughout the operating cycle of the reactor.

The effects of xenon poisoning, samarium poisoning, low cross section fission product poisoning (abbreviated LCSFP), and fuel burnout on the  $K_{eff}$  of the reactor were computed as a function of time. The macroscopic equilibrium thermal absorption cross section of xenon was computed using (ref. B.10)

$$\Sigma_a^{Xe} = \frac{y^{Xe} \bar{\sigma}_a^{Xe} \Sigma_{F,th} \phi_{th}}{\lambda^{Xe} + \bar{\sigma}_a^{Xe} \phi_{th}} \quad (B13)$$

where

$$y^{Xe} \quad 0.0716$$

$$\bar{\sigma}_a^{Xe} \quad 2.93 \times 10^{-18} \text{ cm}^2$$

$$\lambda^{Xe} \quad 2.103 \times 10^{-5} \text{ sec}^{-1}$$

Values of xenon constants were taken from reference B.1. The macroscopic thermal absorption cross section of samarium as a function of time after startup was computed using the following equation (ref. B.10):



$$\Sigma_a^{Sm}(t) = \Sigma_a^{Sm}(\infty) \left[ 1 + \left( \frac{\lambda}{\sigma_{\phi_{th}} - \lambda} \right) \frac{e^{-\sigma_{\phi_{th}} t}}{e^{-\lambda t}} - \left( \frac{\sigma_{\phi_{th}}}{\sigma_{\phi_{th}} - \lambda} \right) \frac{e^{-\lambda t}}{e^{-\sigma_{\phi_{th}} t}} \right] \quad (B14)$$

where

$$\Sigma_a^{Sm}(\infty) = y \Sigma_{F,th}$$

$y$  fission yield of promethium

$\lambda$   $4.1 \times 10^{-6} \text{ sec}^{-1}$ , decay constant of promethium

$\sigma$   $5.3 \times 10^{-20} \text{ cm}^2$ , absorption cross section of samarium

The macroscopic thermal absorption cross section of the LCSFPP was computed by

$$\Sigma_a^{LCSFPP} = (P) \times (t) \times (\sigma_a^{LCSFPP}) \quad (B15)$$

where the specific power is  $1.872 \times 10^{13} \text{ fissions/cm}^3 \times \text{sec}$  and the  $\sigma_a^{LCSFPP}$  is obtained from curves plotted in reference B.11. The fuel burnout was computed by

$$\Delta N^U = (1 + \alpha) \times (P) \times (t) \quad (B16)$$

where  $\alpha$  is the ratio of the radiative capture cross section to the fission cross section of  $U^{235}$ .

Based on the above assumptions and formulas, the excess reactivity requirements presented in table 2.4 of section 2 were obtained. These results are based on the average unit volume in the reactor and thus, neglect the effects due to the nonuniform power distribution.

#### EXCESS REACTIVITY CONTROL BY BURNABLE POISONS

The concept of using fuel assemblies containing a burnable poison, such as boron, to control excess reactivity associated with fuel burnup and low cross section fission product buildup, has been widely studied. For application to power reactors, where long periods of uninterrupted service are desired, use of burnable poisons promises increased core life, more uniform power distributions, and a more economical operation in comparison to use of conventional fuel elements.

Applicability of burnable poisons to research reactors. - The application of burnable poisons to a research reactor of the MTR-type can provide several advantages:

1. After equilibrium xenon has been achieved, the shim rods may not have to be inserted as far as with conventional fuel elements. Insertion depth would be governed principally by transient xenon override requirements. This would permit a greater number or larger core and reflector irradiation facilities to be exposed to reasonably uniform fluxes during the operating cycle of the reactor.

2. Considerable improvement in operating economy and reduction in fuel-element inventory may be achieved. This results from the larger total fuel burnups possible from fuel elements initially loaded with large concentrations of uranium and boron before the elements require reprocessing. An attempt to achieve larger total fuel burnups by increasing uranium concentrations in fuel elements without the use of boron would provide core loadings with initially too much excess reactivity. These loadings would require initially deep insertion of shim rods with associated maldistribution of neutron fluxes. The present MTR system of refueling is to replace partially spent fuel elements with new elements of high uranium concentrations so as to achieve required excess reactivity for each new operating cycle. By this means large fuel burnups per element may result by gradually shifting the partially depleted element toward the center of the core. It will be shown, however, that by the use of boron in MTR-type fuel elements operating for the suggested NACA reactor operating cycle (10 days at 600 watts/cc core), it is possible to operate as long as three cycles (30 days) without replacing any fuel elements at all.

The application of burnable poisons to a research reactor can introduce several problems:

1. The fabrication techniques for such elements are yet to be perfected and their reliability is yet to be proven.

2. Larger average uranium concentrations in the core result in lower thermal fluxes for the core operated at constant average specific power. With reflector fluxes remaining about the same, larger thermal flux gradients will occur at the core-reflector interface where the point of highest heat flux is located. In an unperturbed core this would place a restriction on the total core power by increasing the maximum-to-average specific power. However, for the NACA core with experiments in the horizontal through holes, these flux peaks at the core-reflector interface do not occur.

Specific reactivity calculations with burnable poisons. - Burnable poison in the form of natural boron was added to the MTR-type fuel element array being considered for the core of the NACA research reactor. By this means, a longer operating cycle can be achieved with less shim rod movement required and less excess reactivity present at reactor start-up than with conventional fuel elements.

The calculation was carried out for a 9- by 27- by 24-inch core (3 by 9 fuel element array) which was surrounded successively by a 3/4-inch beryllium tank, 3 inches of beryllium, and an effectively infinite water reflector. An excess reactivity of 10 percent was tentatively aimed for to allow 5 percent for experiments and 5 percent for transient xenon override during most of the cycle. The initial investments of boron and uranium were distributed uniformly. Preliminary homogeneous calculations for this reactor were used to attain the initial investments used. This was taken to be 250 grams of U-235 and 0.25 grams of B-10 (distributed as natural boron) for each fuel element.

All burnup calculations were made on the one-dimensional reactor simulator. The spatial solution was in the direction of the long horizontal 27-inch core dimension with diffusion and leakage in the normal dimensions accounted for. The modified two-group diffusion theory previously described was used for the solutions.

The power distribution is known to vary slowly with burnup and can, therefore, be treated as essentially constant for small burnup intervals. The actual burnup of fuel and poison in any interval of time considered was based on the power distribution at the start of the interval. The error from such an approximation is negligible in this case as small enough intervals of burnup were chosen.

Calculations for the prescribed initial condition and burnups of 300, 600, 1200, and 1800 megawatt-days were carried out. The calculations were made using equilibrium xenon, samarium, and the other fission product concentrations derived from a 60 megawatt power level. The variation in reactivity with operating time is shown in figure B3. The value of  $K_{eff}$  for this core at startup is 1.117. For the first 20 days at 60 Mw (1200 Mw-days) a very small change in reactivity is indicated. For 30 days at 60 Mw the loss of reactivity is only 3.8 percent, with sufficient  $\Delta K$  remaining to permit operation at 1800 Mw-days.

At this time in the operating cycle (1800 Mw-days) the center elements in the long 27-inch dimension, the elements with greatest burnup, were eliminated. The less depleted outside elements were then moved to the center positions and fresh fuel elements were inserted in the outside spaces. Such a procedure should lead to a greater percentage burnup of fuel, and a more uniform power distribution. To simplify the evaluation of the reactivity of the new nonuniform fuel and poison and fission product loading, the remaining fuel and poison in the center elements were redistributed uniformly in these elements.

The result of the diffusion calculation on the simulator for this nonuniform core was to increase the reactivity of the core to a  $K_{eff}$  of 1.109, a level only 0.8 percent below the reactivity of the startup core.

Subsequent operation at 60 Mw with this particular nonuniform loading resulted in a reduction in available reactivity to a  $K_{eff}$  of 1.078 at the end of 2400 total Mw-days and a  $K_{eff}$  of 1.038 at the end of total 3000 Mw-days as shown in figure B-3. The characteristic initial rise in reactivity accompanying the more rapid burnout of boron relative to uranium was not obtained in this second loading. This was due to the fact that the elements shifted to the center of the loading at 1800 Mw-days were practically depleted in boron (only about 15 percent of the initial boron remained). The shifting of these boron depleted elements to the central region of high statistical importance results in a loading in which the advantages of using burnable poisons are lost. It would seem that if outer fuel elements of initially greater boron concentrations were used, subsequent shifting of these to central core locations would improve the core longevity characteristics.

Although studies are not complete at this time, the present results for the addition of burnable poisons look favorable enough to merit further investigation. It would appear that it may be possible to design for a repetitive cycle of refueling by which an element would remain in the core assembly about 40 days at 60 Mw. With 26 fuel assemblies in a loading, this corresponds to an average burnup of about 115 grams of uranium per fuel element, or an average fuel burnup of 40 to 50 percent.

#### REFERENCES

- B.1. Webster, J. W.: ORNL 1631 (classified).
- B.2. Bogart, D., and Soffer, L.: NACA RM E55L23 (classified).
- B.3. McMurtry, H. L.: Nuclear Constants for the MTR as a Function of Fuel Content, Poison Content, and Al/H<sub>2</sub>O Ratio. IDO-16127.
- B.4. Batt, M. L., Webster, J. W., and McMurtry, H. L.: Reflector Savings due to the MTR Water Blanket. IDO-16075.
- B.5. Zweifel, P. F., and Bigelow, S. R.: Numerical Solution of the Neutron Slowing-Down Problem in the Presence of Hydrogen. KAPL-1278.
- B.6. Roberts, Hill, Fitch, and Dabbs: The Slowing Down Distribution to Indium Resonance of Fission Neutrons from a Point Fission Source in Two Mixtures of Aluminum and Light Water, 1:1 and 1:2 by Volume. AECD-3408.
- B.7. Bogart, D., and Soffer, L.: NACA RM E53F30 (classified).
- B.8. Bogart, D., and Hallman, T.: Supplement III. NACA Reactor Facility Hazards Summary. Reactivity Measurements with the Bulk Shielding Reactor. To be published.

- B.9. Henry, A. F.: Computation of Parameters Appearing in the Reactor Kinetic Equations. WAPD-142 NAVY.
- B.10. Glasstone, S., and Edlund, M. C.: Elements of Nuclear Reactor Theory. (Van Nostrand.)
- B.11. Webster, J. W.: The Low Cross-Section Fission Product Poisons. IDO-16100.



APPENDIX CMETEOROLOGICAL ASPECTS OF A PROPOSED NUCLEAR FACILITY

By Scientific Services Division  
U.S. Weather Bureau  
Washington, D. C.

## INTRODUCTION

The proposed facility is located approximately 4 miles south-southeast of Sandusky, Ohio and about 5 miles from Lake Erie. The surrounding terrain is relatively level except for irregularities and bluffs near the Huron River to the southeast.

The purpose of this preliminary report is to review the meteorology of this area for use in the evaluation of the site location and compilation of a hazards analysis.

## SOURCE OF DATA

Meteorological data are not available from the precise location proposed for this facility. However, records have been maintained for many years at the Weather Bureau Office in Sandusky, Ohio. The differences occasioned by the urban location and closer proximity to Lake Erie of the Sandusky station are not of sufficient magnitude to preclude a preliminary description of the proposed site climate based on the Sandusky records. Measurements of vertical temperature gradient are not routinely made at Sandusky. For these data it was necessary to utilize radiosonde data obtained at Toledo, Ohio. Here again the Toledo station is sufficiently similar to the lake shore climatic regime of the proposed site to permit using the data to obtain at least a qualitative picture of the vertical temperature structure.

Attached to this report is a copy of the Local Climatological Data for Sandusky, Ohio (ref. C1). The narrative summary included in the publication is a good general description of the weather of this area. The table headed "Normals, Means, and Extremes" on page 2 of this annual summary presents much data on the temperature, degree days, precipitation, humidity, etc.

## CLIMATOLOGICAL REVIEW

In the present brief report, emphasis will be placed on the meteorological parameters which directly influence the spread of materials through the atmosphere.

## Surface Wind Direction

The hourly observations for a 5 year period, for the Weather Bureau Office, Sandusky, Ohio were studied in detail. Table C1 presents the percentage frequency of the wind direction. The prevailing direction is south-westerly with 55 percent of the winds occurring from the directions south through west, on an annual basis. This predominance of southwesterly winds is true in all seasons, however, the increasing frequency of north and northeasterly winds in the spring and summer deserves notice and explanation.

Table C1 shows that the northerly winds are almost twice as frequent during the summer day as during the summer night. This shift is occasioned by the development, during late spring and summer of the daytime on-shore lake breeze, a phenomenon similar in character and cause to the more familiar coastal sea breezes. The existence of the lake breeze and its intrusion over the site will result in frequent changes in air mass and thus diffusion characteristics. Prior to the on-set of the sea breeze the vertical temperature gradient over the land will usually be quite unstable due to solar heating. The cooler lake air, moving inland, will be less unstable and at the boundary of the lake air an inversion will be formed. Thus the lake breeze will tend to scour out and push ahead any contaminants previously in the air, or to contain within the lake breeze (depth from 200 to 500 ft) contaminants released after its arrival. Further detailed study at the proposed site would be required to accurately evaluate the particular character (i.e., depth, duration, arrival time, extent from lake shore, etc.) of its action in dispersing air borne materials.

TABLE C1. - PERCENTAGE FREQUENCY OF WIND DIRECTION,  
WEATHER BUREAU AIRPORT STATION, SANDUSKY, OHIO

(Based on hourly observations December 1949 - November 1954)

	Winter	Spring	Summer	Fall	Annual (all observed)	Daylight <sup>a</sup>		Night <sup>a</sup>		Annual (during precipitation- 16.2 percent of time)
						Summer	Annual	Summer	Annual	
N	5	9	12	7	8	16	10	9	7	7
NE	6	13	11	8	10	14	12	10	8	10
E	7	15	13	7	11	9	9	15	12	10
SE	5	5	5	5	5	2	3	7	6	6
S	15	12	15	16	15	9	11	19	17	15
SW	32	19	21	30	25	22	25	21	26	25
W	18	17	11	13	15	14	17	10	13	15
NW	11	10	10	11	10	14	13	7	9	11
Calm	1	(b)	2	3	1	(b)	(b)	2	2	1

<sup>a</sup>Daylight - 8 a.m. to 4 p.m.; Night - 5 p.m. to 8 a.m.

<sup>b</sup>Less than 1 percent.



Another factor worthy of mention can be seen from table C1. Contrary to many climatic regimes there is no major shift in wind patterns during precipitating weather. Although precipitation occurred only about 16 percent of the hours considered, the frequency of wind, by directions, is virtually identical with the annual frequencies. Thus, no special consideration of the direction of travel of "washed-out" material is necessary.

Wind direction may also be important when the lower atmosphere is very stable and atmosphere diffusion is a minimum. Examination of the Toledo, Ohio radiosonde data shows that with southerly winds inversions occur 70 to 90 percent of the time at night. Southerly winds also favor daytime inversions, particularly in winter. These conditions are shown in detail in table C3(b).

### Surface Wind Speed

Table C2 presents the frequency of wind speeds in various class intervals. More than 75 percent of the wind speeds are between 4 and 12 mph. The average speed is 9.7 mph with the strongest winds occurring in winter and spring. Winds less than 4 mph are rather common particularly in summer when 13 percent of the values are in this interval. Peak wind speeds reaching more than 50 mph have occurred in all months except May. The highest recorded speed was 77 mph during June.

TABLE C2. - PERCENTAGE FREQUENCY OF WIND SPEED GROUPS (mph),

WEATHER BUREAU AIRPORT STATION, SANDUSKY, OHIO

(Based on hourly observations December 1949 - November 1954)

	Winter	Spring	Summer	Fall	Annual (all observed)	Daylight		Night		Annual (during precipitation- 16.2 percent of time)
						Summer	Annual	Summer	Annual	
0-3	5	6	13	11	9	7	5	16	11	4
4-7	27	35	55	41	39	55	36	55	41	26
8-12	42	39	29	36	37	33	40	26	35	41
13-18	23	18	3	11	14	5	17	3	12	26
19-24	3	2	(a)	1	1	--	2	(a)	1	3
25-31	(a)	(a)	(a)	(a)	(a)	--	(a)	--	(a)	(a)
32-46	(a)	(a)	(a)	(a)	(a)	--	--	--	--	--
47	(a)	(a)	(a)	(a)	(a)	--	--	--	--	--

<sup>a</sup>Less than 1 percent.

Two very localized types of storms which are accompanied by high winds deserve special mention, thunderstorms, and tornadoes. Thunderstorms average 32 days per year occurring primarily in summer. June and July average 7 days apiece with thunderstorms. Thunderstorm activity is extremely variable but a rare severe storm may cause winds in excess of 50 mph, 1 to 3 inches of rain in an hour and hailstones 1/2 inch or larger in diameter. Situations favorable for the formation of severe thunderstorms are also conducive to tornado formation. A 35 year study of United States' tornadoes shows that 111 tornadoes occurred in Ohio during this period with the largest percentage of these storms in the northern and western portions of the state.

E-102

### Precipitation

As indicated in the attached Local Climatological Data, the Sandusky area receives about 33 inches of precipitation per year which will be spread over approximately 138 days. Maximum precipitation occurs during the late spring and summer. The maximum recorded monthly total is 12.51. Sandusky has an average of 12 days per year with an inch or more of snowfall. The yearly average snowfall is 28 inches however, the maximum monthly fall has been 29.8 inches and as much as 12.3 has been recorded in 24 hours.

### Atmospheric Stability

Measurements of vertical temperature gradients are not routinely made in the Sandusky area. However, twice daily radiosondes (10 a.m. and 10 p.m. EST) are made at Toledo, Ohio and five years of these data (from 1946 to 1950) were examined in detail. Salient features of the lapse rate are presented in table C3. The location and climate of Toledo and the proposed site are sufficiently similar to permit at least a good qualitative notion of the lapse rate near Sandusky to be obtained from the Toledo data. In table C3 the 10 p.m. observations are referred to as "night" conditions, the 10 a.m. as "day" conditions. Although these discrete observations do not provide information on inversion duration the above classification is sufficient for a preliminary analysis.

It can be seen that inversions are a common feature of the climate of this area at night and not too infrequent during the day. Summer is the season of the most frequent night inversions but the frequency drops to almost half the summer value by winter. The reverse is true of day inversions with these reaching a maximum during winter. In connection with these frequencies it should be mentioned that the summer inversions will almost always be eliminated by daytime heating while in late fall and winter stable conditions may persist for several days.

TABLE C3. - INVERSION DATA (TOLEDO, OHIO 1946 - 1950)

## a. Percentage Frequency of Base of Inversion

Inversion base	Winter		Spring		Summer		Fall		Annual	
	N	D	N	D	N	D	N	D	N	D
Surface	39	14	49	4	73	1	67	5	57	6
>Surface<1000'	3	19	9	11	2	6	2	19	4	14
1500'	47	41	61	22	75	9	70	31	63	26

## b. Percentage of Inversions with Specified Wind Direction

Wind direction	Winter		Spring		Summer		Fall		Annual	
	N	D	N	D	N	D	N	D	N	D
N	15	4	22	0	41	0	53	6	32	2
NE	20	0	38	2	54	0	50	5	42	2
E	38	14	62	1	65	0	74	2	61	3
SE	73	31	80	8	86	2	92	11	86	11
S	72	47	79	17	86	1	86	13	81	20
SW	48	23	60	2	83	1	71	4	65	8
W	24	8	41	1	70	1	38	4	39	4
NW	13	0	25	1	61	0	47	3	33	1
Calm	83	0	83	0	93	0	86	29	88	14

c. Percentage of Inversions Base at the Surface with  
Specified Wind Speeds

Wind speed	Winter		Spring		Summer		Fall		Annual	
	N	D	N	D	N	D	N	D	N	D
<4 mph	59	28	74	5	83	0	82	13	79	9
All speeds	39	14	49	4	73	(a)	67	5	57	6

<sup>a</sup>Less than 1 percent.

N 2200 EST.

D 1000 EST.

Table C3(b) indicates the frequency that inversions occur with particular wind directions. This tabulation indicates that with southerly

winds inversions can be expected at night between 70 and 90 percent of the time. Inversions occur least frequently with northerly winds. As would be expected stable conditions occur most frequently with light winds, particularly at night. These data are shown in table C3(c).

#### Atmospheric Diffusion

Within the last few years, there have been many reports prepared for the Atomic Energy Commission which have utilized the diffusion equations of O. G. Sutton (refs. C2, C3) in computations of the spread of radioactive wastes, either from a continuous or instantaneous source. These equations, together with the appropriate meteorological parameters are given below:

Continuous point source

$$X = \frac{2Q}{\pi C^2 u x^{2-n}} \exp\left(-\frac{h^2}{C^2 x^{2-n}}\right) \quad (C1)$$

Instantaneous source

$$X = \frac{2Q}{\pi^{3/2} C^3 (ut)^{3/2(2-n)}} \exp\left(-\frac{h^2}{C^2 (ut)^{2-n}}\right) \quad (C2)$$

where

X concentration at the ground, gm or curies/m<sup>3</sup>

Q source strength, gm/sec or curie/sec for continuous sources, gm or curies for instantaneous sources

h stack height, m

x horizontal distance downwind from stack base, m

C virtual diffusion coefficient, m<sup>n/2</sup>

u mean wind speed, m/sec

n dimensionless stability parameter

t time, sec

Values of the parameters C and n follow, according to Sutton's theory, from wind gustiness and velocity profile information. Experience

with above relations at various sites permits a reasonable preliminary estimate to be made of  $C$  and  $n$  values appropriate to the site using climatological data as a guide. The stability parameter,  $n$ , may vary from 0 to 1, such as:

Large lapse	1/5
Zero or small lapse	1/4
Moderate inversion	1/3
Large inversion	1/2

$C^2$  then varies with  $h$ ,  $n$ ,  $u$  such as:

h	n	u(m/sec)		
		1	5	10
25	1/5	0.064	0.046	0.040
	1/4	.021	.014	.012
	1/3	.009	.005	.004
	1/2	.006	.002	.002
50	1/4	.015	.010	.008
100	1/4	.008	.005	.004

From equation (C1) for a continuous source, it is found that the maximum ground concentration,  $X_{\max}$ , would be

$$X_{\max} = \frac{2Q}{e\pi u h^2}$$

and the distance,  $d$ , in meters of this concentration from the stack base would be

$$d = \left( \frac{h^2}{C^2} \right)^{1/2-n}$$

Holland (ref. C4) has tabulated some of the formulae needed most frequently for practical applications and Gifford (ref. C5) has developed an alinement chart which will facilitate most of the desired diffusion computations. This work has been extended to the calculation of radiation dosages from diffusing clouds of hypothetical reactor explosion products (ref. C6).

Concentrations of specific isotopes can be calculated from equations (C1) and (C2) if the quantities released are known, and these concentrations can be compared with tolerance for the appropriate exposure times with the aid of reference (C7).

## REFERENCES

- C1. U.S. Department of Commerce, Weather Bureau: "Local Climatological Data" for 1955, Sandusky, Ohio, U.S. Government Printing Office.
- C2. Sutton, O. G.: "The Theoretical Distribution of Airborne Pollution from Factory Chimneys," 1947, Q. J. Roy. Met. Soc., Vol. 73.
- C3. Sutton, O. G.: "Micrometeorology," 1953, McGraw-Hill, New York.
- C4. Holland, J. Z.: "A Meteorological Survey of the Oak Ridge Area," November 1953, U.S. Atomic Energy Commission, ORO-99, pp. 533-544.
- C5. Gifford, Frank: "An Alignment Chart for Atmospheric Diffusion Calculations," Bulletin of the American Meteorological Society, Vol. 34, March and May 1953, pp. 101-105 and p. 216.
- C6. Meteorology and Atomic Energy, July 1955, Superintendent of Documents, Washington, D. C.
- C7. U.S. Department of Commerce, National Bureau of Standards Handbook 52, March 1953, "Maximum Permissible Amounts of Radioisotopes in the Human Body and Maximum Permissible Concentrations in Air and Water." Superintendent of Documents, Washington, D. C.

# LOCAL CLIMATOLOGICAL DATA

## WITH COMPARATIVE DATA

1955

SANDUSKY, OHIO



### NARRATIVE CLIMATOLOGICAL SUMMARY

The weather records indicate a varied climate for this vicinity. The mean temperature is 50°, the average summer temperature is 72° and the winter months average about 30°. Spring and fall average 47° and 54° respectively. The warmest year of record is 1921 with a mean of 54°, the coldest year was in 1885 with a mean of 47°. The warmest summers were 1931 and 1949 when temperatures of 90° or higher were recorded 31 times each. The longest hot spells occurred in 1949 with temperatures above 90° for 8 consecutive days from June 29 to July 6, inclusive. The coolest summers were in 1882 and 1907 with 90° or above being recorded but once each. The coldest winter was 1884-85 with an average of 16°, the mercury having dropped to zero or lower on 21 days. The next coldest winter was 1935-36 with sub-zero readings on 16 days. The longest cold spell of record occurred in January of 1936 with below zero temperatures on 6 consecutive days, from the 22 to 27 inclusive. The highest temperature ever recorded here was 105° in 1918 and again in 1936. The coldest day was on January 3, 1879 with a reading of 16° below zero. The lowest modern record is 12 below in 1936. The warmest winter day of record was on January 25, 1950 with a temperature of 73°. An oddity of this occasion was the report of a heat prostration case, the first such case to ever occur, according to local insurance officials. There have been 24 winters during which the temperature failed to go below zero.

The growing season in this vicinity extends from about April 15, to October 26, an average of 194 days. The longest season of record was 221 days in 1911 and again in 1921. The shortest were in 1888 and 1946 with but 168 days between killing frosts. The latest killing frost in the spring was on May 9, 1923; the earliest in the fall occurred on September 29, 1942.

Precipitation varies considerably from year to year with an annual average of 39 inches. Spring and fall account for 8

inches each while 10 inches fall in the summer and 7 in the winter. The wettest year was 1950 with over 50 inches, the next highest amount fell in 1937 with a total of 47 1/2 inches, while over 46 inches were recorded way back in 1881. The heaviest rain occurred on June 24-25, 1937, with nearly 6 inches falling in 24 hours. The total for the whole month was over 12 inches, a record for any month. The driest year was 1934 with but 21 inches being recorded. The longest period of rainfall on record was from November 29 to December 10, 1914, with at least 0.01 inch on each of the 12 days. The greatest number of consecutive days without rain was 26 days between October 9 and November 3, 1944.

Snowfall also varies considerably with an average of 29 inches per winter. The heaviest annual amount of record was the 68 inches that fell in 1893, with nearly 30 inches of it in January alone. Other heavy amounts were 61 inches in 1910, and nearly 48 inches in 1940. The heaviest fall in a 24 hour period was 14 inches in April, 1886, the next heaviest being in November, 1950, with a little over 12 inches being recorded on the 25. The least annual snow was 11 inches in 1890, 1919 and 1928.

Sunshine in Sandusky averages about 51% of possible and the average cloudiness is about 6 tenths. There are an average of 90 clear days per year and 152 cloudy days, the rest being partly cloudy. Humidity runs about 63 during the daytime and 76 at night. Thunderstorms occur on an average of 31 days per year, and hail twice. There has been one tornado here in 73 years, that occurring in 1924. Wind averages 10 MPH, the prevailing direction is SW with NE being a close second. Winds of 40 MPH or higher occur several times per year, usually in connection with thundersqualls. The highest ever registered was 77 MPH and occurred in connection with the tornado.

## MONTHLY AND SEASONAL SNOWFALL

SANDUSKY, OHIO  
POST OFFICE BUILDING  
1955

Season	July	Aug.	Sept.	Oct.	Nov.	Dec.	Jan.	Feb.	Mar.	Apr.	May	June	Total
1905-1906	0	0	0	0	0.3	0.9	1.8	6.4	11.6	0	T	0	21.1
1906-1907	0	0	0	0	0.1	4.1	4.4	3.0	2.6	0.8	T	0	15.0
1907-1908	0	0	0	0	0.1	5.1	10.1	15.8	0.1	0.2	T	0	31.4
1908-1909	0	0	0	0	0.1	3.9	15.3	9.1	1.6	0.2	T	0	30.2
1909-1910	0	0	0	T	T	13.1	28.5	18.4	0.1	5.0	0	0	65.1
1910-1911	0	0	0	T	0.8	7.9	3.6	7.9	2.1	1.0	T	0	23.3
1911-1912	0	0	0	0	2.9	5.0	10.4	9.0	8.3	2.4	0	0	38.0
1912-1913	0	0	0	0	0.5	4.3	10.7	13.8	11.5	0	0	0	40.8
1913-1914	0	0	0	0.1	8.3	3.7	16.1	10.4	2.3	0.3	0	0	41.2
1914-1915	0	0	0	0	0.6	12.8	15.3	1.5	0.5	T	0	0	30.7
1915-1916	0	0	0	0	0.4	14.0	3.9	7.6	16.1	2.0	0	0	44.0
1916-1917	0	0	0	0	0.1	7.6	11.8	6.6	7.7	T	0	0	33.8
1917-1918	0	0	0	1.6	4.9	11.5	23.0	1.3	0.5	1.2	0	0	44.0
1918-1919	0	0	0	0	T	0.8	0.7	1.9	4.2	T	0	0	7.6
1919-1920	0	0	0	0	T	4.3	11.5	2.8	2.9	1.8	0	0	23.3
1920-1921	0	0	0	T	3.6	3.2	2.2	7.5	1.7	0.6	0	0	18.8
1921-1922	0	0	0	T	1.8	4.2	4.5	3.2	4.0	0.8	0	0	18.5
1922-1923	0	0	0	0	1.8	12.6	8.0	3.4	5.2	0.1	T	0	31.1
1923-1924	0	0	0	0	T	0.3	10.3	10.0	5.9	2.4	0	0	28.9
1924-1925	0	0	0	0	0.5	4.3	9.1	0.9	1.7	0	0	0	16.5
1925-1926	0	0	0	1.2	0.2	5.3	8.7	12.7	4.9	2.6	0	0	35.6
1926-1927	0	0	0	T	1.5	12.8	7.5	8.6	T	T	0	0	31.2
1927-1928	0	0	0	0	2.4	4.2	3.8	4.5	1.9	0.4	0	0	17.0
1928-1929	0	0	0	0	0.2	0.7	18.6	14.6	0.9	T	T	0	33.0
1929-1930	0	0	0	T	0.9	11.5	5.3	2.2	7.5	T	0	0	27.4
1930-1931	0	0	J	T	1.8	3.5	4.3	1.4	6.9	0.3	0	0	18.2
1931-1932	0	0	0	0	4.0	0.2	T	3.5	4.9	3.8	0	0	16.4
1932-1933	0	0	0	0	2.3	4.5	1.0	1.3	5.2	T	0	0	14.3
1933-1934	0	0	0	0	8.1	6.5	1.6	6.7	4.4	2.0	0	0	29.3
1934-1935	0	0	0	T	T	6.2	0.5	8.9	T	0.3	0	0	15.9

The horizontal lines drawn on the Average Temperature, Total Precipitation, Monthly and Seasonal Degree Days, and Monthly and Seasonal Snowfall tables separate the data according to station location (see Station Location table).

Season	July	Aug.	Sept.	Oct.	Nov.	Dec.	Jan.	Feb.	Mar.	Apr.	May	June	Total
1935-1936	0	0	0	T	0.7	10.5	8.7	7.9	3.6	0.7	0	0	32.1
1936-1937	0	0	0	T	1.1	2.4	5.1	2.1	2.0	T	0	0	12.7
1937-1938	0	0	0	0.1	3.7	2.5	5.9	2.9	0.7	4.4	0	0	20.2
1938-1939	0	0	0	0	8.6	2.7	13.4	8.8	0.5	0.9	0	0	34.9
1939-1940	0	0	0	0.1	T	2.3	9.7	14.8	9.6	3.3	T	0	39.8
1940-1941	0	0	0	T	4.4	5.7	8.1	6.3	3.6	0	0	0	28.1
1941-1942	0	0	0	0	0.1	1.0	2.1	11.4	3.2	0.2	0	0	18.0
1942-1943	0	0	0	0	3.0	8.9	12.1	4.9	5.5	0.7	0	0	35.1
1943-1944	0	0	0	T	0.9	1.1	0.6	8.2	7.1	0.4	0	0	18.3
1944-1945	0	0	0	0	0.3	13.9	14.4	7.3	3.9	T	0	0	38.8
1945-1946	0	0	0	0	0.6	10.4	3.5	2.6	T	0	0	0	17.1
1946-1947	0	0	0	0	0	7.6	4.4	5.2	11.9	T	0	0	29.1
1947-1948	0	0	0	0	3.5	4.0	7.9	3.5	6.0	T	0	0	27.9
1948-1949	0	0	0	0	T	3.1	3.6	0.6	7.1	T	0	0	14.4
1949-1950	0	0	0	0	2.0	1.2	4.7	4.8	7.1	1.7	0	0	21.5
1950-1951	0	0	0	0	19.8	10.5	12.7	4.4	7.5	T	0	0	54.9
1951-1952	0	0	0	0	4.3	20.2	3.1	4.8	2.6	4.7	0	0	39.7
1952-1953	0	0	0	T	0.2	6.2	5.7	3.9	0.7	0.5	0	0	17.2
1953-1954	0	0	0	T	5.2	7.5	4.5	8.1	11.1	T	T	T	36.4
1954-1955	0	0	0	T	T	3.5	5.5	3.5	12.1	T	0	0	24.6
1955-1956	0	0	0	T	5.2	3.9							

## STATION LOCATION

Location	Occupied from	Occupied to	Airline distance and direction from previous location	Latitude	Longitude	Elevation above								REMARKS		
						Sea level		Ground								
						Ground	Actual barometer elevation (H <sub>a</sub> )	Wind instruments	Extreme thermometers	Psychrometer	Telepsychrometer	Tipping bucket rain gage	Weighting rain gage		8" rain gage	
West House Hotel, Cor. Columbus & Market Sts.	8- 1-77	3-31-88		41° 25' N	82° 40' W		629									Reason for move unknown.
P. O. Building, corner of Columbus & Market	4- 1-88	3-13-27	1 block	41° 25' N	82° 40' W											Move due to erection of new P. O. & dismantling of the old.
New P. O. Bldg., corner Washington & Jackson Streets	3-13-27	present	2 blocks	41° 25' N	82° 40' W	603	628	67	7				3	2		Buildings & trees surround location but due to distance involved there is but little effect on the accuracy of the instruments. The sloping effect of the P.O. roof is thought to adversely affect
Prior to the erection of the new P. O. building, the old P. O. building was used for the purpose of the weather station.																

Prior to the opening of the WBO in Sandusky, temperature and precipitation observations were made under the supervision of the Smithsonian Institution in Margaretta Township about 5 miles southwest. Temperature observations were made from 1868 to 1876 and precipitation from 1859 to 1867.



## AVERAGE TEMPERATURE

## TOTAL PRECIPITATION

SANDUSKY, OHIO  
POST OFFICE BUILDING  
1955

Year	Jan.	Feb.	Mar.	Apr.	May	June	July	Aug.	Sept.	Oct.	Nov.	Dec.	Annual
1906	36.0	27.0	29.6	49.6	59.4	69.2	71.7	75.0	68.7	52.0	40.4	31.8	50.9
1907	29.6	23.9	42.3	40.4	52.1	65.4	72.6	69.4	65.0	49.0	40.0	33.2	48.6
1908	28.1	25.4	39.9	48.3	60.4	69.6	73.4	70.7	68.4	54.7	42.0	32.2	51.1
1909	31.3	32.0	35.2	46.4	57.0	68.6	71.8	72.8	63.4	48.7	48.4	24.2	50.0
1910	26.4	24.5	45.6	50.0	55.8	65.9	74.8	71.7	65.8	58.2	36.8	25.2	49.9
1911	30.7	31.4	35.5	46.8	56.8	70.8	74.4	71.8	66.5	52.4	37.2	36.0	51.6
1912	15.4	20.1	28.4	47.6	60.7	66.2	72.6	69.0	66.8	55.4	43.0	33.6	48.2
1913	34.3	24.2	37.2	48.6	58.6	69.5	73.8	73.0	63.5	53.8	45.0	35.2	51.4
1914	32.2	19.8	33.8	46.0	61.4	69.8	73.6	72.9	63.7	57.2	41.6	25.4	49.8
1915	25.0	32.0	31.8	52.8	54.8	64.9	71.0	67.6	67.3	55.1	43.8	30.0	49.7
1916	33.6	23.6	30.0	47.2	59.2	64.8	77.8	74.8	64.6	53.2	42.2	28.2	49.9
1917	26.2	21.6	37.8	45.1	52.0	60.0	73.0	70.8	62.0	45.6	38.6	21.6	46.7
1918	14.6	28.2	41.0	45.9	65.1	68.2	71.3	75.6	58.4	56.0	42.8	38.8	50.5
1919	32.7	31.3	37.6	46.8	56.4	74.1	75.6	71.2	67.8	58.8	40.6	25.2	51.5
1920	18.9	25.0	40.8	42.8	56.3	69.3	70.7	70.8	66.8	60.3	41.0	34.0	49.7
1921	32.8	32.6	45.6	54.8	61.8	72.0	78.7	71.0	70.2	54.1	42.2	32.8	54.0
1922	25.8	31.4	38.6	49.0	62.8	70.0	73.9	71.4	68.6	56.2	44.1	30.7	51.8
1923	30.5	24.4	35.0	46.9	54.0	71.8	73.0	70.5	65.2	52.2	41.9	39.6	50.4
1924	23.4	26.1	34.1	46.4	52.5	66.0	70.7	71.6	60.8	56.8	41.2	26.6	48.0
1925	25.2	34.2	39.9	51.5	54.8	62.0	72.1	71.6	68.6	45.5	39.8	28.8	50.3
1926	27.2	28.1	30.4	42.1	58.2	65.2	72.7	74.0	65.4	52.5	39.9	27.8	48.6
1927	28.4	34.2	41.0	47.6	57.8	64.8	72.9	67.1	68.8	58.2	46.4	31.9	51.4
1928	28.5	28.7	36.1	45.6	58.5	64.6	74.8	74.1	62.7	57.4	44.0	34.1	50.8
1929	33.8	24.2	43.9	52.0	67.0	67.1	73.8	69.2	65.6	52.8	38.3	30.0	49.8
1930	25.4	37.0	36.0	48.3	61.8	71.0	75.2	72.8	67.1	51.3	42.7	31.0	51.7
1931	30.8	33.4	35.0	48.7	58.4	69.8	78.0	73.9	70.6	57.7	48.5	38.9	53.7
1932	39.0	36.0	31.6	44.8	60.1	70.8	73.8	73.8	66.4	54.4	38.6	31.8	51.8
1933	36.8	30.4	35.8	47.5	62.0	74.4	75.4	72.6	68.0	52.9	38.0	32.1	52.2
1934	32.4	17.4	32.6	46.4	62.7	75.0	77.8	71.4	68.0	54.3	45.2	29.2	51.0
1935	28.1	28.8	42.8	45.4	54.4	66.4	77.4	73.4	65.2	53.6	42.6	26.1	50.4
1936	22.4	20.0	39.5	44.6	63.4	68.6	76.2	75.0	68.8	54.0	37.8	35.2	50.5
1937	34.2	30.6	33.2	47.1	60.6	69.2	74.1	75.4	63.8	51.4	39.7	28.8	50.7
1938	28.2	34.4	44.6	50.1	59.9	69.0	75.1	76.0	64.8	55.8	44.8	32.4	52.9
1939	31.3	31.0	37.1	45.5	62.8	72.4	74.0	74.0	69.0	55.8	41.8	34.8	52.5
1940	18.0	28.2	31.4	44.6	57.2	70.3	75.4	72.8	63.6	54.6	40.0	34.8	49.3
1941	28.8	26.8	31.8	52.4	63.6	71.2	75.6	72.2	69.2	57.7	44.0	37.5	52.6
1942	28.0	24.8	40.0	53.4	62.2	70.6	75.4	72.2	65.0	55.4	43.0	26.8	51.4
1943	26.5	30.1	35.9	43.6	58.8	74.2	75.1	73.2	63.0	53.1	39.8	28.8	50.2
1944	32.8	31.2	33.8	44.4	64.6	73.1	74.8	74.8	68.2	54.0	43.8	26.0	51.6
1945	19.8	29.8	49.0	52.0	54.2	67.0	72.2	73.0	67.4	53.2	43.7	25.9	50.6
1946	30.0	30.8	47.4	49.8	58.2	69.2	73.6	69.0	67.0	59.0	46.7	34.5	52.9
1947	33.0	23.6	32.8	47.0	56.3	67.0	71.8	77.8	67.1	62.0	38.5	31.8	50.7
1948	21.4	28.0	37.6	52.6	57.3	66.8	75.0	72.8	68.0	50.8	46.8	34.2	51.1
1949	35.1	34.6	38.0	47.7	62.5	74.9	79.0	74.8	62.2	60.4	42.5	35.4	53.9
1950	37.2	30.1	33.9	43.6	60.3	69.7	72.4	71.8	65.0	58.7	38.2	25.8	50.6
1951	30.3	30.1	38.7	47.2	61.0	70.1	74.5	71.3	64.1	58.5	37.2	31.1	51.2
1952	32.9	32.1	37.0	50.4	68.0	74.3	78.0	72.7	65.6	50.9	44.9	35.6	52.8
1953	33.8	34.3	40.8	45.6	61.4	72.8	74.4	74.7	66.8	58.1	46.1	34.8	53.6
1954	29.5	37.1	36.4	51.4	57.4	73.4	73.7	72.5	68.9	56.9	42.5	32.5	52.9
1955	27.5	30.7	38.9	56.5	63.1	68.5	78.8	77.0	67.8	55.9	38.9	28.8	52.7
RECORD MEAN	27.8	28.2	36.7	47.7	59.2	69.2	74.1	72.2	65.9	54.5	41.7	31.3	50.7
TEMP	34.5	35.2	44.0	55.6	67.6	77.8	82.6	80.4	74.3	62.5	48.4	37.4	58.4
MAX	21.0	20.9	29.3	39.6	50.8	60.8	65.6	64.0	57.4	46.5	34.9	25.2	43.0
MIN													

Year	Jan.	Feb.	Mar.	Apr.	May	June	July	Aug.	Sept.	Oct.	Nov.	Dec.	Annual
1906	.93	1.01	1.87	1.50	1.48	1.53	7.82	6.85	3.12	3.81	2.21	3.10	34.83
1907	4.87	.33	4.39	1.19	2.16	4.64	4.43	1.59	6.83	3.43	1.38	3.40	38.44
1908	2.09	3.70	3.61	2.83	2.12	1.72	3.34	2.96	.75	.97	.62	1.77	26.48
1909	2.52	4.44	2.16	2.50	5.22	4.98	6.52	1.48	1.03	1.56	3.67	2.23	38.31
1910	3.84	2.97	.28	6.24	1.89	1.74	1.76	2.28	3.30	4.91	1.55	1.72	32.48
1911	2.77	1.93	1.66	3.46	1.92	3.90	2.09	5.31	3.53	5.06	2.19	2.20	35.82
1912	1.62	1.60	2.93	2.43	1.94	4.52	4.93	3.57	2.79	3.12	.79	1.52	31.76
1913	6.10	2.07	8.69	2.10	4.89	5.54	2.19	5.42	2.18	2.37	2.25	.83	40.43
1914	2.71	1.86	2.16	3.86	4.03	3.13	1.55	4.73	1.74	1.58	.98	3.08	31.41
1915	2.41	1.89	1.17	.35	3.00	3.48	6.19	2.43	5.11	2.84	1.61	2.61	33.09
1916	3.62	1.07	3.09	1.37	3.60	4.36	.26	2.28	2.03	1.24	2.19	2.09	27.80
1917	2.66	.73	2.72	3.66	3.13	4.21	.46	3.99	2.34	6.22	.79	1.12	32.03
1918	2.77	1.25	1.92	1.39	4.15	1.25	1.32	1.76	4.30	1.13	1.17	2.71	25.12
1919	.74	.94	3.37	3.41	3.46	.91	2.23	5.37	2.17	1.46	1.36	.66	28.78
1920	1.32	.27	1.38	4.77	1.85	4.63	2.01	1.71	2.82	3.30	2.24	1.77	28.07
1921	1.59	1.91	4.07	2.65	2.28	1.73	3.26	3.49	5.04	1.54	3.18	1.55	32.29
1922	1.28	1.00	4.43	3.02	2.58	1.96	2.60	2.52	1.86	3.21	1.27	3.07	26.81
1923	2.50	1.21	2.22	1.86	3.19	2.21	3.32	3.59	3.26	1.79	1.77	4.08	30.00
1924	3.11	1.67	2.93	2.93	2.23	7.68	2.35	2.62	5.44	.64	.66	3.98	36.24
1925	.95	2.34	2.21	1.08	1.23	2.44	3.63	.96	3.59	2.43	3.08	.78	23.52
1926	1.79	1.98	2.18	3.55	.89	1.63	2.61	3.80	7.01	4.08	1.55	1.63	32.64
1927	1.48	2.32	2.97	2.28	3.80	2.82	5.65	2.21	1.32	1.11	6.43	3.29	35.58
1928	1.53	1.79	2.63	2.34	1.92	5.26	4.04	2.92	1.73	3.95	2.57	1.81	30.59
1929	4.00	1.79	3.01	5.76	4.43	4.12	4.15	1.58	2.53	5.90	2.74	3.82	42.93
1930	5.41	1.81	3.71	2.70	2.79	2.94	1.34	1.16	3.88	1.07	1.45	.84	29.10
1931	1.73	1.71	2.16	4.14	2.10	3.59	1.03	6.39	3.63	2.37	2.08	2.37	33.30
1932	4.07	1.06	3.62	2.52	2.73	1.18	3.78	1.83	2.18	4.31	2.54	3.21	33.03
1933	1.34	1.45	3.27	2.48	5.24	1.11	1.46	1.68	4.38	.94	1.90	1.74	26.99
1934	1.19	.75	2.95	4.09	.84	1.48	1.24	2.89	2.57	.98	1.01	1.23	21.12
1935	2.24	1.65	2.07	1.51	3.58	2.71	5.43	2.76	1.79	2.51	2.21	1.71	28.87
1936	1.07	3.02	3.87	2.08	1.26	2.05	3.21	1.83	3.28	2.55	2.20	1.74	28.16
1937	8.58	2.41	1.82	4.41	3.66	12.51	3.54	3.03	3.51	3.29	.99	1.81	47.56
1938	.91	3.25	3.11	2.11	5.38	5.68	4.27	1.68	4.42	.75	3.26	1.71	36.51
1939	2.11	3.43	3.13	4.34	1.08	4.03	5.06	2.28	3.45	2.21	.86	1.40	33.18
1940	1.36	2.68	2.38	4.65	3.43	3.66	1.47	5.83	5.01	2.26	2.28	3.50	36.31
1941	1.30	.65	1.03	1.65	3.47	6.19	6.02	2.76	1.10	3.04	1.34	1.54	30.09
1942	1.09	2.70	2.34	2.70	3.81	4.21	4.91	3.30	2.13	1.48	4.05	2.43	35.13
1943	1.64	1.05	2.20	2.91	9.04	5.41	9.71	2.70	2.78	2.01	.83	.65	40.93
1944	.90	1.62	3.04	3.95	4.31	5.00	.80	2.91	3.30	1.16	2.28	2.29	29.58
1945	1.10	1.57	5.12	2.19	3.35	5.72	1.87	2.39	5.15	3.38	1.61	1.87	35.30
1946	.84	1.58	1.70	.75	6.73	8.64	3.24	2.14	2.20	2.25	1.91	2.58	34.56
1947	4.20	.40	2.12	3.54	5.15	5.30	2.40	4.57	2.88	1.51	1.82	2.08	36.07
1948	1.65	2.36	5.06	2.68	3.95	3.84	3.46	2.92	1.90	2.02	4.33	1.72	35.89
1949	3.09	2.01	2.10	2.96	4.15	1.45	5.15	2.82	3.60	1.24	1.24	2.11	30.02
1950	6.54	4.53	3.37	5.02	1.17	4.77	5.41	2.82	7.72	2.08	4.89	2.18	50.50
1951	2.37	2.67	3.42	2.41	2.46	3.59	2.94	1.30	1.95	2.29	3.59	5.74	34.73
1952	3.97	2.00	4.12	4.03	3.00	1.87	2.72	1.12	2.96	.44	1.86	2.56	30.75
1953	3.20	.82	2.03	2.67	3.01	3.83	3.06	4.65	1.05	.77	1.69	1.94	28.72
1954	2.55	2.89	4.50	3.98	1.14	1.41	1.82	6.76	1.21	4.91	1.44	1.51	34.12
1955	2.02	2.30	4.55	3.37	3.02	2.70	3.92	3.85	.99	2.92	3.32	.74	33.70
RECORD MEAN	2.35	2.12	2.82	2.80	3.29	3.75	3.47	3.14	2.91	2.38	2.34	2.21	33.21

# METEOROLOGICAL DATA FOR THE CURRENT YEAR

LATITUDE 41° 25' N  
LONGITUDE 82° 40' W  
ELEVATION (ground) 603 feet

SANDUSKY, OHIO  
POST OFFICE BUILDING  
1955

Month	Temperature				Degrees days	Precipitation				Relative humidity		Wind				Number of days				Temperatures							
	Averages		Extremes			Total	Greatest in 24 hrs.	Date	Snow, Sleet, Hail	Fastest mile	Average hourly speed	Prevailing direction	Speed	Direction	Date	Sunrise to sunset			Snow, Sleet, Hail	Thunderstorms	Heavy fog	Maximum		Minimum			
	Daily maximum	Daily minimum	Monthly	Lowest												Partly	Cloudy	Cloudy				32° and above	32° and below		Zero and below		
Jan.	32.7	22.3	27.5	15	2.02	1.19	5-9	5.5	2.0	12-13	8.2	34	SW	27	37	7.4	5	18	15	4	0	0	15	25	1		
Feb.	36.9	24.5	30.7	18	2.30	0.48	26-27	3.5	2.1	10-11	7.1	28	NE	2	43	6.9	5	6	17	1	1	0	6	24	0		
Mar.	47.3	30.4	38.9	10	4.55	0.93	20-21	12.1	8.7	25-26	10.5	35	SW	22	58	5.2	13	7	11	15	4	5	17	0	0		
Apr.	56.5	40.4	54.5	13	3.37	0.91	19-21	7	24+	24+	7.5	38	NE	19	78	4.9	12	9	9	10	0	0	0	0	0		
May	71.8	54.4	63.1	27+	3.03	1.00	23-24	0.0	0.0	0.0	6.8	30	NE	4	75	4.7	12	11	8	10	0	0	0	0	0		
June	78.2	58.7	68.5	31	2.70	1.61	30	0.0	0.0	0.0	5.9	18	SW	30	73	4.3	12	13	5	0	1	0	2	0	0		
July	87.4	70.2	78.8	38	3.92	1.98	23-24	0.0	0.0	0.0	6.3	22	N	27	88	3.4	16	13	2	9	0	8	0	0	0		
Aug.	85.1	68.6	77.0	37	3.85	2.06	23-24	0.0	0.0	0.0	6.8	27	NE	13	78	4.3	13	6	8	0	4	0	10	0	0		
Sept.	77.8	57.8	67.8	34	2.89	0.89	23-24	0.0	0.0	0.0	6.8	28	NE	10	78	3.8	18	6	4	7	0	1	0	0	0		
Oct.	64.8	46.9	55.9	30	2.82	1.06	8-11	7	31+	31+	8.3	30	NE	24	54	7.6	10	7	14	11	0	3	0	1	0		
Nov.	47.1	30.6	38.9	13	3.32	1.62	15-16	5.2	4.5	19	7.9	32	SW	17	31	7.2	5	11	17	10	1	5	1	4	0		
Dec.	34.6	23.6	28.6	8	0.74	0.25	3-4	3.9	1.3	14	7.6	38	N	4	38	7.5	2	10	16	8	3	2	0	14	28	0	
Year	60.8	44.5	52.7	29	33.70	2.06	Aug 6	30.2	8.7	25-26	7.6	55	SW	22	60	5.5	123	115	127	120	13	41	7	30	43	115	1

APPENDIX DMEMORANDUM ON THE GEOLOGY AND HYDROLOGY OF A PROPOSEDREACTOR SITE NEAR SANDUSKY, OHIO

By Stanley E. Norris<sup>1</sup>

## INTRODUCTION

## Purpose and Scope

The purpose of this report is to discuss, with special reference to the disposal or unintended loss of radioactive fluid to the ground, the geology, and hydrology of a proposed reactor site at the Plum Brook Ordnance Works near Sandusky, Ohio. The report was prepared at the request of the National Advisory Committee for Aeronautics as an aid to the Committee on Reactor Safeguards of the U.S. Atomic Energy Commission in evaluating the feasibility of operating a nuclear power reactor at the site in question.

## Previous Work and Acknowledgments

Data on which this report is based are from well records in the files of the Ohio Division of Water, from publications and manuscript maps of the Ohio Division of Geological Survey, from publications of the Ohio Division of Shore Erosion, and from engineering data collected by the U.S. Corps of Engineers. A brief reconnaissance was made of the site area by the writer and R. K. Cash, of the Geological Survey, in company with officials of the National Advisory Committee for Aeronautics and personnel of the Plum Brook Ordnance Works. Mr. Cash also spent time in the field collecting well data and information on water use in the area.

This report was prepared under the general supervision of A. N. Sayre, Chief of the Ground Water Branch, U.S. Geological Survey. The writer is indebted to Mr. N. P. Miller of the National Advisory Committee for Aeronautics for his assistance in furnishing engineering data of the site, and to Mr. R. E. Lamborn of the Ohio Division of Geological Survey for making available the manuscript maps prepared by Frank Carney, showing the extent of the beach ridges in the Sandusky area.

---

<sup>1</sup>District Geologist, Ground Water Branch, U.S. Geological Survey, Columbus, Ohio.

## AREA OF INVESTIGATION

## Location and Extent

As shown on figure D1, the Plum Brook Ordnance Works occupies an area of between 15 and 20 square miles, chiefly in Perkins and Oxford townships, Erie County, Ohio. The proposed reactor site lies in the northern part of the ordnance works grounds, five miles south-southeast of the Court House in Sandusky, Ohio.

## Topography and Drainage

The area under discussion lies near the southern shore of Lake Erie, on the flat plain which in glacial time was a portion of the lake bottom. The land surface slopes gently toward the lake, descending from an elevation of 700 feet above sea level at Prout Station, at the southern boundary of the ordnance works, to the level of the lake, about 573 feet<sup>2</sup> above sea level. The topography is very flat, the principal relief being afforded by the old beach ridges and sand hills which mark the former shoreline. The present shoreline, in the vicinity of Sandusky, is one of submergence, characterized by drowned stream mouths and large areas of marshland (Metter, ref. D3, p. 5).

The drainage in the area of the ordnance works is by short streams which flow north across the lake plain in relatively straight courses to empty into Lake Erie. As shown on the map, the streams draining the immediate area of the proposed reactor site include a tributary of Pipe Creek on the western side, an unnamed stream in the central part, and Plum Brook in the eastern portion of the site area. These streams have very low average flows and are intermittent except in their lower courses near the lake where they enter the marshland along the shore.

## GEOLOGY

## Soils

The soils in the general vicinity of the proposed reactor site are derived from very fine sand, silt, and clay, except in areas of the beach ridges where they are developed on deep sand or sand over clay. Natural drainage is classified as good on the beach ridges and poor to very poor in the intervening areas (Conrey et al., ref. D1, pp. 21-25).

## Surficial Deposits

The surficial deposits in the area are comprised of lacustrine clay, thinly underlain by glacial till, with local patches of sand along the

---

<sup>2</sup>During the summer of 1951; Metter, ref. D3, pp. 7-9.

old beach ridges. The unconsolidated deposits generally are thin, not more than about 20 feet in thickness, with bedrock exposed at many places. Within the ordnance works is a fairly extensive area underlain by sand deposits which formerly were a source of molders sand.

The unconsolidated deposits along the lake shore, both in the marshy areas near the stream mouths and beneath the shallow offshore waters, are considerably thicker than the unconsolidated deposits in the area of the ordnance works. As reported by Metter (ref. D3, p. 13):

"The Sandusky city engineers have made a series of auger bore holes in the marshy region from the new Cedar Point entrance road westward to within about 300 yards of Willow Point. The borings were made at 1000-foot intervals in nine north-south rows 1000 feet apart. The westernmost line of borings encountered bedrock at an elevation of approximately 550 feet, overlain by gravel, sand, clays, and swamp muck - approximately 25 feet of unconsolidated material. The next line of probings, 1000 feet farther east, encountered bedrock at an elevation of 545 feet, and there is no more record of bedrock elevations eastward along the shore of the peninsula. Borings at the Plum Brook Intake went down to elevations of 516 feet without encountering rock, giving a minimum thickness here of approximately 60 feet for the unconsolidated material."

#### Consolidated Rocks

Consolidated rocks underlying the area are sedimentary in origin and of Devonian age. A generalized geologic section, compiled from Stout (ref. D5, p. 359) and other sources is as follows:

Name	Approximate thickness, ft
Ohio shale	300
Olentangy shale (includes the Prout limestone member of Stauffer near the top)	40
Delaware limestone	70
Columbus limestone	65

The regional dip of the strata is easterly and younger rocks crop out progressively from west to east. The bedrock is limestone in the western part of the ordnance works property and shale in the eastern part. On the map is shown the line of demarcation between the Columbus and Delaware limestones on the west and the Olentangy and Ohio shales on the east. Also shown on the map are locations of quarries and other exposures of the bedrocks.

The carbonate rocks in the Sandusky area are described by Stout (ref. D6, p. 363, 365-366) as follows:

"The stone in the Columbus formation shows considerable variation, both physical and chemical, in different parts of the section. In composition, it changes upward from a dolomite bearing a little free calcium carbonate to a limestone containing from 10 to 25 percent magnesium carbonate. The stone in the upper part is blue in color and lies in thin to medium beds rather uniform in thickness. Formerly this part was quarried extensively near Sandusky along Mills Creek, was known to the trade as "Sandusky stone," and was employed for building, paving, and flagging purposes. In the middle portion the strata are more massively bedded, are from bluish to light brown in color, and locally contain some chert. The dolomite in the lower portion is well crystallized, massive bedded, and commonly light brown . . ."

"The youngest of the carbonate rock formations in Erie County is the Delaware which extends in a strip from four to five miles in width from the lake and bay near Sandusky southwestward across the area to Huron County. It covers central Portland, western Perkins, southeastern Margareta, western Oxford, and eastern Groton townships. The general color of the Delaware limestone is bluish gray but owing to the effects of organic pigments parts assume brown and dark sooty shales. The stone is finely crystalline, hard, dense, and fossiliferous. Locally it contains chert, usually in the nodular form, localized along bedding planes, and varying much in color depending upon the state of weathering. Ordinarily the strata are rather uniformly bedded in layers from 2 to 10 inches. This formation has been rather extensively quarried south of Sandusky for building stone and crushed rock products."

The Olentangy and Ohio shales were exposed in former years at two localities within the ordnance works, in the railroad cut about a mile north of Prout Station, and along Plum Brook about two miles northeast of Prout Station. Based on the description by Stauffer (ref. D4, p. 120-121), the Olentangy shale, below the Prout limestone member, is at least 30 feet thick and is a soft, blue shale, marly in composition, containing layers and nodules of hard, fossiliferous limestone. At the top of the Olentangy shale is a prominent limestone bed approximately 9 feet thick which Stauffer called the Prout limestone and described (ref. D4, p. 120) as a "very hard silicious blue limestone with a layer of cherty pyrite at the top."

The Ohio shale, which overlies the Olentangy shale, is a black, thinly bedded shale, containing pyrite and much bituminous matter. The upper portion of the Ohio shale was called the Huron shale in older reports.

## GROUND-WATER HYDROLOGY

## Source and Occurrence of Ground Water

E-102

Ground water in the area of the ordnance works has its source in local precipitation. The limestone beds are the principal aquifer and, in areas where they comprise the bedrock, furnish supplies to most of the farms and suburban homes. Yields from the limestone deposits range generally between 5 gallons a minute and 10 gallons a minute, though variations over a considerable range - from 3 gallons a minute or less to more than 25 gallons a minute - are not uncommon. Water in limestone beds occur principally in joint cracks, along bedding planes and in other openings, some of which may be enlarged by solution to form interconnecting passages through which water may move in much the same manner as a surface stream. This is the case at Castalia, about 6 miles west of the proposed reactor site, where water issues in great volume from a famous spring called the "Blue Hole." According to Stout (ref. D6, p. 278):

"The rocks forming the highlands to the south of Castalia are limestones and dolomites of the Columbus and Detroit River formations. They are highly pitted with sink holes as far south as Bellevue, nine miles away. These are the source for the water of the great Blue Hole and other springs issuing in the vicinity of Castalia. The flow into the Blue Hole alone is more than 7,000,000 gallons daily. Water is close to the surface throughout the entire Castalia Prairie of over 4000 acres."

No large limestone springs are known to the writer in the vicinity of the ordnance works, nor do sink holes, such as those which give rise to the underground flow at Castalia, appear to characterize the area. Most wells in the limestone deposits in the vicinity of the ordnance works range between 50 and 80 feet in depth. The quality of the water deteriorates rapidly with increased depth, and wells deeper than about 100 feet generally yield sulphur water.

Ground water conditions change abruptly east of the line which marks the boundary between areas underlain by limestone and those in which the bedrock is shale. The shales are relatively impermeable and wells drilled into these beds generally yield less than about 3 gallons a minute, a quantity barely sufficient for limited farm or domestic use. Many wells drilled into the shales are failures and in such cases property owners commonly resort to cisterns for their water supplies. Wells drilled through the shales, into the underlying limestone beds, generally encounter water of poor quality, unusable in most cases.

Table D1 is a list of representative wells in the Plum Brook Ordnance Works area, compiled from well records in the files of the Ohio Division of Water.

TABLE D1. - RECORDS OF REPRESENTATIVE WELLS, PLUM BROOK ORDNANCE WORKS AREA

Number	Name	Altitude at well, ft above sea level	Depth to bedrock, ft	Depth of well, ft	Principal water- bearing bed	Static water level below land surface, ft	Yield, gal/min	Type of well	Diameter of well, in.	Remarks
1	Diamond Fertilizer Co.	580	25	102	ls		70	Dr	8 5/8	Water sulphurous
2	Joe L. Strickfaden, Jr.	600	11	105	ls			Dr	5 5/8	
3	Seitz Amusement Co.	585	40	94	sh ls	9	3	Dr	6 3/4	"Dry hole"
4	M. Crillis	590	29	135	sh ls			Dr	5 1/16	
5	Albert Schenk	600	2	30	sh	10		Dr	5 5/8	Water sulphurous
6	Elmer Stengor	590	2	279	sh & ls	6		Dr	5 5/8	"Dry hole"
7	Don Christotel	615	14	80	sh & ls			Dr		
8	Wm. C. Young	625	19	35	ls	15	10	Dr	5	
9	Carl Schemenauer	645	3	51	sh	12		Dr	5	
10	Jack Ehrhard	635	4	43	sh	3	1 1/2	Dr	5	
11	J. C. Klaholz, Jr.	630	2	40	sh	4		Dr	5	
12	Wm. Dempsey	645	6	63	sh	10		Dr	5	
13	Clarence Ohlemacher	625	26	45	sh	6		Dr	5	
14	Robert Bennett	615	48	53	sh	10		Dr	5 1/4	
15	Harry Kuhl	630	39	55	sh	8	1	Dr	6 1/4	
16	Don Taylor	630	49	62	sh			Dr	5	
17	Everett Hunter	695	6	40	sh	5	1	Dr	7	
18	C. H. Stanley	705	13	41	sh	4		Dr	5	
19	Robert Stewart	695	7	45	sh	10		Dr	5 1/4	
20	Wensink Brothers	705	7	46	sh	6		Dr	6	
21	Harold Lippus	640	26	43	sh			Dr		"Dry hole"
22	Avery Paper Corp.	650	31	210	sh ls	10	5	Dr	5	
23	Perry Balcom	645	49	68	sh			Dr	5 5/8	
24	F. G. Mileham	638	8	40	sh	5		Dr	6 5/8	
25	J. C. Klaholz	612	11	40	sh	7		Dr	5 5/8	
26	Harold Stevens	620	27	55	sh	11		Dr	6	

Explanation:

Dr - drilled  
ls - limestone  
sh - shale



## Movement of Ground Water

Based on well records and foundation data furnished by the U.S. Corps of Engineers, the water table in the area of the ordnance works is within a few feet of the surface, the general range in depth is between 5 and 15 feet. The configuration of the water table is a subdued replica of the surface topography. The flow of ground water, therefore, is similar in direction to the course of the surface runoff. The average hydraulic gradient in the area is very low, less than about one percent, and the rate of ground water movement probably is no greater than a foot or two per day in the limestone beds, and certainly is much less than this in the shales. These estimates are based in part on percolation rates in typical materials as given by Tolman (ref. D7, p. 219) and on other factors.

## SURFACE WATER SUPPLIES

### Lake Erie

Two principal water supplies in the area of the proposed reactor site are from Lake Erie. These are the Sandusky water supply and the water supply of the Plum Brook Ordnance Works. Both supply intakes are located east of Sandusky, as shown on figure D1. The Plum Brook pumping plant has a capacity of 51 million gallons a day (mgd). Maximum pumpage, when the ordnance works was operating at near capacity was 28 mgd. The City of Sandusky presently uses about 3.3 mgd in the winter and up to 11 mgd in the summer.

Drainage from the area of the proposed reactor site enters the lake about midway between the Sandusky intake and the Plum Brook intake. Crucial questions relative to the hazards of contaminated water entering either the Sandusky intake or the Plum Brook intake involve the effects of dilution by the lake waters and the direction of the lake currents.

Direction of Lake Erie currents. - The Ohio Division of Shore Erosion has been making studies of the Lake Erie shoreline for the past several years in cooperation with the Ohio Division of Geological Survey. Studies in 1951 revealed important facts about the direction of flow of longshore currents in the Sandusky area. As reported by Metter (ref. D3, p. 44):

"The Cedar Point shore line trends nearly N. 45° W., and wind producing waves from north of N. 45° E. would impinge upon the shore in such a manner as to produce an eastward current. Waves must approach from east to N. 45° E. to produce a resultant current toward the west. This concept of the cause of direction of longshore currents was borne out during the summer of 1951, when currents were observed to flow from the west on all but two of the days that the author was in the area, and on those two days, the wind was from the E.N.E.

From the above reasoning, it would follow that during the times that the waves were from N. 45° E. on around to the northwest, longshore currents would carry sediments to the east. During the severe storms usually associated with waves from the east the movement would be to the west."

From Metter's observations, it would follow that the principal hazard associated with the discharge of radioactive fluids into Lake Erie between the Sandusky intake and the Plum Brook intake would be more apt to involve the water supply of the ordnance works than the Sandusky supply. A potential hazard would confront both, however.

#### EARTHQUAKE ACTIVITY

The State of Ohio has experienced at least 11 earthquake shocks which had their epicenters within the State boundary. According to Heck (ref. D2), six of the shocks had an intensity of 6 or more on the Rossi-Forel scale of intensity. All but one of the six most severe earthquakes had their epicenters in northwestern Ohio, in Auglaize and Shelby counties. The area of these epicenters is about 110 miles southwest of Sandusky. Damage from earthquakes does not appear to be an important consideration in the Sandusky area.

#### CONCLUSIONS

Owing to the proximity of Lake Erie, and the absence of any large-scale ground water developments along the principal flow routes between the proposed reactor site and the lake, the hazards of ground water contamination resulting from the spillage of radioactive fluid appear negligible compared to the potential hazards to surface water supplies.

The short flow routes and the poor infiltration properties of the soils and surficial deposits over which a contaminant must move, would seem to assure its entry into the lake with but little prior dilution and perhaps only slight diminution in quantity. The latter condition would hold true especially in times when the ground is frozen or saturated. Conversely, infiltration would be greatest when the soil is dry, such as during periods of large moisture deficiency which commonly occur during the growing season.

The course of a spilled liquid, should it reach the water table, would be toward Lake Erie where it would discharge into the lake through springs and seeps along the shore. In the course of its underground journey, it is possible that a contaminant might, under present conditions, be diverted to wells that supply some of the farms and suburban homes in the area. However, owing to its very slow movement through either the underlying limestone beds or shale deposits, time would be available for

remedial measures. Areas subject to possible ground water contamination are not large and auxiliary supplies doubtless could be provided where required during such an emergency.

If a contaminant were to enter Lake Erie in volume, a much more critical problem would arise. Under average wind and weather conditions, the currents probably would carry the contaminated water in the direction of the Plum Brook intake. If so, it would be a potential hazard to personnel of the ordnance works while in proximity to the intake crib. It might require closing the intake until the contaminant had moved safely to leeward or until dilution to a nonhazardous level had occurred.

Should lake currents carry a contaminant toward the Sandusky intake, hazards would be of similar nature, though perhaps somewhat more critical. The Sandusky intake is closer to the potential source of contamination and it is reasonable to suppose there would be less dilution of wastes at that point than in the vicinity of the Plum Brook intake.

Additional hazards caused by the discharge of radioactive fluids into Lake Erie would involve the safety of bathers at the Sandusky beach and the possible contamination of fish. Sandusky is the center of an important fishing industry which could be adversely affected if fish in the area were contaminated. In this connection it should also be borne in mind that the international boundary between the United States and Canada is in Lake Erie within a few miles of Sandusky.

#### REFERENCES

- D1. Conrey, G. W., Paschall, A. H., and Burrage, E. M.: 1934, A Key to the Soils of Ohio: Ohio Engineering Experiment Station.
- D2. Heck, N. H.: 1947, Earthquake History of the United States (Exclusive of California and Western Nevada) and Alaska: U.S. Dept. of Commerce, Coast and Geodetic Survey, Serial No. 609, Revised Edition, p. 1, Continental United States.
- D3. Metter, R. E.: 1953, Sedimentary Processes along Lake Erie Shore, from Cedar Point to Huron: Chapter 2 in 1951 Investigations of Lake Erie Shore Erosion, Ohio Dept. Nat. Res., Divisions of Shore Erosion and Geol. Surv., Rept. of Investigations No. 18.
- D4. Stauffer, C. R.: 1909, The Middle Devonian of Ohio: Geol. Surv. of Ohio, 4th Ser., Bull. 10.
- D5. Stout, Wilber: 1941, Dolomites and Limestones of Western Ohio, Geol. Surv. of Ohio, 4th ser., Bull. 42.

- D6. Stout, Wilber, Ver Steeg, Karl, and Lamb, G. F.: 1943, Geology of Water in Ohio: Geol. Surv. of Ohio, 4th ser., Bull. 44.
- D7. Tolman, C. F.: 1937, Ground Water: New York, McGraw-Hill Book Co., Inc.

## APPENDIX E

### PRIMARY WATER ACTIVITY

A knowledge of the water activity is necessary to determine (1) the shielding required along the cooling water circuit; (2) water disposal procedures; and (3) water handling procedures during certain operations (for example, when changing fuel elements). The short-lived activities determine the shielding requirements while long-lived activities control the disposal situation.

In the 2-pass cooling system contemplated the water in its passage through the reactor pressure tank is activated both when flowing up and around the reactor and again when flowing down through the reactor. The activity induced during the flow around the reactor is important and has to be evaluated. The flow picture in the pressure tank is not known, and in order to simplify calculations, the following simplified flow pattern is assumed. Referring to figure E.1, water enters near the bottom of the tank and flows upward around the reactor core at a uniform velocity of 18 cm/sec until it reaches the top of the tank. Then it flows downward toward the reactor through a narrow column above the reactor at a uniform velocity of 300 cm/sec. Through the reactor core the velocity is 900 cm/sec. After flowing through the reactor the water exits near the bottom of the tank.

As the water flows upward, around the reactor, its activity at any level varies with the distance radially from the reactor core. The average activity at any level (obtained by mixing the flow over the cross section) occurs along the surface of a streamtube having a constant radius. The average activity of the water at any level in the tank is thus determined by evaluating the activity along this average streamtube surface.

The activation of the water is considered to occur in 6 phases:

- (a) In flowing upward along the average streamtube surface the activating flux is assumed to vary exponentially with the distance below level A (bottom of reactor).
- (b) In flowing between level A and level B (top of reactor) the activating flux is assumed to be constant along the streamtube surface.
- (c) In flowing away from the reactor along the streamtube surface, the activating flux is assumed to vary exponentially with the distance above level B.

(d) As the water flows down toward the reactor it passes through a region where the radiation flux is assumed to vary exponentially with the distance above level B.

(e) Through the reactor the water is activated by a constant flux.

(f) In flowing away from the reactor the water is activated by a flux varying exponentially with the distance below level A.

The  $N^{16}$  activity which is the most predominant in the water is the result of  $O^{16}$  (np) reaction having about a 10 mev threshold. In evaluating this activity the uncollided flux was used. The thermal flux was used for most of the other activities. In the reactor the average thermal flux is about  $5 \times 10^{14}$  n/cm<sup>2</sup>-sec. Above and below the reactor the thermal flux was approximated to vary as  $5 \times 10^{14} e^{-0.12y}$  where  $y$  is the distance above or below the reactor. Along the average streamtube surface the flux was approximated to be  $3.6 \times 10^{13}$  in the region between the top and bottom levels of the reactor. Above and below these levels the flux varied as  $3.6 \times 10^{13} e^{-0.12y}$ .

The uncollided flux in the reactor was evaluated to be  $5.2 \times 10^{14}$  and to vary as  $2.6 \times 10^{14} e^{-0.13y}$  above and below the reactor. Along the streamtube surface between the top and bottom levels of the reactor the flux was evaluated as  $7.8 \times 10^{11}$  and above and below these levels the flux varied according to  $7.8 \times 10^{11} e^{-0.13y}$ .

Consider the case where the flux varies with distance  $y$  from level A according to  $\Phi(y) = \Phi_0 e^{-\mu y}$  where the attenuation coefficient  $\mu$  and flux  $\Phi_0$  are constants. Water flows toward A with constant velocity  $v$  from a distance  $H$ .

If the water at  $H$  has an activity  $\alpha_0$  then at level A its activity will be

$$\alpha = \alpha_0 e^{-\frac{\lambda H}{v}} + \frac{\lambda \Sigma \Phi_0}{\lambda + \mu v} \left[ 1 - e^{-\left(\mu + \frac{\lambda}{v}\right)H} \right]$$

where

$\lambda$  decay constant

$\Sigma$  macroscopic absorption cross section

If water flows away from A and if its initial activity at A is  $\alpha_0$  then at H its activity is

$$\alpha = \alpha_0 e^{-\frac{\lambda H}{v}} + \frac{\lambda \Sigma \Phi_0}{\mu v - \lambda} \left( e^{-\frac{\lambda H}{v}} - e^{-\mu H} \right)$$

If water flows in a region of constant flux  $\Phi_0$  at constant velocity  $v$  for a distance  $H$  then

$$\alpha = \alpha_0 e^{-\frac{\lambda H}{v}} + \Sigma \Phi_0 \left( 1 - e^{-\frac{\lambda H}{v}} \right)$$

These equations were applied to the 6 irradiation phases of the water during each cycle. For each radioactive isotope, its activity after cycling for 1000 hours was computed at a level C below the reactor (fig. E.1). At level C (about 40 cm below level A) the radiation flux has dropped sufficiently so it contributes only negligible activity to the water.

In order to determine activities the concentrations of the impurities in the water must be known. These impurities consist of those originally in the water entering the system, and constituents of the stainless steel, aluminum, and beryllium which corrode into the water. The equilibrium concentrations of impurities in water (attained in about 10 hr running time) are as follows:

Na	0.03 ppm
K	0.005 ppm
Ca	0.005 ppm
Mg	0.002 ppm
SiO <sub>2</sub>	0.02 ppm
Cl	0.06 ppm
Stainless	0.10 ppm
Al	0.07 ppm
Be	0.002 ppm

These are based on:

- a. Corrosion rates of Al =  $0.231 \times 10^{-5}$  lb/hr-sq ft, Stainless =  $0.016 \times 10^{-5}$  lb/hr-sq ft, Be =  $0.0282 \times 10^{-5}$  lb/hr-sq ft, and surface areas of Al = 700 sq ft, Stainless = 15,000 sq ft, Be = 175 sq ft.
- b. Cooling water flow = 16,250 gpm.
- c. Bypass flow to system deionizer = 100 gpm.

- d. Make-up water = 5 gpm.
- e. The water supplied initially to the system, and as make-up contains a total ion concentration = 0.1 ppm  $\text{CaCO}_3$  equivalent.
- f. Water after passing through the system deionizer contains a total ion concentration = 0.1 ppm  $\text{CaCO}_3$  equivalent.

In the reactor many atoms in the aluminum plates upon capturing a neutron and becoming radioactive, recoil out of the aluminum into the water. The activity in the water due to these recoils is an appreciable part of the total water activity. The recoil isotopes consist mainly of the following:  $\text{Al}^{28}$  from  $\text{Al}^{27}$  ( $n\gamma$ ) capture,  $\text{Na}^{24}$  from  $\text{Al}^{27}$  ( $n\alpha$ ) reaction,  $\text{Mg}^{27}$  from  $\text{Al}^{27}$  ( $n\beta$ ) reaction, and  $\text{Mn}^{56}$  from  $\text{Mn}^{55}$  ( $n\gamma$ ) capture (the  $\text{Mn}^{55}$  being an impurity in the aluminum).

A summary of the activities of the important isotopes is presented in table E.1. These activities are the values just after the last irradiation of the water in the cycle (at level C) and are based on an operating time of 1000 hours. For the long half life isotopes, the allowable activities in water based on values given in reference 5.1 are listed. The composition of the stainless steel was taken from reference E.1.

Isotopes of half lives greater than about 15 minutes will have constant activity (at values given in table E.1) during the entire cycle. The activities of shorter half life isotopes may vary appreciably throughout the cycle depending on their half lives. The important short lived isotopes are  $\text{N}^{16}$ ,  $\text{O}^{19}$ ,  $\text{Al}^{28}$ ,  $\text{Mg}^{27}$ . Their activities throughout the cycle are shown plotted in figure E.2. The total cycle time is 90 seconds. After the final irradiation the water spends 9.6 seconds in the pressure tank before exiting, 38 seconds outside the tank, and 4.1 seconds back in the tank before entering the first irradiation region again. In passing around the reactor the first three irradiations occur in succession and last 2.3, 3.5, and 2.3 seconds. The water flows up to the top of the tank during the next 28.2 seconds and down to the start of the final three irradiations in the next 1.7 seconds. The final irradiations take a total time of about 0.3 second.



TABLE E.1. - ACTIVITIES OF RADIOACTIVE ISOTOPES IN PRIMARY COOLING WATER

Radio-active isotopes	Half life	Source	Activity, dis/cm <sup>3</sup> -sec	Allowable* activity, dis/cm <sup>3</sup> -sec
Na <sup>24</sup>	15 h	Recoils in Al plates, Al <sup>27</sup> (na) From Al in water, Al <sup>27</sup> (na) From Na in water, Na <sup>23</sup> (nr)	$7.8 \times 10^3$ 3 $9.6 \times 10^2$	30
Al <sup>28</sup>	2.27 m	Recoils in Al plates, Al <sup>27</sup> (nr) From Al in water, Al <sup>27</sup> (nr) From SiO <sub>2</sub> in water, Si <sup>28</sup> (np)	$4.3 \times 10^4$ $9.5 \times 10^2$ 2	$4.4 \times 10^4$
Mg <sup>27</sup>	9.45 m	Recoils in Al plates, Al <sup>27</sup> (np) From Al in water, Al <sup>27</sup> (np) From Mg in water, Mg <sup>26</sup> (nr)	$4.1 \times 10^4$ 10 65	$4.1 \times 10^4$
Mn <sup>56</sup>	2.6 h	Recoils Mn component in Al plates, Mn <sup>55</sup> (nr) From Mn component in Al in water From Mn component in S.S. in water	$3.5 \times 10^3$ 18 $6.9 \times 10^2$	550
N <sup>16</sup>	7.35 s	From O in water, O <sup>16</sup> (np)	$4.2 \times 10^6$	
O <sup>19</sup>	29.4 s	From O in water, O <sup>18</sup> (nr)	$5.2 \times 10^4$	
Ca <sup>41</sup>	$1.2 \times 10^5$ y	From Ca in water, Ca <sup>40</sup> (nr)	$2.4 \times 10^{-5}$	
Ca <sup>45</sup>	152 d	From Ca in water, Ca <sup>44</sup> (nr)	.37	1.8
Ca <sup>47</sup>	4.8 d	From Ca in water, Ca <sup>46</sup> (nr)	$1.3 \times 10^{-3}$	
Ca <sup>49</sup>	8.5 m	From Ca in water, Ca <sup>48</sup> (nr)	.31	
K <sup>42</sup>	12.4 h	From K in water, K <sup>41</sup> (nr)	15	52
S <sup>35</sup>	87 d	From Cl in water, Cl <sup>35</sup> (np)	9	18
Cl <sup>36</sup>	$4.4 \times 10^5$ y	From Cl in water, Cl <sup>35</sup> (nr)	$1.7 \times 10^{-2}$	8.9
Cl <sup>38</sup>	37.3 m	From Cl in water, Cl <sup>37</sup> (nr)	$3.6 \times 10^2$	
Fe <sup>55</sup>	2.94 y	From Fe component in SS in water, Fe <sup>54</sup> (nr)	6.5	14.8
Fe <sup>59</sup>	45.1 d	From Fe component in SS in water, Fe <sup>58</sup> (nr)	2.4	.41
Cr <sup>51</sup>	27.8 d	From Cr component in SS in water, Cr <sup>50</sup> (nr)	240	1850
Co <sup>60</sup>	5.27 y	From Co component in SS in water, Co <sup>59</sup> (nr)	.65	67
Ta <sup>182</sup>	111 d	From Ta component in SS in water, Ta <sup>181</sup> (nr)	.80	
Nb <sup>94</sup>	$5 \times 10^4$ y	From Nb component in SS in water, Nb <sup>93</sup> (nr)	$2.2 \times 10^{-5}$	
Ni <sup>59</sup>	$8 \cdot 10^4$ y	From Ni component in SS in water, Ni <sup>58</sup> (nr)	$7.6 \times 10^{-4}$	920
Ni <sup>63</sup>	85 y	From Ni component in SS in water, Ni <sup>62</sup> (nr)	.14	
Ni <sup>65</sup>	2.56 h	From Ni component in SS in water, Ni <sup>64</sup> (nr)	7.9	
C <sup>14</sup>	5570 y	From C component in SS in water, C <sup>13</sup> (nr)	$1 \times 10^{-6}$	13

\*Values calculated from ref. 5.1.

In order to facilitate radiation calculations from the water activity the following table is presented. The fraction of disintegrations yielding a photon and photon energies are given for several isotopes.

TABLE E.2. - PHOTON YIELD AND ENERGY FOR SEVERAL  
RADIOACTIVE ISOTOPES

Isotope	Fraction of disintegrations yielding a photon	Photon energy
N <sup>16</sup>	0.74	6.1
	.06	7.1
O <sup>19</sup>	.70	1.6
Al <sup>28</sup>	1.00	1.8
Mg <sup>27</sup>	1.00	.8
	.20	1.0
Mn <sup>56</sup>	1.00	.8
	.25	1.8
Na <sup>24</sup>	.15	2.1
	1.00	2.7
	1.00	1.4

#### REFERENCE

E.1. Reactor Handbook, vol. 2, p. 688.

APPENDIX FANALYSES OF THE BORAX-TYPE EXCURSION IN THE NACA REACTOR

The effectiveness of steam formation as a self-limiting mechanism in a Borax-type excursion has been established by the series of Borax and Spert tests (refs. F.1, F.2, and F.3). Various analyses have been made attempting to predict the results of Borax-type excursions in reactors with Borax (MTR) type fuel elements. A description of the methods of four of these analyses (refs. F.4, F.5, F.6, and F.7) and the results of their application to the NACA reactor will be presented. All four methods attained some limited degree of success in predicting the results of the Borax experiments. Despite the fact that there is considerable question as to the validity of any of these analyses for reactor systems other than the Borax type, they were used for the NACA reactor because no better ones were available.

## BORAX-TYPE EXCURSION ANALYSIS

Edlund and Noderer (ref. F.4) make the following general assumptions for the self-limiting process of a Borax-type excursion. The power rises exponentially with constant period until sufficient steam volume forms to completely compensate for the initial increase in reactivity. Heat is transferred from the fuel plate to the water by nucleate boiling once the saturation temperature is reached. The heat transferred to the water is contained in a layer adjacent to the fuel plate, the thickness of which grows directly as the square root of time. The pressure in the reactor is equal to the saturation pressure corresponding to the average temperature of the heated water layer. The pressure rise is directly proportional to the second derivative of steam volume with respect to time. Equations are derived which permit the estimate of maximum fuel plate temperature, excursion energy, and maximum pressure in a Borax-type excursion.

Gartner and Daane (ref. F.5) make the following general assumptions for the self-limiting process. The power rises exponentially with constant period until sufficient steam volume has formed to completely compensate for the excess prompt reactivity. Heat is transferred from the fuel plate to the water by conduction. The pressure in the reactor is equal to the saturation pressure corresponding to the surface temperature of the fuel plate. The pressure rise is directly proportional to the second derivative of steam volume with respect to time. Equations are derived which permit the estimate of maximum fuel plate temperature, excursion energy, and maximum pressure.

Golian, Bergstralh, Harris, and O'Rourke (ref. F.6) make an analysis of the self-limiting process with the following general assumptions. The

power rises exponentially with constant period until sufficient steam volume has formed to completely compensate for the excess prompt reactivity. Heat is transferred from the fuel plate to the water by conduction until the boiling point is reached. Above the boiling point, heat is assumed to be transferred through a steam film by conduction. The pressure is assumed to remain constant. Equations are derived which permit the estimate of maximum fuel plate temperature and excursion energy.

Booth (ref. F.7) analyzes the self-limiting process with the following general assumptions. The power rises exponentially with a constant period until sufficient steam volume has formed to halt the rise. Heat is transferred from the fuel plate first by conduction and then by nucleate boiling. Booth defines "fully developed boiling" as the condition where the net rate of heat transfer to the boiling water layer adjacent to the fuel plate is zero. That is, the heat transferred from the fuel plate to the layer of water adjacent to the fuel plate in which boiling is taking place is equal to the heat transferred from the boiling water layer to the subcooled water at the center of the passage. The assumption is made that the temperature profile in the subcooled water is related to the temperature profile which existed in the entire water cross section at the time boiling began. The heat transfer from the layer of boiling water to the subcooled water is calculated as equal to the heat conduction into the subcooled water required to give the appropriate slope to the temperature profile of the subcooled water. The correlation of Rohsenow for steady-state nucleate boiling is used to estimate the heat transfer from the fuel plate to the boiling water layer. The heat transfer into the boiling water layer is assumed equal to the heat transfer out of the layer. The resulting equation can be solved for fuel plate temperature and this fuel plate temperature is assumed to correspond to the fuel plate temperature when sufficient steam has formed to halt the nuclear excursion.

The value of the void coefficient of reactivity, which determines the effectiveness of steam volume formation as a self-limiting mechanism, is of considerable importance in the analyses of references F.4, F.5, and F.6. The hydrodynamics of the reactor, which determines the relationship between the steam volume generated and the pressure, is of considerable importance in the analyses of references F.4 and F.5. The void coefficient of reactivity and the hydrodynamics of the NACA reactor will be discussed below.

#### APPLICATION TO NACA REACTOR

##### Void Coefficient of Reactivity

The void coefficient of reactivity has been computed for the NACA reactor as described in appendix B. For uniformly distributed voids the

computed value is  $-0.18 \frac{\Delta K/K}{\Delta V_{\text{void}}/V_{\text{H}_2\text{O}}}$ . Several cases of nonuniformly dis-

tributed voids have been computed corresponding approximately to the type of distribution which might occur in a Borax-type excursion. The ratio of the void coefficient for nonuniform void distribution to the void coefficient for uniform void distribution varied from about 1.35 to 2.00 depending on the degree of concentration. For the analyses of this section it has been assumed that this ratio is 1.5 and the fractional void coefficient in a Borax-type excursion is equal to  $1.5 \times (-0.18)$  or

$$-0.27 \frac{\Delta K/K}{\Delta V_{\text{void}}/V_{\text{H}_2\text{O}}}.$$

The results of experiments in the Bulk Shielding Facility on a reactor configuration which was specifically selected to approximate the NACA reactor are described in supplement III. These results indicate that voiding of water passages in the fuel element at the geometric center of the slab loading produced a fractional void coefficient of

$$-0.64 \frac{\Delta K/K}{\Delta V_{\text{void}}/V_{\text{H}_2\text{O}}};$$

voiding of water passages in the fuel element at the hot-spot position at the core-reflector interface produced a fractional void coefficient of  $-0.41 \frac{\Delta K/K}{\Delta V_{\text{void}}/V_{\text{H}_2\text{O}}}$ . These results indicate the strong

spatial statistical dependence of the void coefficients and the fact that the assumed weighted void coefficient of  $-0.27 \frac{\Delta K/K}{\Delta V_{\text{void}}/V_{\text{H}_2\text{O}}}$  is probably conservative.

#### Hydrodynamics of the Reactor

The hydrodynamics of the reactor, which determines the relationship between the steam volume generated and the pressure, is of considerable importance in the analyses of references F.4 and F.5. The situation in the reactor core is essentially this: When steam is generated in the core, the volume it occupies is many times the volume occupied by an equivalent weight of water. Therefore, a certain amount of water must be expelled from the core to make room for the steam. Similarly, the water outside the reactor core must move to make room for the water expelled from the core. Force is required to overcome the inertia of the water and this force is felt as a pressure.

Assumption A: Water incompressible, bellows. - In references F.4 and F.5 the assumption is made that the water is incompressible, or equivalently that the speed of sound in water is infinite. This assumption leads to the following relation

$$\Delta P(t) = \rho \alpha \ddot{V}_s \quad (F.1)$$

where

$\Delta P(t)$	pressure rise in the reactor core, a function of time
$\ddot{V}_s$	second derivative of steam volume with respect to time
$\rho$	density of water
$\alpha$	a constant which depends on the reactor geometry
$t$	time

The constant,  $\alpha$ , depends on the lengths and cross-sectional areas of the water flow paths in the reactor core, and from the reactor core to the nearest free surface.

The only free surface in the NACA reactor primary water system is in the head tank which is very distant from the reactor core. The value of  $\alpha$  for this system would be very large, which is undesirable. Accordingly, it was considered that bellows might be located in the reactor tank close to the core to provide additional expansion volume. Bellows were designed with sufficient volume and flexibility to provide the equivalent of a free surface and were located  $3\frac{2}{3}$  feet above the top face of the reactor core. Values for the maximum fuel plate temperature, excursion energy, and maximum pressure were calculated for the NACA reactor by the methods of references F.4 and F.5 using a value of  $\alpha$  which took into account the presence of the bellows (the methods of refs. F.6 and F.7 were not affected by the presence or absence of bellows). These results will be discussed later in this appendix.

Assumption B: Water compressible, no bellows. - Since water is actually compressible, the effect of water compressibility will now be considered.

The formation of steam gives rise to pressure waves in the water. The pressure waves compress the water and the change in volume at any given time is the volume occupied by the steam. The relationship between steam volume generated and the pressure, considering only the compressibility of the water and not the bellows system described above, can be expressed

$$V_s = \int \beta \Delta p(l, t) dv \quad (F.2)$$

where

$\Delta p(l, t)$	local pressure rise, a function of position and time
$\beta$	bulk modulus of compressibility of water
$dv$	differential volume element
$V_s$	steam volume

The integral of equation (F.2) is taken over the entire volume of water in the system. For the NACA reactor, only the water in the reactor tank will be considered. This is a conservative assumption.

The exact form of the function,  $\Delta p$ , depends on the geometry of the system under consideration. For the NACA reactor, the following simplifying assumptions will be used. Plane pressure waves will be assumed to originate in the horizontal plane which passes through the reactor center line. These plane pressure waves will extend over the entire cross-sectional area of the reactor tank. The plane pressure waves will travel both up and down and will reflect from the top and bottom, respectively, of the reactor tank. When the reflected waves reach the plane of origin they will be badly broken up by the local structure and therefore no subsequent reflection will be considered.

To account for the fact that the pressure waves actually originate from a small volume in the reactor core and not from a plane across the entire reactor tank, the pressure level of the plane waves will be assumed to be one-ninth the pressure in the reactor core. The value of this factor was obtained by assuming it equal to the reduction in pressure of a spherical wave traveling outward from a one foot diameter sphere representing the volume of origin to the nine foot diameter of the reactor tank. The value of one foot was determined by assuming the surface area of the sphere of origin equal to the surface area of the ends of the fuel elements.

The local pressure rise in the reactor tank may then be expressed

$$\Delta p(l, t) = \frac{1}{9} [\Delta P(t)]_{t=t-\frac{l}{a}} + \frac{1}{9} [\Delta P(t)]_{t=t-\frac{2L-l}{a}} \quad (F.3)$$

where

- $l$  distance from plane of origin of pressure wave (taken positive in both directions)
- $a$  speed of sound in water

$L$  distance to plane of reflection at the top or bottom of the reactor tank (taken positive for both locations)

Equation (F.3) expresses the fact that the pressure at a given time  $t$ , at a distance  $l$  from the plane of origin of the pressure waves, is equal to the pressure which existed at the plane of origin at a time in the past; the time decrement being equal to the time required for the pressure wave to travel from  $l = 0$  to  $l = l$ , namely  $l/a$  for the original wave and  $\frac{2L - l}{a}$  for the reflected wave. The first term on the right hand side of equation (F.3) represents the contribution of the original pressure wave and the second term represents the contribution of the reflected pressure wave.

Using equations (F.2) and (F.3), an expression relating steam volume generated and pressure rise in the reactor core can be found

$$V_s = \frac{\beta A}{9} \int_0^{L_1} \left\{ [\Delta P(t)]_{t=t-\frac{l}{a}} + [\Delta P(t)]_{t=t-\frac{2L_1-l}{a}} \right\} dl + \frac{\beta A}{9} \int_0^{L_2} \left\{ [\Delta P(t)]_{t=t-\frac{l}{a}} + [\Delta P(t)]_{t=t-\frac{2L_2-l}{a}} \right\} dl \quad (F.4)$$

where

$A$  cross-sectional area of reactor tank

$L_1$  distance from plane of origin of pressure waves to top of reactor tank

$L_2$  distance from plane of origin of pressure waves to bottom of reactor tank

Equation (F.4) represents approximately the relation between  $V_s$  and  $\Delta P(t)$  for the NACA reactor considering only the compressibility of the water.

Comparison of assumptions A and B for references F.5, F.6, and F.7. - It is now desired to apply the analyses of references F.4, F.5, F.6, and F.7 to the NACA reactor using assumption B in place of assumption A. This is accomplished by replacing equation (F.1) with equation (F.4) in the analyses. The results will then be compared to the results using equation (F.1) and the bellows system described previously.



The results from references F.6 and F.7 are entirely unchanged since neither analysis uses equation (F.1) or any similar relationship.

The substitution of equation (F.4) for (F.1) is very easily carried out for the method of reference F.5 and figure F.1 compares the values of maximum fuel plate temperature, excursion energy, and maximum pressure in the reactor core as calculated using equation (F.4)(assumption B) and using equation (F.1)(assumption A). It will be noted that the maximum fuel plate temperatures, excursion energies, and maximum pressures calculated using assumption B (water compressible, no bellows) are lower throughout the range of periods considered.

Comparison of assumptions A and B for reference F.4. - The substitution of equation (F.4) for (F.1) is difficult to carry out for the method of reference F.4. This is because there is an approximation in the derivation which is no longer pertinent when equation (F.4) is substituted for equation (F.1) and because, after the derivation is complete, a constant is evaluated by comparison with experimental data. It was felt that the changes resulting from the use of a different approximation in the derivation and the evaluation of a new constant from the experimental data would constitute too much of a change in the original method for the results to be properly comparable with the results of the original method.

Accordingly, a more roundabout method is used. An assumption is made as to the variation with time of the reactor core pressure. Using this assumption, the steam volume is computed for assumptions A and B. The assumption which provides more steam volume for a given set of conditions provides for better self-limiting of Borax-type excursions.

It will be assumed that the variation of pressure rise in the reactor core with time can be approximated by an exponential function

$$\Delta P(t) = \Delta P_0 e^{mt} \quad (F.5)$$

where

$m$  the reciprocal of the period of the pressure

$\Delta P_0$  pressure rise at  $t = 0$

Substituting equation (F.5) in equation (F.1) and integrating twice with respect to  $t$  between the limits  $t = 0$  and  $t = t$  gives

$$V_s = \frac{\Delta P_0 (e^{mt} - mt - 1)}{\rho \alpha m^2} \quad (F.6)$$

Substituting equation (F.5) in equation (F.4) and integrating gives

$$V_s = \frac{\Delta P_o \beta A a e^{mt}}{9m} \left[ \left( 1 - e^{-\frac{2mL_1}{a}} \right) + \left( 1 - e^{-\frac{2mL_2}{a}} \right) \right] \quad (F.7)$$

The ratio of the value of  $V_s$  in equation (F.7) to that in equation (F.6) is

$$R = \frac{V_s(F.7)}{V_s(F.6)} = \frac{\beta A a m \alpha}{9} \left( \frac{e^{mt}}{e^{mt} - mt - 1} \right) \left[ \left( 1 - e^{-\frac{2mL_1}{a}} \right) + \left( 1 - e^{-\frac{2mL_2}{a}} \right) \right] \quad (F.8)$$

For values of  $R$  greater than 1, the steam volume as computed using assumption B (water compressible, no bellows) is greater than the steam volume as computed using assumption A (water incompressible, bellows). Therefore, for  $R$  greater than 1 assumption B provides better self-limiting of Borax-type excursions than assumption A; for  $R$  less than 1, the opposite is true. We wish to show that  $R$  is greater than 1 for the periods of interest.

In order to evaluate  $R$  from equation (F.8) it is necessary to make some assumption as to the value of  $m$ , the reciprocal of the period of the pressure. From the rather uncertain experimental pressure rise data of references F.1, F.2, F.3, and F.7 it would seem that the pressure period is probably shorter than the power period for the periods of interest. Since it turns out that  $R$  increases with increasing  $m$ , the assumption that  $m$  is equal to the reciprocal of the power period is probably conservative.

$R$  also depends on  $mt$  (the time in periods) in the term  $\frac{e^{mt}}{e^{mt} - mt - 1}$ . This term is always greater than one and therefore the value of  $R$  assuming this factor is equal to one is always conservative. However, some indication of the value of the factor may be obtained from the experimental evidence in references F.1, F.2, and F.3. The time interval between the time when the fuel plate temperature reaches the boiling point and the time when the power peak is reached is of the order of 0.3 to 1 period for power periods from 15 to 50 milliseconds for subcooled reactors of the Borax I or Spert I type. The factor  $\frac{e^{mt}}{e^{mt} - mt - 1}$  varies from 27 for  $mt = 0.3$  to 3.8 for  $mt = 1$ .

In table F.1 below, are tabulated the values of  $R$  computed from equation (F.8):

TABLE F.1

Period, sec	m	$R$ (assuming that $e^{mt}/e^{mt} - mt - 1 = 1$ )	$R$ (assuming that $e^{mt}/e^{mt} - mt - 1 = 3.8$ )
0.040	25	0.083	0.32
.020	50	.31	1.2
.010	100	1.05	4.2
.005	200	3.2	12.2

It may be seen from table F.1 that even for the most conservative assumption, the ratio  $R$  is greater than one for periods of 10 milliseconds or less. If a more probable value of the term  $e^{mt}/e^{mt} - mt - 1$  is used, the ratio  $R$  becomes greater than one at still longer periods. For example, for  $mt = 1$ ,  $e^{mt}/e^{mt} - mt - 1 = 3.8$ ,  $R$  is greater than one for periods of about 21 milliseconds or less.

This completes the lengthy digression which was necessary because we could not directly substitute equation (F.4) for equation (F.1) in the analysis of reference F.4. It has been shown, within the limits of the accuracy of the assumptions of the above analysis, that for periods of 10 milliseconds or less water compressibility alone provides more volume for steam, and consequently better self-limiting of Borax-type excursions, than would be provided by the bellows under the assumption that the water is incompressible. Therefore the values of maximum fuel plate temperature, excursion energy, and maximum pressure in the reactor core as calculated under assumption A (water incompressible, bellows) are conservative for periods of 10 milliseconds or less; these are the critical periods for the NACA reactor. It has also been shown that there is a good probability that the values of temperature, energy, and pressure calculated under assumption A are conservative for periods of 21 milliseconds or less and perhaps even for longer periods.

#### Results for the NACA Reactor

It is now possible to give the final comparison of the results of applying the analyses of references F.4, F.5, F.6, and F.7 to the NACA reactor system (no bellows in the reactor tank). The results given for references F.6 and F.7 do not depend on the presence or absence of a bellows. The results which will be given for reference F.5 are those computed by substituting equation (F.4) for equation (F.1) in the analysis

of reference F.5. The results which will be shown for reference F.4 are those computed assuming that the water is incompressible and that the bellows system previously described is present. These results have been shown to be conservative for periods of 10 milliseconds or less and possibly for longer periods.

The critical set of initial conditions for the NACA reactor is the case of a  $\Delta K$  step increase when the reactor is operating at zero power. This condition is critical because the degree of subcooling is greatest and because it is physically possible to obtain a closer approximation to a  $\Delta K$  step as opposed to a  $\Delta K$  ramp. The following results are based on an initial reactor temperature of 50° F and an initial pressure of 135 pounds per square inch absolute. The temperature of 50° F is the lowest temperature it is expected the primary water might attain in the winter. The pressure of 135 pounds per square inch absolute is the average of reactor inlet and outlet design pressures.

Figure F.2 shows the variation of maximum fuel plate temperature with period as predicted by the four different methods. It may be noted that the fuel plates would not melt unless the period were shorter than about 10 milliseconds,  $\Delta K$  greater than about 1.8.

Figure F.3 shows the variation of energy release with period for three of the different methods. The method of reference F.7 does not permit the computation of energy release. It may be noted that the predicted energy release of the NACA reactor is less than 135 megawatt-seconds (the energy release of the Borax explosion) for periods down to about 5 milliseconds,  $\Delta K$  greater than about 2.9.

Figure F.4 shows the variation of maximum pressure in the reactor core with period for two of the different methods. The methods of references F.6 and F.7 did not permit the computation of pressure rise.

#### FINAL REACTOR SHUTDOWN

If a Borax-type excursion occurred due to the insertion of a step  $\Delta K$  into the reactor at a time when the control rods failed to function properly and the formation of steam volume in the reactor core shut down the reactor before any permanent damage could be done, the reactor might again become critical when the steam condensed in the subcooled water, and the entire cycle repeat itself. Some means of shutting down the reactor when the control rods fail to function must be available to prevent this type of occurrence. Various methods of accomplishing this are under consideration and the one which is deemed most suitable will be built into the NACA reactor.

## REFERENCES

- F.1. Dietrich, J. R.: Experimental Investigation of the Self-Limitation of Power During Reactivity Transients in a Subcooled Water-Moderated Reactor, AECD-3668.
- F.2. Dietrich, J. R.: Experimental Determinations of the Self-Regulation and Safety of Operating Water-Moderated Reactors, International Conference on the Peaceful Uses of Atomic Energy (Geneva), Vol. 13, paper 481, pp. 88-101.
- F.3. Nyer, W. E., Forbes, S. G., Bentzen, F. L., Bright, G. O., Schroeder, F., and Wilson, T. R.: Experimental Investigation of Reactor Transients, IDO 16285.
- F.4. Edlund, M. C., and Noderer, L. C.: Analyses of Borax Experiments and Application to Safety Analyses of Research Reactors. To be published.
- F.5. Gartner, L., and Daane, R.: The Self-Regulation by Moderator Boiling in Stainless Steel  $\text{UO}_2\text{-H}_2\text{O}$  Reactors. NDA report 15-H-1.
- F.6. Golian, S. E., Bergstralh, T. A., Harris, E. G., and O'Rourke, R. C.: NRL report 4495 RD 480 (classified).
- F.7. Booth, M. E.: Behaviour of Water-Moderated Reactors During Rapid Transients. M. S. Thesis, MIT.



## APPENDIX G

### POSSIBLE CHEMICAL REACTIONS

As a result of the nuclear energy release in a Borax-type excursion, the fuel plates of the reactor may be heated to a temperature high enough to permit a metal-water reaction to occur between the aluminum and aluminum-uranium alloy of the fuel plates and the water in the core. If this reaction should occur, hydrogen would be liberated. The nuclear and chemical energy released by the nuclear excursion and concurrent metal-water reaction would undoubtedly rupture the reactor pressure tank and hurl a portion of the contents of the reactor pressure tank into the air-filled dome of the containment tank. The hydrogen liberated by the metal-water reaction might react with the air in the dome of the containment tank. A discussion of the potential metal-water reaction and the potential hydrogen-air reaction occurring will be discussed below.

### METAL-WATER REACTION

Mills (ref. G.1) first noted that if metal-water reactions actually occurred during a nuclear runaway, the heat released would be comparable in magnitude to that released by nuclear reaction. Further, if the chemical reactions went explosively, there would be the possibility of spreading radioactivity over a large area. Numerous experimental investigations have been undertaken subsequently to establish whether or not the reactions really proceeded under conditions that might be attained in reactors. It may be noted that the free energy change is negative for the reaction of all metals commonly used in reactors with the exception of nickel. In the NACA reactor we are concerned with aluminum and an aluminum-uranium alloy (~10 percent uranium).

### Literature

Several types of experiments have been performed that are pertinent. West and Weills (ref. G.2) forced molten aluminum (3kg) into water by sudden application of air pressure. The nozzle through which the aluminum was forced was perforated by a large number of 1/16 inch diameter holes. No detectable steam pressure was produced and there was no evidence of significant chemical reaction even when the aluminum was heated to 1000° C.

Milich and King (ref. G.3) melted metal rods inductively in an argon atmosphere. The molten metal (~10 gm) was allowed to drop into varying amounts of water (10-140 ml). Aluminum, zirconium, 304 stainless steel, and mild steel were tested. No violent reactions or detonations were observed. Slight reaction was observed with zirconium, 304 stainless, and

mild steel. No reaction was observed with aluminum except in one case in which the dish containing the water was insulated to retain the heat.

In aluminum foundry practice, water is used as a quench to form ingots from the molten metal. Several serious explosions have occurred, however, and Russell (ref. G.4) has investigated the conditions under which explosions take place. He found aluminum poured from a 1 inch diameter opening will not explode under conditions where that poured from a 3 inch diameter opening would explode violently. Also there appeared to be a correlation between higher temperature of the molten metal and increasing tendency to explode. No explosions occurred if water depth was greater than 30 inches.

Higgins (ref. G.5) poured the following molten metals, in a 1 inch diameter stream into water: aluminum, nickel, zirconium, stainless steel, magnesium, and an aluminum-lithium alloy. None reacted violently though a thin oxide coating was formed on the globules in each case. In an attempt to obtain dispersion of the molten metal, a blasting cap was inserted beneath the surface of the water, provided with a timing circuit. With this setup, violent reactions were obtained with zirconium, Zircaloy-2, an aluminum-lithium alloy, and magnesium. However, aluminum and nickel yielded no violent reactions; only the formation of a thin oxide film occurred. The particle size of the nickel and aluminum globules was such that 87 and 81 percent, respectively, passed through a 4-mesh screen.

Shidlovski (ref. G.6) was able to induce explosive reactions in mixtures of water (43 percent by weight) and magnesium powder (57 percent by weight) by providing confinement and detonating them with a blasting cap. A mixture of 50 percent water and 50 percent fine aluminum powder did not explode under the same conditions. However, with an auxiliary detonating charge of tetryl in addition to the blasting cap, a true explosion was initiated. Some  $\text{Al}_2\text{O}_3$  powder was recovered from the products along with some unreacted aluminum.

Higgins (ref. G.5) extended the work of Shidlovski in a different apparatus employing smaller sample size, a lesser degree of confinement, and a larger booster charge. He obtained explosions with 50-50 slurries of magnesium in water and in methanol. However, the following slurries could not be exploded:  $\text{Al-H}_2\text{O}$ ,  $\text{Al-CH}_3\text{OH}$ ,  $\text{Zr-H}_2\text{O}$ , and  $\text{Al-Mg-CH}_3\text{OH}$ .

Ruebsamen, Shon, and Chrisney (ref. G.7) heated metal wire and foil samples while immersed in water by means of a high voltage condenser discharge. Samples were heated to about  $2500^\circ\text{C}$ . The extent of the chemical reaction was calculated from measurements of the amount of  $\text{H}_2$  found and the weight of metal lost. Explosive reactions were observed with substantial amounts (up to 100 percent) of the metal reacting for: uranium, zirconium, aluminum, aluminum-lithium, and aluminum-uranium (10 and



25 percent U). No outstanding differences in reactivity were observed. Nickel did not give explosive reaction nor react to any great extent.

Experiments are in progress at the MTR (ref. G.8) in which aluminum-uranium alloy samples (26 to 50 percent by weight U-235) 1/8-inch diameter and 0.10-inch thick with aluminum cladding on one side only are mounted in a small ceramic cup and exposed to water on only one face. The test cup is glued to a pressure capsule containing the water and fitted with a pressure transducer. The sample is lowered into the reactor lattice for 6-12 second irradiations. Indications are that explosive reactions are obtained just above the melting point of the alloy, though not at higher temperatures (ref. G.9).

#### Discussion of Literature

It appears that aluminum is the most difficult of the reactive metals with which to induce an explosive reaction in water. This is undoubtedly due to the very protective  $Al(OH)_3$  formed on its surface. This hydrated oxide is practically completely protective on solid aluminum and almost as protective on molten aluminum. However, the literature indicates that an explosion can be obtained under two sets of conditions:

A. When a massive blob of molten aluminum is dropped into a comparable amount of water, not deep enough to cool the aluminum substantially before striking the bottom of the container. Whether this is a steam explosion or a metal-water explosion has not been demonstrated. In any event these conditions are not possible in the NACA reactor.

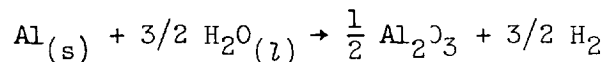
B. When the aluminum is very finely dispersed as in a fine powder or when atomized (i.e., heated above the boiling point).

The aluminum-uranium alloy will give an explosive metal-water reaction more readily than pure aluminum. The greater the percentage of uranium, the more easily will the explosion occur. The 10 percent uranium alloy is probably only slightly more reactive than pure aluminum. This no doubt depends on how much the protective  $Al(OH)_3$  is altered by the 10 percent uranium.

#### Explosion Problem Arising from $Al-H_2O$ Reaction in NACA Reactor

A. Weight of aluminum: It may be assumed that only the aluminum in the fuel plates will be heated enough during a runaway to be considered here. This amounts to 90kg. About 1/3 of this is aluminum-uranium (90-10 percent) alloy and 2/3 pure aluminum cladding.

B. Heat evolved from reaction:

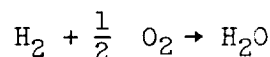


$$-\Delta H_{298} = 195 \text{ kcal}$$

$$Q_{(90\text{kgAl})} = 1350 \text{ megawatt secs}$$

C. Hydrogen evolution: Approximately 4100 cu ft of hydrogen at standard conditions (23 lb) would be evolved.

D. Heat evolved from reaction:



$$-\Delta H_{298} = 68.3 \text{ kcal}$$

$$Q (\text{H}_2 \text{ from } 90 \text{ kg Al}) = 1600 \text{ megawatt secs}$$

E. Estimate of fraction of metal that will react:

From examination of residue of Borax experiment (ref. F.1, appendix F) and from drop size measurements obtained by Higgins (ref. G.5) it appears that molten metal dispersed by an explosion in water is not so finely divided (as in powders) than an autocatalytic reaction is to be expected in the case of aluminum. Hence the fraction of the molten aluminum that reacts would probably be small. The situation is, however, far from clear. The assumption made in the body of the report (section 6.4.3) that 50 percent of the metal in the fuel plates reacts appears to be conservative for the case of little or no metal vaporization.

#### HYDROGEN - AIR REACTION

Following a detonation in which the reactor pressure tank is destroyed, a jet of water,  $\text{H}_2$ , and metal will issue into the containment tank dome. The exact composition of this jet is unknown since it depends on the extent of the reactions which have preceded its emergence. The course of the jet is also not known since debris, protective equipment and the like will serve, in some measure at least to deflect and disrupt it. It is known that in the absence of such deflectors the jet would issue vertically with little spreading.

Two questions are of paramount importance: (1) is there enough inert gas in the jet to render the  $\text{H}_2$ -gas mixture nonflammable under all conditions and (2) if an explosion does occur would it rupture the containment tank.

With regard to the flammability of H<sub>2</sub>-air-inert mixtures, some data exist on the effect of water vapor and the limits of flammability (ref. G.10). There are also some data on the detonation limits of H<sub>2</sub>-air mixtures in the absence of water (ref. G.11). These data are shown in figure G.1. For the flammability limit data straight lines have been drawn between the H<sub>2</sub>-air limits and the single point for nonpropagation irrespective of fuel-air ratio for mixtures containing water vapor. Similar data on other fuels suggest that straight lines are a reasonable approximation (ref. G.10). The point of major interest, however, is the one at which no fuel-air mixture is flammable. This mixture contains 60 percent water by volume and 10 percent H<sub>2</sub> by volume or a H<sub>2</sub>/H<sub>2</sub>O ratio of about 0.17 by volume and about 0.02 by weight. Since the water must be in the vapor state or at worst in the form of a very fine mist it seems unlikely that this condition would exist following a catastrophe.

If one assumes that the detonation limit curves are parallel to the flammability limit curves, it is possible to find a corresponding non-detonation limit for water mixtures. There is no particular justification for this assumption. Nevertheless, a cross-over occurs at a volumetric water vapor concentration of about 32 percent and a H<sub>2</sub> concentration of 21 percent of a H<sub>2</sub>/H<sub>2</sub>O ratio of about 0.66 by volume or 0.07 by weight. It again appears unlikely that this condition would exist in a catastrophe. It must therefore be assumed that it is possible, during the mixing of the jet from the reactor tank into the containment tank, that flammable and possibly detonable mixtures of H<sub>2</sub> and air would at some time occur. It does not, of course, mean that these mixtures would occur at a time and place containing an ignition source nor does it mean that a large volume of the total mixture would exist in the flammable range.

A part of the same problem concerns the ultimate mixture which would result if the jet is uniformly mixed in the chamber. To be nonflammable the ultimate mixture of H<sub>2</sub>-air would have to contain less than 4 percent hydrogen by volume. The containment tank has an air volume of 451,000 cu ft; the 23 pounds of hydrogen produced if all the metal in the fuel plates reacted would result in a concentration of hydrogen of about 1 percent by volume in the containment tank. It appears, therefore, that the ultimate uniform mixture would be well below the flammability limit. The probability of explosion is thus considerably reduced since even flammable concentrations will exist only as a transient. This transient condition must also occur in the presence of an ignition source. Since the upward thrust of the original jet is great, little mixing will probably occur in the early stages so that some cooling will take place before the flammable mixtures form.

Assuming that an explosion might occur, what will be its severity. The minimum concentration of hydrogen which will form a detonable mixture is about 18 percent. In the body of the report (section 6.4.3) it is

assumed that 50 percent of the metal in the fuel plates reacts. This would produce about 11.5 pounds of hydrogen; the volume of hydrogen would be approximately 2500 cubic feet. The explosion which would most severely try the containment tank is that which would occur if some portion of the detonable mixture were in contact with the containment tank. The pressure-time history which the containment tank would see if a hydrogen-air mixture in contact with it were to detonate is discussed in appendix H.

## REFERENCES

- G.1. Mills, M. M.: NAA-SR-31, 1949 (classified).
- G.2. West, J. M., and Weills, J. T.: ANL-4503, Oct., 1950; ANL-4549, Dec. 1950.
- G.3. Milich, M., and King, E. C.: "Molten Metal-Water Reactions," Tech. Rep. 44, Mine Safety Appliances Co., Callery, Pa., Nov. 9, 1955. Contract nos. -65426, Index no. NS-200-021.
- G.4. Russell, A. G.: Aluminum-Water Explosions, (memorandum) Aluminum Company of America, New Kensington, Pa., April 14, 1950.
- G.5. Higgins, H. M.: A Study of the Reaction of Metals and Water, AECD-3664, April 15, 1955.
- G.6. Shidlovski, A. A.: Explosive Methyl Alcohol-Water Mixtures with Magnesium and Aluminum, Zhur. Prik. Him. 19, 371-17 (1946).
- G.7. Ruebsamen, W. C., Shon, F. J., and Chrisney, J. B.: "Chemical Reaction Between Water and Rapidly Heated Metals," NAA-SR-197, Oct. 27, 1952.
- G.8. MTR Technical Branch Quarterly Rep. Fourth Quarter pp. 16-17, 1954.
- G.9. Personal communication with A. W. Brown at MTR, March 15, 1956.
- G.10. Bureau of Mines Bulletin 503.
- G.11. Pigford, T. H.: "Explosion and Detonation Properties of Mixtures of Hydrogen, Oxygen, and Water Vapor.

## APPENDIX H

### FORCES ON THE REACTOR CONTAINMENT STRUCTURE

The forces acting on the reactor containment structure are discussed below. Included in this discussion are the forces due to a 400 pound TNT explosion at the reactor location, the forces which might act on the reactor containment tank if a hydrogen explosion occurred in the air above the shielding pool, and the equilibrium pressure in the containment tank after an excursion.

#### FORCES DUE TO A 400 POUND TNT EXPLOSION

An explosion of 400 pounds of TNT was assumed to occur at the location of the reactor core. Pressure-time histories were calculated for the reactor pressure tank and the shielding pool floor and walls by use of reference H.1. The results are shown in figure H.1. The impulse-time histories for the shielding pool floor and walls are shown in figure H.2.

##### The Reactor Pressure Tank

The pressure on the bottom is that due to 400 pounds doubled for full reflection. That at the top was taken to be that due to 800 pounds, thus allowing for some focusing by the side walls. This should be a reasonable estimate. The side pressures are faired between these two charge weights.

##### Shielding Pool Floor

The 9-foot steel tank and accompanying concrete are assumed to offer no resistance whatever and are henceforth ignored. According to reference H.1 (pp. 255-259), the pressure on the floor should vary from double that due to 400 pounds of TNT directly below the reactor to that due to 800 pounds of TNT at the intersection with the side wall. By a comparison with reference H.1, figure 7.19, this variation was established. Because of the free surface, there will be a rarefaction wave from the surface hitting the floor at a later time. This simply cuts the initially high pressure due to the shock to zero. As the shock travels at about 5000 fps, the times at which the shock wave and rarefaction wave arrive are given by

$$t_{\text{shock}} = r/5 \text{ milliseconds}$$

$$t_{\text{rarefaction}} = \frac{\sqrt{2500 + r^2}}{5} \text{ milliseconds}$$

r radial distance from reactor measured along floor

depth of water 25 feet

Because of reflection from the side walls, the wave recrosses any point on the floor, repeating the pressure history at a time after the initial wave

$$t = \frac{2(30 - r)}{5} \text{ milliseconds}$$

for the short floor and

$$t = \frac{2(40 - r)}{5} \text{ milliseconds}$$

for the long floor. The distance to the side wall is assumed to be about 30 feet for the short floor and about 40 feet for the long floor.

#### Shielding Pool Walls

Assume that the floor of the tank is flat and a perfect reflector. Then at the walls, the effect of the bottom is allowed for by considering the blast as 800 pounds of TNT at floor level. Then from reference H.1, the pressure-time histories at the wall distances can be found directly. These pressures should then be doubled to account for reflection from the wall. Because of the free surface, there will be a rarefaction wave hitting the wall at a later time. The times at which the shock wave and rarefaction arrive are given by

$$\left. \begin{aligned} t_{\text{shock}} &= \frac{\sqrt{x^2 + 900}}{5} \text{ milliseconds} \\ t_{\text{rarefaction}} &= \frac{\sqrt{900 + (50 - x)^2}}{5} \text{ milliseconds} \end{aligned} \right\} \text{ Short side wall}$$

$$\left. \begin{aligned} t_{\text{shock}} &= \frac{\sqrt{x^2 + 1600}}{5} \text{ milliseconds} \\ t_{\text{rarefaction}} &= \frac{\sqrt{1600 + (50 - x)^2}}{5} \text{ milliseconds} \end{aligned} \right\} \text{ Long side wall}$$

x height on the side wall measured from the floor

## Remarks

The effects of the secondary pulses and gas bubble have been ignored in the hope that they will dissipate themselves. In any case, their effect should be small. The assumptions throughout of perfect reflection from the walls and floor are sufficiently conservative so as to allow a considerable margin for error in this respect.

The pressures computed as described above should be at least as accurate as the initial number of 400 pounds of TNT.

If the side wall is allowed to expand and leak, but not break, the containment tank wall 15 feet beyond this will feel no appreciable load due to the blast.

## FORCES DUE TO A HYDROGEN EXPLOSION

Experiments have been run at the NACA (ref. H.2) to determine the pressure-time histories in hydrogen explosions. A twenty-four inch diameter pipe closed at both ends was filled with hydrogen-oxygen mixtures and the mixture was then detonated. Side-on and face-on pressures were measured. Some of the runs were made with the pipe full of water spray. The water spray somewhat reduced the detonation pressures but did not prevent detonation. Figure H.3 shows the variation of face-on pressure with time for a typical run with water spray and with a stoichiometric mixture of hydrogen and oxygen. Mixtures of hydrogen and oxygen leaner than stoichiometric give somewhat lower pressures. In the NACA reactor the mixture will probably be below stoichiometric and the reaction will be between hydrogen and air rather than hydrogen and oxygen. The pressure-time history of figure H.3 should therefore be conservative as applied to the case of a hydrogen explosion in the NACA reactor.

## EQUILIBRIUM PRESSURE AFTER AN EXCURSION

The equilibrium pressure in the containment tank after an excursion was estimated in two different manners.

The value of 400 pounds for the TNT charge was chosen because its total energy was equivalent to about 820 megawatt seconds. The energy released by the reaction of the hydrogen evolved from the reaction of 50 percent of the metal in the fuel plates is about 800 megawatt-seconds. The sum of the two energies is 1620 megawatt-seconds.

The first method of estimating the equilibrium pressure assumed that the air in the containment tank was originally at 75° F and 50 percent relative humidity. For the equilibrium conditions after the excursion it

was assumed that this air was saturated with moisture, and that the enthalpy of the air had increased 1620 megawatt-seconds. The air pressure increased about 0.9 psi and the vapor pressure increased about 1.0 psi, making a total pressure rise of about 1.9 psi.

The second method used was to assume that all the energy released goes into generating saturated steam and that the steam compressed the air adiabatically and without mixing. The maximum pressure arrived at by this method of computation is coincidentally also about 1.9 psi. The steam would, of course, eventually mix with the air, some of it would condense out, and the final condition would correspond to the final condition of the first method.

The maximum pressure in the containment tank after an excursion has, therefore, been assumed to be about 2 psi.

#### REFERENCES

- H.1. Cole, R. H.: Underwater Explosions, Princeton University Press, 1948.
- H.2. Ordin, P. M.: Hydrogen-Oxygen Explosions in Exhaust Ducts, NACA report in preparation.



APPENDIX ISTRUCTURAL ANALYSIS

The philosophy of the containment design has been to make the structure inside the containment tank shield the containment tank as much as possible from the forces associated with a Borax-type excursion.

The containment tank and the structure inside it are shown in figures 2.12 and 2.13. The ability of this containment structure to resist the forces due to the 400 pound TNT explosion, the concurrent hydrogen-air explosion, and the resultant equilibrium pressure, will be considered below in the following order:

1. The reactor tank and adjacent concrete
2. The radial quadrant walls of the shielding pool
3. The shielding pool wall
4. The floor of the sub-pile room
5. The fillet between the sub-pile room walls and the floor of the shielding pool
6. The shielding pool floor
7. The shrapnel shield
8. The debris from the 400 pound TNT explosion
9. The hydrogen-air explosion
10. The resultant equilibrium pressure
11. The containment tank

The presentation will outline the types of loads considered on the various portions of the structure and the methods used to estimate the ability of the structure to resist these loads. Many of the assumptions used in the following analyses are necessarily approximate; all assumptions were selected with the aim of being conservative.

#### Reactor Tank and Adjacent Concrete

The pressures due to the 400 pound TNT explosion on the nine-foot diameter reactor tank and the two-foot thick concrete surrounding

the reactor tank sides are quite high (see fig. H.1(a)) and no attempt was made to design these structures to hold. It is accordingly assumed that the reactor tank and the two-foot thick concrete surrounding the reactor tank sides will fail immediately. To be completely conservative, no credit has been taken for the energy absorbed by this structure. Subsequent calculations concerning the effect of the blast on other structural members were carried out with no diminution in blast pressures due to the resistance of the reactor tank or the concrete surrounding the reactor tank sides.

### Radial Quadrant Walls of the Shielding Pool

As can be seen in figure 2.12(a), the reactor tank is not in the center of the shielding pool, and consequently, two of the radial quadrant walls are shorter than the remaining two. These two shorter walls, having less resistance to the forces being considered, will govern the design. The ends of these walls adjacent to the reactor tank were assumed to be subjected to the forces shown in figure H.1(a) for the side of the reactor tank (see sketch in fig. I.1). The distance  $h$ , in figure I.1, is the height above the floor of the center of gravity of the pressure forces on the end of the quadrant wall. The total integrated pressure force is shown as  $F$ . The moment  $Fh$  tends to rotate the wall about a neutral axis at point  $o$  in figure I.1, while the force  $F$  tends to shift the wall laterally. Steel reinforcing bars are placed in the wall vertically to resist rotation, and diagonally to resist lateral shift.

It will be noted in figure H.1(a) that peak pressures for the entire height of the wall are above the crushing strength of concrete. To induce local weakening of concrete adjacent to the tank, horizontal reinforcing steel will be formed and arranged as shown in section B-B of figure I.1. By this means it is believed that except for the initial shock wave of very brief duration, pressures exceeding the crushing strength of concrete would not be transmitted to the body of the wall.

We will first consider the resistance of the wall to rotation, and then the resistance of the wall to lateral drift.

Resistance against rotation. - The moment,  $M = Fh$ , produces a rotation of the quadrant wall about the neutral axis,  $o$ , shown in figure I.1. This tendency to rotate is resisted by the vertical steel bars and the concrete. The concrete and steel would be in compression at the base of the wall to the left of the neutral axis,  $o$ . The steel to the right of  $o$  would be in tension. The concrete is, of course, assumed to have no resistance in tension.

The amount of overturning of the quadrant wall can be computed from

$$\left[ \frac{1}{2}(M_n + M_{n-1}) - W_a - M_R \right] (t_n - t_{n-1}) = J_o(\dot{\theta}_n - \dot{\theta}_{n-1}) \quad (11)$$

where

$M$	applied moment due to the blast forces = $Fh$ (see fig. I.1)
$W$	weight of the wall
$a$	distance from center of gravity of wall to centroid of the compression area at the base of the wall
$M_R$	resisting moment due to the material of the wall
$t_n - t_{n-1}$	increment of time
$J_o$	polar moment of inertia of wall about neutral axis through o (see fig. I.1)
$\dot{\theta}$	derivative of the angle of rotation of the wall with respect to time

and the subscripts

$n$  value at time,  $t_n$

$n-1$  value of time,  $t_{n-1}$

The resisting moment of the material may be expressed

$$M_R = M_s + M'_s + M_c \quad (I2)$$

where

$M_s$  resisting moment due to the portion of the vertical steel bars which are placed in tension

$M'_s$  resisting moment due to the portion of the vertical steel bars which are placed in compression

$M_c$  resisting moment due to the concrete in compression

When the material is in the elastic range, the values of the individual resisting moments may be expressed

$$M_s = f_s \frac{A}{g} (x_1^2 + x_2^2 + x_3^2 + \dots) \quad (I3)$$

$$M'_s = \frac{n-1}{n} f_s \frac{A}{g} (y_1^2 + y_2^2 + y_3^2 + \dots) \quad (I4)$$

$$M_c = \frac{1}{3} \frac{f_s}{n} \frac{k^3 b}{g} \quad (I5)$$

where

- $f_s$  unit stress in tension bar at greatest distance from neutral axis, elastic range
- $A$  cross section area of one vertical steel bar
- $g$  distance from neutral axis to farthest tension bar
- $x$  distance from neutral axis to particular tension bar
- $n$  ratio of modulus of elasticity of steel to that of concrete
- $y$  distance from neutral axis to particular compression bar
- $k$  distance from neutral axis to farthest compression fiber of concrete
- $b$  wall thickness

When the material reaches the plastic range, the individual resisting moments are

$$M_s = f_{sp} N_s A \bar{x} \quad (I6)$$

$$M'_s = (n - 1) f_{cp} N'_s A \bar{y} \quad (I7)$$

$$M_c = \frac{1}{2} f_{cp} k^2 b \quad (I8)$$

where

- $f_{sp}$  unit stress in tension bar, plastic range
- $N_s$  number of vertical bars on the tension side
- $\bar{x}$  distance from centroid of steel tension forces to neutral axis
- $f_{cp}$  unit stress in concrete on compression side, plastic range
- $N'_s$  number of vertical bars on compression side
- $\bar{y}$  distance from centroid of steel compression forces to neutral axis

The neutral axis can be located, both in the elastic and the plastic range, by application of the principle that the summation of the vertical forces on the base of the wall is zero and the summation of the moments is zero.

Using equations (I1) through (I8), and a time increment in equation (I1) of one quarter millisecond, it was found that the quadrant wall would rotate 0.00074 radian which results in it lifting about 0.15 inch at the reactor end. The quadrant wall is, therefore, safe from the point of view of rotation.

Resistance to lateral drift. - Under influence of the blast forces (see fig. I.1) the quadrant wall, in addition to rotating, will be forced to shift laterally. This lateral movement is assumed to be resisted by the diagonal reinforcing bars and the inertia of the wall. The lateral drift can be computed from

$$\left[ \frac{1}{2} (F_n + F_{n-1}) - \frac{1}{2} (V_n + V_{n-1}) \right] (t_n - t_{n-1}) = m(v_n - v_{n-1}) \quad (I9)$$

where

F lateral blast force

V total shear value of all diagonal bars

m mass of wall

v velocity of wall

Substituting appropriate values in equation (I9) and using time increments of one quarter millisecond, the lateral shift was computed as 0.35 inch. The quadrant wall is, therefore, safe against lateral shift.

#### Shielding Pool Wall

As can be seen in figure 2.12 the reactor tank is not in the center of the shielding pool, and, consequently, the design of the shielding pool wall will be governed by the forces and impulses on the section of the wall nearest the reactor tank. The shortest distance between the center of the reactor tank and the shielding pool wall is 30 feet. Forces and impulses at a radius of 30 feet are shown in figures H.1(d) and H.2(c). In the following calculations, the shielding pool wall will be assumed to be a ring 30 feet in diameter.

The elongation of the reinforcing hoops in the shielding pool wall can be calculated from

$$\left[ \frac{1}{2} (P_n + P_{n-1}) - \frac{1}{2} (Q_n + Q_{n-1}) \right] (t_n - t_{n-1}) = \frac{m}{2\pi R} (v_n - v_{n-1}) \quad (I10)$$

where

P                      pressure on the wall

Q                      resistance of structural members expressed as an equivalent external pressure

$t_n - t_{n-1}$           increment of time

m                      mass of the wall

R                      radius of the wall

v                      radial velocity of the wall

and the subscripts

n                      value at time,  $t_n$

n-1                   value at time,  $t_{n-1}$

In the elastic range

$$Q = \frac{AE_s r}{R^2} \quad (I11)$$

In the plastic range

$$Q = \frac{f_{sp} A}{R} \quad (I12)$$

where

A                      cross sectional area of steel hoops

$E_s$                     modulus of elasticity of steel

r                      radial displacement of the wall

$f_{sp}$                    dynamic yield point of steel

Substituting appropriate values in equation (110) and using increments of time of one quarter millisecond, the elongation of the steel reinforcing hoops in the shielding pool wall was found to be about eight percent. The elongation to rupture of the material in the hoops is sixteen percent, and the shielding pool wall, though it might crack badly, would not fail in a gross sense. Because the shielding pool wall would hold, the containment tank would be almost unaffected by the blast forces transmitted laterally through the water of the shielding pool.

#### Floor of the Sub-pile Room

The sub-pile room beneath the reactor tank is shown in figure 2.13. Between the reactor tank and the sub-pile room is a section of concrete and lead. The lead is about one foot thick and the total concrete thickness about twenty inches. The shock wave in the water of the reactor tank due to the equivalent TNT explosion would be transmitted through this mass of concrete and lead. The peak pressure of the shock would be well above the crushing strength of the concrete and the shock wave in passing through the concrete-lead mass would crush the concrete, break the entire mass loose, and impart a velocity to it. When the shock reaches the concrete-air interface at the ceiling of the sub-pile room, a rarefaction wave is propagated back through the concrete and lead increasing the velocities of these materials. The final velocity imparted to the crushed concrete below the lead is greater than that imparted to the lead and the crushed concrete strikes the floor of the sub-pile room first transmitting a pressure wave to the concrete of the sub-pile room floor. A short time later, the lead strikes the crushed concrete layer which has just fallen and transmits a pressure wave through it to the concrete of the sub-pile room floor. The resistance of the concrete below the sub-pile room to these impacts will be considered.

When a strong, normal shock wave reaches the interface of two different materials, and both transmitted and reflected shock waves are propagated, the equations approximately relating the pressures and material velocities are

$$u_2 = \frac{2u_1}{1 + \frac{\rho_2 a_2}{\rho_1 a_1}} \quad (113)$$

$$P = \rho a u \quad (114)$$

where

- $\mu$  material velocity
- $\rho$  density
- $a$  speed of sound
- $P$  pressure

and the subscripts

- 1 the material in which the incident shock is propagating
- 2 the other material

In equation (I14), the quantities are all evaluated in the same material. The values used for  $\rho$  and  $a$  are listed below.

	$\rho$ (slugs/cu ft)	$a$ (ft/sec)
Water	2.05	4,500
Concrete	5.24	13,000
Lead	21.3	4,000
Crushed concrete (sand)	1.94	2,000

When the shock wave reaches the concrete-air interface at the ceiling of the sub-pile room, a rarefaction wave is propagated back through the concrete doubling its velocity.

Using equations (I13) and (I14), taking into account geometrical attenuation where appropriate, and also the doubling of the concrete velocity due to the rarefaction wave from the concrete-air interface at the sub-pile room ceiling, the initial velocity of the lead plug is found to be about 83 ft/sec, while the velocity of the crushed concrete below it would be about 140 ft/sec. The velocities when the lead and the crushed concrete strikes the floor, will be about 89 ft/sec and 143 ft/sec, respectively.

The crushed concrete will hit first, and then the lead plug will hit the crushed concrete layer which will transmit the shock to the floor. The equation approximately relating the material velocities when a falling body strikes a stationary one is

$$u_s = \frac{u_f}{1 + \frac{\rho_s a_s}{\rho_f a_f}} \quad (\text{I15})$$

where the symbols are the same as before, and the subscript  $f$  refers to the falling material, and the subscript  $s$  to the stationary material. Equation (I14) again relates pressure and material velocity in the material.

Equation (I15) governs the shock wave propagated in the concrete of the sub-pile room floor when it is hit by the falling crushed concrete. It also governs the shock wave propagated in the fallen crushed concrete layer when it is hit, a short time later, by the falling lead. Equation



(I13) still governs the transmission, from the crushed concrete to the floor, of the shock wave set up in the crushed concrete when it is struck by the lead.

Using equations (I13), (I14), and (I15), the resultant pressure on the floor of the sub-pile room was found to be about 3400 psi due to the impact of the crushed concrete, and a short time later about 4300 psi due to the impact of the lead. The geometrical attenuation factor from the bottom of the sub-pile room to the containment tank skin eight feet below can be estimated from an equation given by Morse (ref. I.1, p. 313) as about equal to 2. The maximum resultant pressure on the concrete just above the containment tank skin is about 2150 psi. The dynamic crushing strength of concrete is about 5000 - 6000 psi (ref. I.2). The floor of the sub-pile room would, therefore, not crush through to the skin of the containment tank.

The containment tank skin is backed by the limestone bedrock with all cracks in the limestone pressure grouted. Therefore, even if the concrete in the sub-pile room floor were crushed through to the containment tank skin, the metal skin would not move much and, being ductile, would not fail.

#### Fillet Between Sub-pile Room Walls and Shielding Pool Floor

The shielding pool floor beyond a radius of about 20 feet from the reactor vertical centerline is constant in thickness (see fig. 2.13). From this radial distance inward, the thickness of the shielding pool floor increases rapidly until the pool floor finally blends into the walls of the sub-pile room. For convenience, this mass of concrete of varying thickness will be referred to as the fillet.

The resistance of the fillet to the blast is best considered on an energy basis. The energy release from the 400 lb TNT explosion is about  $5.55 \times 10^8$  ft lbs. Most of this energy is degraded into waste heat by the time the shock wave reaches the surface of the reactor tank at the fillet location. Approximately 10 percent of the energy will remain in the form of kinetic energy and pressure energy (ref. I.3). Furthermore, the fillet subtends only about 27 percent of the  $4\pi$  solid angle around the reactor. The energy available to do work in the shock wave when it reaches the fillet is then about  $1.5 \times 10^7$  ft lbs.

Not all of this energy is transmitted to the fillet. A portion of the energy goes into the reflected wave in the water. The portion of the total energy transmitted to the concrete is given approximately by

$$\frac{E_c}{E_1} = \frac{\rho_w a_w}{\rho_c a_c} \left( \frac{2}{1 + \frac{\rho_w a_w}{\rho_c a_c}} \right)^2 \quad (I16)$$

where

$E_c$  energy transmitted to concrete

$E_1$  energy in incident shock wave

and the subscripts

c concrete

w water

The portion of the energy going into the concrete is about 40 percent. The energy going into the concrete of the fillet is, therefore, about  $6.0 \times 10^6$  ft lbs.

The volume of concrete in the fillet down to the skin of the containment tank is about 15,000 cu ft. The energy required to crush a cubic foot of concrete can be found by integrating the stress-strain curve up to the dynamic crushing stress. This gives a value of about 540 ft lbs/cu ft. The energy required to crush all the concrete would be about  $8.1 \times 10^6$  ft lbs. Therefore, the  $6.0 \times 10^6$  ft lbs of energy which is transmitted to the fillet would not crush the concrete through to the skin of the containment tank.

The containment tank skin is backed by the limestone bedrock with all cracks in the limestone pressure grouted. Therefore, even if the concrete in the fillet were crushed through to the containment tank skin, the metal skin would not move much and, being ductile, would not fail.

#### Shielding Pool Floor

The resistance to the blast of the shielding pool floor beyond the fillet is best considered on an energy basis in a similar manner to the fillet. The quadrant in which the shielding pool wall is thirty feet from the reactor centerline is the critical one. Approximately five percent of the energy in the shock wave will be available in the form of kinetic and pressure energy (ref. I.3). The section of the floor beyond the fillet in this quadrant subtends about 3.3 percent of the  $4\pi$  solid angle around the reactor. The portion of the energy transmitted to the concrete is again about forty percent. The total energy transmitted to the concrete is about  $3.6 \times 10^5$  ft lbs. The volume of concrete is about 2600 cu ft. The energy required to crush the concrete is about  $4.6 \times 10^5$  ft lbs. Therefore, the concrete will not be crushed through to the skin of the containment tank.

The containment tank skin is backed by the limestone bedrock with all cracks in the limestone pressure grouted. Therefore, even if the concrete in the shielding pool floor were crushed through to the containment tank skin, the metal skin would not move much and, being ductile, would not fail.

### Shrapnel Shield

The 400 lb TNT explosion will rupture the reactor tank top and the water and tank-top debris will move upward and be caught in the shrapnel shield. The amount the shrapnel shield would be lifted can be estimated from

$$x_n - x_{n-1} = \left( \frac{v_n + v_{n-1}}{2} \right) (t_n - t_{n-1}) \quad (I17)$$

$$m(v_n - v_{n-1}) = \left[ A \left( \frac{P_n + P_{n-1}}{2} \right) - W \right] (t_n - t_{n-1}) \quad (I18)$$

where

x	distance shrapnel shield is lifted
v	velocity of shrapnel shield
$t_n - t_{n-1}$	increment of time
m	mass of shrapnel shield
A	area of shrapnel shield subjected to pressure
P	pressure
W	weight of shrapnel shield

and the subscripts

n      value at time,  $t_n$

n-1    value at time,  $t_{n-1}$

Substituting appropriate values in equations (I17) and (I18) and using increments of time of one quarter millisecond, the shrapnel shield was found to rise about 15 feet. Since the distance from the shrapnel shield to the top of the dome of the containment tank is about 50 feet, the rise of the shrapnel shield will cause no damage to the containment tank.

## Debris

Most debris from the blast will be slowed down by the water in the shielding pool to the point where it can do no damage. Debris from the reactor-tank top will be caught by the shrapnel shield. Of the other debris, that in the shielding quadrant (assuming the quadrant happens to be dry) will have the highest velocities. The maximum velocity of this debris will be in the part of it which comes from the concrete and steel directly opposite the reactor. The maximum velocity of the concrete and steel can be estimated from equation (113) assuming that the steel, being relatively thin, takes on the velocity of the concrete (this assumption is conservative). The maximum velocity of the steel and concrete fragments is found to be about 160 ft/sec.

The largest piece of concrete likely to be dislodged would be about the size of a cube with side equal to the spacing of the reinforcing bars. This piece would weigh about 6 lbs. A similar sized piece of steel would weigh about 18 lbs. Suppose by chance a piece of debris of this type hit the containment tank without any diminution of velocity. The steel fragment is obviously critical. Using an equation given in reference I.4, the velocity required for an 18 lb fragment of steel to pierce the containment tank is about 1000 ft/sec. Even though the equation of reference I.4 was intended for velocities much greater than 160 ft/sec, the safety factor is sufficiently great to assure the safety of the containment tank.

## Hydrogen-Air Explosion

If the hydrogen-air explosion occurs at all, it is difficult to estimate where the explosion might occur or what portion of the hydrogen would detonate. The explosion would be most dangerous if it occurred right up against the containment tank. The pressure-time history of the explosion as would be felt by the containment tank for this condition is shown in figure H.3. The area of the containment tank which would be affected would depend on the area of contact between the containment tank and the hydrogen. Two areas of contact, typical of those which might occur, will be considered: a circular area two feet in diameter and a circular area twenty feet in diameter.

The case of a circular area, two feet in diameter, was investigated experimentally in reference H.3 for hydrogen-oxygen mixtures. The tests in reference H.3 were carried out in a long pipe two feet in diameter. One end of the pipe was sealed with mild steel sheet of different thicknesses. A series of experimental detonations in the two foot diameter pipe indicated that while a 16 gage (0.065 in.) sheet would fail, both 12 gage (0.109 in.) and 14 gage (0.083 in.) sheets would not rupture. The edge of the steel sheet was clamped and the maximum unit strain would be expected to be greater than the maximum unit strain for the comparable two foot circular area in the containment tank whose edge has a greater degree of freedom.

Since the thickness of the containment shell, 0.75 inch, is many times the thickness of the 12 and 14 gauge sheets which did not rupture in the experiments, it may be concluded that the containment tank would readily contain a hydrogen-air explosion with a two foot diameter area of contact.

The case of a twenty foot diameter area of contact was checked analytically. The elongation of the material can be approximately determined by integrating the equation

$$\frac{d^2h}{dt^2} = \frac{2g}{\rho H} P - \frac{8gsh}{\rho R^2} \quad (119)$$

where

- h height of the center of the contact area above the edge of the contact area
- t time
- g acceleration of gravity
- $\rho$  weight density of steel
- H containment shell thickness
- P pressure
- s dynamic yield point of steel
- R outer radius of the contact area

This equation assumes that the material is stressed in the plastic range throughout and that the mode shape is parabolic. The first term on the right represents the effect of the pressure load and the second term on the right represents the resistance of the material. Equation (119) was integrated numerically to determine the maximum  $h$  and this  $h$  was used to determine the maximum biaxial elongation. The maximum biaxial elongation was found to be about 4.8 percent and the containment tank would not fail.

#### Equilibrium Pressure

The equilibrium pressure in the containment tank has been estimated in appendix H to be about 2 psi. The hoop stress in a 100 foot diameter cylinder with a 3/4-inch thick wall due to an internal pressure of 2 psi

would be 1600 psi. The stress in a 100 foot diameter sphere would be 800 psi. The doors in the containment tank are all designed for a steady internal pressure of 5 psi with a safety factor of 3. The containment shell would, therefore, readily contain the equilibrium pressure.

### Containment Tank

The entire philosophy of the containment design has been to make the structure inside the containment tank shield the containment tank as much as possible from the forces associated with a Borax-type excursion. The preceding results will be reviewed with this in mind.

The equivalent 400 lbs TNT explosion would destroy the reactor tank and the concrete adjacent to its sides. The radial quadrant walls, though badly damaged, would not move appreciably as a unit. The concrete in the shielding pool wall might be badly cracked but the steel reinforcing hoops would hold and there would be no gross failure of the shielding pool wall. Because the shielding pool wall does not fail in a gross sense, the containment tank would be almost unaffected by the blast forces transmitted laterally through the water of the shielding pool.

The equivalent 400 lb TNT explosion would crush a good deal of the concrete in the sub-pile room floor, the shielding pool floor, and the fillet between them. However, though the concrete might crack clear through to the skin of the containment tank, the concrete will not crush clear through to the containment tank skin. Since the containment tank skin is backed by the limestone of the local terrain, which has been pressure grouted to fill all cracks and topped with a layer of concrete to eliminate rough spots, the skin of the containment tank below the floor levels will suffer little or no distortion.

The equivalent 400 lb TNT explosion would break the top of the reactor tank, but the tank-top debris and the water behind it will be trapped by the shrapnel shield. This entire mass will rise in the air perhaps as much as fifteen feet, but it will not reach the dome of the containment tank.

There are forces which the structure inside the containment tank could not shield from the containment tank. These are the forces due to some of the debris from the 400 lb TNT explosion, the forces due to the hydrogen-air explosion, and the forces due to the equilibrium pressure. It has been shown in the preceding sections that the debris from the 400 lb TNT explosion would not pierce the containment shell; the hydrogen-air explosion would not rupture it; the equilibrium pressure would be contained.

In conclusion it may be stated that, though the structure inside the containment tank would be severely damaged, the containment tank itself would survive, its integrity would be maintained, and it would contain all solids, liquids, and gases present inside of it.

## REFERENCES

- I.1. Morse, P. M.: Vibration and Sound. McGraw Hill.
- I.2. Watstein, D.: Properties of Concrete at High Rates of Loading.  
ASTM preprint 93b, 1955.
- I.3. Porzel, F. B.: Hydrodynamics of Strong Shocks. Armour Research  
Foundation, Report D917. To be published.
- I.4. Tolch, N. A., and Bushkovitch, A. V.: Penetration of Mild Steel by  
Bomb Fragments. BRL Report 568.





APPENDIX JRADIOLOGICAL HAZARDS FROM THE RELEASE OF FISSION PRODUCTS

The extreme importance of containing a Borax-type excursion which is of sufficient magnitude to melt the fuel plates is indicated by a study of the hazards associated with the release of fission products. The hazards resulting from the release of fission products to the ground diluted in water, or to the air as a gaseous cloud are discussed below, as are the hazards resulting if all the fission products are contained in the reactor containment tank.

## HAZARDS DUE TO RELEASE OF FISSION PRODUCTS DILUTED IN WATER

If the reactor containment tank were to fail and fission products diluted in water were released to the ground, the radioactive water would be contained by the surrounding dike (see section 3.5) and would leave the site only by seepage through the ground. This is the first case considered. The other case considered is the combination of conditions which could cause the maximum conceivable contamination of Lake Erie.

## Hazards Due to Ground Water Seepage

In the event of a major accident, it is possible that all of the nonvolatile fission products from the reactor core would become dissolved in all of the reactor water, i.e., both quadrant and cooling water. This water would seep into the ground and move as a unit toward Lake Erie, following the route indicated on figure D.1, appendix D, at the rate of 1-2 feet per day.

Assuming this concentration, direction, and rate, two potential hazard extremes exist. The first is represented by the active water in well number 8 (fig. D.1, appendix D) and the second by the radioactive water entering the City of Sandusky water supply via the Sandusky intake.

Since the flow rate at the water table level is 1-2 feet per day, the slug of water would take approximately 10 years to reach well number 8 and approximately 40 years to reach the lake. This establishes the criterion for choosing the fission products. That is, products with half lives long enough so that the activities built up will be large enough to be significant, but not too short that the activities will have decayed out completely.

Assuming 1000 grams burn up, the important fission products and their activities are:

Nuclide	Activity in curies after		
	10 Years	20 Years	40 Years
Cs <sup>137</sup> Ba <sup>137m</sup> }	440	360	236
Sm <sup>151</sup>	105	91	70
Sr <sup>90</sup> Y <sup>90</sup> }	490	380	237
Cd <sup>113m</sup>	No information as to yield		
Nb <sup>93m</sup>	1470	280	11
Sb <sup>125</sup> Te <sup>125m</sup> }	110	10	.07
Pm <sup>147</sup>	1000	5	-----

The specific activity at well number 8 is then  $0.49 \mu\text{c}/\text{cm}^3$ . The specific activity at the lake is then  $0.077 \mu\text{c}/\text{cm}^3$ .

Although these activities appear to be well above tolerance, i.e., above  $10^{-7} \mu\text{c}/\text{cm}^3$  (ref. J.1), two factors have been omitted in the calculation that tend to reduce the hazard. The first is that no ion-exchange has been assumed to take place in the ground. And second, is that this active water will be diluted considerably between the time it reaches the lake and the time it actually reaches the Sandusky water intake. The factors have been omitted because no information is available on either at present.

#### Maximum Conceivable Contamination of Lake Erie

##### by Surface Water Run-Off

A dire picture of Lake Erie contamination results if every possible adverse circumstance occurs simultaneously with an explosion. This may be shown by the following analysis which depends upon several crude assumptions:

1. That a catastrophic explosion of the reactor occurs toward the end of an operating cycle.

2. That the containment tank ruptures and releases a major portion of the fission products to the surrounding area.

3. That the ground is frozen and a heavy rain follows shortly after the explosion.

4. That the valves in the surrounding dike (see section 3.5) remain open and permit most of the released activity to reach Lake Erie.

All of these assumptions can be summarized by assuming that the maximum activity in the reactor is somehow released promptly to Lake Erie waters.

According to Glasstone (ref. J.2, p. 120) the maximum reactor activity is given roughly by the quantity

$$1.4P \left[ (\tau - T_0)^{-0.2} - \tau^{-0.2} \right] \text{ curies}$$

where

P      $60 \times 10^6$  watts

$T_0$    10 days

$\tau$      10 days + run-off time of perhaps 1 day

for the case considered here. The maximum activity released to Lake Erie is accordingly about  $32 \times 10^6$  curies.

Obviously this activity cannot be dispersed throughout Lake Erie very quickly and in the meantime considerable decay can occur. However, in the absence of water flow data for the lake, no detailed study of the eventual distribution of this activity seems worthwhile. The emergency 30 day contamination levels for potable water is about  $3 \times 10^{-2}$   $\mu\text{c/cc}$  (ref. J.3) or about  $8.5 \times 10^2$   $\mu\text{c/ft}^3$ . Neglecting decay, the released activity therefore would contaminate about  $4 \times 10^{10}$  cubic feet. Each square mile of water 70 feet deep embraces about  $2 \times 10^9$  cubic feet. Evidently about 20 square miles of lake water could be so contaminated, using an average lake depth of 70 feet. The waters of Sandusky Bay and its environs are much shallower, thereby extending the contaminated area several fold. According to reference J.4, ordinary city water treatment is unlikely to reduce this possible hazard to potable waters very appreciably.

If the intermediate level of 10 mc per  $10^6$  gallons of water (ref. J.5) is chosen as a permissible contamination limit, the results are much more adverse. This limit is about  $10^{-4}$  times the emergency limit. Since Lake Erie has an area of about  $10^4$  square miles, it follows that the released activity assumed above is more than sufficient to contaminate the whole lake by a factor of about 20.

There are a number of mitigating circumstances which could be assumed here which would make the situation somewhat more favorable, but not enough so to warrant detailed consideration here. It was this kind of treatment, crude though it is, that led to the provision of the dike around the reactor site as described in section 3.5.

#### HAZARDS DUE TO RELEASE OF FISSION PRODUCTS AS A GASEOUS CLOUD

In the event of a large-scale reactor disaster, if the containment tank is pierced, some fission products will be diffused in the atmosphere as a highly radioactive cloud.

Calculations have been made of the radiation dosages received by an individual at various distances directly downwind of the accident. The total dosage received would be the sum of the external radiation dosage of the cloud passing overhead; the surface deposition dosage due to "fall-out" or "rain-out;" and the inhalation dosage due to breathing contaminated air. In addition, there would be the additional hazard of ingesting radioactive food or water. The ingestion hazard is difficult to calculate accurately and its estimation has not been attempted here.

Dosages have been calculated for a severe inversion and a small lapse atmospheric diffusion conditions using the Sutton parameters and equations. Two types of reactor accidents have been assumed; a clean reactor power excursion of 150 MW-sec, and a saturated reactor steady power accident at 60 MW. Six cases were computed. The table below is a detailed listing of the cases.

Case number	Type of reactor accident	Atmospheric diffusion condition	Type of release	Height of release, h, meters	Stability parameter, n	Sutton diffusion coefficient, $C^2$	Mean wind velocity, $\frac{\text{meters}}{\text{sec}}$
I	Power excursion Clean reactor	Severe inversion	Instantaneous	15	0.5	0.008	1
II	Power excursion Clean reactor	Small lapse	Instantaneous	15	.25	.020	5
III	Steady power Saturated reactor	Severe inversion	Instantaneous	15	.5	.008	1
IV	Steady power Saturated reactor	Small lapse	Instantaneous	15	.25	.020	5
V	Steady power Saturated reactor	Severe inversion	Continuous over 24 hours	Ground level	.5	.008	1
VI	Steady power Saturated reactor	Small lapse	Continuous over 24 hours	Ground level	.25	.020	5

In all cases, 1 percent of the total fission product activity is assumed to be released into the atmosphere.

### Results

The radiation dosages received by an individual directly downwind of a radioactive airborne cloud are shown in figures J.1 to J.9.

The first three figures show the external dosages in roentgens, the next three show the deposition initial dosage rates in roentgens per hour for maximum rain-out and maximum fall-out, while the last three indicate the inhalation dosages in roentgens. An inversion and a lapse condition are plotted on each figure. The distance to the nearest residents, 1000 meters, and the distance to the center of Sandusky, 7200 meters, is indicated on each figure by arrows for easy reference.

It is apparent from the figures that, as might be expected, a power excursion starting with a clean reactor does not represent as great a radiation hazard to outlying areas as a steady power accident starting with a saturated reactor. This is due, of course, to the much larger amount of fission products present in the saturated reactor and the more rapid rate of decay of power excursion products compared to steady power products ( $t^{-1.21}$  as compared to  $t^{-0.21}$ , respectively). The worst dosages, for all cases except one, occur when steady power products are released instantaneously under severe inversion conditions. The worst inhalation dosage to the nearest residents occurs when steady power products are released over a twenty-four hour period under severe inversion conditions. In the table below are indicated the greatest possible dosages received by an individual at 3 distances of interest.

WORST POSSIBLE DOSAGES

	External, roentgens	Deposition, roentgens/hr	Inhalation, roentgens
Nearest residents, 1000 meters = 3200 ft	38	170	12,500
State Soldiers Home, 3000 meters = 9600 ft	17	18	2,700
Center of Sandusky, 7200 meters = 4.5 miles	7	3.5	690

## Computation of External Dosage

The gamma dosages were computed from the nomograms due to J. Z. Holland, listed as figures 8.1 and 8.3 in reference J.6. For the NACA reactor operating at a steady power of 60 MW for an infinite time, the total gamma activity contained in 1 percent of the fission products was

$$Q_\gamma = 5.46 \times 10^6 t^{-0.21} \text{ curies}$$

The source strength used in all calculations of hazards due to release of fission products in a gaseous cloud is taken from reference J.7. If this is released at a constant rate over 24 hours, this becomes

$$\frac{dQ_\gamma}{dt} = 0.0632 t^{-0.21} \text{ Kilocuries/sec}$$

This was multiplied by the dosage per Kilocurie as obtained from the nomogram and integrated over the total time of exposure of the observer.

$$D_Y(\text{roentgens}) = \int_{t=\frac{d}{\bar{u}}}^{t=\frac{d}{\bar{u}}+86,000} \frac{\text{Dosage/Kilocuries} \times \bar{u}_0 \times 0.0632 t^{-0.21}}{\bar{u}} dt$$

where  $\bar{u}_0$  is a mean wind velocity of 1 meter/sec,  $\bar{u}$  is the mean wind velocity in meters/sec, and  $d$  is the distance from the reactor to the observer in meters. The total integrated beta dosage in roentgens/MW-sec listed in reference J.6 was used to calculate the surface body beta dosage for the case of a clean reactor power excursion.

$$D_\beta(r/\text{MW-sec}) = \frac{4.8 \times 10^{-16} \times 0.64 E_r \bar{u}^{-0.21}}{6.8 \times 10^{-10} \pi C_z^2 d^{(2-n)+(1.21)}} \exp\left(\frac{-h^2}{C_z^2 d^{2-n}}\right)$$

where a release,  $E_r$ , of 150 MW-sec was assumed.

where

$h$  is the height of release in meters

$n$  is the dimensionless stability parameter

$C_z$  is the Sutton virtual diffusion coefficient in meters<sup>n/2</sup> in the z-direction

Since this is a surface body dosage, and in addition, takes no account of clothing shielding, an attempt was made to take these factors into account to give a total body dose.

Since the penetration of the betas into the body is small (0.15 in.), the ratio of tissue affected by beta radiation to total body tissue is calculated to be 1/10. This multiplied by an arbitrary clothing shielding factor of 0.5, yields a combined total body and clothing shielding factor of 0.050, which was applied to all the beta dosages.

The total integrated beta dosage, in roentgens, listed in reference J.6 was used for the saturated reactor steady power case.

$$D_\beta(\text{roentgens}) = \frac{0.64 Q_\beta}{\pi \bar{u} C_y C_z d^{2-n} 6.8 \times 10^{-10}} \exp\left(\frac{-h^2}{C_z^2 d^{2-n}}\right)$$

where  $C_y$  is the Sutton virtual diffusion coefficient in the y-direction. For infinite operation at 60 MW steady power

$$Q_\beta = 1.37 \times 10^{19} t^{-0.21} \text{ Mev/sec}$$

For a continuous release at a constant rate over 24 hours

$$\frac{dQ_{\beta}}{dt} = 1.585 \times 10^{12} t^{-0.21} \text{ Mev/sec}^2$$

and again we integrate over the exposure time of the observer to obtain a total dosage.

#### Computation of Surface Deposition Dosage

Using the conversion factor cited in reference J.6, that a uniformly contaminated slab of 1 curie/m<sup>2</sup> emitting gamma radiation of 0.7 Mev produces a dosage rate of 10r/hr at a point 1 meter above it, the source strengths were calculated and substituted into the deposition equations.

$$\omega_{\text{rain-max}} = \frac{Q}{e\pi^{\frac{1}{2}} C_y d^{2-(n/2)}}$$

$$\omega_{\text{dry-max}} = \frac{n}{2} \omega_{\text{rain-max}}$$

where  $Q$  is source strength in curies or curies/second and  $\omega$  is ground concentration in curies/m<sup>2</sup> or curies/meters<sup>2</sup> sec. In this manner the gamma deposition dosage rates were calculated for both maximum rain-out and maximum fall-out.

For the beta radiation, an attenuation of 0.325 Mev/meter in air was assumed. The average beta energy upon arrival at the body surface was estimated to be 0.25 Mev. Correcting for total body dosage, clothing shielding, and geometry, it is estimated that a surface uniformly contaminated with 1 curie/m<sup>2</sup> of fission product betas would produce a dosage rate of 25 mr/hr for a human being assumed to be entirely concentrated at a point 1 meter above the surface.

#### Computation of Inhalation Dosage

An observer breathing in a radioactive cloud as it passes by will receive a dosage due to the entry of radioactivity into the respiratory tract. A rough rule taken from reference J.6, which has been used here, is that 10 curie sec/m<sup>3</sup> of mixed gamma and beta fission product activity would produce an internal dosage of 25 roentgens. The Total Integrated Dosage formula (ref. J.6) is used to compute the number of curie sec/m<sup>3</sup> that the observer is exposed to.



$$T.I.D. = \frac{2Q}{\pi C^2 \bar{u} d^{2-n}} \exp\left(\frac{-h^2}{C^2 d^{2-n}}\right)$$

where  $C$  is the Sutton generalized diffusion coefficient assuming isotropic turbulence. The source  $Q$  in curies is  $Q_\gamma + Q_\beta$  for each particular case and type of release. The source strength and method of integration over time for a continuous source is listed and described previously.

#### HAZARDS IF ALL THE FISSION PRODUCTS ARE CONTAINED

An accident resulting in the release of a large amount of fission products would constitute a serious hazard even if it were contained in the reactor containment tank. The fission products would be present both in the quadrant water and in the air in the containment tank. This would result in a hazard to individuals both inside and outside the building.

The basic assumption made for the evaluation of this hazard is that the integrity of the containment shell is not violated. With this assumption in mind, two cases will be considered. Case I involves the hazards due to the gamma radiation from gaseous fission products within the shell. Case II involves hazards due to gamma radiation from nonvolatile fission products dissolved in the quadrant water.

Case I: Hazards due to gamma radiation from gaseous fission products. The assumptions for this case are:

1. The containment shell is a cylinder of volume and diameter equal to that of the actual shell.

2. The fission gases which are important are:

Br <sup>84</sup>	Kr <sup>85</sup>	I <sup>131</sup>	Xe <sup>135</sup>
Br <sup>87</sup>	Kr <sup>87</sup>	I <sup>132</sup>	
	Kr <sup>88</sup>	I <sup>133</sup>	
		I <sup>134</sup>	
		I <sup>135</sup>	
		I <sup>136</sup>	

The criteria for these choices are that only gamma emitters are considered, that no isotopes of gamma energy less than 0.1 mev are considered, and that isotopes with extremely small yields are neglected.

3. The fission products are at equilibrium values. These were obtained from Clark (ref. J.8) for 1000 hours of reactor operation.

## 4. Instantaneous uniform dispersion of the gases in the shell.

The gamma flux at a distance "a" from the edge of a cylinder due to a volume gamma source within the cylinder, is given by Moteff (ref. J.9) as

$$\phi(E) = \frac{BS(E)_v C^2}{2(a+z)} \int_0^\theta e^{-(\mu_a z + \mu_1 t_1 + \mu_2 t_2) \sec \theta} d\theta$$

where

$\phi(E)$	gamma flux, mev/cm <sup>2</sup> sec watt
B	buildup factor
$S(E)_v$	volume source, mev/cm <sup>3</sup> sec watt
C	radius of the cylinder, cm
a	distance from the edge of the cylinder to the detector, cm
z	self shielding factor, cm
$\mu_a = \mu_2$	linear absorption coefficient for air, cm <sup>-1</sup>
$\mu_1$	linear absorption coefficient for steel, cm <sup>-1</sup>
$t_1$	thickness of steel, cm
$t_2$	a, cm
$\theta$	arctan [height of cyl/2 (a + z)]

The dose is then computed from this flux by means of tables given by Moteff (ref. J.9).

The results of this calculation are plotted on two graphs. Figure J.10 shows the dose rate as a function of distance from the edge of the containment tank at various decay times. Figure J.11 shows the integrated dose as a function of time for various radial distances.

Case II: Hazards due to gamma radiation from fission products in the quadrant water. The assumptions for this case are:

1. All of the fission products which are not gaseous are dissolved in the water. This is approximately 80 percent of all of the fission products.

2. All gaseous products have been removed from the shell.

3. The reactor has been operating for 1000 hours. The activity values as a function of decay time were obtained from Moteff (ref. J.9) and from Rockwell (ref. J.11) using a 6-group energy distribution.

Dose rates were calculated at three positions in the reactor building (a) 1 meter above the center of the pool, (b) just outside the shell 1 meter above the floor, and (c) in the control room. Dose rates are also obtained outside the reactor building as a function of radial distance from the reactor.

For the three positions inside the reactor building, the surface of the water is assumed to be an isotropic disc source of gamma radiation of strength.

$$S(E)_A = \frac{S(E)_v}{2\mu_w}$$

The gamma flux is given at:

Position (a) by

$$\phi(E) = S(E)_A \left[ E_i(\mu_A h) - E_i(\mu_A \sqrt{h^2 + c^2}) \right] \quad (\text{ref. J.10})$$

Position (b) by

$$\phi(E) = \int_A \frac{S(E)_A e^{-\mu_s \bar{t}}}{4\pi\rho_b^2} dA$$

and

Position (c) by

$$\phi(E) = \int_A \frac{S(E)_A e^{-(\mu_s \bar{t} + \mu_A t_A)}}{4\pi\rho_c^2} dA$$

where

$\phi(E)$	gamma flux, mev/cm <sup>2</sup> sec megawatt
$S(E)_A$	area source strength, mev/cm <sup>2</sup> sec megawatt
$S(E)_V$	volume source strength, mev/cm <sup>3</sup> sec megawatt
$\mu_w$	Compton coefficient for water, cm <sup>-1</sup>
$\mu_a$	Compton coefficient for air, cm <sup>-1</sup>
$\mu_s$	linear absorption coefficient for steel, cm <sup>-1</sup>
$\bar{t}$	average thickness of steel, cm
$t_A$	average thickness of air, cm
$h$	height above the water, cm
$\rho_b$	distance from dA to position (b)
$\rho_c$	distance from dA to position (c)
$E_i(x)$	$\int_x^{\infty} \frac{e^{-y}}{y} dy$

For the dose rate outside the reactor building as a function of radial distance, the source was assumed to be a point source with single air scattering followed by exponential attenuation. The resulting dose rates were plotted and faired into the value of the dose rate just outside the reactor shell (position (b)) as calculated above.

The results of these dose rate calculations for fission products released and contained in the quadrant water are shown in three figures. Figure J.12 shows the dose rate as a function of time for positions (a), (b), and (c). Figure J.13 shows the dose rate as a function of radial distance for various decay times. Figure J.14 shows the integrated dose as a function of time for various radial distances.

Figure J.15 shows the sum of the integrated doses due to both the gaseous and nongaseous fission products as a function of time.

The results in all the figures for both gaseous and nongaseous fission products have been shown "per megawatt," that is, for fission products resulting from 1000 hours of operation at one megawatt. These fission products could originate either in the core or in an experiment. Therefore, in order to evaluate the hazard from an accident, whether to

the core or to an experiment, one needs only to multiply the dose rate found on the proper graph by the operating power in megawatts of the fuel involved.

Dose rates and integrated doses for significant locations and times, and for the gaseous and nongaseous fission products resulting from 1000 hours of operation at sixty megawatts are tabulated below.

Time, days after release of fission products	Just outside the containment tank		Nearest point of NACA fence - 920 ft (see fig. J.16)		Nearest point of Ordnance Works fence - 3000 ft (see fig. J.16)	
	Dose rate, r/hr	Integrated dose from time zero, r	Dose rate, r/hr	Integrated dose from time zero, r	Dose rate, r/hr	Inte- grated dose from time zero, r
0	39,000	-----	35	---	0.18	-----
1/4	8,600	200,000	6.9	50	.027	0.060
1	3,700	450,000	4.0	140	.011	.160
7	1,700	1,200,000	.91	410	.0013	.630
14	840	1,300,000	.34	470	.00045	.930
25	270	1,500,000	.10	550	.00011	1.080

The following conclusions may be drawn from the above tabulation concerning the effects of the contained release of the fission products resulting from 1000 hours of operation at sixty megawatts.

In view of the extremely high initial dose rate just outside the containment tank, it is doubtful that anyone in the reactor building near the containment tank would survive unless they happen to be shielded. Other personnel on the site further removed from the containment tank would have to be evacuated as rapidly as possible.

The dose rates at the nearest point of the NACA fence are high and certain portions of Plum Brook Ordnance Works would have to be blocked off. The portions closest to the site would have to be blocked off for a period in excess of twenty-five days. Calculations for longer times indicate that the period will not exceed ninety days. There would be ample time available to warn Ordnance Works personnel who happen to be in the vicinity of the site since the integrated dose in the first six hours is 50 r. Also, as may be seen from figure J.16, the sections of the Ordnance Works which would have to be blocked off would not seriously hamper the operation of the works.

The dose rate at the nearest point of the Ordnance Works fence, which represents the closest approach that the general public can make to the

reactor, is not too high. The integrated dose which would be picked up at this point in the first week (168 hours) is about 630 mr which is only about twice the allowable continuous exposure dose of 300 mr/week. The integrated dose for the second week (168 hours) is down to about 300 mr.

#### REFERENCES

- J.1. National Bureau of Standards: Maximum Permissible Amounts of Radioisotopes in the Human Body and Maximum Permissible Concentration in Air and Water. Handbook 52.
- J.2. Glasstone: Principles of Nuclear Reactor Engineering.
- J.3. U.S. Department of Health, Education, and Welfare: Handbook of Radiological Health, Nov. 1954, p. 135.
- J.4. Morton, R. J., and Straub, Conrad P.: Removal of Radionuclides from Water by Water-Treatment Processes. Preprint 172 of American Water Works Association Presented at the Nuclear Science and Engineering Congress in Cleveland, Ohio, Dec. 12-13, 1955.
- J.5. Federal Register for July 16, 1955, p. 5101.
- J.6. U.S. Department of Commerce, Weather Bureau: Meteorology and Atomic Energy, July, 1955.
- J.7. Fitzgerald, J. J., and Chappell, D. G.: Graphic Aids to Estimate Nuclear Radiation Hazards. KAPL-1178 (unclassified), August 30, 1954.
- J.8. Clark, F. H.: Decay of Fission Product Gammas. NDA-27-39, Nuclear Development Associates, Inc., White Plains, New York, Dec. 30, 1954.
- J.9. Moteff, John: Miscellaneous Data for Shielding Calculations. Apex-176, Aircraft Nuclear Propulsion Department, Atomic Products Division, General Electric Company, Cincinnati, Ohio, Dec. 1, 1954.
- J.10. Foderaro, A., and Obenshain, F.: Fluxes from Regular Geometric Sources, WAPD-TN-508.
- J.11. Rockwell, T.: Reactor Shielding Design Manual TID-7004.

APPENDIX KEMERGENCY PROCEDURES IN EVENT OF SERIOUS FISSION PRODUCT RELEASE

E-102 The discussion of emergency procedures in the event of serious fission product release is divided into two parts: the emergency procedures with respect to the area open to the public surrounding the reactor site, and the emergency procedures with respect to the reactor site and Plum Brook Ordnance Works. These are of a preliminary nature only. More time and study are needed to provide a detailed comprehensive plan.

## THE AREA OPEN TO THE PUBLIC

The probability of an accident which can endanger a great many people away from the reactor site is believed to be low. However, the consequences of some conceivable accidents, should the containment tank fail, can be very serious. This means that some thought should be given to planning for such a disaster. This planning is worthless if the system is impractical to maintain over long periods of time because of (1) waning interest among those responsible, (2) personnel changes (both at the reactor facility and among public officials in nearby communities), and (3) the common human tendency to become less aware of a problem the longer people live with it. The long term practicality is most important. Someone has said that the safest reactor is one that has just started operating.

Any extensive disaster planning is likely to involve the general public. For this reason all disaster planning probably should include local public officials.

There is another aspect of disaster planning which is also difficult to assess, namely, public opinion. Public reaction could easily become one of unreasoning fear and objection to having a reactor anywhere near them, as soon as the subject of disaster planning is presented.

Complete dependence upon the reactor staff for executing a disaster plan has much to commend it. Long term maintenance of the plan would be easier to control. Less hazardous accidents can be handled effectively by reactor personnel. There is one major weakness, however. Such planning assumes a substantially intact staff which remains organized following a major explosion. While a major accident might incapacitate a large majority of the staff at the reactor site, the guardhouse, 920 feet away, and an administration area 5000 feet away where representatives of the Health Physics Section will be stationed, will serve as points from which effective action could be taken immediately.

As explained in appendix J, the chief immediate hazard to neighboring communities which accompanies a catastrophic reactor explosion which ruptures the containment tank is the radioactive cloud which drifts away from the site. This cloud can be very dangerous under certain atmospheric conditions even as far away as Sandusky. Under more usual atmospheric conditions and wind directions, the cloud would be less dangerous and would not pass over Sandusky at all. Moreover, the cloud is unlikely to carry any large fraction of the fission products present in the reactor at the time of the accident. Under the worst possible conditions it might be better to attempt the evacuation of communities lying along the path of the cloud. To do so effectively requires very specific instructions to the populace within a very short interval, either day or night. Carefully designed evacuation plans have to be worked out beforehand and the proper one announced when needed. There is always the possibility of mixup and subsequent confusion which might be worse than no plan at all. This approach requires very swift evacuation to be effective.

The best plan appears to be for everyone to stay indoors for a number of hours at least. The heavier the fall-out or rain-out, the longer the severe hazard period in a given locality. This approach may result in excessive radiation dosages within buildings under very special circumstances, but for the average case is probably adequate and certainly more practical to achieve compliance.

Sandusky and the other communities in the area have no civil defense organization of record. Any off-site assistance in warning to the populace, therefore, must come primarily from the local and state police with some help from local radio stations. Disaster planning thus far is limited, and probably will continue to be limited to cooperative arrangements between the laboratory staff and these police organizations.

In case a catastrophic accident does occur, some mechanism for informing the public will be necessary if there is danger to specific communities. Reliance on radio instruction is likely to be very ineffective, particularly between 10 P.M. and morning. Some more positive warning system is necessary to supplement radio instructions.

The whole question about when and how to warn the public is fraught with many uncertainties. The advice of the AEC Safeguards Committee as regards a reasonable disaster coverage would be very helpful. Even very limited provisions for a disaster can consume a fair amount of effort and expense if the warning system is to have any hope of being usable when needed, perhaps many years in the future.

#### THE REACTOR SITE AND PLUM BROOK ORDNANCE WORKS

Disaster planning for the reactor site can be somewhat more realistic, inasmuch as at least a portion of the staff will remain which can assume



responsibility and provide the necessary effort. Here again, detailed planning must await further study in terms of work being done, the safety and monitoring equipment available, and better information about the personnel available and their training.

According to appendix J, an explosion which is contained by the shell provided for the purpose is also a very serious radiation hazard, particularly to those working at the site. For example, the following maximum initial dosage rates have been estimated for a contained explosion:

<u>Distance</u>	<u>Dosage rate</u>
50'	4800 r/hr
100'	1900 r/hr (includes most of site personnel neglecting shielding by buildings)
920'	35 r/hr (applies to NACA gate guard and nearest non-site workers)
3000'	180 mr/hr

These data indicate that some reliance for emergency service can be placed upon the gate guard and the Health Physics representative. These personnel can warn off-shift personnel and notify Ordnance Works officials. Those at the site may also be able to help in this respect because radiation damage effects will not be evident immediately after an explosion. It must be borne in mind that some of them may be sufficiently shielded that a lethal dose is unlikely. All site personnel must be instructed to proceed promptly to the best locations in this respect.

Certain selected personnel can be provided with radiation instruments to be kept at home in anticipation of serious accidents. The same is true of the gate house and the administration area. By the use of such instruments, these people can approach hazard areas with discretion and thereby avoid excessive exposures to themselves. Briefly, several teams can be organized within the various shifts with detailed instructions as to what they should and can do in an emergency. They would be given responsibility for rendering all possible aid to site personnel and for evacuating surrounding inhabitants as prevailing conditions dictate. The composition and leadership of these teams would be based in part upon location of homes of members so as to insure having at least one team intact in time of need.

The Health Physics people would provide the leadership for executing on-site disaster operations. They would be assisted by other groups arranged in teams composed of people who are least likely to be injured or irradiated by an accident. The facility should be provided with a loud speaker system, for emergency use only which can be operated from several points, one of which includes the Health Physics Office at the site. It would also help to have all radiation monitoring systems give a limit

warning in this same office and in the administration area. These Health Physics offices at the site should have a permanently connected off-site telephone provided with underground leads for a reasonable distance.

As presently conceived, on-site disaster operations planning will include a detailed study of what can happen, with some decisions as to what immediate steps can be taken. This is particularly desirable for each type of fueled experiment. With a properly designed monitoring system it should be easy to visualize what kind of accident has happened and proceed with the proper control measures. These include warnings as needed to on-site and off-site people, a check on automatic shutdown operations (and, if necessary, supplementing these), evaluating the hazard level at various check points, and organizing such rescue or contamination control measures as are indicated.

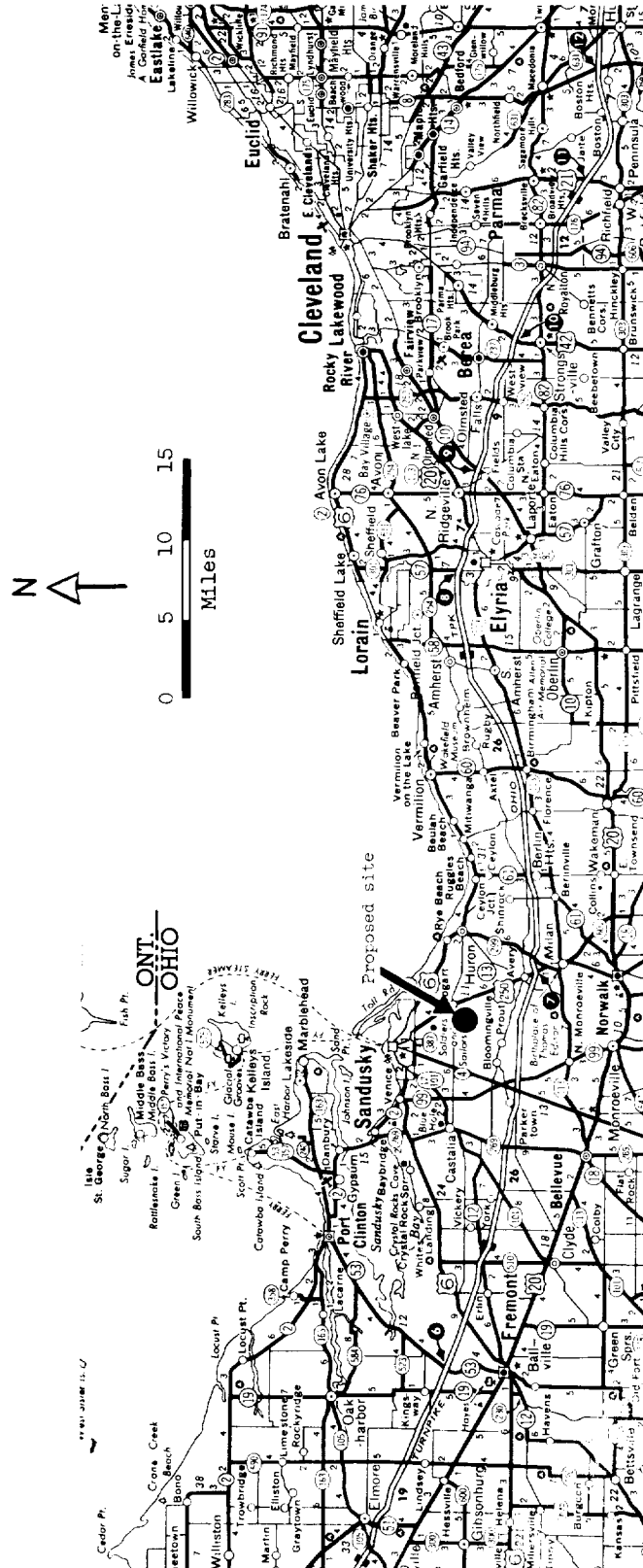


Figure 2.1 - Map showing location of site relative to Cleveland and Sandusky.

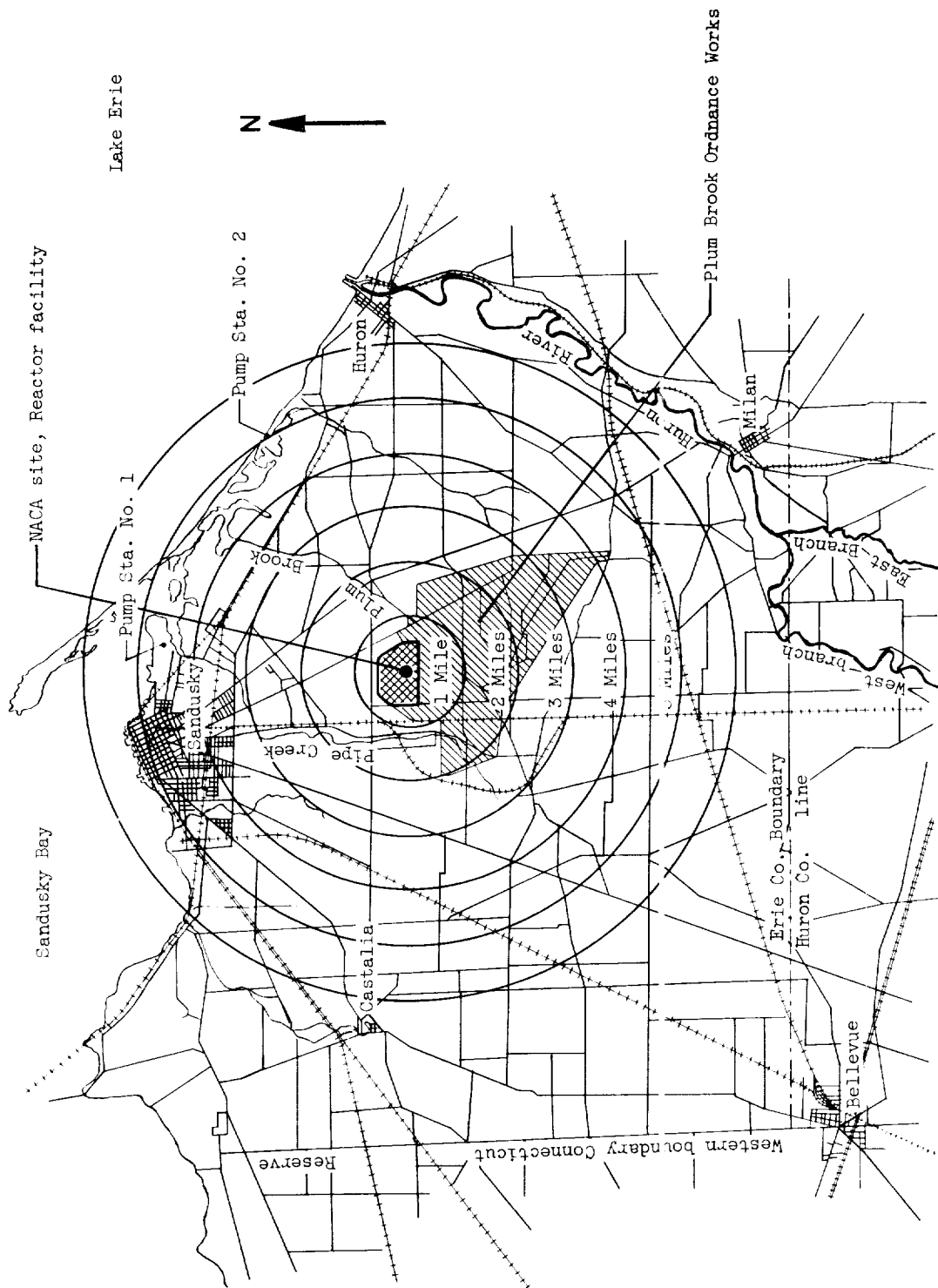


Figure 2.2 - Map showing location of site relative to Sandusky.

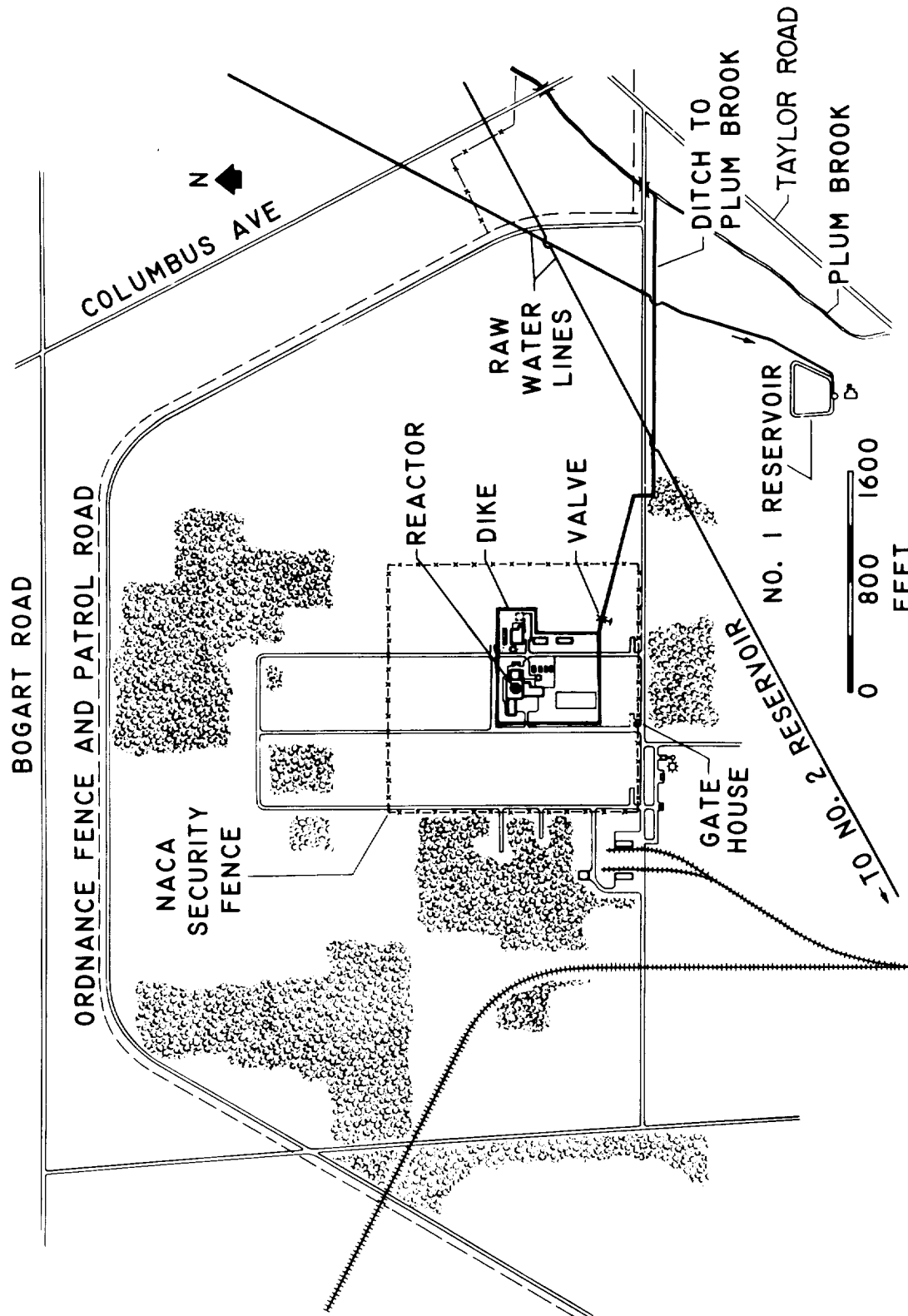


Figure 2.3 - Reactor facility on NACA site.

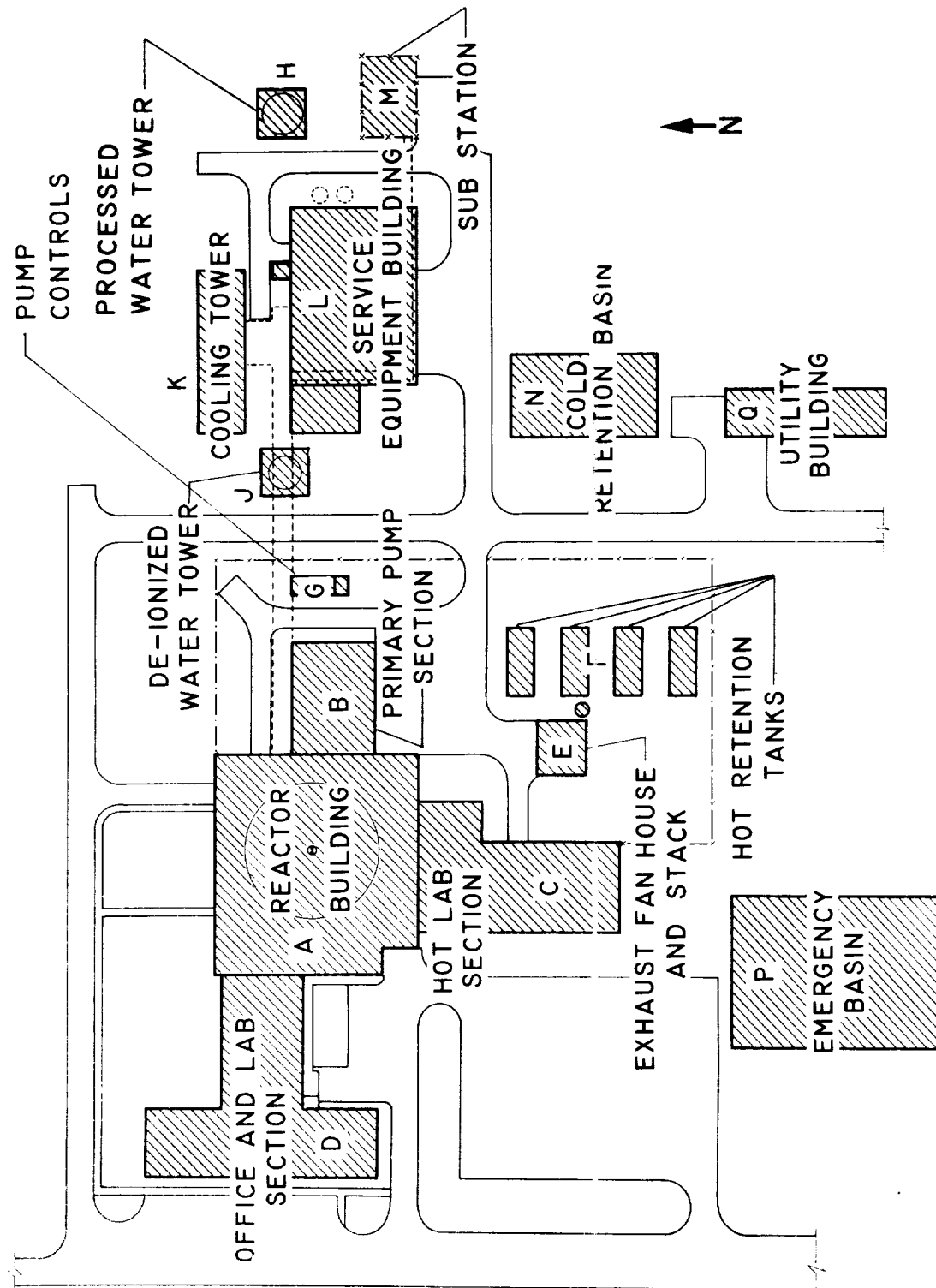


Figure 2.4. - Plot plan of reactor facility.

C-42503

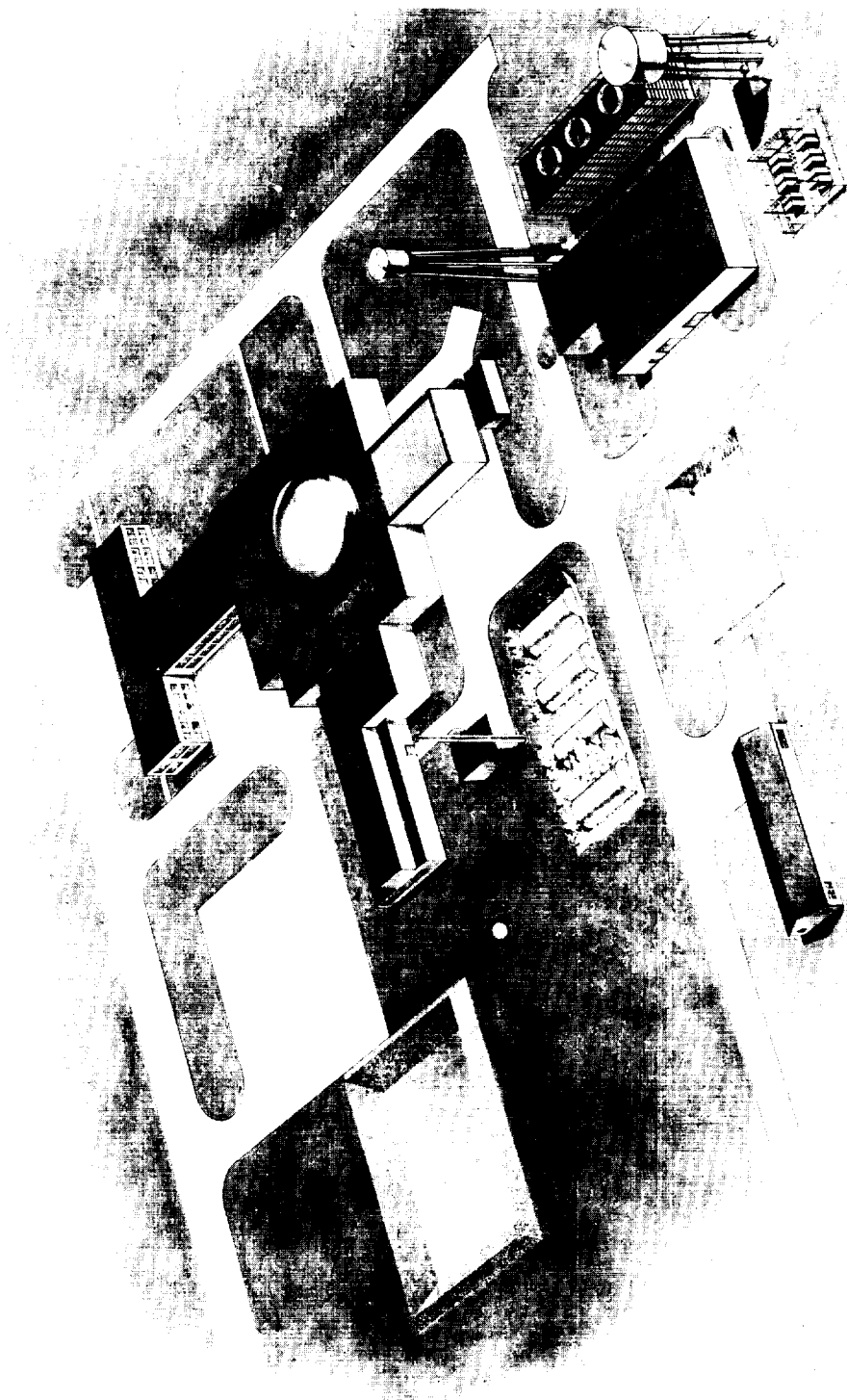


Figure 2.5 - Perspective drawing of reactor facility.

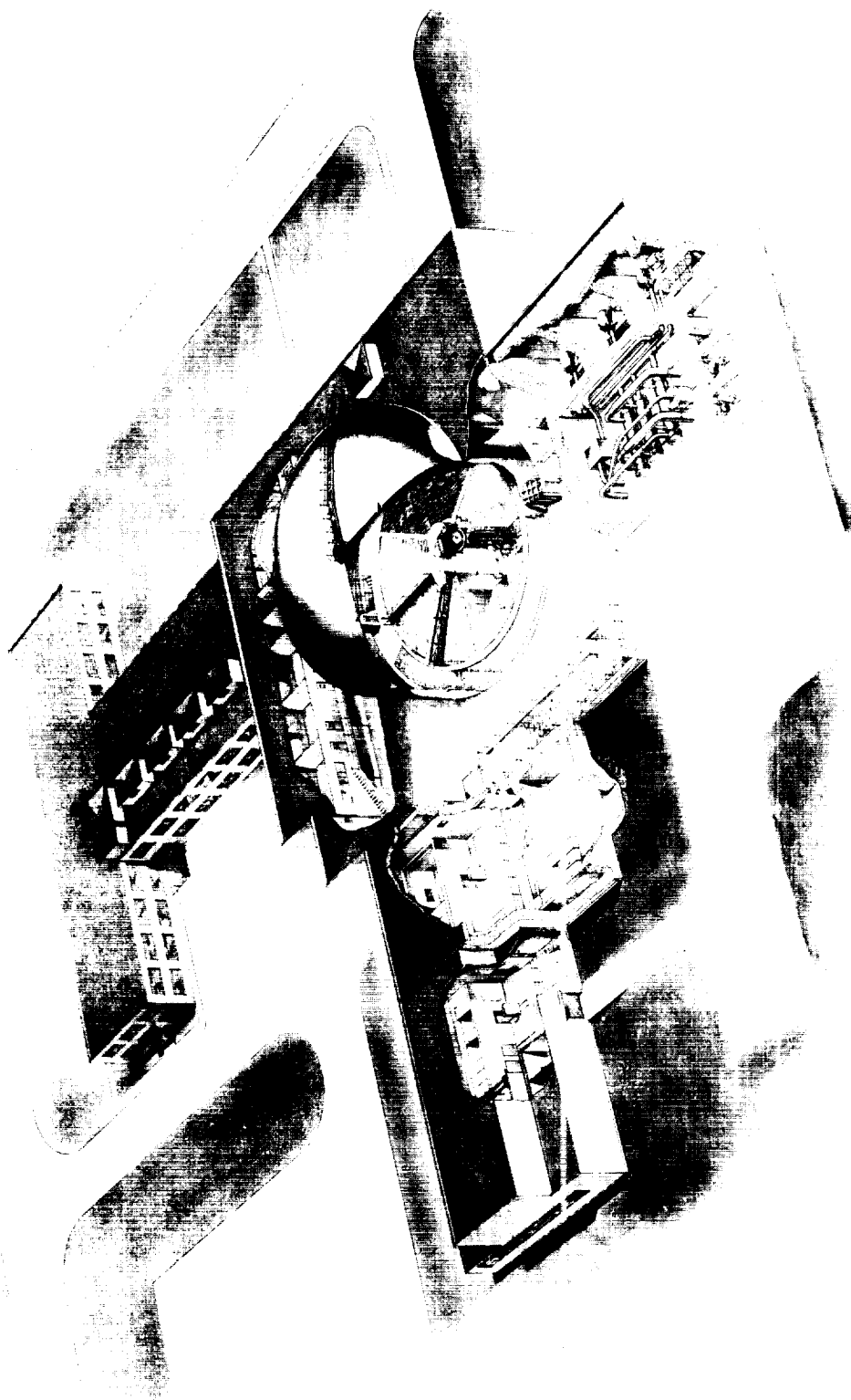


Figure 2.6 - Artists conception of reactor building.



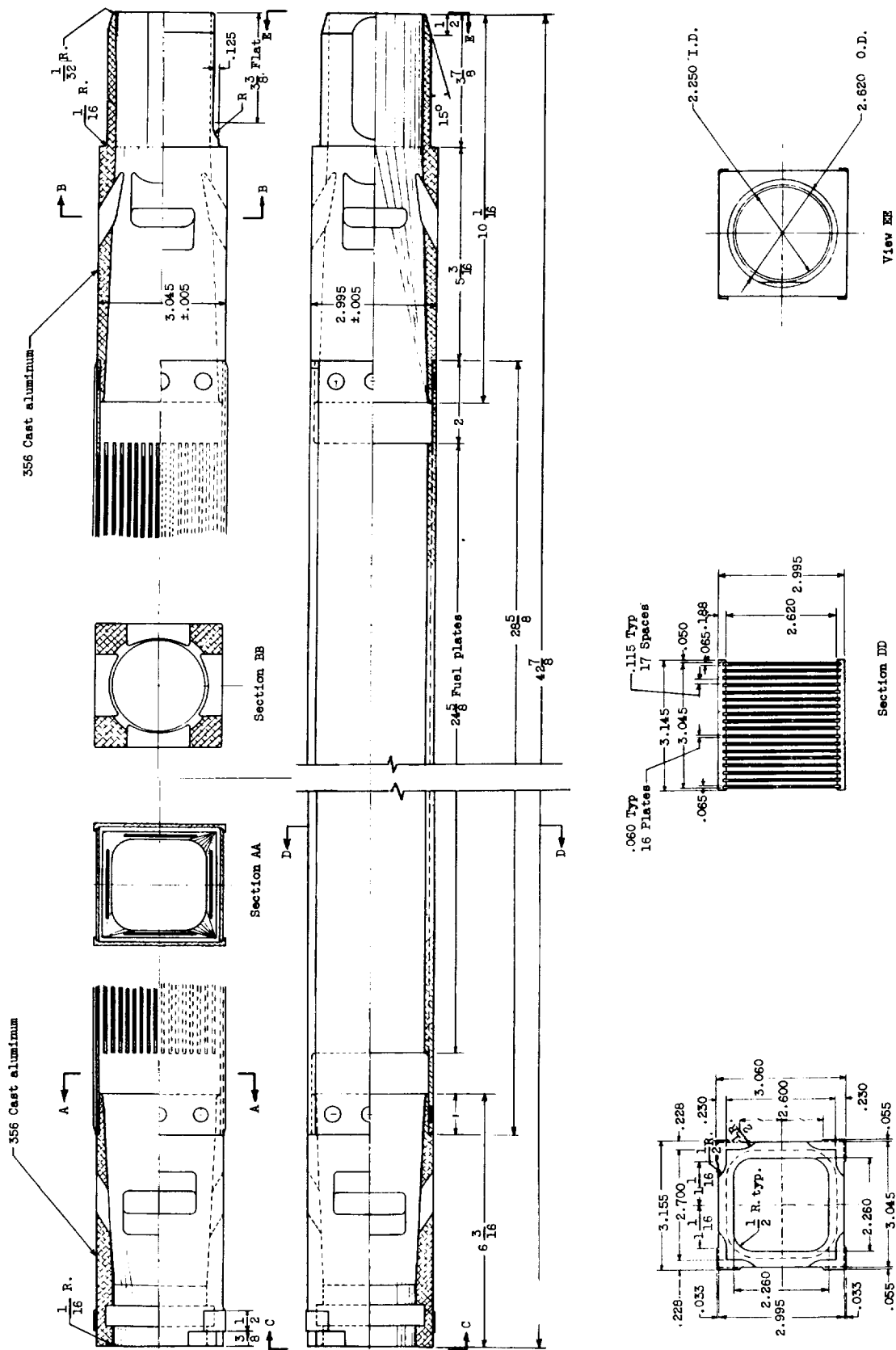
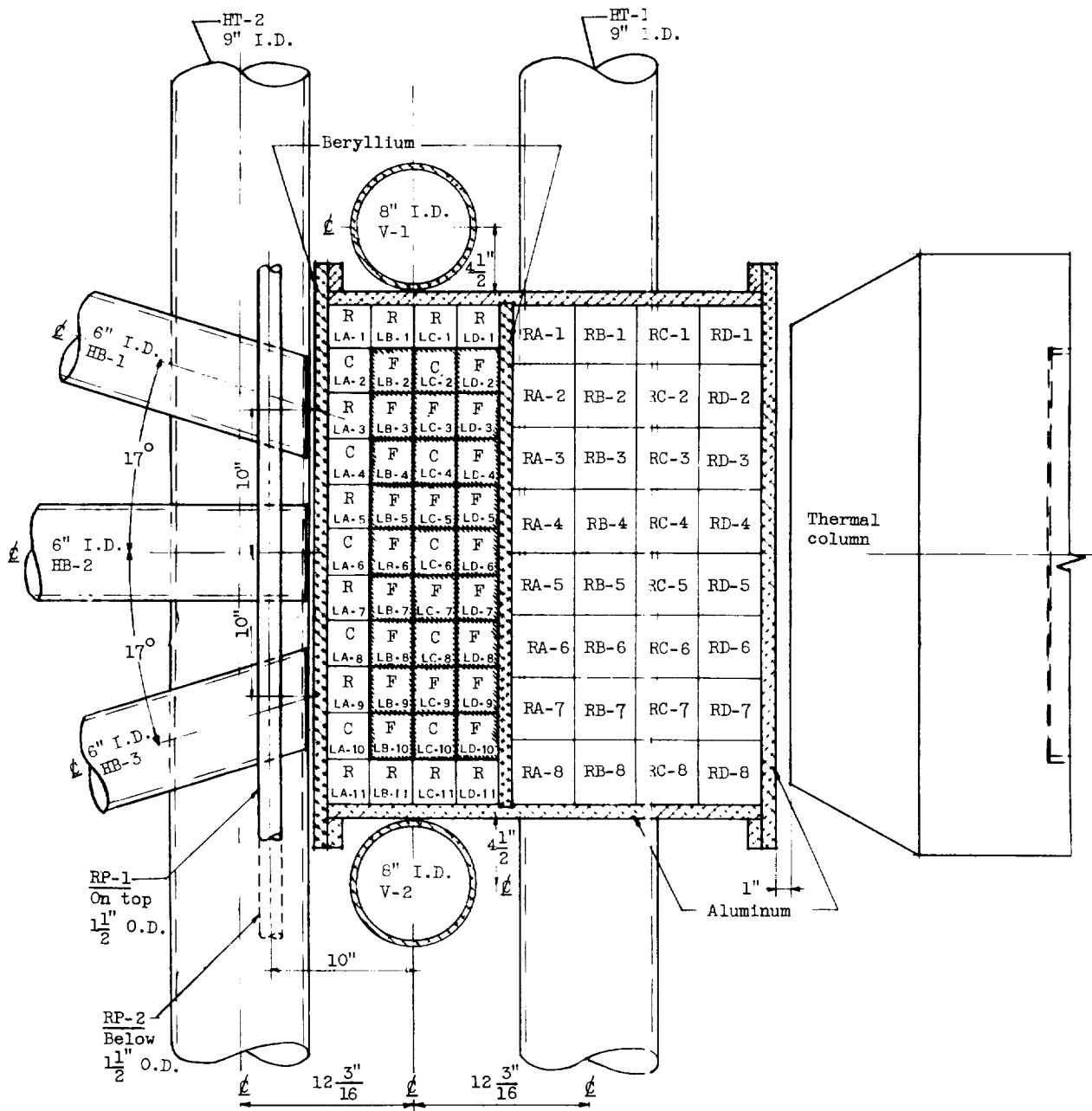


Figure 2.7 - Fuel element.

N ←



(a) Horizontal section

Figure 2.8 - Reactor core.

E-102

U2-52 back

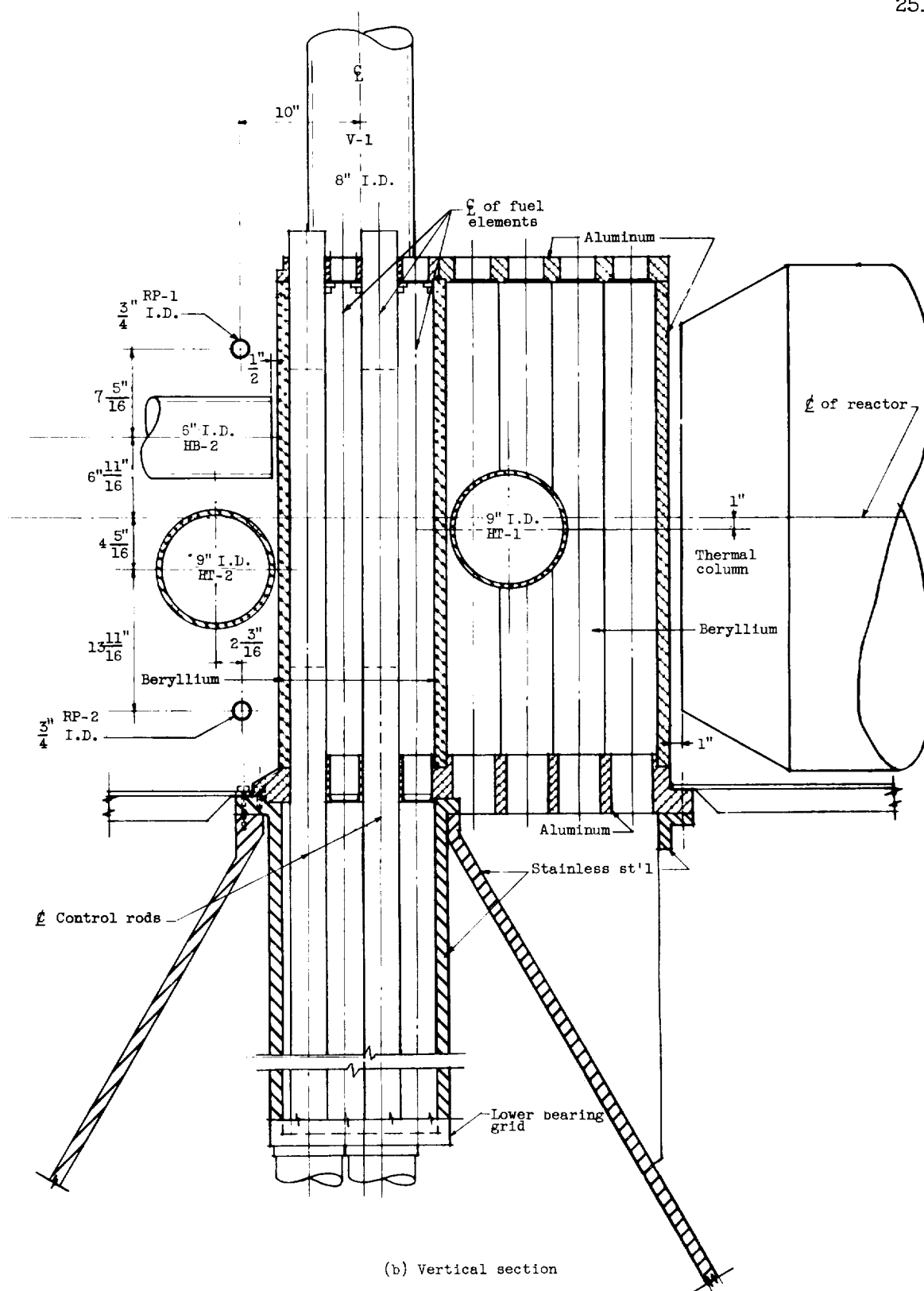
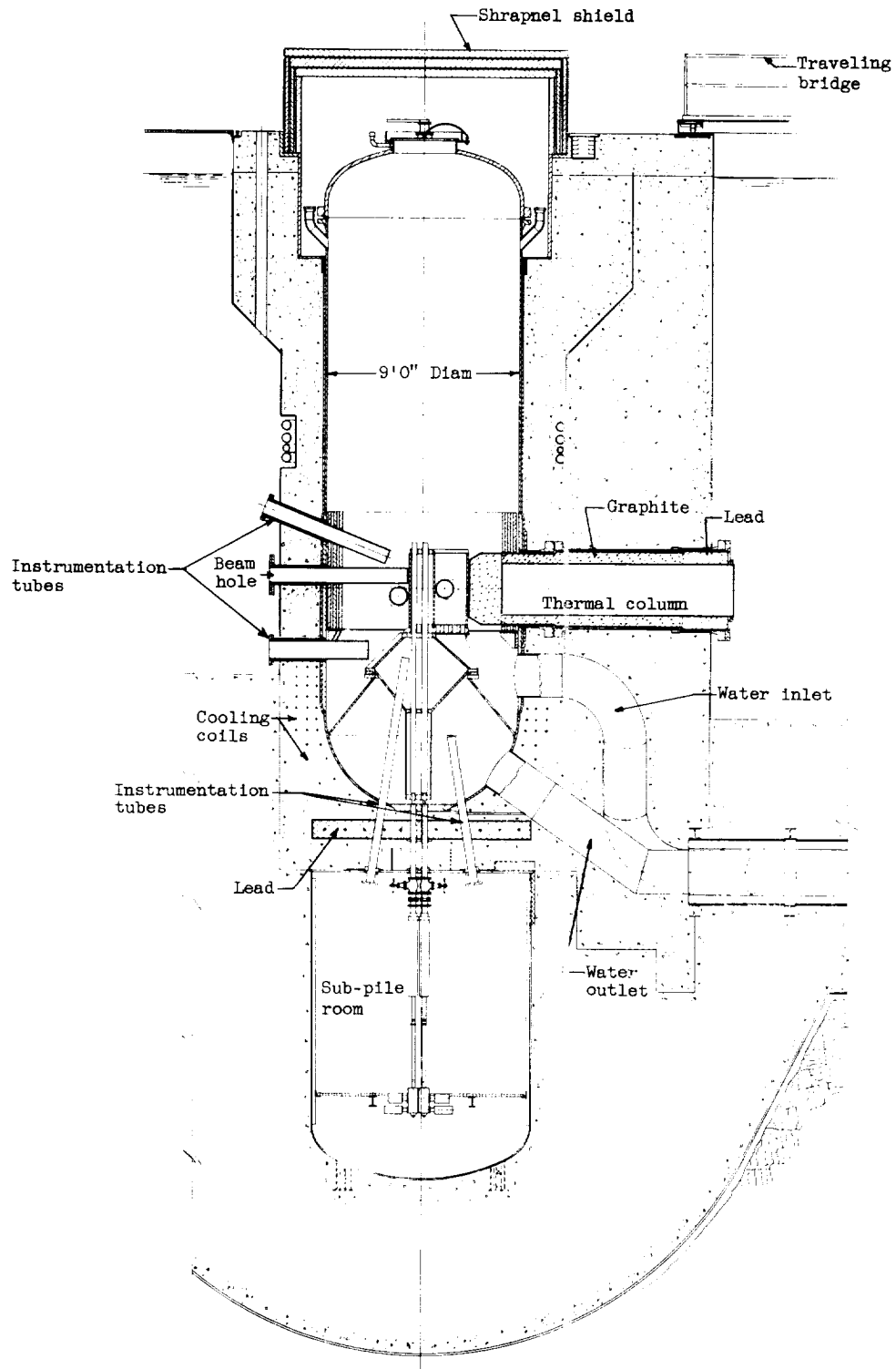


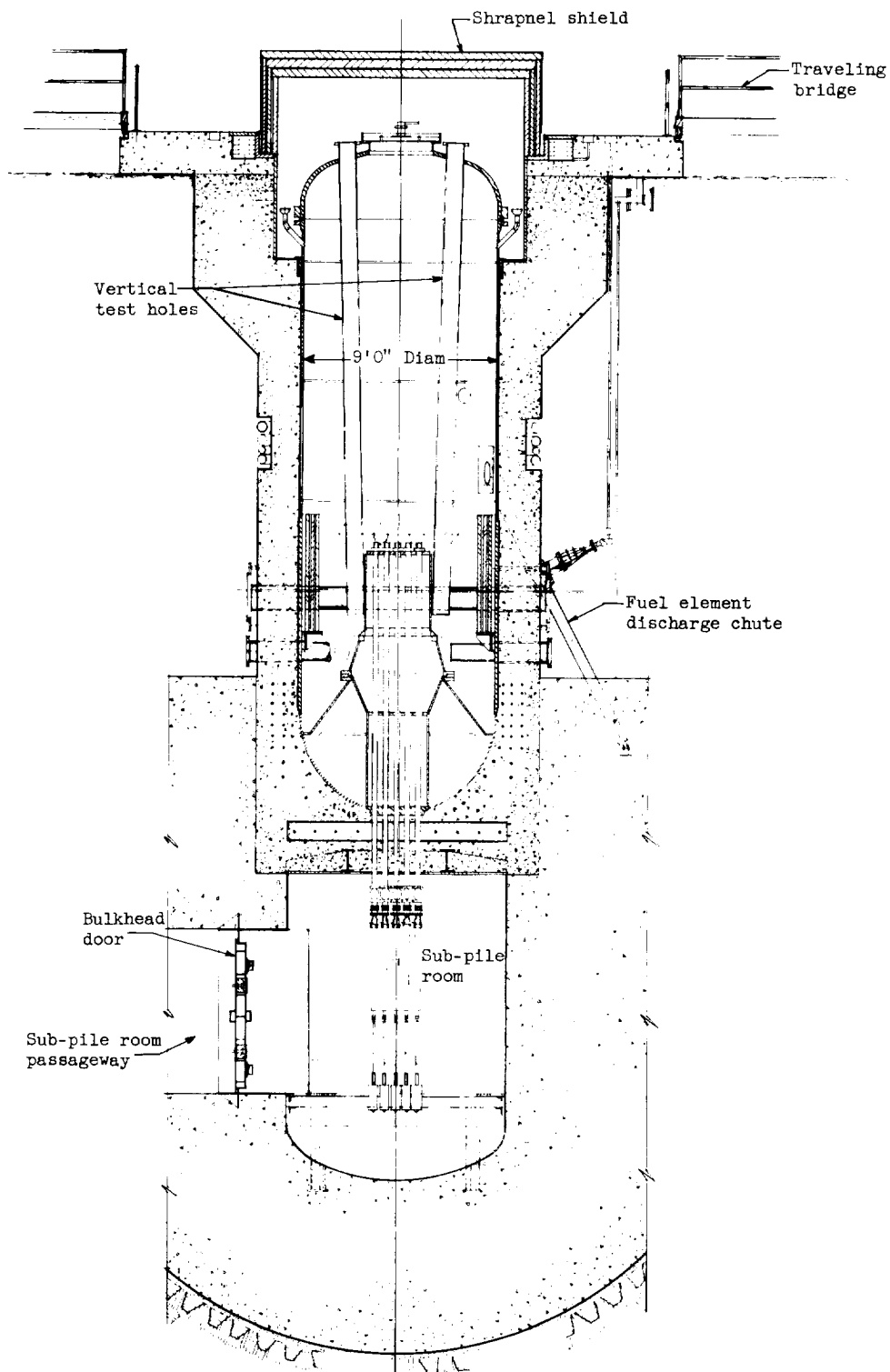
Figure 2.8 - Concluded. Reactor core.



(a) Vertical section perpendicular to wide face of reactor.

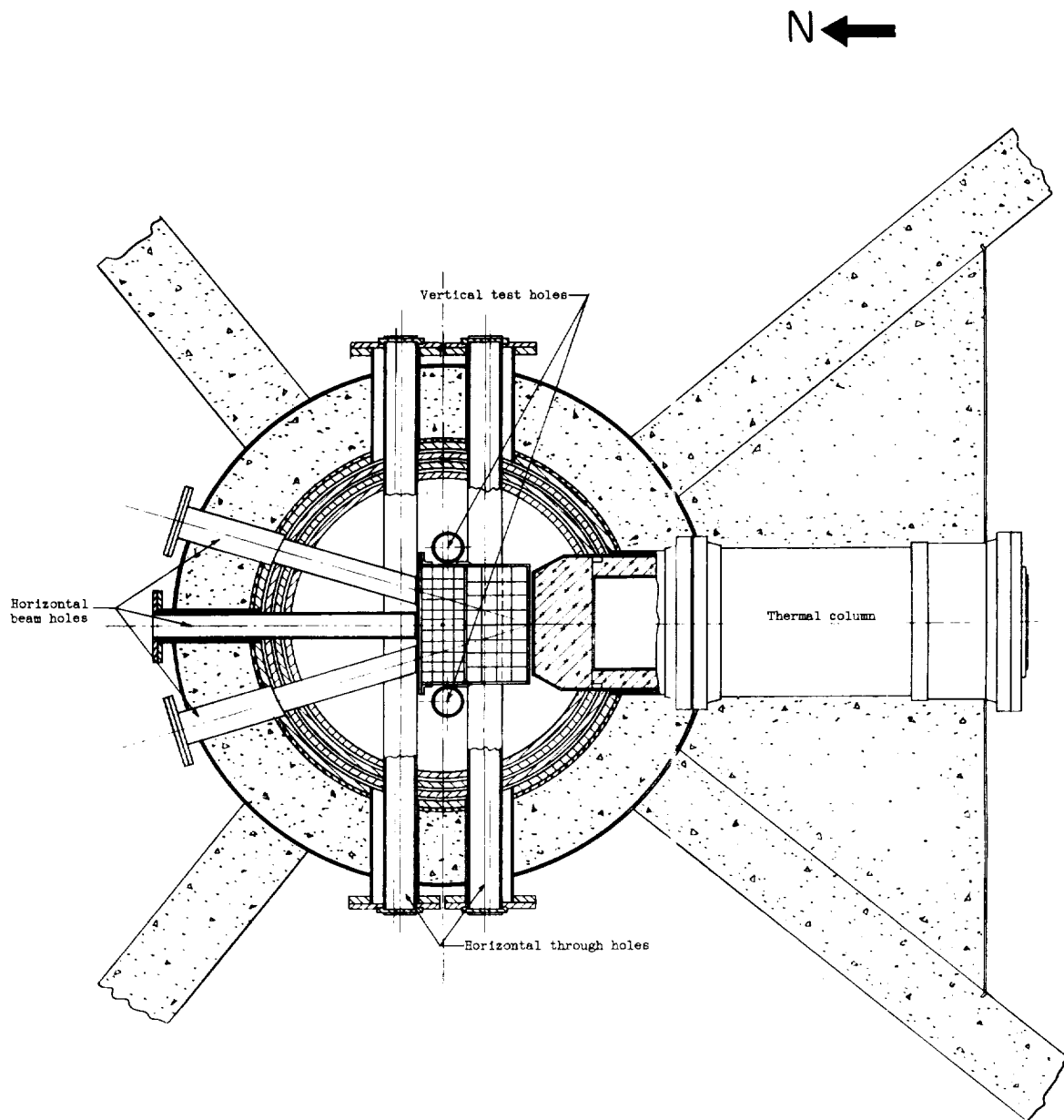
Figure 2.9 - Reactor assembly.

E-102



(b) Vertical section perpendicular to narrow face of reactor.

Figure 2.9 - Reactor assembly.



(c) Horizontal section at reactor level.

Figure 2.9 - Reactor assembly.







E-102

CZ-33

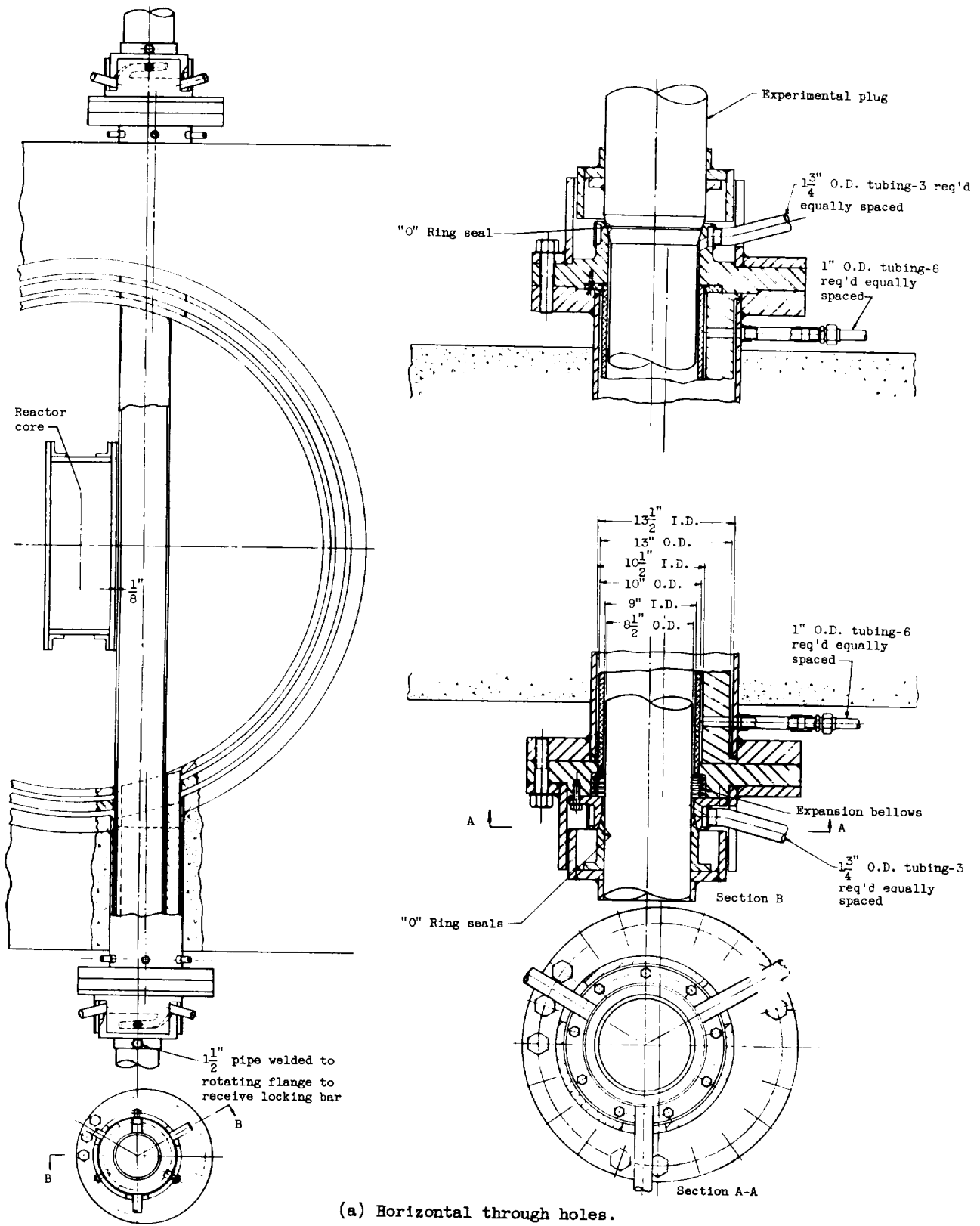
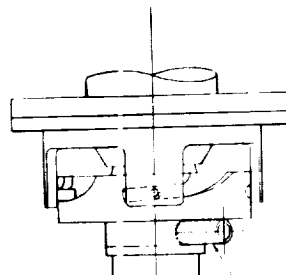
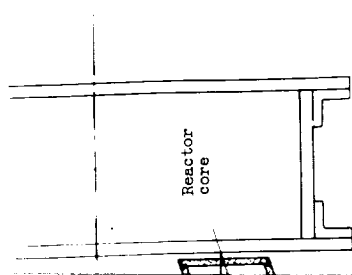
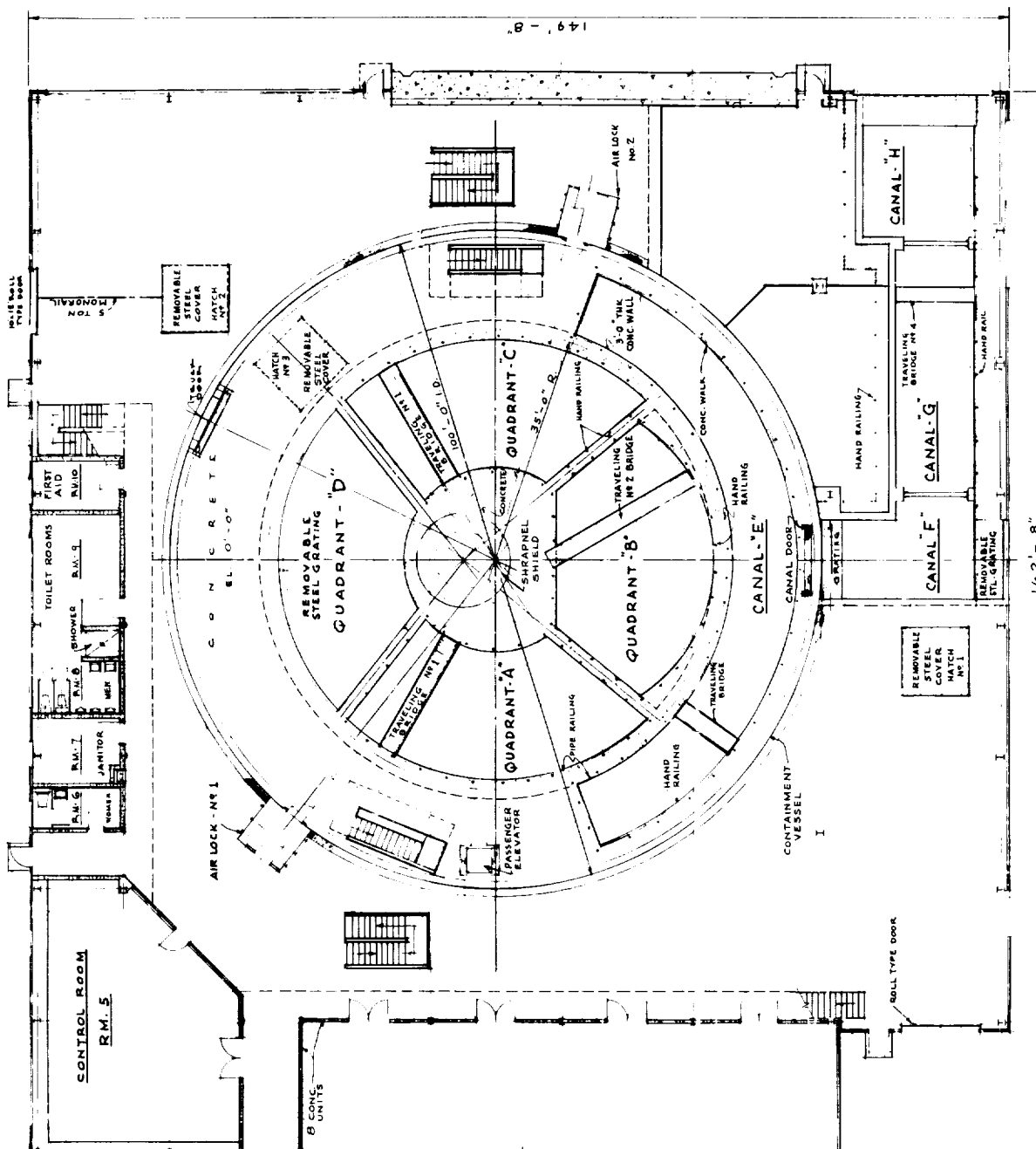


Figure 2.11 - Details of experimental test holes.

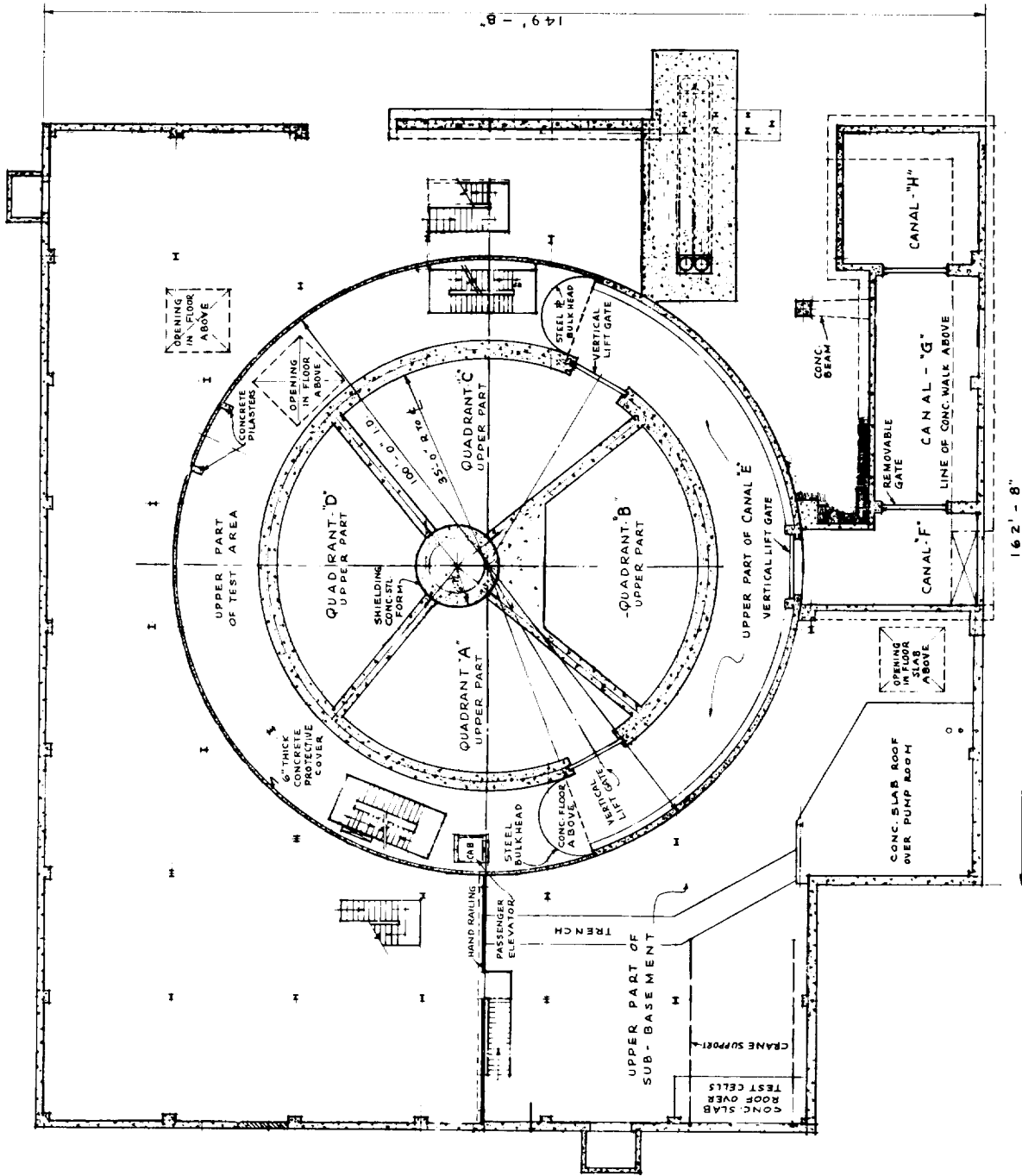


Auxiliary view "C-C"



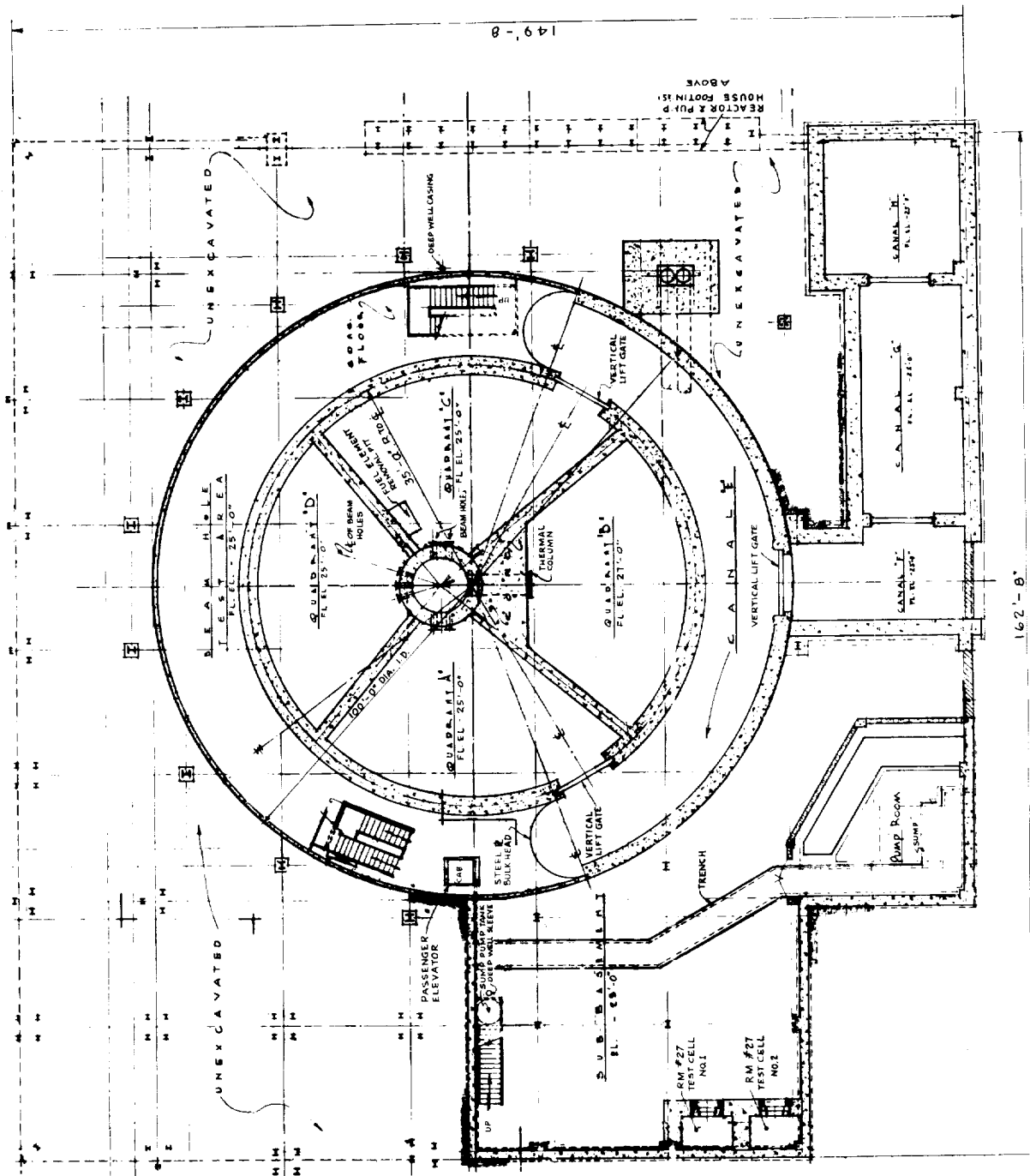
(a) First floor plan.

Figure 2.12 - Horizontal section of the reactor building.



(b) Basement plan (-15 ft elevation)

Figure 2.12 - Continued. Horizontal section of the reactor building.



(c) Basement plan (-25 ft elevation)  
Figure 2.12 - Continued. Horizontal section of the reactor building.

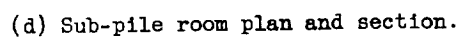


Figure 2.12 - Concluded. Horizontal section of the reactor building.



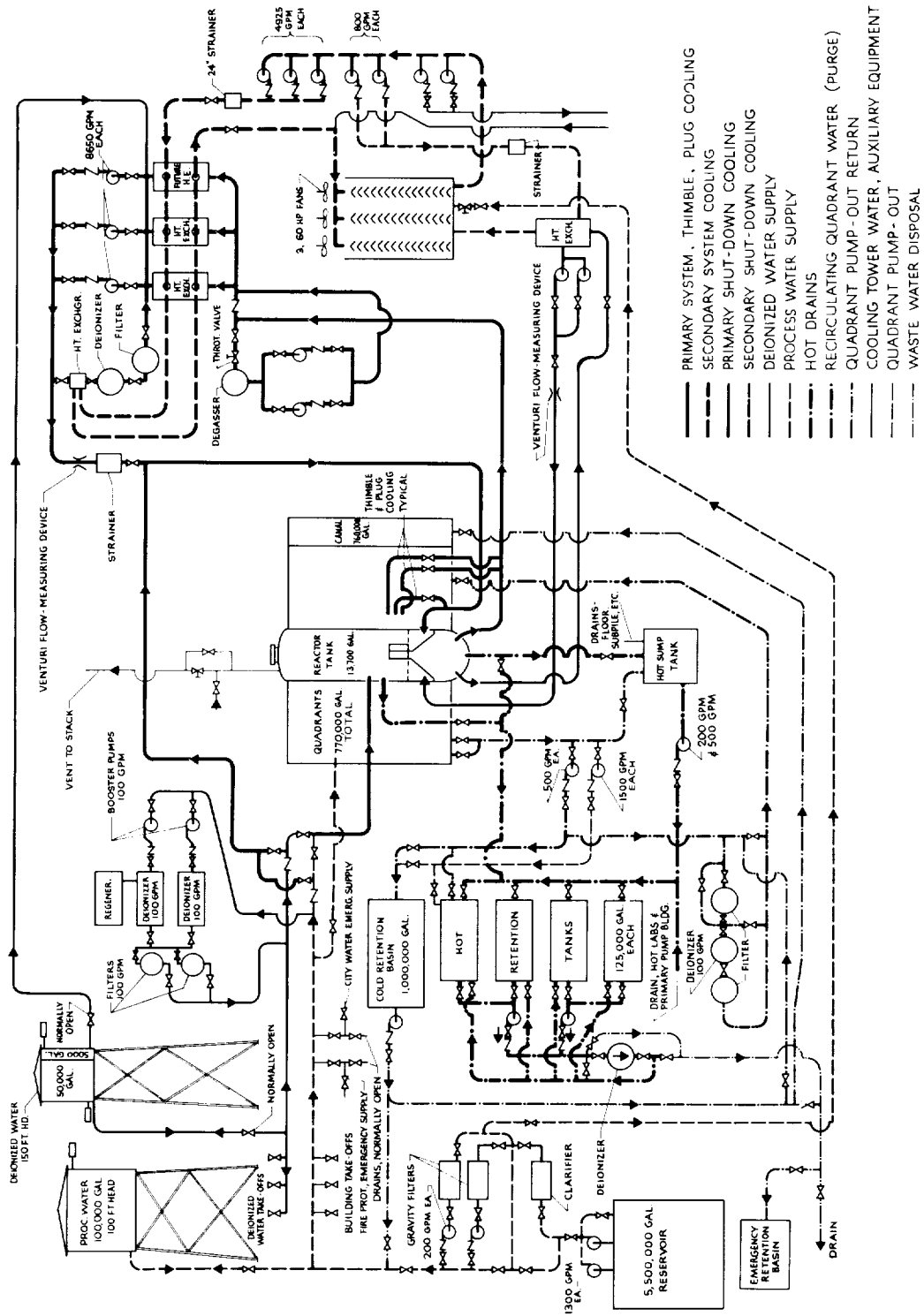


Figure 2.14 - Schematic drawing of water systems.

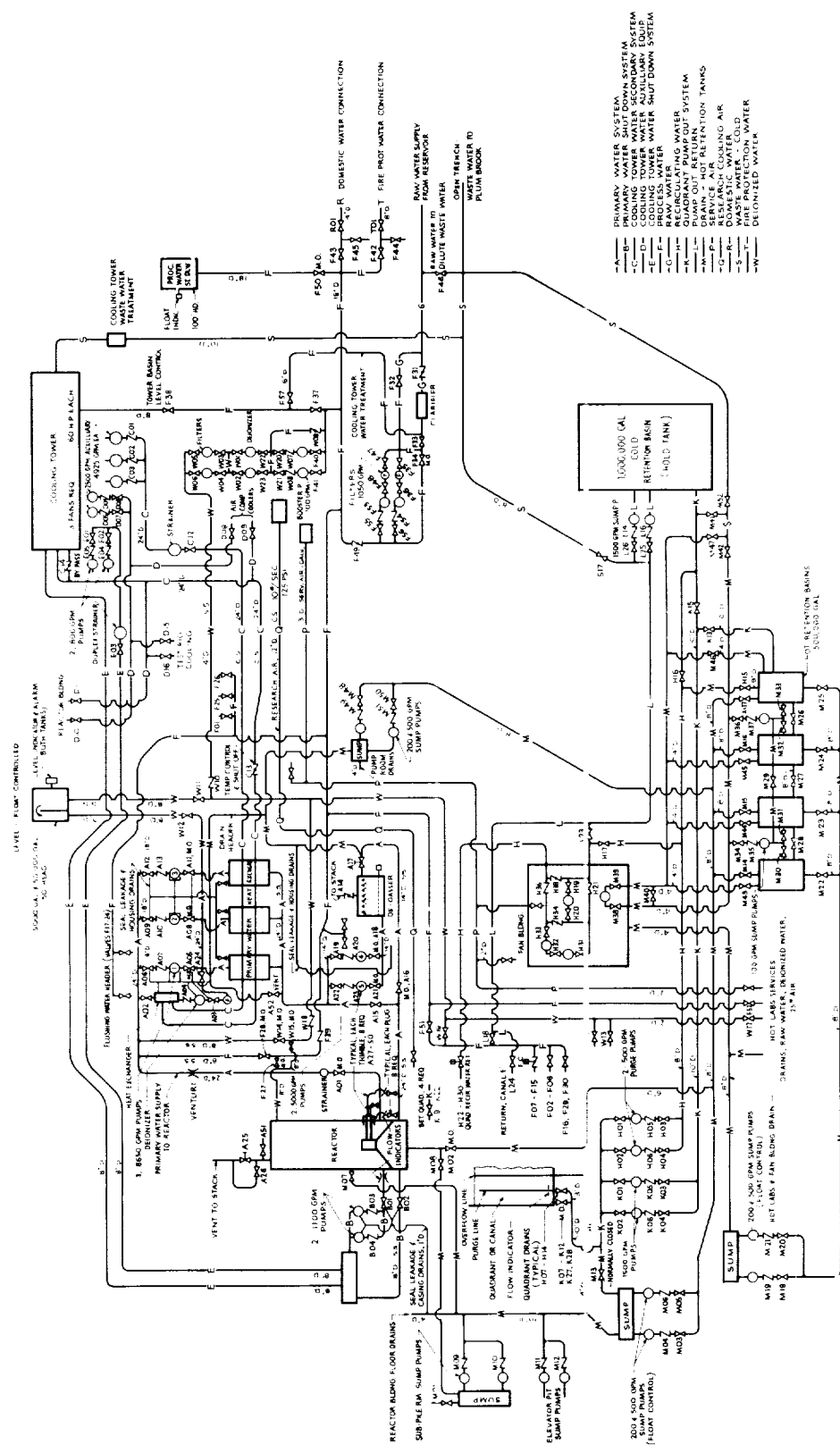
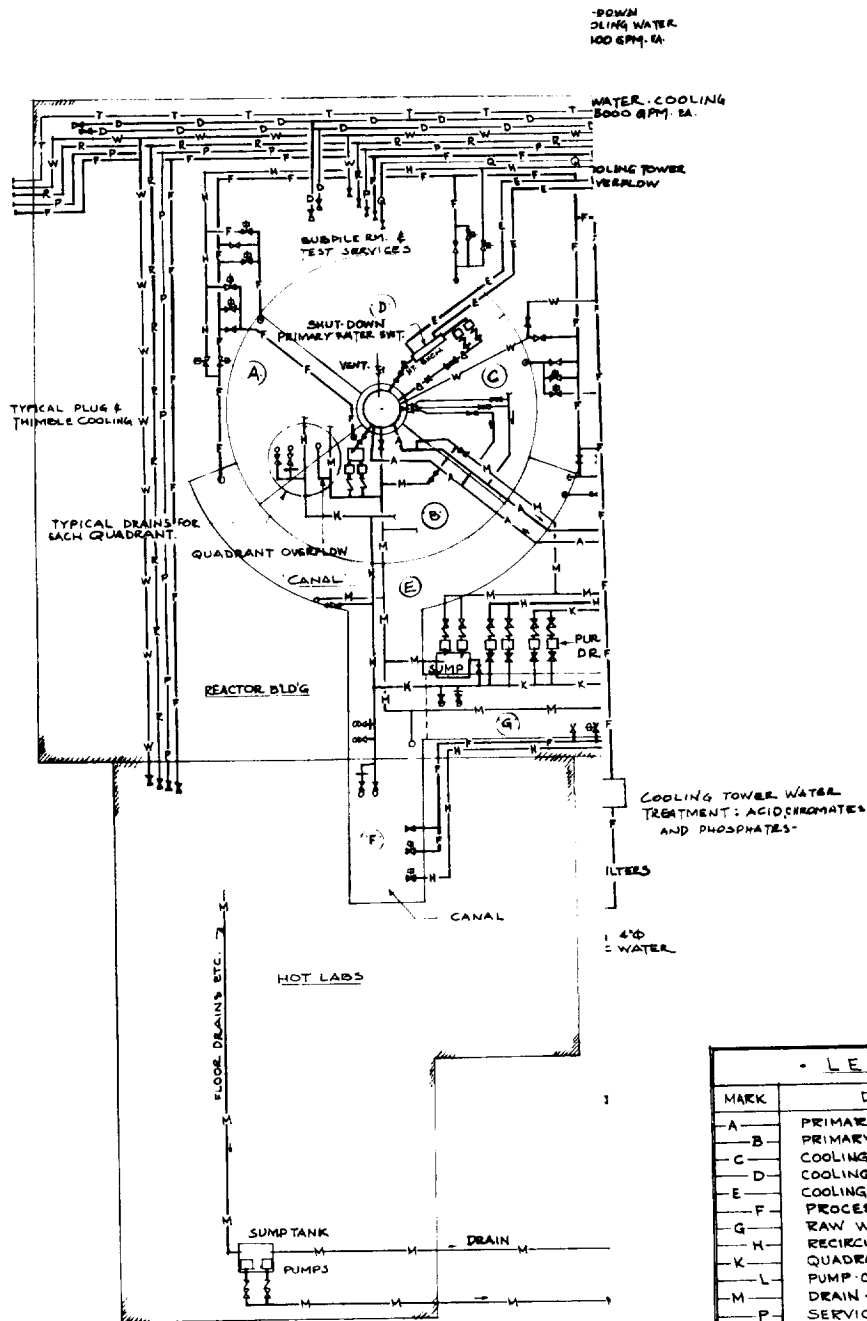


Figure 2.15 - Schematic drawing of piping and valves for water system.



E-102



## • LEGEND •

MARK	DESCRIPTION
A	PRIMARY WATER SYSTEM
B	PRIMARY WATER - SHUT DOWN SYSTEM
C	COOLING TOWER WATER - SECONDARY SYSTEM
D	COOLING TOWER WATER - AUXILIARY EQUIPMENT
E	COOLING TOWER WATER - SHUT DOWN SYSTEM
F	PROCESS WATER
G	RAW WATER
H	RECIRCULATING WATER
K	QUADRANT PUMP-OUT SYSTEM
L	PUMP-OUT RETURN
M	DRAIN - HOT RETENTION TANKS
P	SERVICE AIR
Q	RESEARCH COOLING AIR
R	DOMESTIC WATER
S	WASTE WATER (COLD)
T	FIRE PROTECTION SYSTEM
W	DEIONIZED WATER

Figure 2.16



E-102

CZ-35

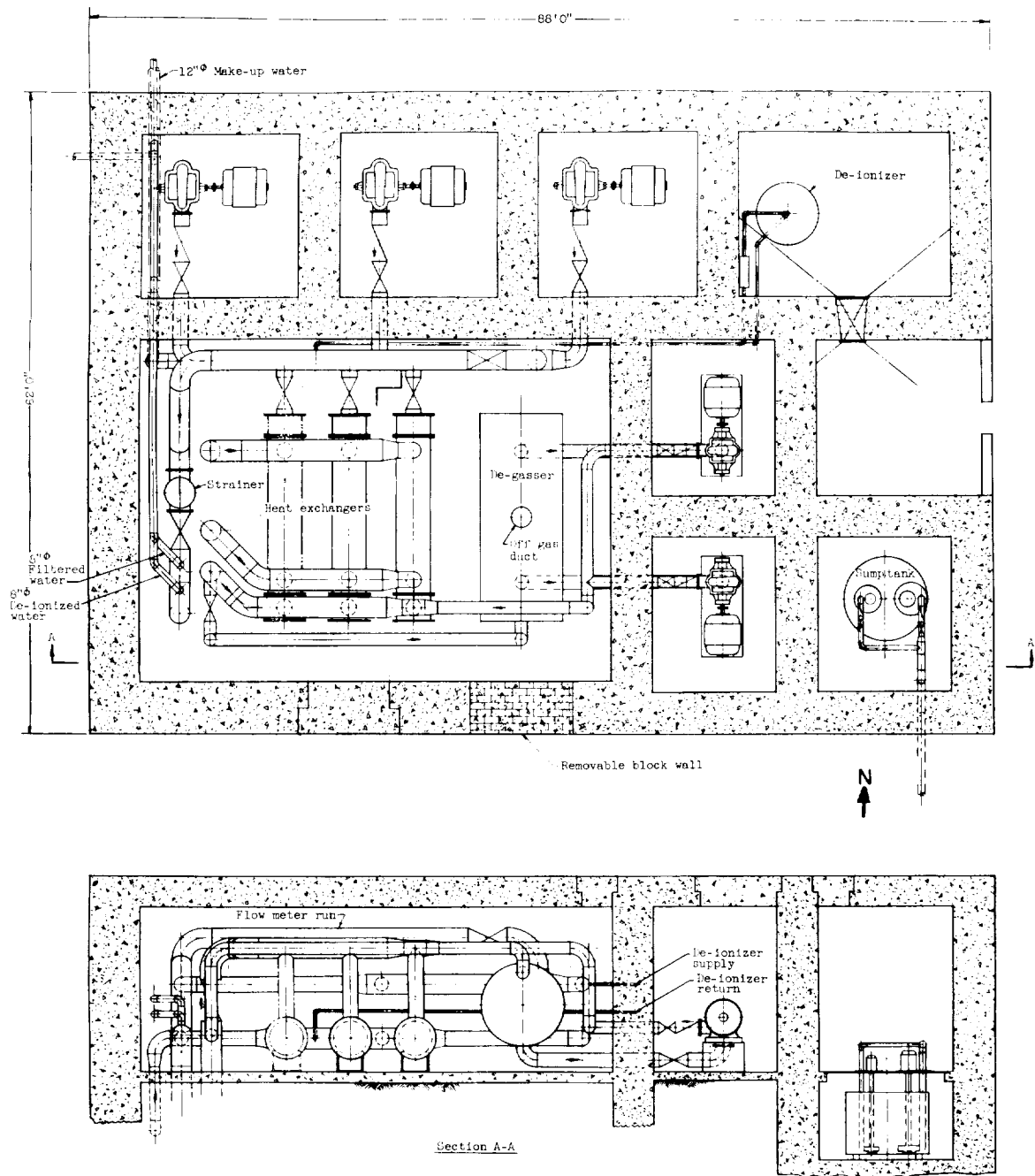


Figure 2.17 - Primary water pump house.

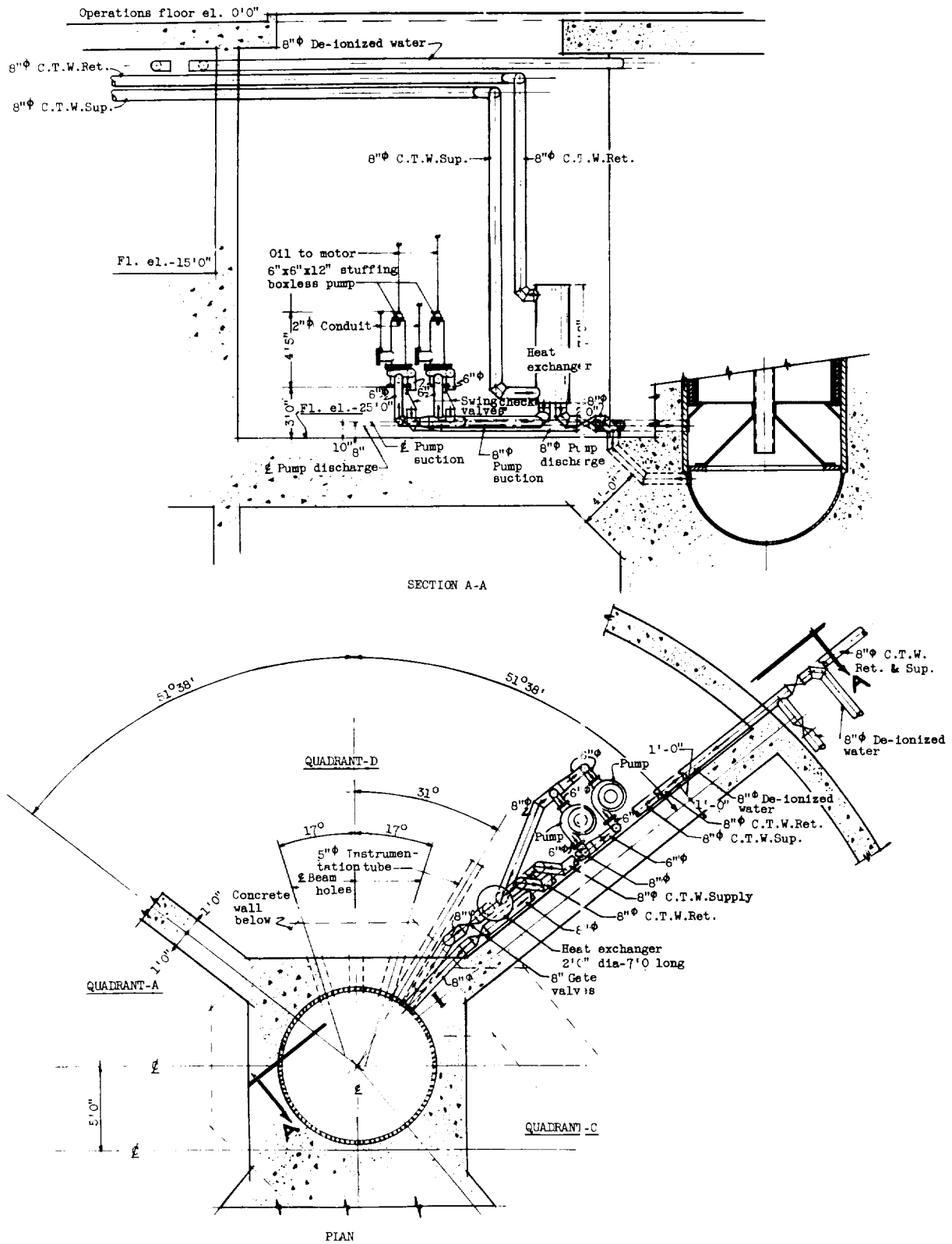


Figure 2.18 - Shut-down cooling system.

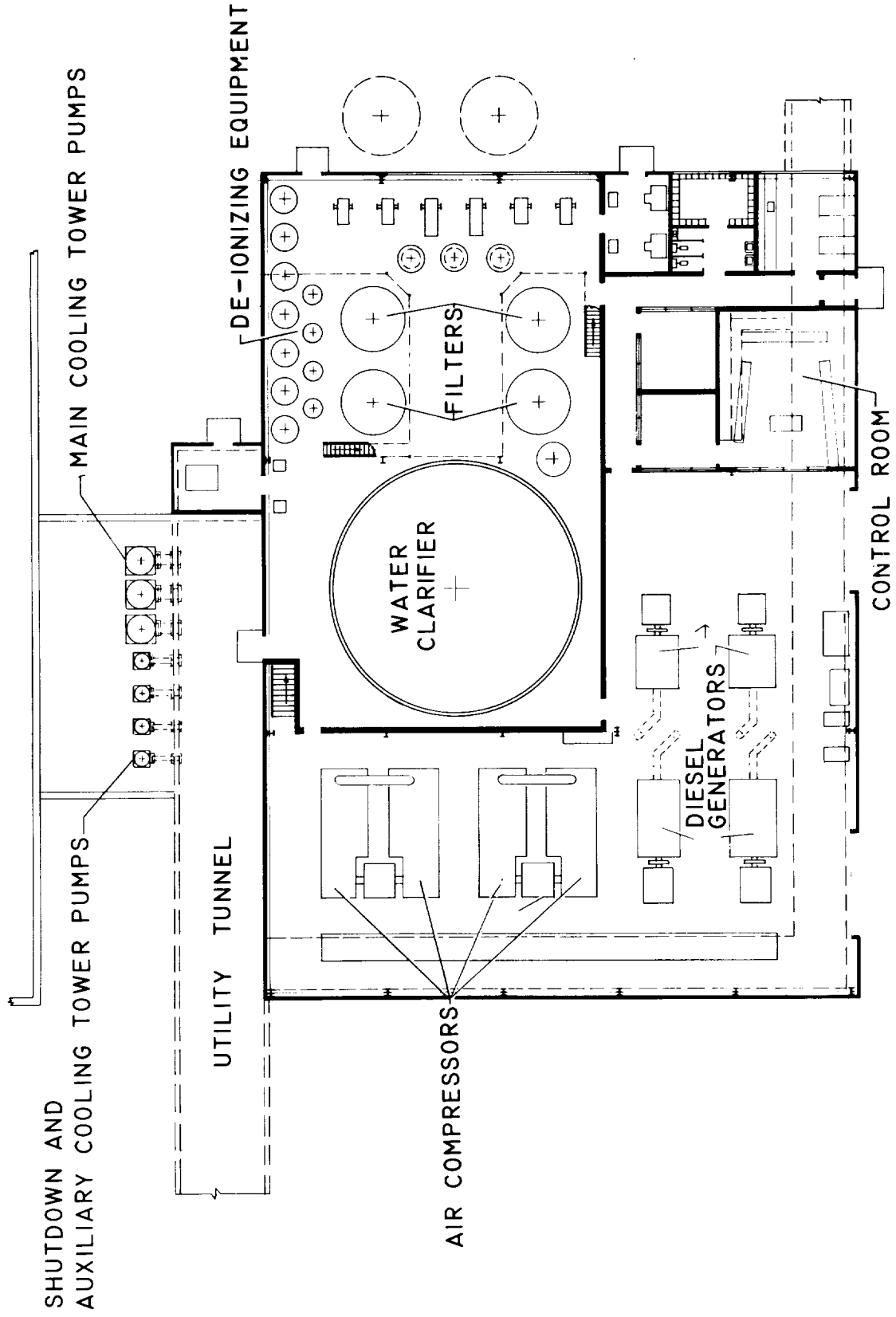
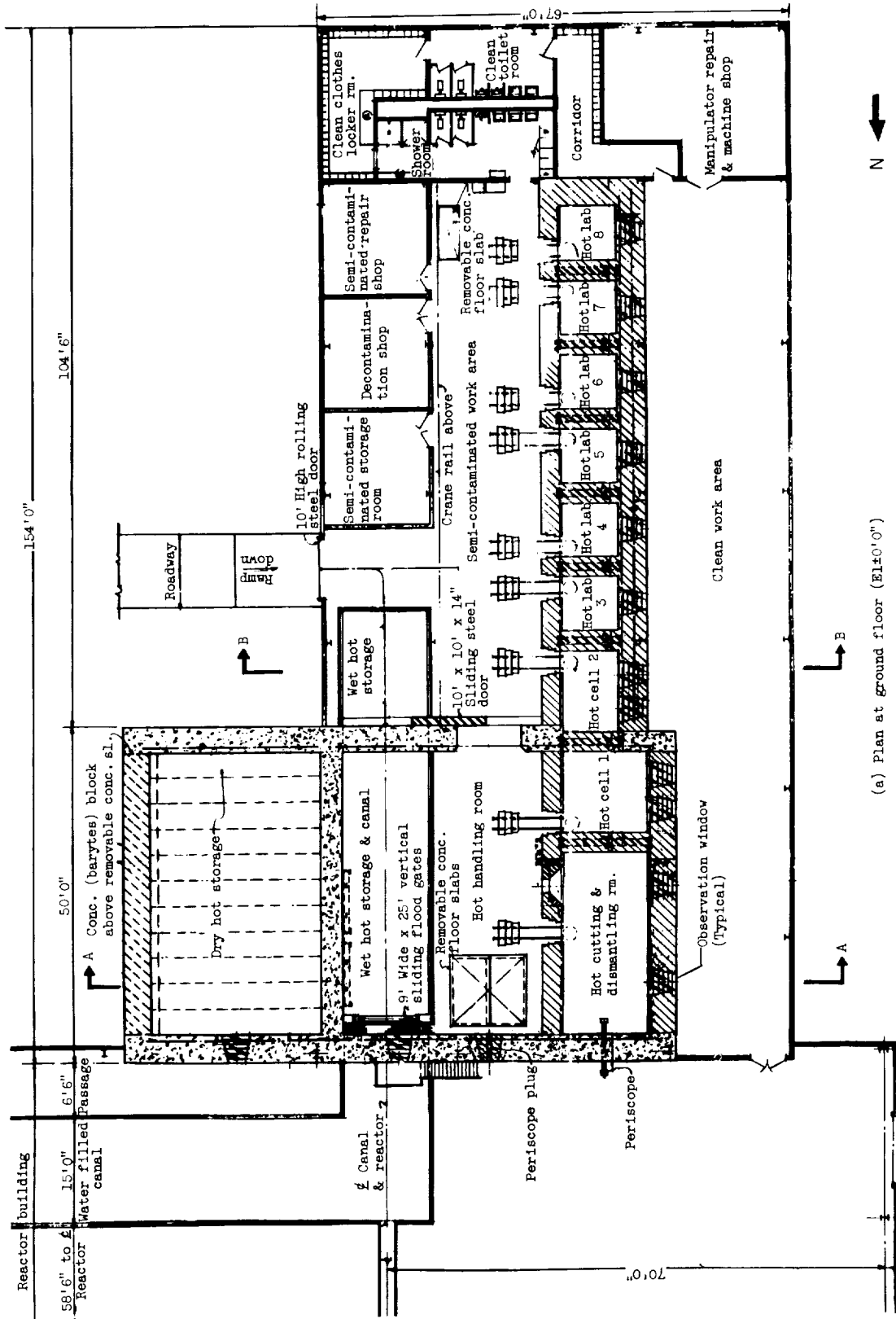


Figure 2.19 - Service equipment building.



(a) Plan at ground floor (El±0'0")

Figure 2.20 - Layout drawing of hot laboratory.

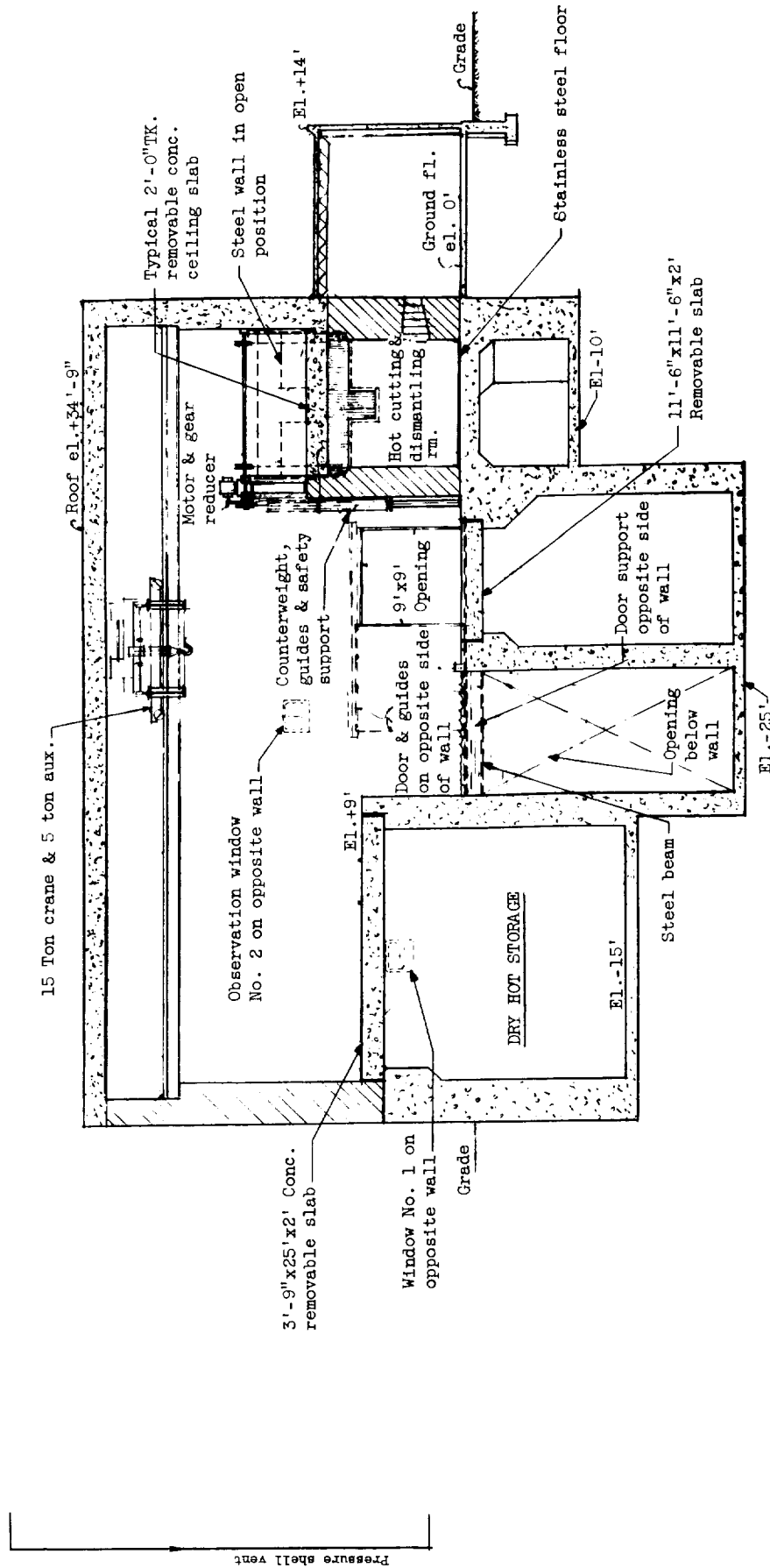


Figure 2.20 - Layout drawing of hot laboratory.







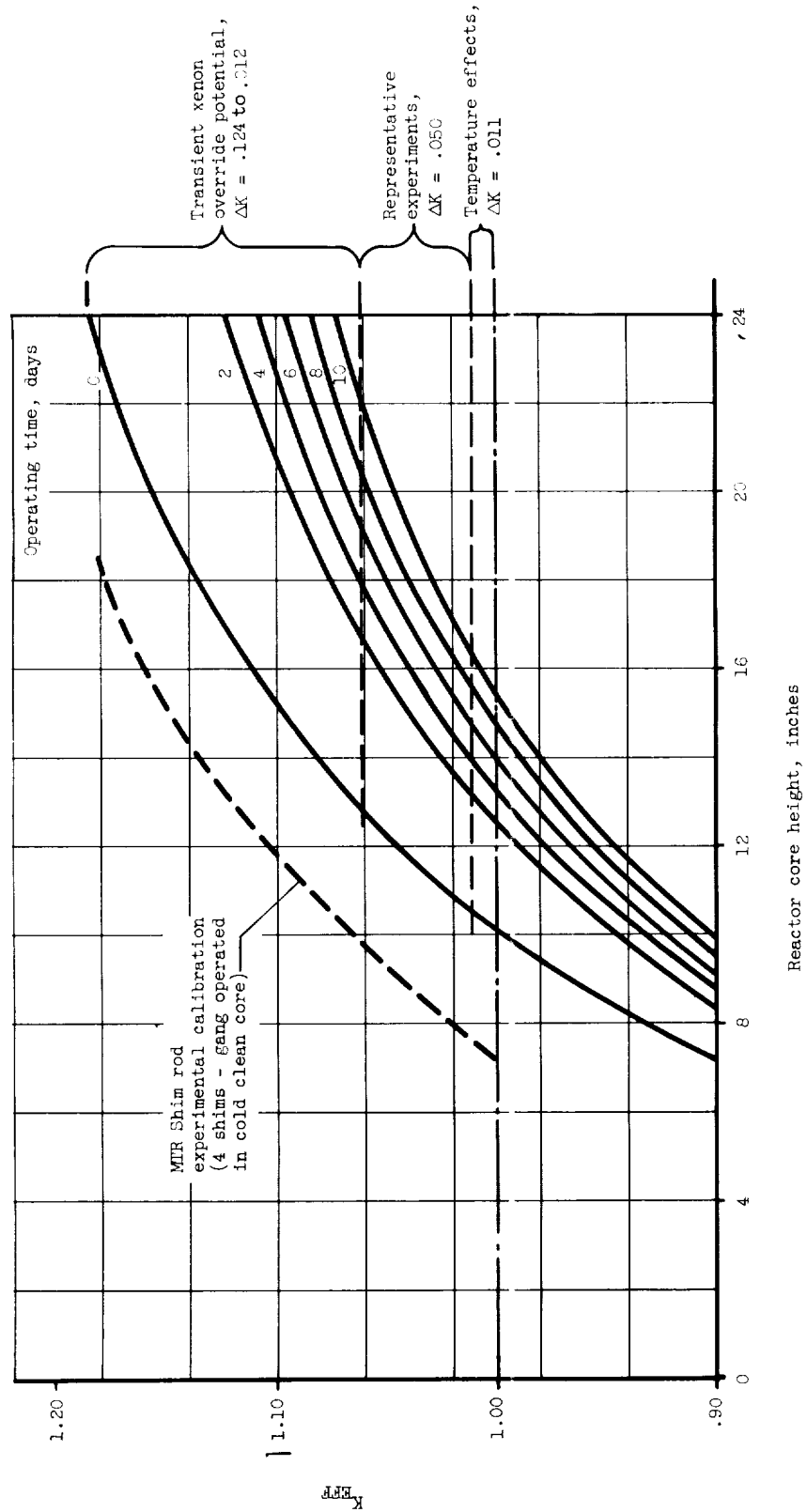


Figure 2.23 - Critical core height and reactivity potential during operating cycle.

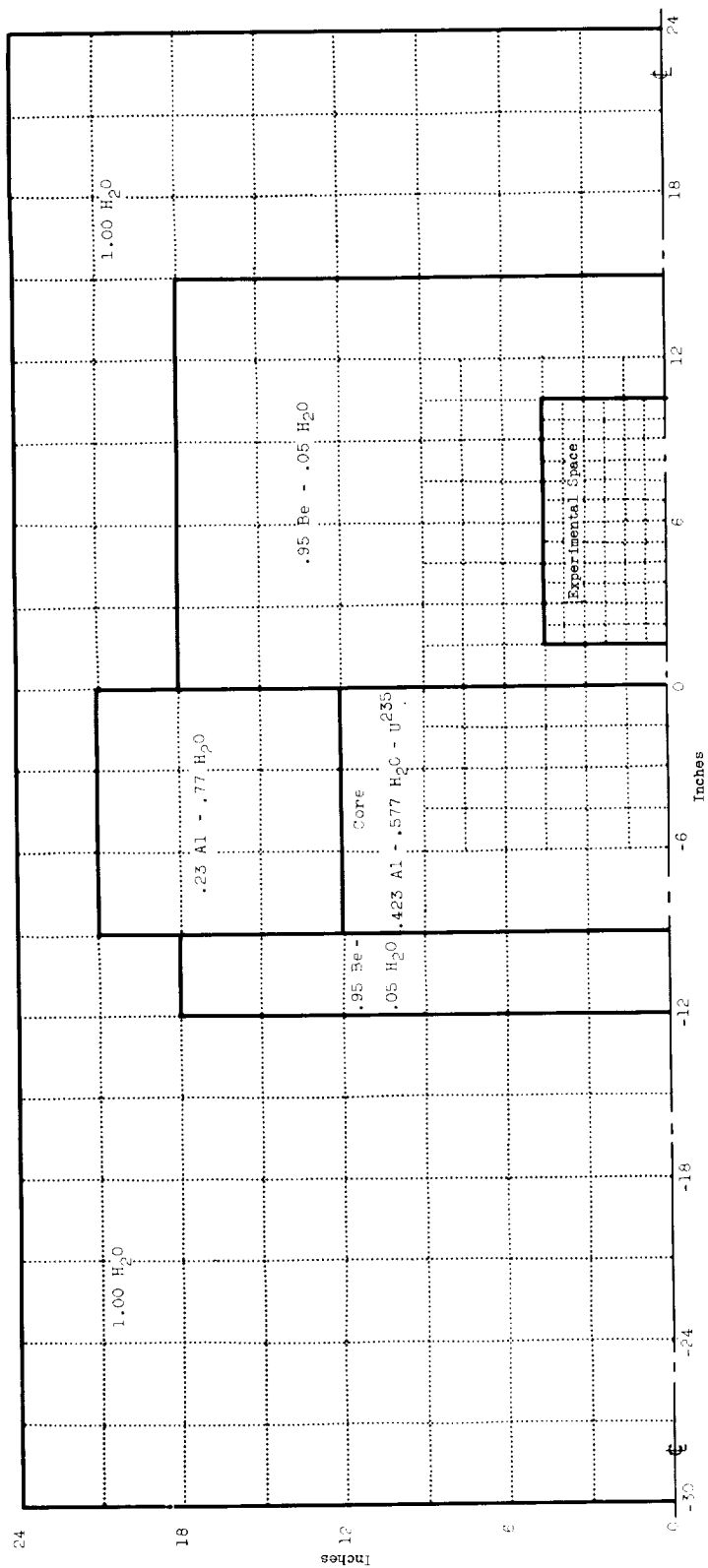


Figure 2.24. - Reactor geometry for two-dimensional simulator, vertical section. (Each dotted area represents a grid point of solution.)

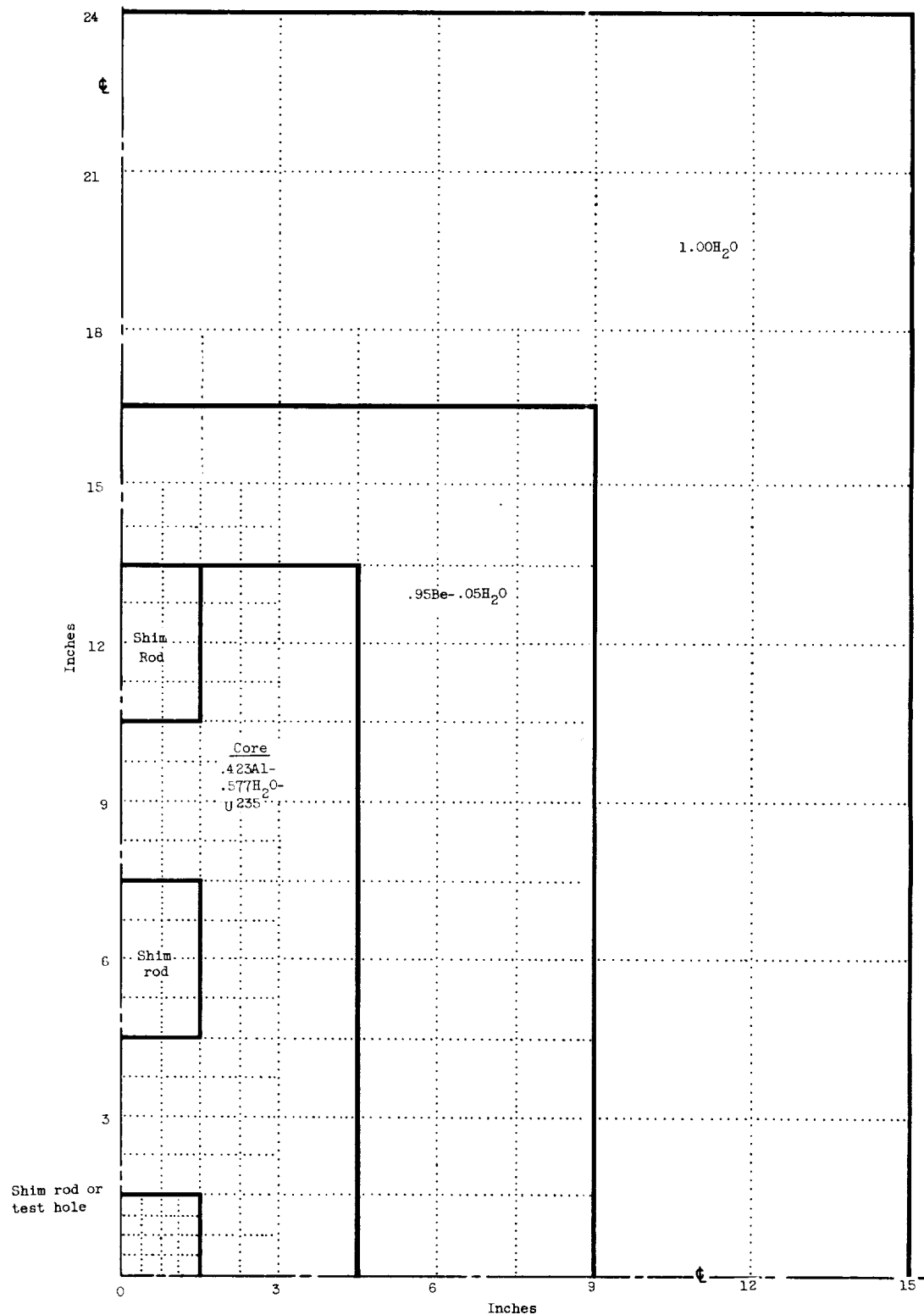


Figure 2.25 - Reactor geometry for two dimensional simulator, horizontal section.  
(Each dotted area represents a grid point of solution.)

**FOI-7**

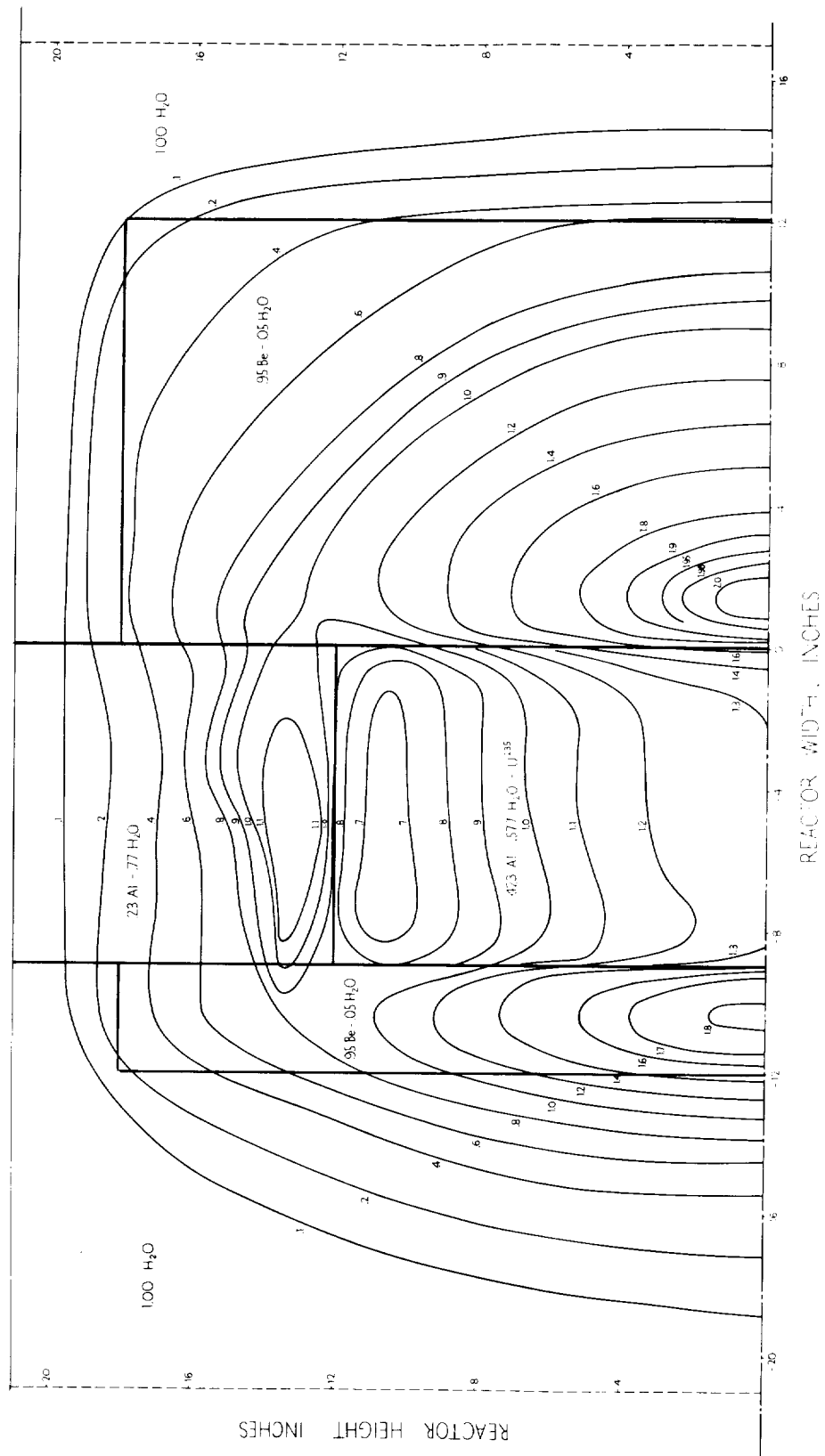


Figure 2.26(a) - Thermal neutron flux distribution for vertical section of unperturbed reference reactor. (Relative to average thermal flux of unity over core volume.)

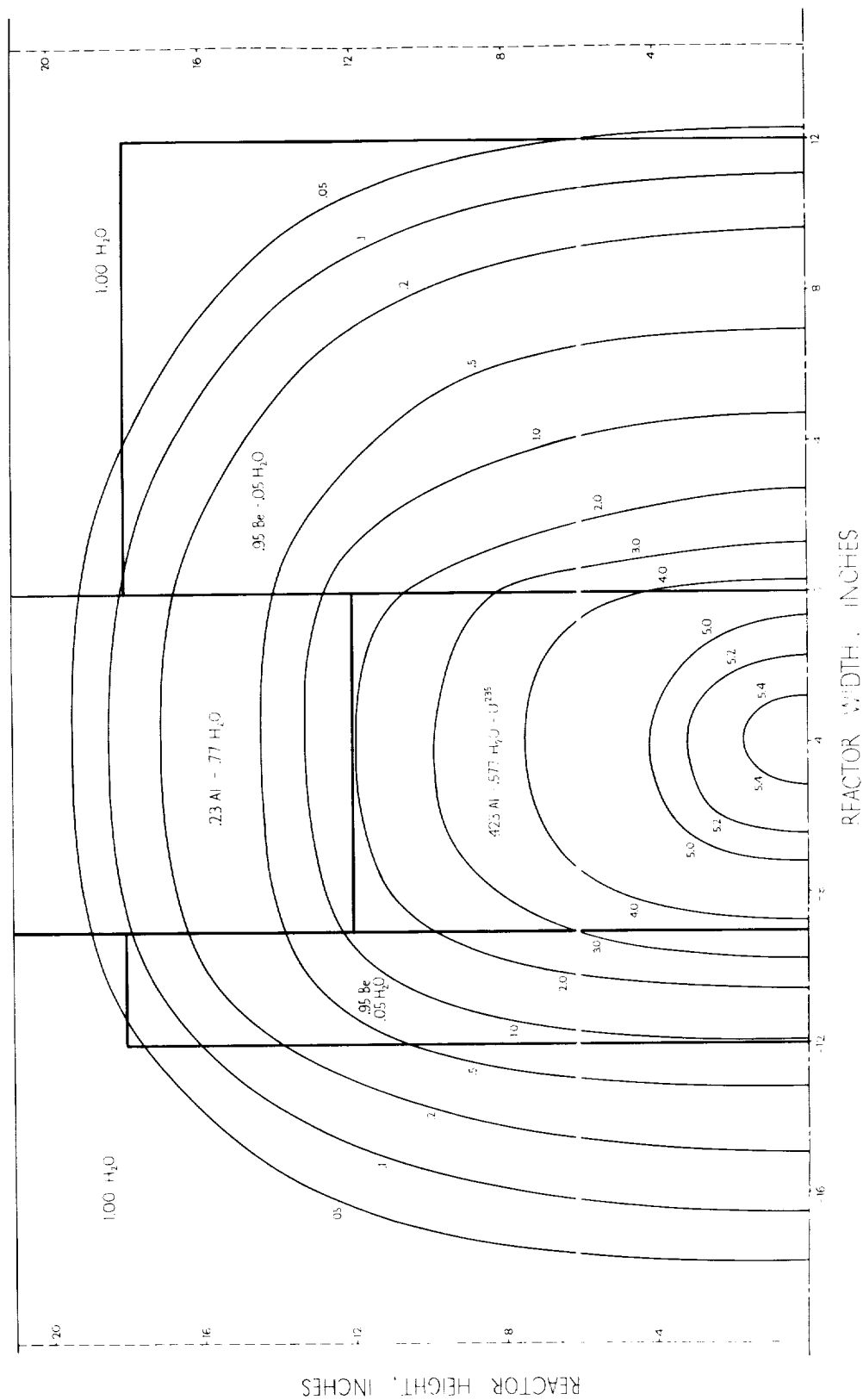


Figure 2.26(b) - Fast neutron flux distribution for vertical section of unperturbed reference reactor. (Relative to average thermal flux of unity over core volume.)

E-102

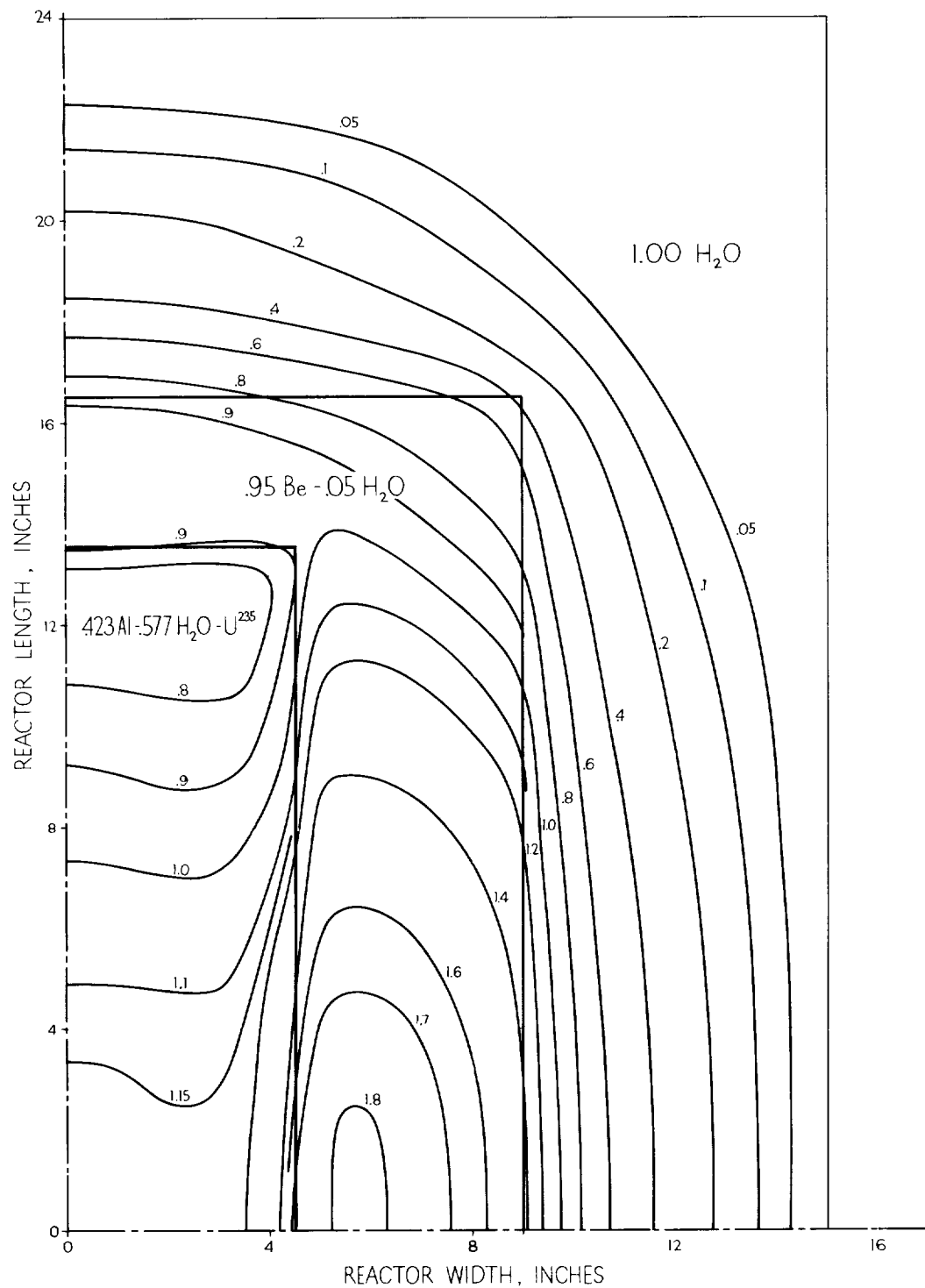


Figure 2.27(a) - Thermal neutron flux distribution for horizontal section of unperturbed reference reactor. (Relative to average thermal flux of unity over core volume.)

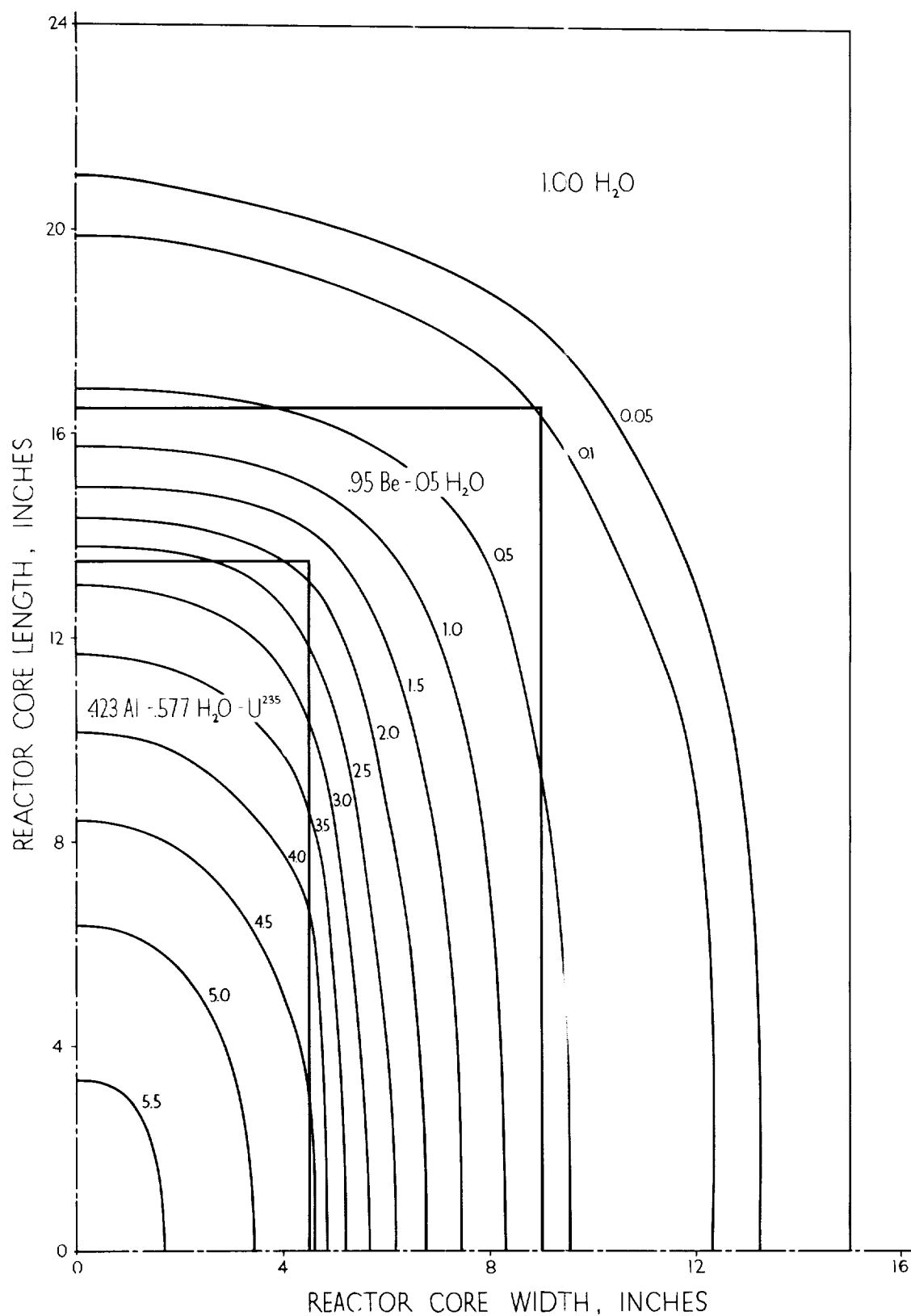


Figure 2.27(b) - Fast neutron flux distribution for horizontal section of unperturbed reference reactor. (Relative to average thermal flux of unity over core volume.)



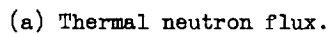
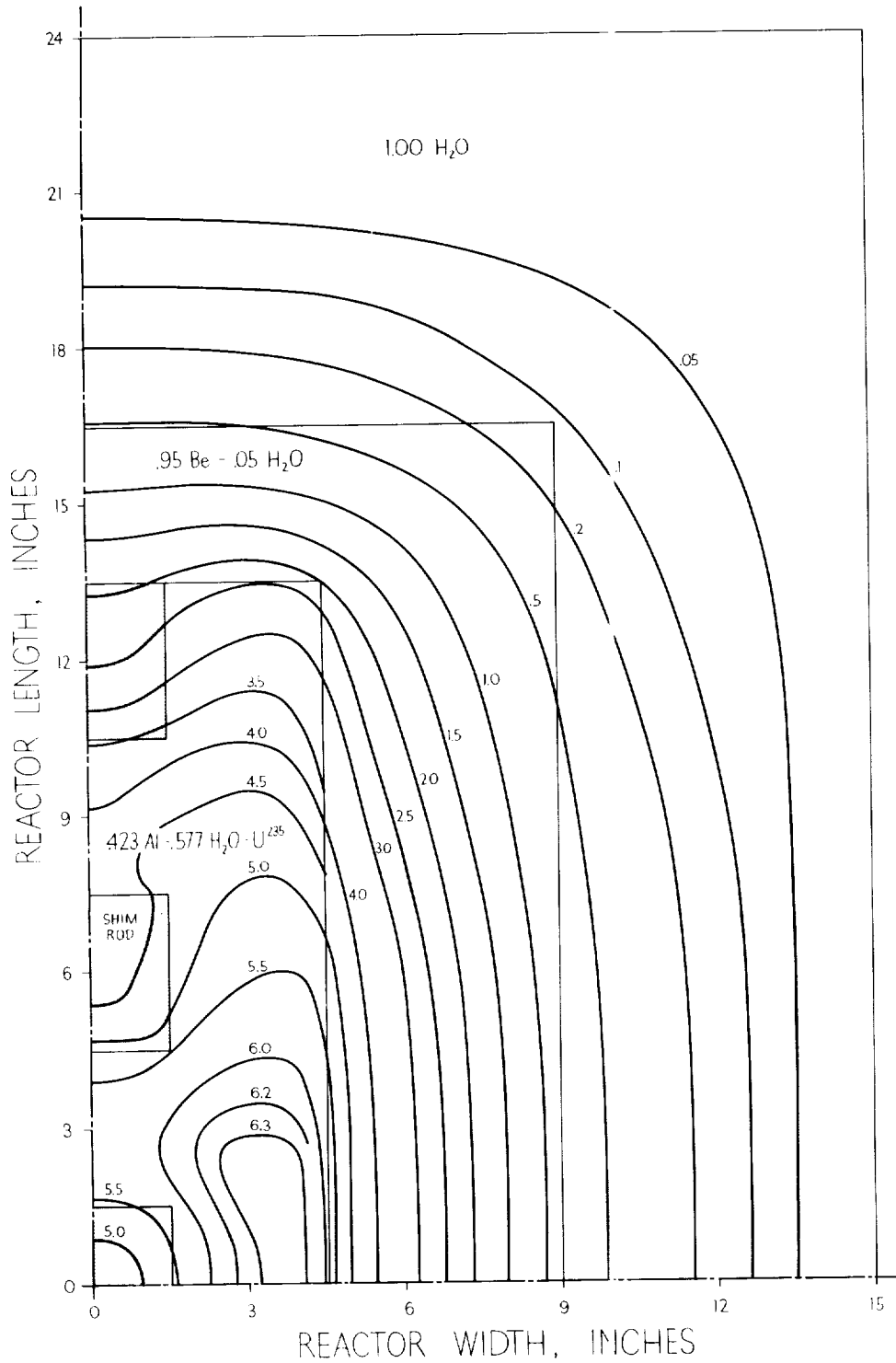


Figure 2.28 - Neutron flux distribution for horizontal section of reactor with cadmium sections of the five core shim rods fully inserted. (Relative to average thermal flux of unity over core volume.)



(b) Fast neutron flux.

Figure 2.28 - Concluded. Neutron flux distribution for horizontal section of reactor with cadmium section of the five core shim rods fully inserted. (Relative to average thermal flux of unity over core volume.)

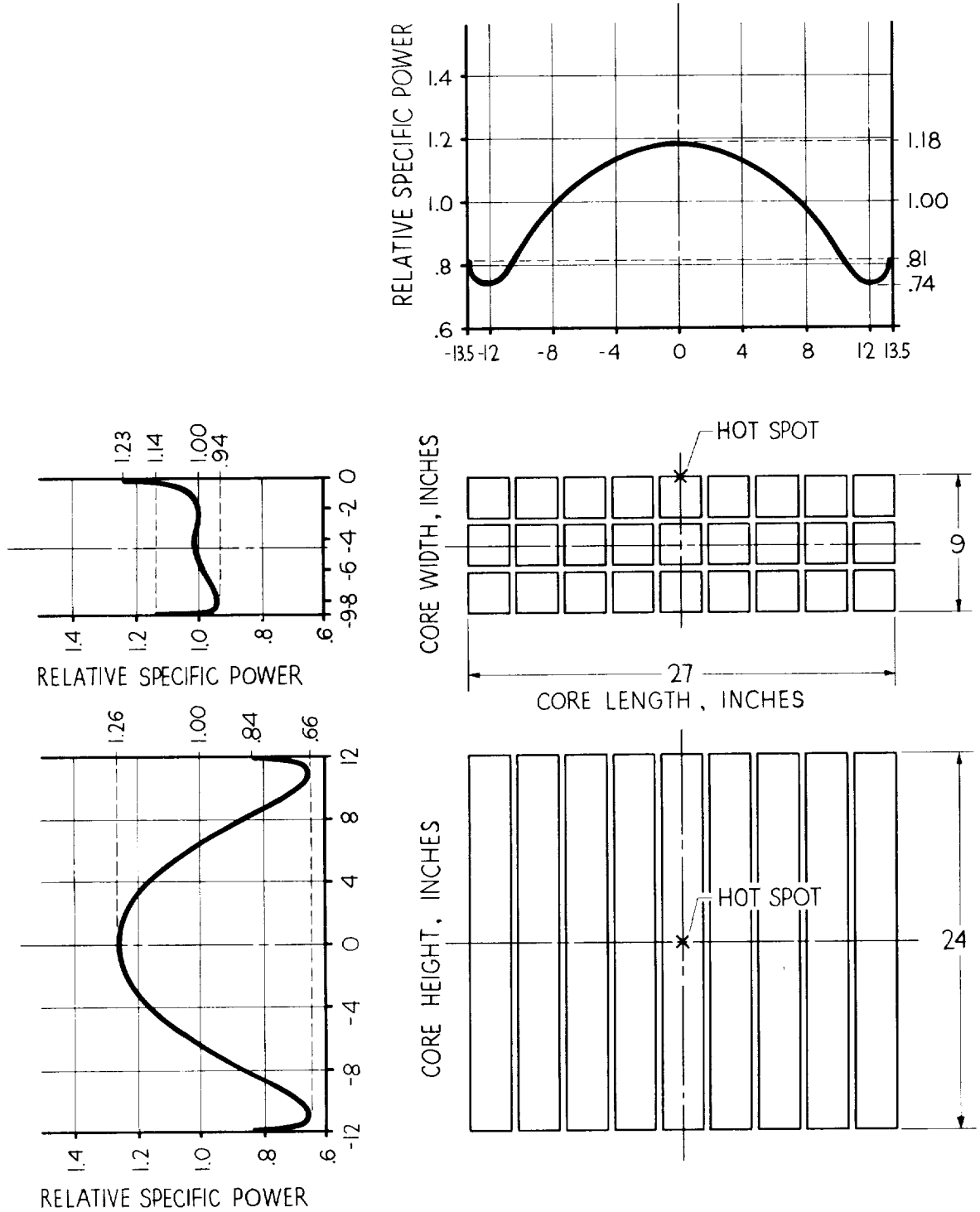


Figure 2.29 - Specific power distributions along axes of unperturbed reference reactor. (Relative to average of unity over core volume.)

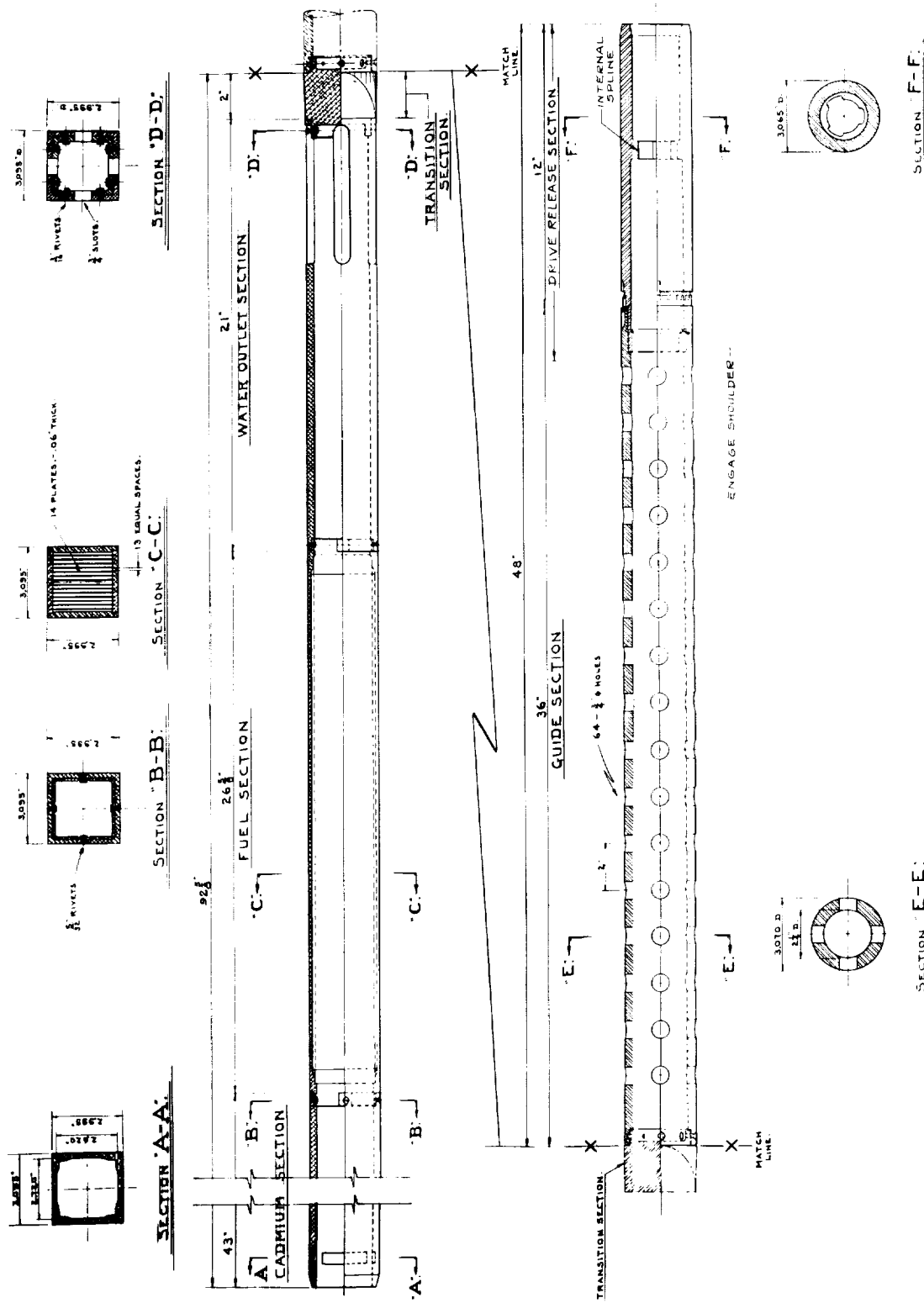
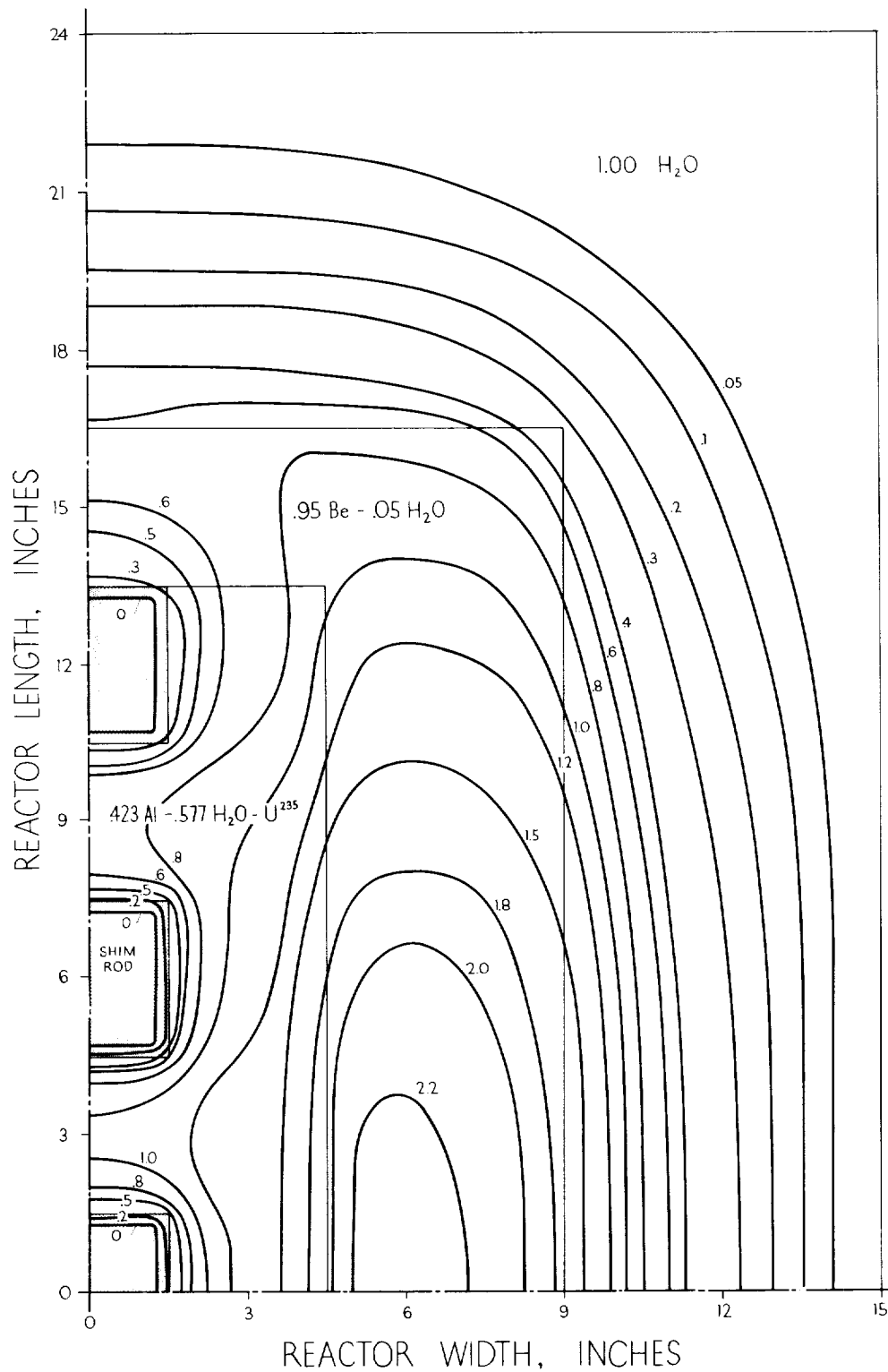
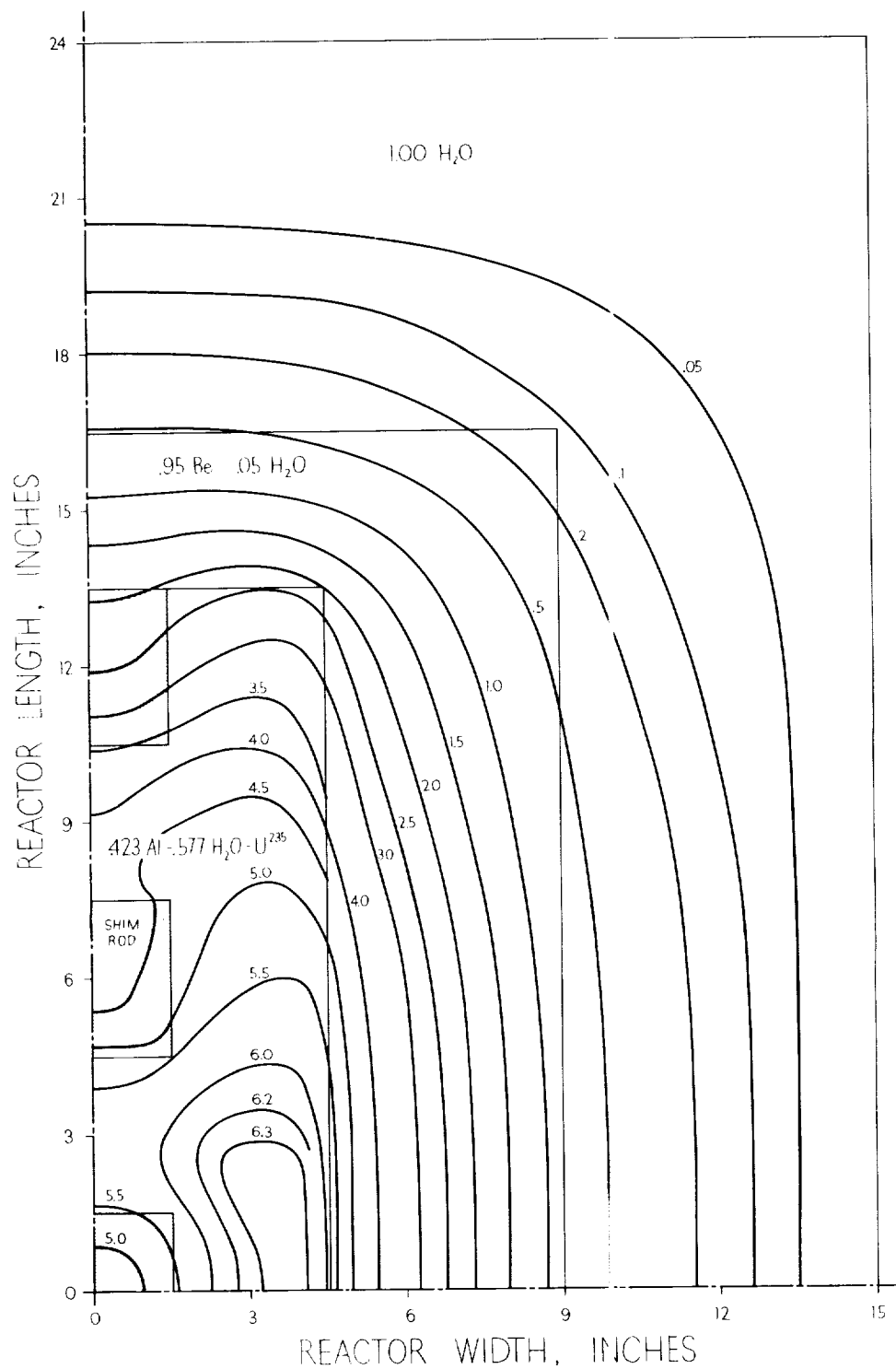


Figure 2.30 - Fuel-slab shim-safety rod.



(a) Thermal neutron flux.

Figure 2.28 - Neutron flux distribution for horizontal section of reactor with cadmium sections of the five core shim rods fully inserted. (Relative to average thermal flux of unity over core volume.)



(b) Fast neutron flux.

Figure 2.28 - Concluded. Neutron flux distribution for horizontal section of reactor with cadmium section of the five core shim rods fully inserted. (Relative to average thermal flux of unity over core volume.)

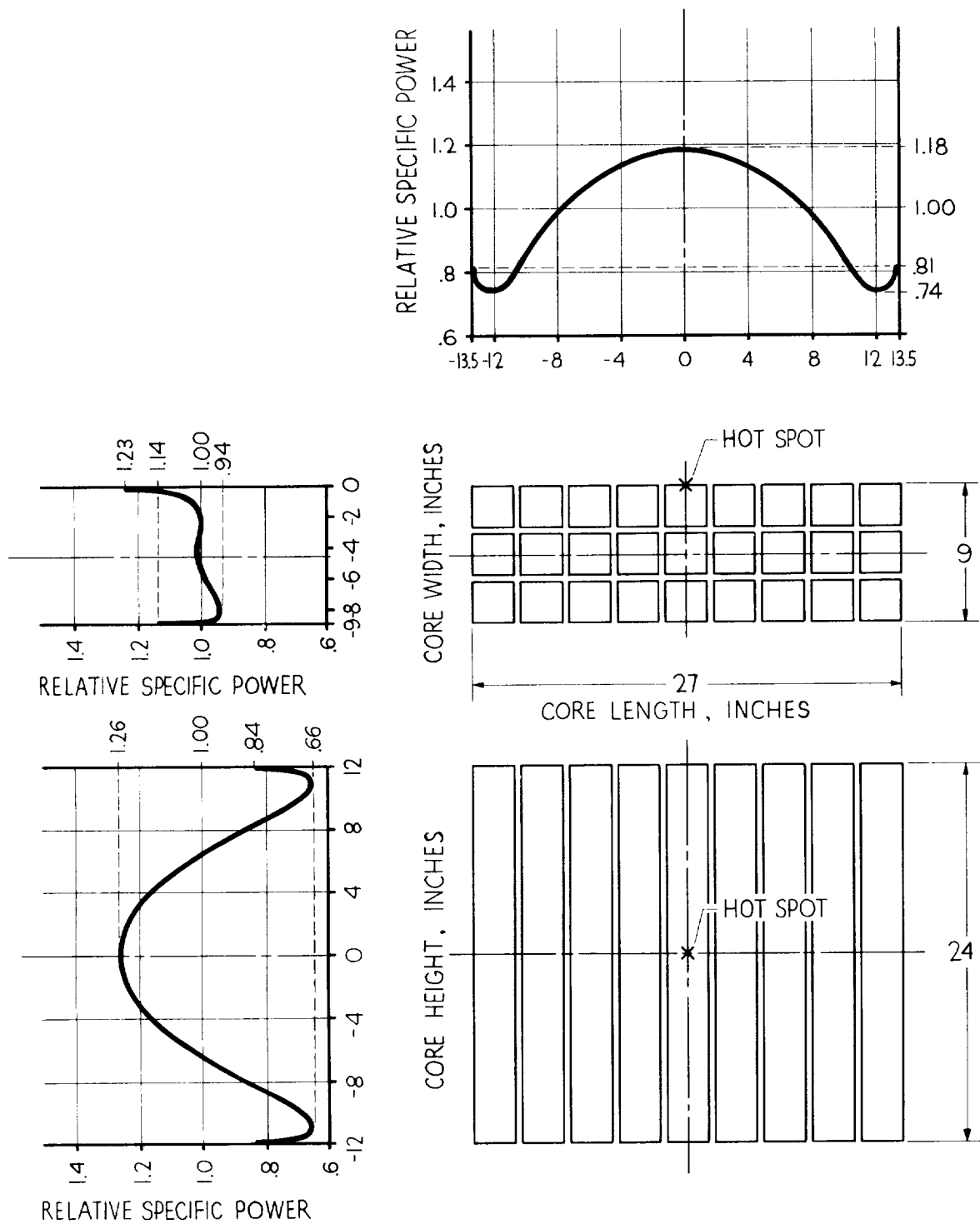


Figure 2.29 - Specific power distributions along axes of unperturbed reference reactor. (Relative to average of unity over core volume.)





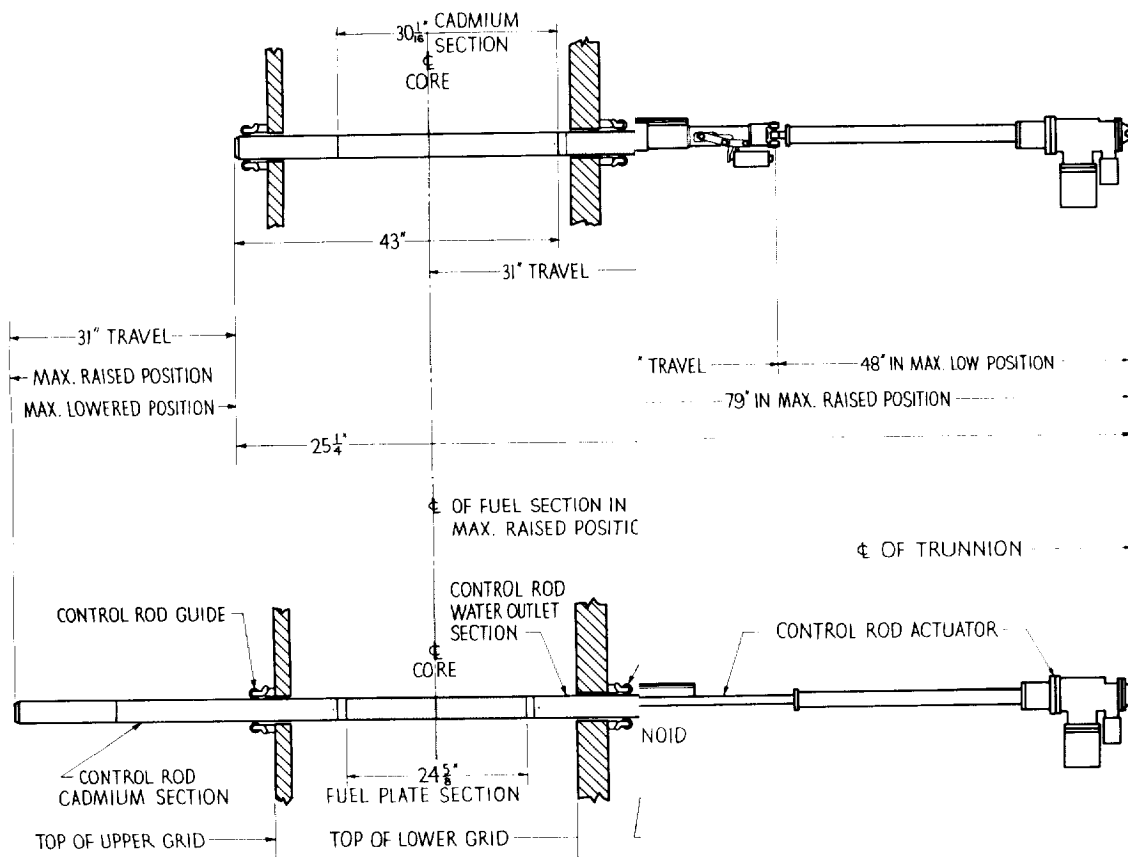


Figure 2.31



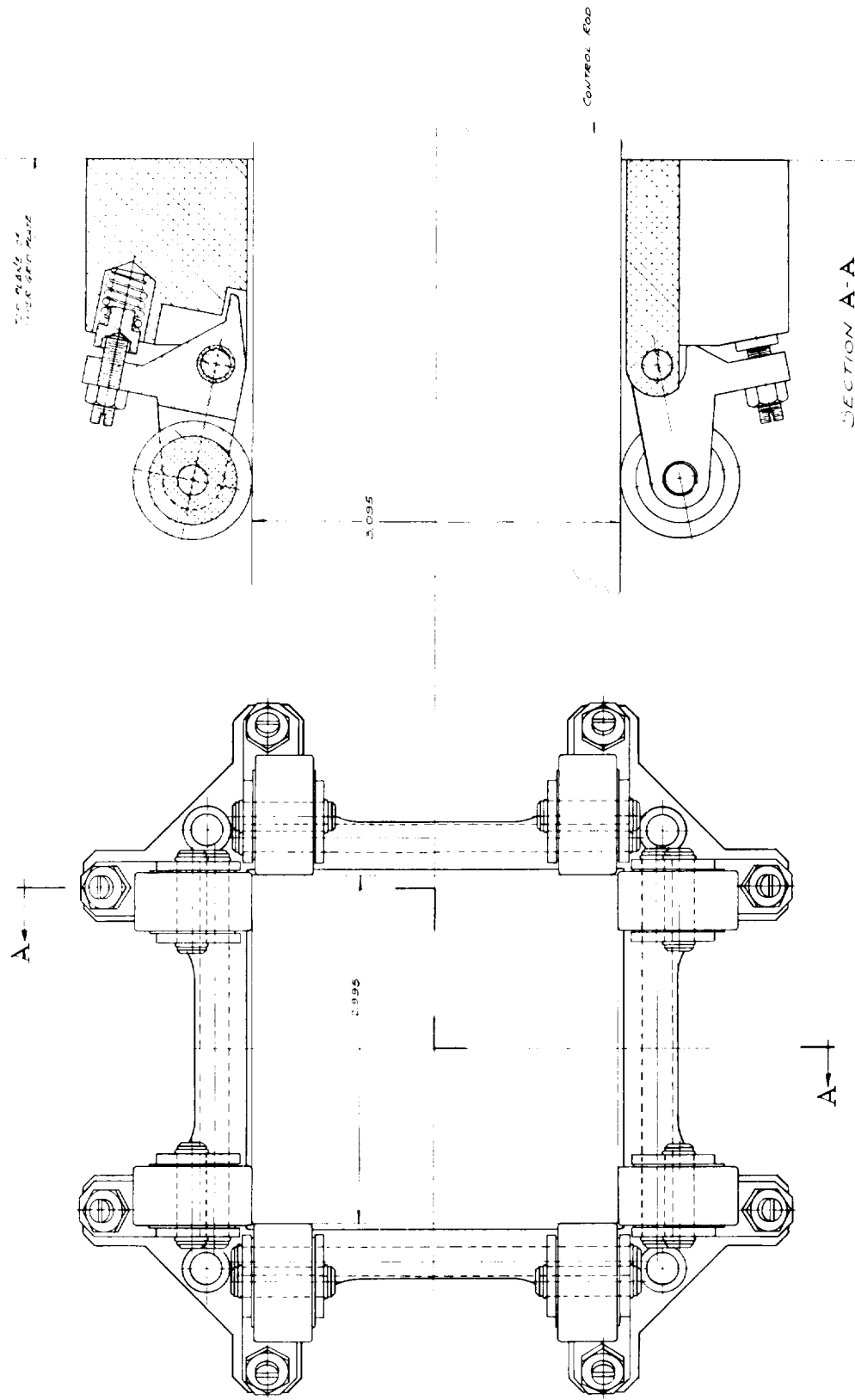


Figure 2.32 - Shim-rod floating-guide bearing.



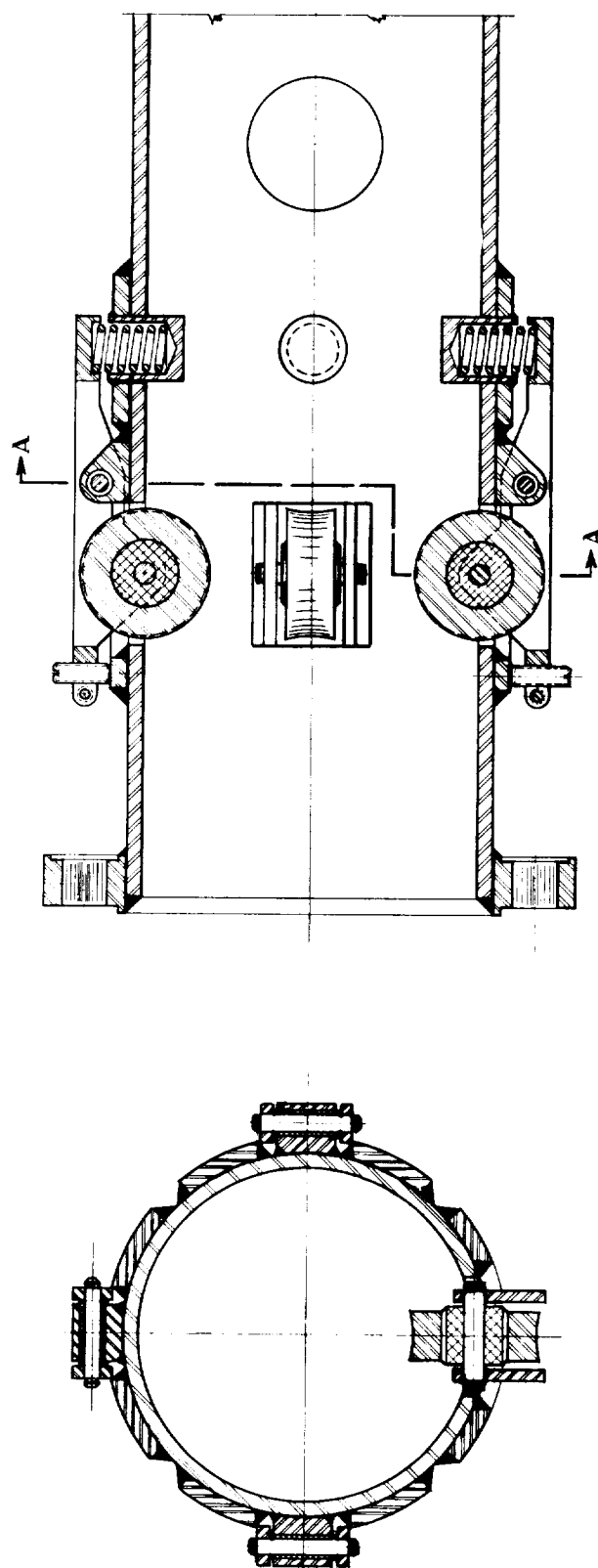


Figure 2.34 - Lower shim-rod guide bearing.

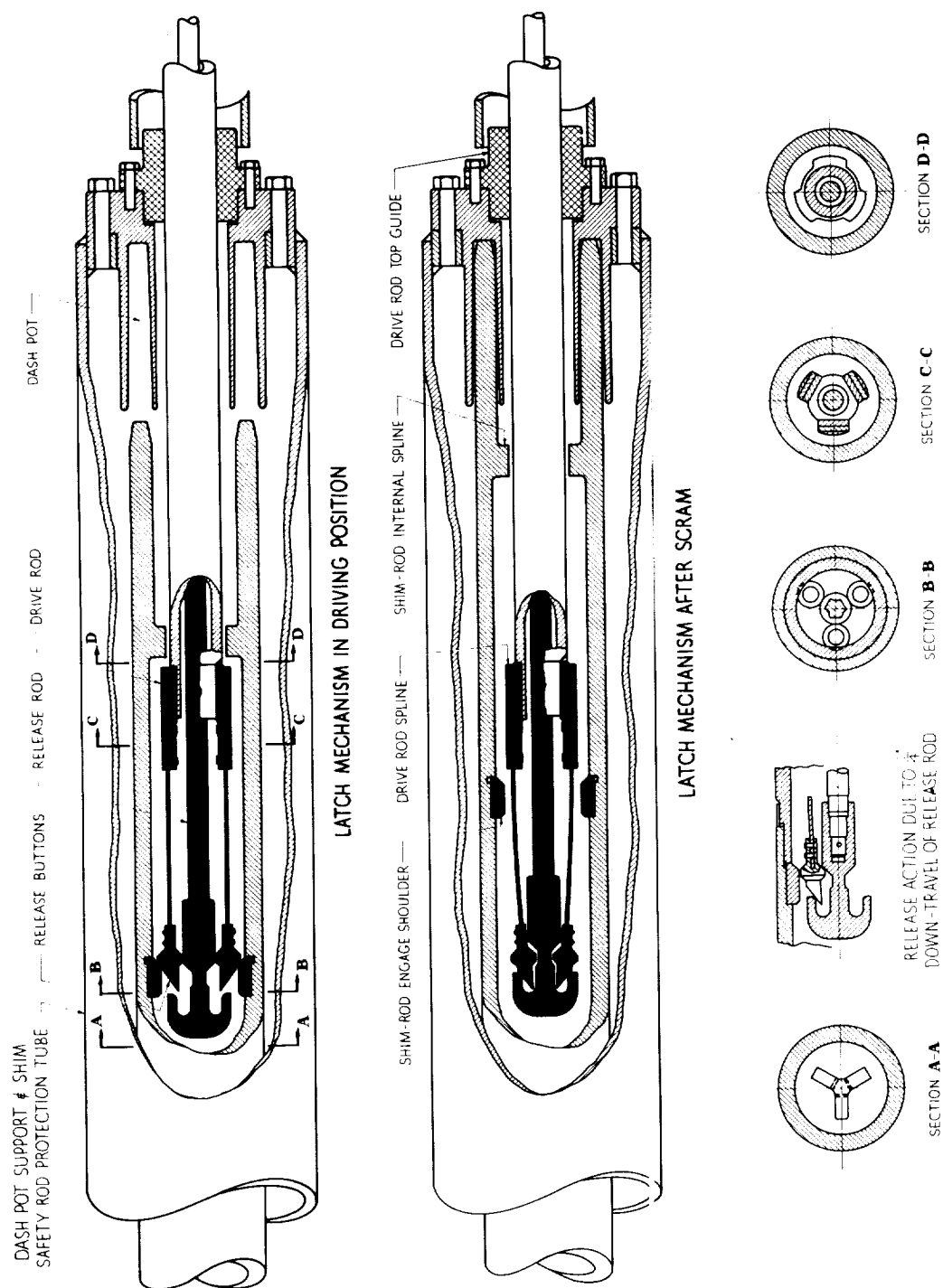


Figure 2.35 - Shim-safety rod scram release.

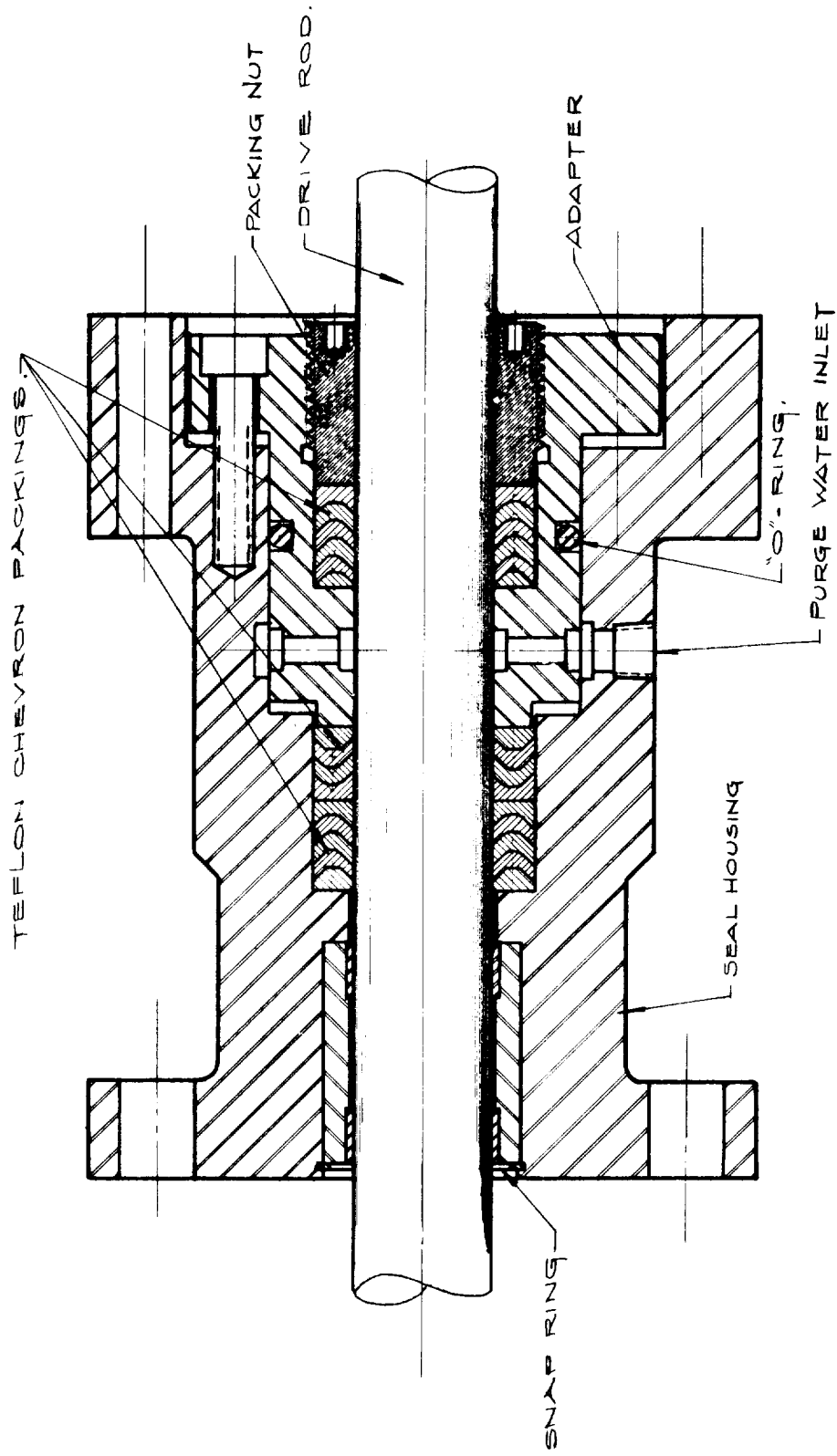


Figure 2.36 - Drive-rod seal assembly.





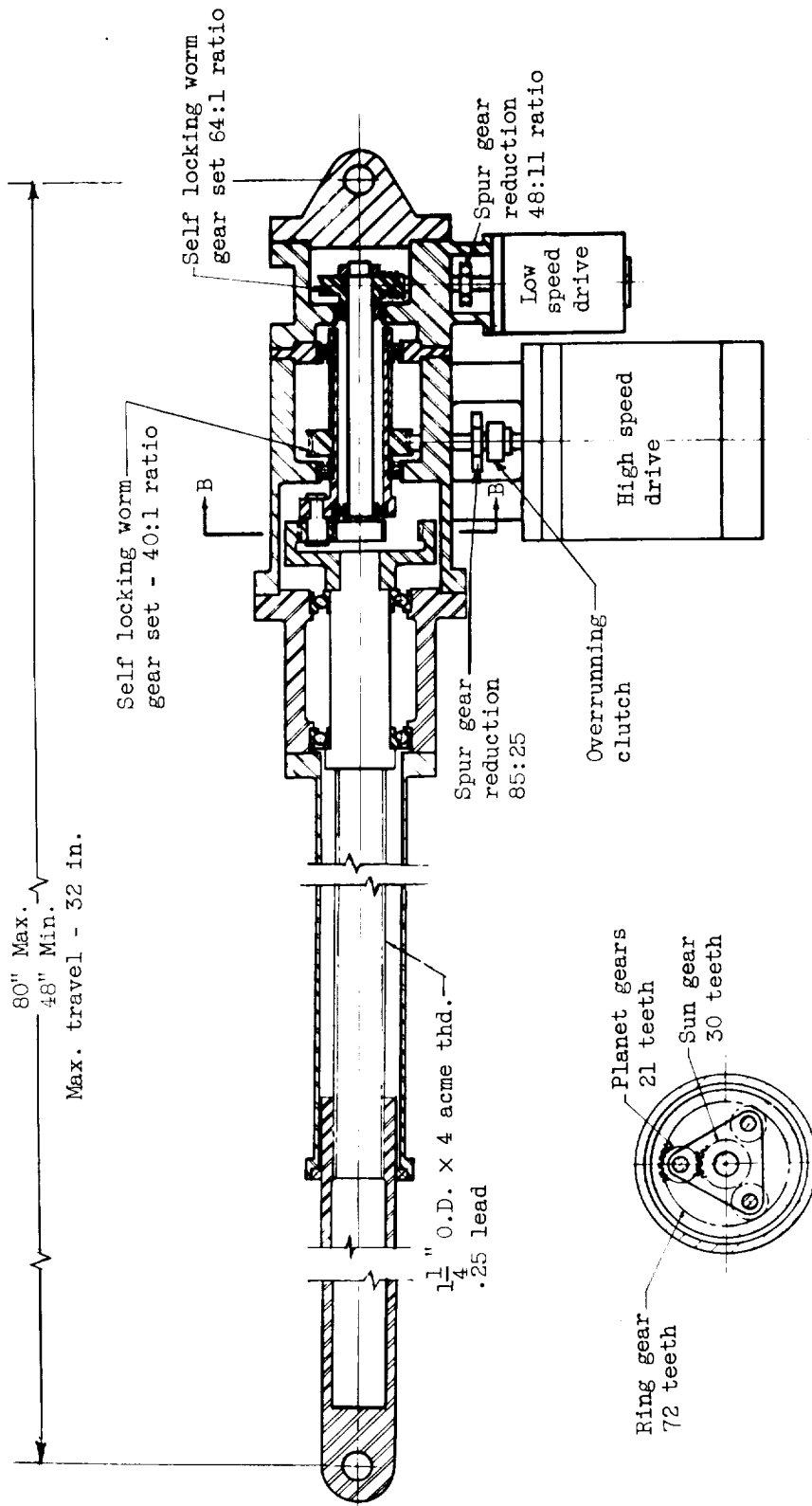


Figure 2.38 - Drive-rod actuator.

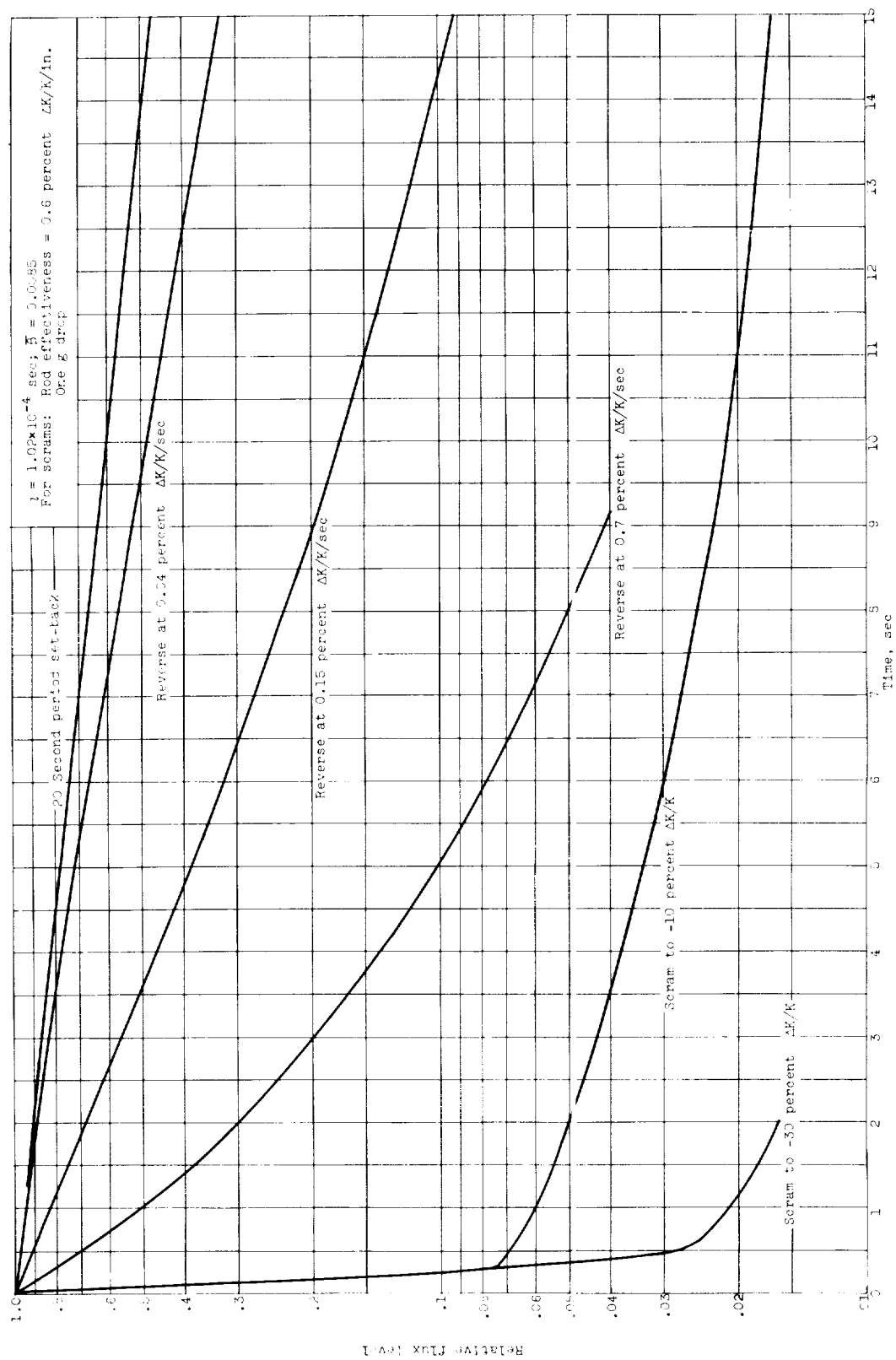


Figure 2.39 - Effect of cut-backs on flux level.

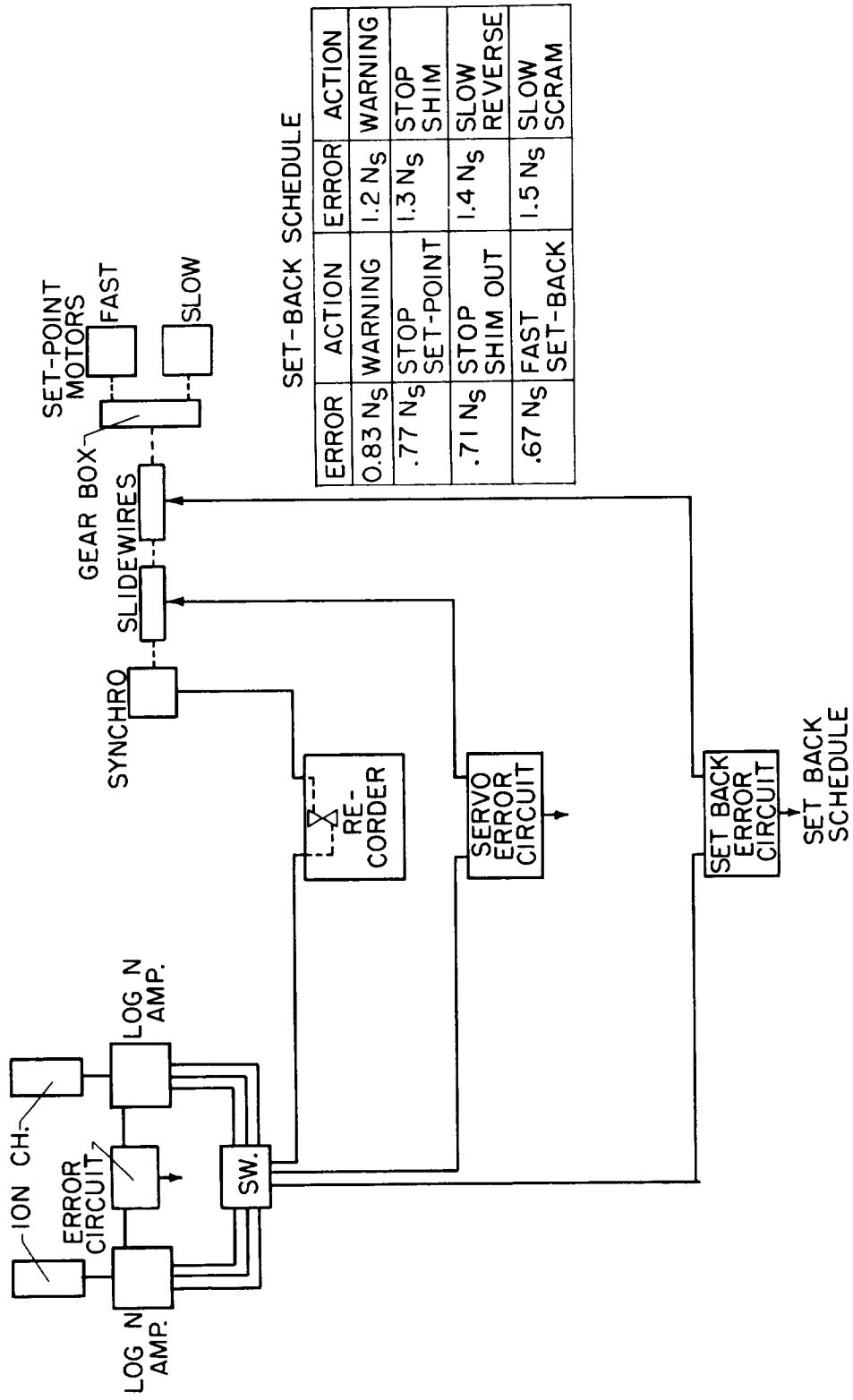


Figure 2.40 - Set back schedule.

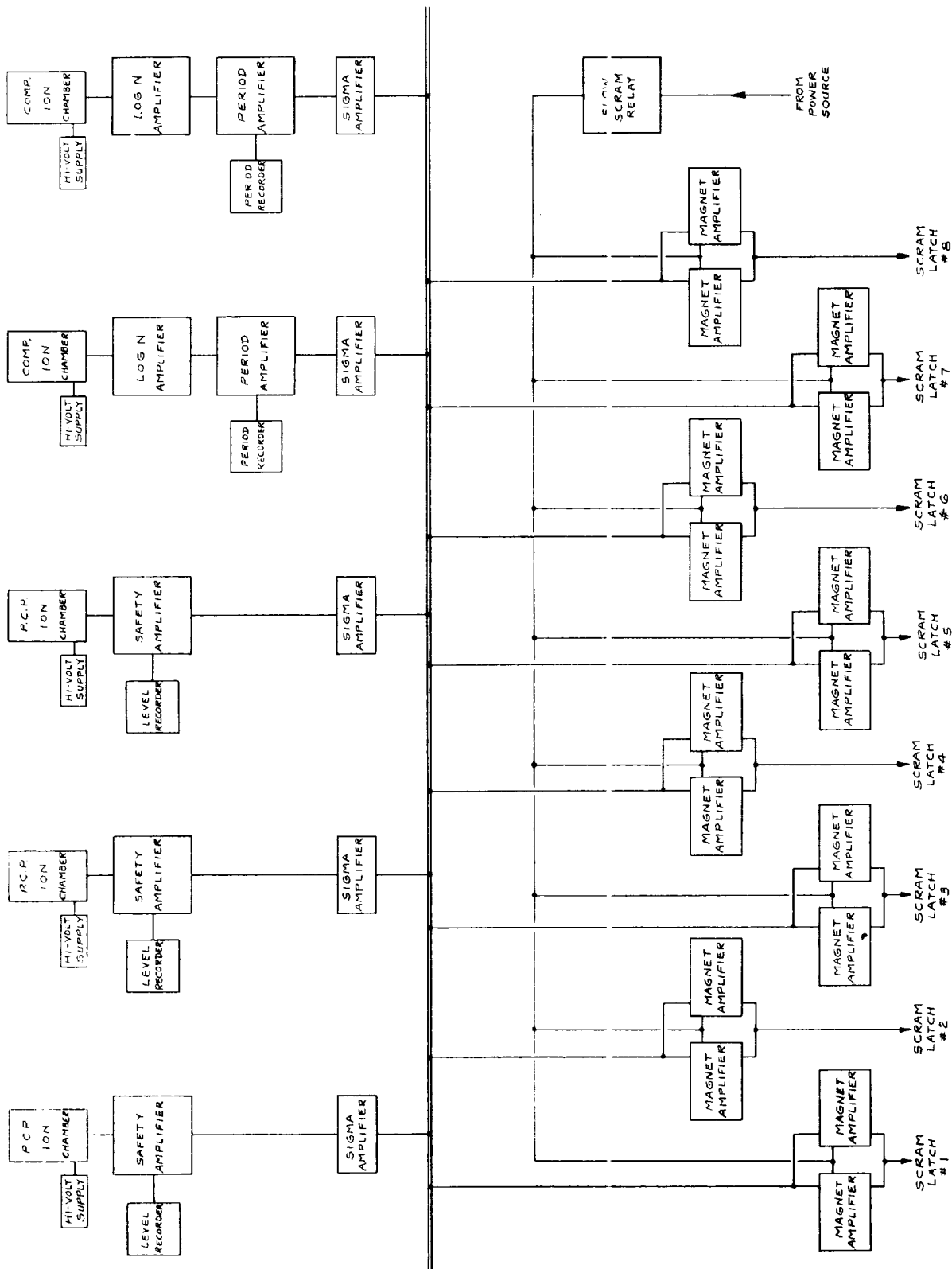


Figure 2.41 - Fast scram safety system.

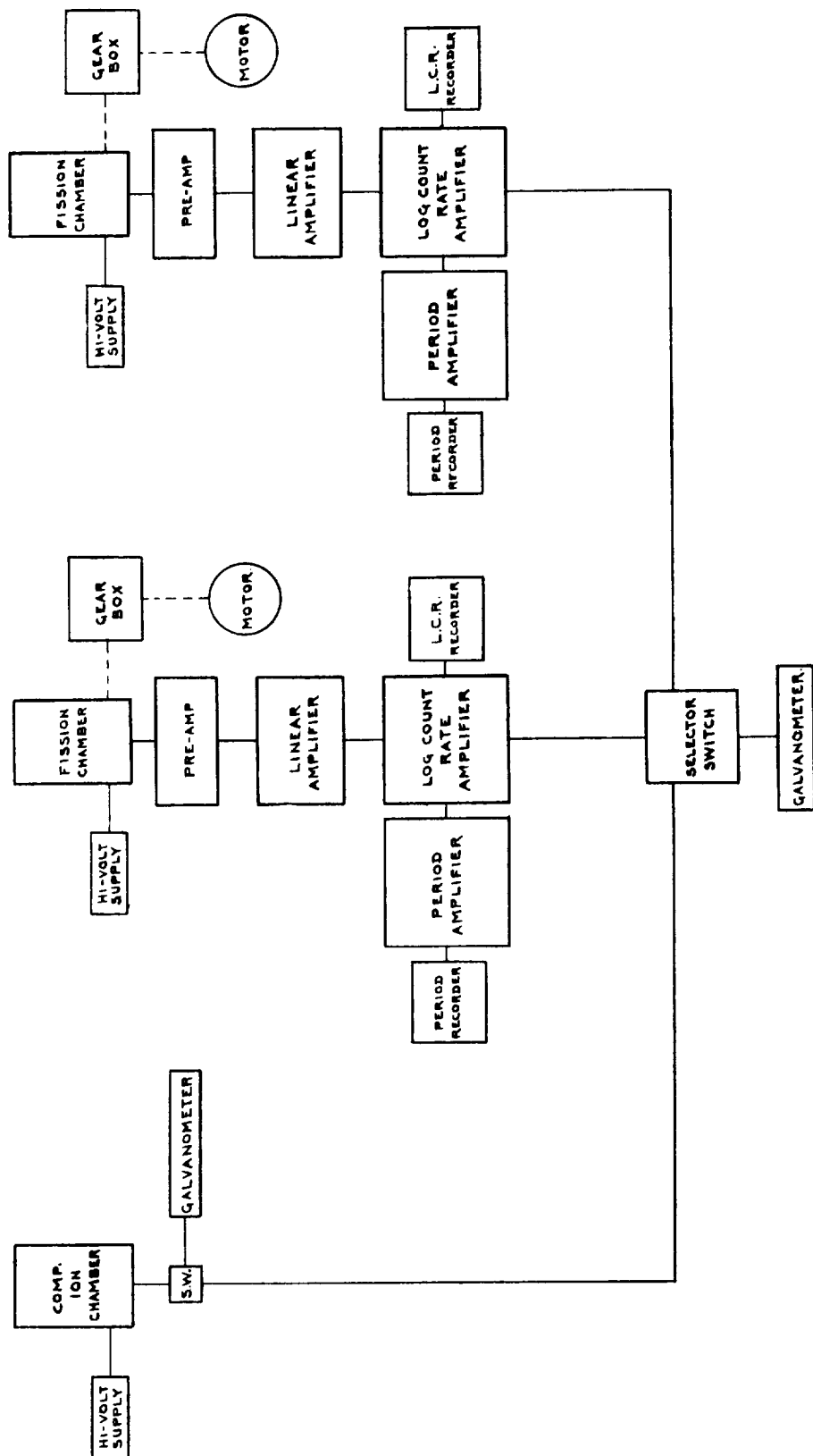


Figure 2.42 - Galvanometer system.

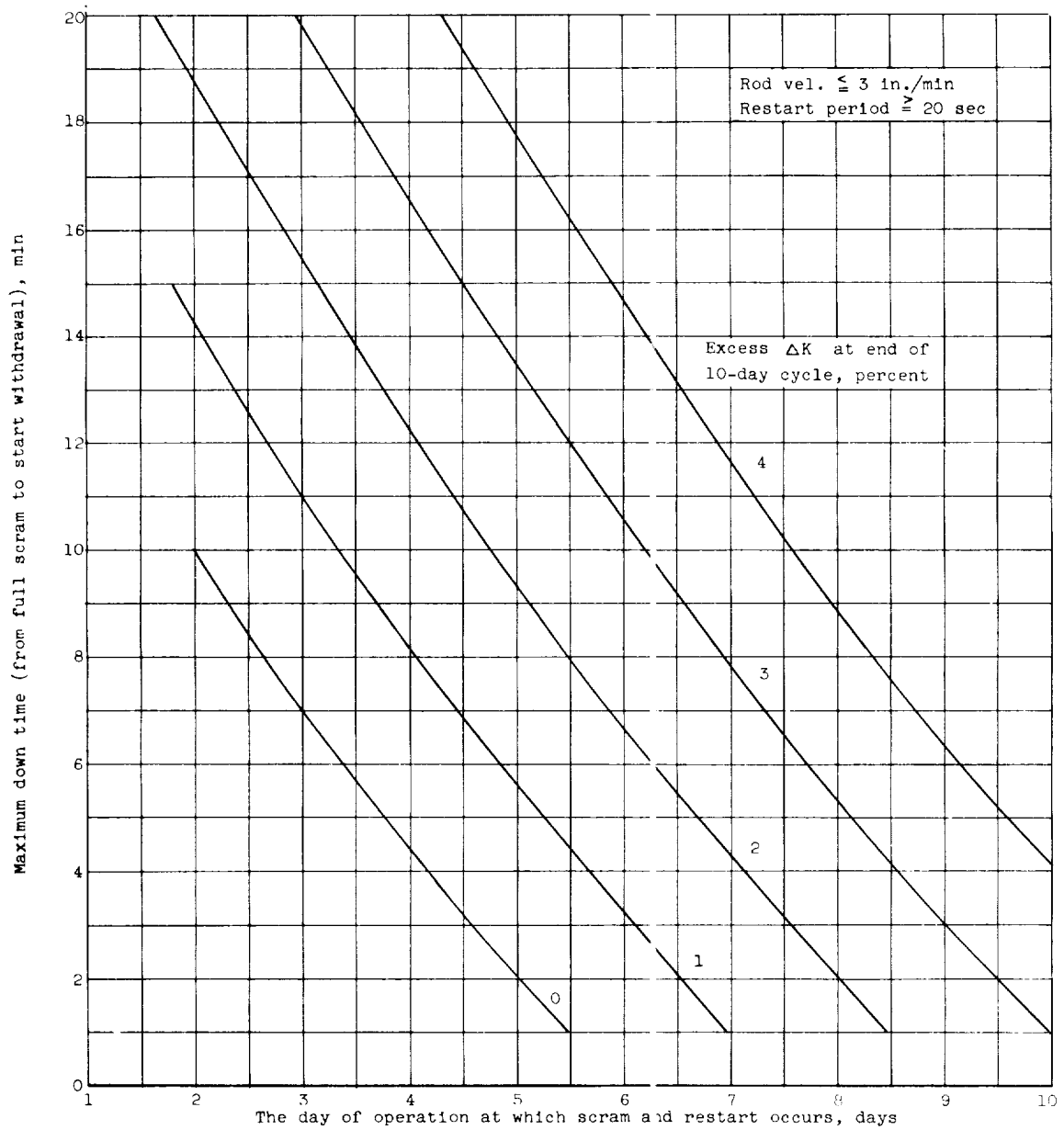


Figure 2.43 - Allowable times in which to restart after a recent shutdown.

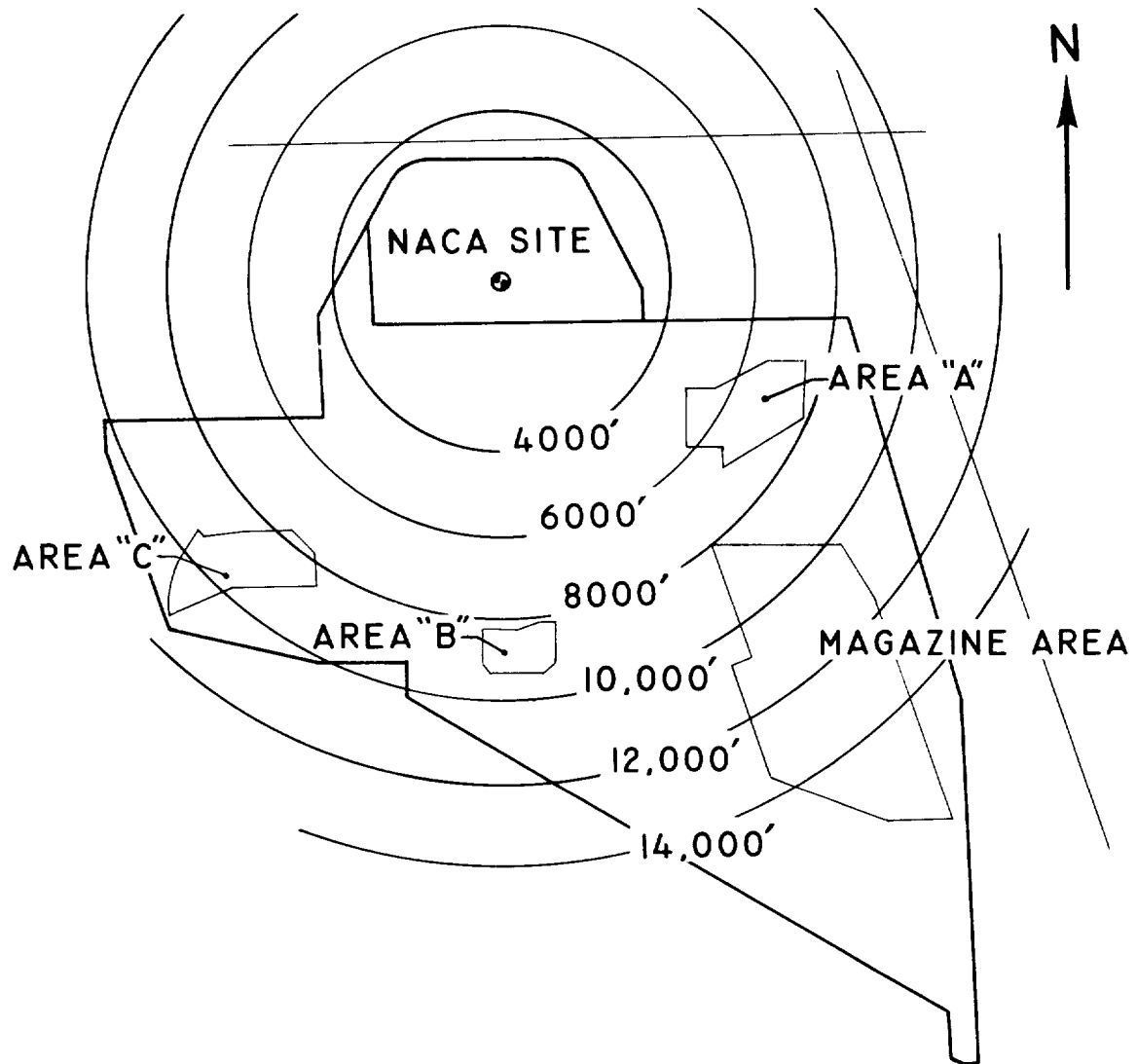


Figure 3.1 - Map of Plum Brook Ordnance Works.

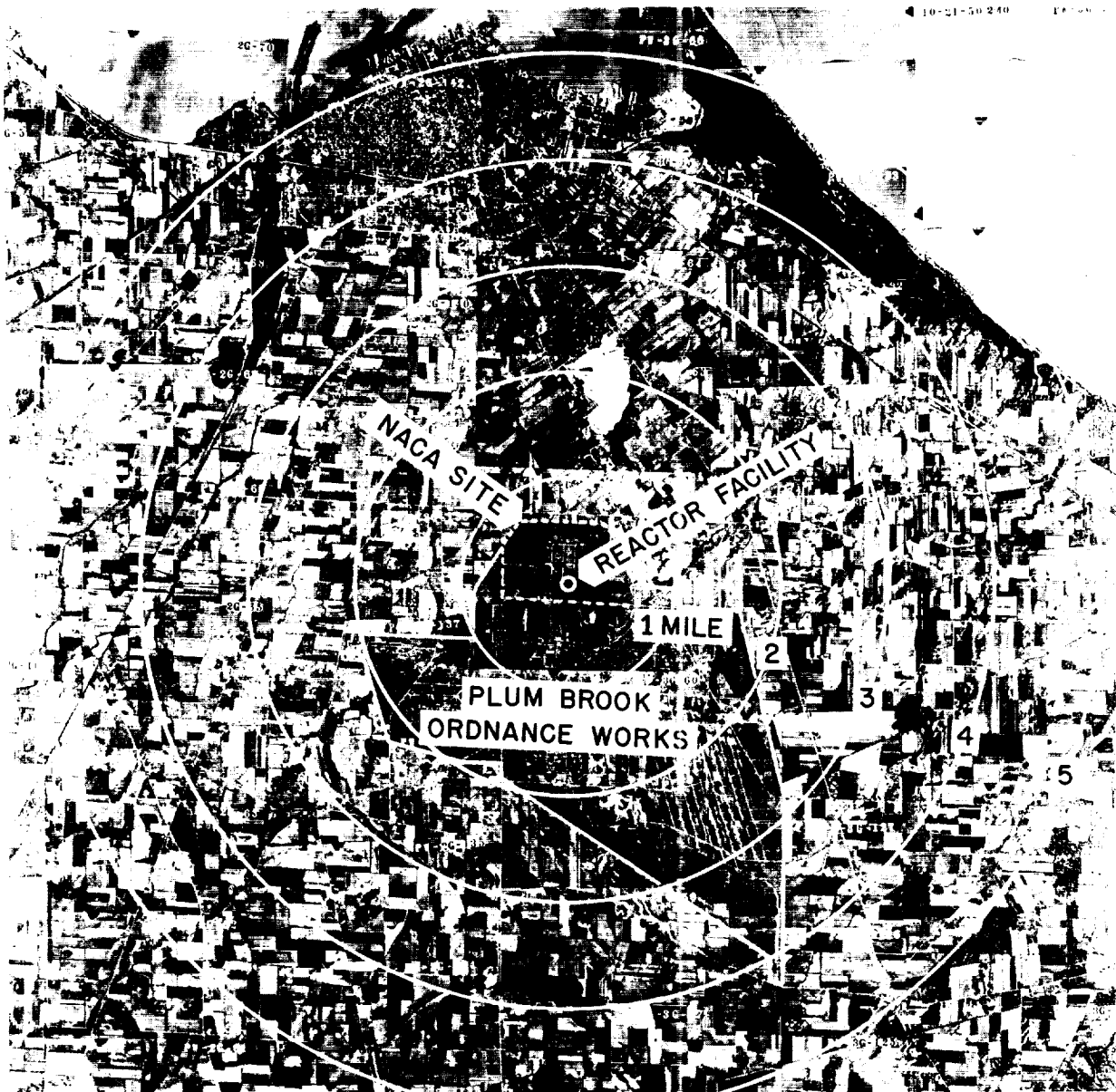


Figure 3.2 - Aerial mosaic of site area.



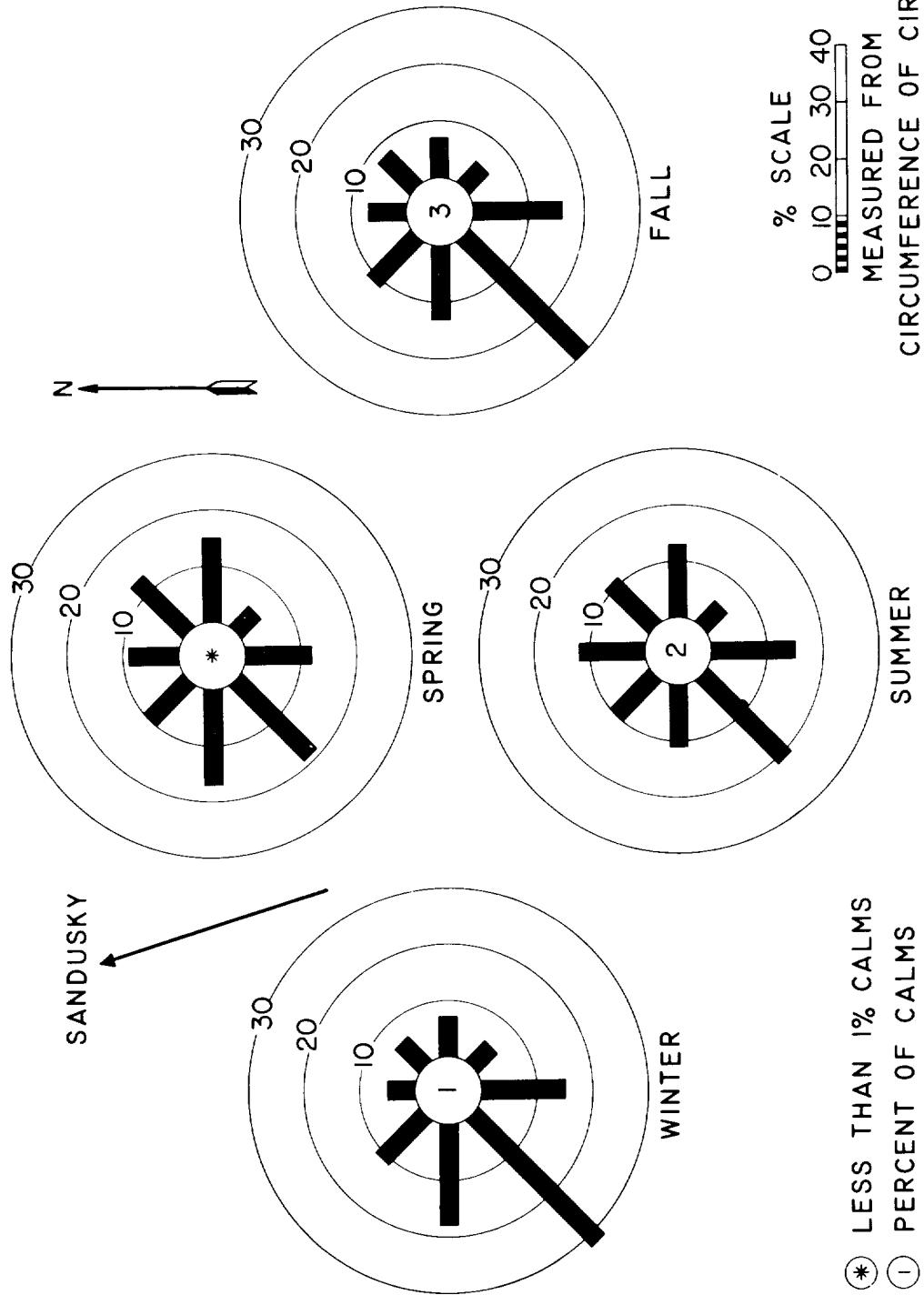


Figure 3.3 - Percentage frequency of surface winds from directions shown. New post office building, Sandusky, Ohio. Hourly observations December, 1949 - November, 1954.

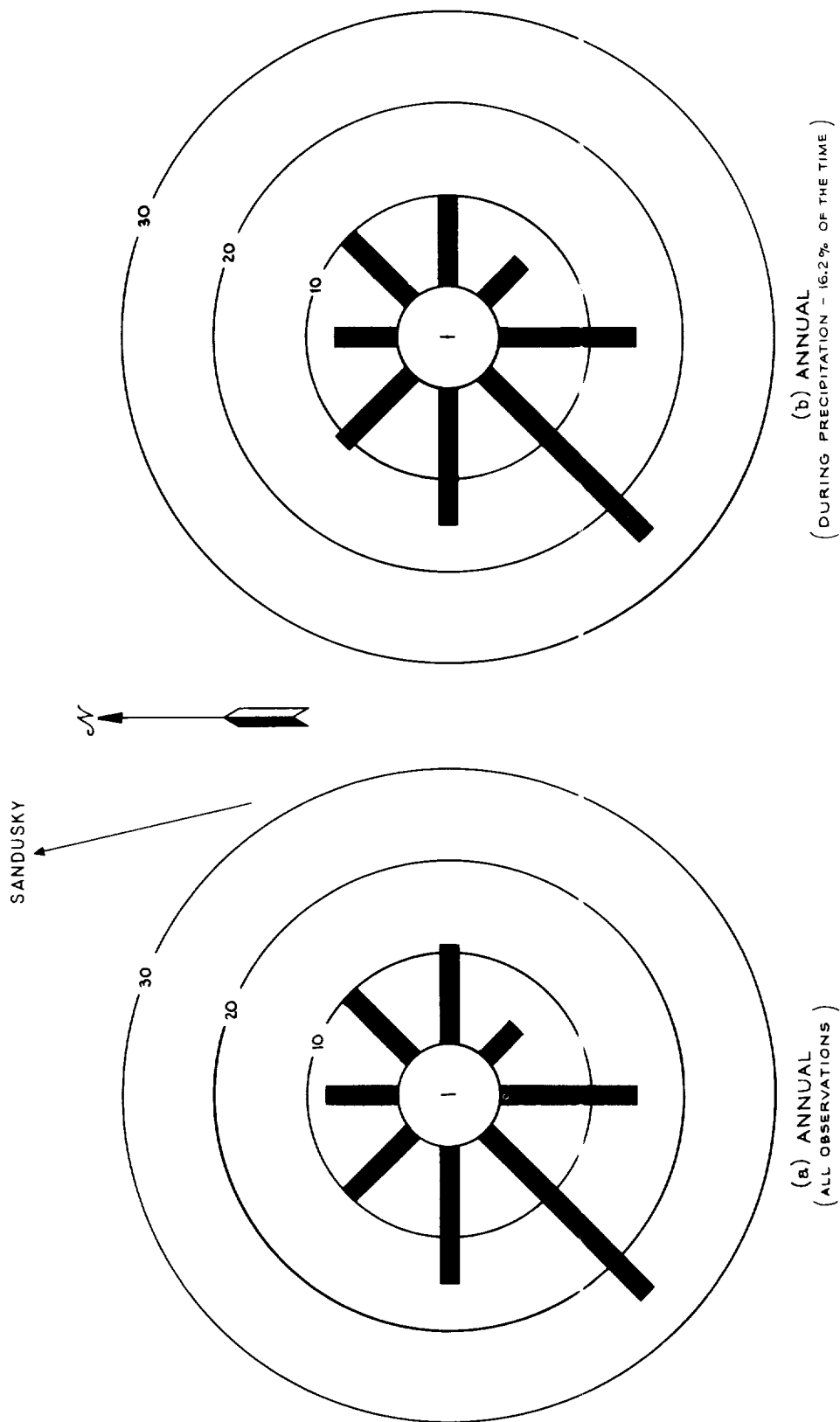
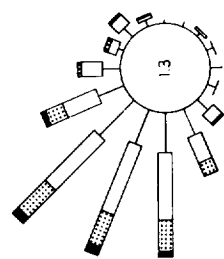
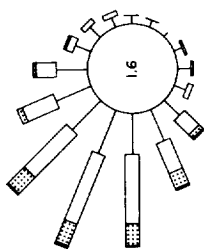


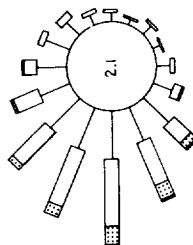
Figure 3.4 - Percentage frequency of surface winds for a) all observations, and b) during precipitation from directions shown. New post office building, Sandusky, Ohio. Hourly observations. December, 1949 - November, 1954.



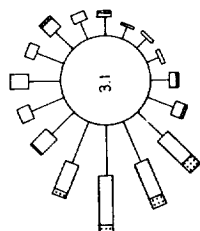
5000 METERS



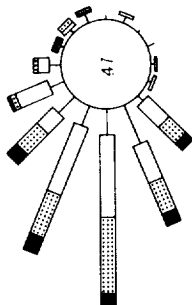
3000 METERS



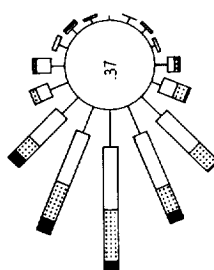
2000 METERS



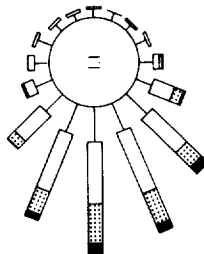
1000 METERS



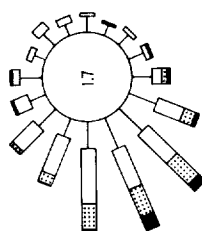
5000 METERS



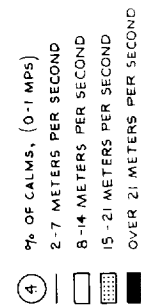
3000 METERS



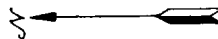
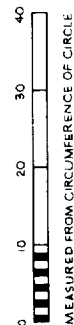
2000 METERS



1000 METERS

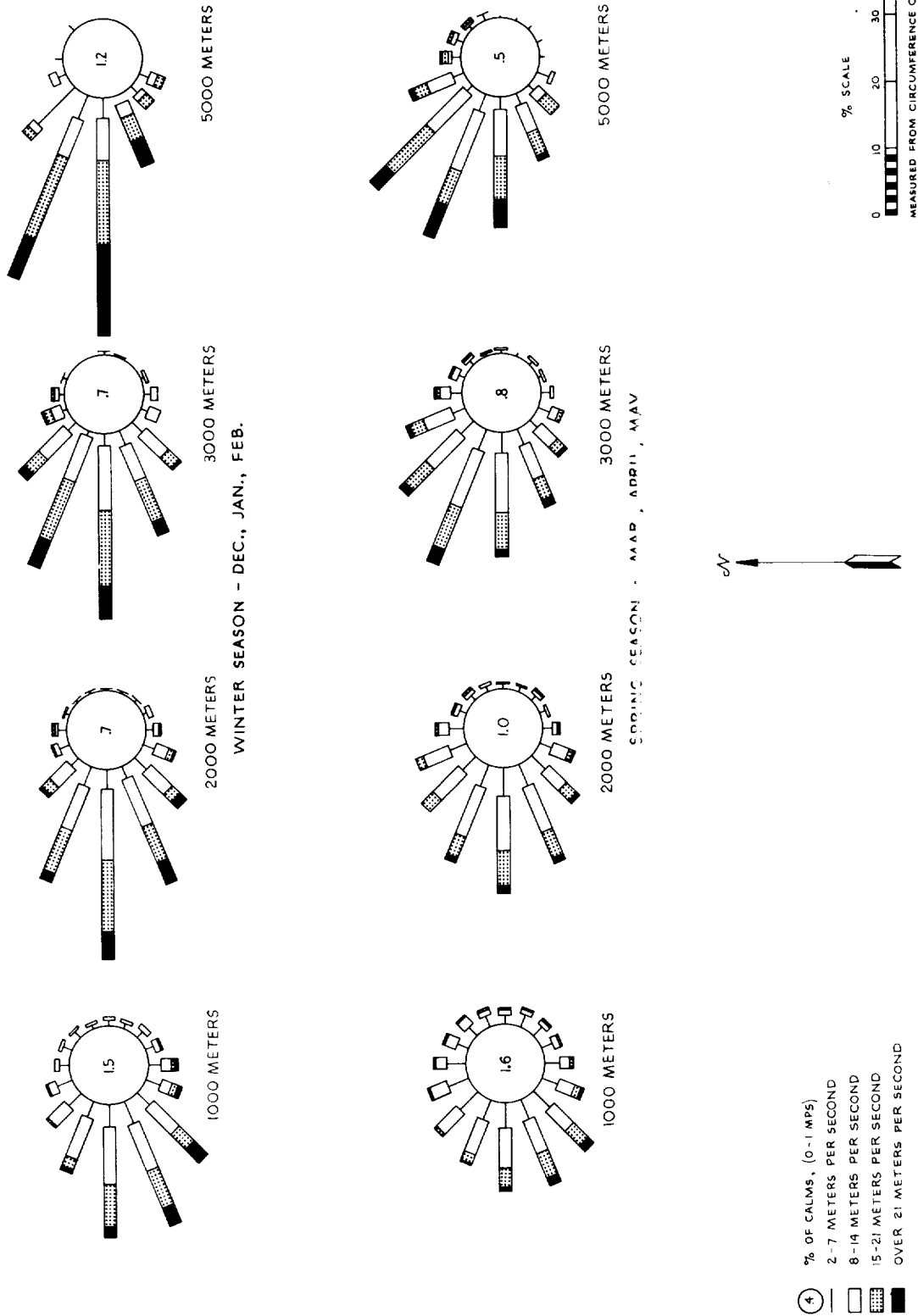


% SCALE



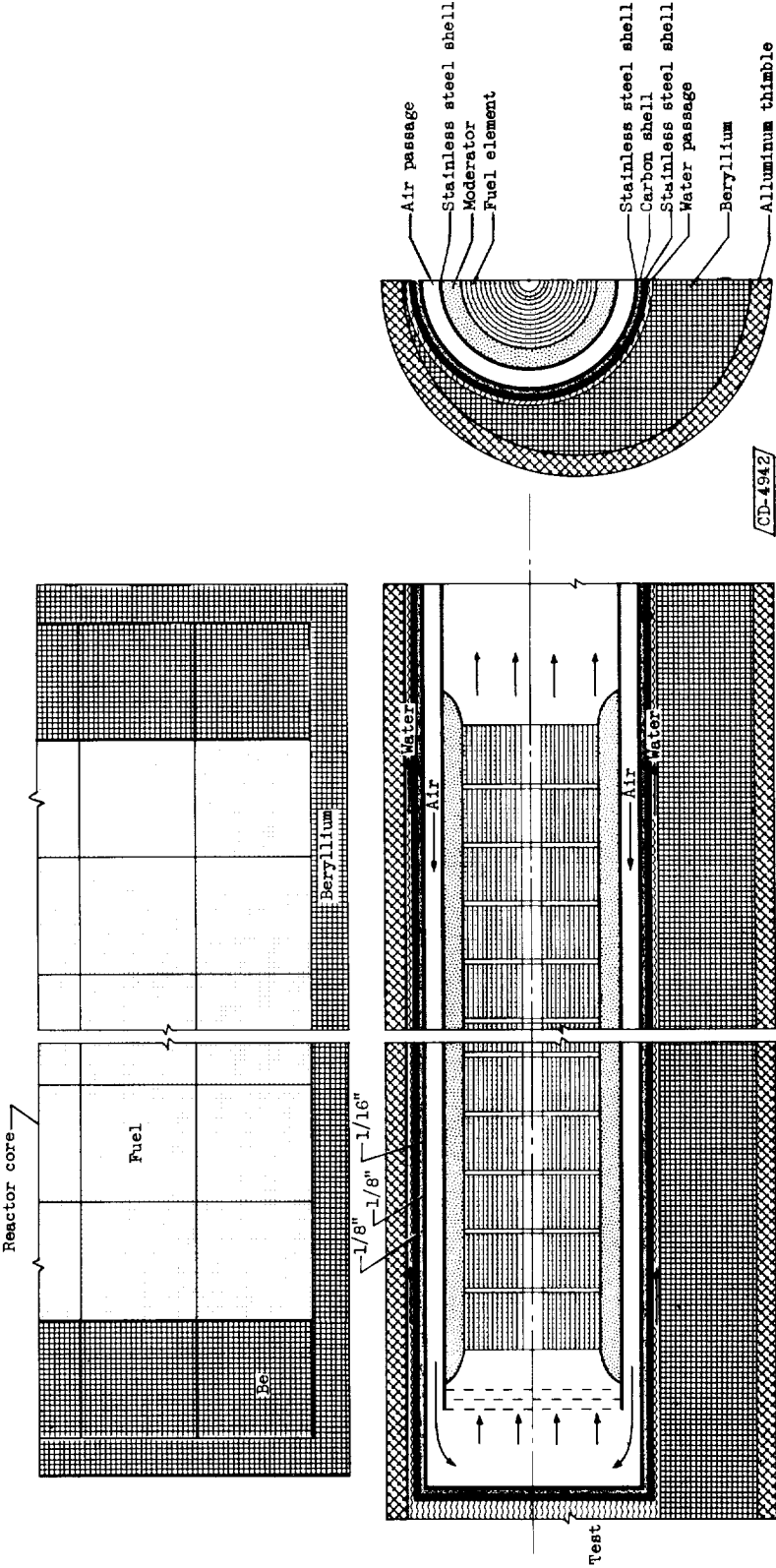
(a) Summer and fall

Figure 3.5 - Upper air wind roses for Cleveland, Ohio, 1926 through 1938 (ref. 3.1).



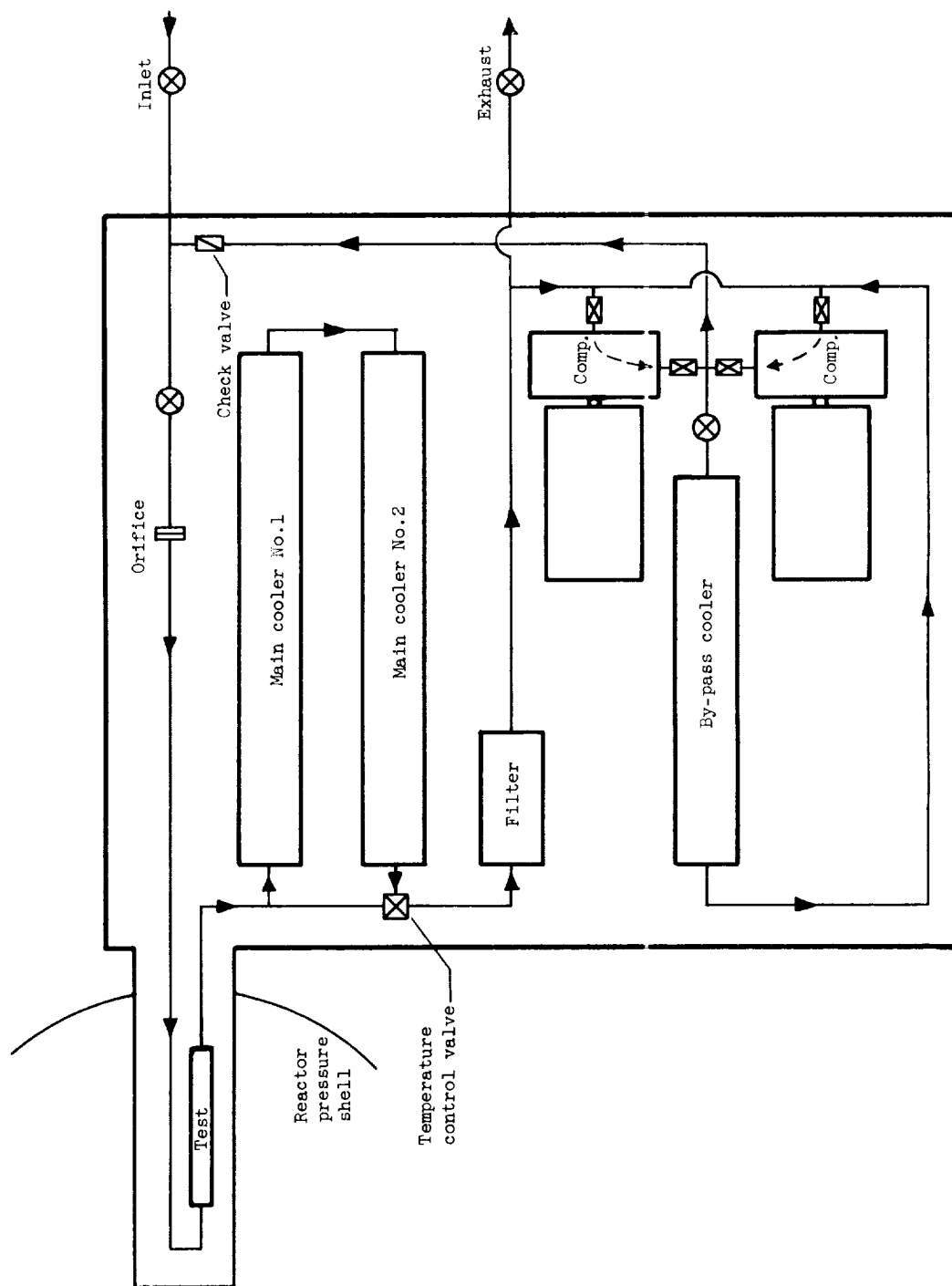
(b) Winter and spring.

Figure 3.5 - Concluded. Upper air wind roses for Cleveland, Ohio. 1926 through 1938. (ref. 3.1).



(a) Arrangement of test element in HTI hole.

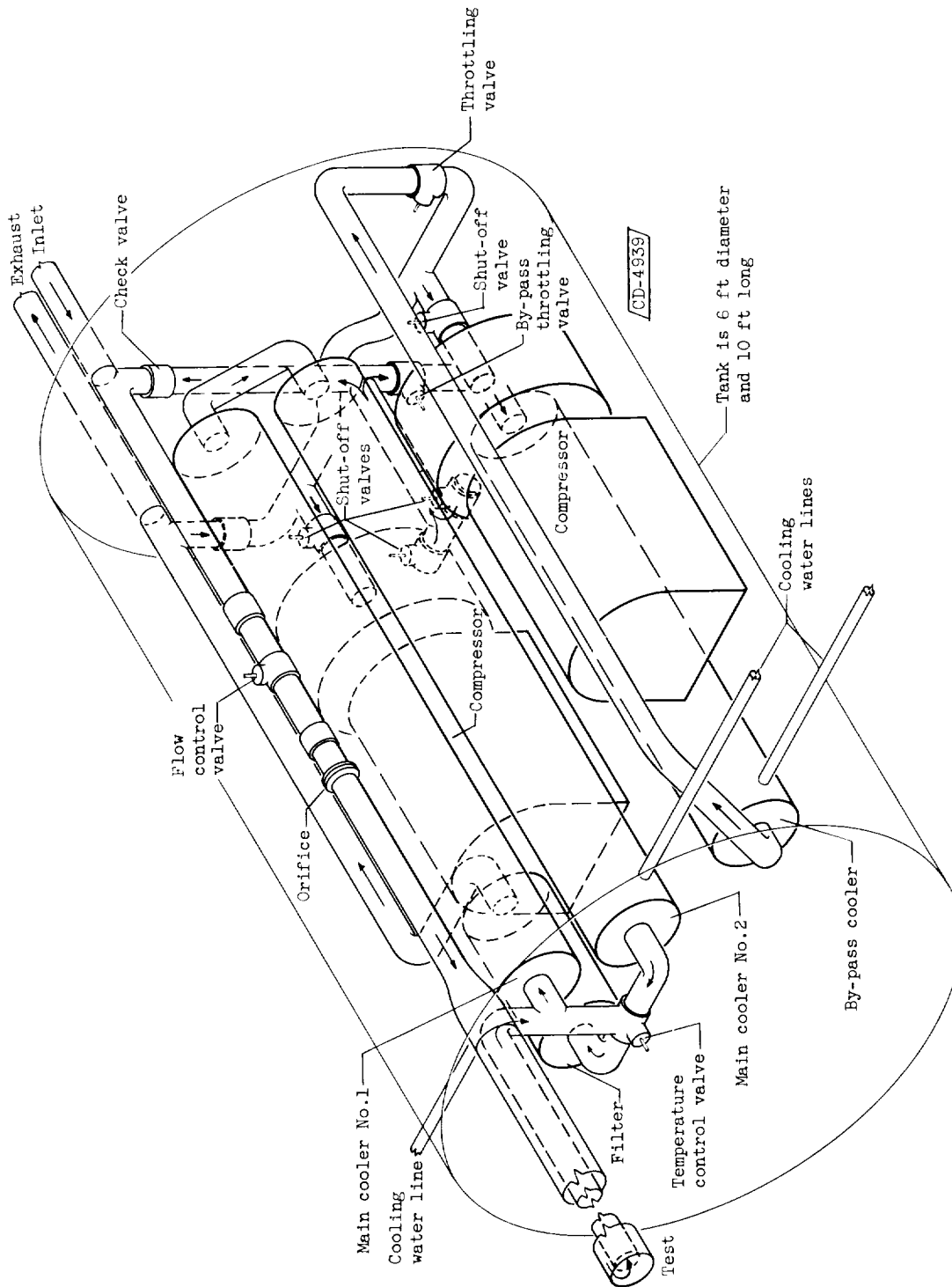
Figure 4.1 - Air-cooled fuel element experiment.



/CD-4944/

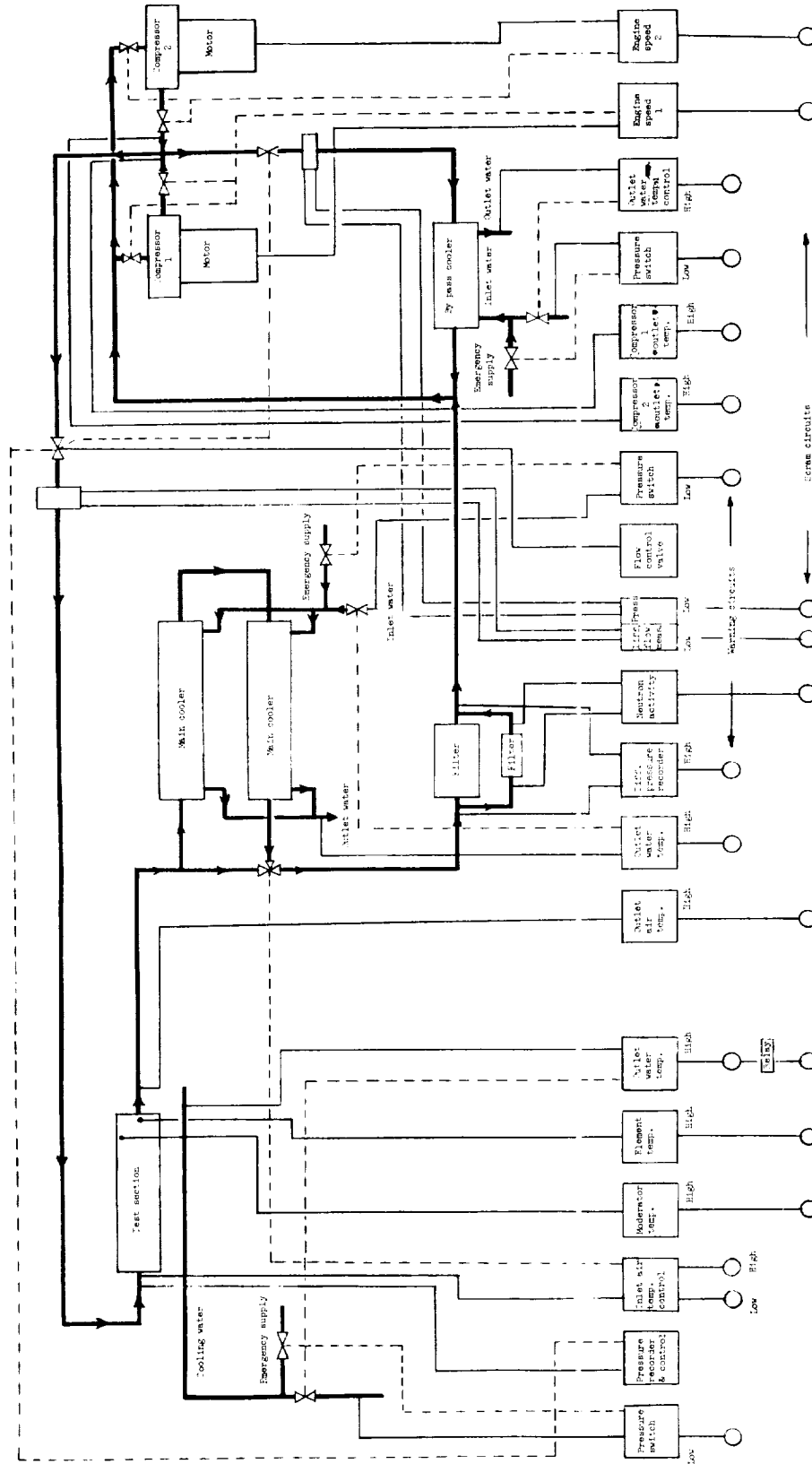
(b) Flow diagram.

Figure 4.1 - Continued. Air-cooled fuel element experiment.



(c) Arrangement of auxiliary equipment.

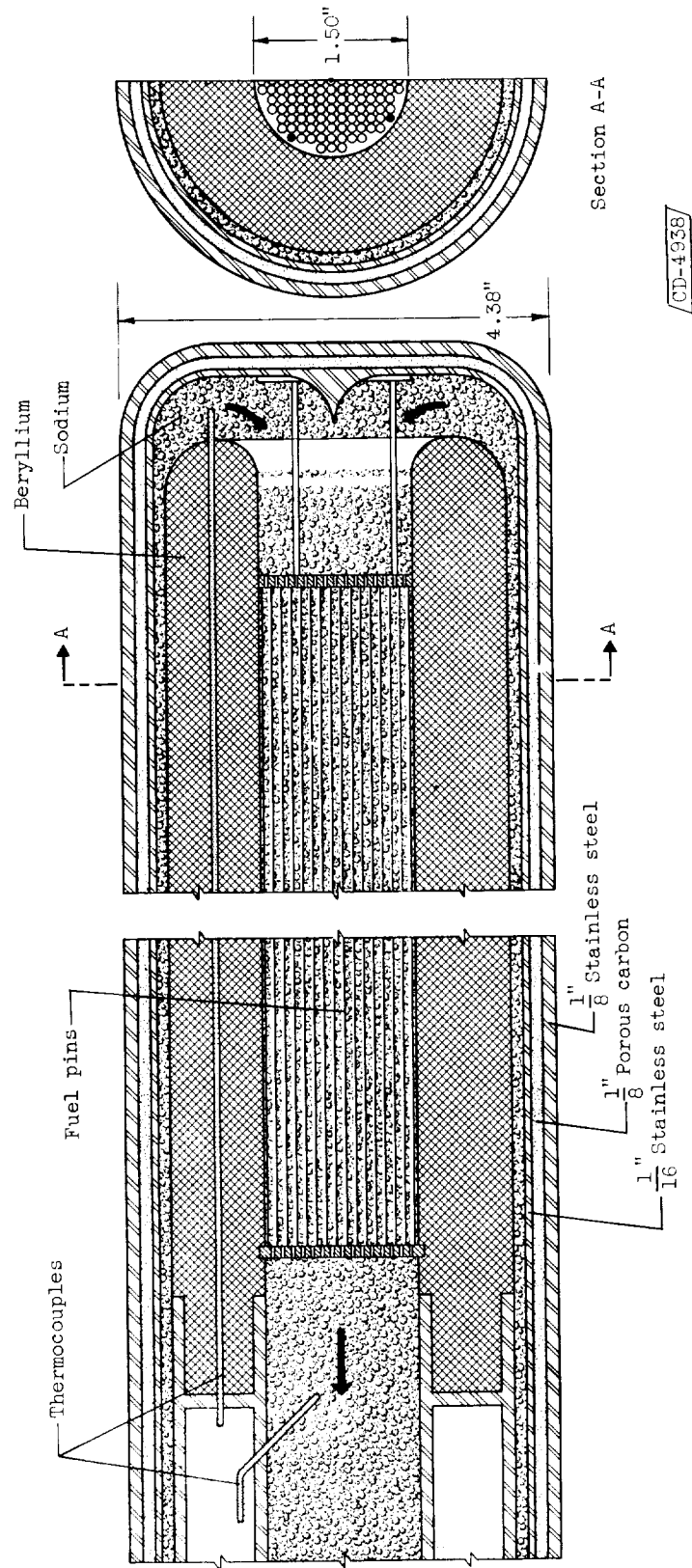
Figure 4.1 - Continued. Air-cooled fuel element experiment.



(d) Safety and control instrumentation.

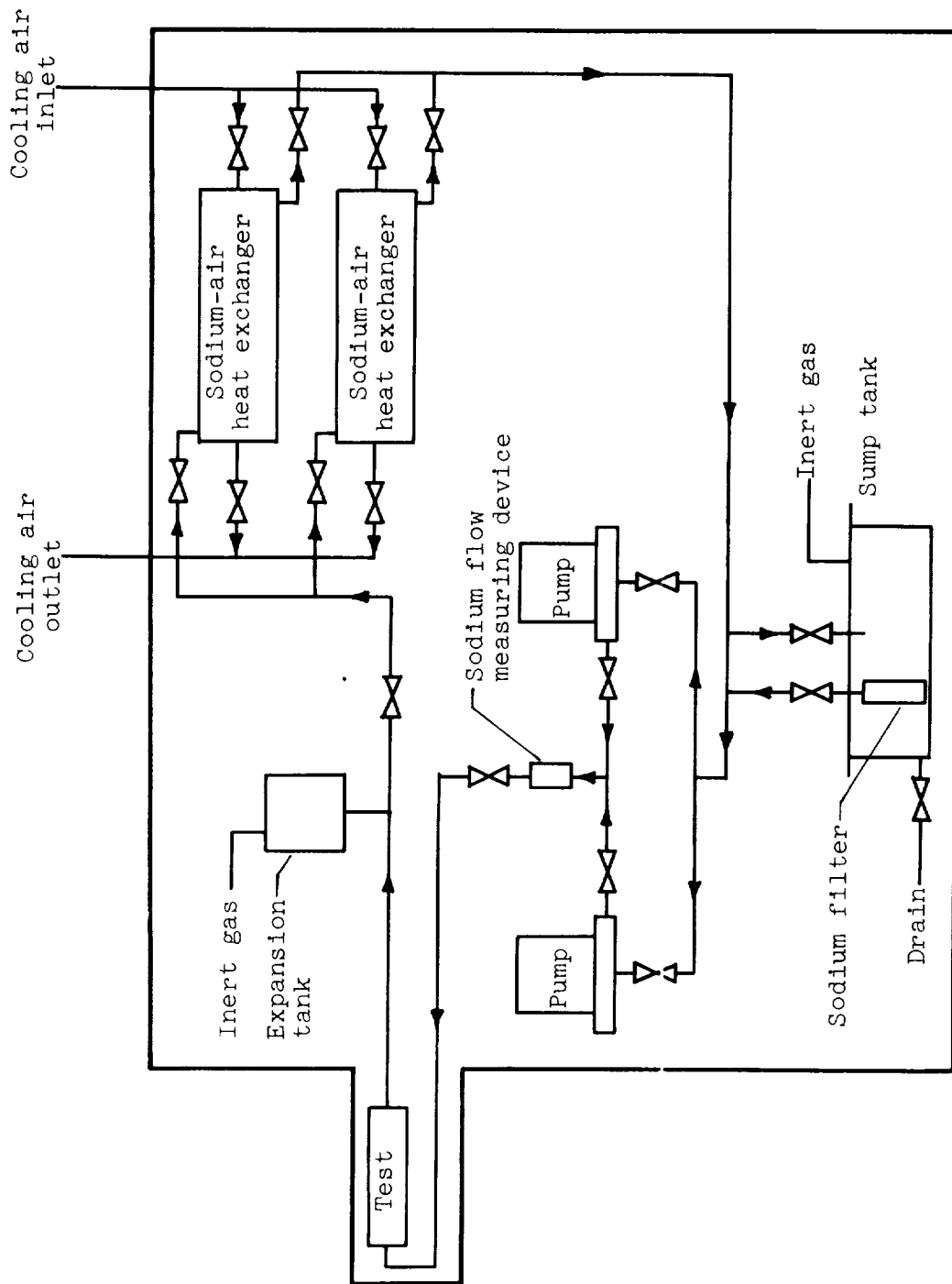
Figure 4.1 - Concluded. Air-cooled fuel element experiment.





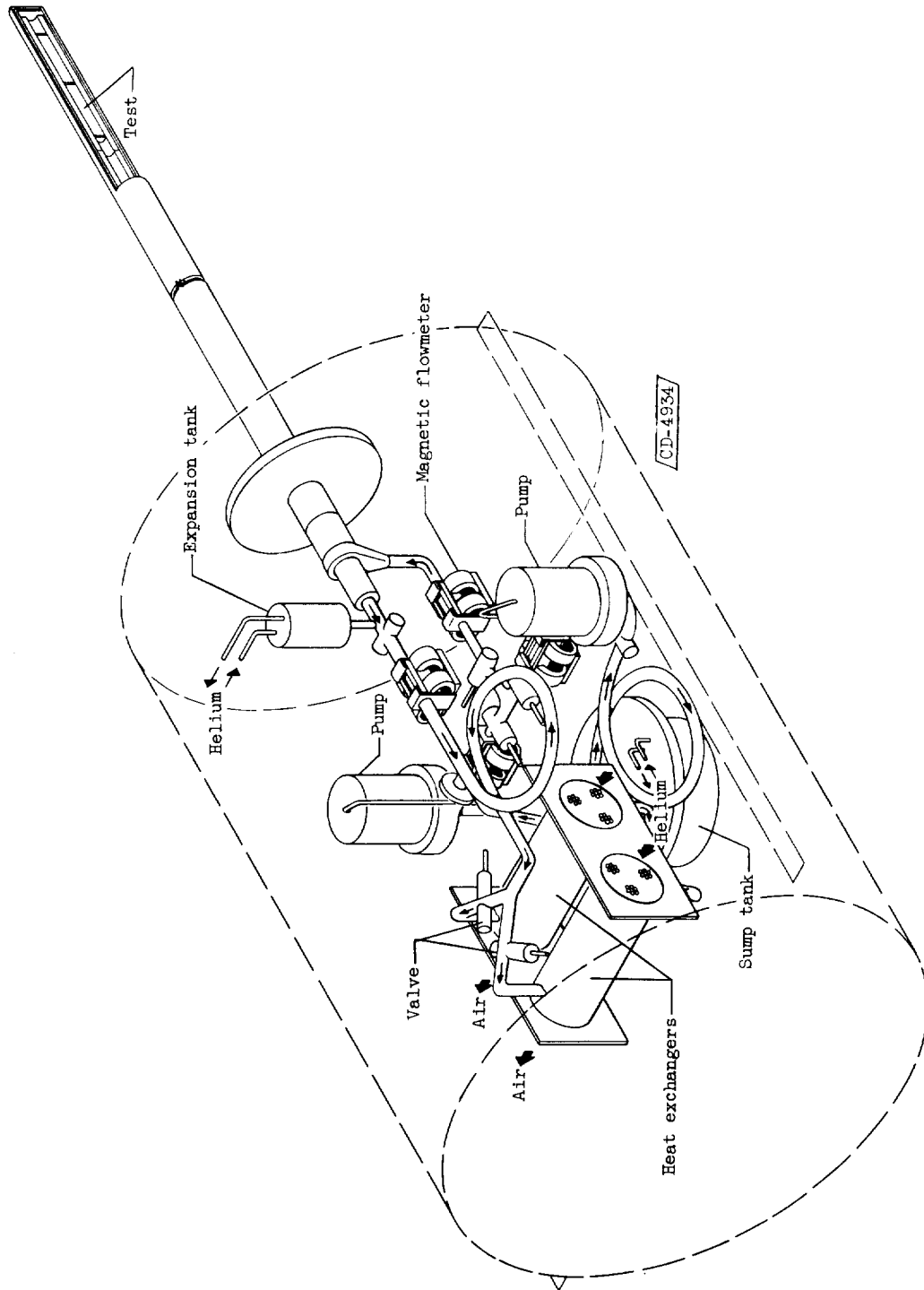
(a) Arrangement of test element.

Figure 4.2 - Liquid-cooled fuel element experiment.



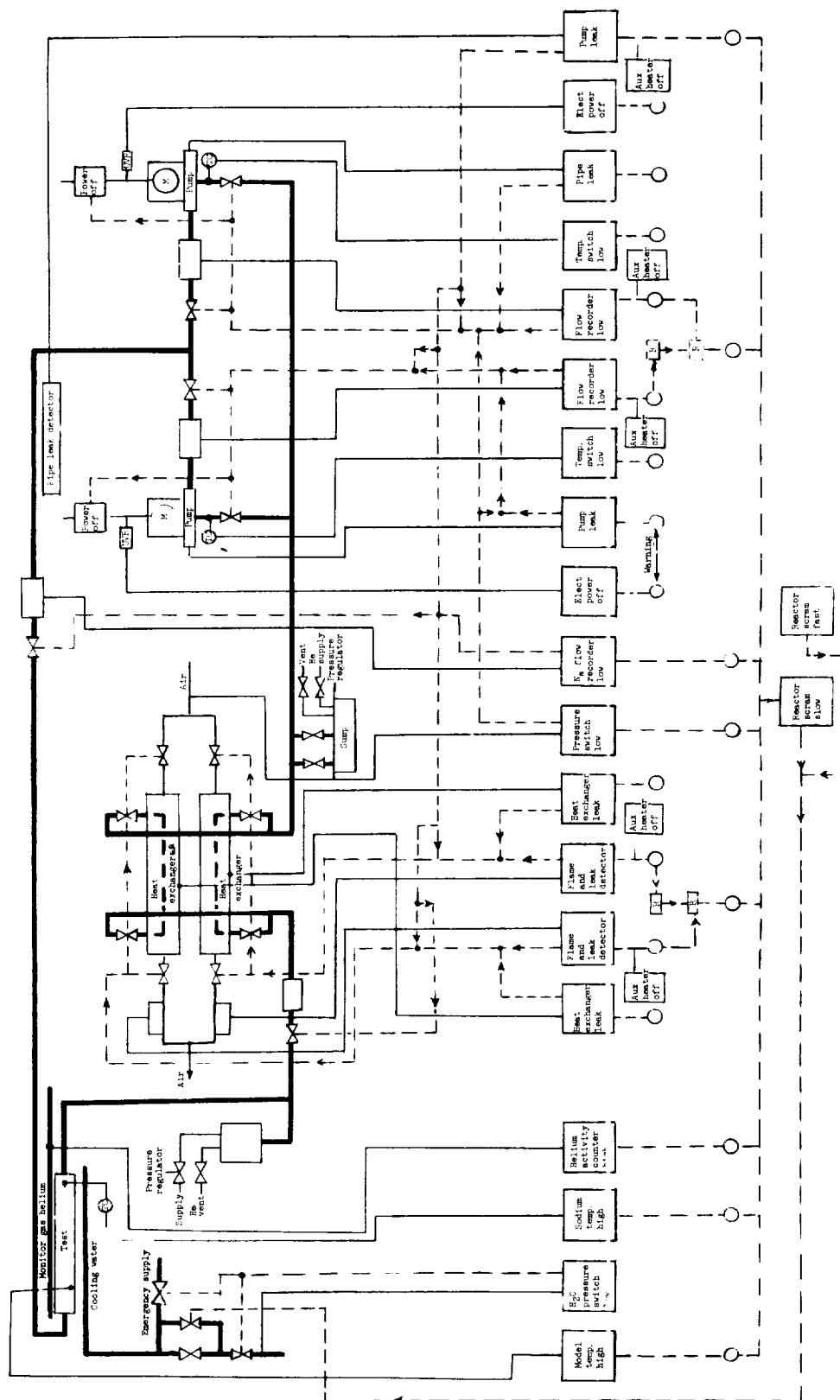
(b) Flow diagram.

Figure 4.2. - Continued. Liquid-cooled fuel element experiment.



(c) Arrangement of auxiliary equipment.

Figure 4.2 - Continued. Liquid-cooled fuel element experiment.



(d) Safety and control instrumentation

**Figure 4.2 - Concluded. Liquid-cooled fuel element experiment.**

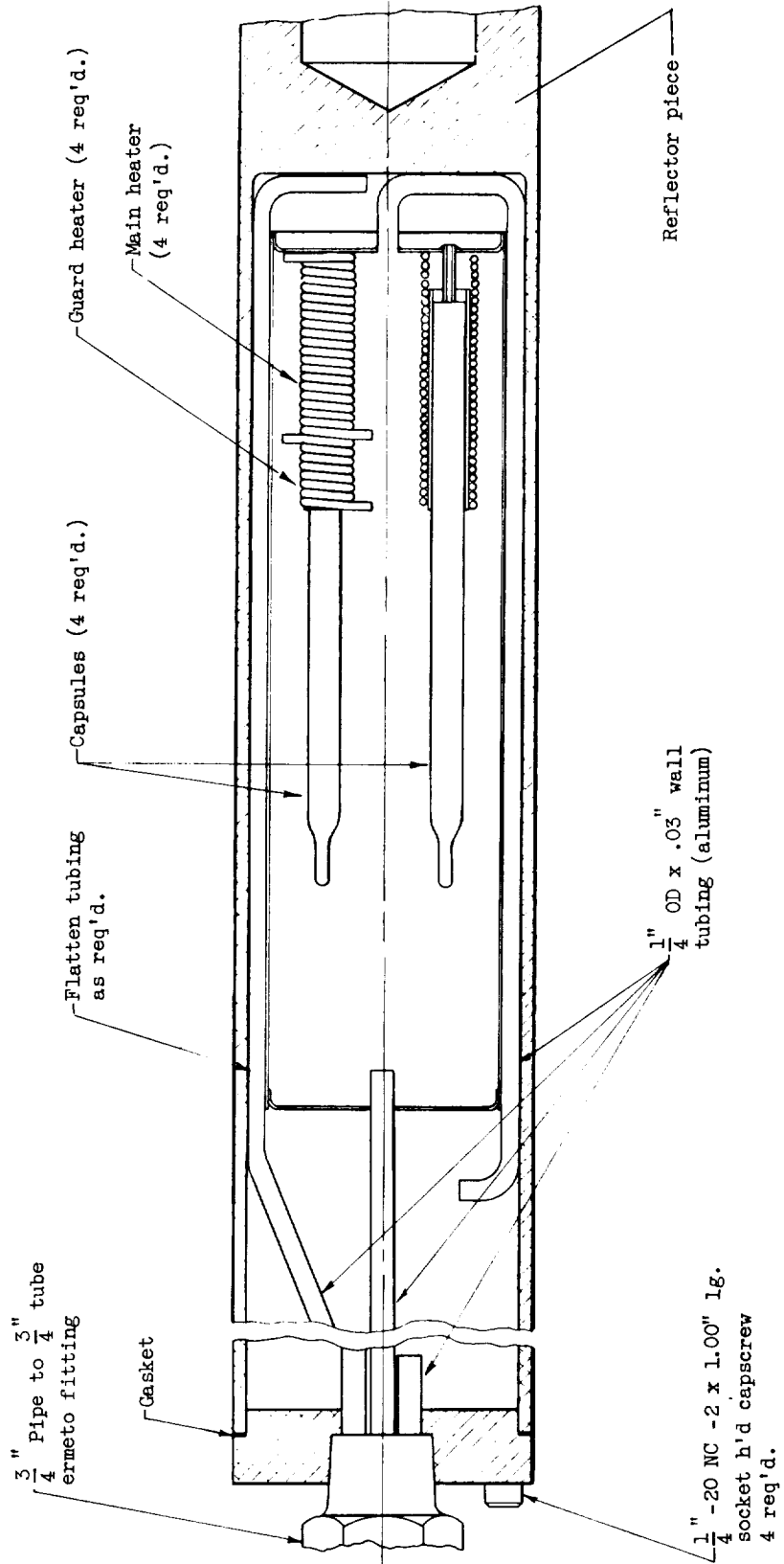


Figure 4.3 - Corrosion capsule experiment.

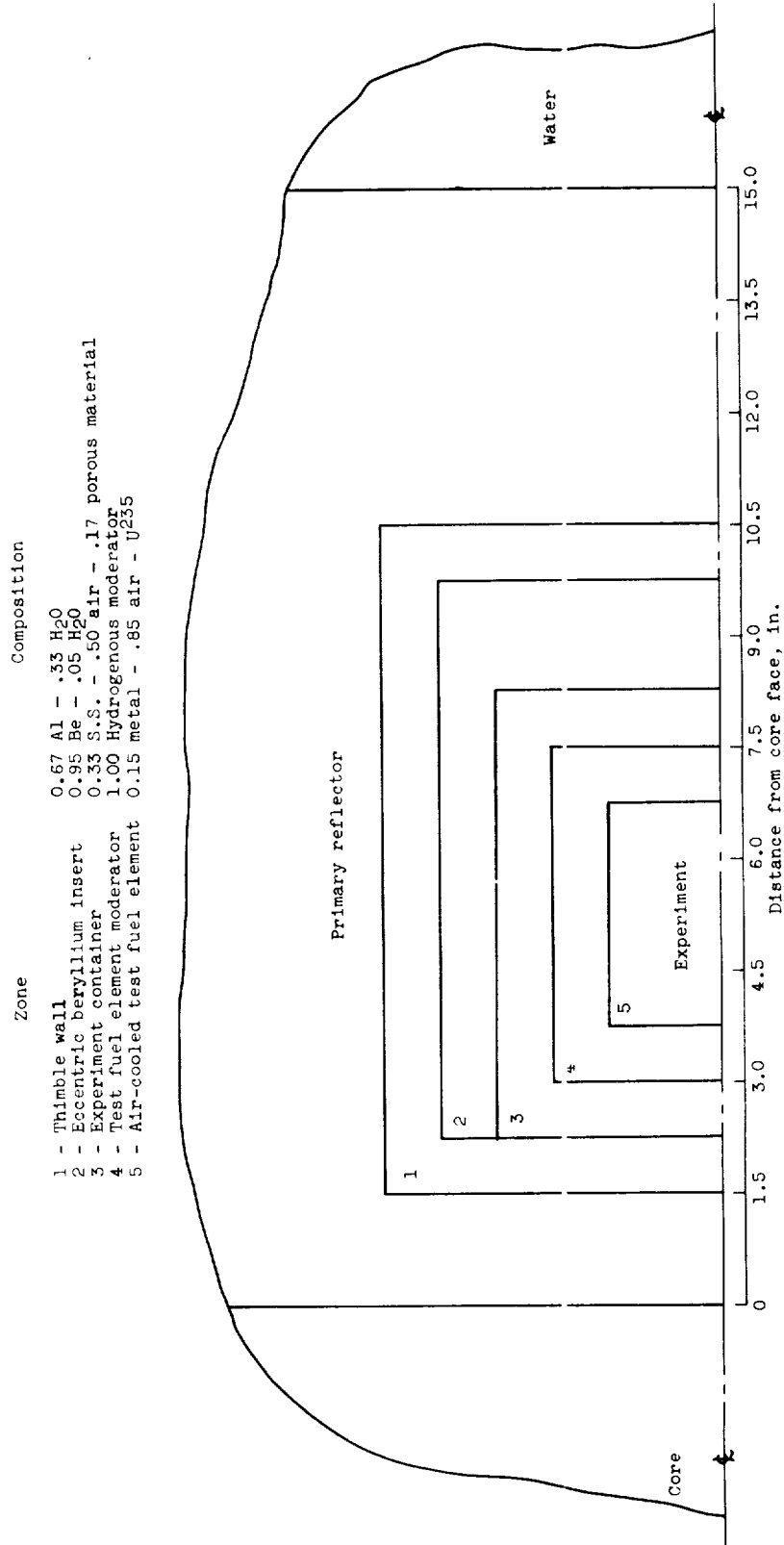


Figure 4.4. - Composition of air-cooled fuel element experiment in horizontal through hole. Modified geometry used in two-dimensional simulator calculations.

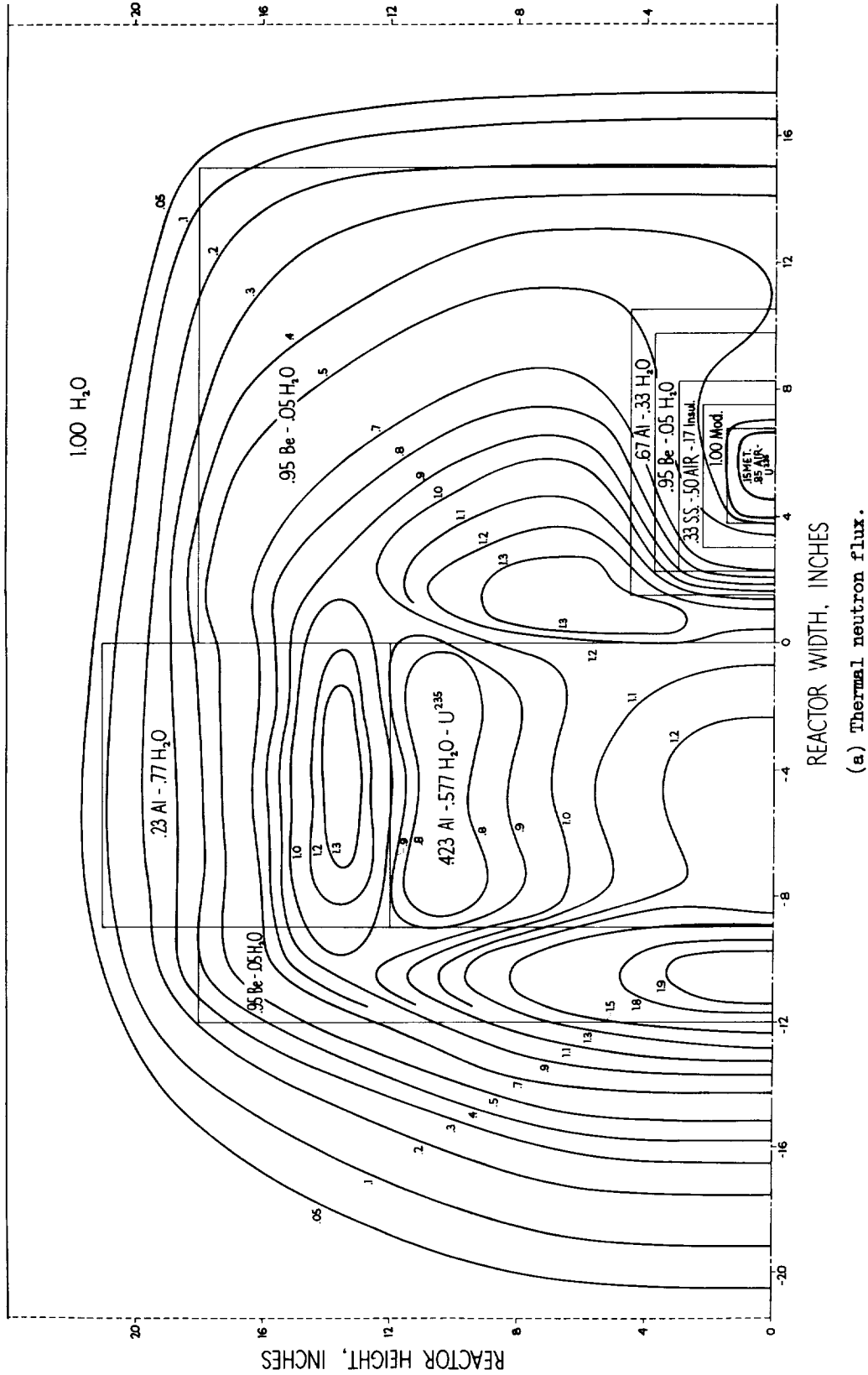
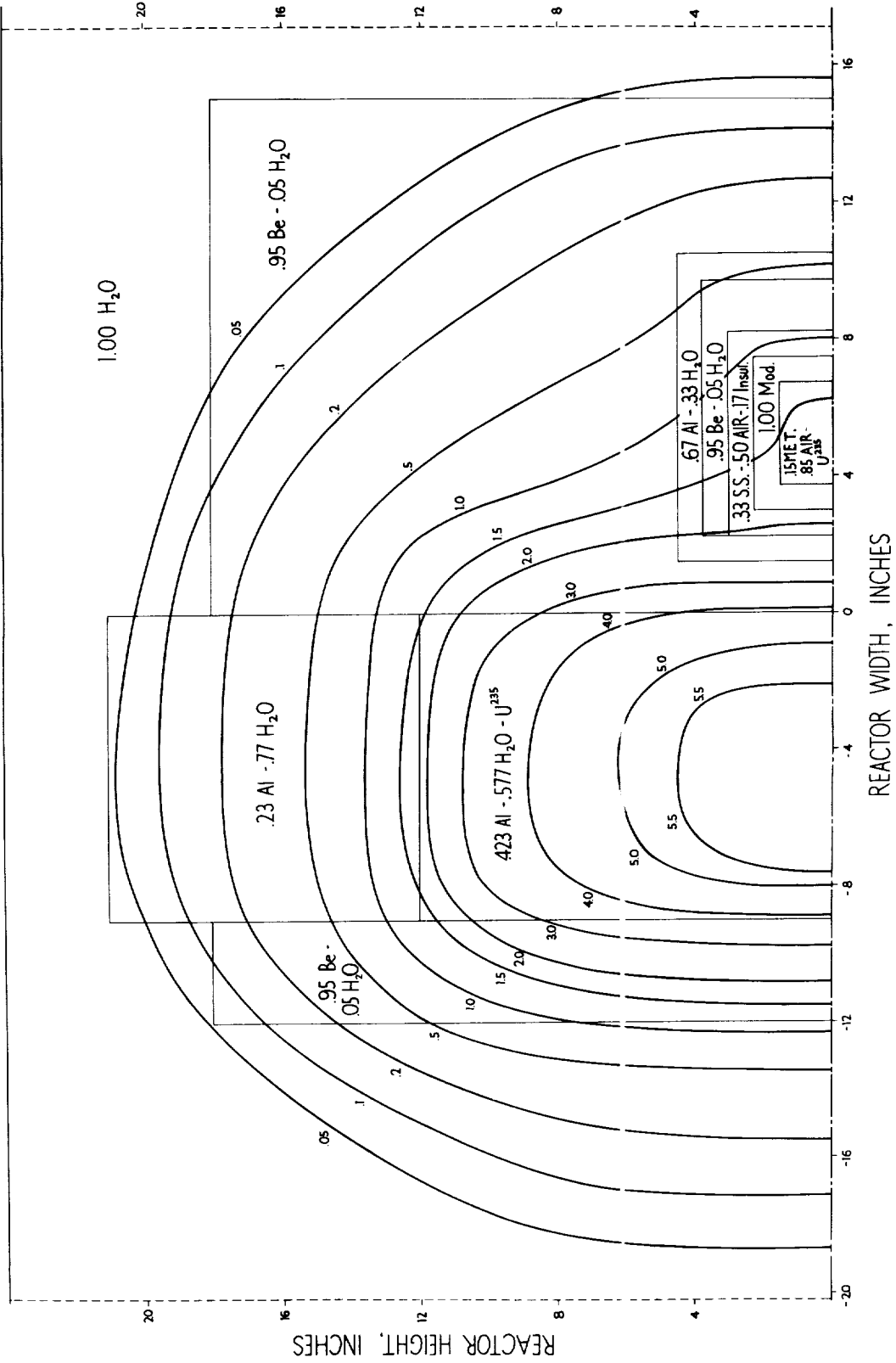


Figure 4.5 - Flux distribution for vertical section of reactor with air-cooled fuel-element experiment in HT-1 hole in closest position to face of core. (Fluxes are relative to an average thermal flux of unity over the core volume.)



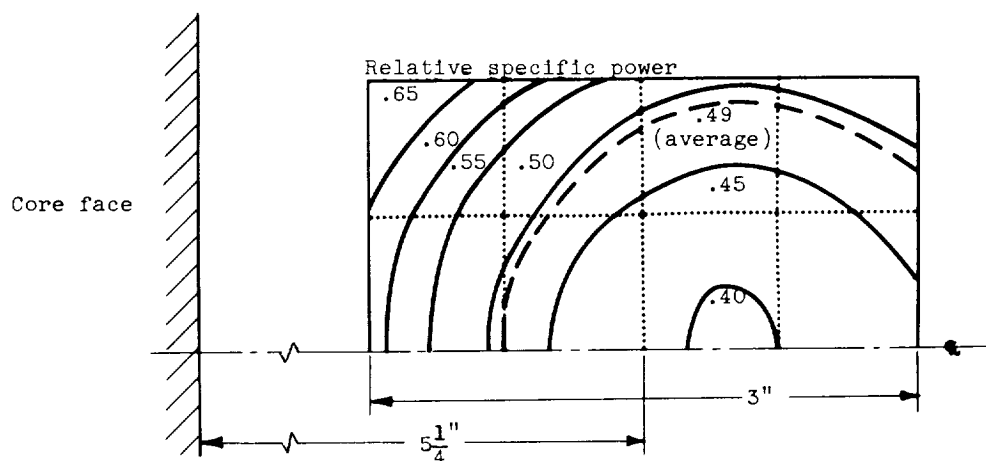
(b) Fast neutron flux.

Figure 4.5 - Concluded. Flux distribution for vertical section of reactor with air-cooled fuel-element experiment in H-1 hole in closest position to face of core. (Fluxes are relative to an average thermal flux of unity over the core volume.)

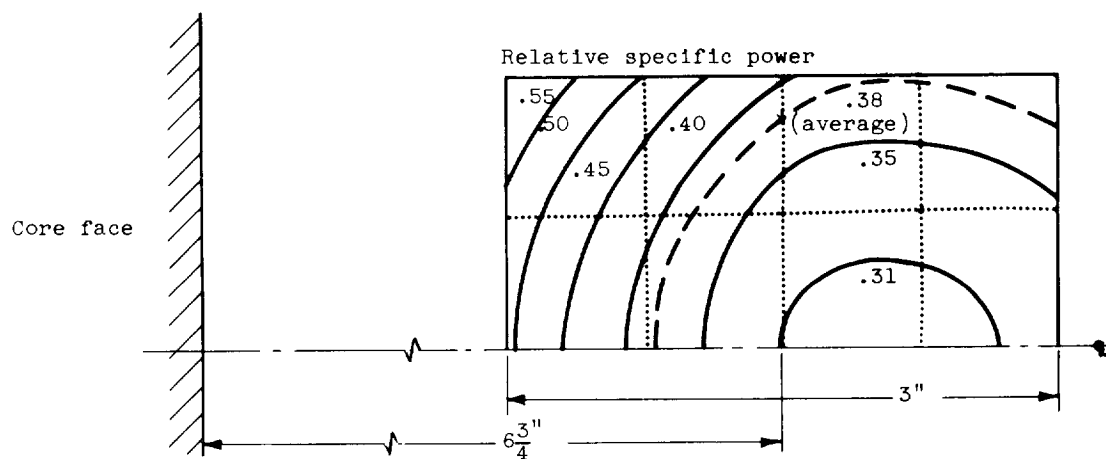


E-102

CZ-42

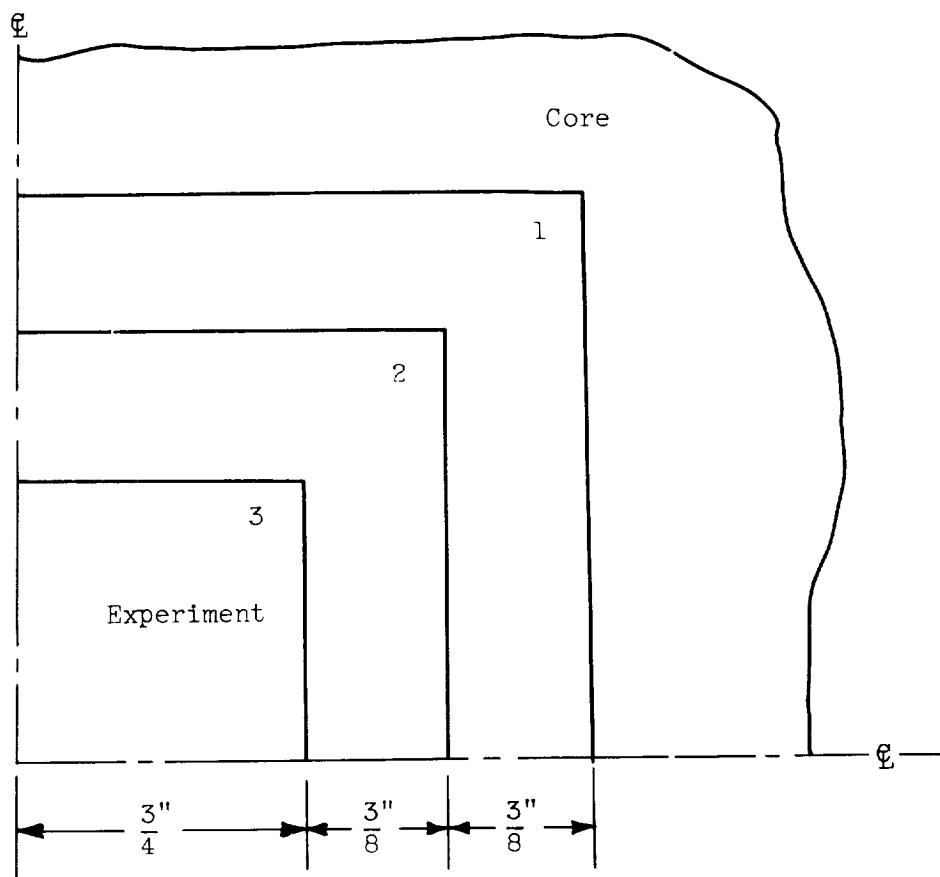


(a) Closest position to core of test fuel element in HT-1.



(b) Farthest position from core of test fuel element in HT-1.

Figure 4.6. - Specific power distribution in air-cooled fuel element experiment in HT-1. Specific power is relative to average specific power of unity in core.



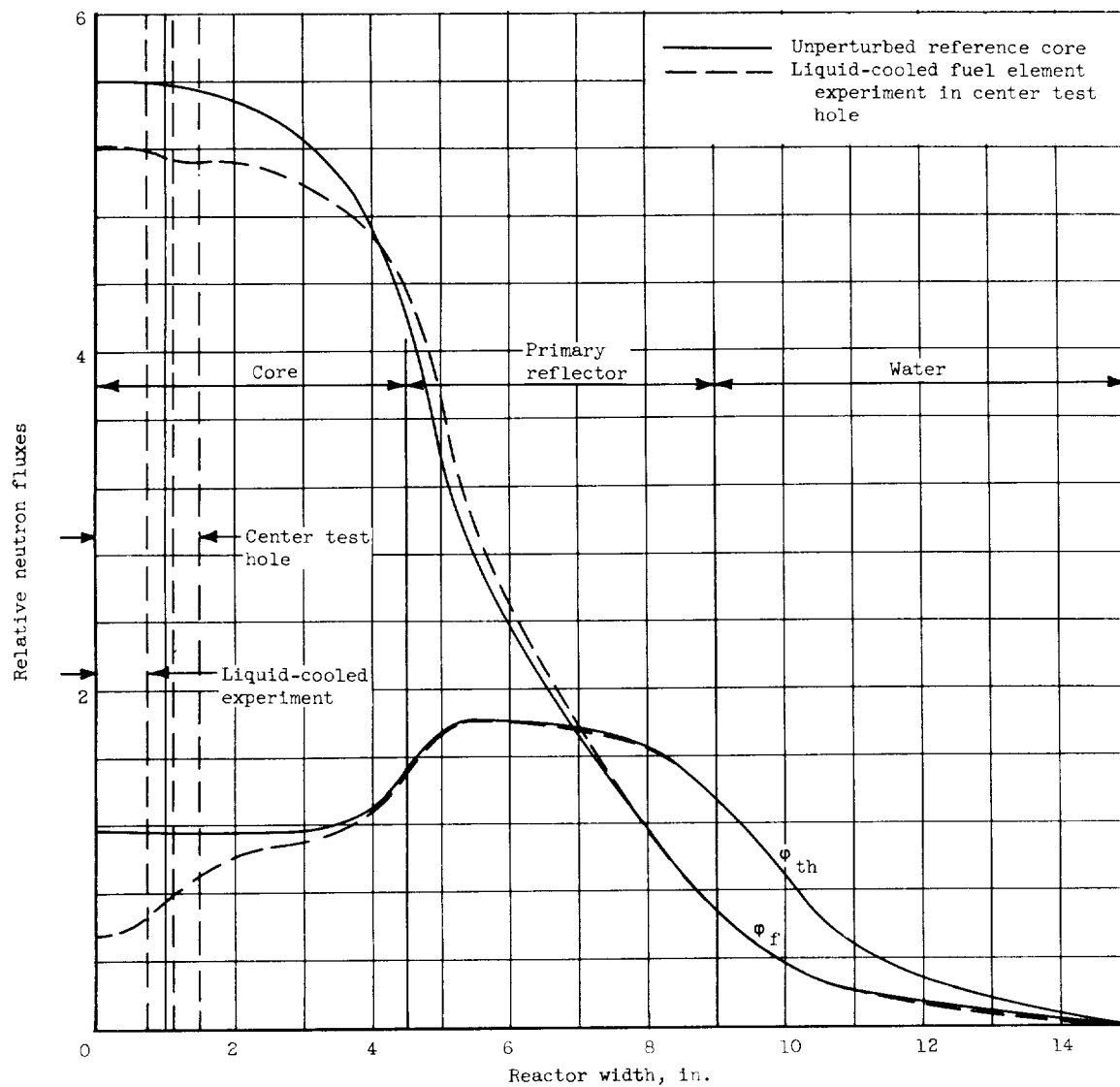
Liquid-cooled center test hole experiment

Zone	Composition
1	0.67Al - 0.33 H <sub>2</sub> O
2	0.25 Stainless steel - 0.42 insulation - 0.33 void
3	U <sup>235</sup> - 0.90 Liquid 0.10 Metal

Figure 4.7 - Composition of center test hole experiment.  
Modified geometry used in two-dimensional simulator calculations.

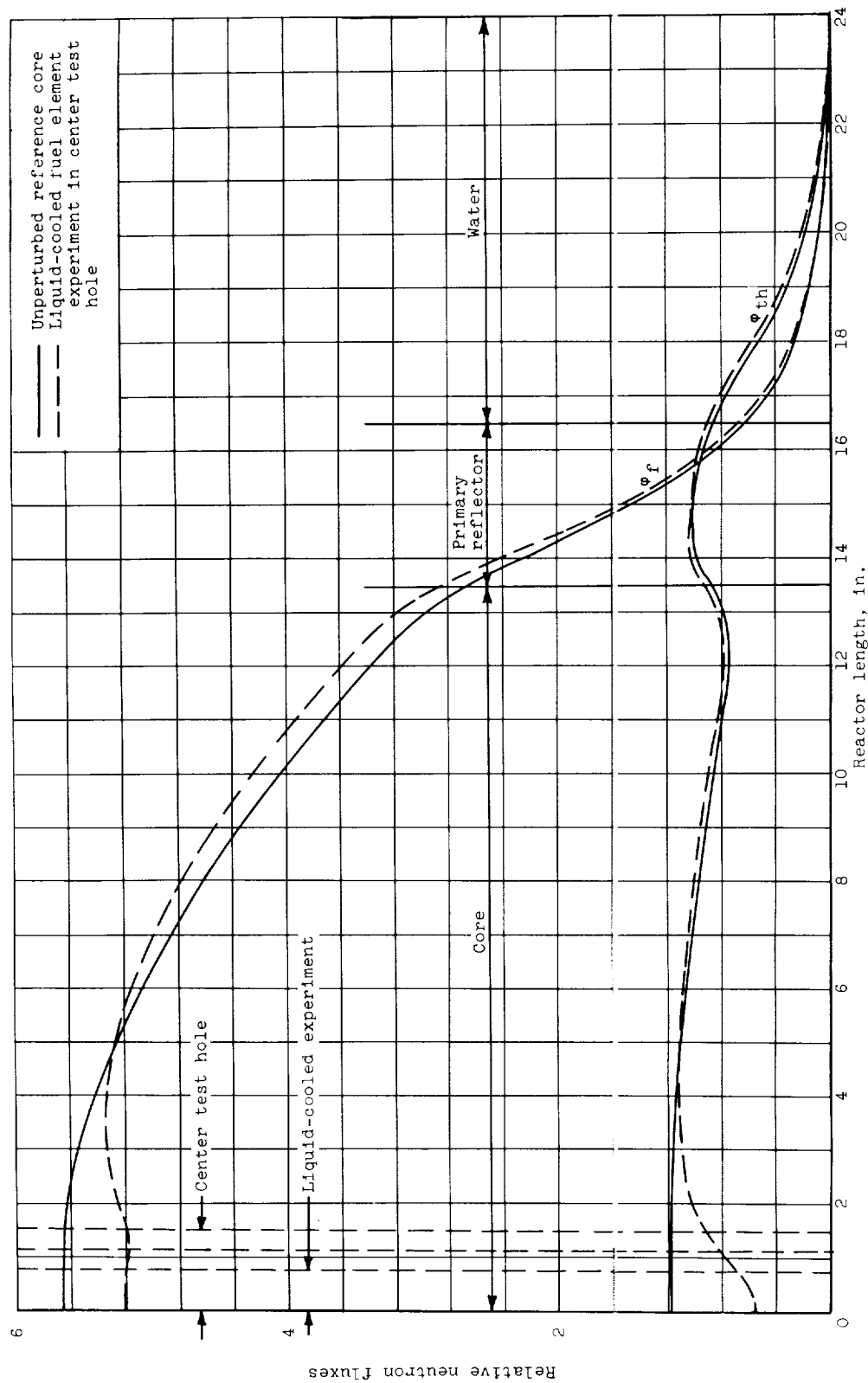
E-102

CZ-42 back



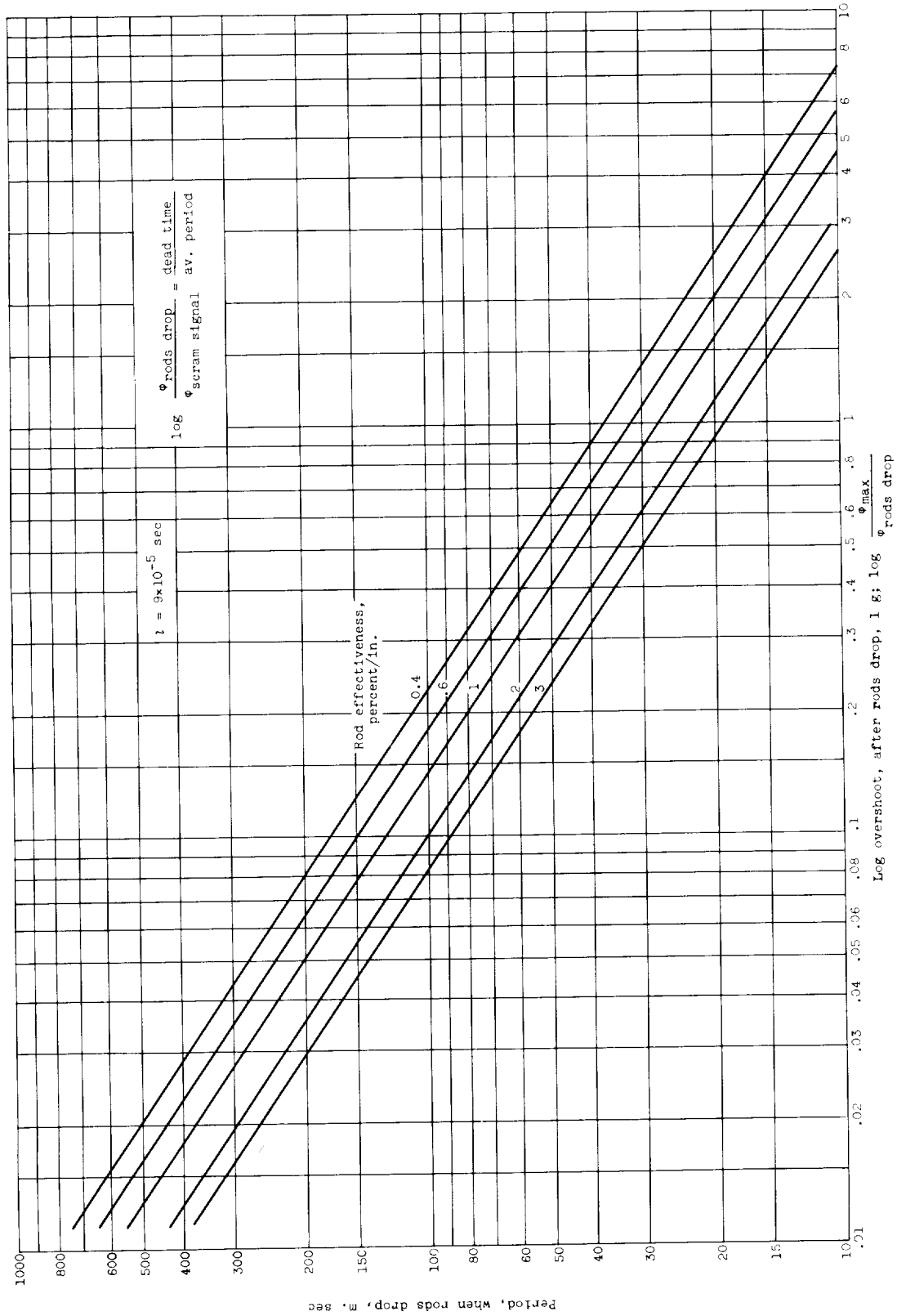
(a) Fluxes along width.

Figure 4.8 - Two-group neutron flux distributions along reactor width and length with and without liquid-cooled fuel element experiment. (Fluxes relative to average thermal flux of unit, over core volume.)



(b) Fluxes along length.

Figure 4.8 - Concluded. Two-group neutron flux distributions along reactor width and length with and without liquid-cooled fuel element experiment. (Fluxes relative to average thermal flux of unity over core volume.)



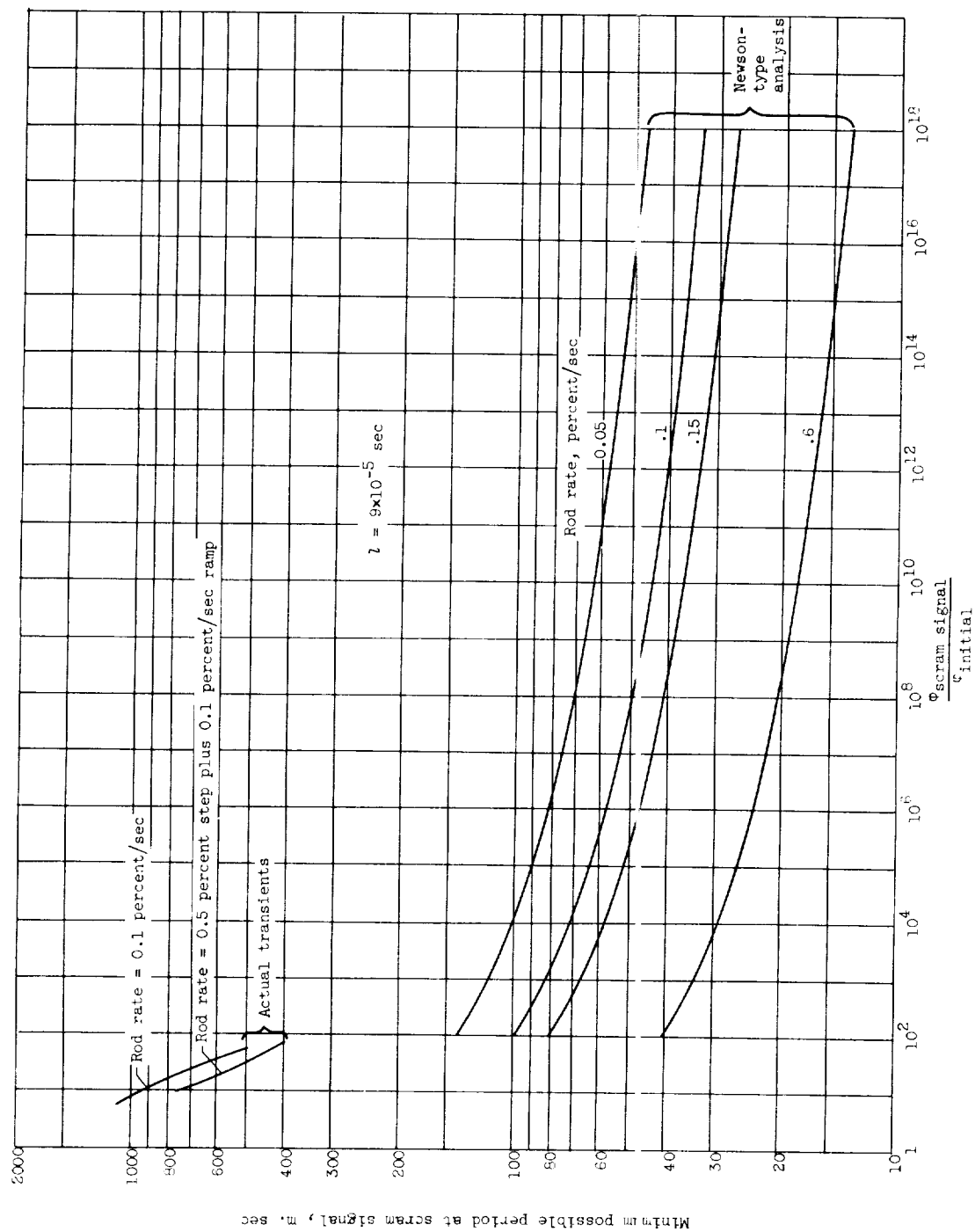


Figure 6.2. - Reactor periods at scram signal power levels during start-up accident.

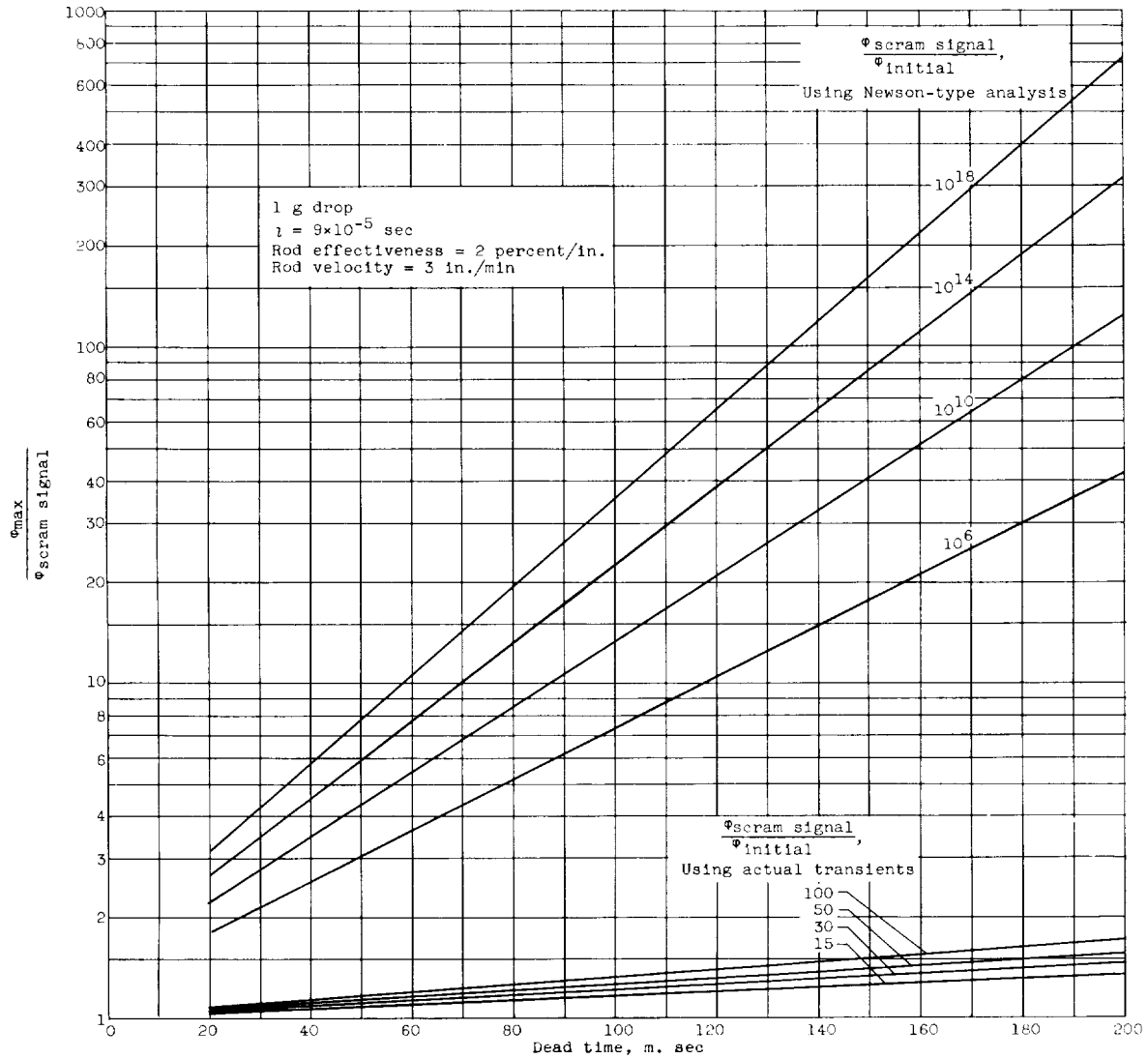


Figure 6.3. - Total overshoots above the scram signal power level for the start-up accident.

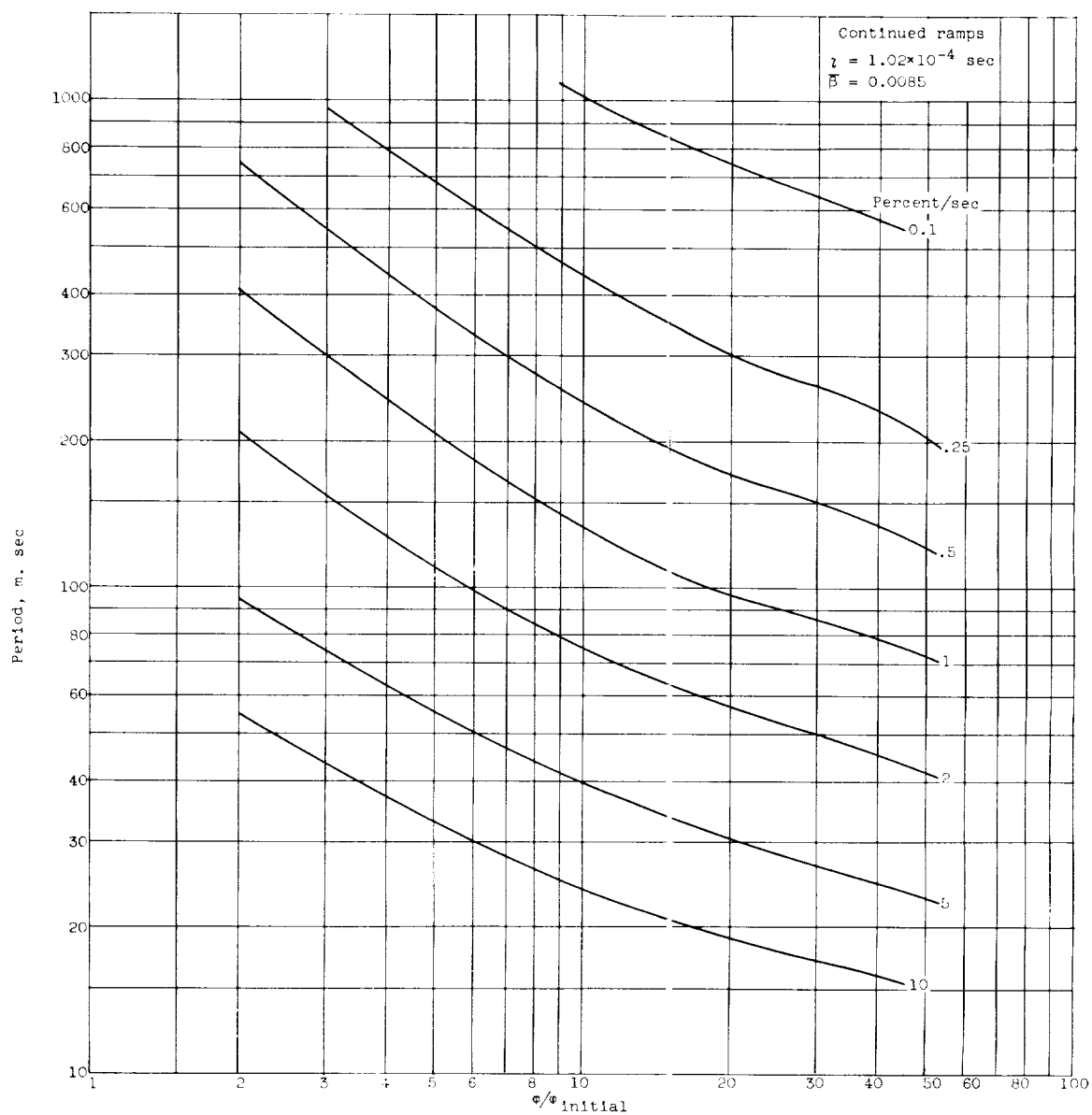


Figure 6.4. - Relation between reactor period and power level for continued insertion of reactivity at constant rates.



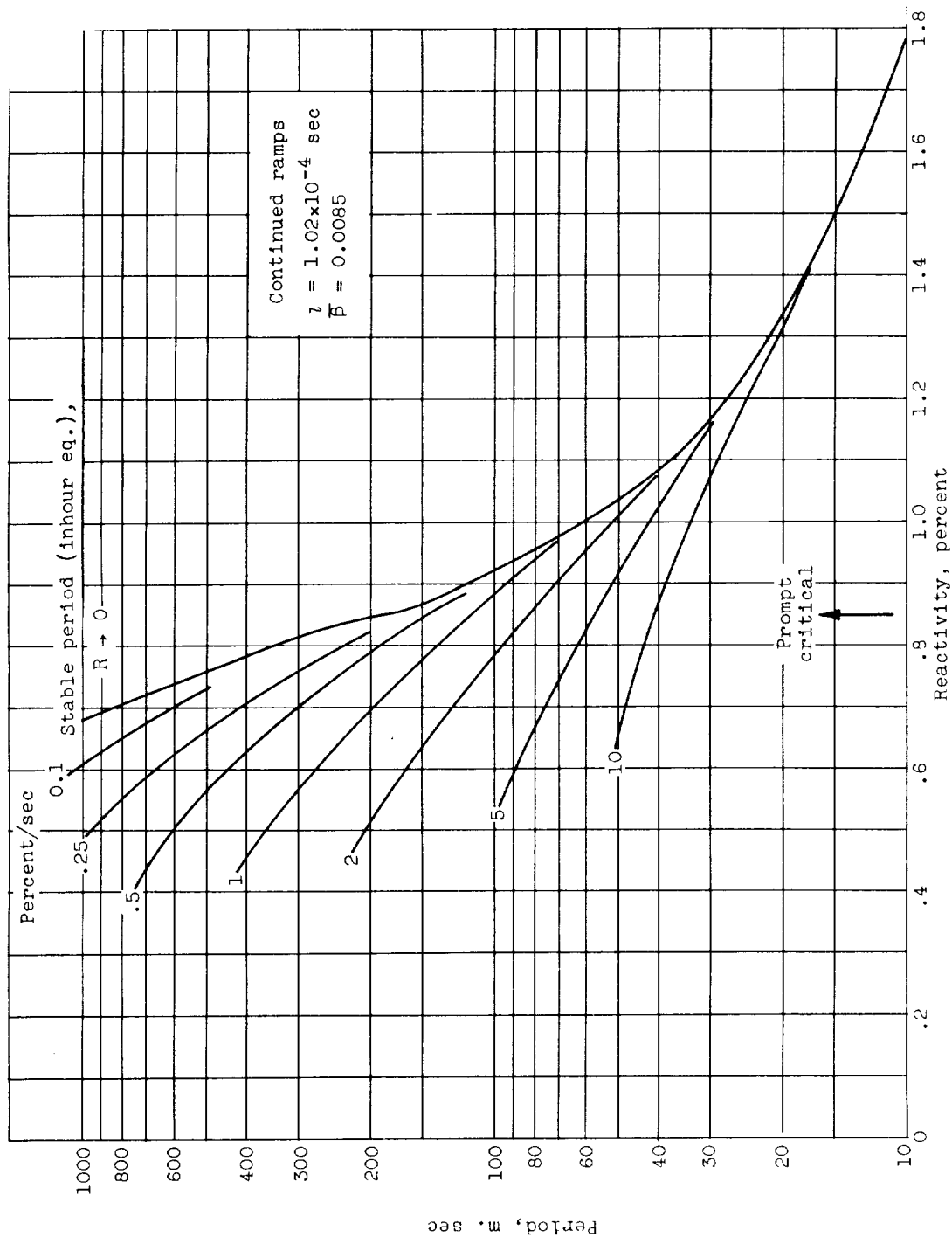


Figure 6.5. - Relation between reactor period and reactivity for continued insertion of reactivity at constant rates:  $\lambda = 1.02 \times 10^{-4} \text{ sec}$ .

FOR LEAST FAVORABLE LEVELS AT START OF ACCIDENT  
 SHIM-SAFETY ROD EFFECTIVENESS, 0.4 %  $\Delta k$ /IN.  
 $\phi_{MAX} < 2.5 \phi_f$

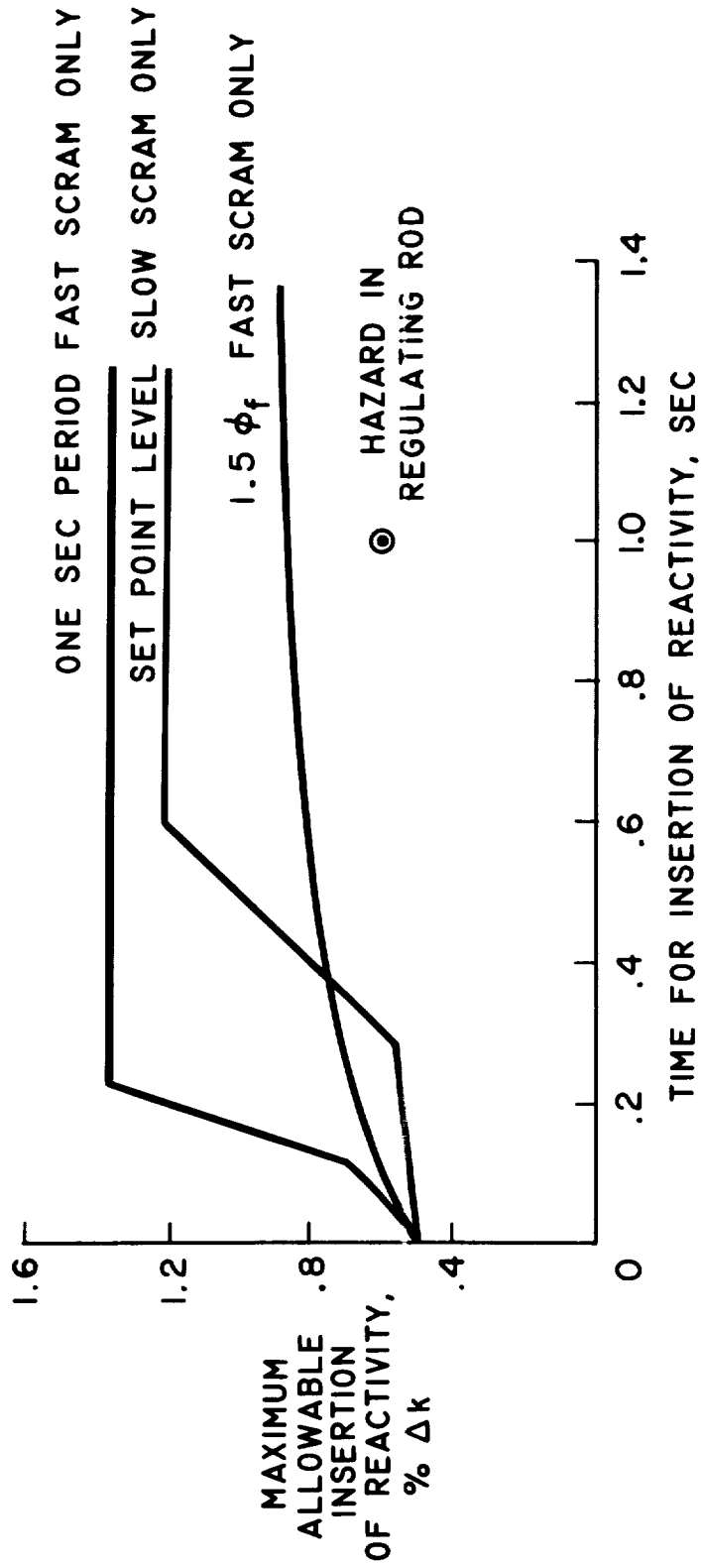


Figure 6.6 - Controllable accidental insertions of reactivity.

E-102

CZ-43 back

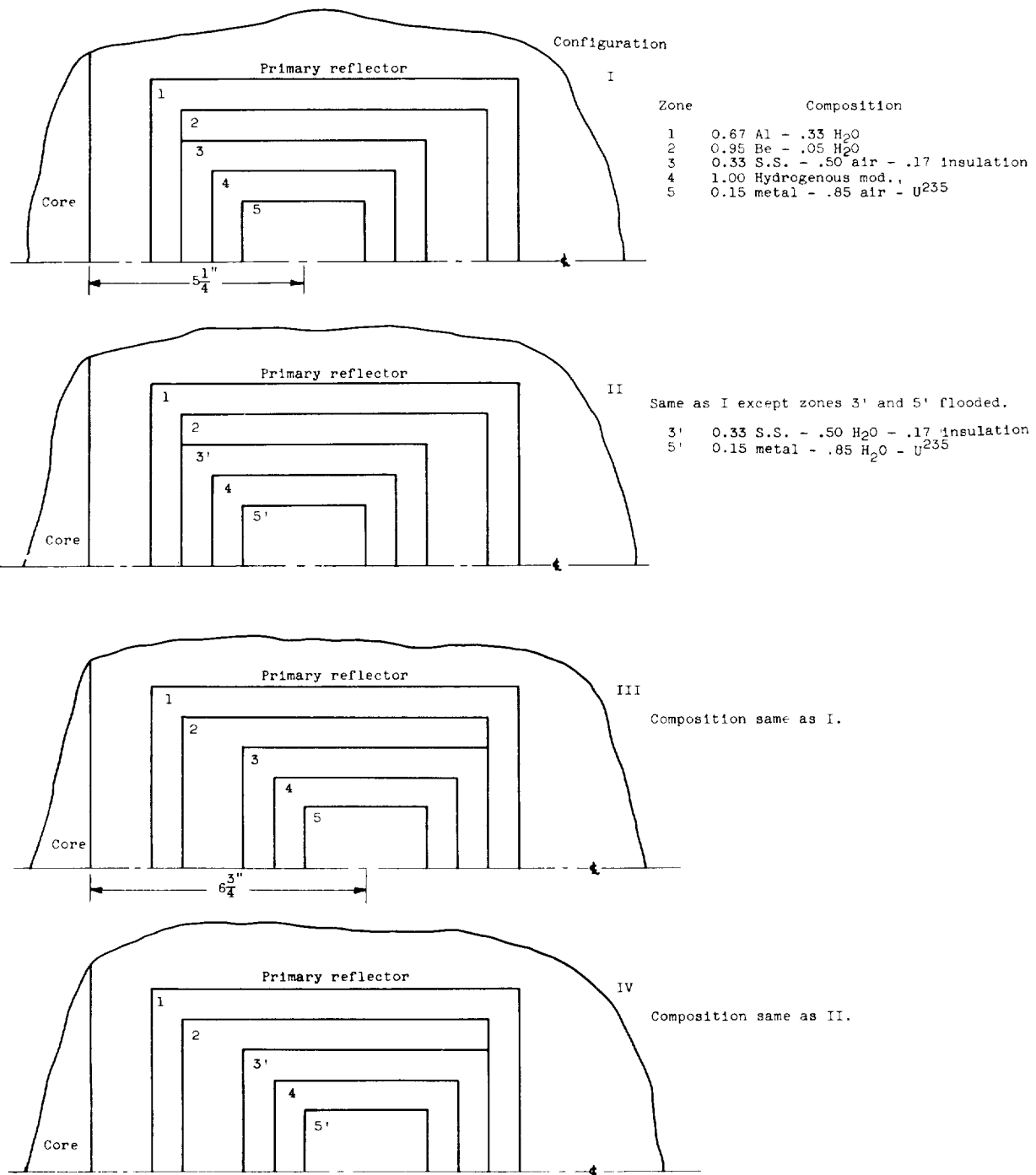


Figure 6.7. - Compositional and geometrical changes to air-cooled experiment in horizontal through hole for evaluation of reactivity effects on two-dimensional space simulator.

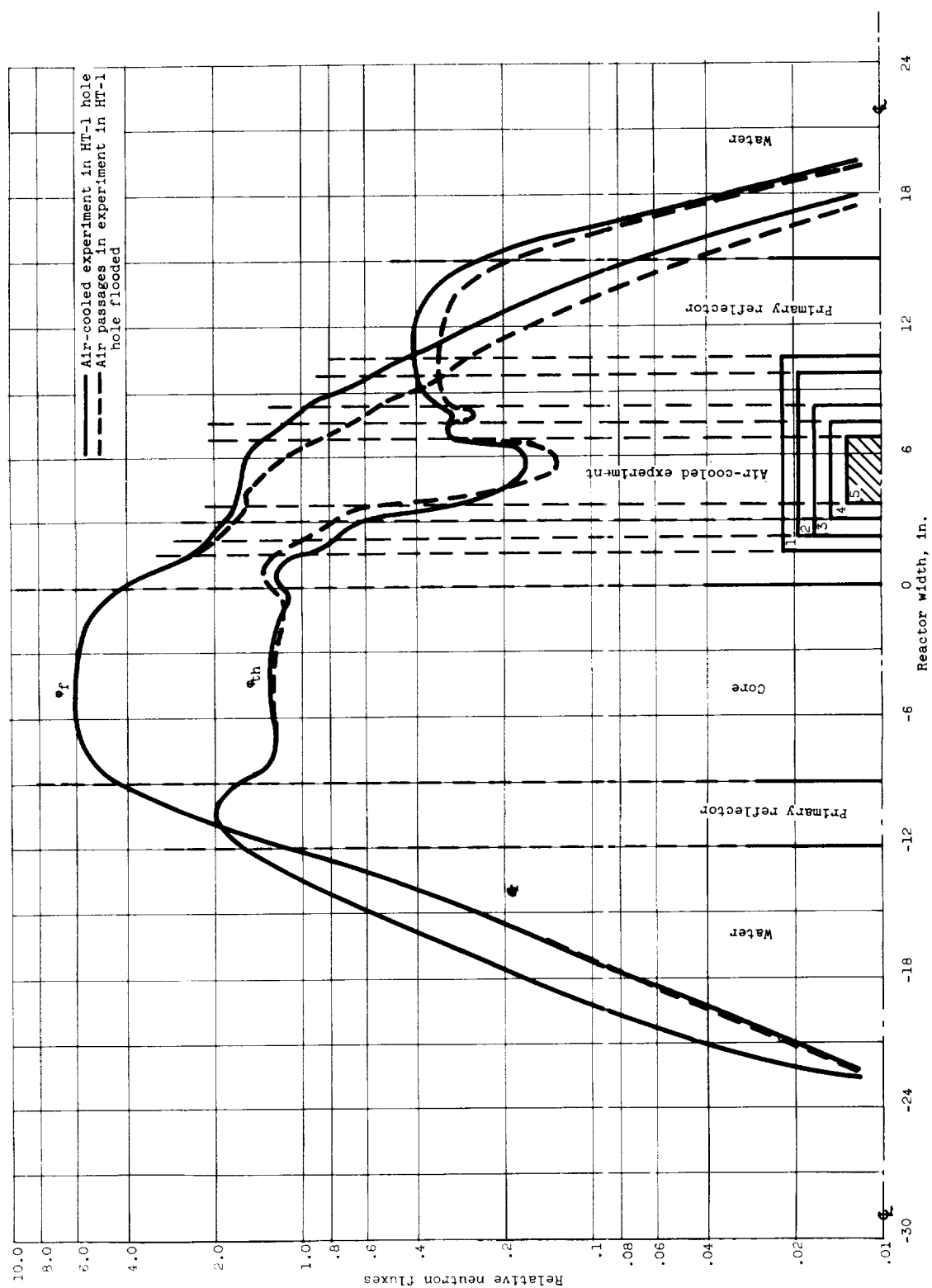


Figure 6.8. - Two-group neutron flux distributions across reactor horizontal midplane with air-cooled fuel element experiment in HT-1 hole. (Fluxes are relative to an average thermal flux of unity over the core volume.)

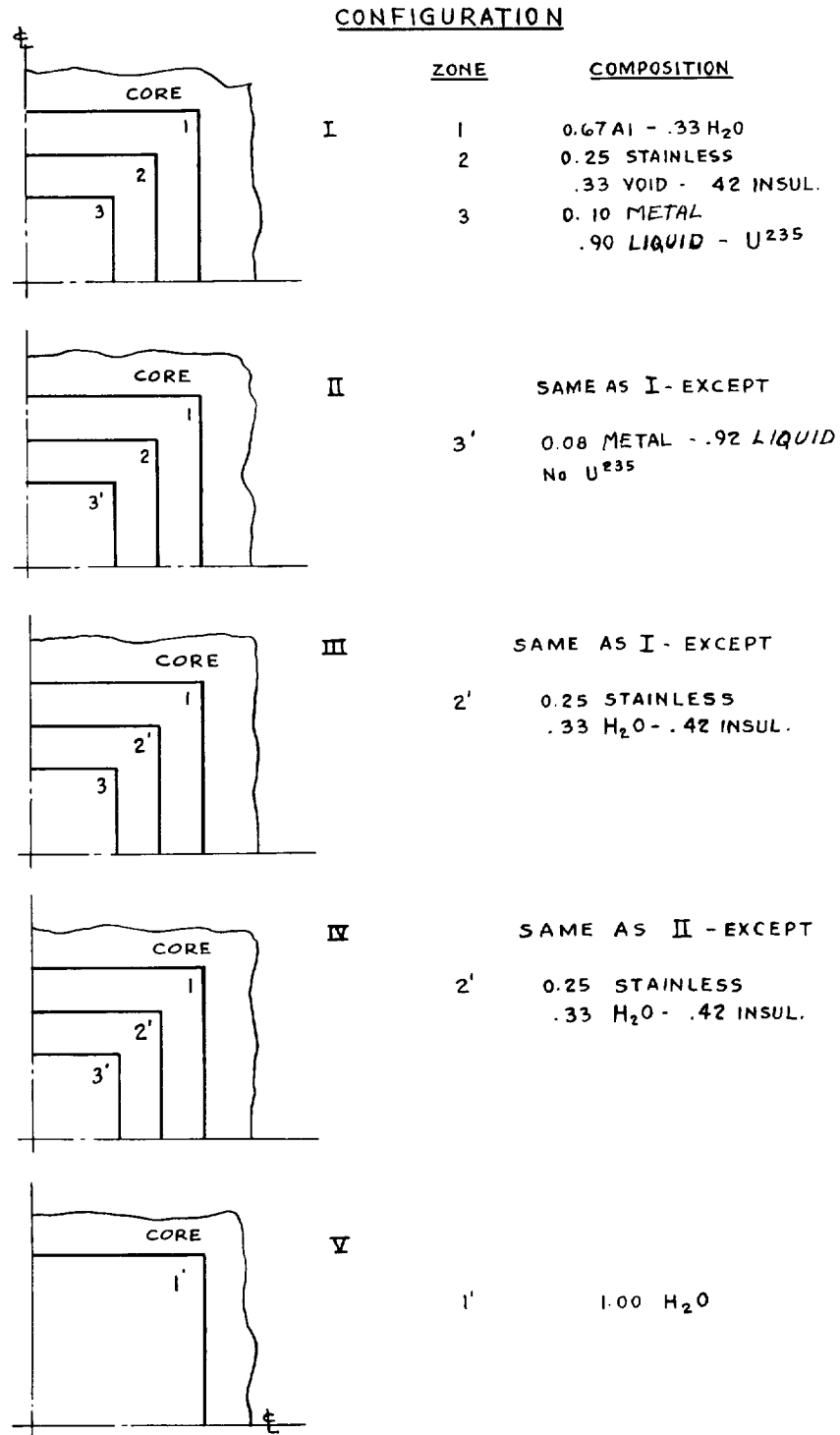


Figure 6.9 - Compositional changes to liquid-cooled experiments in reactor core center test hole, for evaluation of reactivity effects on two-dimensional simulator.

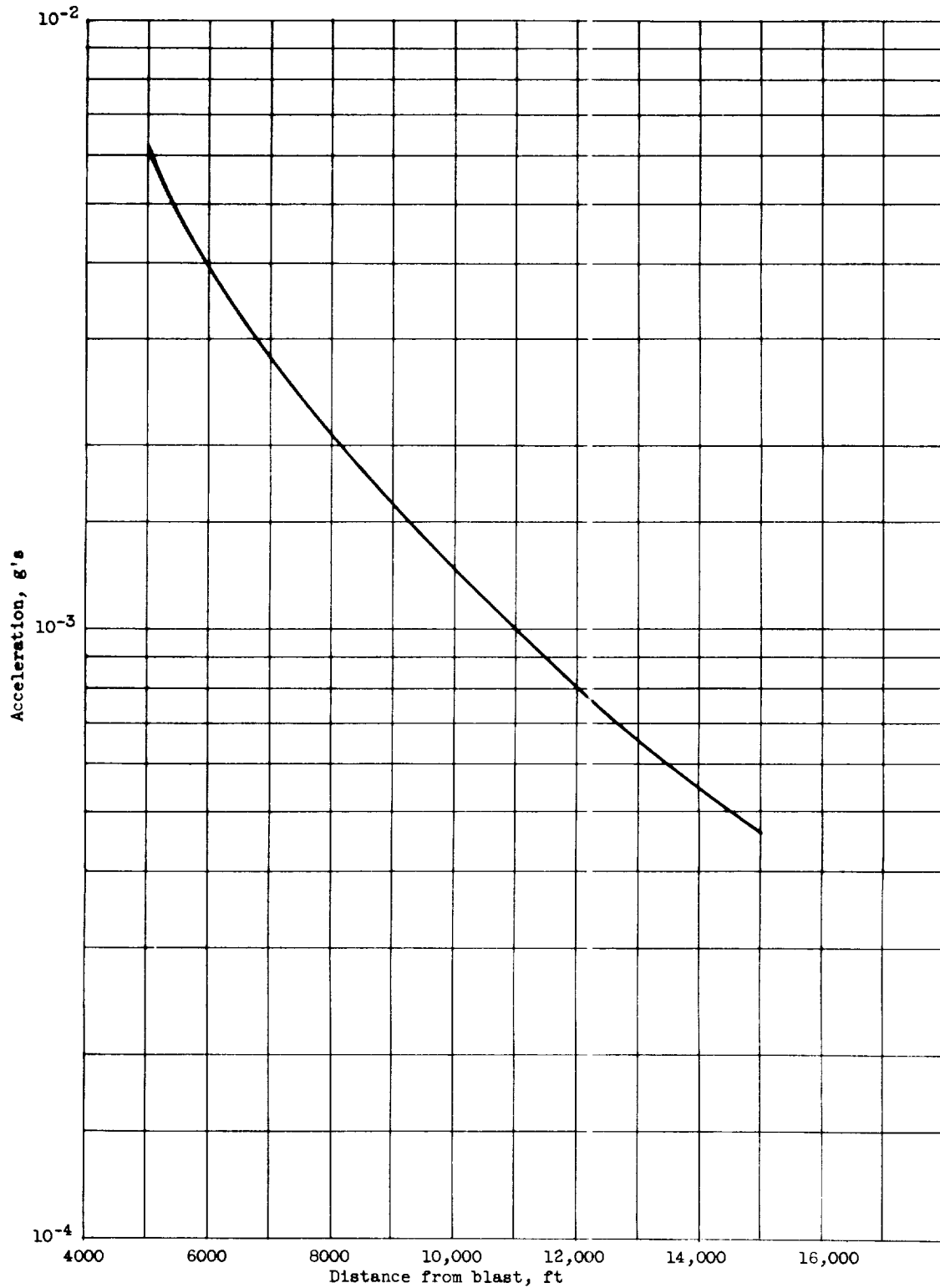


Figure 6.10. - Horizontal acceleration against distance from a 250,000 pound TNT explosion for volcanic rock with 20 feet overburden of sand and gravel.

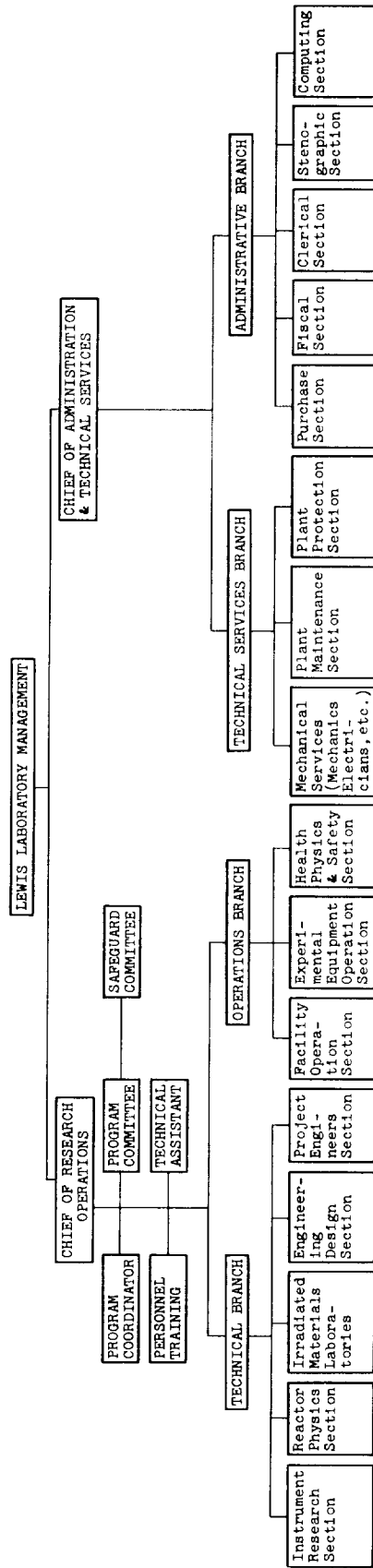


Figure 7. 1. - Diagram of administrative organization.

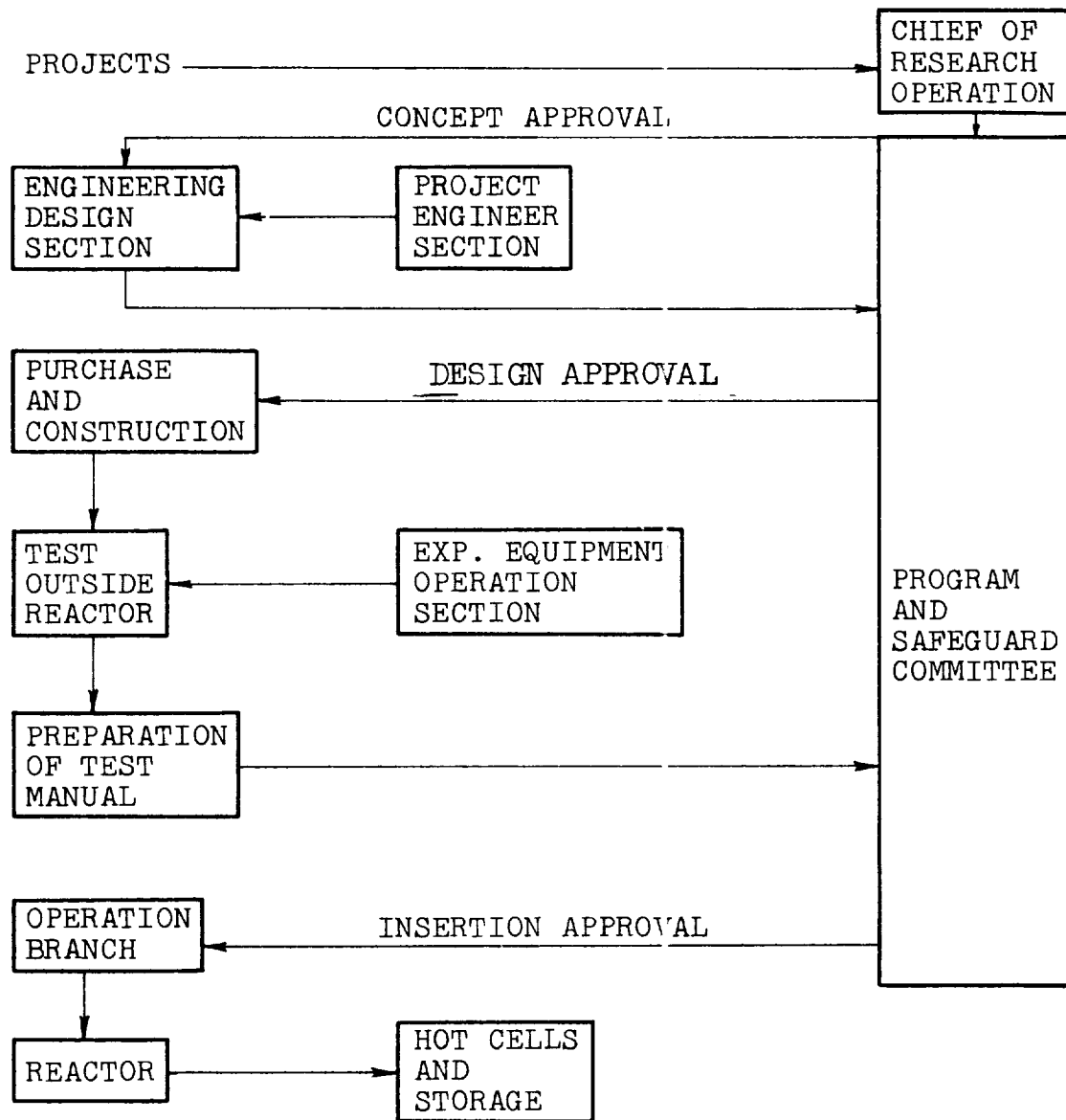


Figure 7.2. - Project flow diagram.



E-102

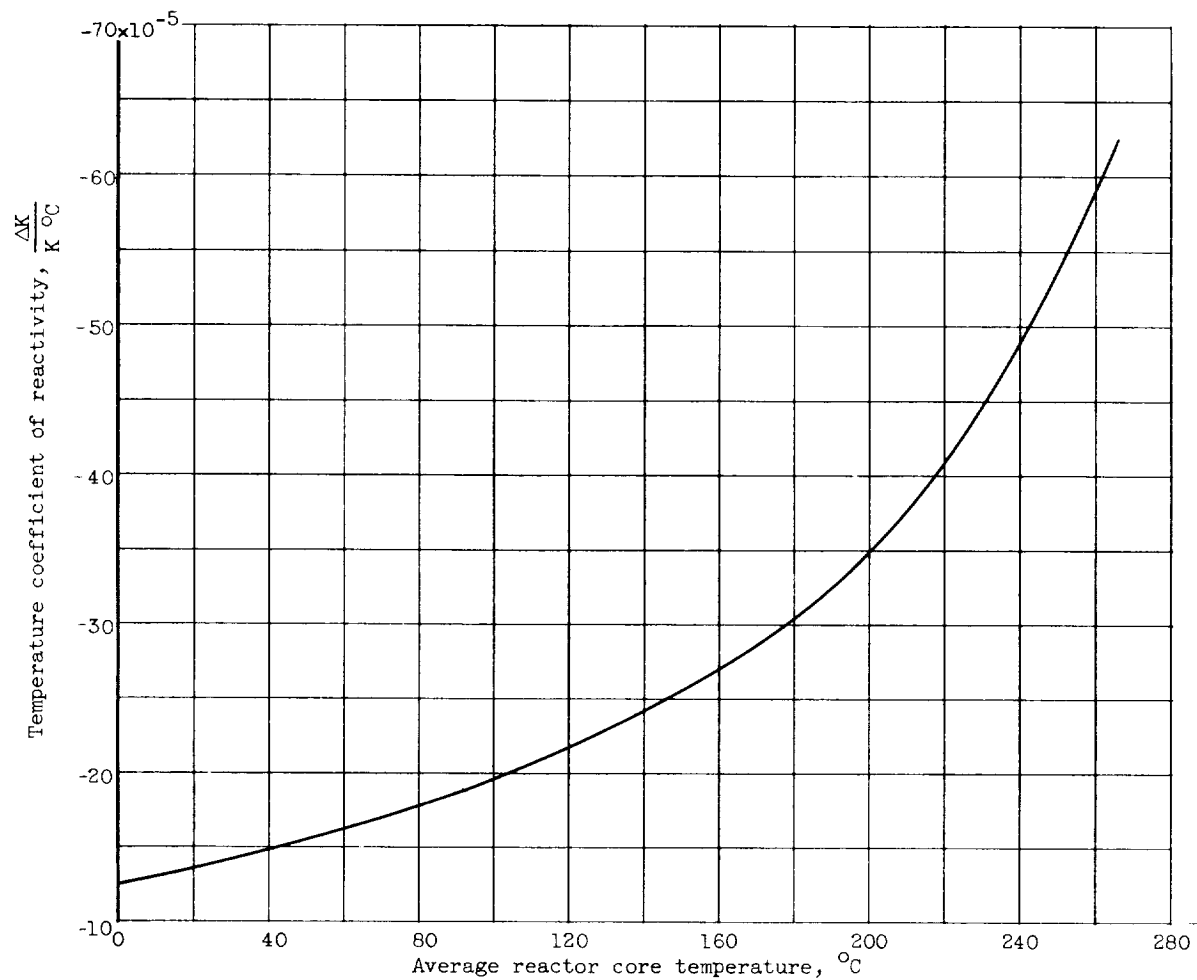


Figure B.1. - Temperature coefficient of reactivity as a function of average reactor core temperature.

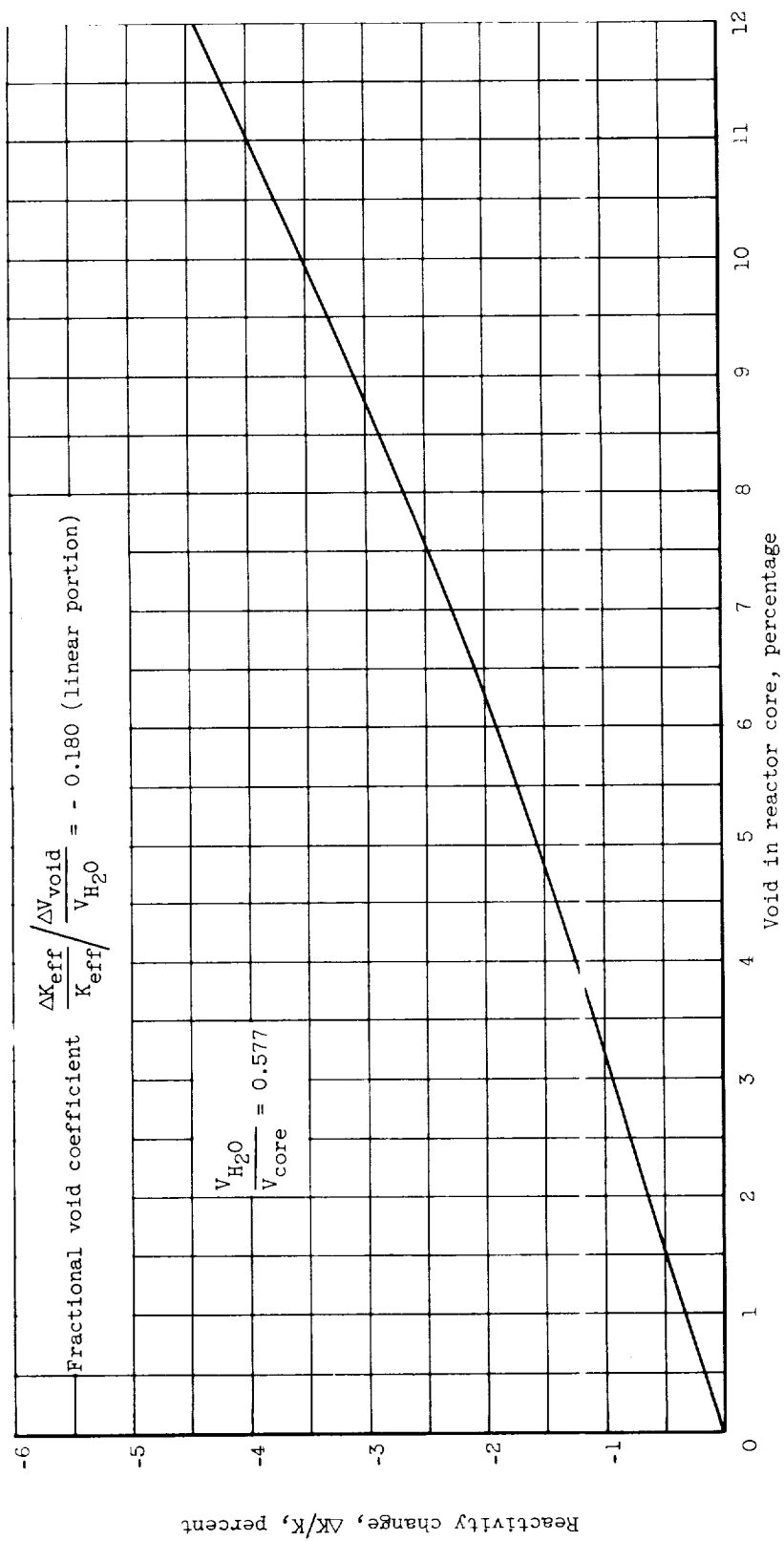


Figure B.2. - Reactivity change due to addition of voids in reactor core.

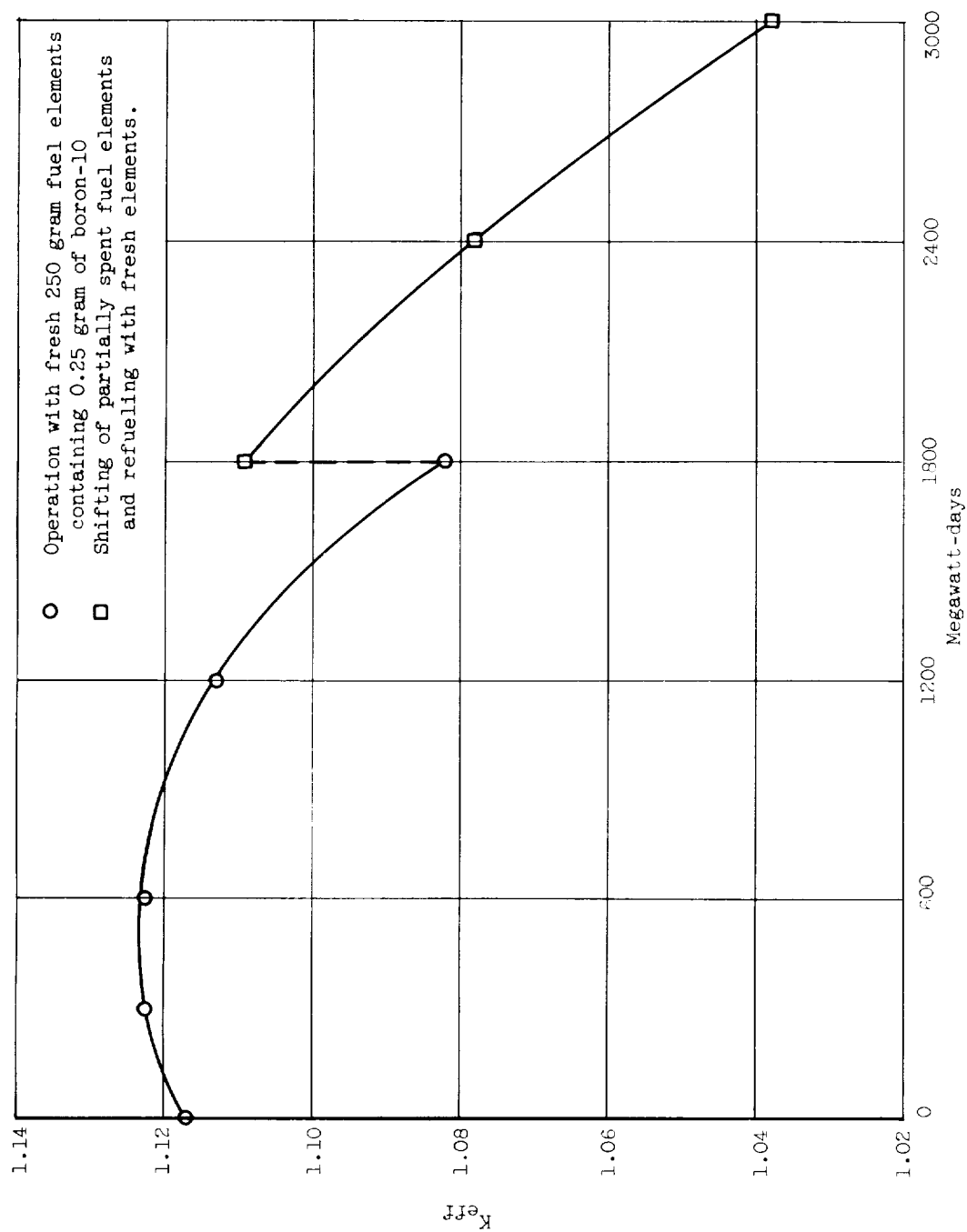
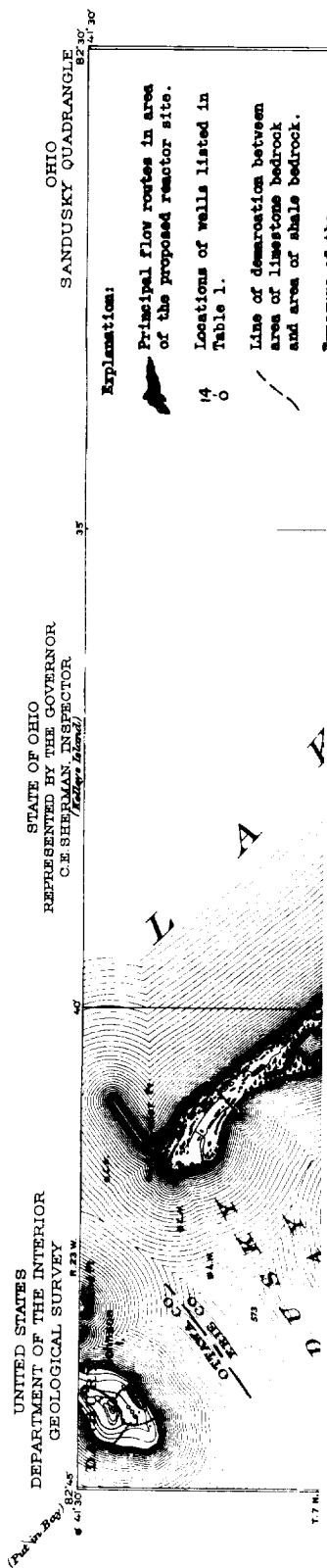


Figure B.3 - Variation of reactivity with operating time for reactor using burnable poisons (boron) in fuel elements.







E-102

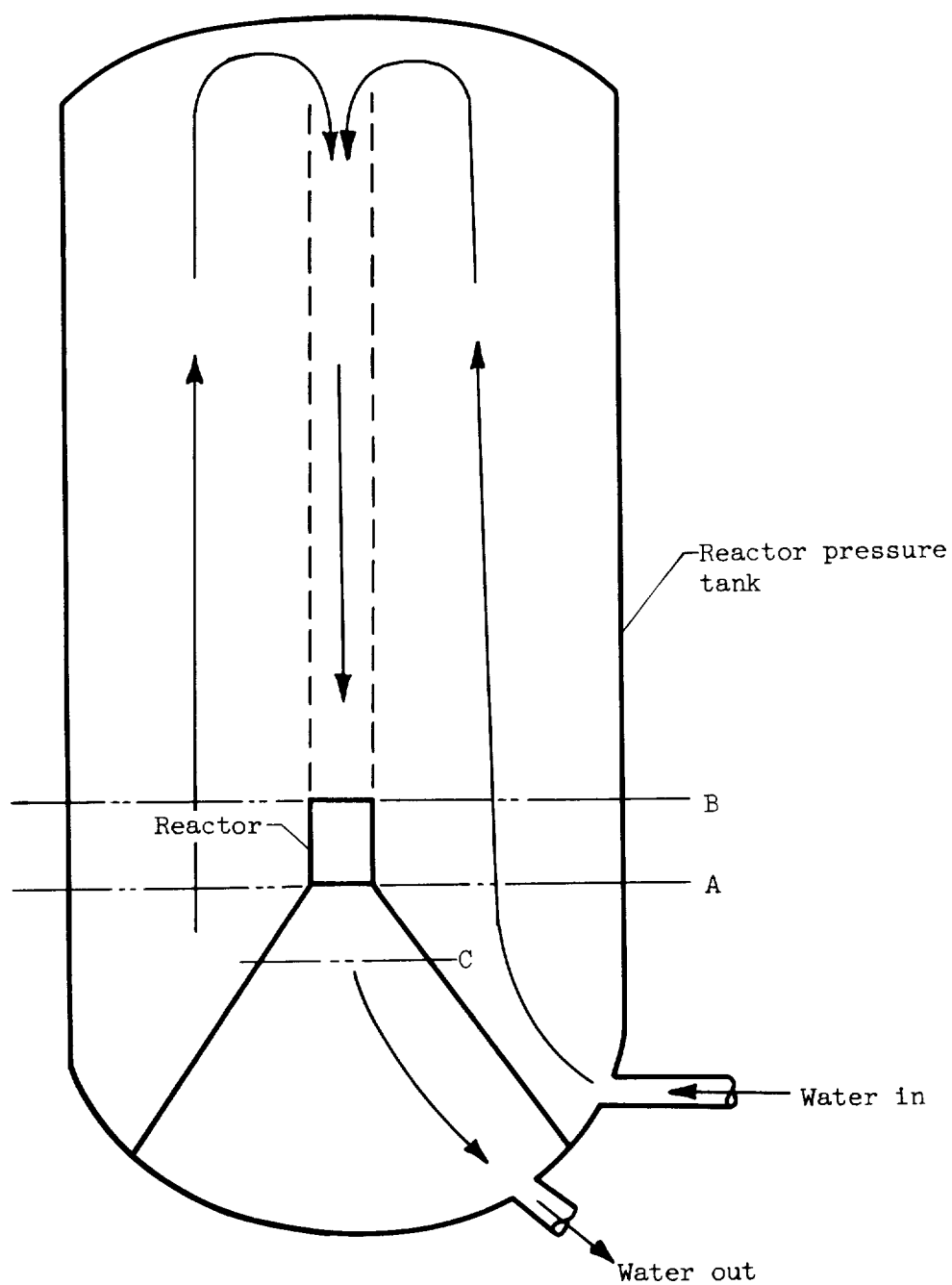


Figure E.1. - Simplified primary water flow pattern in reactor pressure tank.

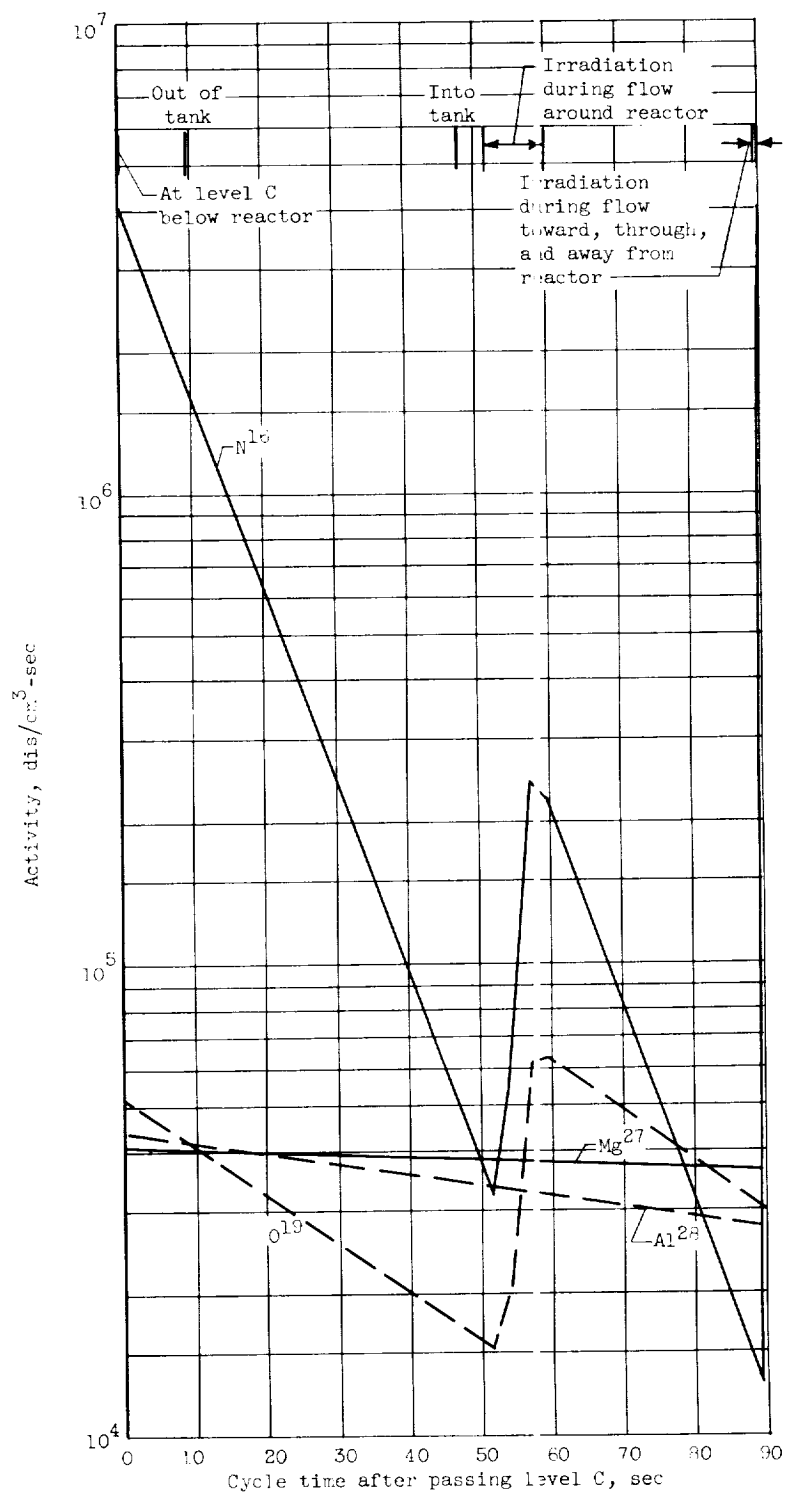


Figure E.2. - Variation of several short-lived activities during a complete cycle of primary water.



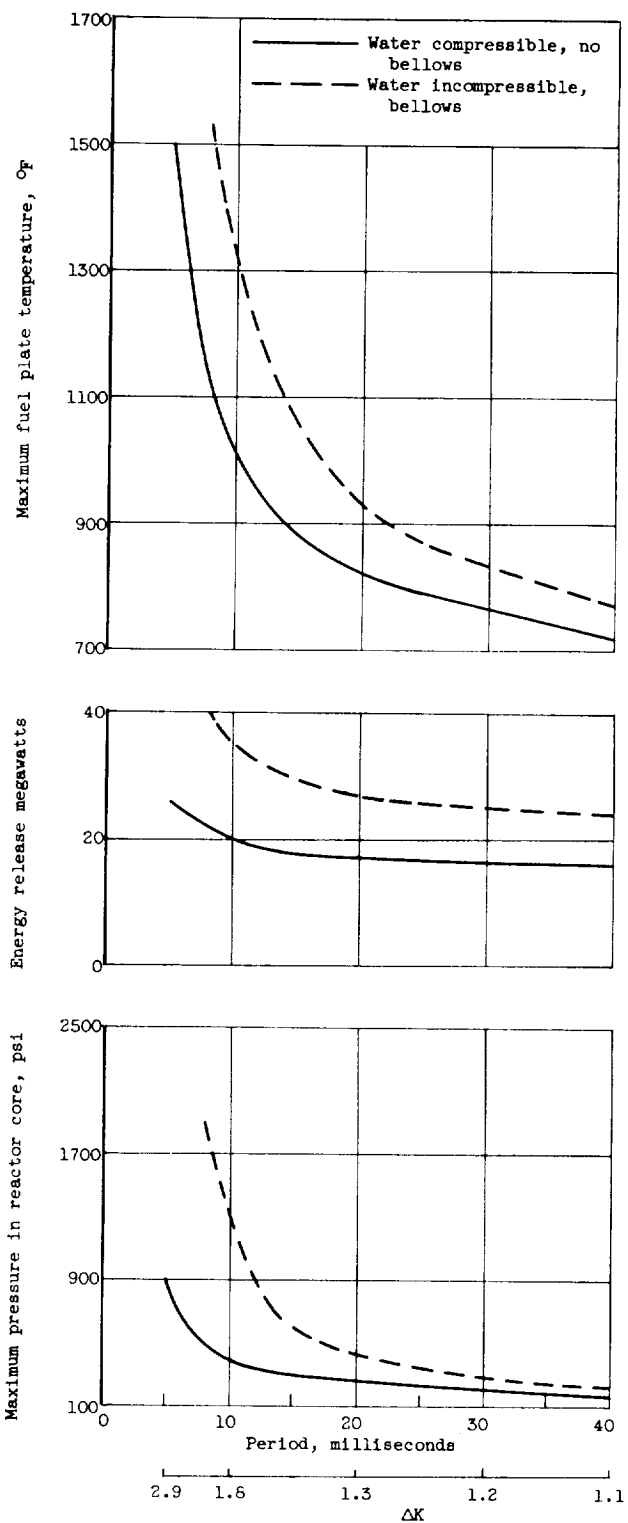


Figure F.1 - Comparison in the analysis of reference F.5 of the two assumptions: water compressible, no bellows and water incompressible, bellows.

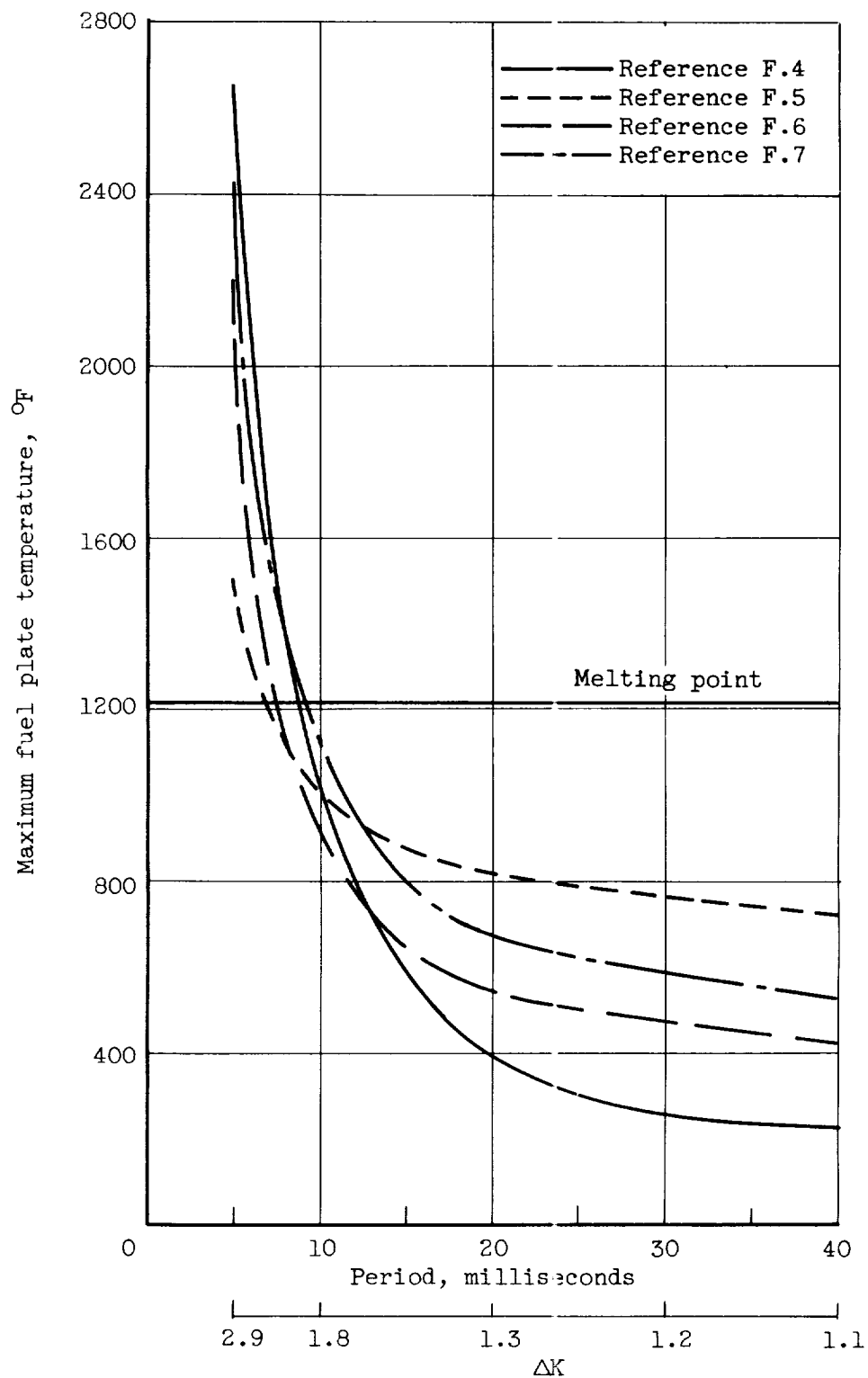


Figure F.2 - Variation of maximum fuel plate temperature with period for Borax-type excursions.

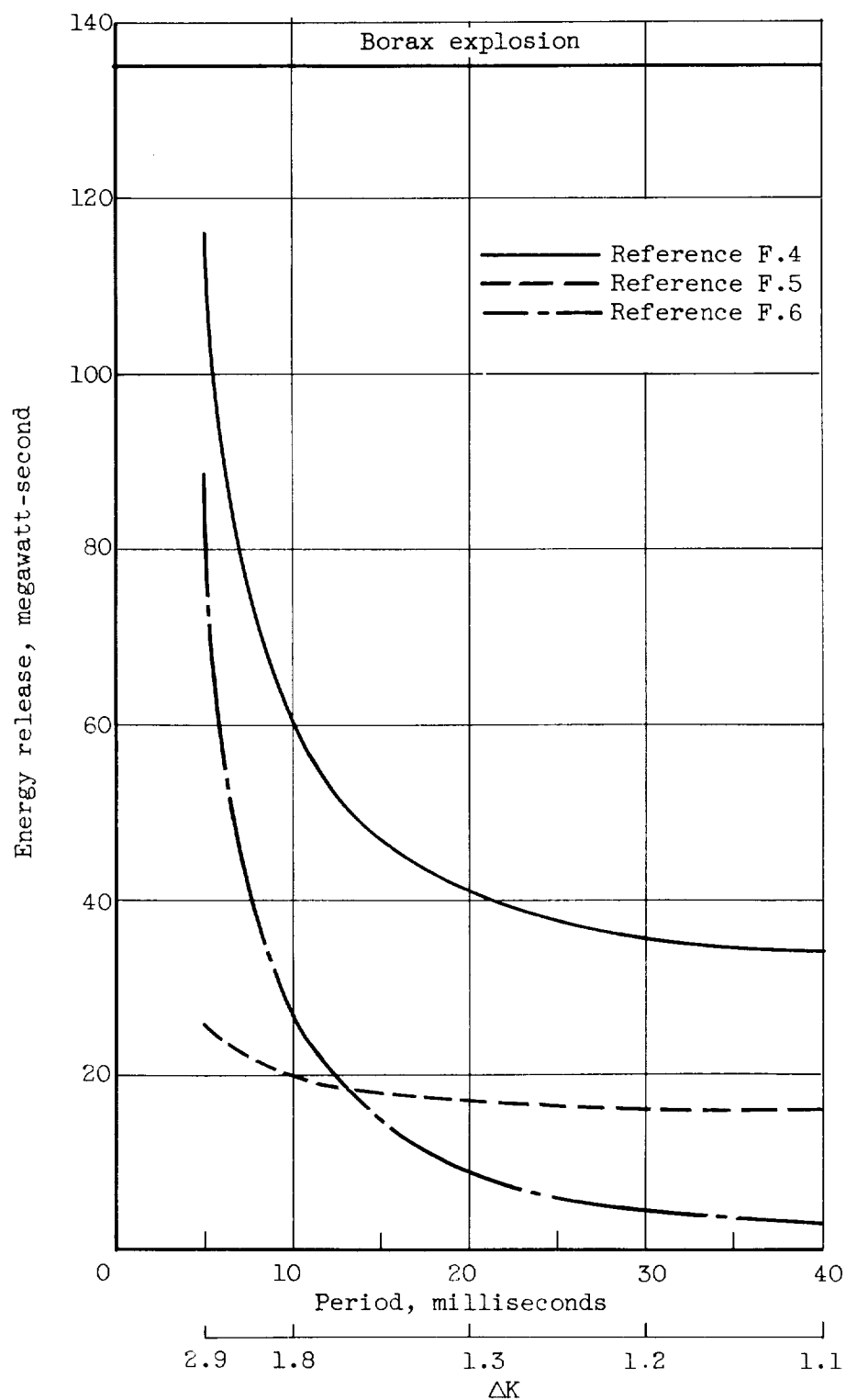


Figure F.3 - Variation of nuclear energy release with period for Borax-type excursions.

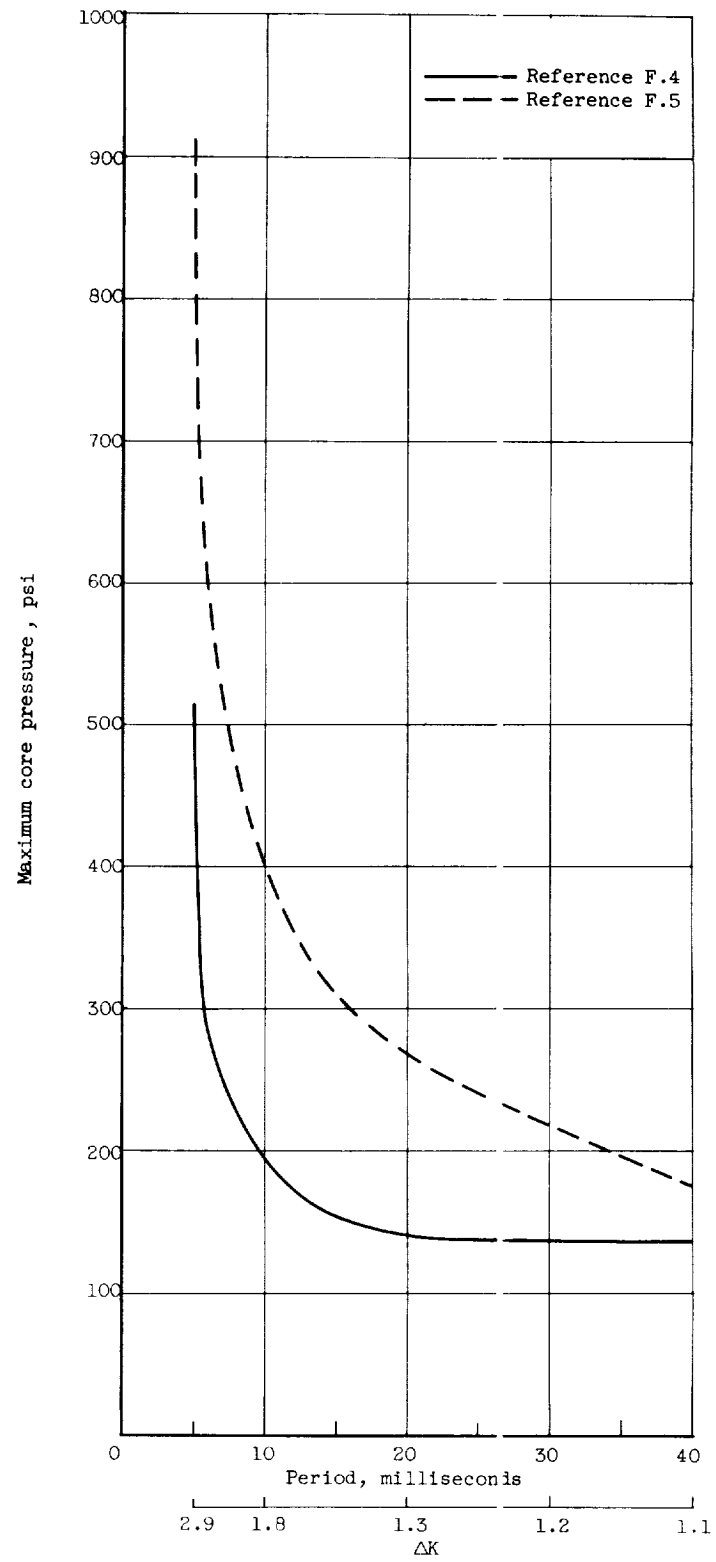


Figure F.4 - Variation of maximum pressure with period for Borax-type excursions.

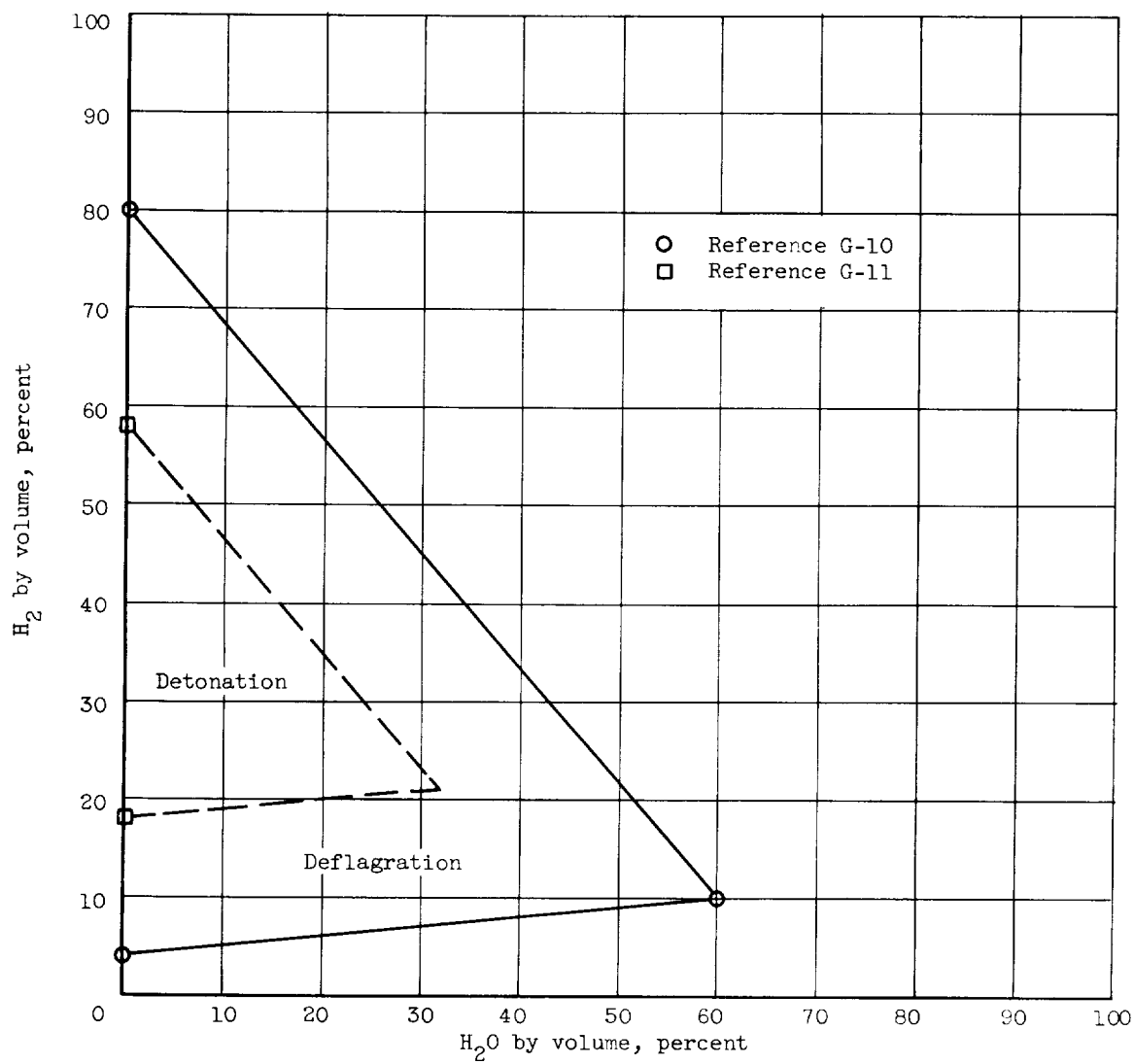
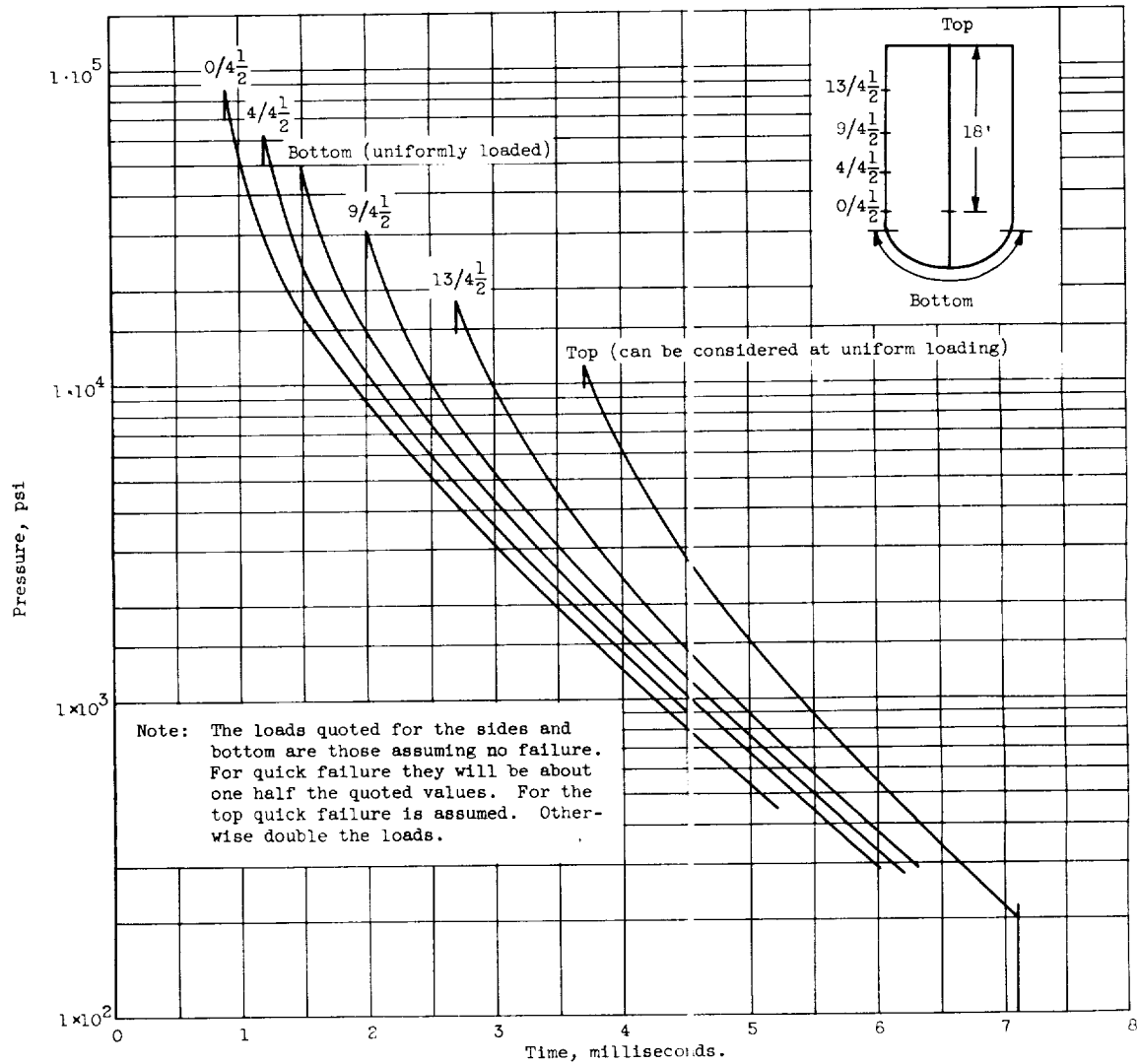
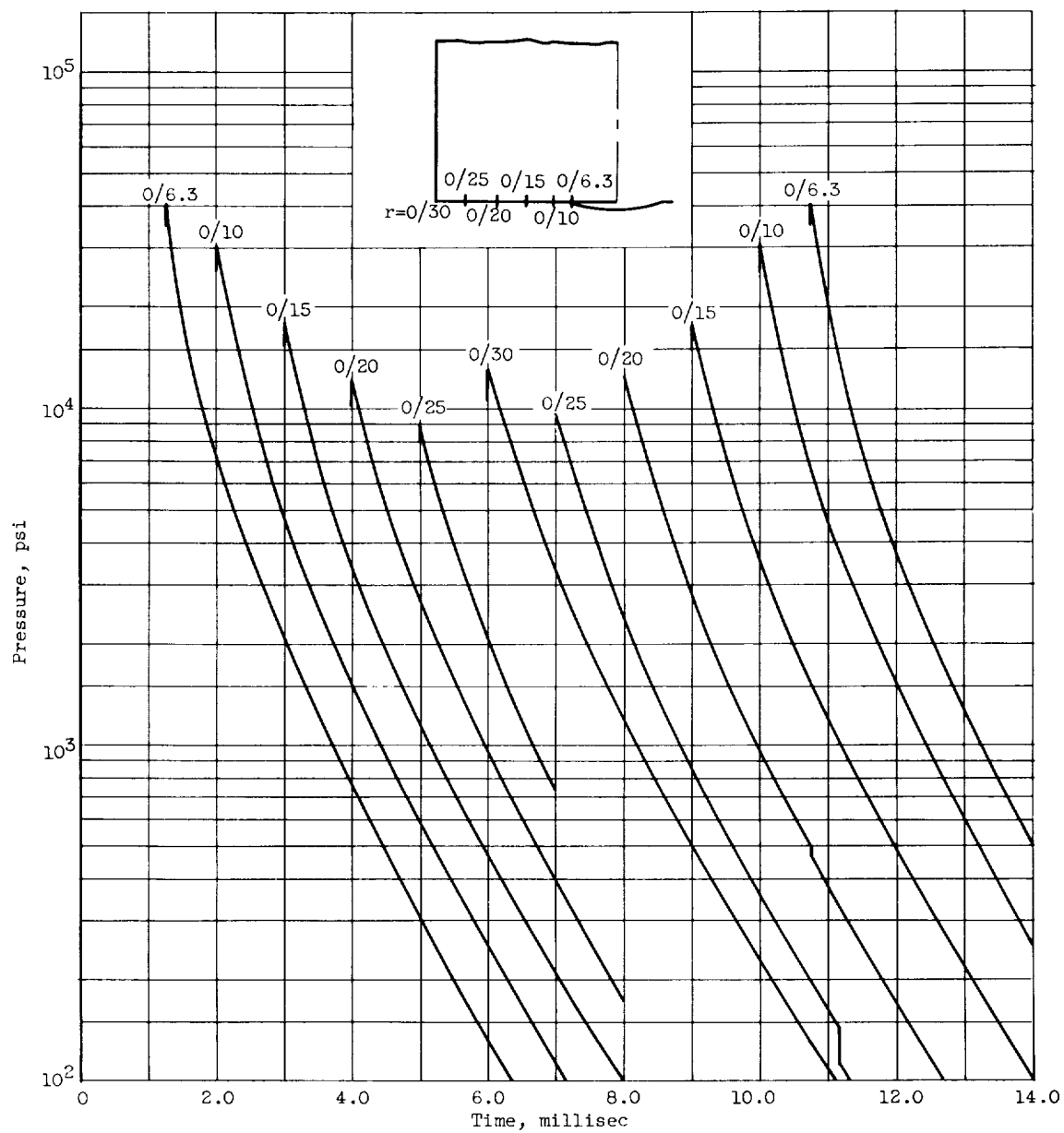


Figure G.1. - Estimated detonation and flammability limits for hydrogen-water mixtures.



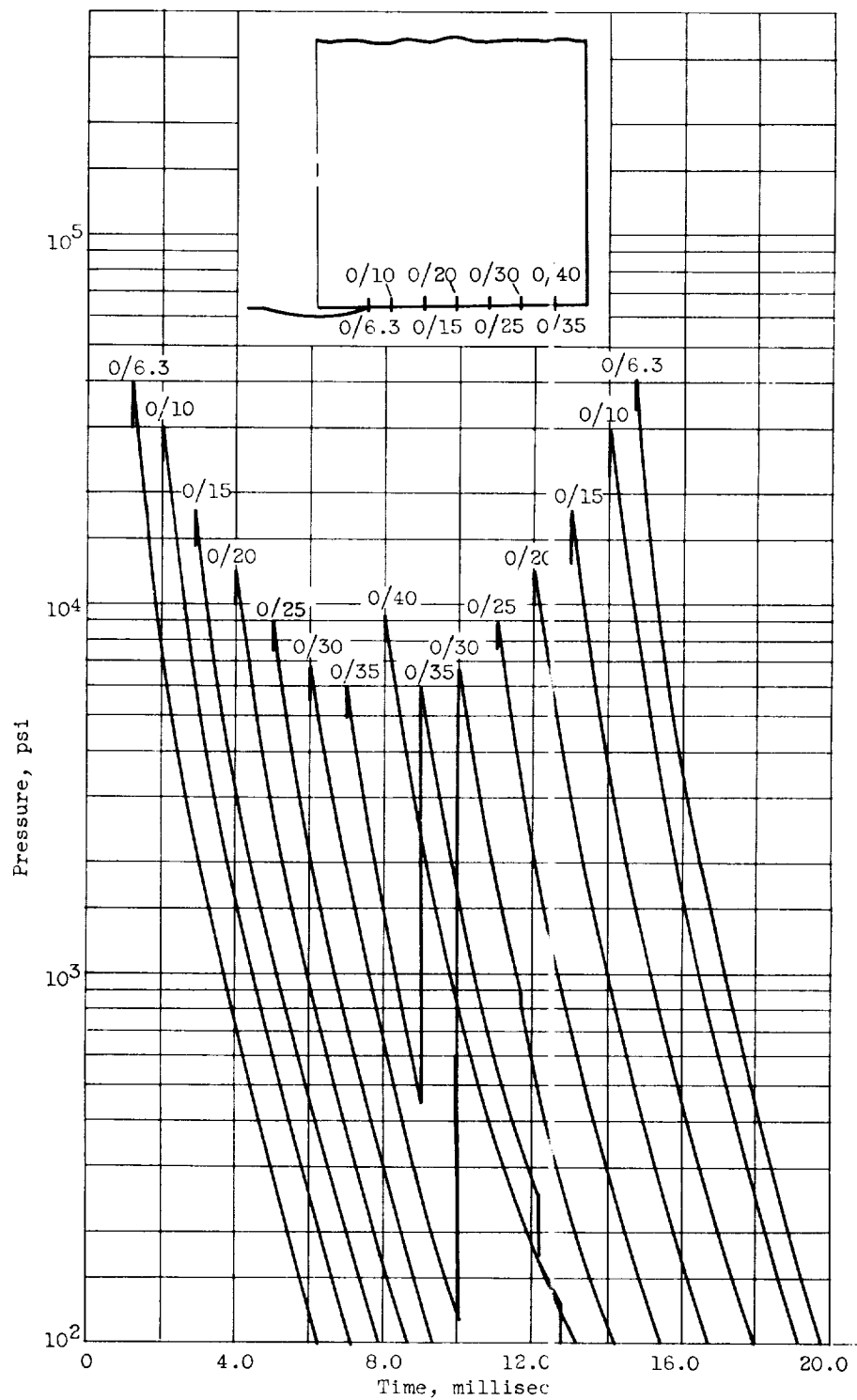
(a) Reactor pressure tank.

Figure H.1. - Pressure time histories for a 400 pound TNT explosion.



(b) Shielding pool floor; short side.

Figure H.1. - Continued. Pressure time histories for a 400 pound TNT explosion.



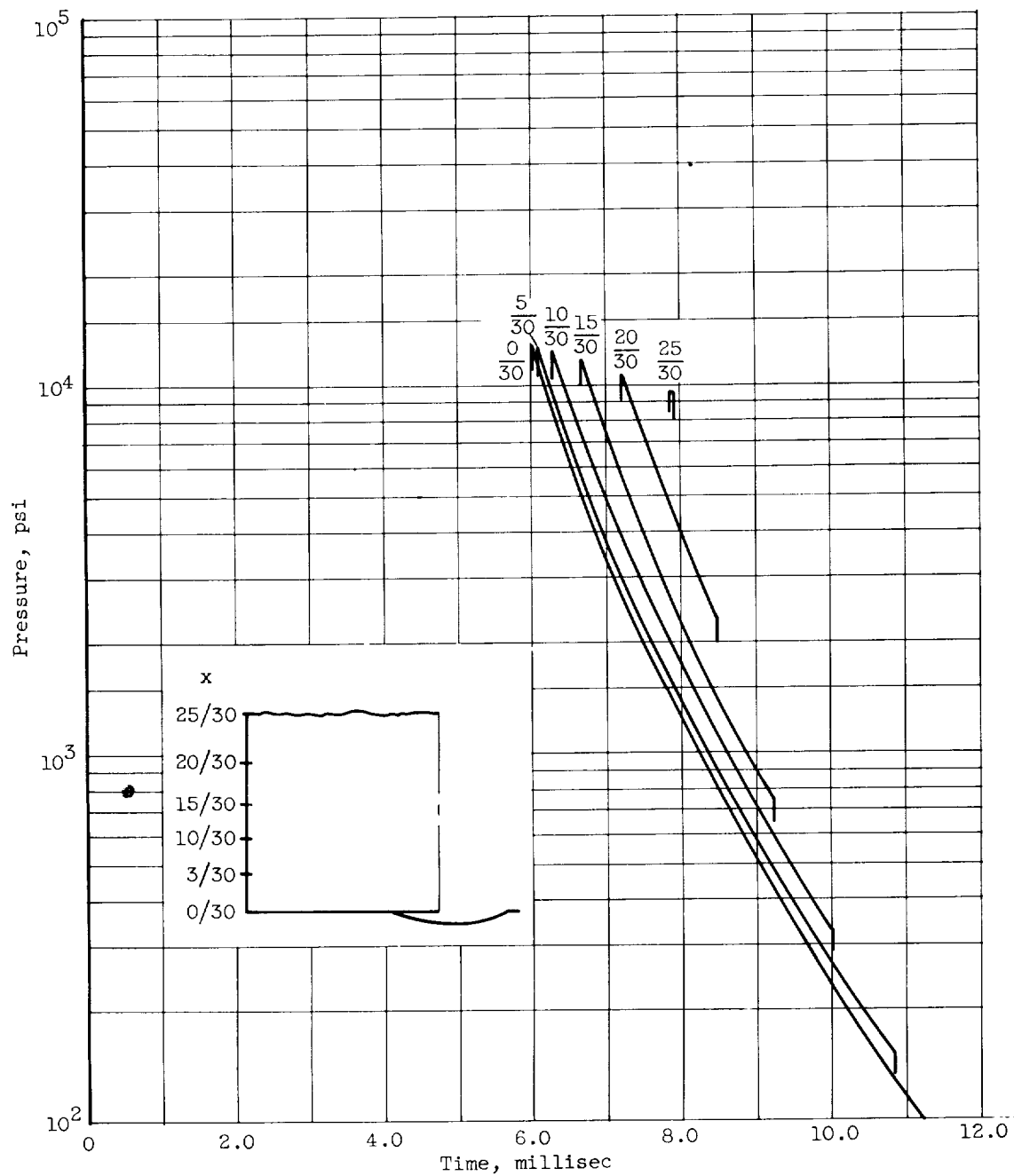
(c) Shielding pool floor; long side.

Figure H.1. - Continued. Pressure time histories for a 400 pound TNT explosion.



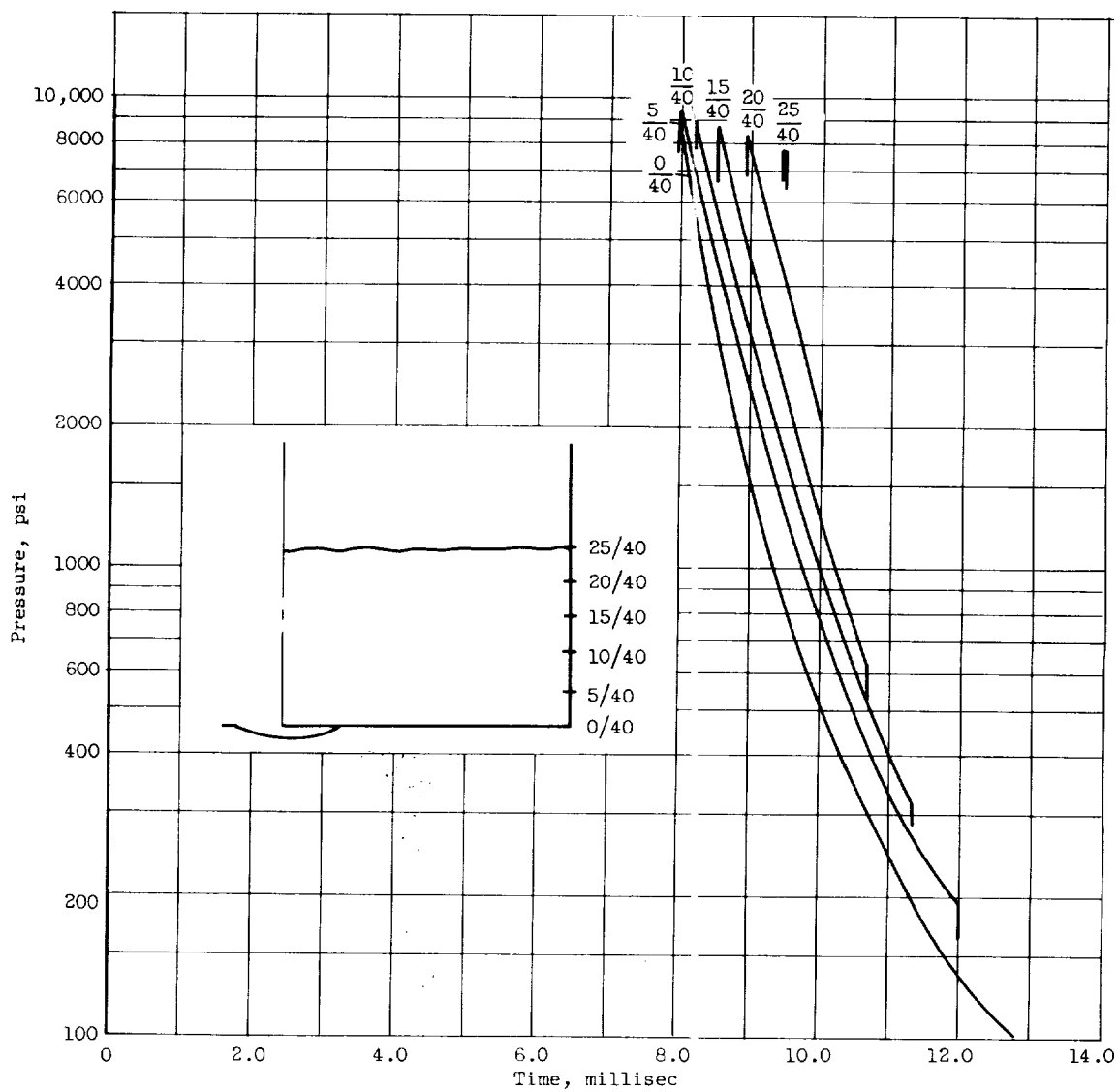
E-102

CZ-46



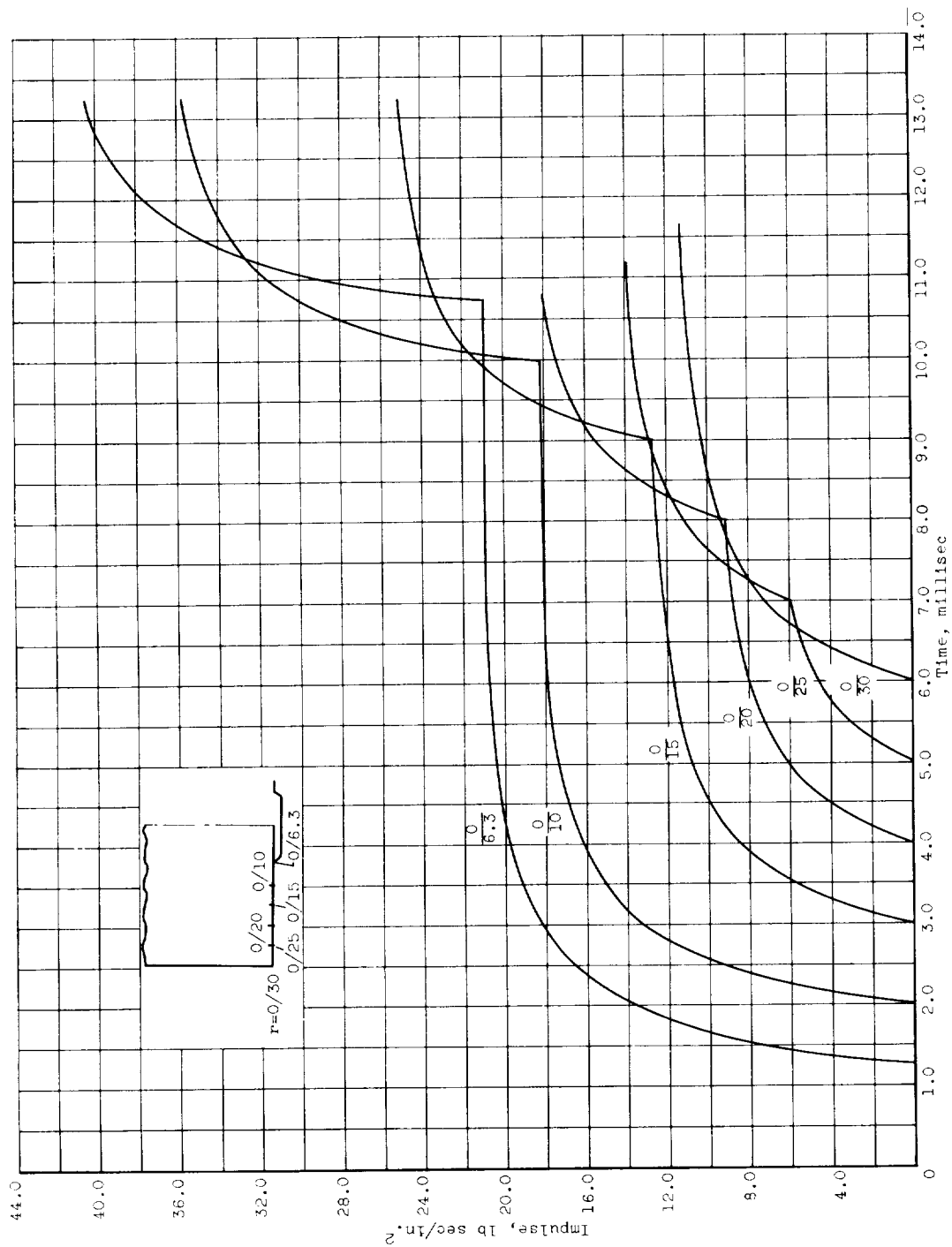
(d) Shielding pool wall; short side.

Figure H.1. - Continued. Pressure time histories for a 400 pound TNT explosion.



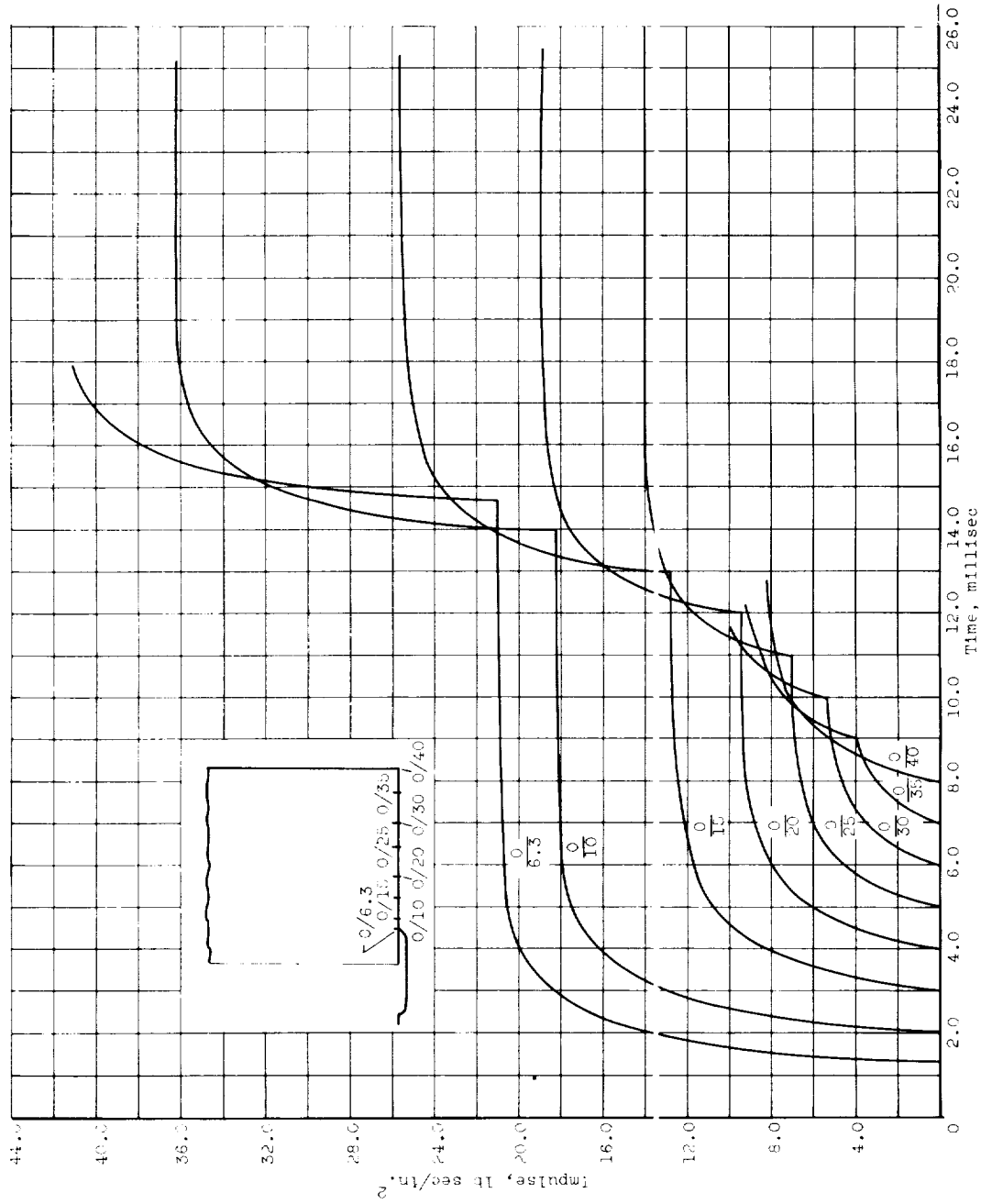
(e) Shielding pool wall; long side.

Figure H.1. - Concluded. Pressure time histories for a 400 pound TNT explosion.



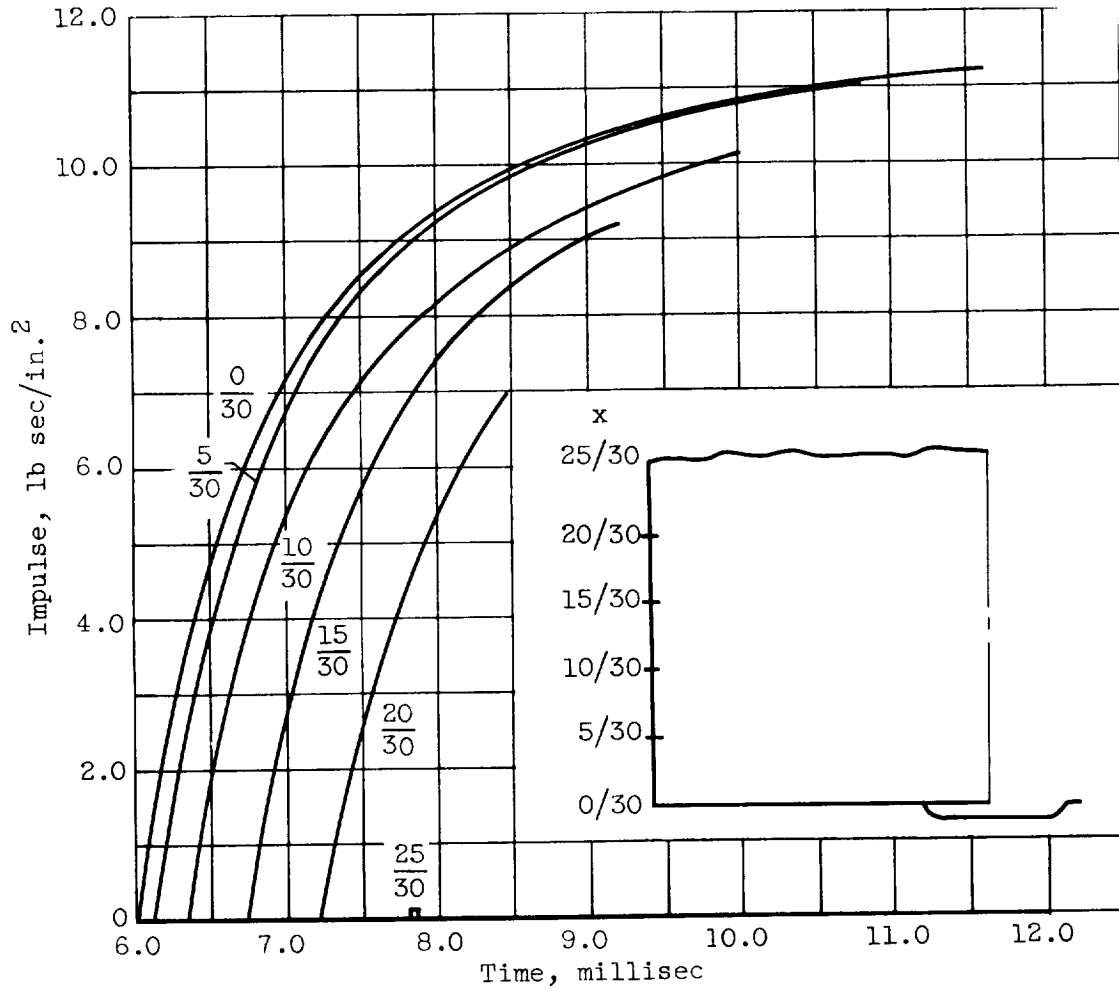
(a) Shielding pool floor; short side.

Figure H.2. - Impulse time histories for a 400 pound TNT explosion.



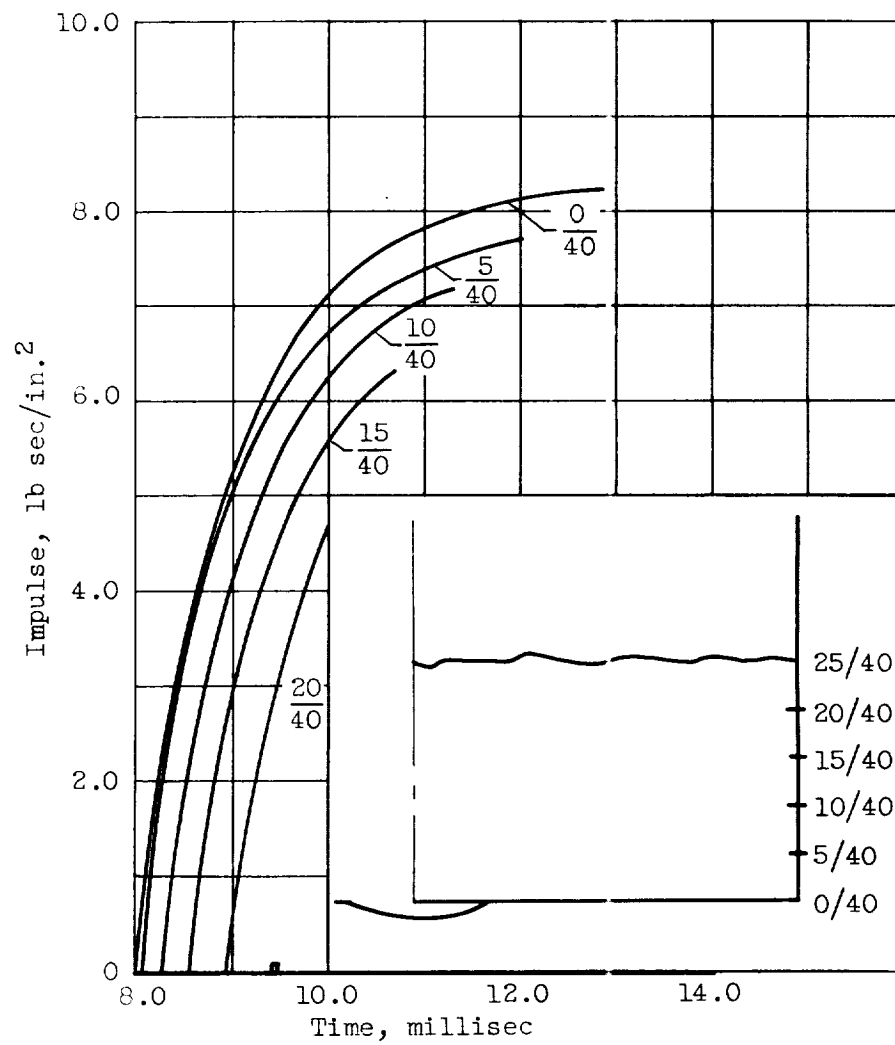
(b) Shielding pool floor; long side.

Figure H.2. - Continued. Impulse time histories for a 400 pound TNT explosion.



(c) Shielding pool wall; short side.

Figure H.2. - Continued. Impulse time histories for a 400 pound TNT explosion.



(d) Shielding pool wall; long side.

Figure H.2. - Concluded. Impulse time histories for a 400 pound TNT explosion.

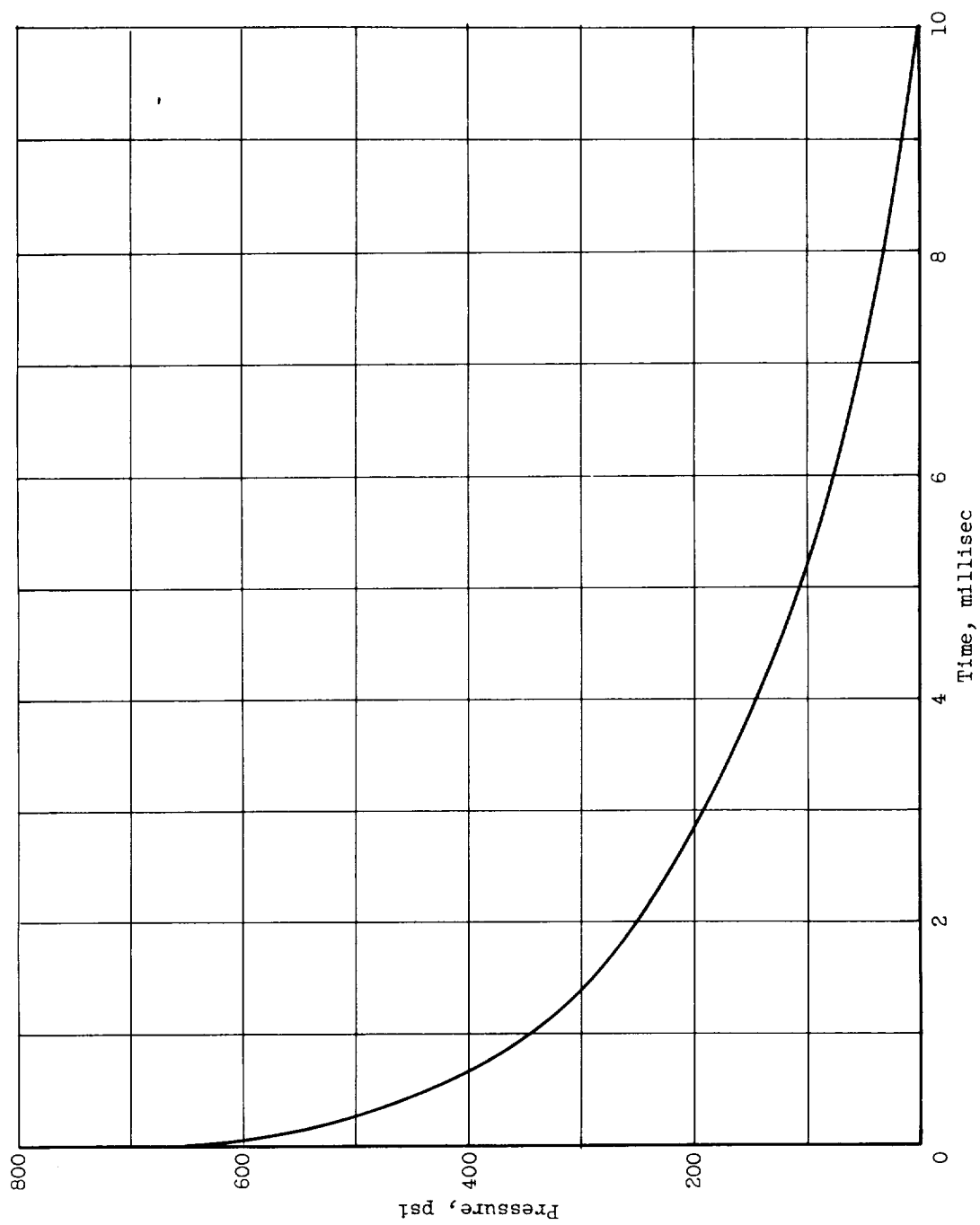


Figure H.3. - Pressure-time history of a hydrogen-oxygen explosion with water spray present.

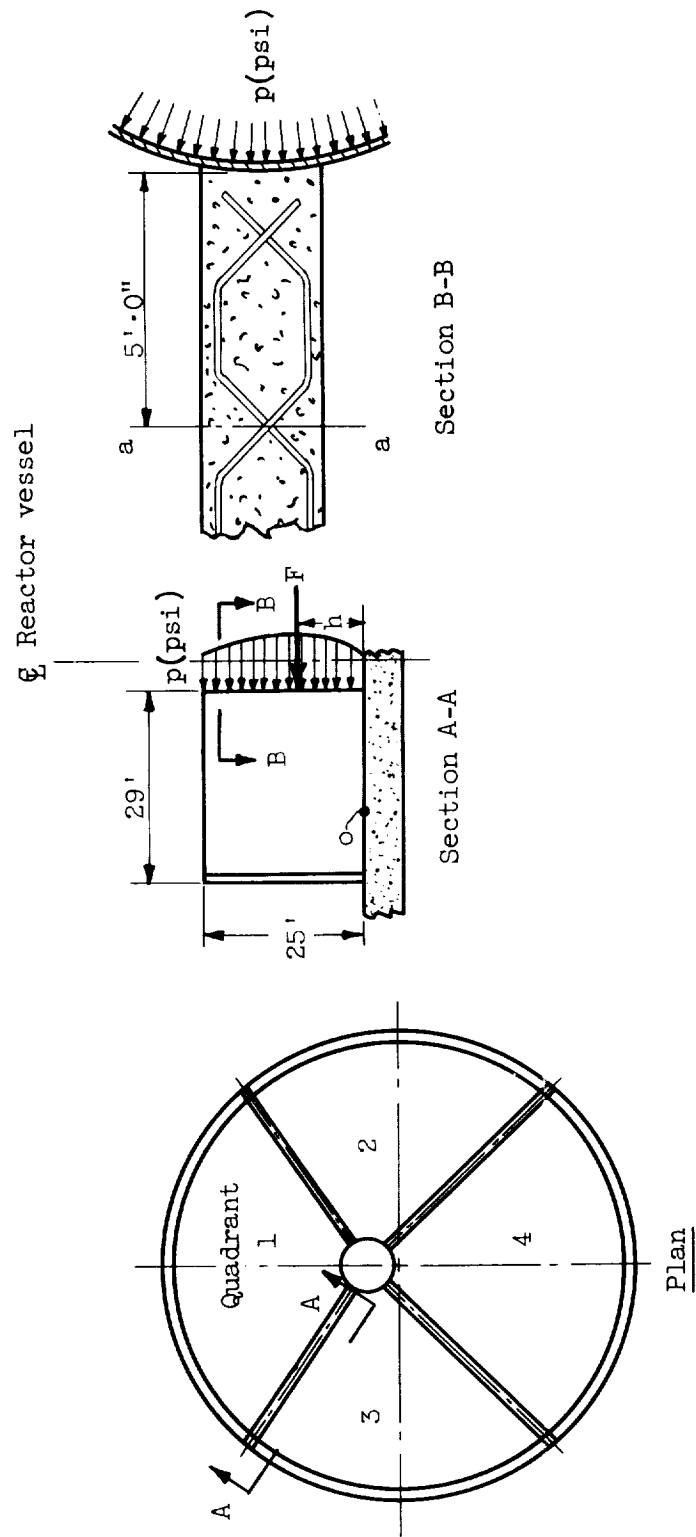


Figure I.1. - Sketch relating to the structural analysis of the quadrant walls.



E-102

CZ-47

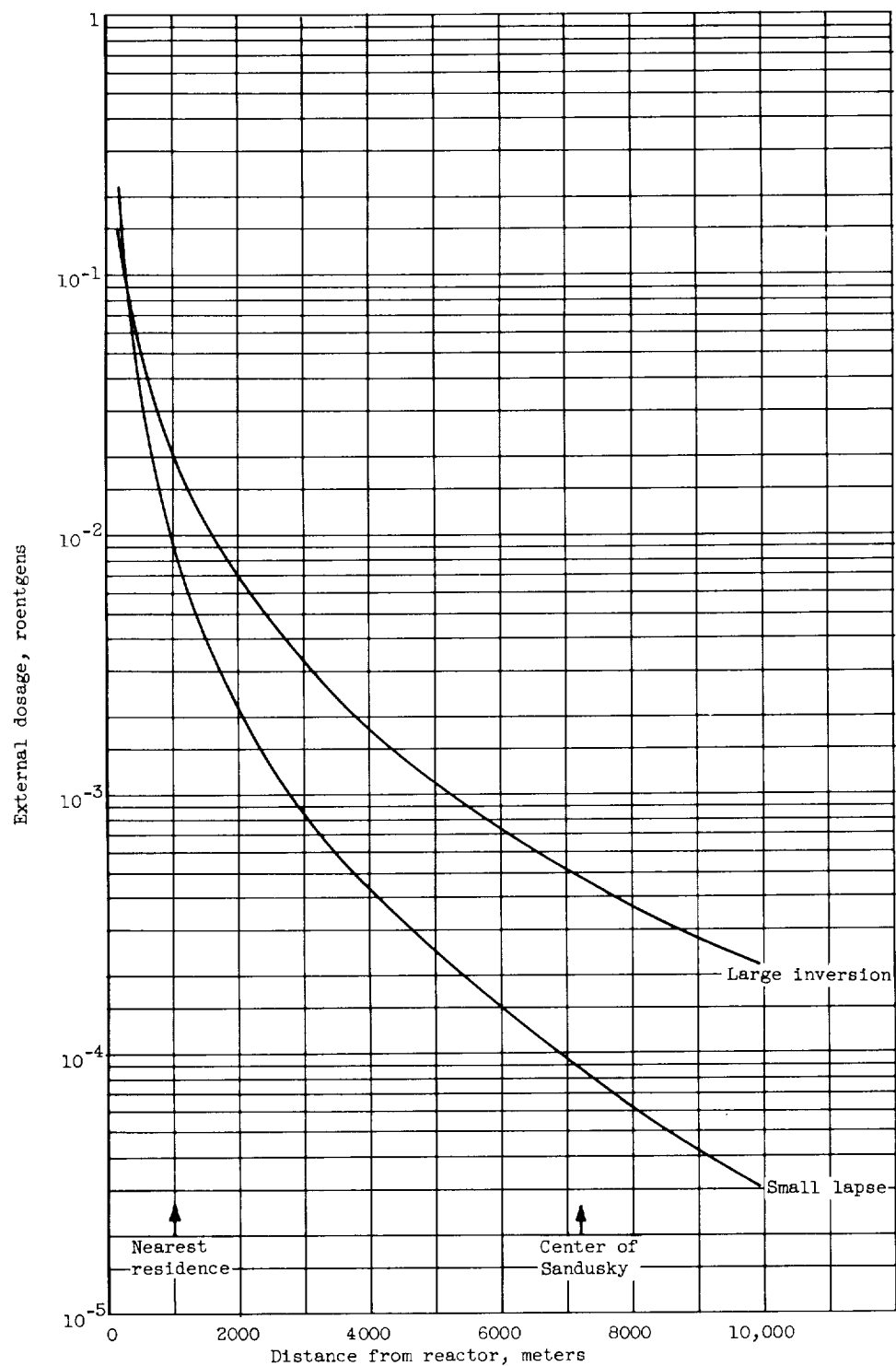


Figure J.1. - External dosage from cloud containing 1 percent of fission products. Clean power excursion of 150 megawatts - seconds. Initial cloud height, 15 meters. Instantaneous release.

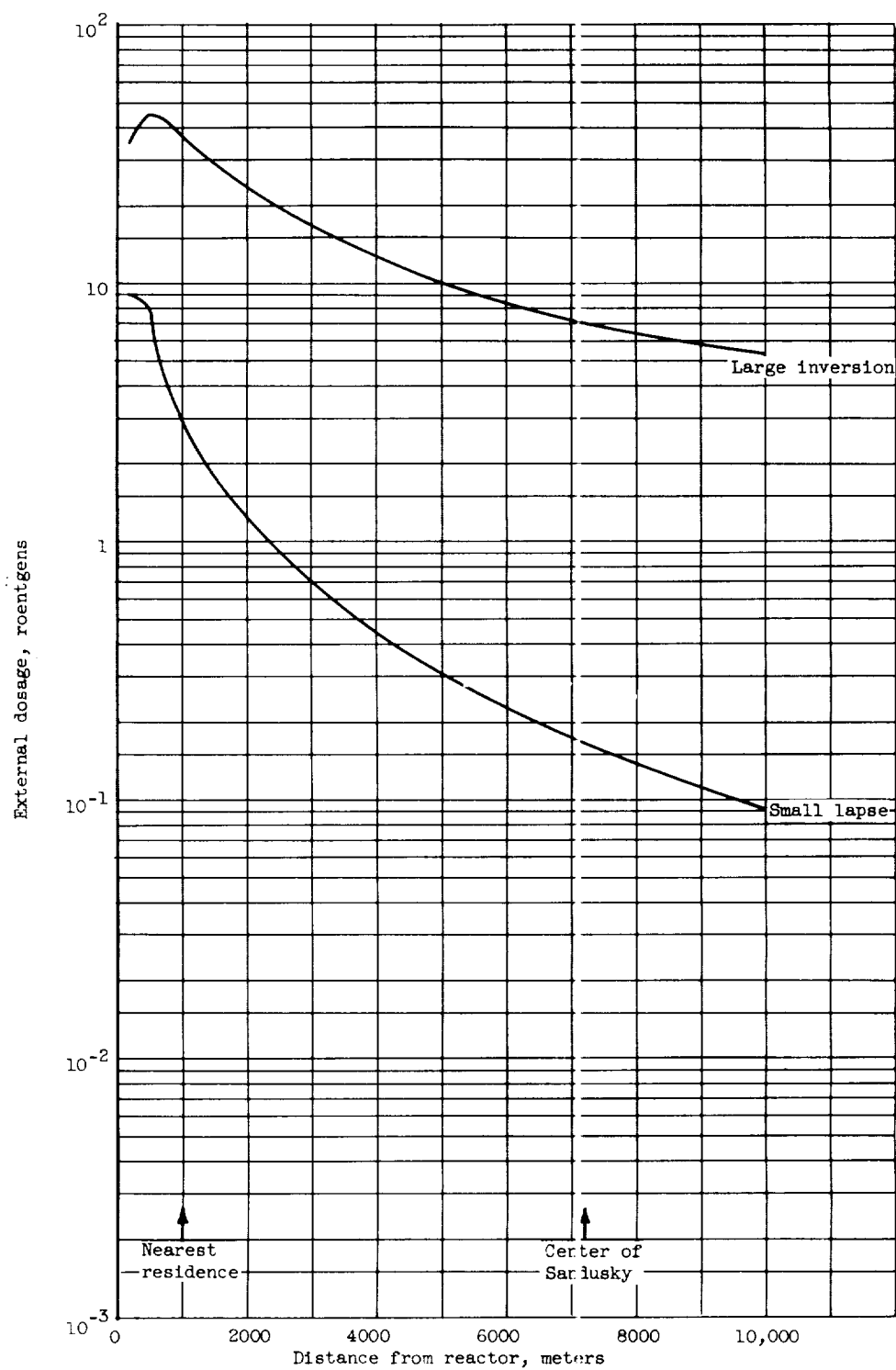


Figure J.2. - External dosage from cloud containing 1 percent of fission products. Saturated steady power (60 mw) accident. Initial cloud height, 15 meters. Instantaneous release.

E-102

CZ-47 back

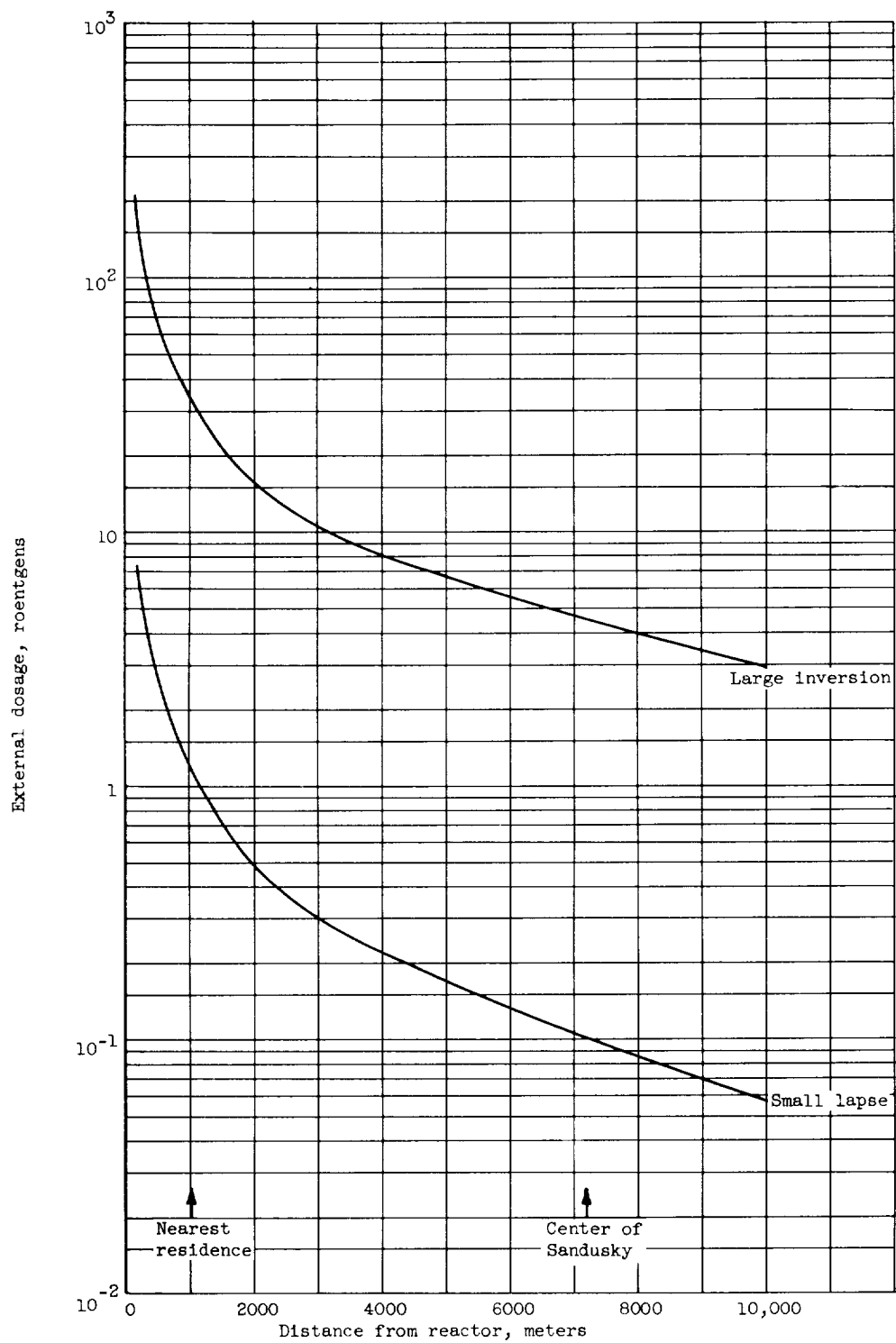


Figure J.3. - External dosage from cloud containing 1 percent of fission products. Saturated steady power (60 mw) accident. Initial cloud height at ground level. Continuous release over 24 hours.

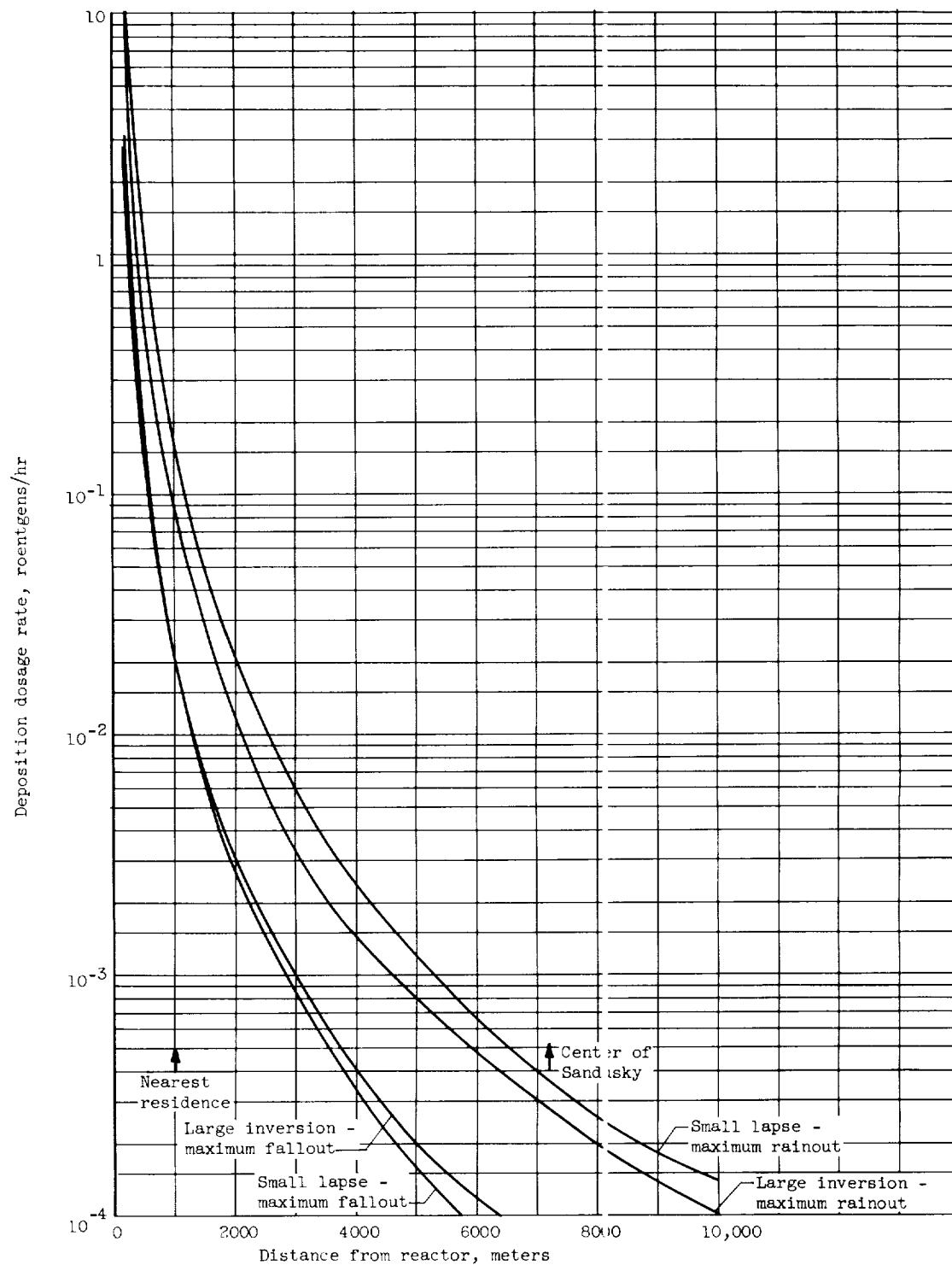


Figure J.4. - Deposition dosage rate from cloud containing 1 percent of fission products. Clean power excursion of 150 megawatts - seconds. Initial cloud height, 15 meters. Instantaneous release.

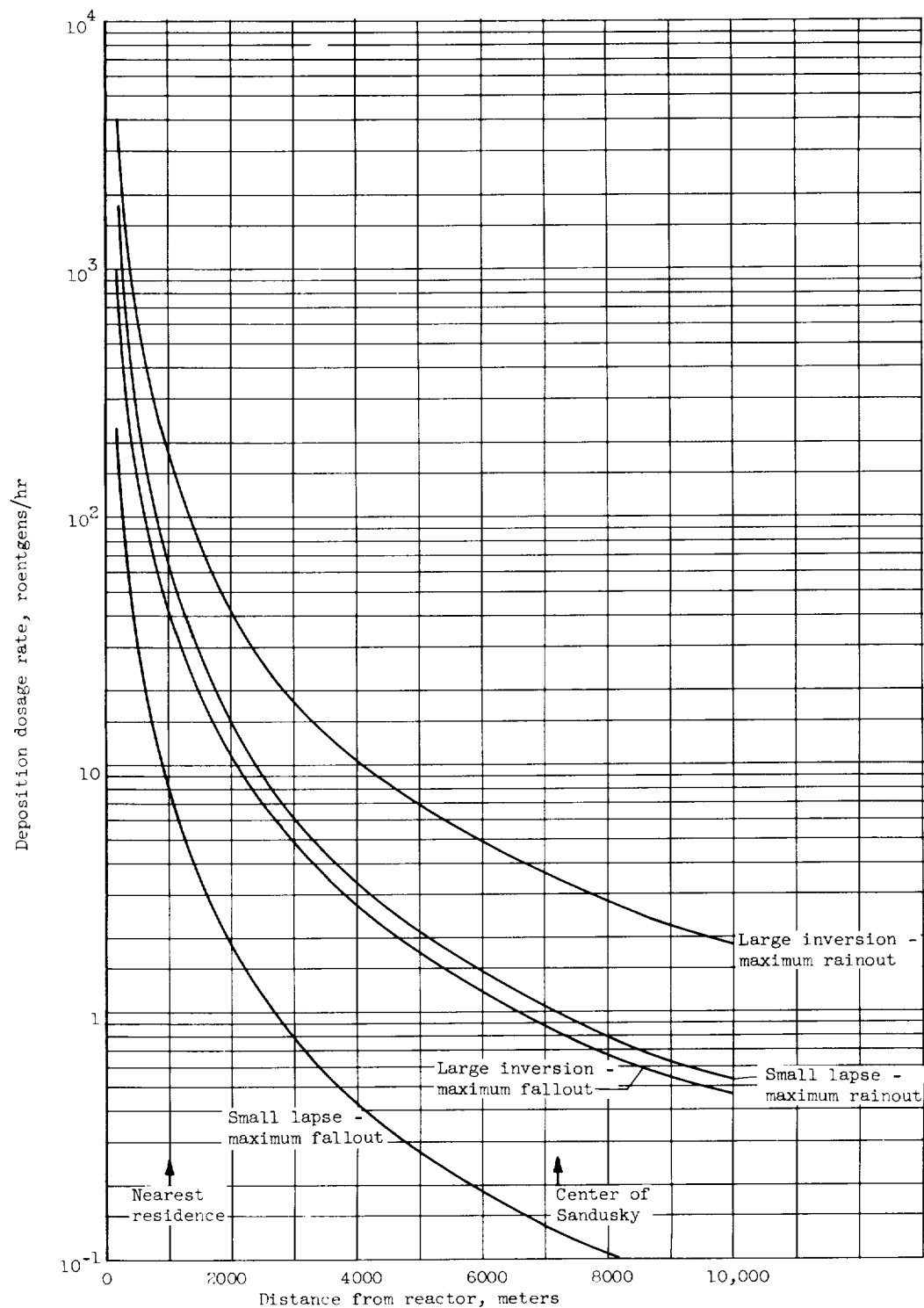


Figure J.5. - Deposition dosage rate from cloud containing 1 percent of fission products. Saturated steady power (60 mw) accident. Initial cloud height, 15 meters. Instantaneous release.

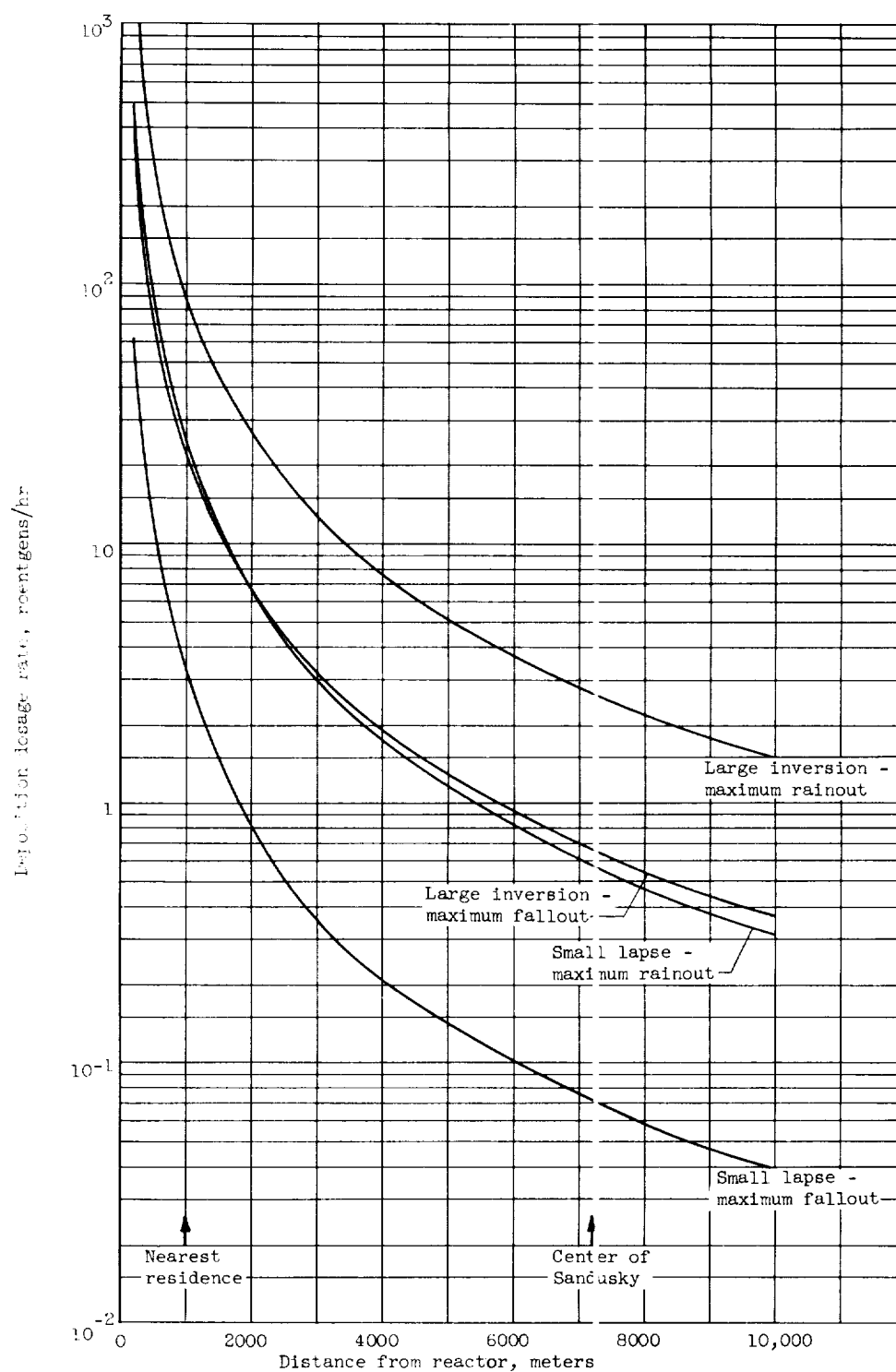


Figure J.6. - Deposition dosage rate from cloud containing 1 percent of fission products. Saturated steady power (60 mw) accident. Initial cloud height at ground level. Continuous release over 24 hours.

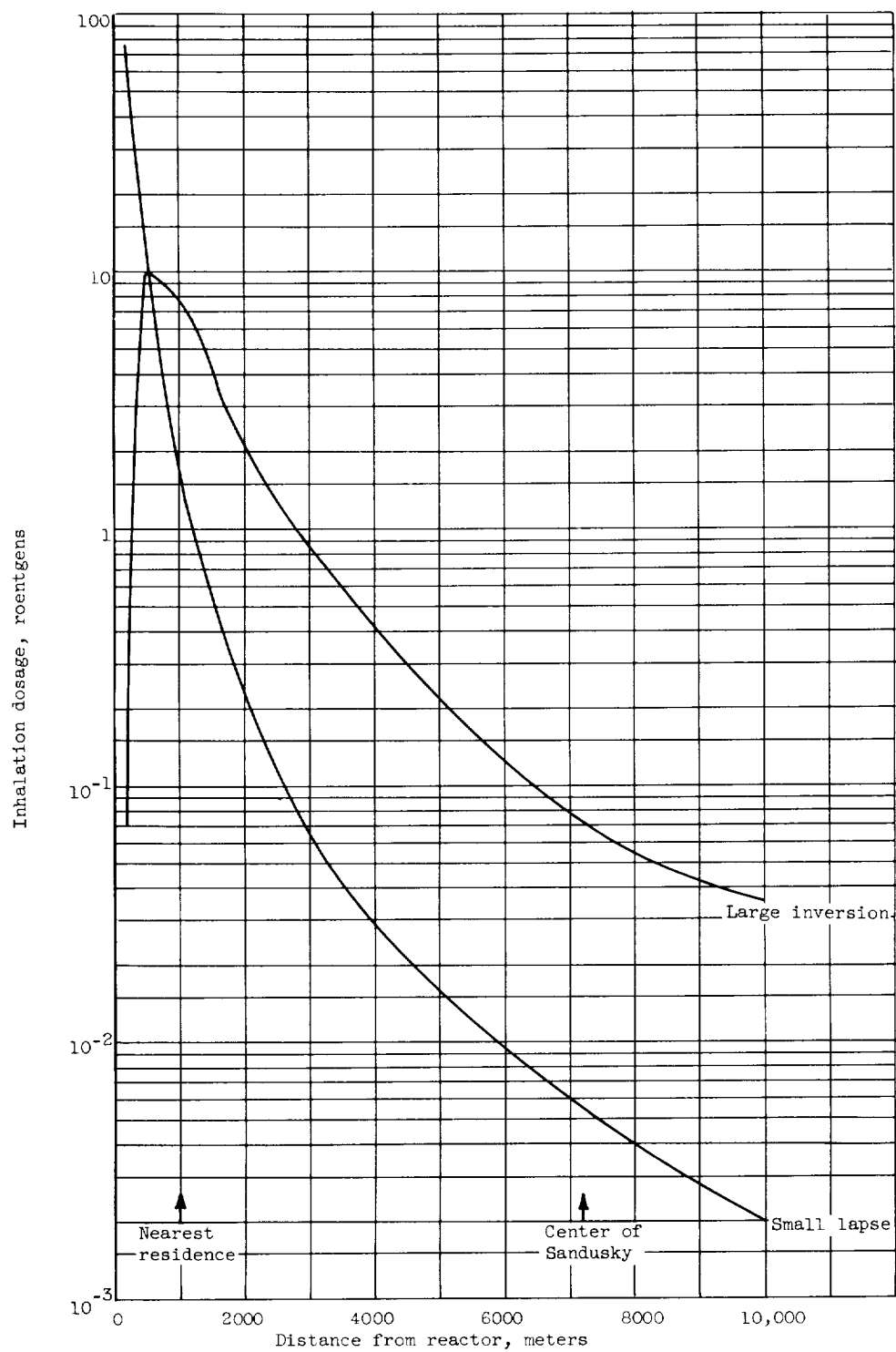


Figure J.7. - Inhalation dosage from cloud containing 1 percent of fission products. Clean power excursion of 150 megawatts - seconds. Initial cloud height, 15 meters. Instantaneous release.

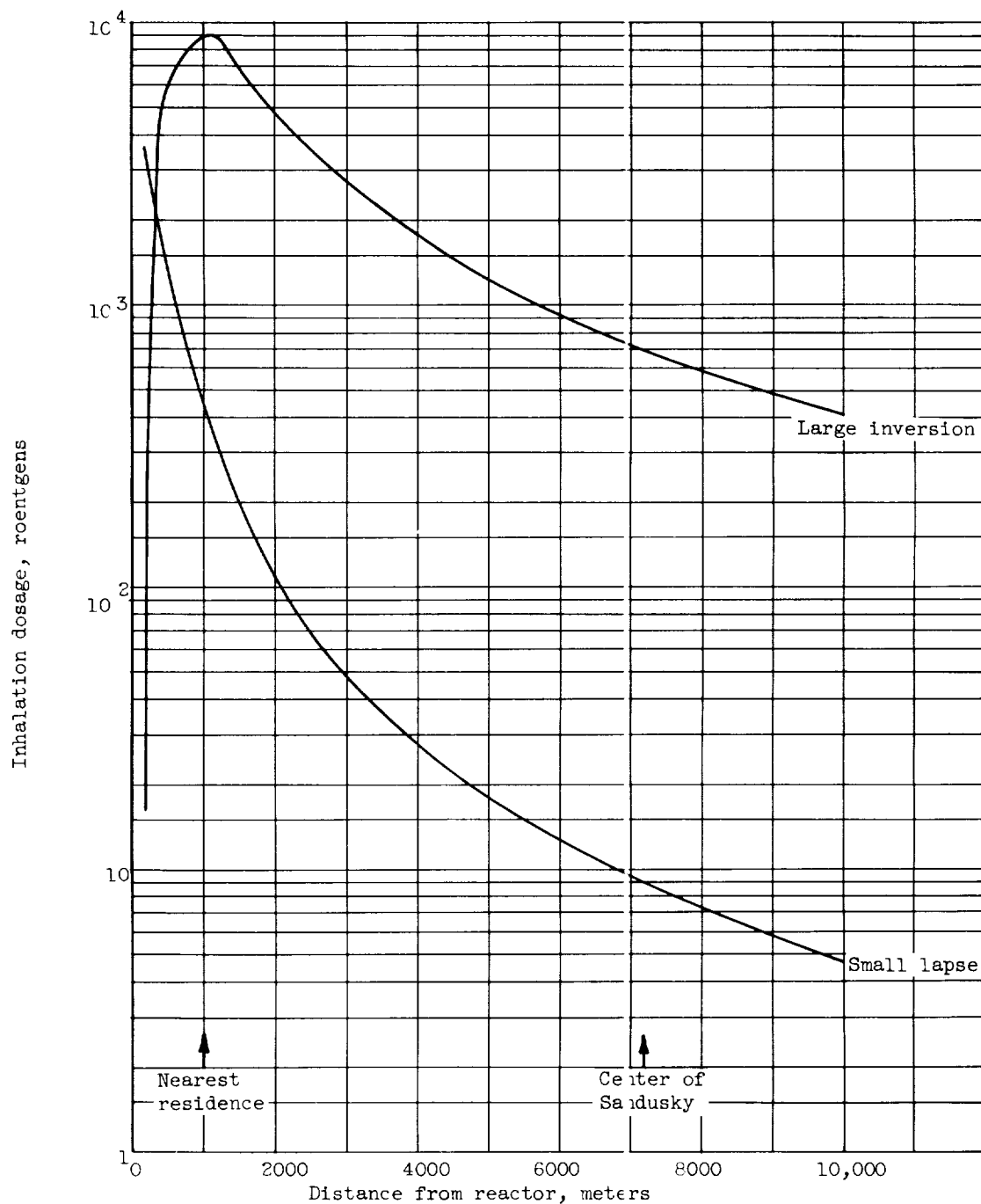


Figure J.8. - Inhalation dosage from cloud containing 1 percent of fission products. Saturated steady power (60 mw) accident. Initial cloud height, 15 meters. Instantaneous release.



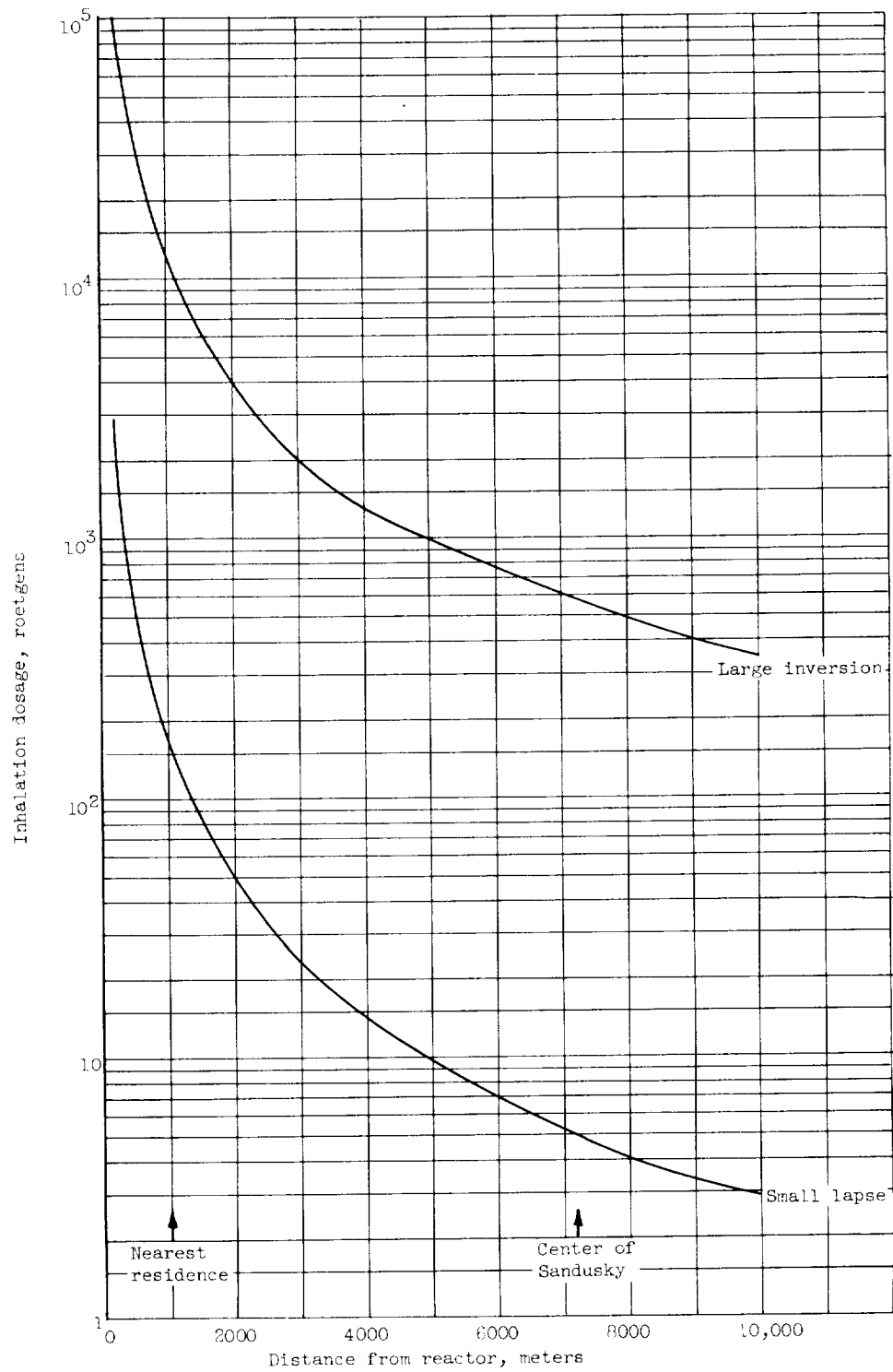


Figure J.9. - Inhalation dosage from cloud containing 1 percent of fission products. Saturated steady power (60 mw) accident. Initial cloud height at ground level. Continuous release over 24 hours.

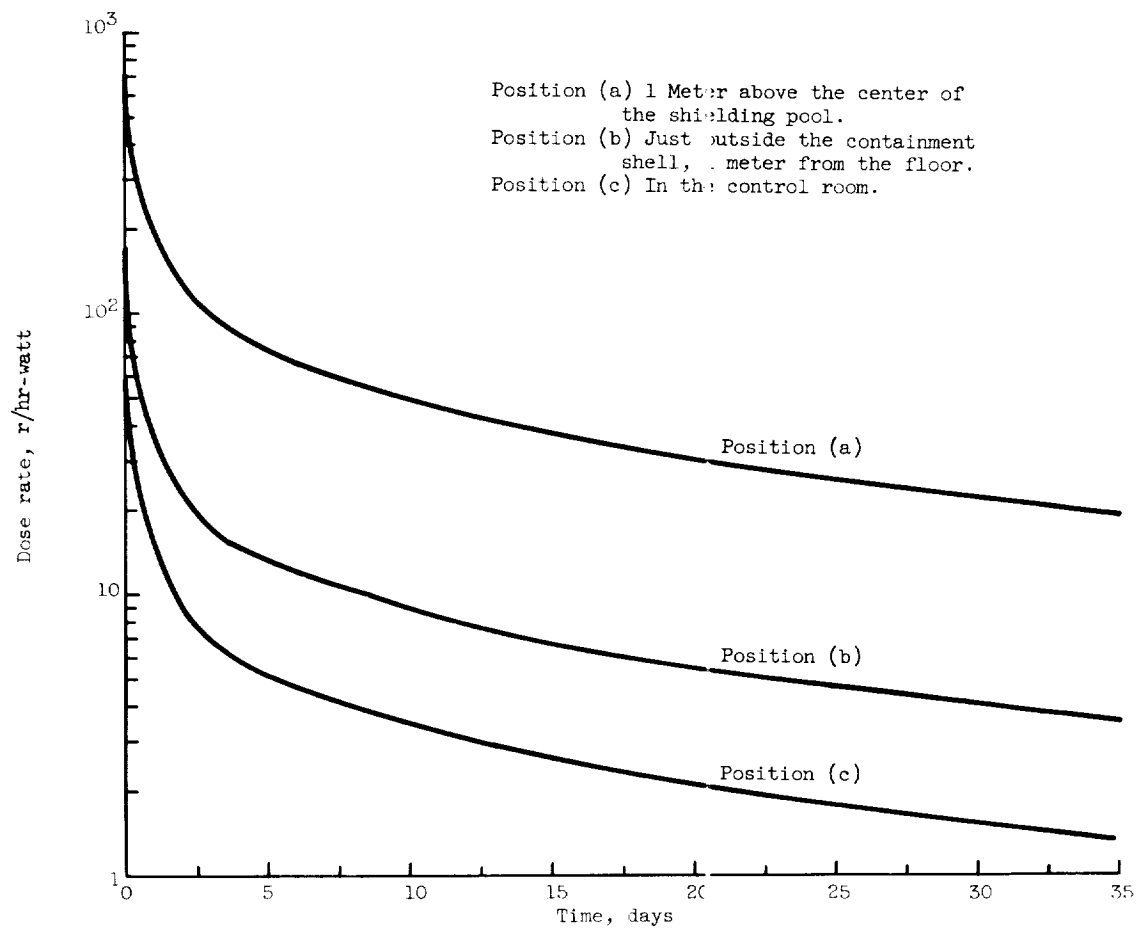


Figure J.12 - Dose rate due to contaminated quadrant water.

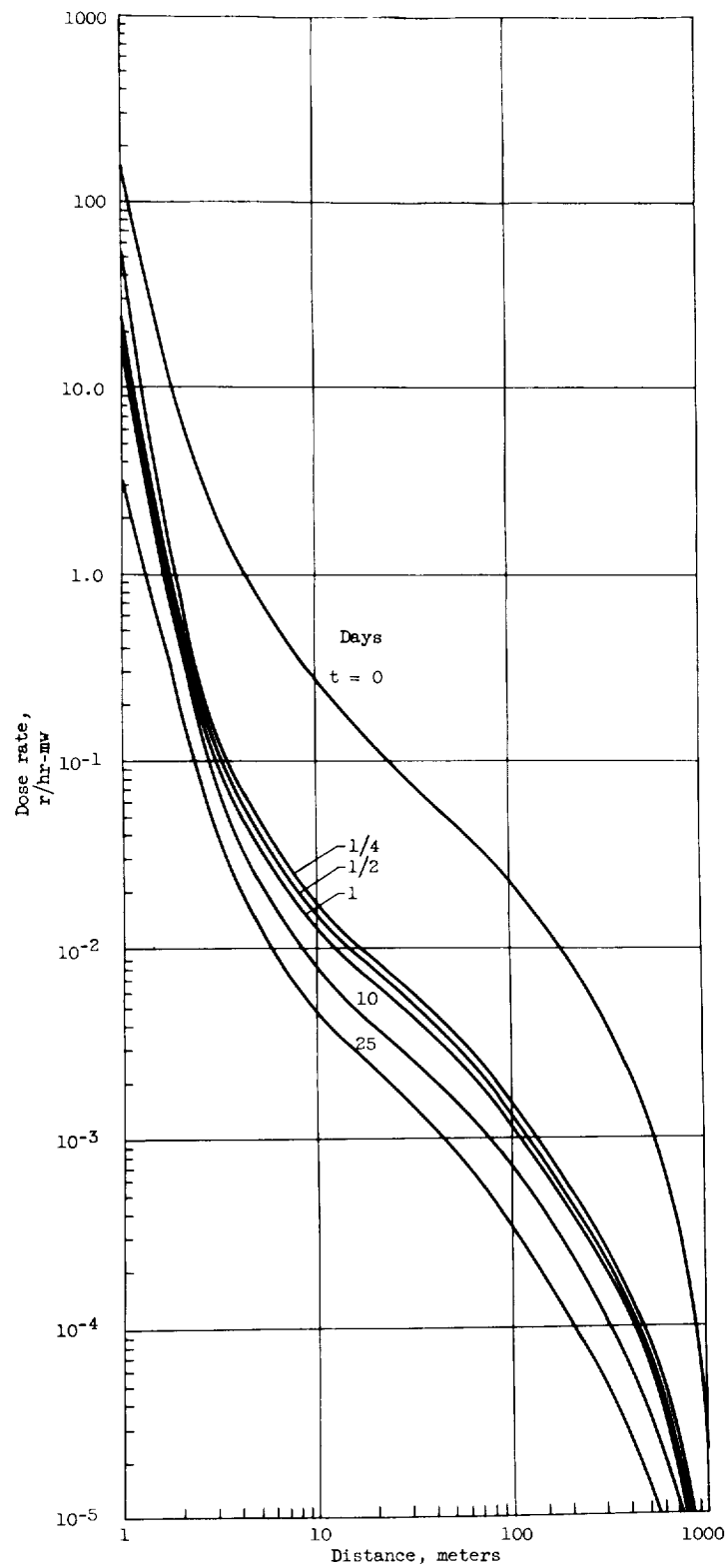


Figure J.13 - Gamma dose rate due to nonvolatile fission products in the quadrant water.

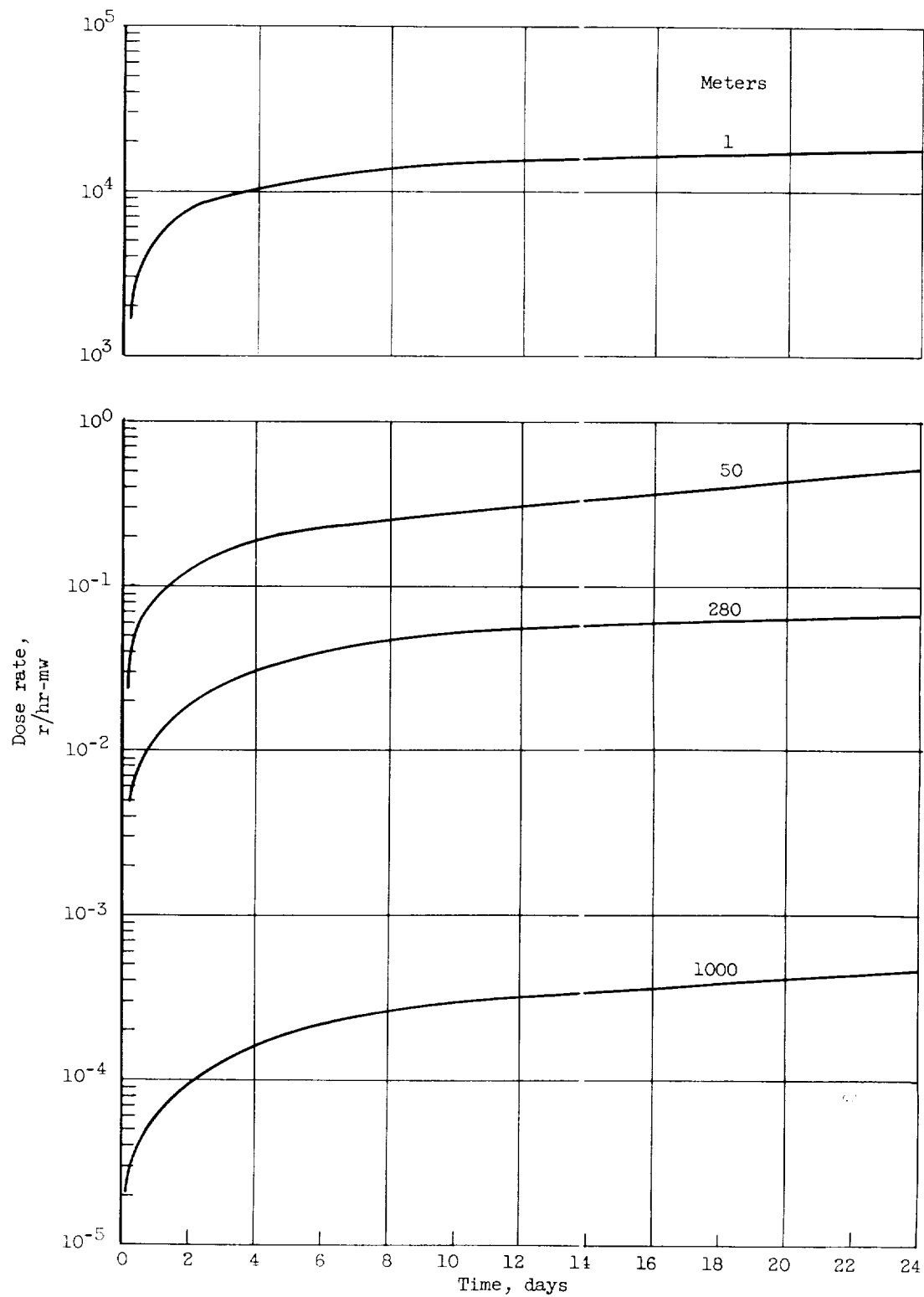


Figure J.14 - Integrated gamma dose due to nonvolatile fission products in the quadrant water.

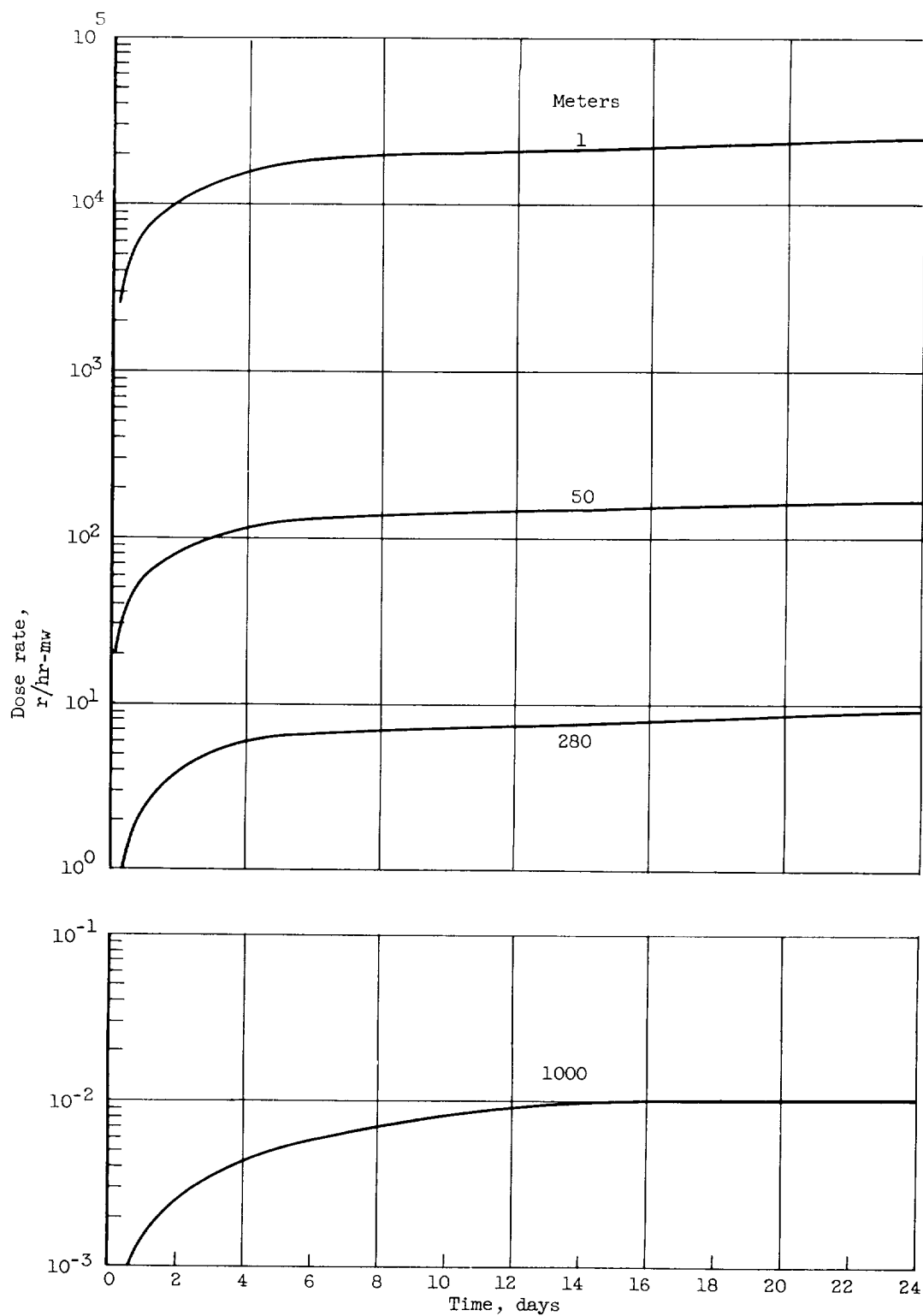
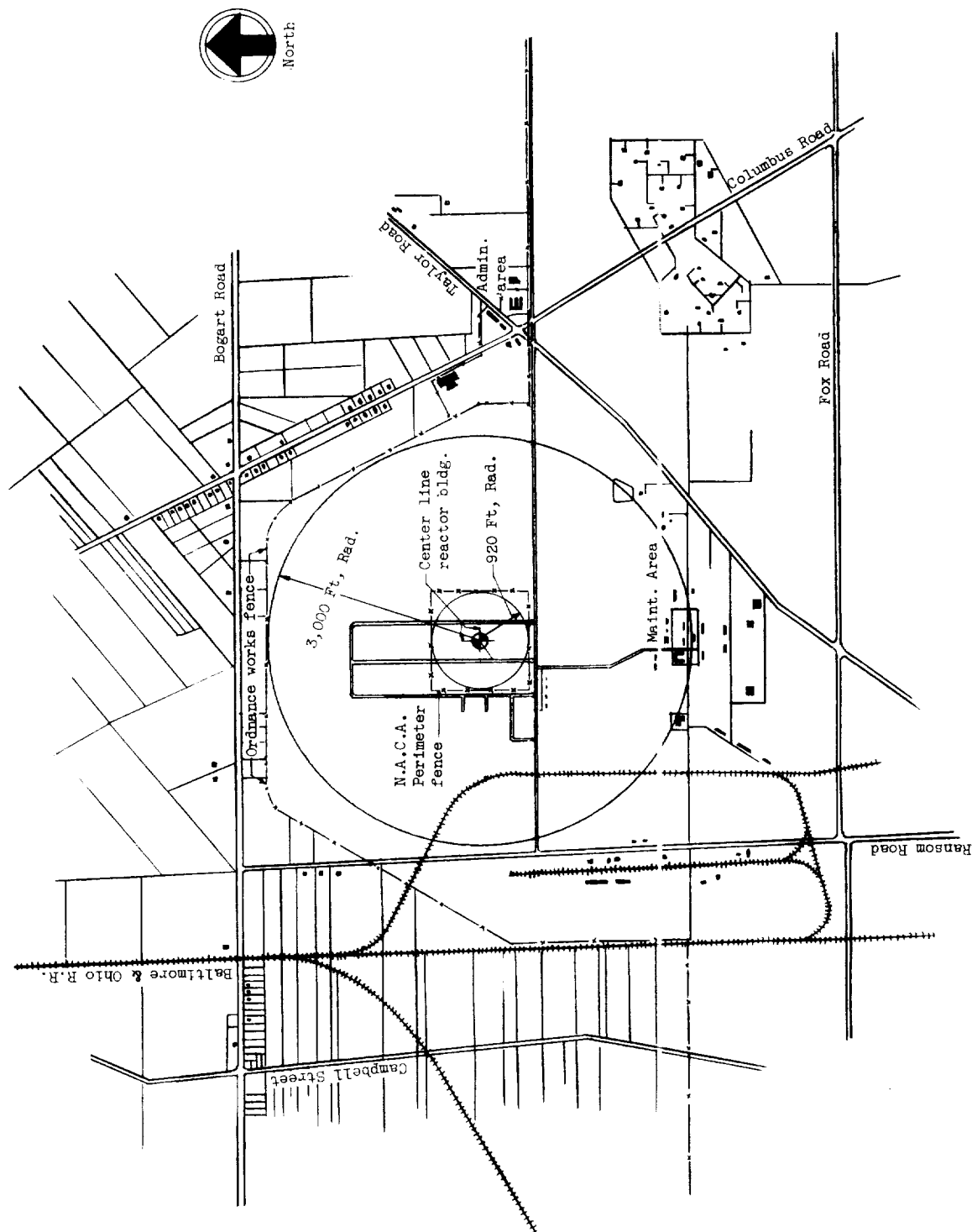


Figure J.15 - Total integrated gamma dose due to volatile and nonvolatile fission products.



920' Radius - Nearest point of arsenal property  
 3000' Radius - Nearest point of public property

Figure J.16 - The reactor site and surrounding area showing the 920 and 3000 foot radius circles.